ANNUAL REPORTS ON NMR SPECTROSCOPY

Volume 19

ANNUAL REPORTS ON

NMR SPECTROSCOPY

This Page Intentionally Left Blank

ANNUAL REPORTS ON

NMR SPECTROSCOPY

Edited by

G. A. WEBB

Department of Chemistry, University of Surrey, Guildford, Surrey, England

VOLUME 19

1987

ACADEMIC PRESS

LIST OF CONTRIBUTORS

Dr E. W. Bastiaan, *Department of Physical Chemistry, Free University, Amsterdam, The Netherlands.*

Professor A. A. Bothner-By, *Department of Chemistry, Carnegie-Mellon University, Pittsburgh, Pennsylvania, USA.*

Professor J. F. Hinton, *Department of Chemistry, University of Arkansas, Fayetteville, Arkansas 72701, USA.*

Professor S. S. Krishnamurthy, *Department of Inorganic and Physical Chemistry, Indian Institute of Science, Bangalore 560 012, India.*

Professor C. MacLean, *Department of Physical Chemistry, Free University, Amsterdam, The Netherlands.*

Dr K. G. Orrell, *Department of Chemistry, The University, Exeter EX4 4QD, UK.*

Dr V. Šik, *Department of Chemistry, The University, Exeter EX4 4QD, UK.*

Dr P. C. M. van Zijl, *Department of Physical Chemistry, Carnegie-Mellon University, Pittsburgh, Pennsylvania, USA.*

Dr M. Woods, *Department of Inorganic and Physical Chemistry, Indian Institute of Science, Bangalore 560 012, India.*

This Page Intentionally Left Blank

PREFACE

The catholic nature of NMR spectroscopy is adequately demonstrated by the four areas chosen for review in the present volume. Three of these areas are receiving specific coverage for the first time in this series.

The first chapter is a very timely one on ^{33}S NMR. This topic is one that has attracted considerable attention in the past two years and is likely to continue expanding rapidly in the near future. Thus the present account should serve to attract attention to an important field of NMR applications. High-resolution NMR of liquids and gases and the effects of magnetic-field-induced molecular alignment are comprehensively covered in the second chapter. This is another area where rapid developments are generating much interest. Following this is a review of dynamic NMR spectroscopy in inorganic and organometallic chemistry that both complements and provides an update of an earlier report in Volume 12 of this series. The final chapter deals with the NMR spectroscopy of cyclophosphazenes, which is another new area of coverage for *Annual Reports on NMR Spectroscopy*.

It gives me great pleasure to be able to thank all of the authors concerned for the careful preparation of their manuscripts and for the promptness with which they were delivered. I am also grateful to various members of the staff of Academic Press (London) for their kind assistance on several occasions during the preparation of this volume.

University of Surrey   G. A. WEBB
Guildford, Surrey
England

This Page Intentionally Left Blank

CONTENTS

Sulphur-33 NMR Spectroscopy

J. F. HINTON

High-Resolution NMR of Liquids and Gases: Effects of Magnetic-Field-Induced Molecular Alignment

E. W. BASTIAAN, P. C. M. van ZIJL, C. MACLEAN AND A. A. BOTHNER-BY

Dynamic NMR Spectroscopy in Inorganic and Organometallic Chemistry

K. G. ORRELL AND V. ŠIK

Nuclear Magnetic Resonance of Cyclophosphazenes

S. S. KRISHNAMURTHY AND MICHAEL WOODS

This Page Intentionally Left Blank

Sulphur-33 NMR Spectroscopy

J. F. HINTON

Department of Chemistry, University of Arkansas, Fayetteville, Arkansas 72701, USA

I. INTRODUCTION

The ubiquitous nature of sulphur secures a place of considerable importance for this element in chemistry and biochemistry. Consequently, there is always the desire for the development of new techniques to be used in the investigation of the chemical and physical properties of sulphur. The advent of pulsed fast Fourier transform (FFT) nuclear magnetic resonance spectroscopy, high-field magnets and sophisticated pulse sequences have opened the periodic table of the elements to investigation in a remarkable manner. With a few exceptions, any nuclide with spin can now be observed routinely in the NMR experiment. One of the exceptions is the [33]S nucleus. Although there are formidable obstacles to overcome in attempting to observe this nucleus in a routine manner, the chemical and biochemical importance of the element demand every effort be expended to determine the limits to which NMR techniques can be applied to the direct observation of the [33]S nucleus.

The purpose of this review is to present the difficulties involved in the observation of the [33]S nucleus, to suggest some solutions to overcome these difficulties, and then to discuss the applications and results of [33]S NMR spectroscopy. It is hoped that the review will be useful in indicating what is currently possible in [33]S NMR spectroscopy and that it will also be of some heuristic value.

II. NMR PROPERTIES OF ^{33}S

Table 1 gives the properties of the ^{33}S nucleus pertinent to the NMR experiment. The combination of low natural abundance, moderate quadrupole moment and small magnetogyric ratio make the ^{33}S nucleus intrinsically insensitive in the NMR experiment. The receptivity of ^{33}S relative to ^{1}H and ^{13}C is 1.7×10^{-5} and 9.7×10^{-2} respectively. These represent the highest receptivity values for the ^{33}S nucleus (i.e. they assume spherical electron symmetry about the ^{33}S nucleus); in actual practice, the receptivity can be lower by several orders of magnitude as a result of electron asymmetry about the nucleus.

TABLE 1

NMR properties of the ^{33}S nucleus.

Isotope	Spin I	Natural abundance (%)	Magnetogyric ratio $\gamma/10^7$ (rad T^{-1}s^{-1})	Magnetic moment u/μ_N	Quadrupole moment $Q/10^{-28}$ m^2
^{33}S	$\frac{3}{2}$	0.76	2.0517	0.8296	-6.4×10^{-2}

III. EXPERIMENTAL TECHNIQUES

Although the unfortunately low receptivity of the ^{33}S nucleus makes its experimental observation very difficult in most sulphur-containing molecules, a number of ^{33}S NMR studies have been reported in the literature. In fact, the first direct observation of the ^{33}S nucleus was reported only five years after the landmark papers of Bloch[1] and Purcell[2] in 1946. Dharmatti and Weaver[3] observed the ^{33}S NMR signal (line width about 10^{-4} T) of CS$_2$ and used it to calculate the magnetic moment of the nucleus. In 1953 Dehmelt[4] observed the pure quadrupole resonance of ^{33}S in rhombic sulphur powder. The four absorption lines attributable to the nuclear quadrupole resonance of the ^{33}S isotope were used to determine an average quadrupole coupling constant of 45.8 MHz. In 1965 Kushida and Silver[5] indirectly observed the ^{33}S resonance line in CdS using the double resonance technique in the rotating frame. The spectra-averaging (i.e. time-averaging) technique was employed to obtain the ^{33}S NMR spectra of the solid compounds CdS,[6] ZnS[6] and MnS.[7] The study of the temperature dependence of the ^{33}S resonance signal in the paramagnetic state of the cubic antiferromagnetic MnS over the temperature range of 175–300 K produced a Curie–Weiss temperature of -630 K and a transferred hyperfine coupling of 1.65×10^{-4} cm^{-1}.

   With the apparent success of these early ³³S NMR investigations, especially with solids, it may seem peculiar that more has not been achieved with ³³S since then. However, it must be realized that these solids represent compounds of cubic symmetry, and therefore produce ³³S NMR lines that are relatively narrow. The high concentration of ³³S in solids, compared with neat liquid sulphur compounds or solutions, and the relatively narrow line widths in these particular solids enhance the capability of observing the NMR signal. This condition is the exception rather than the rule.

   As alluded to previously, it is the combination of low natural abundance, small magnetogyric ratio and moderate quadrupole moment of the ³³S nucleus that make the NMR experiment so difficult. With some nuclei, the problem of low natural abundance can be overcome by using isotopic enrichment. However, the cost of ³³S-enriched elemental sulphur is high, about $200 per milligram for 90% enrichment. The cost of obtaining enough of a particular compound through some synthetic scheme, starting with enriched elemental sulphur, would seem to be prohibitive. Even though a suitable amount of compound could be synthesized, the line width of the ³³S NMR signal might be so broad that no resonance could be observed.

   There is nothing that we can do about the small magnetogyric ratio — we must take what Nature gives. However, the effect of the quadrupole moment on the difficulty of the ³³S NMR experiment is variable, depending upon several factors. The line width at half-height, $\Delta v_{1/2}$, of a quadrupolar nucleus of spin I in the extreme narrowing limit is given by

$$\Delta v_{1/2} = \frac{3\pi}{10} \frac{2I_x + 3}{I_x^2(2I_x - 1)} \chi^2(1 + \tfrac{1}{3}\eta^2)\tau_c \tag{1}$$

χ is the nuclear quadrupole coupling constant defined as

$$\chi = e^2 q_{zz} Q/h \tag{2}$$

where Q is the nuclear electric quadrupole moment, q_{zz} is the largest component of the electric field gradient tensor at the ³³S nucleus, e is the charge of the electron, $\eta = (q_{xx} - q_{yy})/q_{zz}$ is the asymmetry parameter and τ_c is the isotropic tumbling correlation time of the molecule. Despite the moderately small quadrupole moment of ³³S, one does not often encounter sulphur atoms in molecules with high electron charge symmetry about them. Therefore broad resonance lines are characteristic of ³³S NMR spectroscopy. If a broad line spectrum is anticipated, the only way to narrow the resonance line is to reduce the correlation time by raising the temperature and/or using a nonviscous solvent.

   There is an insidious problem that arises in the observation of a quadrupolar nucleus with a small magnetogyric ratio (i.e. a low resonance frequency). The most efficient accumulation of NMR spectra (FIDs) requires

a probe of high sensitivity. However, the recovery time of a high-sensitivity probe is normally too long to observe an undistorted FID of a quadrupolar nucleus that relaxes very fast. A low-sensitivity probe is necessary for a fast recovery, but obviously the much needed sensitivity is lost with such a probe. The long recovery time of a high-sensitivity probe used with short, high-power r.f. pulses has associated with it acoustical ringing, which is an added component to the NMR signal. The source of the acoustical ringing is the electromagnetic generation of ultrasonic waves in metals.[8-10] This acoustic signal normally occurs when the r.f. is below about 20 MHz, and can last for as long as 2 ms at very low frequencies. Acoustic ring of this duration can completely mask any NMR signal broader than about 160 Hz. The acoustic ringing produces a signal that has the appearance of the FID of an NMR signal. This can be very frustrating when searching for the signal of a low-frequency quadrupolar nucleus. The Fourier transform of the acoustic-ringing signal generates a spectrum with a rolling base-line that can obliterate the real NMR signal. Figure 1 shows the "FID" and the Fourier transform of the acoustic-ringing signal in a probe tuned for a ^{33}S resonance frequency of 6.83 MHz (i.e. a field of 2.11 T). With a sample of neat CS_2, the signal from acoustic ringing is so much stronger than the ^{33}S NMR signal that the spectrum produced is of little use, as seen in Fig. 2.

Obviously, it is very important to eliminate the acoustic-ringing effect but retain the high sensitivity of the probe for the study of a low-magnetogyric-ratio quadrupolar nucleus. There are several approaches that one can take to achieve this. A simple technique involves inserting a delay between the end of the r.f. pulse and the beginning of the data acquisition. This method will not
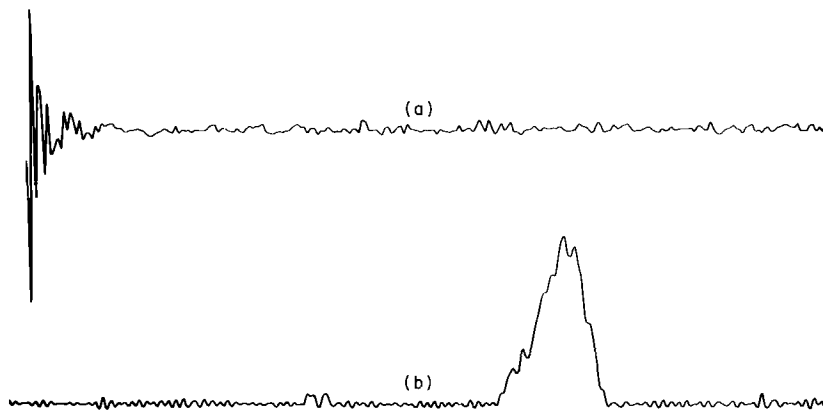
FIG. 1. (a) Acoustic-ringing FID, no sample in the probe. 16 pulses with a 1 μs delay between the end of the r.f. pulse and data acquisition, 28 000 Hz spectral width. (b) Fourier transform of acoustic-ringing FID.
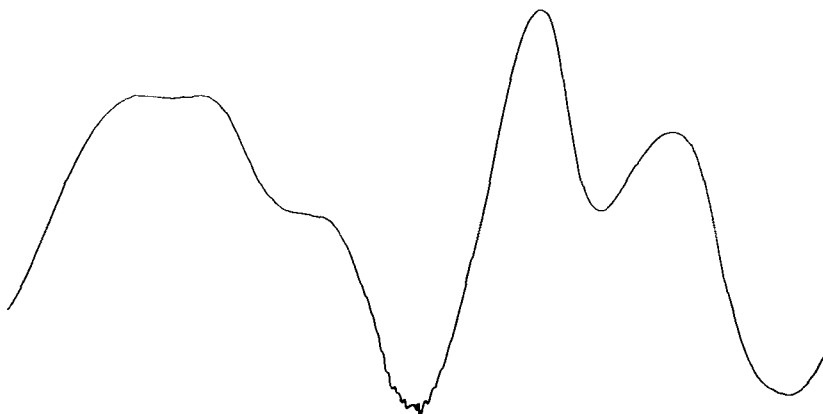
FIG. 2. Fourier-transformed signal of a CS_2 sample, showing the effect of acoustic ringing. 10 000 pulses are taken, and the spectral width is 28 000 Hz.

work if the NMR relaxation is much faster than the acoustic-ringing time (i.e. the delay should be less than $1/\pi\Delta\nu_{1/2}$) or part of the NMR FID will be lost. The effect of the length of the delay on the ^{33}S spectrum of CS_2 is shown in Fig. 3. A better solution to the problem involves the use of a pulse sequence, a
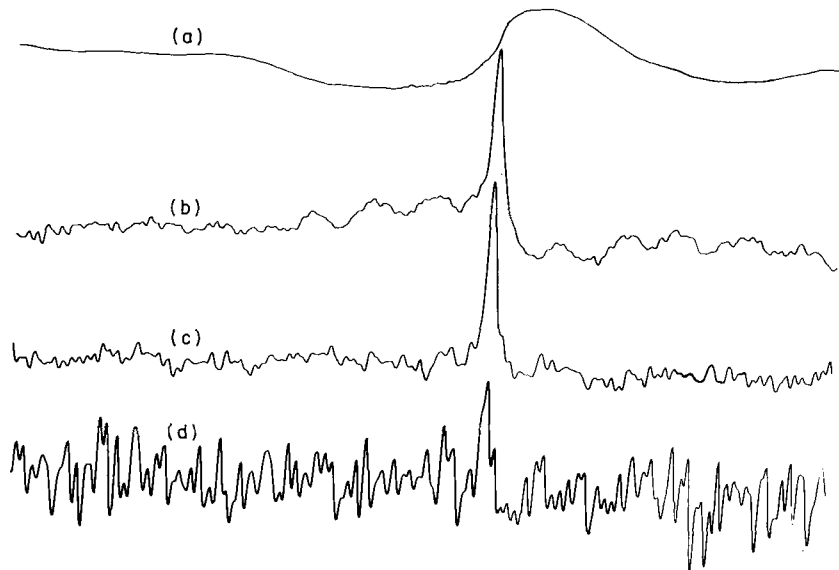
FIG. 3. Effect of a delay between the end of the r.f. pulse and data acquisition. (a) 100 μs delay; (b) 500 μs delay; (c) 1000 μs delay; (d) 3000 μs delay. The sample is neat CS_2, 10 000 pulses are taken and the spectral width is 28 000 Hz for each spectrum.
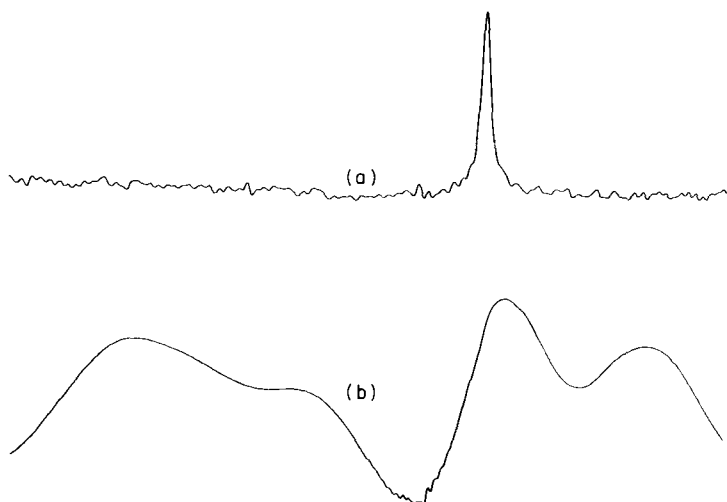
FIG. 4. (a) Spectrum of neat CS_2 obtained with the phase-shifted spin-echo pulse sequence. The delay between the 90° and 180° pulses in the echo sequence is 25 μs. 10 000 FIDs taken with a spectral width of 28 000 Hz. (b) Spectrum of the same sample under the same conditions except that a spin-echo technique is not used.

number of which are described in the literature.[10-14] The very efficient sequence of Ellis[13] involves a combination of the spin-echo and phase-alternation techniques. Figure 4 illustrates the effectiveness of this procedure by comparing the ^{33}S spectrum of CS_2 without the pulse sequence to eliminate the acoustic ringing with that obtained with the spin-echo, phase-alternation pulse sequence. There is a limit, however, to the effectiveness of this technique when working at very low frequency with very broad NMR signals. If the relaxation of the nucleus is very fast, such that the NMR signal vanishes in the same time frame as the ringing, then the results will be poor. For example, the line width at half-height of the ^{33}S NMR signal for $(CH_3)_2SO$ is about 5000 Hz. At a field strength of 2.11 T (i.e. 6.83 MHz resonance frequency for ^{33}S), the NMR signal for this compound cannot be observed.

Since the amplitude of the acoustic-ringing signal is inversely proportional to the pulse frequency, the deleterious effect of this signal can be attenuated by performing the ^{33}S NMR experiments at as high a magnetic-field strength as possible. Even then, some pulse sequence is required to eliminate as much of the acoustic-ringing effect as possible when the NMR signal is very broad. The ^{33}S NMR signal for $(CH_3)_2SO$ can be observed at 7.05 T with the aid of the spin-echo, phase-alternation sequence.

It should be remembered that INEPT-type pulse sequences cannot be used

to increase the sensitivity of detection of ^{33}S where quadrupolar relaxation dominates and effectively decouples, or nearly so, the ^{33}S nucleus from neighbouring ^{1}H nuclei.

IV. APPLICATIONS AND RESULTS OF ^{33}S NMR

The parameters of chemical shift, coupling and relaxation are all significant components of ^{33}S NMR spectroscopy, but to varying degrees. As one might anticipate, the chemical shift and relaxation are the most significant parameters for the ^{33}S nucleus, although a few couplings have been measured. Of the two parameters, chemical shift and relaxation, the relaxation dominates ^{33}S NMR spectroscopy, to the probable dismay of the chemist, because it determines the extent to which an NMR signal can be observed and the accuracy to which the chemical shift of the signal can be measured.

A. ^{33}S relaxation

Values of ^{33}S quadrupole coupling constants that have been experimentally determined are given in Table 2. The magnitude of the values of these quadrupole coupling constants clearly suggest that ^{33}S NMR spectroscopy will be very difficult for many compounds.

TABLE 2

Quadrupole coupling constants for ^{33}S.

Compound	Quadrupole coupling constant (MHz)	Ref.
OCS	−29.07	15, 16
CS	12.84	17
HNCS	−27.5	18
H_2S	40	19, 20
SO_2	25.7	20, 21
S_8	45.8	4
SO	−15.9	22
CS_2	14.9	23
$C_4H_8SO_2$	1.34	24
SO_4^{-2}	0.53	31

The quadrupole coupling constant for ^{33}S in CS_2 is determined from a combination of the ^{33}S NMR line width and the correlation time for the molecule.[23] For this linear molecule, where the asymmetry parameter η is

zero, the quadrupole coupling constant is

$$\frac{e^2qQ}{h} = \left(\frac{5\Delta v_{1/2}}{2\pi\tau_c}\right)^{1/2} \tag{3}$$

where $\Delta v_{1/2}$ is the full line width at half-height of the ^{33}S NMR signal and τ_c is the correlation time for the reorientation of the ^{33}S quadrupole coupling tensor in CS_2. The correlation time for the reorientation of the quadrupole coupling tensor is identical to the reorientation correlation time of the ^{13}C chemical-shielding tensor previously determined.[25] Table 3 shows the line width of the ^{33}S NMR signal as a function of temperature along with the calculated quadrupole coupling constant and the reorientation correlation time. A comparison of the quadrupole coupling constant of CS_2 with those of OCS and HNCS suggests that it is also negative, but smaller because the electronegativity of sulphur is less than that of oxygen or nitrogen. A least-squares fit of the line-width–temperature data to the Arrhenius equation gives an activation energy for the reorientation process of $5.36\,kJ\,mol^{-1}$. The molecular reorientation of CS_2 is discussed in terms of the hydrodynamic slip model for molecular reorientation in liquids of Hu and Zwanzig.[26]

TABLE 3

^{33}S NMR line width and associated quadrupole relaxation data as functions of temperature.

T (K)	$\Delta v_{1/2}$ (Hz)	e^2qQ/h (MHz)	τ_c (ps)[a]
311.3	312	15.23	1.12
301.2	347	15.43	1.25
288.6	358	14.86	1.29
278.6	370	14.45	1.33
273.5	402	14.75	1.45
268.0	426	14.75	1.53
257.7	494	15.07	1.78
245.6	553	14.87	1.99
234.4	600	14.44	2.16

[a] Calculated using the line widths and the average value of the quadrupole coupling constant, 14.87 MHz.

The effects of solution viscosity on the ^{33}S NMR line width and molecular reorientation correlation time of CS_2 have been investigated.[27] Table 4 contains the pertinent data showing this correlation. Different diffusion models are used to describe the neat liquid and the solutions.

The quadrupole coupling constant of ^{33}S in sulpholane ($C_4H_8SO_2$) has

TABLE 4

^{33}S line widths and correlation times for CS$_2$ in alkanes.

Solvent^a	Viscosity n (cP)	$\Delta v_{1/2}$ (Hz)	τ (ps)
n-C$_6$H$_{14}$	0.318	310	1.12
neat CS$_2$	0.365	353	1.27
C(C$_2$H$_5$)$_4$	0.807	478	1.72
n-C$_{12}$H$_{26}$	1.443	533	1.92
n-C$_{14}$H$_{30}$	2.180	657	2.36
n-C$_{16}$H$_{34}$	3.454	686	2.47

^{a}All solutions are 5% v/v of CS$_2$ in alkanes, 303 K.

been determined by using the very elegant electric-field NMR technique.[24] A polar molecule, in the presence of a very strong electric field, will be partially oriented by the interaction of the field with the permanent molecular dipole moment. The effect of the partial orientation manifests itself in the NMR spectrum through anisotropic spin interactions. For quadrupolar nuclei, the Hamiltonian, $\hat{H}_Q$, describing the anisotropic interaction between the nuclear quadrupole moment and the electric-field gradient at the nucleus is given by

$$\hat{H}_Q = \frac{eQ}{4(2I-1)} V_{z'z'}(3I_{z'}^2 - I^2) \tag{4}$$

In this equation eQ is the nuclear quadrupole moment, I is the nuclear spin quantum number, $I_{z'}$ the component of the nuclear spin along the magnetic-field direction (z') and $V_{z'z'}$ the electric-field gradient along the z-axis. The electric-field gradient can be expressed in terms of gradients in a molecular frame of reference (x, y, z) as follows:

$$V_{z'z'} = \langle \tfrac{3}{2} \cos^2 \theta_{z'z} - \tfrac{1}{2} \rangle_E V_{z'z} \tag{5}$$

where V_{zz} is the electric-field gradient along the direction of the molecular dipole moment, the angle-bracketed term represents the alignment and $\theta_{z'z}$ is the instantaneous angle between the dipole moment and magnetic field. The brackets $\langle \rangle$ indicate averaging over molecular tumbling in the liquid. The quadrupole interaction produces line splitting ($2I$ total lines) in the NMR spectrum. For parallel electric and magnetic fields, the frequency difference (in Hz) between adjacent lines is

$$\Delta v = \frac{3}{2I(2I-1)} \frac{eQV_{zz}}{h} \langle \tfrac{3}{2} \cos^2 \theta_{z'z} - \tfrac{1}{2} \rangle_E \tag{6}$$

For deuteriated sulpholane the deuteron NMR signal will also be split, and the frequency difference will be defined according to the above equation. It is

clear that the ratio of line splittings for ^{33}S and ^{2}H is related to the ratio of the corresponding eQV_{zz}/h terms. Since the necessary parameters for ^{2}H are known or can be experimentally determined, the quadrupole coupling constant for ^{33}S may be obtained from the line-splitting ratio. Assuming the asymmetry parameter of the electric field gradient to be zero for deuterons, the following relationship holds:

$$\frac{eQV_{zz}}{h} = (\tfrac{3}{2} \cos \alpha_{zz''} - \tfrac{1}{2}) \frac{eQV_{z''z''}}{h} \tag{7}$$

where $\alpha_{zz''}$ is the angle between the dipole moment and the z'' axis and $(eQ/h)V_{zz}$ is the major principal component of the quadrupole coupling tensor, which is found to lie along the carbon–deuteron bond. The value of these parameters were obtained from an electron diffraction–MINDO-optimized molecular-structure determination and the literature value for the average quadrupole coupling constant for a deuteron bonded to an sp^3 hybridized carbon. The splitting in the ^{33}S and ^{2}H resonance lines for the partially oriented sulpholane in an electric field of 8.3×10^{6} V m^{-1} at 5.87 T is shown in Fig. 5. The quadrupolar line splittings are 17.8 Hz and 74 Hz for the α-deuteron and sulphur respectively. No splitting is observed for the β-deuteron owing to the unfavourable orientation of the carbon–β-deuteron bond with respect to the molecular dipole moment. A value of 1.34 MHz is obtained for the quadrupole coupling constant by this technique for sulpholane. Spin–lattice relaxation-time measurements as a function of temperature for both the α- and β-deuterons and ^{33}S give activation energies of 15.4 ± 1.5, 14.5 ± 1.5 and 17.2 ± 2.5 kJ mol^{-1} respectively for the reorientation process. These results indicate that the molecular tumbling is isotropic.
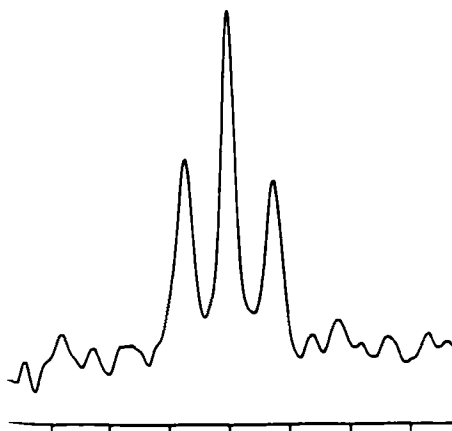

FIG. 5. ^{33}S NMR spectrum of partially oriented sulpholane.

The line width and reorientation correlation time of sulpholane have been found to be concentration-, temperature- and solvent dependent.[14,28] The line width and correlation time change from 32 Hz and 12.8 ps, respectively, in neat sulpholane (10 M) to about 16 Hz and 6.4 ps for a 1 M solution of sulpholane in acetone[14] at 294 K. The inversion-recovery technique was used to obtain the spin–lattice relaxation times of sulpholane, sulpholene and methylsulphone, in the same solution, as functions of temperature in DMSO and CDCl$_3$.[28] Figure 6 shows the ^{33}S NMR spectrum of a DMSO solution containing these three compounds. From the relation between $1/T_1$ and the viscosity–temperature ratio n/T, the activation energies for the reorientation process were obtained for both solvents. Figure 7 shows the Arrhenius plot for the three compounds in DMSO. The activation energies for sulpholane, sulpholene and methylsulphone in DMSO are 16.97, 11.87 and 20.73 kJ mol^{-1}, and in CDCl$_3$ they are 18.10, 9.70 and 9.32 kJ mol^{-1} respectively. These results indicate differences in molecular association in the two solvents. The line widths and correlation times for these molecules in DMSO and CDCl$_3$ at the temperature extremes are shown in Table 5.
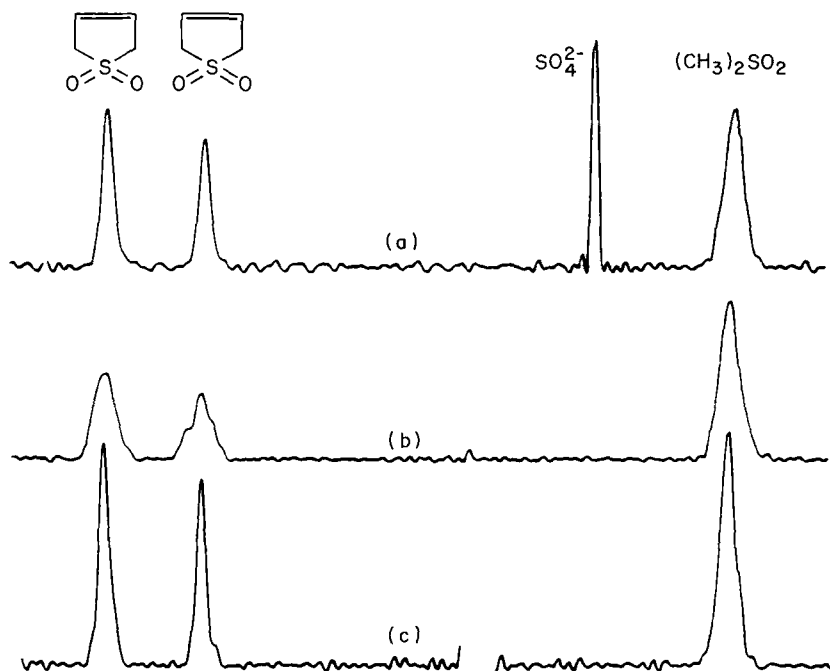

FIG. 6. (a) ^{33}S NMR spectrum of sulpholane, sulpholene and methylsulphone with ^{1}H decoupling with respect to the reference SO$_4^{2-}$ anion. (b) Spectrum of the three compounds without ^{1}H decoupling, showing evidence for ^{1}H coupling to ^{33}S. (c) ^{1}H-decoupled spectrum.
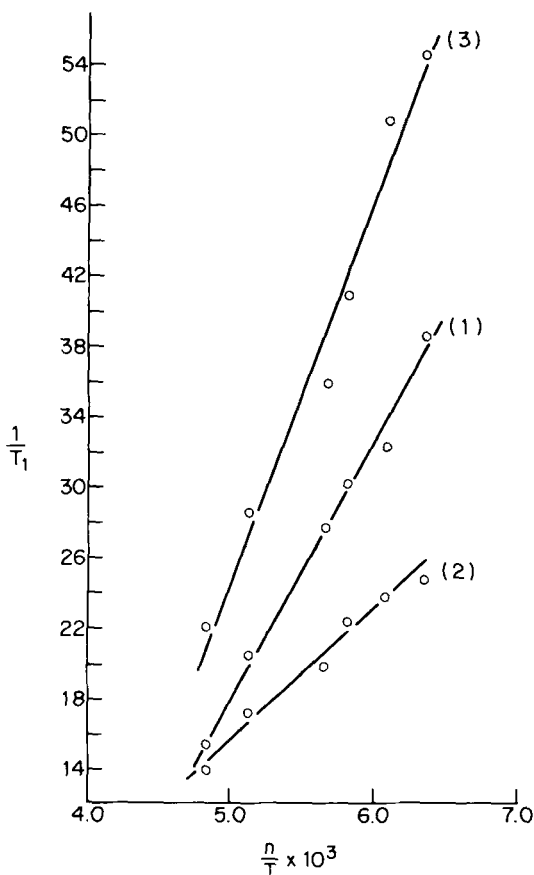
FIG. 7. Plot of $1/T_1$ as a function of n/T for the compounds sulpholane (1), sulpholene (2) and methylsulphone (3) in DMSO.

The tetrahedral symmetry about the sulphur nucleus in the SO_4^{2-} anion suggests that the quadrupole coupling constant in this species is small and that the ^{33}S NMR line width should be relatively narrow. The value of the quadrupole coupling constant (0.53 MHz) shown in Table 2 corroborates this prediction. Because the line width is in fact relatively narrow and the NMR signal easy to obtain, the ^{33}S spin–lattice relaxation time T_1 of the SO_4^{2-} anion has been determined using the inversion-recovery technique (Fig. 8) as a function of cation, concentration and temperature (Table 6).[29-31] Hertz[32] has shown that T_1 should increase with decreasing concentration. This was observed for both $(NH_4)_2SO_4$ and Cs_2SO_4. The probability of producing transient electron-cloud distortion about the sulphur nucleus due to ion-pair

TABLE 5

^{33}S relaxation times T_1, line widths $\Delta v_{1/2}$ and correlation times τ for some sulphur-containing compounds in DMSO and CDCl$_3$ as solvents.

Compound	DMSO (307 K)			DMSO (349 K)		
	T_1 (ms)	$\Delta v_{1/2}$ (Hz)	τ (ps)	T_1 (ms)	$\Delta v_{1/2}$ (Hz)	τ (ps)
Sulpholane	28.5	11.2	4.5	64.4	4.9	2.0
Sulpholene	40.3	7.9	3.2	71.2	4.5	1.8
Methylsulphone	16.2	19.7	7.9	45.1	7.1	2.8

Compound	CDCl$_3$ (303 K)			CDCl$_3$ (323 K)		
	T_1 (ms)	$\Delta v_{1/2}$ (Hz)	τ (ps)	T_1 (ms)	$\Delta v_{1/2}$ (Hz)	τ (ps)
Sulpholane	40.4	7.9	3.2	66.9	4.8	1.9
Sulpholene	39.4	8.1	3.2	52.7	6.0	2.4
Methylsulphone	25.9	12.3	4.9	33.5	9.5	3.8

formation or collisions between ions increases with increasing salt concentration; hence T_1 for the ^{33}S nucleus should be sensitive to concentration changes. Relaxation is faster in the presence of Cs$^+$ ions than for an equal concentrations of NH$_4^+$ ions — probably because of greater ion pairing with Cs$^+$. The relationship between temperature and the ^{33}S T_1 value for the NH$_4^+$ solutions again fits the Arrhenius equation. Activation energies of 10.95 and
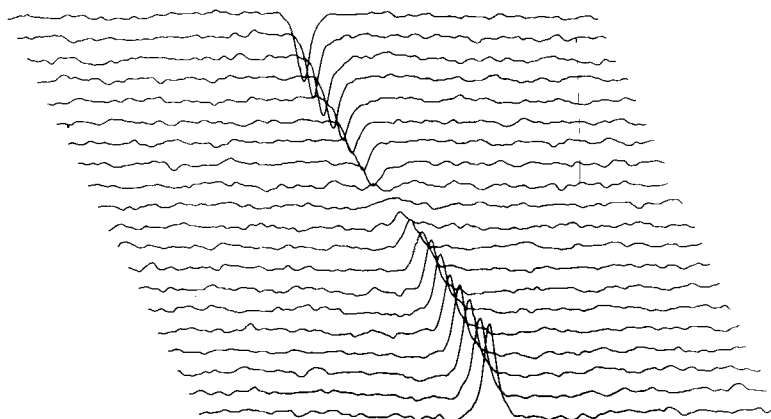

FIG. 8. Typical inversion-recovery experiment for determining the T_1 of the SO$_4^{2-}$ anion.

TABLE 6

^{33}S relaxation time T_1, line width $\Delta v_{1/2}$ and correlation time τ for two salts.

Salt	Concentration (M)	Temperature (K)	T_1 (ms)	$\Delta v_{1/2}$ (Hz)	τ (ps)
$(NH_4)_2SO_4$	0.9	297	138.5	2.3	6.6
	0.9	311	161.8	2.0	5.7
	1.0	311	157.7	2.0	5.7
	0.9	327	204.4	1.6	4.6
	0.9	339.5	239.9	1.3	3.7
	4.0	297	98.9	3.2	9.1
	4.0	311	125.2	2.5	7.1
	4.0	327	149.5	2.1	6.0
	4.0	339.5	165.2	1.9	5.4
Cs_2SO_4	1.0	299	91	3.5	10.0
	2.0	299	76	4.2	12.0
	3.0	299	65	4.9	14.0
	4.0	299	36	8.8	25.0

10.12 kJ mol^{-1} are obtained for 0.9 and 4.0 M solutions respectively. The ^{33}S NMR signal from an aqueous solution of Rb_2SO_4 solution has been used to determine the magnetic moment of that nucleus.[33] The moment is calculated from the ratio of the Larmor frequencies of ^{33}S and ^{85}Rb and the known magnetic moment of ^{85}Rb.

The line width of the ^{33}S NMR signal of liquid SO_2 has been determined as a function of the temperature (Table 7).[34]

An Arrhenius plot of these data produces an activation energy of

TABLE 7

Temperature dependence of ^{33}S NMR line width in SO_2.

Temperature (K)	Half-height line width (Hz)
294	375
274	410
270	420
257	450
238	615
223	735
215	860
206	1130
202	1175
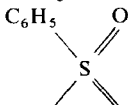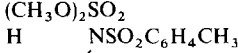
$6.9 \, \text{kJ} \, \text{mol}^{-1}$ for the reorientation process. The ^{33}S quadrupole coupling constant and the asymmetry parameter for SO_2 have been determined to be 25.7 MHz and 0.87 respectively.[20] Using equation (1), an effective rotational correlation time of 0.3 ps at 294 K is obtained. A value for the effective rotational correlation time of 0.41 ps at 295 K has been determined for OCS from the ^{33}S line width (440 Hz) and quadrupole coupling constant.[35]

From the data presented so far, it is obvious that the difficulty encountered in observing ^{33}S NMR signals is intimately related to the electric field gradient about the quadrupolar ^{33}S nucleus; the larger the electric field 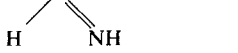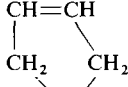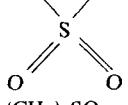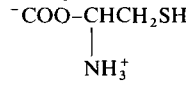gradient, the broader the signal. Experimentally searching for the ^{33}S NMR signal in a type of compound that has no ^{33}S literature precedent can be frustrating, particularly if the line width is very broad. A knowledge of the magnitude of the electric-field gradient about the ^{33}S nucleus correlated with the experimental line width would be a very useful guide for initiating such a search. The method of Townes and Dailey[36] can be used to calculate approximate values for the electric-field gradient about a nucleus.[37-40] Calculations of the electric-field gradient for the ^{33}S nucleus have been made for several compounds,[41] and are given in Table 8 along with the experimentally determined ^{33}S line widths, where available. The agreement between the calculated electric-field gradient and the experimentally determined line width is satisfactory. However, more correlations are necessary before the calculated electric field gradient can be reliably employed to predict line widths.

There is one example in ^{33}S NMR spectroscopy where the calculated electric-field gradient can be used to make the correct peak assignment in a spectrum. The ^{33}S NMR spectrum of the $S_2O_3^{2-}$ anion exhibits only *one* peak. This peak was assigned earlier to the thiosulphur atom.[42] A subsequent study provided evidence that the observed ^{33}S peak should be assigned to the internal sulphur atom.[43] The results of the latter study are based upon the synthesis of $S_2O_3^{2-}$ in which the thiosulphur atoms are depleted in ^{33}S from the natural abundance value of 0.076% to 0.02%. The essence of the experiment is to compare the ^{33}S signal obtained from a sample of ^{33}S-depleted $S_2O_3^{2-}$ with that of the normal (i.e. both sulphur atoms at the same natural abundance, 0.76%) $S_2O_3^{2-}$ anion. If the ^{33}S signal disappears for the sample containing 0.02% ^{33}S in the thiosulphur position then the signal observed in the normal solution of natural abundance can be assigned to the thiosulphur atom. However, if identical signals are observed for both samples, then they must be assigned to the internal sulphur atom. Figure 9 shows the result of the experiment. The ^{33}S NMR signal is the same in both solutions. Therefore the one signal observed can be assigned to the internal sulphur atom. A comparison of the electric-field gradients about the two sulphur atoms would also suggest the same assignment. The thiosulphur has

TABLE 8

Some calculated electric-field gradients and observed line widths for ^{33}S.

Compound	Electric-field gradient	Line width (Hz)
SO_4^{2-}	0	2–4
$(CH_3)_2SO_2$	0.0027	7
$C_3H_6O_2SO$	0.0024	
$S^*SO_3^{2-}$	0.00308	18–59
$^*SSO_3^{2-}$	0.909	
$\begin{array}{c} C_6H_5 \quad\; O \\ \diagdown \quad \diagup\!\!= \\ S \\ \diagup \quad \diagdown\!\!\!\!\diagdown \\ C_6H_5 \quad NH \end{array}$	0.00599	
$(CH_3O)_2SO_2$	0.0280	
$\begin{array}{c} H \qquad NSO_2C_6H_4CH_3 \\ \diagdown \quad \diagup\!\!= \\ ^*S \\ \diagup \quad \diagdown\!\!\!\!\diagdown \\ H \qquad NH \end{array}$	0.04686	
$\begin{array}{c} H \qquad N^*SO_2C_6H_5CH_3 \\ \diagdown \quad \diagup\!\!= \\ S \\ \diagup \quad \diagdown\!\!\!\!\diagdown \\ H \qquad NH \end{array}$	0.15513	
CS_2	0.0607	340–360
SO_2	0.0714	
$(C_6H_5)_2S(NH)_2$	0.0883	
OCS	0.1877	440
$\begin{array}{c} CH\!=\!CH \\ \mid \qquad \diagdown \\ CH_2 \quad CH_2 \\ \diagdown \quad \diagup \\ S \\ \diagup\!\!= \;\; =\!\!\diagdown \\ O \qquad O \end{array}$	0.00526	4–8
$(CH_3)_2SO$		2500–4900
Staggered	0.2102	
Eclipsed	0.5725	
$\begin{array}{c} ^-COO\text{-}CHCH_2SH \\ \mid \\ NH_3^+ \end{array}$	0.6618	
H_2S	1.0702	<2000

FIG. 9. (a) ^{33}S spectrum of commercial $Na_2S_2O_3$. (b) ^{33}S spectrum of $Na_2S_2O_3$ prepared from Na_2SO_3 and elemental sulphur (^{33}S is 0.76% abundant). (c) ^{33}S spectrum of $Na_2S_2O_3$ prepared from Na_2SO_3 and elemental sulphur (^{33}S is 0.02% abundant). All solutions are 0.58 M.

a predicted electric-field gradient of 0.909 compared with 0.00308 for the internal sulphur atom.

The spin–lattice relaxation time of the internal sulphur atom in the $S_2O_3^{2-}$ anion is found to be dependent on the temperature and salt concentration as shown in Table 9.[43] The activation energy for the reorientation process for $S_2O_3^{2-}$ is 21.8 kJ mol^{-1}.

This discussion of the relaxation behaviour of the ^{33}S nucleus in a variety of compounds has not been exhaustive. The intent has been to present a summary of the general trends found in ^{33}S NMR spectroscopy. Although ^{33}S line widths can be very narrow, the narrowest being 0.03 Hz for SF$_6$,[35] broad lines are certainly much more prevalent. In the next section, where ^{33}S chemical shifts are discussed, the chemical-shift data tables also contain line-width (i.e. relaxation-time) information for each compound, where available. It is hoped that the combination of chemical-shift and line-width information will be an effective guide for those contemplating the possible use of ^{33}S NMR spectroscopy.

B. ^{33}S chemical shifts

Acknowledging the fact that ^{33}S NMR lines are usually broad, limiting the accuracy of chemical-shift measurements, the known chemical shift range of

TABLE 9

^{33}S T_1 values and line widths $\Delta v_{1/2}$ of $S_2O_3^{2-}$ at various concentrations and temperatures.

Concentration (M)	Temperature (K)	T_1 (ms)	$\Delta v_{1/2}$ (Hz)
1.0	298	10.42	30.6
2.0	298	8.4	38
3.0	298	7.5	44.5
3.0	309.2	10.23	31.1
3.0	316	11.18	28.5
3.0	321.2	14.53	21.9
3.0	332	17.46	18.2
3.8	297.4	5.40	59.0
3.8	304	6.66	48.0
3.8	312.5	8.93	35.7
3.8	316.7	9.29	34.3
3.8	322	12.7	25.0

about 1000 ppm is sufficiently large to make the chemical shift a useful parameter for chemical studies. The spectra[28,43] displayed in Fig. 6 demonstrate this point. Table 10 (p. 21) gives the chemical shifts and line widths of the sulphur compounds that have been reported in the literature. All chemical shifts (in ppm) are referenced to the SO_4^{2-} anion[33] at 0 ppm (negative sign refers to low frequency). It must be understood that the reference resonance is slightly cation-, concentration- and temperature-dependent.

Although the SO_4^{2-} anion is presented as the ^{33}S reference in Table 10, Wasylishen[35] has established an "approximate" absolute ^{33}S nuclear magnetic shielding scale based upon the shielding constant of OCS. Using the ^{33}S nuclear spin-rotation constant of OCS measured by molecular-beam electric resonance and the procedure of Flygare,[55-57] an absolute ^{33}S shielding constant of 843 ± 12 ppm is calculated for OCS, permitting the establishment of an "approximate" absolute shielding scale. This shielding scale is presented in Fig. 10 along with that based on the SO_4^{2-} anion. In the absolute shielding scale of Wasylishen, the shielding constants for CS_2 and 4 M $(NH_4)_2SO_4$ are 581 and 249 ppm respectively. Theoretical calculations of the ^{33}S shielding constant have been reported.[58-60] Using a pseudopotential technique, the average ^{33}S shielding constant for H_2S has been determined to be 734.6 ppm.[59] A value of 721 ppm has been calculated.[60] These values compare very favourably with that of 752 ppm on the absolute shielding scale of Wasylishen.

(a) $\delta(^{33}S)$

$(NH_4)_2SO_4$

SO$_2$ SOCl$_2$ (CH$_3$O)$_2$SO$_2$ SO$_2$F$_2$ SF$_6$ CS$_2$ CH$_3$SH H$_2$S OCS

|————|————|————|————|————|————|————|
400   200   0   -200   -400   -600

ppm

(b) $\sigma(^{33}S)$

SO$_2$ $(NH_4)_2SO_4$ CS$_2$ OCS

|————|————|————|————|————|
-150   0   250   450   650   850
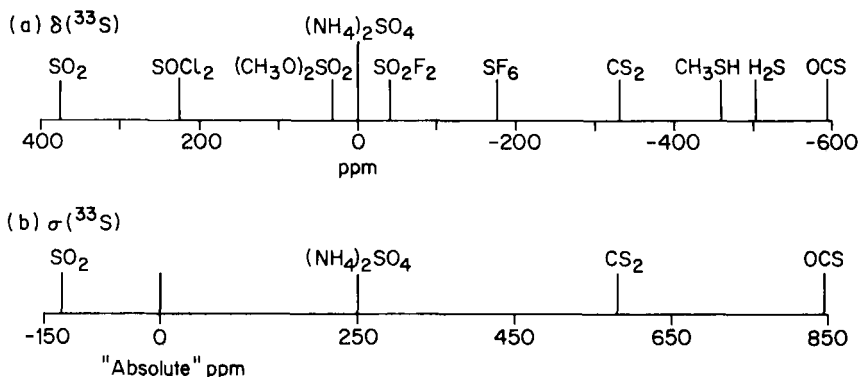
"Absolute" ppm

FIG. 10. (a) Chemical-shift scale based on SO$_4^{2-}$. (b) "Approximate" absolute chemical-shift scale.

Although the volume of chemical-shift data is relatively small, there are some unmistakable trends. Harris[14] identifies four distinct regions between the transition-metal compounds and the polysulphide. In order of increasing frequency, they are: (1) singly bonded sulphur; (2) multiply bonded sulphur; (3) sulphur participating in a delocalized system; and (4) sulphur bonded to one or more oxygen atoms. The low-frequency resonance of the polysulphide anion is rationalized as being due to the negative charge and not being subjected to electron-withdrawing effects, while the high-frequency resonance of the tetrathiomolybdate ion may be due to the mixing of the sulphur and metal d-orbitals.[14]

For a given type of sulphur functionality, one can observe chemical-shift phenomena similar to those seen with the more commonly studied nuclei. For example, Hinton[55] has observed a correlation between the ^{33}S chemical shift and the Hammett substituent parameter, sigma, for substituted benzenesulphonic acids. The relatively narrow line width of the ^{33}S signal for sulphones makes these compounds good candidates for the study of substituent effects on the ^{33}S chemical shift. The ^{33}S chemical shifts of a series of symmetrical dialkyl and diaryl sulphones as well as cyclic sulphones have been determined as well as the magnitude of the β-methyl substituent effect.[47] In the acyclic aliphatic sulphones a systematic symmetrical replacement of the hydrogens attached to the α-carbons by methyl groups produces a shielding decrease of the ^{33}S nucleus. This β-methyl effect is nearly additive, averaging 7–8 ppm per methyl group and mirrors the trend in the ^{13}C chemical shift of the carbonyl carbons for an analogous series of dialkyl ketones. The replacement of a hydrogen atom γ to the sulphur with a methyl group in open-chain sulphones appears to produce a shielding effect of 2 ppm.[50] (With dimethyl sulphone, the β-substituent effects for methyl and

phenyl groups are found to be 7–8 ppm and about 6 ppm respectively, while the replacement of a methyl group by a vinyl or a phenyl group produces a low-frequency shift of 7–8.5 or 4–5 ppm respectively.[51]) With an increase in alkyl-chain length, the ^{33}S chemical shift is essentially invariant, indicating that alkyl substitution resulting in chain lengthening beyond the β-carbon exerts a minimal effect on the ^{33}S chemical shift. This observation seems to support the presumption that, beyond the β-carbon, influence of a methyl or methylene group on the sulphonyl ^{33}S nucleus is likely to be transferred through the sulphonyl oxygens rather than through the bonds. Therefore steric and electronic perturbations on the ^{33}S nucleus produced by alkyl substituents *outside* the γ *anti/gauche* conformations involving β-carbons and the SO_2 oxygens are not expected to be of significant influence.

Substituent effects on the ^{33}S chemical shifts of some sulphonic acids and their corresponding sulphonates have been determined.[53] A reasonably linear correlation is found to exist between the ^{33}S chemical shift in sodium sulphonates and the ^{13}C chemical shift of the carboxylic carbon in the related carboxylates, indicating that substituent effects on $-SO_3$ and $-COO$ ^{33}S and ^{13}C chemical shifts are closely related. This suggests that the ^{33}S chemical shifts observed for these compounds can be rationalized on the same basis as the current theory provides for substituent effects on ^{13}C chemical shifts in carbonyl groups. In $CH_3SO_3^-$ the substitution of a hydrogen atom by a methyl group produces a *deshielding* of 9.8 ppm (i.e. a β-effect). The substitution of a methyl group for a hydrogen atom in $CH_3CH_2COO^-$ is found to produce a *shielding* effect of 2 ppm (i.e. a γ-effect). A small *deshielding* of about 1.2 ppm is observed for substitution at the δ position.

The ^{33}S chemical shift in cyclic compounds shows a dependence on both ring size and substitution.[14,46,47,50] For example, in the series $(CH_2)_{n-1}SO_2$, where $n = 4$, 5, 6 and 11, the ^{33}S chemical shift is -2.3, 34.7, -11.4 and 6.0 ppm respectively. The ^{33}S chemical shift of $C_5H_{10}S$ is about 30 ppm to the low-frequency side of that for C_4H_8S. Six-membered sulphone rings have chemical shifts in the same region as open-chain sulphones; however, the five-membered sulphone rings are deshielded by about 40–50 ppm. Methyl substitution appears to affect the chemical shift of five-membered rings more than six-membered rings, presumably because of the geometric variability of the five-membered ring with substitution compared with the geometrical stability of the six-membered ring. The ^{33}S chemical-shift differences found in bicyclic sulphones indicate that they could be very useful in making stereochemical assignments.[47]

In the thiotungstate and thiomolybdate anion series, where the ^{33}S chemical shift becomes more positive as the sulphur content increases, it is found that the chemical shift is dominated by the paramagnetic term and that the variations in the chemical shifts can be explained, to a first approxi-

mation, by changes in the lowest electronic transition energy of the complex.[61] It is also interesting to note that the line width of the ³³S NMR signal in these compounds becomes smaller as the sulphur content decreases, this is possibly due to changes in the amount of π-bonding, with a resultant decrease in the quadrupole coupling constant.

The small database and the difficulty in measuring chemical shifts very accurately due to the broad line characteristic of ³³S NMR spectroscopy inhibit the formulation of general concepts for the understanding and prediction of ³³S chemical shifts for all sulphur compounds at the present time.

³³S chemical shifts can be solvent-dependent (see Table 10 for examples). The chemical shift of sulpholane changes by 12 ppm when trifluoroacetic acid is used as the solvent rather than chloroform.[47] The ³³S chemical shift of sulpholane is also concentration-dependent, changing by 1.7 ppm in going from a 1 to a 10 M solution in acetone.[14] As mentioned earlier in this discussion of ³³S chemical shifts, one must be very careful with the use of the sulphate ion as a chemical-shift reference. The effects of counter ion, pH and viscosity on the line width, chemical shift and relaxation times of the ³³S resonance of the inorganic sulphate anion have been studied.[62,63] Even weak ion-pairing interactions with the sulphate anion are found to have significant effects on the chemical shift and resonance line width. Interactions with cations such as Ce(IV) and Al⁺ produce large effects. Changes in solution pH from 6.4 to 0.9 cause a 3 ppm variation in the chemical shift and an increase in line width of 190 Hz.

TABLE 10
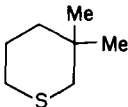
Some ³³S chemical shifts and line widths.

Compound	Solvent	Chemical shift (ppm)	Line width (Hz)	Ref.
OCS		−593.8	440	35
Na₂S	H₂O	−592	1600	45
Ammonium polysulphide	H₂O	−584	2200	14
ZnS (powder)		−562	53	31, 44
(solid)		−561	65	45
H₂S		−503.0		35
S₂(C₂H₅)₂		−499	5200	45
CH₃SH		−458.3		35
	CHCl₃	−366	2500	50

TABLE 10 (*cont.*)
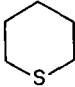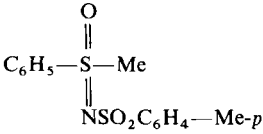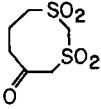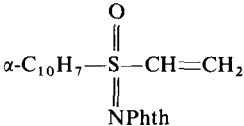
Compound	Solvent	Chemical shift (ppm)	Line width (Hz)	Ref.
	CHCl$_3$	-363	5500	50
Tetrahydrothiophene		-354	4800	14
		-422	2600	45
	CHCl$_3$	-330	5500	50
1-Butanethiol		-415	2100	14
Ethyl isothiocyanate		-340	4300	14
CS$_2$		-332		35
		-331	360	33
		-333	350	14
		-330	400	49
		-328	284	54
3-Bromothiophene		-197	1600	45
2-Methylthiophene		-153	1300	45
3-Methylthiophene		-134	1600	45
thiophene	CS$_2$	-111	620	45
		-119	1450	14
SF$_6$		-176.6	0.03	35
sulphuryl chloride		-47	600	14
(CH$_3$)$_2$SONC$_6$H$_5$	CHCl$_3$	-46	274	54
SO$_2$Cl$_2$		-44.7		35
SO$_2$F$_2$		-40.8		35
C$_6$H$_5$—S(=O)—Me, NSO$_2$C$_6$H$_4$—Me-*p*	CHCl$_3$	-39^a	690	50
	CHCl$_3$	-35	644	50
C$_6$H$_5$SONCH$_3$CH$_3$	CHCl$_3$	-31	1196	50
p-CH$_3$C$_6$H$_4$SO$_2$NH$_2$	CHCl$_3$	-30	1380	50
α-C$_{10}$H$_7$—S(=O)—CH=CH$_2$, NPhth	CHCl$_3$	-29	1500	50
E-C$_6$H$_5$SO$_2$CHCHF	CHCl$_3$	-29	160	51
C$_6$H$_5$SO$_2$CHCHCH$_3$	CHCl$_3$	-28	115	50
	CHCl$_3$	-23	50	54

TABLE 10 (cont.)

Compound	Solvent	Chemical shift (ppm)	Line width (Hz)	Ref.
p-$CH_3C_6H_4SONHCH_3$	$CHCl_3$	-28	1196	50
E-$C_6H_5SO_2CHCHBr$	$CHCl_3$	-27	110	51
Z-$C_6H_5SO_2CHCHBr$	$CHCl_3$	-26	140	51
E-$C_6H_5SO_2CHCHCl$	$CHCl_3$	-26	200	51
$(CH_2{=}CH)_2SO_2$	DMSO	-26	60	46
	$CHCl_3$	-30	60	50
$C_6H_5SO_2CHCH_2$	$CHCl_3$	-25	50	51
E-$C_6H_5SO_2CHCHC_6H_5$	$CHCl_3$	-24	80	51
$(C_6H_5)_2SO_2$	DMSO	-23	130	46
	Acetone	-24.5	42	14
	$CHCl_3$	-21	120	47
	DMSO	-28	130	47
	$CHCl_3$	-21	161	50
	$CHCl_3$	-23	70	51
	$CHCl_3$	-21		51
	$CHCl_3$	-22	48	54
p-MeC$_6$H$_4$—$\overset{\overset{O}{\|}}{\underset{\underset{NPhth}{\|}}{S}}$—Me	$CHCl_3$	-23	1100	50
(Phth = phthalimido)				
HFSO$_3$		-22.4		35
$C_6H_5SO_2CHC(CH_3)_2$	$CHCl_3$	-22	60	51
$CH_3SO_2NCH_3$	$CHCl_3$	-22	69	50
$(p$-$CH_3C_6H_4)_2SO_2$	$CHCl_3$	-22	140	47
$(p$-$HOC_6H_4)_2SO_2$	$CHCl_3$	-20		47
$C_6H_5SO_2CH_3$	DMSO	-20	120	46
	$CHCl_3$	-17	35	54
DMSO		-20	4900	14
		-100	2600	45
		-8	5620	50
$(CH_3O)_2SO_2$		-12.6	1400	14
		0.0	2000	49
		32.2		35
p-chlorophenyl methyl sulphone	Acetone	-19.4	87	14
$CH_3C_6H_4SO_2CO_2CH_3$	Acetone	-19	284	54
p-MeC$_6$H$_4$—$\overset{\|}{S}$—Me NSO$_2$C$_6$H$_4$—Me-p	$CHCl_3$	-18	1200	50
$(C_6H_5SO_2)_2CH_2$	$CHCl_3$	-18	586	54
$CH_3C_6H_4SO_2CH_3$	$CHCl_3$	-18	48	54

TABLE 10 (cont.)

Compound	Solvent	Chemical shift (ppm)	Line width (Hz)	Ref.
$C_6H_5SO_2CH_3$	CHCl$_3$	-17	30	51
m-NO$_2$C$_6$H$_4$SO$_3$Na	H$_2$O	-16.5	100	53
1-naphthalenSO$_3$Na	H$_2$O	-15.2	12	53
$(CH_3)_2SO_2$	DMSO	-7	50	46
	Acetone	-13.6	8.5(6)	14
	CHCl$_3$	-13	50	47
	CF$_3$COOH	-1	275	47
	DMSO	-12	50	47
	DMSO	-11	6.8	54
	CHCl$_3$	-18	46	50
	CHCl$_3$	-13	20	51
	CHCl$_3$	-14		52
$C_6H_5CH_2$—S—C_6H_5 $\parallel$ NSO$_2$C$_6$H$_4$—Me-p	CHCl$_3$	-13^a	2500	50
$C_6H_5SO_2CH_2$c$_6$H$_5$	CHCl$_3$	-13	92	50
CH_2CHSO_3Na	H$_2$O	-13.4	35	53
p-ClC$_6$H$_4$SO$_3$Na	H$_2$O	-13.2	12	53
p-toluenesulphonic acid	H$_2$O	-12	65	14
		-10	90	46
$CH_3SO_2CH_2CO_2CH_3$	CHCl$_3$	-12	78	54
Benzenesulphonic acid	H$_2$O	-11.9	24	14
	H$_2$O	-11.7	15	53
m-NH$_2$C$_6$H$_4$SO$_3$Na	H$_2$O	-11.5	26	53
2-naphthaleneSO$_3$Na	H$_2$O	-11.5	15	53
CH_2=$CHSO_3Na$	D$_2$O	-11	70	46
$(CH_2)_5SO_2$	CHCl$_3$	-11.4	44	14
	CHCl$_3$	-11	50	47
	CHCl$_3$	-12	92	50
$C_6H_5SO_2CH_2C_6H_5$	CHCl$_3$	-11	100	51
$C_6H_5SO_2CH_2CH_3$	CHCl$_3$	-11	161	50
p-NH$_2$C$_6$H$_4$SO$_3$Na	H$_2$O	-10.5	16	53
p-CH$_3$OC$_6$H$_4$—S—Me $\parallel$ NSO$_2$C$_6$H$_4$—Me-p	CHCl$_3$	-10^a	1500	50
p-CH$_3$C$_6$H$_4$SO$_3$Na	D$_2$O	-10	90	46
	H$_2$O	-11.1	32	53
$CH_2CHCH_2SO_2C_6H_5$	CHCl$_3$	-10	50	54
NaOOCCH$_2$SO$_3$Na	H$_2$O	-9.6	10	53
L-Cysteic acid	D$_2$O	-9	80	46
	H$_2$O	-10	29	14
sodium methylsulphate	H$_2$O	-10	700	14
$C_6H_5SO_2CH_2CH_3$	CHCl$_3$	-9	100	51

TABLE 10 (*cont.*)
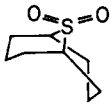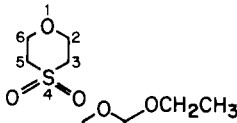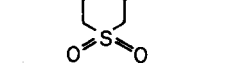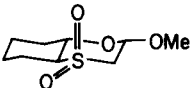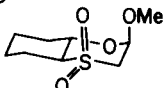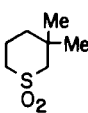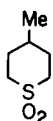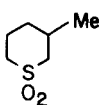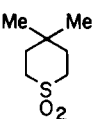
Compound	Solvent	Chemical shift (ppm)	Line width (Hz)	Ref.
$(NH_4)NH_2SO_3$	H_2O	-9	300	49
$CH_3SO_2N(CH_3)_2$	$CHCl_3$	-9		51
H_2SO_4 5 M	H_2O	-8.8		35
4 M	H_2O	-8	340	33
10 M	H_2O	-17	500	33
Conc.	H_2O	-106	2300	45
Conc.	H_2O	0	1200	49
	$CHCl_3$	-8	190	47
	$CHCl_3$	-18	100	47
	$CHCl_3$	-18	20	54
	$CHCl_3$	-18	100	47
	$CHCl_3$	-10	200	47
	$CHCl_3$	-20	200	47
	$CHCl_3$	-13	115	50
	$CHCl_3$	-12	69	50
	$CHCl_3$	-11	92	50
	$CHCl_3$	-11	138	50

TABLE 10 (*cont.*)
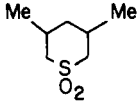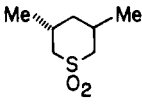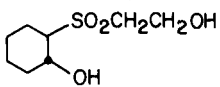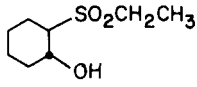
Compound	Solvent	Chemical shift (ppm)	Line width (Hz)	Ref.
[structure: dimethyl tetrahydrothiopyran dioxide, Me...Me, SO₂]	CHCl₃	−11	92	50
[structure: dimethyl tetrahydrothiopyran dioxide, Me,,,Me, SO₂]	CHCl₃	−12	69	50
$(n\text{-}CH_3CH_2CH_2)SO_2CH_3$	CHCl₃	−7	92	50
$[n\text{-}CH_3(CH_2)_3]SO_2CH_3$	CHCl₃	−7	92	50
CH_3SO_3Na	H₂O	−5.6	28	53
CH_3SO_3H	D₂O	−5	150	46
$C_6H_5SO_2CH_2CHCHCOOEt$	CHCl₃	−5	207	50
$(C_6H_5CH_2)_2SO_2$	CHCl₃	−3	120	47
	CHCl₃	−2	100	51
$(CH_2)_3SO_2$	CHCl₃	−2.3	15	14
$H_2NCH_2SO_3Na$	H₂O	−2.3	80	53
$(CH_3CH_2CH_2)_2SO_2$	CHCl₃	0	180	47
	DMSO	2	130	47
	CHCl₃	−2	92	50
$C_6H_5SO_2N(CH_3)_2$	CHCl₃	−1		51
	Acetone	−1		51
$(CH_3CH_2)_2SO_2$	CHCl₃	1	70	47
	CHCl₃	2	92	50
	CHCl₃	1	100	51
$C_6H_5CH_2\!-\!S\!-\!Me$, $\|\,NSO_2C_6H_4\!-\!Me\text{-}p$	CHCl₃	2[a]	1100	50
$CH_3(CH_2)_2SO_3Na$	H₂O	2.2	200	53
$[CH_3(CH_2)_3]_2SO_2$	CHCl₃	3.0	180	47
	Acetone	0.4	52	14
$CH_3(CH_2)_3SO_3Na$	H₂O	3.4	350	53
$CH_3CH_2SO_3Na$	H₂O	4.2	160	53
t-Butylphenyl sulphone	Acetone	5.9	144	14
$(CH_2)_{10}SO_2$	CHCl₃	6.0	60	14
$(n\text{-}C_3H_7)_2SO_2$	DMSO	7	130	46
[structure: cyclohexyl, SO₂CH₂CH₂OH, OH]	Acetone	5	150	47
	CH₃OH	4	250	47
[structure: cyclohexyl, SO₂CH₂CH₃, OH]	CH₃OH	10	250	47
	DMSO	7	600	47
	CHCl₃	7	1000	47

TABLE 10 (*cont.*)
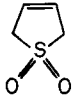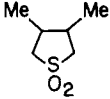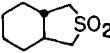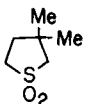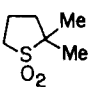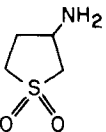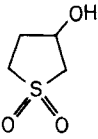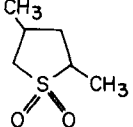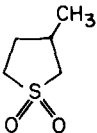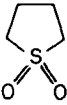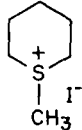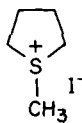
Compound	Solvent	Chemical shift (ppm)	Line width (Hz)	Ref.
$(CH_3)_2CHSO_2CH(CH_3)_2$	$CHCl_3$	18	160	47
$[(CH_3)_3C]_2SO_2$	$CHCl_3$	33	160	47
	Acetone	27.1	46	14
	DMSO	32	50	46
	Acetone	26.5	18(7)	14
	$CHCl_3$	28	50	47
	$CHCl_3$	29	14	54
	$CHCl_3$	25	115	50
	$CHCl_3$	25	92	50
	$CHCl_3$	29	69	50
	$CHCl_3$	32	207	50
	DMSO	33	80	46
$(NH_4)_2S_2O_3$	H_2O	34.5	36	42
$Na_2S_2O_3$	H_2O	33.5	37	14
	D_2O	34	60	49
Na_2S (high pH)		34	60	49
$(CH_2)_4SO_2$	$CHCl_3$	34.7	15	14
	$CHCl_3$	37	50	47
	$CHCl_3$	35	69	50
	DMSO	36	100	46
	DMSO	37	90	46

J. F. HINTON

TABLE 10 (cont.)

Compound	Solvent	Chemical shift (ppm)	Line width (Hz)	Ref.
(structure: 3-methyl sulfolane)	DMSO	37	60	46
(structure: sulfolane)	DMSO	42	50	46
		36.7	32	14
		37	50	47
		37.6		35
	CHCl$_3$	38	9.8	54
	CHCl$_3$	35	69	50
Isothiazole		53.7		35
[WS$_n$O$_{4-n}$]$^{-2}$				
$n = 4$	H$_2$O	159	13	14
$n = 3$	H$_2$O	57	140	14
$n = 2$	H$_2$O	-56	220	14
$n = 1$	H$_2$O	-186	300	14
SOCl$_2$		224		35
[MoS$_n$O$_{4-n}$]$^{-2}$				
$n = 4$	H$_2$O	345	38	14
		343	40	48
$n = 3$	H$_2$O	240	170	14
$n = 2$	H$_2$O	123	250	14
$n = 1$	H$_2$O	-25	200	14
(structure: 1-methylthianium iodide)	CHCl$_3$	337	9200	50
SO$_2$		374.9		35
(structure: 1-methylthiolanium iodide)	CHCl$_3$	417	9200	50

^{a}Only one signal observed and assigned to the non-SO$_2$ sulphur atom. This is in agreement with electric-field-gradient calculations; see Table 8.

C. ³³S couplings

The very rapid relaxation of the ^{33}S nucleus in most chemical (i.e. electronic) environments prevents the direct observation of heteronuclear spin–spin couplings. A few couplings, however, have been measured. The first coupling reported is that between ^{33}S and ^{19}F in the SF_6 molecule where $^1J(F, S)$ is found to be 251 Hz.[63] This value is confirmed through direct observation of the ^{33}S signal in SF_6, where a value of 251.8 Hz is obtained (see Fig. 11).[35] The first observation of ^{33}S coupling to ^1H is reported to be 6 Hz for the vicinal interaction between sulphur and olefinic protons in butadiene sulphone.[64] This coupling has been confirmed several times in the literature.[28,14] A value of $^2J(S, H) = 4.5$ has been reported for the sulpholane molecule,[24] and a value of $^2J(S, H) = 3$ Hz for dimethyl sulphone.[54]
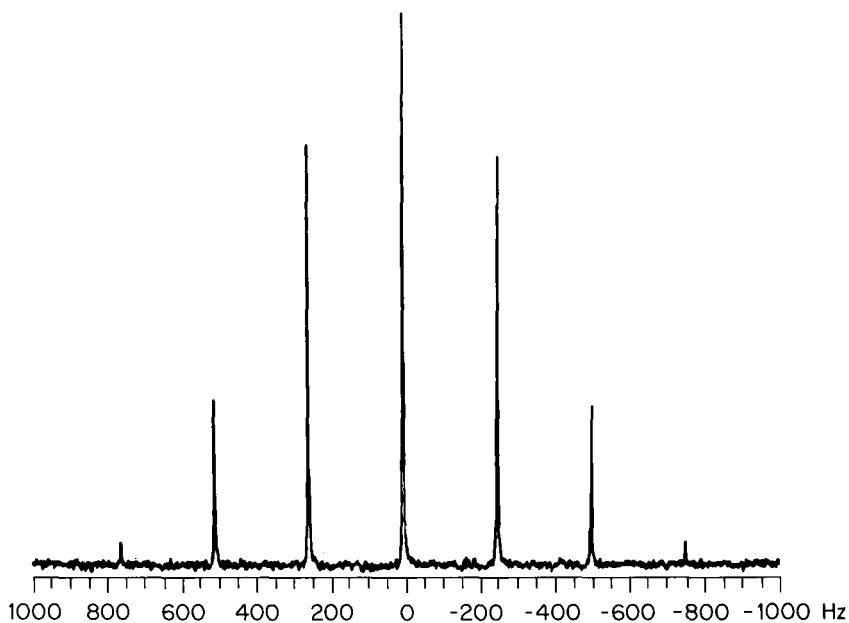

FIG. 11. ^{33}S spectrum of SF_6, showing ^{33}S coupling to ^{19}F.

D. Reaction-product identification

^{33}S has the potential of being quite useful in identifying the products of reactions. In the study of the chemistry of acyl sulphones, the carbomethoxy sulphone $[RS(=O)_2CO_2CH_3]$ was assumed to have been prepared; however, the chemistry of the species seemed better suited to the compound

[RS(=O)OCO$_2$CH$_3$]. Although ^{1}H-, ^{13}C-NMR and infrared spectroscopy seem to support the sulphone structure, they are not definitive. ^{33}S NMR spectroscopy shows that RS(=O)$_2$CO$_2$CH$_3$ is actually prepared.[54]

V. ^{33}S NMR STUDIES OF SOLIDS

As mentioned at the beginning, some of the first ^{33}S NMR spectra obtained were those of a few solid compounds.[6,7,31,44,45,65] The first detailed ^{33}S NMR study of a variety of metal sulphides and sulphates, including naturally occurring minerals, has been reported that tends to dispel the pervading pessimism concerning solid-state ^{33}S NMR studies.[66] The success of this investigation is due to a number of important factors. The spectra are

TABLE 11

Compound	Chemical shift (ppm)	Line width (Hz)	Quadrupole moment (MHz)
Li$_2$S	−680	1380	
Na$_2$S	−671	500	
MgS	−507	300	
CaS	−361.5	100	
SrS	−290.2	100	
BaS	−42	250	
PbS (Oklahoma)	−630	580	
(Kansas)	−626	300	
ZnS (sphalerite)	−561	800	
(wurtzite)	−564		
CdS (wurtzite)	−617		
Na$_2$SO$_4$	−3	2300	0.82
Na$_2$Ca(SO$_4$)$_2$	5	1700	0.71
Na$_2$Mg(SO$_4$)$_2$4H$_2$O	−12	16 000	2.2
CaSO$_4$	−7	3500	1.0
CaSO$_4$2H$_2$O	−4	2000	0.77
BaSO$_4$		18 000	2.3
K$_2$SO$_4$	1	4300	1.13
Rb$_2$SO$_4$	−4	3500	1.01
Cs$_2$SO$_4$	2	3200	0.97
Tl$_2$SO$_4$	−13	3600	1.03
(NH$_4$)$_2$SO$_4$	−5	1200	0.59
KAl(SO$_4$)$_2$12H$_2$O	−6	2100	0.79
RbAl(SO$_4$)$_2$12H$_2$O	1	1050	0.56
CsAl(SO$_4$)$_2$12H$_2$O	−2	950	0.53
NH$_4$Al(SO$_4$)$_2$12H$_2$O	0	950	0.53
TlAl(SO$_4$)$_2$12H$_2$O	−1	1050	0.56

obtained at a magnetic field strength of 11.74 T (500 MHz for ^1H and 38.372 MHz for ^{33}S). This not only provides additional sensitivity, but also minimizes second-order nuclear quadrupole coupling effects. The line width arising from the broadening effect of the second-order quadrupole interaction on the $\frac{1}{2}$ to $-\frac{1}{2}$ transition decreases in a manner proportional to the increase in the Larmor frequency. Even at this high magnetic field strength, the pulse sequence of Ellis[13] was used to eliminate acoustic-ringing effects. The use of composite pulses provided a wider range of effective excitation, compensated for r.f. field inhomogeneities, flip-angle missetting and improved sensitivity. It is also well to remember that theoretically the 90° pulse length for the central transition of an $I = \frac{3}{2}$ nucleus becomes one half of the normal value, as measured in liquids, when the satallite transitions (i.e. $\frac{3}{2}$ to $\frac{1}{2}$ and $-\frac{3}{2}$ to $-\frac{1}{2}$)
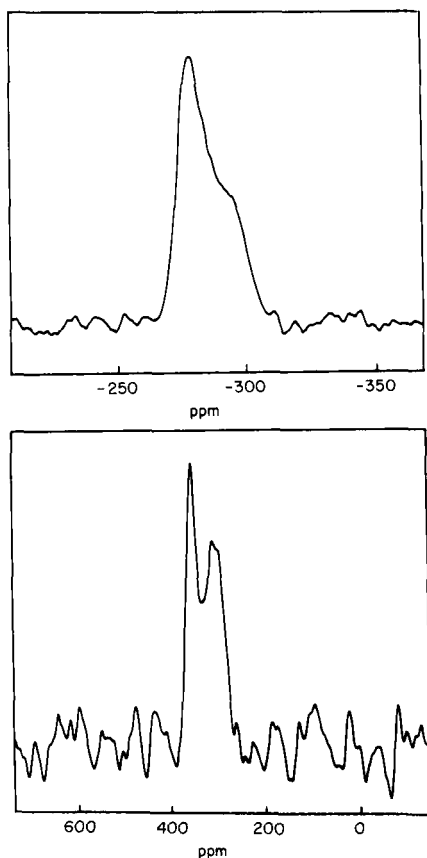

FIG. 12. Solid-state ^{33}S NMR spectra of CdS (top) and Cs_2SO_4 (bottom).

are not excited by the r.f. pulse.[67] This behaviour is observed for all of the compounds studied. Table 11 gives the NMR parameters, chemical shift, line width and quadrupole coupling constant determined for the compounds listed.

From an inspection of the data in Table 11, it can be seen that the sulphate chemical shifts are nearly identical and very nearly the same in value as that for the sulphate ion in solution. However, a very large chemical-shift range, of about 600 ppm, exists for the metal sulphide compounds. Chemical-shielding anisotropies of 23 and 28 ppm are measured for ZnS and CdS respectively (see Fig. 12 for the spectrum of CdS). The explanation of the chemical shifts of the metal sulphides involves a consideration of the crystalline ionicities and the effects of orbital overlap. The more covalently bonded sulphides, ZnS, CdS and PbS, are appropriately described in terms of the bond-orbital model.[68,69]

For the alkali and alkaline earth sulphides, an extended Kondo–Yamashita[70] approach is found to provide a satisfactory description of the chemical shifts. The temperature dependence of the shielding of some of the sulphide compounds supports the chemical-shift analysis presented.

ACKNOWLEDGMENTS

REFERENCES

1. F. Bloch, W. W. Hansen and M. Packard, *Phys. Rev.*, 1946, **69**, 127.
2. E. M. Purcell, H. C. Torrey and R. V. Pound, *Phys. Rev.*, 1946, **69**, 37.
3. S. S. Dharmatti and H. E. Weaver, *Phys. Rev.*, 1951, **83**, 845.
4. H. G. Dehmelt, *Phys. Rev.*, 1953, **91**, 313.
5. T. Kushida and A. H. Silver, *Phys. Rev.*, 1965, **137**, A1591.
6. C. Karr and H. D. Schultz, The Pittsburgh Conference on Analytical Chemistry and Applied Spectroscopy, Cleveland, Ohio, 1968 (*Spectrosc. Lett.*, 1968, 205).
7. K. Lee, *Phys. Rev.*, 1968, **172**, 284.
8. W. D. Wallace, *Int. J. Nondestructive Testing*, 1971, **2**, 309.
9. E. Fukushima and S. B. Roeder, *J. Magn. Reson.*, 1979, **33**, 109.
10. C. Brevard, in *NMR of Newly Accessible Nuclei*, Vol. 1 (P. Laszlo, ed.), Academic Press, New York, 1983, p. 3.
11. D. Canet, J. Brondeau, J. P. Marchal and B. Robin-Lherbrier, *Org. Magn. Reson.*, 1982, **20**, 51.

12. S. L. Patt, *J. Magn. Reson.*, 1982, **49**, 161.
13. P. D. Ellis, in *The Multinuclear Approach to NMR Spectroscopy* (J. B. Lambert and F. G. Riddell, eds), Reidel, Dordrecht, 1983.
14. P. S. Belton, I. J. Cox and R. K. Harris, *J. Chem. Soc., Faraday Trans.*, 1985, **81**, 63.
15. J. R. Eshbach, R. E. Hillger and M. W. P. Strandberg, *Phys. Rev.*, 1952, **85**, 532.
16. C. H. Townes and S. Geschwind, *Phys. Rev.*, 1948, **44**, 1113.
17. R. C. Mockler and G. R. Bird, *Phys. Rev.*, 1955, **98**, 1837.
18. G. C. Dousmanis, T. M. Sanders, C. H. Townes and H. J. Zeiger, *J. Chem. Phys.*, 1953, **21**, 1416.
19. K. Ohno, Y. Mizuno and M. Mizushima, *J. Chem. Phys.*, 1958, **28**, 691.
20. G. R. Bird and C. H. Townes, *Phys. Rev.*, 1954, **94**, 1203.
21. R. Van Reit, *Ann. Soc. Sci. Bruxelles*, 1962, **76**, 56.
22. T. Amano, E. Hirota and Y. Morino, *J. Phys. Soc. Jpn*, 1967, **22**, 399.
23. R. R. Vold, S. W. Sparks and R. L. Vold, *J. Magn. Reson.*, 1978, **30**, 497.
24. B. H. Ruessink, W. J. van der Meer and C. MacLean, *J. Am. Chem. Soc.*, 1986, **108**, 192.
25. H. W. Spiess, D. Schweitzer, U. Haeberlen and K. H. Hausser, *J. Magn. Reson.*, 1971, **5**, 101.
26. C. M. Hu and R. Zwanzig, *J. Chem. Phys.*, 1974, **60**, 4354.
27. B. Ancian, B. Tiffon and J.-E. Dubois, *Chem. Phys. Lett.*, 1979, **65**, 281.
28. J. F. Hinton, *J. Magn. Reson.*, 1984, **59**, 469.
29. E. Haid, D. Kohnlein, G. Kossler, O. Lutz and W. Schich, *J. Magn. Reson.*, 1983, **55**, 145.
30. J. F. Hinton and D. Shungu, *J. Magn. Reson.*, 1983, **54**, 309.
31. O. Lutz, in *The Multinuclear Approach to NMR Spectroscopy* (J. B. Lambert and F. G. Riddell, eds), Reidel, Dordrecht, 1983, p. 389.
32. H. G. Hertz, *Ber. Bunsenges. Phys. Chem.*, 1973, **77**, 688.
33. O. Lutz, A. Nolle and A. Schwenk, *Z. Naturforsch.*, 1973, **28a**, 1370.
34. R. E. Wasylishen, J. B. MacDonald and J. O. Friedrich, *Can. J. Chem.*, 1984, **62**, 1181.
35. R. E. Wasylishen, C. Connor and J. O. Friedrich, *Can. J. Chem.*, 1984, **62**, 981.
36. C. H. Townes and B. P. Dailey, *J. Chem. Phys.*, 1949, **17**, 782.
37. J. M. Lehn and J. P. Kintzinger, in *Nitrogen NMR* (G. A. Webb and M. Witanowski, eds), Plenum Press, London, 1973, p. 96.
38. A. Carrington, B. J. Howard, D. H. Levy and J. C. Robertson, *Mol. Phys.*, 1968, **15**, 187.
39. H. Uehara and Y. Morino, *Mol. Phys.*, 1969, **17**, 239.
40. E. A. C. Lucken, *Nuclear Quadrupole Coupling Constants*, Academic Press, New York, 1969.
41. G. A. Webb, Private communication.
42. O. Lutz, W. Nepple and A. Nolle, *Z. Naturforsch.*, 1976, **31a**, 978.
43. J. F. Hinton and D. Buster, *J. Magn. Reson.*, 1984, **58**, 324.
44. M. Haller, W. E. Hertler, O. Lutz and A. Nolle, *Solid State Commun.*, 1980, **33**, 1051.
45. H. L. Retcofsky and R. A. Friedel, *J. Am. Chem. Soc.*, 1972, **94**, 6579.
46. R. Faure, E. J. Vincent, J. M. Ruiz and L. Lena, *Org. Magn. Reson.*, 1981, **15**, 401.
47. D. L. Harris and S. A. Evans, *J. Org. Chem.*, 1982, **47**, 3355.
48. P. Kroneck, O. Lutz and A. Nolle, *Z. Naturforsch.*, 1979, **35a**, 226.
49. P. P. Mahendroo and D. Sherry, *Magn. Reson. Chem.*, 1985, **23**, 503.
50. R. Annunziata and G. Barbarella, *Org. Magn. Reson.*, 1984, **22**, 250.
51. L. Cassidei, V. Fiandanese, G. Marchese and O. Sciacovelli, *Org. Magn. Reson.*, 1984, **22**, 486.
52. A.-M. Hakkinen and P. Ruostesuo, *Magn. Reson. Chem.*, 1985, **23**, 424.
53. L. Cassidei and O. Sciacovelli, *J. Magn. Reson.*, 1985, **62**, 529.
54. T. C. Farrar, B. M. Trost, S. L. Tang and S. E. Springer-Wilson, *J. Am. Chem. Soc.*, 1985, **107**, 262.
55. W. H. Flygare and J. Goodisman, *J. Chem. Phys.*, 1968, **49**, 3122.
56. T. D. Gierke and W. H. Flygare, *J. Am. Chem. Soc.*, 1972, **94**, 7277.

57. W. H. Flygare, *Chem. Rev.*, 1974, **74**, 653.
58. S. Rothenberg, R. H. Young and H. F. Schaefer, *J. Am. Chem. Soc.*, 1970, **92**, 3243.
59. J. Ridard, L. Levy and P. Mille, *Mol. Phys.*, 1978, **36**, 1025.
60. R. Holler and H. Lischka, *Mol. Phys.*, 1980, **41**, 1041.
61. P. S. Belton, I. J. Cox, R. K. Harris and M. J. O'Connor, Private communication.
62. P. S. Belton, I. J. Cox and R. K. Harris. *Magn. Reson. Chem.*, 1986, **24**, 171.
63. P. T. Inglefield and L. W. Reeves, *J. Chem. Phys.*, 1964, **40**, 2425.
64. J. Cox, R. K. Harris and P. S. Bolton, 6th International Meeting on NMR Spectroscopy, Edinburgh, Scotland, July 1983.
65. H. Suzuki, T. Komaru, T. Hihara and Y. Koi, *J. Phys. Soc. Jpn.*, 1971, **30**, 288.
66. H. Eckert and J. P. Yesinowski, *J. Am. Chem. Soc.*, 1986, **108**, 2140.
67. A. Abragam, *Principles of Nuclear Magnetism*, Clarendon Press, Oxford, 1967, p. 37.
68. W. A. Harrison, *Phys. Rev. B*, 1973, **8**, 4487.
69. W. A. Harrison and S. Ciraci, *Phys. Rev. B*, 1974, **10**, 1516.
70. J. Kondo and J. Yamashita, *J. Phys. Chem. Solids*, 1959, **10**, 245.

Since completion of the manuscript, several ^{33}S NMR papers have appeared in the literature:

1. H. Duddeck, U. Korck, D. Rosenbaum and J. Drabowicz, *Mag. Reson. Chem.*, 1986, **24**, 792.
2. P. S. Belton, I. J. Cox and R. K. Harris, *Mag. Reson. Chem.*, 1986, **29**, 1004.
3. P. S. Belton and J. D. Woollins, *Mag. Reson. Chem.*, 1986, **24**, 1080.
4. D. D. McIntyre and O. P. Strausz, *Mag. Reson. Chem.*, 1987, **25**, 36.

High-Resolution NMR of Liquids and Gases: Effects of Magnetic-Field-Induced Molecular Alignment

E. W. BASTIAAN AND C. MACLEAN

Department of Physical Chemistry, Free University, Amsterdam

P. C. M. VAN ZIJL AND A. A. BOTHNER-BY

Department of Chemistry, Carnegie-Mellon University, Pittsburgh

I. INTRODUCTION

High-resolution NMR experiments are normally performed with liquid or gaseous samples. In interpreting the spectra obtained, it has usually been assumed that the solute molecules tumble randomly in solution, so that directionally dependent nuclear interactions are motionally averaged and

only mean values can be inferred from the spectra. With this assumption, chemical shifts and indirect spin–spin couplings are predicted to behave as scalar quantities and magnetic dipolar and electric quadrupolar interactions to average to zero.

On the other hand, if the solute molecules do not tumble randomly, but are subjected to some aligning influence, much more information becomes available from the spectra. Such an alignment may result from a variety of conditions.

For example, in liquid-crystal solutions subjected to moderately strong electric or magnetic fields, the probe molecules experience an anisotropic environment due to the oriented solvent, and different molecular orientations are not equally probable.[1-4] It is important to realize that in normal liquids and gases alignment may be induced by applying either a strong external electric[5-7] or magnetic[7-9] field. In contrast, the field exerts orienting torques directly on the solute molecules.

The reason that NMR spectra of these anisotropic liquid media are well resolved is that the solute molecules are highly mobile. The alignment is counteracted by the thermal molecular motion, but since the tumbling is not random an incomplete (or partial) orientation results that is dynamic in nature, not static. Hence anisotropic intramolecular interactions, such as the dipolar and quadrupolar spin couplings, are partly preserved, leading to additional structure in the spectra.

The extra information that is available from these spectra explains the interest in NMR alignment experiments: investigation of the anisotropic nuclear interactions enables the determination of molecular properties and the study of intermolecular interactions. For example, dipolar spin interactions can be used for structure elucidation,[10,11] and quadrupolar effects can give information on quadrupole coupling in molecules.[12-14] When external fields are used to induce the alignment, electric[15,16] or magnetic[7,17-20] properties of compounds can be studied: these experiments are the NMR analogues of the Kerr[21] and the Cotton–Mouton[22] effects, by which the double refraction of a liquid (or a gas), partially aligned by an electric or a magnetic field, is measured.

In order to align molecules, it is necessary that they possess certain anisotropic properties. Therefore the effective molecular symmetry, which may be affected by vibrations,[23] must be lower than tetrahedral.[2] Depending on the orienting mechanism, further requirements must be fulfilled. Thus in an electric field only molecules that have an electric dipole moment are oriented. The dipole moment can be permanent (μ),[6,7] or induced in molecules with an anisotropic polarizability tensor (α),[24] and both mechanisms have to be considered. Analogously, when molecules have an anisotropic magnetic susceptibility they tend to be aligned by the magnetic field of the spectrometer.[7]

The use of liquid-crystal solvents leads to a rather large degree of orientation of the probe molecules. For direct alignment by an external electric or magnetic field it is much smaller. To make these remarks more quantitative, consider the average $\langle \frac{1}{2}(3 \cos^2\theta - 1) \rangle$, the value of which measures the degree of alignment of an axially symmetric molecule; θ is the angle between the applied field and the principal molecular axis (see Fig. 1)
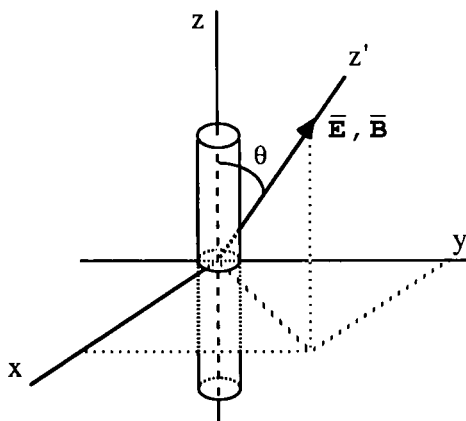

FIG. 1. The principal axis z of an axially symmetric molecule, represented by a cylinder, makes an instantaneous angle θ with the applied electric (E) or magnetic (B) aligning field. The alignment $\langle \frac{1}{2}(3\cos^2\theta - 1) \rangle$ can take values from $-\frac{1}{2}$ to $+1$. The extremes are attained for completely oriented molecules; the value zero indicates absence of average orientation, i.e. the molecules are tumbling randomly.

and the brackets denote averaging over the molecular tumbling. Representative values of $\langle \frac{1}{2}(3 \cos^2\theta - 1) \rangle$ for some alignment mechanisms are given in Table 1. Despite the fact that partial alignment induced directly by external fields is normally some orders of magnitude less than in a liquid crystal, it has an important advantage: the orienting mechanism is simpler than for the liquid-crystal technique,[25] where the influence of the solvent on the properties (e.g. quadrupole coupling constant, structure, relaxation) of the probe molecules may be complex.[2]

Whereas liquid crystals for NMR alignment experiments were first introduced in 1963 by Saupe and Englert,[1] the use of external fields in normal liquids and gases is relatively new. After initial experiments by Buckingham and McLauchlan,[26a] Sears and Hahn[26b] and Waugh et al.,[26c] the first successful electric-field studies in NMR were performed in 1969 by Hilbers and MacLean.[5] The first magnetic-field alignment effects in NMR were detected in 1978 by Lohman and MacLean.[8,9] The principal reason for this late date is the requirement of very strong magnetic fields of sufficient homogeneity.

TABLE 1

Orders of magnitude of the alignment $\langle \frac{1}{2}(3 \cos^2 \theta - 1)\rangle$ attainable in liquids and liquid crystals.

Alignment mechanism	$|\langle \frac{3}{2}\cos^2 \theta - \frac{1}{2}\rangle|$	Notes
Liquid crystals		
thermotropic	10^{-1}–1	(a)
lyotropic	10^{-2}	(a)
Electric field		
polar molecules	10^{-5}–10^{-4}	(b)
apolar molecules	10^{-6}	(b, c)
Magnetic field		
paramagnetic molecules	10^{-5}–10^{-4}	(d)
diamagnetic molecules	10^{-6}–10^{-5}	(c, d)

(a) magnetic field of a few tenths of a tesla; (b) electric field strength of about $5 \times 10^6 \, \text{V m}^{-1}$; (c) for aromatic molecules (e.g. naphthalene, triphenylene); (d) magnetic field of 10 T.

The main driving force to reach stronger magnetic fields in NMR spectrometers lies in the increased resolution of the spectra and in the higher sensitivity that can be obtained. At the fields nowadays available, up to 14.57 T (^{1}H frequency 620 MHz), the partial orientation of molecules possessing an anisotropic magnetic susceptibility can affect the high-resolution spectrum significantly. It is with the study and application of these effects that this review is concerned.

The alignment of the molecules in a liquid or a gas may become apparent in the NMR spectrum through anisotropic interactions of the nuclear spins. Two such interactions have been investigated extensively and have already been mentioned: the direct magnetic dipole–dipole interaction between nuclear spins and the interaction of a nuclear quadrupole with the local electric-field gradient caused by its surroundings. A specific example is the ^{2}H spectrum of a deuteriated aromatic compound: when a strong magnetic field is applied the ^{2}H resonances of the different deuterons are split into doublets owing to incompletely averaged quadrupolar couplings (Figs. 2, 6, 12). The line splittings depend on the angles between the respective C–D bonds and the principal axes of the magnetic susceptibility tensor; they are proportional to the quadrupole coupling constants of the deuterons and to the square of the magnetic field strength; they also depend on the anisotropy ($\Delta\chi = \chi_{zz} - \frac{1}{2}(\chi_{xx} + \chi_{yy})$) and the asymmetry ($\delta\chi = \chi_{xx} - \chi_{yy}$) in the susceptibility tensor.

NMR magnetic-field-alignment studies of molecules at a low concentration in an inert solvent provide a simple and efficient method to measure molecular magnetic-susceptibility anisotropies. At higher concentrations, or in noninert solvents, intermolecular interactions (e.g. cluster formation) may play a role.[27, 28] The inferred susceptibilities then have to be regarded as
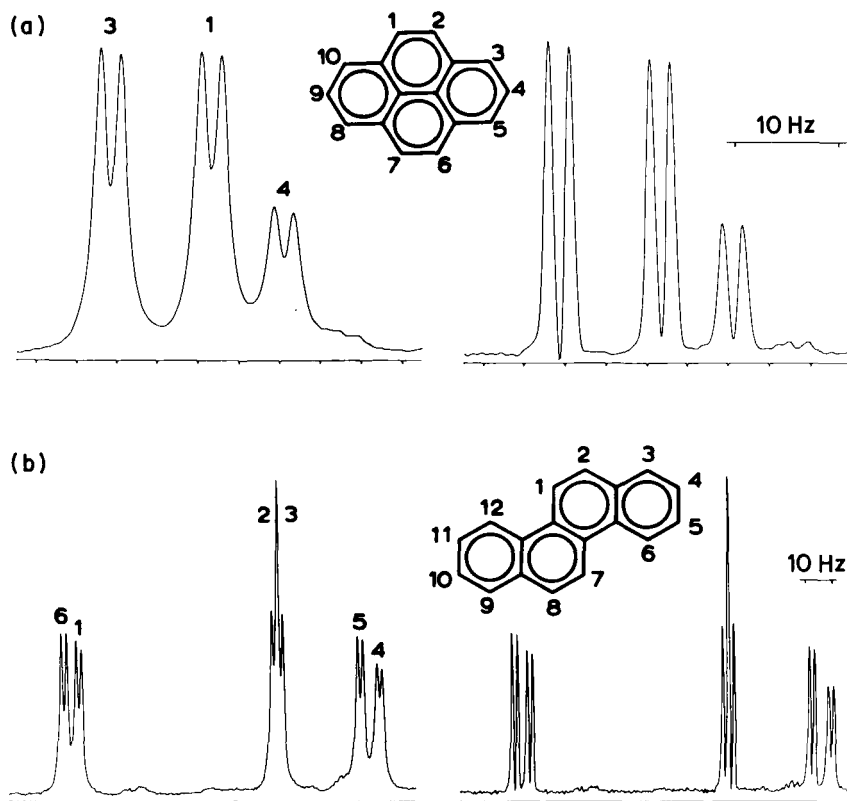
FIG. 2. Normal and resolution enhanced deuterium NMR spectra of pyrene-d_{10} in cyclohexane (a) and of chrysene-d_{12} in diethyl ether (b) in a field of 14.57 T ($T = 296$ K).

effective quantities, in which these interactions are reflected. In specific situations gas-phase molecules can also be studied by NMR. Molecular association is generally, though not always, unimportant in the gas phase.

NMR alignment studies to determine magnetic susceptibility anisotropies can be compared with other techniques:[29,30] the Cotton–Mouton effect,[31] the second-order Zeeman effect in microwave spectroscopy[32] and the solid-state flip-angle method.[33] The NMR approach has some advantages over the other techniques: it is simple to implement on standard NMR spectrometers, and, being a spectroscopic method, offers the opportunity of individually studying different compounds in a mixture. The main problem is the smallness of the measured effects, which limits the attainable accuracy; many molecules cannot be studied successfully yet. Nevertheless, with the availability of high-field spectrometers and of advanced resolution-enhancement

techniques, many compounds have been measured. A more detailed dis-
cussion and review of these aspects is given in Section IV. First, in Section II a
theoretical description of NMR of anisotropic systems is presented. The
general theory of alignment effects has been described in earlier
publications[6,7,34-39] and reviewed several times.[40-44] Here the special
application of alignment in liquids and gases by the static magnetic field, used
for high-resolution NMR spectroscopy, is discussed. In Section III experi-
mental aspects are described. Applications to diamagnetic compounds are
reported in Section IV, and applications to paramagnetic compounds in
Section V. Conclusions are rehearsed in Section VI.

II. THEORY

A. The spin Hamiltonian

The Hamiltonian of a nuclear spin system in a magnetic field is generally
expressed as a sum of contributions, each representing a specific interaction
of the spins.[45,46] The principal term for the magnetic inductions of interest
(2–14 T), is given by the Zeeman interaction $\mathscr{H}_Z$. The remaining terms
account for the nuclear shielding, $\mathscr{H}_\sigma$; indirect spin–spin couplings, $\mathscr{H}_J$; direct
magnetic dipole–dipole interactions, $\mathscr{H}_D$; and electric quadrupole couplings,
$\mathscr{H}_Q$:

$$\mathscr{H} = \mathscr{H}_Z + \mathscr{H}_\sigma + \mathscr{H}_J + \mathscr{H}_D + \mathscr{H}_Q \tag{1}$$

In liquids and gases the Brownian motion causes the spin interactions to be
rapidly fluctuating functions of time, and consequently the Hamiltonian (1)
has to be averaged over the molecular tumbling. Except for $\mathscr{H}_Z$, the
interactions in (1) are based on tensorial properties, which means that, if
random tumbling occurs, they are characterized by the trace of the corre-
sponding tensors. Since $\mathscr{H}_D$ and $\mathscr{H}_Q$ are described by traceless tensors, these
interactions would average to zero, whereas $\mathscr{H}_\sigma$ and $\mathscr{H}_J$ would be given in
terms of scalar quantities, the shielding factor σ and the scalar coupling
constant J. This leads to the "normal" high-resolution Hamiltonian. If,
however, restrictions are imposed on the motion of the molecules, thereby
modifying the average, the tensorial nature of the interactions will be
manifest in the NMR spectrum.

The static magnetic field of the spectrometer imparts a preferential
orientation to all molecules with anisotropic magnetic susceptibilities; in
normal liquids and gases the degree of alignment expected is relatively small,
but increases with the square of the magnetic induction. For the compounds
investigated so far in this type of experiment, the spectral effects of anisotropy

of the nuclear shielding[47] and of the indirect coupling[2] are negligibly small, so that $\mathscr{H}_\sigma$ and $\mathscr{H}_J$ can be treated as scalar interactions. Attention is therefore focused on the dipolar[48] and the quadrupolar[8,9] interactions. These become manifest as splittings of the resonance lines in the NMR spectrum; equations describing the magnitude of these splittings will be derived.

At this point it is necessary to introduce some conventions. The Hamiltonian (1) is usually expressed in a laboratory frame (x', y', z') in which the interactions are measured. As usual, the z'-axis is chosen in the direction of the static magnetic induction B, so that the spins are quantized along the z'-axis.

It has already been mentioned that the spin interactions in (1) have to be averaged over the molecular tumbling. This is most conveniently done by an axes transformation to a molecular frame (x, y, z) fixed in the rigid molecule. In this frame the molecular properties are constant in time and the averaging is only performed over the transformation matrix.[38,39] Strictly speaking, properties in the molecular frame are averages over the molecular vibrations, and may therefore be affected by the molecular tumbling through vibration–rotation interactions. These effects are small and completely negligible in the present situation, but appear in liquid-crystal solutions.[23]

The orienting mechanism considered here is due to the interaction of the external magnetic induction B and the anisotropic magnetic susceptibility of the molecules under study. The latter quantity is described by a second rank tensor χ, which therefore enters into the expressions of the averages to be taken. As a consequence, in order to prevent unwieldly expressions, it is advantageous to take the molecular frame to be the principal frame of the susceptibility tensor, i.e. the frame in which χ is diagonal.

This choice of molecular axes, however, does not necessarily lead to the simplest mathematical form of the spin interactions. A second transformation to a suitable local frame of reference (x'', y'', z'') will in general be required. The local axes are chosen to coincide with the principal axes of the tensor describing the nuclear interaction under study.

B. The dipolar Hamiltonian

From the classical interaction energy between two magnetic dipoles, the following expression can be obtained for the dipolar Hamiltonian of two coupled spins I and S:[46]

$$\mathscr{H}_D = h\mathbf{I} \cdot \mathbf{D} \cdot \mathbf{S} = h \sum_{p',q'} D_{p'q'} I_{p'} S_{q'} \qquad (2)$$

in which

$$D_{p'q'} = -\frac{\mu_0}{4\pi} \frac{\gamma_I \gamma_S h}{2\pi^2 r^3} \left(\frac{3}{2} \frac{r_{p'} r_{q'}}{r^2} - \frac{1}{2} \delta_{p'q'} \right) \qquad (3)$$

The indices p' and q' label the laboratory axes (x', y', z'), so that (2) contains the nine components of the dipolar interaction tensor $\boldsymbol{D}$ (in frequency units, Hz) and of the (dimensionless) spin vectors $\boldsymbol{I}$ and $\boldsymbol{S}$ with respect to the laboratory frame. In (3) γ_I and γ_S are the magnetogyric ratios of the spins, h is Planck's constant and r is the internuclear distance. The projections of $\boldsymbol{r}$ along the axes are labeled by subscripts $(r_{p'})$; δ_{pq} is the Kronecker delta (1 for $p = q$, 0 for $p \neq q$). It is noteworthy from (3) that the tensor $\boldsymbol{D}$ has two useful properties, being symmetrical

$$D_{p'q'} = D_{q'p'} \tag{4}$$

and traceless

$$\sum_{p'} D_{p'p'} = 0 \tag{5}$$

As already mentioned, the Zeeman interaction is the dominant term in the Hamiltonian (1): for alignment effects caused by currently available fields $(\mathcal{H}_Z/h \approx 10^8 \text{ Hz})$ the order of magnitude of H_D/h and $\mathcal{H}_Q/h$, averaged over the molecular tumbling, rarely exceeds a few Hertz. This means that off-diagonal components of the interaction tensors in $\mathcal{H}_D$ and $\mathcal{H}_Q$ can be neglected to a very good approximation. This so-called "high-field limit" leads to a simplified dipolar Hamiltonian given by[46]

$$\mathcal{H}_D = hD[I_{z'} S_{z'} - \tfrac{1}{4}(I'_+ S'_- + I'_- S'_+)] \tag{6}$$

where $D = D_{z'z'}$ is the dipolar coupling constant (in Hz). The observable D is now to be related to molecular properties via transformations to the molecular and the local frames.

For any cartesian second rank tensor $\boldsymbol{A}$ the transformation properties can be expressed as[49]

$$A_{ab} = \sum_{\alpha, \beta} l_{a\alpha} l_{b\beta} A_{\alpha\beta} \tag{7}$$

The indices a, b label the axes in the original reference system and α, β those in the new frame, to which the transformation is carried out. The quantities $l_{a\alpha}$ are direction cosines: $l_{a\alpha} = \cos \theta_{a\alpha}$ is the cosine of the angle between the a-axis and the α-axis.

Applying (7) to the dipolar coupling constant in (6), the transformation from the laboratory to the molecular frame can be made:

$$D = D_{z'z'} = \sum_{p, q} l_{z'p} l_{z'q} D_{pq}$$

$$= \tfrac{1}{3} \sum_p D_{pp} + \tfrac{2}{3} \sum_{p, q} (\tfrac{3}{2} l_{z'p} l_{z'q} - \tfrac{1}{2} \delta_{pq}) D_{pq} \tag{8}$$

where the subscripts p and q label the molecular axes (x, y, z) and the
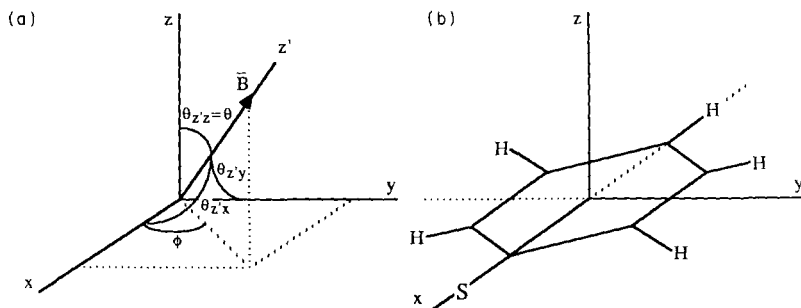
(a)

(b)

FIG. 3. (a) The transformation from the laboratory frame (x', y', z') to the molecular frame (x, y, z) can be described in terms of the angles $\theta_{z'p}$ ($p \in x, y, z$) that the laboratory z'-axis, chosen along the magnetic field **B**, makes with the molecular axes. Alternatively, the polar angles (θ, ϕ) between the laboratory z'-axis and the molecular axes can be used (see also Section II.D). These are related to the direction cosines by: $l_{z'x} = \sin \theta \cos \phi$; $l_{z'y} = \sin \theta \sin \phi$; $l_{z'z} = \cos \theta$. (b) The molecular frame is adapted to the molecular symmetry. For example, in the frame shown for a substituted benzene the diamagnetic susceptibility χ is diagonal ($\chi_{xy} = \chi_{xz} = \chi_{yz} = 0$).

components D_{pq} are given by an equation analogous to (3). Since **D** is traceless, the first part of the last term in (8) can be omitted. The direction cosines $l_{z'p}$ or $l_{z'q}$ in (8) contain the angles between the laboratory z'-axis and the molecular axes (see Fig. 3). The molecular tumbling causes these angles to fluctuate rapidly in time, and consequently an averaging over them must be performed, giving

$$D = \tfrac{2}{3} \sum_{p,q} S_{pq} D_{pq} \tag{9}$$

with

$$S_{pq} = S_{qp} = \langle \tfrac{3}{2} l_{z'p} l_{z'q} - \tfrac{1}{2} \delta_{pq} \rangle \tag{10}$$

The brackets $\langle ... \rangle$ denote the averaging.

The S_{pq} are elements of the order matrix S defined by Saupe[38] and, together with the related c-coefficients defined by Snyder[39] and the elements of the Wigner rotation matrices,[50] are often referred to as motional constants or order parameters. In general, the S_{pq} all have a finite value for nonrandom tumbling, but for the special case of magnetic-field-induced alignment, taking the molecular frame to be the frame in which the magnetic-susceptibility tensor is diagonal (see Section II.D), all the off-diagonal elements are zero, i.e. $S_{pq} = S_{pp}\delta_{pq}$, and

$$D = \tfrac{2}{3} \sum_{p} S_{pp} D_{pp} \tag{11}$$

From (10) it can be seen that the matrix S is traceless (by definition) and therefore two independent order parameters suffice, which might be taken as S_{zz} and $\frac{2}{3}(S_{xx} - S_{yy})$.

The second transformation from the molecular to the local frame can easily be performed without the use of (7), because a very obvious choice of local axes (x'', y'', z'') exists: taking the z''-axis along the internuclear distance vector
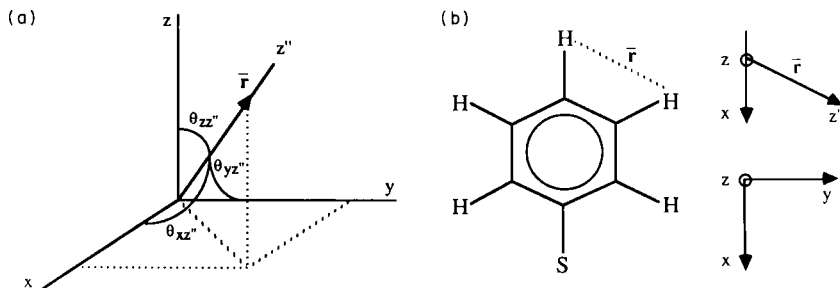

FIG. 4. (a) The choice of the local frame (x'', y'', z'') for the dipolar interaction: the local z''-axis is along the internuclear-distance vector r and makes angles $\theta_{pz''}$ $(p \in x, y, z)$ with the molecular axes. The angles $\theta_{pz''}$ are determined by the molecular geometry. (b) A specific proton pair in a substituted benzene (Fig. 1b). Since the molecule is planar $\theta_{zz''} = \frac{1}{2}\pi$. Assuming a regular hexagon for the aromatic ring, it follows that $\theta_{xz''} = \frac{1}{3}\pi$, $\theta_{yz''} = \frac{1}{6}\pi$.

r and noting that then $r_p/r = l_{pz''}$ (see Fig. 4), it is found that (see also (3))

$$D_{pp} = - \frac{\mu_0}{4\pi} \frac{\gamma_I \gamma_S h}{2\pi^2 r^3} \Gamma_p \tag{12}$$

with Γ_p a geometrical factor, depending only on the molecular structure:

$$\Gamma_p = (\tfrac{3}{2}l_{pz''}^2 - \tfrac{1}{2}) \tag{13}$$

Combining (11) and (12), the expression for the dipolar coupling constant between spins I and S becomes

$$D = - \frac{\mu_0}{4\pi} \frac{\gamma_I \gamma_S h}{2\pi^2 r^3} \frac{2}{3} \sum_p S_{pp} \Gamma_p \tag{14}$$

Equations (6) and (14) thus give the Hamiltonian that forms the basis for the interpretation of dipolar effects in the spectrum.

C. The quadrupolar Hamiltonian

The interaction of the nuclear quadrupole of a spin I $(I > \frac{1}{2})$ with the electric field gradient generated by surrounding charges can be described by the

Hamiltonian[46]

$$\mathcal{H}_Q = \frac{eQ}{2I(2I-1)} \mathbf{I} \cdot \mathbf{V} \cdot \mathbf{I} = \frac{eQ}{2I(2I-1)} \sum_{p',q'} V_{p'q'} I_{p'} I_{q'}$$ (15)

Here eQ is the nuclear quadrupole moment of the spin I. $\mathbf{V}$ is the electric field gradient tensor evaluated at the nucleus; it is symmetrical and, in the absence of electronic charge density at the nucleus so that the Laplace equation is satisfied, traceless (see also (4) and (5)). The indices p' and q' again label the laboratory axes (x', y', z').

Applying the high-field approximation, the quadrupolar Hamiltonian simplifies to

$$\mathcal{H}_Q = \frac{eQ}{4I(2I-1)} V_{z'z'}[3I_{z'}^2 - I^2]$$ (16)

The component $V_{z'z'}$ of the electric-field gradient at the nucleus, defined in the laboratory frame, is a rapidly varying function of time. To obtain the average value, $V_{z'z'}$ is related to molecule-fixed local field gradients by the two-step transformation procedure given above for the dipolar case. Thus, following the lines along which (11) was obtained, in going to the molecular frame (x, y, z) in which χ is diagonal (see also Fig. 3), the order parameters are introduced:

$$V_{z'z'} = \tfrac{2}{3} \sum_p S_{pp} V_{pp}$$ (17)

In order to perform the second step, a suitable local frame has to be available: a convenient choice is the principal-axes system of the field-gradient tensor. The off-diagonal elements being zero, $\mathbf{V}$ has only two independent components, since the tensor is traceless. It is customary to define the symbols

$$eq = V_{z''z''}$$ (18)

the major component of the field gradient tensor, and

$$\eta = \frac{V_{x''x''} - V_{y''y''}}{V_{z''z''}}$$ (19)

the asymmetry parameter. The local axes are taken to satisfy the convention $|V_{z''z''}| \geqslant |V_{y''y''}| \geqslant |V_{x''x''}|$. Using the transformation equation (7), it is found that the components of the field gradients in the molecular frame $(p = x, y, z)$ depend as follows on the symbols eq and η and on the angles between the p-axis and the local axes (see Fig. 5):

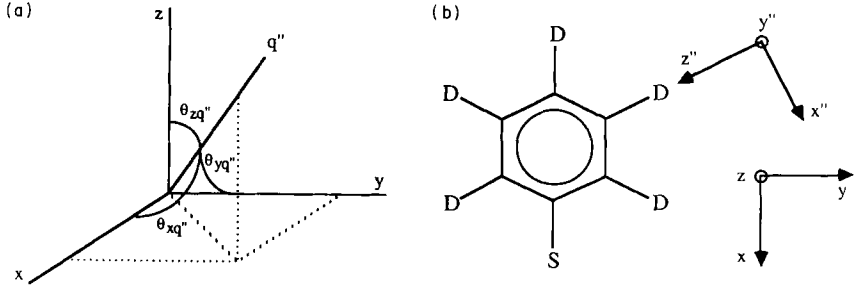$$V_{pp} = eq(\Gamma_p + \tfrac{1}{2}\eta\Omega_p),$$ (20)

FIG. 5. (a) The relation between the molecular frame (x, y, z) and the local frame (x'', y'', z'') for the quadrupolar interaction. The local q''-axis $(q'' \in x'', y'', z'')$ makes angles $\theta_{pq''}$ $(p \in x, y, z)$ with the molecular axes; the angles $\theta_{pq''}$ can be inferred from the molecular geometry. (b) A specific deuterium nucleus in a deuterated substituted benzene. The local frame coincides with the principal axes of the electric-field-gradient tensor at the nucleus $(V_{z''z''} = eq)$. The angles $\theta_{xy''}$, $\theta_{yy''}$, $\theta_{zx''}$ and $\theta_{zz''}$ are all $\frac{1}{2}\pi$, and $\theta_{zy''} = 0$, because of the planar structure. The remaining angles, assuming a regular hexagon as in Fig. 4(b), are $\theta_{xx''} = \theta_{yz''} = \frac{1}{6}\pi$ and $\theta_{xz''} = \theta_{yx''} = \frac{1}{3}\pi$.

with Γ_p and Ω_p geometry factors; Γ_p and Ω_p are defined by

$$\Gamma_p = (\tfrac{3}{2}l^2_{pz''} - \tfrac{1}{2}) \tag{13}$$

$$\Omega_p = (l^2_{px''} - l^2_{py''}) \tag{21}$$

Substituting (20) into (17), it follows that

$$V_{z'z'} = \tfrac{2}{3}eq \sum_p S_{pp}(\Gamma_p + \tfrac{1}{2}\eta\Omega_p) \tag{22}$$

Equations (16) and (22) specify the quadrupolar Hamiltonian to be used for spectral interpretation. The product of quadrupole moment eQ and major field gradient $V_{z''z''}$, i.e. (e^2qQ), in the Hamiltonian is often called the quadrupole coupling constant (in frequency units: e^2qQ/h).

D. The order parameters

The order parameters S_{pq} $(p, q \in x, y, z)$ defined in (10), are averages over the molecular tumbling. They may be calculated by applying Boltzmann statistics. This is most conveniently done by expressing the functions to be averaged in terms of the polar angles (θ, ϕ) between the laboratory z'-axis and the molecular axes (x, y, z) (see Fig. 3). This leads to

$$S_{xx} = \langle \tfrac{3}{2}l^2_{z'x} - \tfrac{1}{2} \rangle = \langle \tfrac{3}{2} \sin^2\theta \cos^2\phi - \tfrac{1}{2} \rangle \tag{23a}$$

$$S_{yy} = \langle \tfrac{3}{2}l^2_{z'y} - \tfrac{1}{2} \rangle = \langle \tfrac{3}{2} \sin^2\theta \sin^2\phi - \tfrac{1}{2} \rangle \tag{23b}$$

$$S_{zz} = \langle \tfrac{3}{2}l^2_{z'z} - \tfrac{1}{2} \rangle = \langle \tfrac{3}{2} \cos^2\theta - \tfrac{1}{2} \rangle \tag{23c}$$

$$S_{xy} = S_{yx} = \langle \tfrac{3}{2} l_{z'x} l_{z'y} \rangle = \langle \tfrac{3}{4} \sin^2 \theta \sin 2\phi \rangle \tag{23d}$$

$$S_{xz} = S_{zx} = \langle \tfrac{3}{2} l_{z'x} l_{z'z} \rangle = \langle \tfrac{3}{4} \sin 2\theta \cos \phi \rangle \tag{23e}$$

$$S_{yz} = S_{zy} = \langle \tfrac{3}{2} l_{z'y} l_{z'z} \rangle = \langle \tfrac{3}{4} \sin 2\theta \sin \phi \rangle \tag{23f}$$

The average of an arbitrary function $F(\theta, \phi)$ is given by

$$\langle F(\theta, \phi) \rangle = \frac{\int_0^\pi \int_0^{2\pi} F(\theta, \phi) \exp\left[-W(\theta, \phi)/kT \right] \sin\theta \, d\theta \, d\phi}{\int_0^\pi \int_0^{2\pi} \exp\left[-W(\theta, \phi)/kT \right] \sin\theta \, d\theta \, d\phi} \tag{24}$$

W is the aligning potential, k Boltzmann's constant and T the absolute temperature. For random tumbling, i.e. for constant W, all order parameters are zero, but whenever (partial) alignment of the molecules occurs the S_{pq} may have finite values.

For alignment induced by a magnetic field, it is possible to evaluate the average in (24), since an analytical expression for W is available. The orienting torques that the field exerts on the molecules are described by an interaction energy[51,52]

$$W = \frac{1}{\mu_0} (-\tfrac{1}{2} \mathbf{B} \cdot \boldsymbol{\chi} \cdot \mathbf{B}) \tag{25}$$

Using a molecular frame in which the susceptibility tensor is diagonal and choosing $\mathbf{B}$ along the laboratory z'-axis (see Fig. 3), the aligning potential (25) can also be expressed in terms of the polar angles (θ, ϕ):

$$W = \frac{1}{\mu_0} \left[-\tfrac{1}{2}\chi_{AV} B^2 - \tfrac{1}{3}\Delta\chi \, B^2 (\tfrac{3}{2} \cos^2 \theta - \tfrac{1}{2}) - \tfrac{1}{4}\delta\chi \, B^2 (\sin^2 \theta \cos 2\phi) \right] \tag{26}$$

The quantities

$$\chi_{AV} = \tfrac{1}{3}(\chi_{xx} + \chi_{yy} + \chi_{zz}) \tag{27}$$

$$\Delta\chi = \chi_{zz} - \tfrac{1}{2}(\chi_{xx} + \chi_{yy}) \tag{28}$$

and

$$\delta\chi = \chi_{xx} - \chi_{yy} \tag{29}$$

are respectively the average of the susceptibility, the anisotropy and the asymmetry of the magnetic susceptibility; the molecular axes are taken such that $|\Delta\chi| > |\delta\chi|$. Hence in a molecule like benzene the z-axis is chosen to be perpendicular to the aromatic plane.

Expressions for the elements of the order matrix can now be obtained by straightforward calculation. Since $|\chi B^2/\mu_0 kT| \approx 10^{-4} - 10^{-2}$ ($B \approx 10 \, T$; room temperature), the high-temperature limit ($kT \gg W$) applies and the exponential in the integrals in (24) can be expanded in a Taylor series, keeping only the first terms. It follows that all off-diagonal components are zero, whereas

for the diagonal elements it is found, to first order in W/kT, that

$$S_{xx} = \frac{1}{15}\frac{B^2}{\mu_0 kT}(-\tfrac{1}{2}\Delta\chi + \tfrac{3}{4}\delta\chi) \tag{30a}$$

$$S_{yy} = \frac{1}{15}\frac{B^2}{\mu_0 kT}(-\tfrac{1}{2}\Delta\chi - \tfrac{3}{4}\delta\chi) \tag{30b}$$

and

$$S_{zz} = \langle \tfrac{3}{2}\cos^2\theta - \tfrac{1}{2}\rangle = \frac{1}{15}\frac{\Delta\chi}{\mu_0 kT}\frac{B^2}{} \tag{30c}$$

As has already been remarked, the S-matrix is traceless (from (10)) and so there are only two independent order parameters for alignment by a magnetic field. These will be taken as S_{zz} and $\tfrac{2}{3}(S_{xx} - S_{yy})$, with

$$\tfrac{2}{3}(S_{xx} - S_{yy}) = \langle \sin^2\theta \cos 2\phi \rangle = \frac{1}{15}\frac{\delta\chi}{\mu_0 kT}\frac{B^2}{} \tag{30d}$$

Expressing eqns. (14) and (22) in terms of these order parameters:

$$D = -\frac{\mu_0}{4\pi}\frac{\gamma_I\gamma_S h}{2\pi^2 r^3}[\langle \tfrac{3}{2}\cos^2\theta - \tfrac{1}{2}\rangle\Gamma_z + \tfrac{1}{2}\langle \sin^2\theta \cos 2\phi \rangle(\Gamma_x - \Gamma_y)] \tag{31}$$

and

$$V_{z'z'} = eq[\langle \tfrac{3}{2}\cos^2\theta - \tfrac{1}{2}\rangle(\Gamma_z + \tfrac{1}{2}\eta\Omega_z)$$
$$+ \tfrac{1}{2}\langle \sin^2\theta \cos 2\phi \rangle\{(\Gamma_x + \tfrac{1}{2}\eta\Omega_x) - (\Gamma_y + \tfrac{1}{2}\eta\Omega_y)\}] \tag{32}$$

The molecular symmetry also affects the order parameters: when effective axial symmetry applies, as for example in benzene, one has $\chi_{xx} = \chi_{yy}$, so that $\delta\chi$ equals zero. Then only one order parameter survives, i.e. $\langle \tfrac{1}{2}(3\cos^2\theta - 1)\rangle$, simplifying the expressions in (31) and (32).

Sometimes another notation is used, in which the sums containing the S_{pp} have been converted into sums of χ_{pp} values:

$$\sum_p S_{pp}\Gamma_p = \frac{B^2}{10\mu_0 kT}\sum_p \chi_{pp}\Gamma_p \tag{33a}$$

$$\sum_p S_{pp}\Omega_p = \frac{B^2}{10\mu_0 kT}\sum_p \chi_{pp}\Omega_p \tag{33b}$$

In general, however, use has been made of (31) and (32).

E. Spectral interpretation

Having arrived at convenient expressions for the Hamiltonians $\mathscr{H}_D$ and $\mathscr{H}_Q$, the only point left is to investigate the way in which the dipolar and

quadrupolar couplings affect the NMR spectrum. From (1) the energy levels, and thus the transition frequencies, can be determined for any spin system. Here some simple examples of NMR spectra of partially oriented molecules are given.

To illustrate the effect of the dipolar coupling, consider the four transition frequencies and intensities in the high-resolution NMR spectrum of a system of two spin-$\frac{1}{2}$ nuclei. Relative to the centre of the multiplet, the transitions have frequencies and intensities given by

$$\nu_1 = \tfrac{1}{2}(-J - D + C), \quad I_1 = 1 + (J - \tfrac{1}{2}D)/C$$

$$\nu_2 = \tfrac{1}{2}(-J - D - C), \quad I_2 = 1 - (J - \tfrac{1}{2}D)/C$$

$$\nu_3 = \tfrac{1}{2}(+J + D - C), \quad I_3 = 1 + (J - \tfrac{1}{2}D)/C$$

$$\nu_4 = \tfrac{1}{2}(+J + D + C), \quad I_4 = 1 - (J - \tfrac{1}{2}D)/C$$

where J and D are the indirect and dipolar coupling constants, and $C = [(\Delta\nu)^2 + (J - \tfrac{1}{2}D)^2]^{1/2}$. This specifies a symmetrical quartet, with lines 2 and 4 at the extremes and 1 and 3 in the middle. Except under unusual circumstances (large D, such that $3D(J + \tfrac{1}{4}D) > (\Delta\nu)^2$, causing scrambling of the line positions), the spacing $\Delta\nu_C$ of the left- and right-hand doublets is

$$\Delta\nu_C = J + D \qquad\qquad (34a)$$

The spacing of the central lines is $J + D - C$. For an A_2 case, transitions 2 and 4 have zero intensity; the result is a doublet consisting of lines 1 and 3, with a splitting

$$\Delta\nu_D = \tfrac{3}{2}D \qquad\qquad (34b)$$

According to (30) and (31), the magnetic-field-induced dipolar coupling gives rise to a quadratic magnetic-field dependence of the apparent doublet splitting $\Delta\nu_C$ or $\Delta\nu_D$. Depending on the geometrical factors Γ_p, the dipolar coupling constant may add to or subtract from the indirect coupling J, as has been established experimentally (see Fig. 7, Section IV.A).[48] Thus, unless the coupled spins are equivalent, dipolar couplings can only be found from field-dependent measurements.

Owing to the factor $\gamma_I\gamma_S/r^3$, dipolar couplings are important between closely spaced nuclei, which have large magnetic moments. Thus ^{13}C—H and CH_2 groups are especially favourable cases for study (see Fig. 7). In general, when studying protons, the spin systems encountered consist of more than two spins. Then spectral interpretation in terms of simple relations, like (34), is usually not possible, and spectra should be analysed by numerical simulation methods to extract the NMR parameters.

The quadrupolar coupling plays a role for any spins with $I > \frac{1}{2}$, but until now attention has been restricted to deuterium ($I = 1$), since so far only for

this quadrupolar nucleus have line widths turned out to be sufficiently small to permit detection of magnetic-field-induced alignment. For a single spin there are two possible transitions, which in the absence of alignment are degenerate. Upon orientation of the molecules, the transition frequencies become unequal, leading to two lines with a doublet splitting given by

$$\Delta v_Q = \frac{3}{2} \frac{eQV_{z'z'}}{h} \tag{35}$$

Equations (30) and (32) show that the magnetic-field-induced quadrupolar splittings Δv_Q also vary with the square of the field. Again the sign depends on the geometrical factors Γ_p and Ω_p. It should be noted that for a single deuteron the NMR spectrum gives no information about the sign of the observed splitting. The sign, however, can be derived from physical arguments concerning the ordering parameters (or susceptibility values).

When considering a spin system of several quadrupolar nuclei, indirect
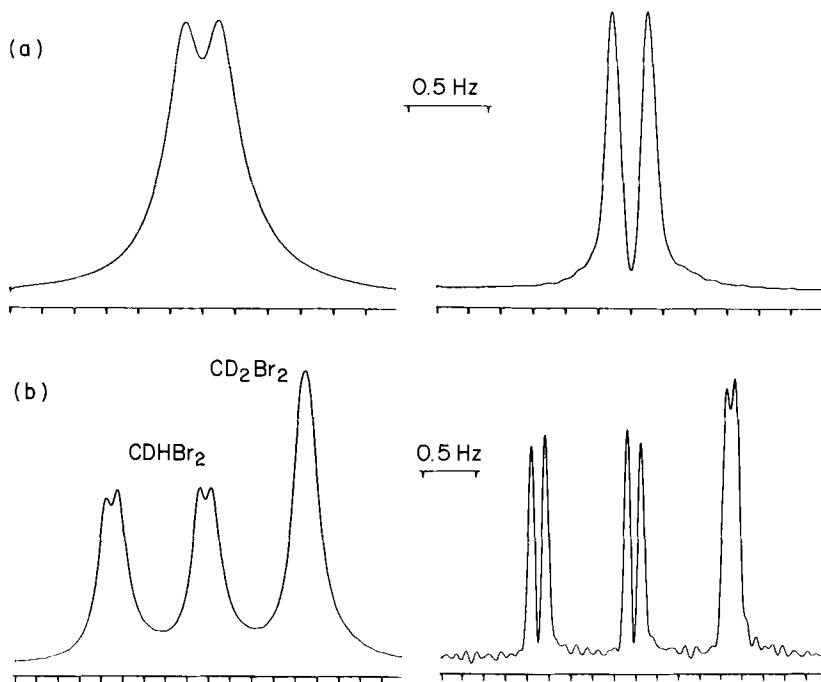
FIG. 6. Normal and resolution-enhanced deuterium spectra (14.35 T; 296 K) of pure $CDCl_3$ (a) and of a mixture of $CHDBr_2$ and CD_2Br_2 (b) at 5 mol% in cyclohexane. The obscuring of the quadrupolar splitting in CD_2Br_2 as a consequence of interference of scalar deuteron–deuteron couplings is clearly visible.

couplings between the spins might interfere with the quadrupolar couplings, thereby complicating the splitting pattern and obscuring the doublet splittings.[53] However, relaxation rates for quadrupolar nuclei are often large compared with the indirect couplings, which are therefore partially or completely averaged out (self-decoupling). A borderline case arises for deuteriated benzenes and methylene halides, where quadrupolar splittings and indirect deuterium–deuterium couplings are of the same order of magnitude (about 0.2 Hz).[53,54] This effect can be seen clearly in Fig. 6(b), where the deuteron resonance of $CHDBr_2$ is already split, but that of CD_2Br_2 is not. This phenomenon is discussed in detail in ref. 54.

Should there be effects due to indirect couplings of the quadrupolar nuclei with protons, these can be eliminated by proton decoupling, so that (35) still applies.

III. EXPERIMENTAL ASPECTS

To induce alignment effects with an external magnetic field, no specific experimental precautions are required. Standard high-field/high-resolution equipment can be used. However, the effort necessary to obtain accurate small line splittings should not be underestimated. In many cases the line width exceeds the splitting, and special techniques have to be used to deconvolute the lines, giving rise to additional uncertainties.

A. Determination of small line splittings

The optimal situation to obtain accurate splittings consists of the simultaneous occurrence of small line widths, a strong field and a large suspectibility anisotropy $\Delta\chi$. The highest field strength currently available in NMR is 14.57 T (^{1}H: 620 MHz; ^{2}H: 95.18 MHz); almost all data in Section IV were obtained at field strengths between 14.10 and 14.57 T. In a previous review,[7] data at 11.75 T were reported. In general, both the line width and $\Delta\chi$ increase with the size of the molecule studied. For instance, the smallest ^{2}H line width measured at room temperature for an aromatic compound like benzene is about 0.35 Hz,[27,53] while for small rapidly reorienting molecules like haloforms and methylene halides[55] it is 0.1–0.2 Hz (Fig. 6). These widths determine whether splittings can be observed; for example for $CHDBr_2$ in cyclohexane at 14.35 T the quadrupolar deuterium splitting of 0.125 Hz[55] can be resolved using line-narrowing techniques (Fig. 6b), and this is about as difficult as resolving the 0.48 Hz ^{2}H splitting in benzene-^{2}H$_1$.[27,53]

The use of resolution enhancement in spectra of compounds with more than one deuteron can be misleading, since the indirect ^{2}H–^{2}H coupling may

interfere.[53] It has been demonstrated that for aromatic molecules larger than benzene, resolution enhancement provides the correct splittings.[27] This was accomplished by means of experiments on monodeuteriated analogues, where simulation as well as resolution enhancement lead to the same quadrupolar effects as for the perdeuteriated species. The explanation for this phenomenon is that the ^2H relaxation rates in these compounds are large enough to cause self-decoupling, whereby the indirect couplings are partially averaged out.[54]

A method to detect splittings smaller than those obtainable by resolution enhancement has been discussed.[56] It consists of the measurement of the field dependence of the amplitude of a merged doublet. For two identical overlapping Lorentzian lines, the amplitude at the centre of the resulting line, as a function of the line splitting Δv, is

$$A(\Delta v) = cT_2^*\{1 + (\pi\Delta vT_2^*)^2\}^{-1} \tag{36}$$

with T_2^* the effective transverse relaxation time and c a scaling constant. The amplitude ratio of the resonance lines of the molecule under investigation and a nonaligning reference compound ($\Delta\chi \approx \delta\chi \approx 0$, therefore $\Delta v \approx 0$) is then measured at different magnetic fields. The ratio of the splitting at two fields is known from their proportionality to B^2, so Δv can be calculated from the experimentally determined amplitudes and T_2^* values of the probe molecule and the internal standard.

Recently a new method to obtain small line splittings has been introduced.[57] It is a deconvolution technique, which has the advantage that no assumption is made about line shape; partially overlapping doublets can clearly be decomposed into their components. Basically, for a doublet the method consists of division of the free induction decay (FID) by $\cos\frac{1}{2}\omega_s t$, with ω_s a trial doublet separation. If ω_s is chosen close to the correct value, Fourier transformation will give a single line for the merged doublet. The correct value of ω_s can be identified by iteration to a final spectrum with smallest line width (greatest amplitude) and absence of base-line modulation. Splittings are obtained with an accuracy increased substantially compared with resolution enhancement.[57] The data in Section IV were obtained before the introduction of this new technique. Other deconvolution techniques are presently under investigation.

When measuring dipolar effects, two different situations may arise: the nuclei under study are either magnetically equivalent or not. In the former case the same consideration as for deuterium apply to the line splittings, since the indirect coupling does not appear in the spectrum. In the latter situation both indirect and dipolar couplings are manifest, and it may be necessary to perform magnetic-field-dependent measurements to separate J and D. Two advantages nevertheless accrue: (i) measurement of $J + D$ provides a simple

method to determine the relative signs of J and D; (ii) the resonances are already separated by J, and in principle very small superimposed dipolar effects can be measured.[58]

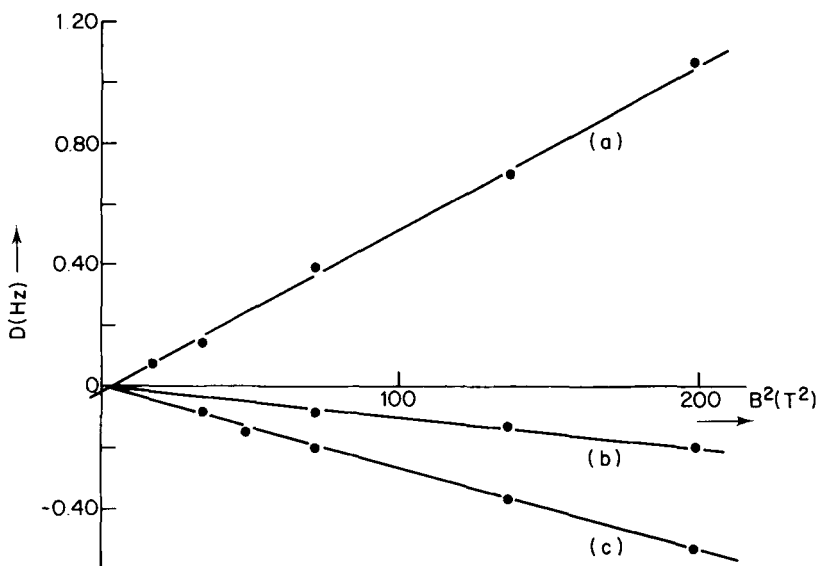In Fig. 7 the magnetic field dependence of D is illustrated for coronene and a porphyrin.

FIG. 7. Quadratic field dependence of the dipolar coupling for: (a) a CH_2 group ($R_{HH} = 1.80$ Å; $\theta_{zz''} = 0°$) in a porphyrin; (b) two neighbouring protons in an aromatic ring ($R_{HH} = 2.45$ Å; $\theta_{zz''} = 90°$) in coronene; (c) a ^{13}C—H group ($R_{HH} = 1.10$ Å; $\theta_{zz''} = 90°$) in coronene. (Reproduced, with permission, from ref. 48.)

In the study of ^{13}C–^1H dipolar couplings first-order spectra are likely to be encountered, the coupling between the spins (150–200 Hz) being much smaller than their resonance-frequency difference. Spectral interpretation, and thus separation of J and D, is then straightforward. For ^1H–^1H interactions second-order effects may play a role, and exact simulation is necessary to obtain the coupling constants.

In general, the accuracy of quadrupolar and dipolar splittings (determined by the line width) is about 2–5%. The recent availability of a deconvolution method to precisely determine couplings[57] will increase the accuracy. This technique will enable the extension to smaller molecules, like the ones generally studied with microwave spectroscopy.

IV. DIAMAGNETIC MOLECULES

A. Magnetic-susceptibility anisotropies and asymmetries

1. Determination by NMR

The first application arising from the equations in Section II is the determination of magnetic susceptibility anisotropies and asymmetries. The method is very straightforward, but a few important considerations must be kept in mind.

First, if molecular susceptibilities are to be determined, the compound should be dissolved in a nonaligning and noninteracting solvent, at a concentration low enough to ensure that solute molecules do not aggregate. If this is not so (Section IV.C) the definition of the geometry of the aggregates and thus of the principal frame of the magnetic susceptibility is not straightforward, and the interpretation of the splittings becomes complex.[27,28] Available data suggest[27] that ether, hexane and cyclohexane are virtually inert solvents for magnetic-field-alignment studies of aromatic molecules and the haloforms. In Table 2 the compounds investigated to date have been summarized. For the monosubstituted benzenes[27,28] and the halomethanes[55] the molecular susceptibilities are derived from dilute solutions, at mole fractions where no concentration dependence of the splitting appears. For the larger aromatic systems all concentrations are below 0.5 mol%. Systems like porphyrins[11] and coronene may be liable to complexation at concentrations as low as 0.1–0.01 mol%. The porphyrins are discussed in Section IV.C.3.

A second prerequisite for determining $\Delta\chi$ is knowledge of the relevant nuclear constants. For dipolar couplings the internuclear distances must be available (equation 31); these can often be obtained from microwave, electron-diffraction or X-ray structure determinations, or deduced from standard bond lengths and angles. In the case of quadrupolar effects (equation 32) the quadrupole coupling constant and the asymmetry parameter must be known. In the last decade, many values of ^{2}H quadrupole coupling constants have been determined, and the values are mostly in the range $e^2qQ/h = 186 \pm 6\,\text{kHz}$ and $\eta = 0.05 \pm 0.02$ for aromatic molecules in the liquid or solid phases.[59] [62] For aliphatic species $(e^2qQ/h) = 165 \pm 5\,\text{kHz}$, assuming $\eta = 0$.[59,63] The value of η used in Table 2 differs from that in most previous papers (before 1985), where the asymmetry parameter of ^{2}H in aromatics is neglected.[7] An illustration that these values are justified is given by coronene, where ^{2}H, ^{13}C–^{1}H and ^{1}H–^{1}H couplings all give the same value of $\Delta\chi$ to within a few per cent.[7,48] It should be noted that for aromatic ions like fluorenyl carbanion and the anthracenyl carbonium ion, altered

TABLE 2

Magnetic-susceptibility anisotropies and asymmetries (in m^3; note that $\chi^{SI}(m^3) = 4\pi \times 10^{-6}\chi^{cgs}(cm^3$, emu)) measured by the NMR method ($T = 296$ K), in comparison with literature data. Molecular-axes definition as well as the quadrupolar splittings of the newly measured species are given in the appendix.

Compound	NMR			Literature		
	$10^{34}\Delta\chi$	$10^{34}\delta\chi$	Ref.	$10^{34}\Delta\chi$	$10^{34}\delta\chi$	Ref.
Hydrogencyanide[a,h,(1/2)]	(−1.0)		56	−0.88		32[i,l]
Chloroform[a,f,3]	3.19		55			
Bromoform[a,f,3]	4.80		55			
Iodoform[a,f,3]	8.39		55			
Methylene bromide[a,f,3]	0.00[n]	3.74[n]	55			
Methylene iodide[a,f,3]	0.00[n]	5.89[n]	55			
Pyridine[a,e,1]	−13.3	0.1	28	−11·9	−0.4	114[i,l]
				−13.3	—[p]	115[j,m]
Benzene[a,e,1]	−12.7		27	−13.2		116[l,o]
				−13.1		117[j,l]
				−13.3		115[j,m]
				−12.4		118[k]
Fluorobenzene[a,e,1]	−13.1	−0.1	28	−12.2	−0.8	119[i,l]
				−11.9	—[p]	120[j,m]
Chlorobenzene[a,e,1]	−12.8	−0.6	28	−9.4	—[p]	120[j,m]
Bromobenzene[a,e,1]	−12.4	−0.8	28	−9.7	—[p]	121[j,m]
Aniline[a,e,1]	−11.9	−0.6	28			
Toluene[a,e,1]	−13.7	−0.5	27	−12.6	—[p]	29[j,m]
Nitrobenzene[a,e,1]	−15.7	−0.9	27	−20.0	—[p]	112[j,m]
Metadinitrobenzene[a,g,1]	−18.2	0.5	q	−15.1	—[p]	123[k]
[5]-Metacyclophane[a,e,1]	−18.7	—[p]	77			
Biphenyl[a,e,1]	−20.6	3.6	124	−24.9[r]	−1.3[r]	125[k]
Naphthalene[a,g,3]	−25.0	0.6	q	−25.0	0.5	125[k]
Acenaphtene[a,g,3]	−26.0	0.0	q	−23.9	0.4	125[k]
Fluorene[a,g,3]	−28.8	0.3	q	−25.3	—[p]	125[k]
Fluorenyl lithium[a,d,1]	−36.8	1.8	64			
Anthracene[a,e,1]	−36.9	1.4	65	−38.1	2.8	125[k]
Anthracenium ion[a,e,4]	−35.2	1.0	65			
Phenanthrene[a,g,3]	−37.4	−0.1	q	−34.6	—[p]	125[k]
Pyrene[a,g,1,3]	−49.6	−1.0	q	−46.4	—[p]	125[k]
Triphenylene[a,g,3]	−47.6		q	−49.3		126[j,m]
Chrysene[a,g,1]	−47.8	−1.1	q	−47.0	—[p]	125[k]
Perylene[a,g,1]	−43.0	−0.6	q	−50.0	—[p]	125[k]
Coronene,[d] a, 2	−94		7	−81		125[k]
a, 8	−93		7			
b, h, 2	−90		48			
c, h, 2	−93		48			
Porphine,[a,d,2]	−148		7			
s	−126		11			

TABLE 2 (cont.)

	NMR			Literature		
Compound	$10^{34}\Delta\chi$	$10^{34}\delta\chi$	Ref.	$10^{34}\Delta\chi$	$10^{34}\delta\chi$	Ref.
VPE,[c,h,s,5]	−161		11			
6	−93		11			
ZnVPE[c,h,t,7]	−119		11			
HMPDA[b,h,u,5]	−122		11			
MPPA[c,h,v,2]	−101		48			
MPDME[w]				−122		127
PPDME[x]				−124		125

[a]Deuterium; [b]^{13}C–^{1}H couplings; [c]^{1}H–^{1}H couplings; [d]11.75 T; [e]14.11 T; [f]14.35 T; [g]14.57 T; [h]From field-dependent measurements; [i]Zeeman effect in microwave spectroscopy; [j]Cotton–Mouton effect; [k]Krishnan critical-angle method (solid); [l]Gas; [m]Liquid; [n]As a consequence of choice of molecular frame (see Appendix); [o]Estimated from Zeeman data of a series of substituted fluorobenzenes; [p]$\delta\chi = 0$ assumed; [q]This work; [r]Planar structure assumed; [s]Calculated (ref. 11); [t]Vinylphylloerythrin methyl ester (Fig. 10); [u]1,2,3,4,5,8-hexamethyl-a-^{13}C-porphyrin-6,7-dipropionic acid dimethyl ester,[11] [v]Methylpyropheophorbide a;[48] [w]Mesoporphyrin dimethyl ester;[11] [x]Protoporphyrin dimethyl ester.
Solvents: (1) diethylether; (2) methylene chloride; (3) cyclohexane; (4) hydrogen fluoride; (5) chloroform; (6) trifluoroacetic acid; (7) pyridine; (8) acetone/CS_2.

charge densities in the compound may influence e^2qQ/h and η. This is discussed in detail in refs. 64 and 65.

The $\Delta\chi$ value of DCN[56] in the table is placed between brackets as the error may be quite large. The DCN deuteron line splitting was determined from the magnetic-field dependence of line intensities (Section III).[56] This method is completely correct, but the substances chosen for study in ref. 56 are not suitable. The main restrictions for the applicability of the method are that $\Delta\chi \approx \delta\chi \approx 0$ for the reference and that there is only one coupling causing the line splitting of the solute molecule. The authors use benzene-^{2}H$_6$ and DCN as solutes, with CD_2Cl_2 as a reference. However, CD_2Cl_2 is not an ideal reference: by comparison with the haloforms and methylene halides ($X = I$, Br), the deuteron splitting for CD_2Cl_2 can be estimated to be 0.05 Hz at 11.75 T, which is the same as for DCN, making the results questionable. Also the interference of scalar ^{2}H–^{2}H couplings affects the intensity of the standard. In benzene-^{2}H$_6$ the scalar couplings of the deuterons interfere with the quadrupolar coupling[53] and the method fails. Here the correct susceptibility arises from measurements on benzene-d$_1$ under proton decoupling.[27,53,66]

For the other compounds the quadrupolar splittings can almost always be resolved completely by resolution enhancement; a few examples are given in Figs. 2 and 6. Including maximum errors in the splitting (Section III), in e^2qQ/h or r^3 (2–4%) and in η (1–2%), the maximum error in $\Delta\chi$ will be about

10%. The uncertainty in $\delta\chi$ is relatively large if $\delta\chi$ is close to zero; the absolute errors are the same as for $\Delta\chi$.

Comparison between literature values and NMR data shows that agreement with microwave and solid-state methods is within 5–10%. In the case of the Cotton–Mouton experiments larger differences sometimes arise, which has been explained in terms of the complexity of this technique.[27,28] This is partly discussed in the next subsection.

2. Comparison with other techniques

Relative to other techniques for determining $\Delta\chi$, such as the Cotton–Mouton effect, microwave spectroscopy or the flip-angle method, the NMR method is simple and in principle applicable to any molecule in the liquid or gas phase. Of course there are limitations: the effects must be large enough to be measurable. Deuteriated compounds as well as a strong magnetic field are often necessary. However, with the recent availability of a method for the accurate determination of small splittings,[57] the restrictions on measuring compounds in the liquid phase are expected to be less stringent. Only in the gas phase, where high pressures are necessary to obtain narrow NMR lines and where the insensitivity of NMR becomes a burden, a limited number of compounds can be measured, mainly because of vapour-pressure restrictions.

Another advantage of the NMR method is that the constants used in the formulae are well known. This is in contrast with the Cotton–Mouton effect, which is experimentally difficult and where quantities like the polarizability anisotropy and the hyperpolarizability, which are difficult to obtain accurately, have their place in the working equations. Recently the local field factor arising in the Cotton–Mouton effect has been accurately established[67] — this previously constituted an extra difficulty. In NMR the unknown quantity most likely to cause trouble is the geometry of the molecule; in most cases, however, the structure is well known.

A final advantage is that NMR does not measure a bulk property of a mixture, but provides a means to study separately the different components in a mixture and different nuclei in a molecule. The power of the method is also demonstrated by the fact that a variety of molecules not yet studied by other methods have yielded measured susceptibility anisotropies and asymmetries: for example the haloforms,[55] aromatic ions[64,65] and a series of porphyrins in solution.[11]

B. Aromaticity

A property closely related to the magnetic susceptibility of a molecule is its aromaticity.[68] Although no general definition of aromaticity is available, a

commonly accepted description is in terms of π-electron delocalization in a ring, causing resonance stabilization.[69-71] Besides criteria such as structure of the ring (planarity, bond length), heat of formation of the compound and reactivity of ring substituents, the magnetic susceptibility, which is directly related to the electronic structure of a molecule, is valuable as a measure of aromaticity. In particular the increased value of one of the principal components of χ, χ_{zz}, in an aromatic compound relative to a nonaromatic reference (localized model) is of importance; χ_{xx} and χ_{yy} do not differ much in the aromatic and nonaromatic species.[72,73] The increase in χ_{zz}, and thus in $\Delta\chi$ or χ_{AV}, has been related to the resonance energy of the ring.[72,73] Thus comparison of the experimental susceptibility (or splitting for negligible $\delta\chi$-values) with that for a nonaromatic reference will provide information concerning aromaticity.

The method has been applied by Flygare *et al.*,[74,75] who used accurate microwave results to evaluate bond susceptibilities[76] for nonaromatic compounds. Using these it is possible to calculate the molecular susceptibility values χ_{ij} in the localized model: they are related to the bond susceptibilities (χ_{aa}, χ_{bb} and χ_{cc}) via the transformation formula

$$\chi_{ij}(\text{local}) = \sum_n \left[l_{ia}^n l_{ja}^n \chi_{aa}^n + l_{ib}^n l_{jb}^n \chi_{bb}^n + l_{ic}^n l_{jc}^n \chi_{cc}^n \right] \tag{37}$$

in which a summation is made over all n bonds in the molecule; l_{ia}^n is the direction cosine between the molecular i-axis and the local a-axis of bond n. The susceptibility frame can be found from a diagonalization procedure. The method has been shown to be valid for a large series of nonaromatic compounds[74,75] and is expected to hold for any localized model.

For small polar molecules, microwave spectroscopy can be used to determine $\Delta\chi$, but for larger species of interest, for example cyclophanes (Fig. 8) or other strained compounds, the microwave spectra are too complex. In these cases high-field NMR offers a convenient alternative. As an example [5]-metacyclophane (Fig. 8; $n = 5$) and some compounds that are certainly aromatic have been investigated.[77] In Table 3 the experimental quadrupolar splitting is compared with that calculated for the nonaromatic reference, and
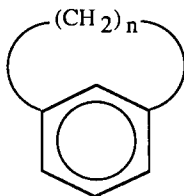
FIG. 8. Structural formula of [n]-metacyclophane (n is an integer).

TABLE 3

Comparison of experimental quadrupolar splittings (*para* deuteron, in Hz) with those calculated for a nonaromatic reference. Some probe species that are certainly aromatic as well as [5]-metacyclophane are given.[77]

Compound	Experiment	Reference
Benzene	0.48	0.21
m-Dimethylbenzene	0.51	0.26
m-Diethylbenzene	0.54	0.26
m-Diisopropylbenzene	0.64	0.27
[5]-Metacyclophane	0.63	0.11–0.21[a]

[a] Depending on structure used.[77]

the differences are unambiguous. The results and assumptions made are discussed in more detail in ref. 77. The experiments, together with available evidence concerning bond lengths, show beyond doubt that [5]-metacyclophane is aromatic.

C. Angular correlation in liquids

1. Introduction

As mentioned in Section IV.A, the magnetic susceptibility measured in the liquid phase is often an effective quantity. Molecular values can only be obtained from studies in inert phases (e.g. gas, low concentration of solute in an inert solvent). At higher concentrations angular correlation with neighbouring molecules may become important. This phenomenon is illustrated in Fig. 9, where the deuteron quadrupolar splitting of perdeuteriated nitrobenzene dissolved in diethylether is given as a function of the concentration.[27] For quantities like the magnetic susceptibility χ or the electric polarizability α the effect is normally represented by a Kirkwood g_2 factor,[78] which is the ratio of the observable in the pure liquid and in an inert environment.

As a consequence of the intermolecular interactions, the interpretation of the splittings becomes more complicated, the main problem being the orientation of the principal frame of the magnetic-susceptibility tensor.[27,28] For instance, if molecular complexes are formed the susceptibility frame of the cluster need not coincide with the molecular frame of a single solute molecule, and the electric field gradient values $V_{\alpha\alpha}$ of the complex must be available in order to calculate the effective susceptibilities. In general, however, only $(\Delta\chi)_{eff}$ values using the single-molecule geometry can be
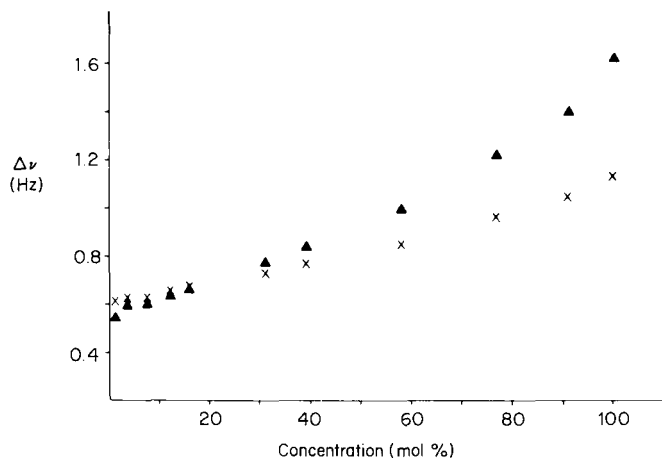
FIG. 9. Concentration dependence of Δv, for perdeuterated nitrobenzene: $\blacktriangle$, *para*; $\times$, average of *ortho* and *meta* splitting. (Reproduced, with permission, from ref. 27.)

obtained.[27,28] In evaluating these parameters, the above limitation should be kept in mind. If cluster formation appears, reliable information can be obtained from the concentration dependence of the observed line splittings, by fitting the curve to trial complex formation constants. The splitting measured will be a weighted average over all species (monomers, dimers, etc.) present; when rapid exchange of molecules between the clusters occurs, assuming a single complex formation constant for attachment of an additional molecule, it is given by

$$\Delta v_i = x^{(1)} \Delta v_i^{(1)} + x^{(2)} \Delta v_i^{(2)} + \cdots + x^{(n)} \Delta v_i^{(n)} \tag{38}$$

$$x^{(n)} = \frac{nC_{(n)}}{C_{(1)} + 2C_{(2)} + \cdots + nC_{(n)}} \tag{39}$$

with $C_{(n)}$ the concentration of *n*-mer and $x^{(n)}$ its mole fraction.[27] The presence of many complexes will make the g_2 values difficult to interpret.

A more detailed description of molecular correlation is possible by assuming that only the orientation of a solute molecule is influenced by its neighbours, but that the single-molecule geometry and principal axis system can still be applied to obtain $(\Delta \chi)_{\text{eff}}$. A directional Kirkwood factor $g_2(p)$ can be defined:[27,28]

$$g_2(p) = \frac{(S_{pp})_{\text{eff}}}{S_{pp}} = \frac{[\Delta \chi(p)]_{\text{eff}}}{\Delta \chi(p)} \tag{40a}$$

Here $g_2(p)$ gives the influence of correlation on $\Delta \chi(p) = \chi_{pp} - \frac{1}{2}(\chi_{qq} + \chi_{rr})$, with

(p, q, r) a permutation of the molecular axes (x, y, z). In addition to the $g_2(p)$'s, describing the influence on the order parameters S_{xx}, S_{yy}, S_{zz}, one can also define a g_2^{pp} describing the change of the effective susceptibility along one axis p:

$$g_2^{pp} = \frac{(\chi_{pp})_{\text{eff}}}{\chi_{pp}} \tag{40b}$$

Under the assumption of an unchanging principal susceptibility frame, (40a, b) can be applied to obtain six correlation factors instead of a single one when applying methods such as the Cotton–Mouton effect,[79-81] the Kerr effect,[80,81] depolarized Rayleigh scattering[82-84] and dielectric studies.[85] NMR alignment experiments using electric fields (EFNMR) could in principle also give more than one g_2 factor, but for dipolar molecules only $g_2(p)$, with p along the dipole-moment direction, is of importance.[6] Recently, the first polarizabilities of apolar aromatic molecules have been measured using EFNMR,[24] which will provide additional $g_2(p)$ factors. In evaluating the physical meaning of the $g_2(p)$ and g_2^{pp} factors the restrictions imposed in obtaining these parameters should not be forgotten.

The next question is how to compare the different $g_2(p)$ values with the g_2's obtained by other methods. For bulk observables (O) the measured quantity is an average of contributions in all directions; for molecules of C_{2v}, D_2 or higher symmetry one can deduce[28,86]

$$g_2 = \frac{(O)_{\text{eff}}}{O} = \frac{\sum_p g_2(p)O(p)}{\sum_p O(p)} \tag{41}$$

In our NMR experiments $O(p) \sim \Delta\chi(p)\,\Gamma_p$, in the Cotton–Mouton effect $O(p) \sim \Delta\chi(p)\,\Delta\alpha(p)$, and for Rayleigh scattering $O(p) \sim [\Delta\alpha^\lambda(p)]^2$. Here α denotes the optical polarizability and α^λ the polarizability for the frequency of the orienting light beam. The formula assumes the same principal frame for the polarizability α and the susceptibility χ and that $g_2(p)$ is a molecular parameter, which is necessary to avoid the definition of separate effective susceptibilities and polarizabilities. This assumption is in agreement with experiment.[87] Equation (41) can be applied to see if the experimental g_2's from the different methods are in agreement with those calculated from our $g_2(p)$'s. If so, this will support the assumptions made.

2. Substituted benzenes

Recently the NMR method has been applied to a group of substituted benzenes and to pyridine.[27,28] For all compounds $g_2(p)$ and g_2^{pp}, data have been obtained. The interpretation of the g_2^{pp} data is quite complex, and this

problem has not been completely solved. In obtaining the g_2^{pp}'s, a second main assumption has to be made. To calculate $(\chi_{pp})_{\text{eff}}$, it is necessary to know $\chi_{AV} = \frac{1}{3}\Sigma_p \chi_{pp}$; these values are only known for the pure liquids, and although there is theoretical support[32] that $(\chi_{AV})_{\text{eff}} = \chi_{AV}$, experimental evidence is not available to our knowledge. Therefore we shall concentrate on the $g_2(p)$ values; they are summarized in Table 4. To check the assumptions made, g_2

TABLE 4

Comparison of bulk g_2 values from Rayleigh scattering and the Cotton–Mouton effect with those calculated from the NMR $g_2(p)$ data.

| Compound | $g_2(x)$ | $g_2(y)$ | $g_2(z)$ | $g_2(\text{Rayleigh})^a$ | | $g_2(\text{C–M})^a$ | |
				Calc.[b]	Exper.	Calc.	Exper.
Nitrobenzene	3.00	1.46	2.17	2.63	$2.3^{c,d}$	2.46	3.2^g
					$2.77^{c,e}$		
					$3.0^{f,e}$		
Toluene	1.18	0.82	0.99	0.95	$1.05^{c,e}$	0.97	1.0^g
					$1.00^{f,e}$		
Fluorobenzene	1.15	0.91	1.03	1.03	$1.00^{c,e}$	1.03	
					$0.94^{f,e}$		
Chlorobenzene	1.21	0.99	1.09	1.13	$1.10^{c,e}$	1.11	
					$1.09^{f,e}$		
Bromobenzene	1.24	0.96	1.09	1.16	$1.10^{c,e}$	1.13	
					$0.89^{f,e}$		
Benzene	0.85	0.85	0.85	0.85	$0.95^{c,e}$	0.85	0.8^g
					$0.79^{f,e}$		

[a] Using $\Delta\alpha$ values from Le Fèvre[88] and taking $\alpha^\lambda = \alpha = \alpha^0$ (α^0 = static polarizability).
[b] Differ slightly from ref. 28, in that Le Fèvre's corrected values are used now.
[c] Ref. 82.
[d] From relaxation times.
[e] From line intensities.
[f] Ref. 84.
[g] Ref. 79.

values for Rayleigh scattering and the Cotton–Mouton effect have been calculated from our data using (41).[28,87] Their agreement with the measured quantities is within experimental error, supporting the approach described above.

For some compounds, (38) and (39) have been applied, substituting different complex formation models. This is discussed in detail in ref. 27. For benzene a fit could be obtained assuming a dimer model. The calculated parameters are $K^{(2)} = 0.13 \pm 0.051\,\text{mol}^{-1}$ (complex formation constant); $\Delta\nu^{(2)} = 0.30 \pm 0.05\,\text{Hz}$; $\Delta\chi^{(2)} = -0.63 \times 10^{-28}\,\text{emu}$ and $x^{(1)} = 0.62 \pm 0.06$ in

the pure liquid. These data correspond to an angle of 73.2° between two benzene rings in a dimer. In an X-ray study of the liquid,[89] three possible dimer geometries are reported: 90°, 41° and 64°. The value of 73.2° can be regarded as the average over the contributions of the three dimers.

Calculations assuming different complex-formation models for nitrobenzene and toluene are unsuccessful in fitting the experimental splittings.

3. Porphyrins

Biologically important molecules for which stacking phenomena are well known are DNA's and porphyrins. The latter are particularly suited for investigation by our NMR method, since they possess a large $\Delta\chi$, effective axial symmetry ($\delta\chi = 0$) and form dimers or polymers of simple geometry (planes stacked parallel). Using (38), one can calculate $\Delta\chi^{(2)} = (1 + x^{(2)})\Delta\chi^{(1)}$ for dimers (mole fraction $x^{(2)}$). As the splitting is proportional to $\Delta\chi$, NMR provides a simple way to study the stacking if the monomer value $\Delta\chi^{(1)}$ is known. At any concentration the amount of stacking can easily be calculated. This procedure has been demonstrated for a series of porphyrins.[11]

D. Deduction of molecular geometry

The formulae for the dipolar and quadrupolar line splittings (equations 31 and 32) indicate some possible applications of the NMR alignment technique. They contain the structure of the molecule as well as a nuclear coupling constant c_a [$-(\mu_a/4\pi)(\gamma_i\gamma_j h/2\pi^2 r_{ij}^3)$ or c^2qQ/h and η]. The latter quantity is discussed in the next subsection; here we shall focus on geometry.

If the order parameters S_{pp}, the nuclear coupling constant and the experimental line splittings are known, the position of a certain nucleus in a molecule can be calculated, and vice versa: the geometry can be used to calculate the alignment (S_{pp} values). However, in large molecules with many groups, the position of some nuclei can be used to determine S_{pp}'s, while the unknown location of some other nuclei can be calculated from these S_{pp} values. An extremely simple situation occurs for axially symmetric molecules, where the line splitting Δv_a ($\Delta v_a = \Delta v_D$ for the dipolar case and $\Delta v_a = \Delta v_Q$ for the quadrupolar case) is given by

$$\Delta v_a = c_a S_{zz} \Gamma_z^a \qquad (42)$$

with c_a the nuclear constant; $\Gamma_z = \frac{1}{2}(3\cos^2\theta_{zz''} - 1)$ (see equation 13). So in the ratio of the splittings of two nuclei in the same molecule the order parameter vanishes:

$$\frac{\Delta v_a}{\Delta v_b} = \frac{c_a\Gamma_z^a}{c_b\Gamma_z^b} \qquad (43)$$
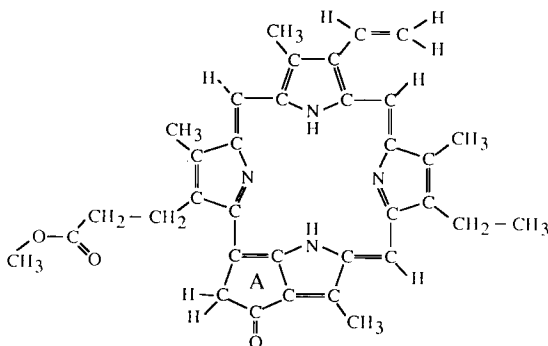
FIG. 10. Structural formula of vinylphylloerythrin methyl ester.

This procedure has been applied to the porphyrin in Fig. 10.[11] Here the CH_2 group in ring A and the geminal proton pair in the vinyl side chain both show a dipolar coupling $[c_a = -(\mu_0/4\pi)(\gamma_i\gamma_j h/2\pi r_{ij}^3)]$. The internuclear distances in both pairs as well as the orientation of the dipolar vector of the CH_2 group are well known. It can then be calculated that $\cos\theta_{zz''} = \pm 0.407$ for the geminal vinyl protons. This direction cosine is related to the dihedral angle α between the planes of the vinyl group and the porphyrin ring and the angle β between the internuclear axis and the rotational axis of the vinyl group through the expression

$$\cos\theta_{zz''} = \sin\alpha\cos\beta. \tag{44}$$

Normal geometry for a vinyl group gives $\beta \approx 31.5°$, yielding $51°$ for the average value of α. This result is obtained for the porphyrin–zinc complex in pyridine as well as for the free porphyrin in chloroform.[11] To our knowledge, no solution studies of the vinyl-group orientation have been made. X-ray diffraction data[90] give $\alpha = 15°$ for methyl pyropheophorbide and $\alpha = 31°$ for ethyl chlorophyllide, but in the solid the rotation may be restricted, as is suggested by the differing α values, and comparison with the liquid state is not warranted.

E. Quadrupole coupling constants

Arguments analogous to those used in the previous subsection for the geometry also hold for the nuclear constant c_a. For quadrupolar nuclei the situation is slightly more complex, since the asymmetry parameter η has to be accounted for in the geometrical part. Two situations can be distinguished. In the first, dipolar and quadrupolar splittings are combined to obtain the

quadrupolar coupling constant, or, if e^2qQ/h is known, some distance r between two dipolarly coupled nuclei. An illustration is given in Section IV.A, where measurements on ^{2}H, ^{13}C–^{1}H and ^{1}H–^{1}H couplings are reported for coronene, all producing the same value of $\Delta\chi$,[7,48] indicating the correctness of the c_a values used.

In the second situation, comparison is made of the same type of nuclear constant in two different phases or in different binding positions. An example, which has recently been published,[14] is that of comparison of the quadrupole coupling constants between the gas phase and the liquid phase. These first gas-phase alignment experiments in NMR were performed for fluorobenzene and benzene.[14] The results are summarized in Table 5. It is remarkable that

TABLE 5

Gas-phase quadrupole coupling constants, calculated from comparison of liquid-phase and gas-phase deuteron splittings (14.11 T; 296 K).[14]

Compound	Liquid		Gas	
	$\Delta\nu$ (Hz)	e^2qQ/h (kHz)	$\Delta\nu$ (Hz)	e^2qQ/h (kHz)
C_6H_5D	0.48 ± 0.02^a	$186 \pm 6^{b,c}$	0.62 ± 0.03^d	$240 \pm 20^{c,e}$
C_6D_5F				
ortho	0.50 ± 0.02^f	$186 \pm 6^{b,c}$	0.48 ± 0.05^d	179 ± 26^c
meta	0.50 ± 0.02^f	$186 \pm 6^{b,c}$	0.48 ± 0.05^d	179 ± 26^c
para	0.50 ± 0.02^f	$186 \pm 6^{b,c}$	0.68 ± 0.03^d	253 ± 21^c

[a] Ref. 27.
[b] Average literature value[59 62].
[c] $\eta = 0.05$.
[d] Ref. 14.
[e] Microwave data: 223 ± 12 kHz. Ref. 91.
[f] Ref. 28.

for the benzene deuteron and the *para* deuteron in fluorobenzene e^2qQ/h is about 30% larger in the gas phase than in the liquid, while the *ortho* and *meta* values remain virtually the same. For monodeuteriobenzene, recent microwave data[91] give $e^2qQ/h = 223 \pm 12$ kHz, which is the same, within experimental error, as that determined from NMR. The liquid-phase constant of 186 ± 6 kHz is also well established,[59-62] so the effect is expected to be reliable. The difference has been tentatively explained in terms of the reaction field of the solute molecules[14] at the site of the deuteron.

V. PARAMAGNETIC MOLECULES

A. Introduction

As can be seen from Table 1, alignment effects of paramagnetic compounds can easily be a factor of 100 larger than those of diamagnetic compounds. However, it was not until two years after the work of Lohman and MacLean[8,17] on diamagnetic species that Domaille[92] measured a deuterium splitting in a solution of the paramagnetic bis[phenyl-d_5-tris(1-pyrazolyl)borato]cobalt(II) system (Co(PTPB-d_5); Fig. 11). At 8.45 T the
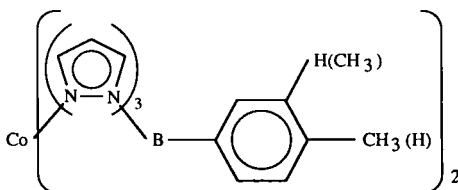
FIG. 11. Structural formula of bis[phenyl-d_5-tris(1-pyrazolyl)borato]cobalt(II): Co(PTPB-d_5).

quadrupolar splitting of the *para* deuteron is already 54.0 Hz, compared with 0.17 Hz calculated for benzene-d_1 at this field. For the *para*-CD_3 group it is 18.0 Hz ($\theta_{zz''} = 109.47°$). Shortly after these initial experiments, the first dipolar splittings[93] were measured for this compound: $\Delta\nu_D(^1H-^1H) = 16.0$ Hz at 17.106 T for the *para*-CH_3 group ($\theta_{zz''} = 90°$), in agreement with the quadrupolar effect.

Domaille *et al.*[92,93] also suggest a special application for paramagnetic systems; namely the evaluation of the dipolar (or pseudocontact) contribution to the paramagnetic isotropic shift. This is discussed in the next subsection. Of course, all applications mentioned for diamagnetic species in the preceding section will also be possible for paramagnetics, provided that the NMR line widths are sufficiently small, which may be a problem on account of slow electron-spin relaxation.

B. Evaluation of dipolar contribution to isotropic paramagnetic shifts

The pure isotropic paramagnetic shift δ can in principle be divided into three contributions:[94-96]

$$\delta = \delta_d + \delta_F + \delta_c \tag{45}$$

with δ_d the dipolar, δ_F the Fermi contact and δ_c the complex formation

contributions to the shift. The latter arises from environmental changes around a substrate molecule upon binding to a complex and can be determined from diamagnetic complexes. The separation of the first two terms in (45) is in general problematic.[94 96] However, the dipolar contribution originates from the anisotropic paramagnetic susceptibility, and our technique may be very useful in its determination. For a nucleus at a distance R from a magnetic point dipole, one can write the following expression for the dipolar shift:[94-96]

$$\delta_d = -\frac{1}{4\pi}\frac{2}{3R^3}\sum_p \chi_{pp}\Gamma_p^R \qquad (46)$$

which shows a strong resemblance to the formulae for the dipolar or quadrupolar coupling (Section II):

$$\Delta v_a = \frac{B^2}{10\mu_0 kT}c_a\sum_p \chi_{pp}\Gamma_p \qquad (47)$$

c_a is a constant describing the nuclear interaction (see also Section IV.D). Γ_p is defined in (13): $\Gamma_p^R = (\frac{3}{2}\cos^2\theta_{Rp} - \frac{1}{2})$, with R the vector from the paramagnetic centre of the molecule (point dipole) to the nucleus under consideration. Therefore a combination of (46) and (47) may give valuable information about the different shift contributions.

Before discussing the experiments, we first outline the conditions and assumptions that are necessary to obtain reliable results: (i) the point-dipole formula for δ_d is valid; (ii) the nuclear constants are known; (iii) there is a single stoichiometric species with a single average geometry; (iv) the distance R and sometimes the bond angles have to be available; (v) in most cases the orientation of the principal susceptibility frame has to be known; (vi) if condition (v) applies, there should be a sufficient number of nuclei to determine $\Delta\chi$ and $\delta\chi$.

The first assumption is correct if $R > 3.0\,\text{Å}$.[97,98] Therefore the nuclei studied should be taken as far from the paramagnetic centre as possible. Nuclear constants are well known (Section IV), and in the quadrupolar case e^2qQ/h and η, as measured from liquid-phase data on diamagnetic systems, can be assumed to be the same in the paramagnetic at large distances from the paramagnetic centre. The importance of the other requirements depends upon the system under investigation. A favourable situation arises if $\Gamma_p^R = \Gamma_p$, meaning that (46) and (47) can be combined directly to give

$$\delta_d = -\frac{\mu_0}{4\pi}\frac{20kT}{3c_a B^2 R^3}\Delta v_a \qquad (48)$$

so that only the averaged distance R need be known. If the geometrical factors are not equal all requirements mentioned are of importance.

In a pioneering study of a transition-metal complex, X-ray studies were performed to obtain bond angles and distances.[99] However, it appears not to be possible to obtain a good fit between all splitting data and the geometry. This is attributed to the existence of several isomers in solution, in rapid equilibrium with each other. No concentration-dependent measurements were made.[99]

In a recent investigation[100,101] of lanthanide shift reagents (Ln(dpm)$_3$; dpm = dipivalomethanato) in chloroform/pyridine solution the evaluation was more successful, although small discrepancies remain. In these solutions rapid exchange takes place between pyridine in solution and in the complex, and the resulting NMR spectrum (Fig. 12) is an average. Concentration-dependent measurements are performed in the concentration region where
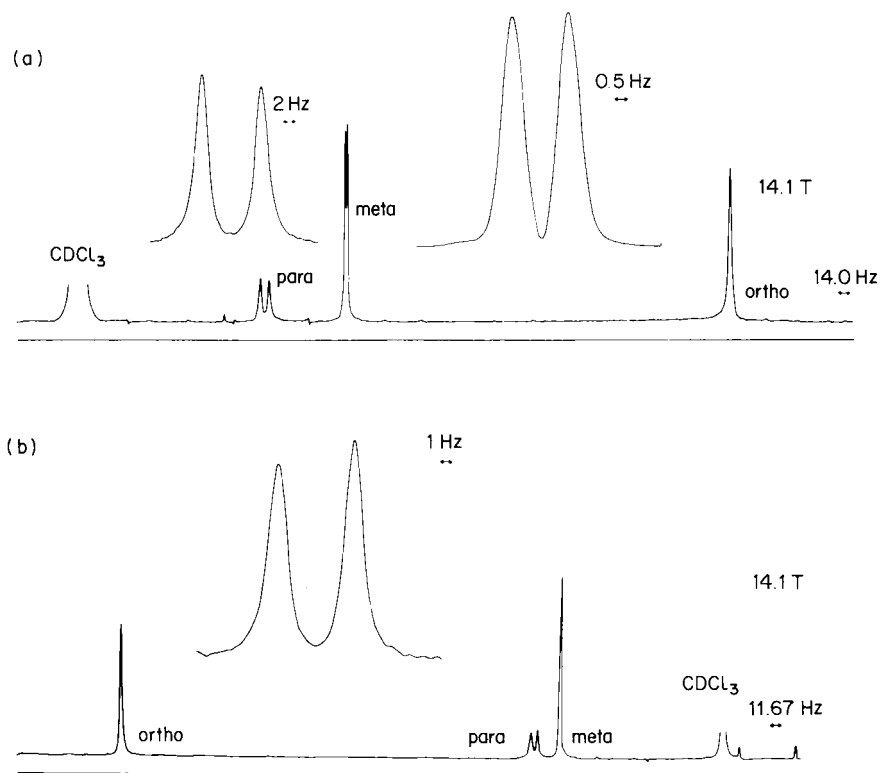
FIG. 12. Deuterium NMR spectra of pyridine-d$_5$ in a solution of Ln(dpm)$_3$(pyridine-d$_5$)$_2$ in pyridine-d$_5$/CDCl$_3$ for Ln = Pr (a) and Ln = Eu (b). The spectrum is an average of bound and free pyridine (rapid exchange), which is reflected in the unequal intensities of the resonances in the quadrupolar doublet.[101]

only 1:2 adducts are formed. Condition (i) also applies, since $R > 6.2$ Å for the *para* deuteron in complexed pyridine-d_5, and the lower limits for *meta* and *ortho* deuterons are 5.4 Å and 3.2 Å respectively. In a first approximation one can assume that the C—D bond (z''-axis) is parallel to R(Ln—D) for the *para* deuteron. It can also be calculated that for the *para* deuteron η ($= 0.05$) gives a negligible contribution for the geometry of the complex.[102,103] These two conditions are equivalent to $\Gamma_p^R = \Gamma_p$. The resulting δ_d's, obtained from the splittings (Fig. 13a), are compared with the experimental shifts (Fig. 13b) in Table 6. The δ and $\Delta v/B^2$ values are obtained from the slopes of the concentration curves. It is clear that the dipolar contribution is dominant. The small deviations can be discussed in terms of a small tilt angle for the pyridine moiety,[102,103] a somewhat different R value in the liquid as compared to the solid, or small deviation in e^2qQ. This has been done in refs. 100 and 101.

Other investigators[104,105] have applied the same method to obtain information about the geometry of palladium transition-metal complexes. However, the assumption of an axially symmetric susceptibility χ is made, which cannot be the case for the system under study. Therefore only qualitative information is obtained in this case.

TABLE 6

Comparison of δ_d, calculated from quadrupolar splittings Δv (see equation (48); assumption of parallel R and C–D bond), with experimental shifts δ for the *para* deuteron in Ln(dpm)$_3$(pyridine-d_5)$_2$ (298 K).[101]

Ln	Δv (Hz)^a	δ_d (ppm)^b	δ (ppm)^c	δ/δ_d
Pr	−28.19	7.715	7.929	1.028
Nd	−15.16	4.191	4.053	0.967
Eu^d	16.44	−4.258	−4.550	1.069
Tb	−143.3	40.58	44.64	1.100
Dy	−204.7	58.67	63.48	1.082
Ho	−97.4	28.46	30.19	1.061
Er	52.37	−15.12	−16.48	1.091
Yb	46.22	−13.63	−14.21	1.043

^{a}Magnetic induction of 14.106 T; including diamagnetic contribution.
^{b}Obtained after correction for Δv(complex formation $= 0.88$ Hz, from the diamagnetic Lu(dpm)$_3$(pyridine-d_5)$_2$.
^{c}After correction for δ(complex formation) $= -0.393$ ppm, from Lu(dpm)$_3$(pyridine-d_5)$_2$.
^{d}Low-lying excited state involved
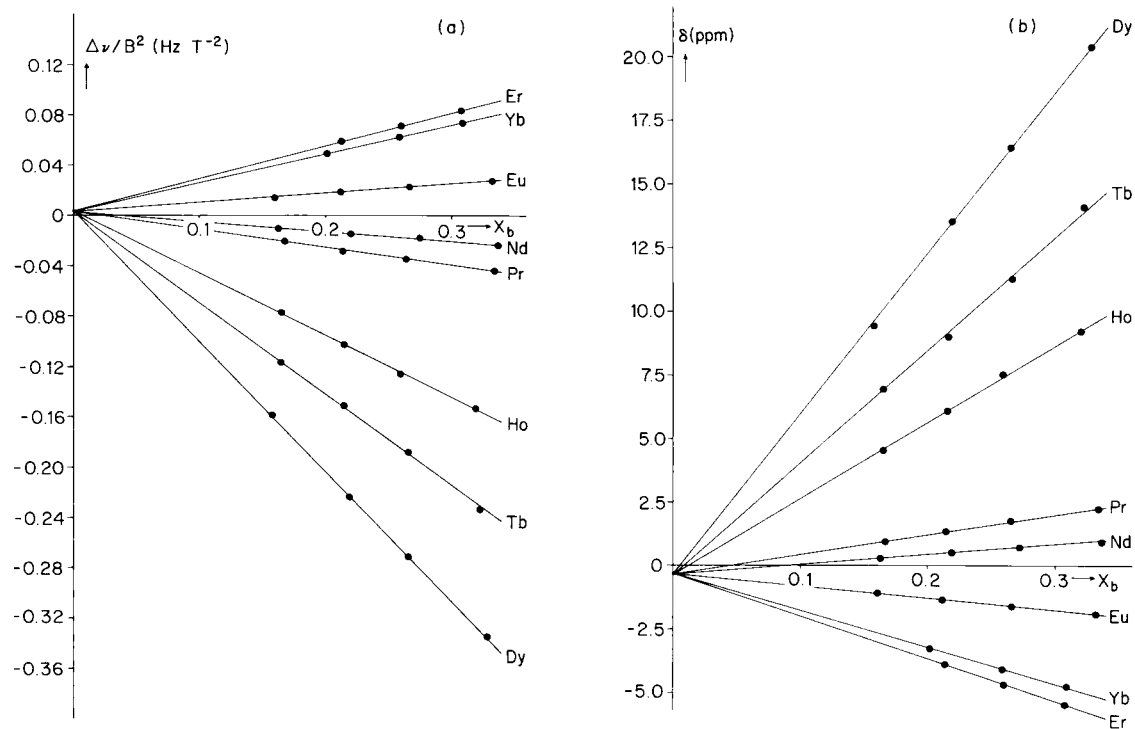
FIG. 13. Concentration dependence of $\Delta v/B^2$ and δ of the *para* deuteron in $Ln(dpm)_3(pyridine-d_5)_2$ for some different lanthanides.

VI. CONCLUSIONS

In the short time that it has been known (since 1978), the NMR analogue of the Cotton–Mouton effect has developed into an accurate and well-established method to study $\Delta\chi$, the anisotropy, and $\delta\chi$, the asymmetry, of the magnetic susceptibility (Sections IV.A,B), geometrical parameters (Section IV.D) and quadrupolar coupling constants (Section IV.E). This is mainly a consequence of the inherent simplicity of the method, which allows good accuracy to be obtained. Measurements have been performed in the liquid phase as well as in the gas phase. Possibilities for the investigation of angular-correlation effects in liquids have been discussed in Section IV.C. The evaluation of the dipolar contribution to the isotropic paramagnetic shift induced by lanthanide shift reagents (Section V.B) is another illustration of the possibilities of the technique. A further important application is the study of pretransitional alignment effects in liquid-crystal formers in the isotropic phase, extensively discussed in refs. 106 and 107.

Future research will partly be directed to both small and large molecules. The recent availability of accurate methods to determine small NMR line splittings,[57,58] as well as of the better resolution attainable on commercial spectrometers[108-110] will greatly facilitate studies on small molecules. For these compounds, comparison with the accurate microwave Zeeman technique, which is restricted to small polar gas-phase molecules, will be possible. A proposal has been filed to develop a 900 MHz (21.2 T) NMR spectrometer,[111] which will enlarge the range of molecules to be studied. Present investigations are focused upon the determination of shielding anisotropies and upon structure and stacking properties of biological systems like porphyrins and short DNA sequences. Extension of the method to other nuclei (^{14}N, ^{19}F) will be explored.

An important role for the NMR method also lies in linking it with other techniques such as the Cotton–Mouton effect, Kerr effect, electric-field NMR and Rayleigh scattering. The accuracy of Cotton–Mouton and Kerr measurements has recently been dramatically improved.[67,79,112] Determination of polarizabilities, hyperpolarizabilities and local field factors in the other methods will be possible if NMR results are available to eliminate the unknowns in the working equations. Previously the number of unknowns arising in combining the methods was still too large; in this respect the NMR magnetic-field alignment technique may be the missing link.

The experiments also imply a warning for NMR spectroscopists in the sense that they should be alert to the influence of these effects upon NMR spectra. Thus the dipolar coupling masquerades as an apparent field dependence of the scalar coupling.[48] Anisotropic shift contributions may begin to appear, especially if accuracies of 10 mHz are available.[113] Splitting

of the lock signal of deuteriated locking agents may well affect lock stability and shimming procedures at high fields.[54,55]

In summary, the relatively new NMR alignment method has already shown a wide range of applications, of interest for both chemists and physicists; its potential for future research seems very promising.

ACKNOWLEDGMENTS

APPENDIX

The values of the susceptibility anisotropies and asymmetries are of course dependent on the choice of the molecular axes. For the compounds studied the following axis definitions (right-handed frame: Fig. 1) have been used:
   (a) symmetry C_{3v} or higher: z along axis of highest symmetry; x, y does not make any difference (only one order parameter);
   (b) aromatics: z perpendicular to the aromatic plane;
       (i) C_{2v} symmetry: x along C_{2v} axis;
       (ii) D_{2h} symmetry: as in Fig. 3 for a substituted benzene, but then for n unsubstituted rings (n is an integer):
   (c) methylene halides: z along C_{2v} axis; y in the plane of the two halide atoms;
   (d) chrysene and biphenyl: as in ref. 7.
   It should be kept in mind that these definitions may differ from those in the original papers. In Table 7 the deuteron splittings in the compounds remeasured for this review are given. For the numbering of the nuclei the reader is referred to the original papers (given in the table) and to Fig. 14. The solvents are given in Table 2.

TABLE 7

Quadrupolar splittings and bond angle $\theta_{z''x}$ for the deuterons in the compounds remeasured at 14.57 T (296 K). All compounds are perdeuteriated.

Compound	Nucleus[a]	Ref.	$\theta_{z''x}$	Δv (Hz)
m-Dinitrobenzene	2	128	0°	0.76 ± 0.02
	5		0°	0.77 ± 0.02
	4, 6		60°	0.72 ± 0.02
Naphthalene	1	18	0°	1.04 ± 0.02
	2		60°	0.99 ± 0.02
Acenaphthene	3	20	60°	1.05 ± 0.02
	4		60°	1.05 ± 0.02
	5		0°	1.05 ± 0.02
Fluorene	1	64	18°	1.16 ± 0.02
	2		78°	1.15 ± 0.02
	3		138°	1.15 ± 0.02
	4		198°	1.17 ± 0.02
Phenanthrene	1	9	30°	1.50 ± 0.03
	2		90°	1.52 ± 0.03
	3		30°	1.48 ± 0.03
	4		30°	1.52 ± 0.03
	9		30°	1.52 ± 0.03
Pyrene (Fig. 2)	1	18	60°	2.03 ± 0.03
	3		60°	2.03 ± 0.03
	4		0°	1.95 ± 0.03
Triphenylene (Fig. 14)	1		—[b]	1.93 ± 0.03
	2		—[b]	1.91 ± 0.03
Chrysene (Fig. 2)	1	19	135°	1.95 ± 0.03
	2[c]		75°	(2.08)[c]
	3[c]		75°	(2.05)[c]
	4		15°	1.88 ± 0.03
	5		45°	1.88 ± 0.03
	6		105°	1.98 ± 0.03
Perylene (Fig. 14)	1		0°	1.70 ± 0.02
	2		60°	1.75 ± 0.02
	3		60°	1.75 ± 0.02

[a] Numbering of nuclei can be found in references given in next column (note: axes definition may differ here).

[b] Not of importance, only one order parameter.

[c] Overlapping, not used in the susceptibility calculation.
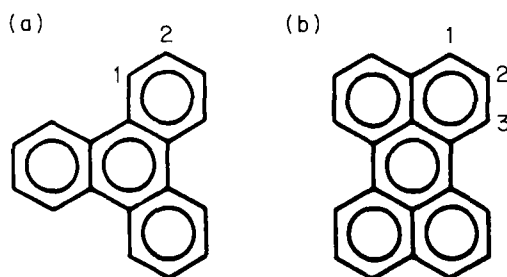
FIG. 14. Structural formulae and numbering of the nucleï for triphenylene (a) and perylene (b).

REFERENCES

1. A. Saupe and G. Englert, *Phys. Rev. Lett.*, 1963, **11**, 462.
2. J. W. Emsley and J. C. Lindon, *NMR Spectroscopy Using Liquid Crystal Solvents*, Pergamon Press, Oxford, 1975.
3. C. L. Khetrapal, A. C. Kunwar, A. G. Tracey and P. Diehl, in *NMR, Basic Principles and Progress*, Vol. 9, Springer, Berlin, 1975.
4. P. Diehl and W. Niederberger, in *Specialist Periodical Reports NMR*, Vol. 3, (P. Diehl, E. Fluck and R. Kosfeld, eds), Chem. Soc., 1974, p. 1.
5. C. W. Hilbers and C. MacLean, *Mol. Phys.*, 1969, **16**, 275.
6. C. W. Hilbers and C. MacLean, in *NMR, Basic Principles and Progress*, Vol. 7, (P. Diehl, E. Fluck and R. Kosfeld, eds), Springer, Berlin, 1972, p. 1.
7. P. C. M. van Zijl, B. H. Ruessink, J. Bulthuis and C. MacLean, *Acc. Chem. Res.*, 1984, **17**, 172.
8. J. A. B. Lohman and C. MacLean, *Chem. Phys.*, 1978, **35**, 269.
9. J. A. B. Lohman and C. MacLean, *Chem. Phys.*, 1979, **43**, 144.
10. P. Diehl, J. Jokisaari and G. Dombi, *Org. Magn. Reson.*, 1979, **12**, 438.
11. A. A. Bothner-By, C. Gayathri, P. C. M. van Zijl, C. MacLean, J. J. Lai and K. M. Smith, *Magn. Reson. Chem.*, 1985, **23**, 935.
12. M. J. Gerace and B. M. Fung, *J. Chem. Phys.*, 1970, **53**, 2984.
13. B. H. Ruessink, W. J. van der Meer and C. MacLean, *J. Am. Chem. Soc.*, 1986, **108**, 192.
14. P. C. M. van Zijl, C. MacLean, C. M. Skoglund and A. A. Bothner-By, *J. Magn. Reson.*, 1985, **65**, 316.
15. T. M. Plantenga, B. H. Ruessink and C. MacLean, *Chem. Phys.*, 1980, **48**, 359.
16. T. M. Plantenga and C. MacLean, *Chem. Phys. Lett.*, 1980, **75**, 294.
17. J. A. B. Lohman and C. MacLean, *Chem. Phys. Lett.*, 1978, **58**, 483.
18. J. A. B. Lohman and C. MacLean, *Chem. Phys. Lett.*, 1979, **65**, 617.
19. J. A. B. Lohman and C. MacLean, *Mol. Phys.*, 1979, **38**, 1255.
20. J. A. B. Lohman and C. MacLean, *J. Magn. Reson.*, 1981, **42**, 5.
21. J. Kerr, *Phil. Mag.*, 1875, **4**, 337.
22. A. Cotton and M. Mouton, *C. R. Acad. Sci. Paris*, 1905, **141**, 317.
23. E. E. Burnell and C. A. de Lange, *J. Chem. Phys.*, 1982, **76**, 3474.
24. B. H. Ruessink and C. MacLean, *J. Chem. Phys.*, 1986, **85**, 93.
25. J. G. Snijders, C. A. de Lange and E. E. Burnell, *Isr. J. Chem.*, 1983, **23**, 269.
26. (a) A. D. Buckingham and K. A. McLauchlan, *Proc. Chem. Soc.*, 1963, 144.

(b) R. E. J. Sears and E. L. Hahn, *J. Chem. Phys.*, 1966, **45**, 2753; *ibid.*, 1967, **47**, 348.

(c) J. D. Macomber, N. S. Ham and J. S. Waugh, *J. Chem. Phys.*, 1967, **46**, 2855.

27. P. C. M. van Zijl, C. MacLean and A. A. Bothner-By, *J. Chem. Phys.*, 1985, **83**, 4410.

28. P. C. M. van Zijl, C. MacLean and A. A. Bothner-By, *J. Chem. Phys.*, 1985, **83**, 4978.

29. B. R. Appleman and B. P. Dailey, in *Advances in Magnetic Resonance*, Vol. 7, Academic Press, New York, 1974, p. 231.

30. R. Ditchfield, in *International Review of Science: Physical Chemistry*, (A. D. Buckingham and G. Allen, eds), Butterworths, London, 1972, p. 91.

31. J. W. Beans, *Rev. Mod. Phys.*, 1932, **4**, 133.

32. W. H. Flygare, *Chem. Rev.*, 1974, **74**, 653.

33. K. Lonsdale and K. S. Krishnan, *Proc. R. Soc. Lond.*, 1936, **A156**, 597.

34. A. D. Buckingham and E. G. Lovering, *Trans. Faraday Soc.*, 1962, **58**, 2077.

35. M. W. P. Strandberg, *Phys. Rev.*, 1962, **127**, 1162.

36. A. M. Vasil'ev, *Zh. Eksp. Teor. Fiz.*, 1962, **43**, 1526 (Engl. transl.).

37. A. D. Buckingham and J. A. Pople, *Trans. Faraday Soc.*, 1963, **59**, 2421.

38. A. Saupe, *Z. Naturforsch.*, 1964, **19a**, 161.

39. L. C. Snyder, *J. Chem. Phys.*, 1965, **43**, 4041.

40. A. D. Buckingham and K. A. McLauchlan, in *Progress in NMR Spectroscopy*, (J. W. Emsley, J. Feeney and L. H. Sutcliffe, eds), Vol. 2, Pergamon Press, Oxford, 1967.

41. A. Saupe, *Angew Chem., Int. Ed. Engl.*, 1968, **7**, 107.

42. G. R. Luckhurst, *Q. Rev.*, 1968, **22**, 179.

43. S. Meiboom and L. C. Snyder, *Science*, 1968, **162**, 1337.

44. P. Diehl and C. L. Khetrapal, in *NMR, Basic Principles and Progress*, Vol. 1, (P. Diehl, E. Fluck and R. Kosfeld, eds), Springer, Berlin, 1969, p. 1.

45. A. Abragam, *The Principles of Nuclear Magnetism*, Clarendon Press, Oxford, 1985.

46. C. P. Slichter, *Principles of Magnetic Resonance*, 2nd edn., Springer, Berlin, 1980.

47. J. Lounila and J. Jokisaari, *Prog. NMR Spectrosc.*, 1982, **15**, 249.

48. C. Gayathri, A. A. Bothner-By, P. C. M. van Zijl and C. MacLean, *Chem. Phys. Lett.*, 1982, **87**, 192.

49. G. Arfken, *Mathematical Methods for Physicists*, 2nd edn., Academic Press, New York, 1970.

50. D. M. Brink and G. R. Satchler, *Angular Momentum*, Clarendon Press, Oxford, 1968.

51. J. H. van Vleck, *The Theory of Electric and Magnetic Susceptibilities*, Oxford University Press, Oxford, 1932.

52. H. Eyring, J. Walter and G. E. Kimball, *Quantum Chemistry*, Wiley, London, 1946.

53. A. A. Bothner-By, C. Gayathri, P. C. M. van Zijl and C. MacLean, *J. Magn. Reson.*, 1984, **56**, 456.

54. P. C. M. van Zijl, submitted to *J. Magn. Res.*

55. A. A. Bothner-By, J. Dadok, P. K. Mishra and P. C. M. van Zijl, *J. Am. Chem. Soc.*, in press.

56. P. R. Luyten, J. Bulthuis and C. MacLean, *Chem. Phys. Lett.*, 1982, **89**, 287.

57. J. Dadok and A. A. Bothner-By, *J. Magn. Reson.*, in press.

58. F. A. L. Anet, *J. Am. Chem. Soc.*, 1986, **108**, 1354.

59. A. Loewenstein, in *Advances in Nuclear Quadrupole Resonance*, Vol. 5, (J. A. S. Smith, ed.), Heyden, London, 1983, p. 53.

60. R. G. Barnes, in *Advances in Nuclear Quadrupole Resonance*, Vol. 1, (J. A. S. Smith, ed.), Heyden, London, 1974, p. 335.

61. M. Rinné and J. Depireux, in *Advances in Nuclear Quadrupole Resonance*, Vol. 1, (J. A. S. Smith, ed.), Heyden, London, 1974, p. 357.

62. J. P. Jacobsen and E. J. Pedersen, *J. Magn. Reson.*, 1981, **44**, 101.

63. A. C. Kunwar, H. S. Gutowsky and E. Oldfield, *J. Magn. Reson.*, 1985, **62**, 521.

64. P. C. M. van Zijl, N. H. Velthorst and C. MacLean, *Mol. Phys.*, 1983, **49**, 315.
65. P. C. M. van Zijl, G. B. M. Kostermans and C. MacLean, *J. Am. Chem. Soc.*, 1985, **107**, 2641.
66. P. C. M. van Zijl, C. MacLean and A. A. Bothner-By, in *Proc. 22nd Congress Ampère, Zürich* (K. A. Müller, R. Kind and J. Roos, eds), 1984, p. 578.
67. W. Hüttner, T. Köder and H. Müller, *Chem. Phys.*, to appear.
68. D. Lewis and D. Peters, *Facts and Theories of Aromaticity*, MacMillan Press, 1975, and references therein.
69. E. Hückel, *Z. Phys.* 1931, **70**, 204.
70. E. Hückel, *Z. Phys.*, 1931, **72**, 310.
71. E. Hückel, *Grundzüge der Theorie Ungesättigter und Aromatischer Verbindungen*, Verlag Chemie, Berlin, 1938, p. 71.
72. J. Aihara, *J. Am. Chem. Soc.*, 1979, **101**, 558.
73. J. Aihara, *J. Am. Chem. Soc.*, 1981, **103**, 5704.
74. D. H. Sutter and W. H. Flygare, *Top. Curr. Chem.* 1976, **63**, 89.
75. T. G. Schmaltz, C. L. Norris and W. H. Flygare, *J. Chem. Phys.*, 1973, **95**, 7961.
76. P. Pascal, *Chimie Generale,* Masson, Paris, 1949.
77. P. C. M. van Zijl, L. W. Jenneskens, E. W. Bastiaan, C. MacLean, W. H. de Wolf and F. Bickelhaupt, *J. Am. Chem. Soc.*, 1986, **108**, 1415.
78. J. G. Kirkwood, *J. Chem. Phys.*, 1939, **7**, 911.
79. U. Oesterle, S. Pferrer and W. Hüttner, *J. Mol. Struct.*, 1983, **97**, 165.
80. M. R. Battaglia, T. I. Cox and P. A. Madden, *Mol. Phys.*, 1979, **37**, 1413.
81. T. I. Cox, M. R. Battaglia and P. A. Madden, *Mol. Phys.*, 1979, **38**, 1539.
82. S. J. Bertucci, A. K. Burnham, G. R. Alms and W. H. Flygare, *J. Chem. Phys.*, 1977, **66**, 605.
83. H. Versmold, in *Organic Liquids* (A. D. Buckingham, E. Lippert and S. Bratos, eds), Wiley, New York, 1978.
84. C. Clement, *J. Chim. Physique*, 1978, **75**, 747.
85. C. J. F. Böttcher and P. Bordewijk, *Theory of Electric Polarization*, Vols. I, II, Elsevier, Amsterdam, 1978, and literature cited therein.
86. A. D. Buckingham, *Discuss. Faraday Soc.*, 1967, **43**, 205.
87. P. C. M. van Zijl, to be published.
88. R. J. W. Le Fèvre and B. P. Rao, *J. Chem. Soc.*, 1958, 1465.
89. A. H. Narten, *J. Chem. Phys.*, 1968, **48**, 1630.
90. H.-C. Chow, R. Serlin and C. E. Strouse, *J. Am. Chem. Soc.*, 1975, **97**, 7230.
91. M. Oldani, T.-K. Ha and A. Bauder, *Chem. Phys. Lett.*, 1985, **115**, 317.
92. P. J. Domaille, *J. Am. Chem. Soc.*, 1980, **102**, 5392.
93. A. A. Bothner-By, P. J. Domaille and C. Gayathri, *J. Am. Chem. Soc.*, 1981, **103**, 5602.
94. F. Inagaki and T. Miyazawa, *Prog. NMR Spectrosc.*, 1981, **14**, 67.
95. G. A. Webb, in *Annual Reports on NMR Spectroscopy*, Vol. 6B (E. F. Mooney, ed.), Academic Press, London, 1975, p. 1.
96. M. C. M. Gribnau, C. P. Keyzers and E. de Boer, *Magn. Reson. Rev.*, 1985, **10**, 161.
97. A. D. Buckingham and P. J. Stiles, *Mol. Phys.*, 1972, **24**, 99.
98. R. M. Golding and L. C. Stubbs, *J. Magn. Reson.*, 1980, **40**, 115.
99. P. J. Domaille, R. L. Harlow, S. D. Ittel and W. G. Peet, *Inorg. Chem.*, 1983, **22**, 3944.
100. P. C. M. van Zijl, R. P. van Wezel, C. MacLean and A. A. Bothner-By, *J. Phys. Chem.*, 1985, **89**, 204.
101. E. W. Bastiaan, C. MacLean, P. C. M. van Zijl and A. A. Bothner-By, to be published.
102. W. D. Horrocks, J. P. Sipe, and J. R. Luken, *J. Am. Chem. Soc.*, 1971, **93**, 5258.
103. R. E. Cramer and K. Seff, *Acta Crystallogr.*, 1972, **B28**, 3381.
104. J. W. Faller, C. Blankenship and S. Sena, *J. Am. Chem. Soc.*, 1984, **106**, 793.
105. J. W. Faller, C. Blankenship, B. Whitmore and S. Sena, *Inorg. Chem.*, 1985, **24**, 4483.

106. G. S. Attard, P. A. Beckmann, J. W. Emsley, G. R. Luckhurst and D. L. Turner, *Mol. Phys.*, 1982, **45**, 1125.
107. G. S. Attard, J. W. Emsley and G. R. Luckhurst, *Mol. Phys.*, 1983, **48**, 639.
108. A. Allerhand, R. E. Addleman and D. Osman, *J. Am. Chem. Soc.*, 1985, **107**, 5809.
109. A. Allerhand, R. E. Addleman, D. Osman and M. Dohrenwend, *J. Magn. Reson.*, 1985, **65**, 361.
110. S. R. Marple and A. Allerhand, *J. Magn. Reson.*, 1986, **66**, 108.
111. J. Dadok and A. A. Bothner-By, Private communication.
112. M. R. Battaglia and G. L. D. Ritchie, *J. Chem. Soc., Perkin Trans. II*, 1977, 901.
113. E. W. Bastiaan, J. Bulthuis and C. MacLean, *Magn. Reson. Chem.*, 1986, **24**, 723.
114. J. H. S. Wang and W. H. Flygare, *J. Chem. Phys.*, 1970, **52**, 5636.
115. M. R. Battaglia and G. L. D. Ritchie, *J. Chem. Soc., Faraday Trans. II*, 1977, **73**, 209.
116. D. Sutter, *Z. Naturforsch.*, 1971, **26a**, 1644.
117. H. Geschka, S. Pferrer, H. Häussler and W. Hüttner, *Ber. Bunsenges. Phys. Chem.*, 1982, **86**, 790.
118. J. Hoarau, N. Lumbroso and A. Pacault, *C. R. Acad. Sci. Paris*, 1956, **242**, 1702.
119. W. Hüttner and W. H. Flygare, *J. Chem. Phys.*, 1969, **50**, 2863.
120. C. L. Cheng, D. S. N. Murthy and G. L. D. Ritchie, *Mol. Phys.*, 1971, **22**, 1137.
121. R. J. W. Le Fèvre and D. S. N. Murthy, *Austr. J. Chem.*, 1966, **19**, 179.
122. R. J. W. Le Fèvre, P. H. Williams and J. M. Eckert, *Austr. J. Chem.*, 1965, **18**, 1131.
123. A. Lasheen, *Acta Crystallogr.*, 1968, **A24**, 289.
124. C. Gayathri and A. A. Bothner-By, Unpublished results (see ref. 7).
125. A. A. Bothner-By and J. A. Pople, *Ann. Rev. Phys. Chem.*, 1965, **16**, 43.
126. R. J. W. Le Fèvre and D. S. N. Murthy, *Austr. J. Chem.*, 1969, **22**, 1415.
127. R. Havemann, W. Haberditzl and P. Grzegorzewski, *Z. Phys. Chem. (Leipzig)*, 1961, **217**, 91.
128. T. M. Plantenga, H. Bulsink, C. MacLean and J. A. B. Lohman, *Chem. Phys.*, 1981, **61**, 271.

This Page Intentionally Left Blank

Dynamic NMR Spectroscopy in Inorganic and Organometallic Chemistry

K. G. ORRELL AND V. ŠIK

Department of Chemistry, The University, Exeter EX4 4QD, UK

I. INTRODUCTION

The primary aims of this review are to survey the recent developments in dynamic NMR (DNMR) techniques and to describe their applications to inorganic and organometallic chemistry. Literature coverage has been based on issues of *Chemical Abstracts* for the period January 1981–December 1985, and thus the review serves as an update of the article by Mann[1] in Volume 12 of these *Annual Reports*. The present review emphasizes the challenges presented to NMR spectroscopists by the diverse and often complex stereodynamical rearrangements displayed by many inorganic and organometallic compounds. No attempt at an exhaustive literature coverage is made. Papers are chosen where they describe either (i) an important development of DNMR theory, or (ii) an important advance in DNMR bandshape, relaxation time or magnetization transfer technique, or (iii) new and accurate rate constant/energy barrier data, or (iv) new and novel dynamic processes. Purely qualitative studies of established types of molecular rearrangements are excluded. Emphasis is given to intramolecular

rearrangements. Certain types of ligand exchange processes are covered, but solvent-exchange kinetics are excluded.

The five-year period of this review has seen some dramatic developments in NMR techniques, a number of which have important consequences for dynamic studies. The increasing use of multinuclear DNMR together with the techniques of spin-polarization transfer and, particularly, two-dimensional exchange spectroscopy, have made NMR measurements sensitive to slower-rate processes than hitherto and more able to distinguish between alternative mechanistic pathways. Section II of this article describes these developments in some detail, while the wide range of applications to inorganic structural chemistry is the subject of Section III.

II. DEVELOPMENTS IN DNMR TECHNIQUES

A. Exchange theory and total bandshape analysis

Two important works of general interest to dynamic NMR spectroscopists appeared during the period covered. First, a monograph by Kaplan and Fraenkel[2] gives a unified density matrix formalism for calculating NMR lineshapes for many kinds of exchanging systems. The theory is illustrated for a variety of conditions (e.g. high r.f. power and double resonance), and is applicable to both liquids and liquid crystals. Starting from the classical Bloch equations, derivation of the total density-matrix equation and its reduction to that of the spin density-matrix equation is given. Relaxation and exchange operators are then introduced and the resulting theory applied to typical exchanging spin systems.

Secondly, a book by Sandström[3] dealing with the methodology and chemical applications of dynamic NMR has appeared. This provides a very readable introduction to DNMR and well illustrates its range of applications to organic molecules, mainly using protons as nuclear probes. In addition, a review[4] by Lambert covers the areas of software development for complex spin systems, multinuclear DNMR, kinetics derived from relaxation-time data, and dynamic processes in the solid state.

Schotland and Leigh[5] have presented exact solutions of the Bloch equations with n-site chemical exchange with initial data corresponding to arbitrary tip angles of the z-component of the magnetization.[5] A multisite exchange treatment of solid-state NMR powder lineshapes has been developed[6] in cases where motional processes of more than one type occur simultaneously. The method is illustrated for the case of bisphenol-A polycarbonate, where one type of motion involves rotational diffusion, libration or oscillation over a limited range, whereas the other includes jumps of larger amplitudes between potential minima.

Two authors have returned to the problem of 2-site exchange. Kuespert[7] has developed a new formulation of the NMR lineshape with exact evaluations of parameters for the paripartite uncoupled $A \rightleftharpoons B$ system. By rearranging the Gutowsky–Holm NMR lineshape equation he has derived several new parameters of the lineshape useful for direct evaluation of the rate constant without recourse to iterative or trial-and-error simulations. The problem of energetically strongly asymmetrical two-site systems without coupling was discussed by Laatikainen.[8] This author also used the Gutowsky–Holm equation as his starting point and developed a new iterative program, DNMRS, for calculating activation-energy parameters. The program takes as input data a set of simultaneously given digitized spectra measured for up to 20 temperatures or different magnetic-field strengths. The procedure is especially useful in cases when the signal of the energetically less favoured site is not observed. Another computer program, LESHI, for evaluating rate constants of systems with up to three uncoupled exchange sites has been described.[9] The program, which uses a least-squares algorithm and classical lineshape functions in preference to a density-matrix treatment, includes phase angle as a parameter and allows for different line widths at different sites. The same authors find an interesting method of estimation of natural line widths in exchange-broadened spectra.[10] The method is based on measurements of T_1, which in many cases are inversely proportional to correlation time τ_c. Since τ_c is normally proportional to η/T (viscosity/absolute temperature), it follows that T_1 is proportional to T/η. Because the spin–spin and spin–lattice relaxation rates are proportional, plots of $\ln T_2$ and $\ln T_1$ against $1/T$ should be parallel, making it possible to extrapolate for T_2, which is especially useful for viscosity-broadened spectra.

NMR lineshapes of $I = \frac{5}{2}$ and $I = \frac{7}{2}$ nuclei were investigated,[11] assuming quadrupole relaxation and nonextreme narrowing conditions. Such quadrupolar nuclei can exhibit so-called dynamic frequency shifts arising from the fact that, for example, the $-\frac{1}{2} \rightarrow \frac{1}{2}$ transition does not necessarily have the same frequency and line widths as $\frac{1}{2} \rightarrow \frac{3}{2}$ and $-\frac{3}{2} \rightarrow -\frac{1}{2}$ transitions. This leads to deviation of lineshapes from Lorentzian form. The authors discuss chemical exchange effects contributing to transverse relaxation and find the behaviour of half-height widths $\Delta v_{1/2}$ rather complex. For instance, the temperature dependence of $\Delta v_{1/2}$ does not follow that expected for a $I = \frac{1}{2}$ nucleus exchanging between two sites and can be virtually constant over a very wide range of temperatures. Kaplan and Garroway[12] have drawn attention to the difference in exchange lineshapes for homogeneous and inhomogeneous distributions of correlation times. Whenever observed relaxation cannot be described by a single correlation time, it is important to distinguish between these two cases. Computer simulation for 2-site exchange shows that in the case of an inhomogeneous distribution, as the temperature

is raised, a central narrow peak begins to grow into the resonance in addition to the two broad "shoulders" on the sides. There is therefore no true coalescence point. For the homogeneous distribution the coalescence point occurs at a higher temperature.

The use of molecular symmetry in the theory of dynamic NMR spectra has been discussed extensively by Szymanski.[13] Taking the example of intra-molecular rearrangements in octahedral transition-metal complexes, the author demonstrates how the lineshape calculations can be simplified by taking advantage of symmetry invariances.

Total bandshape analysis continues to attract considerable attention both from theoretical and experimental points of view. However, considerable caution has to be exercised when $\Delta H^{\neq}$ and $\Delta S^{\neq}$ values are derived from bandshape analysis alone, unless performed over a wide range of temperatures.[14] Martin et al.[14] have re-examined carbamates and thiocarbamates exhaustively using different spectrometers, multinuclear experiments, bandshape fitting procedures, and saturation transfer experiments. They find $\Delta S^{\neq}$ for C–N bond rotation to be nearly zero, in contrast with earlier reports.

B. Spin–lattice relaxation-time measurements

Spin–lattice relaxation studies can yield useful information about rapid molecular motions on a time scale that is far shorter than is associated with bandshape analysis. The usual method is to measure T_1 by the inversion-recovery technique as a function of temperature. Semilogarithmic plots of T_1 versus reciprocal temperature then yield activation energies for internal motions as well as overall molecular reorientation. Aksnes and Ramstad[15] have measured ^{13}C relaxation times in substituted 1,3,2-dioxarsolanes (1) and were able to interpret the data in terms of isotropic overall molecular reorientation, internal rotation about the As–Ph bond and internal methyl rotation.
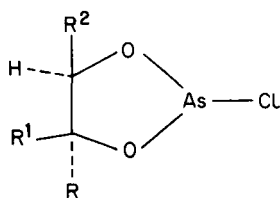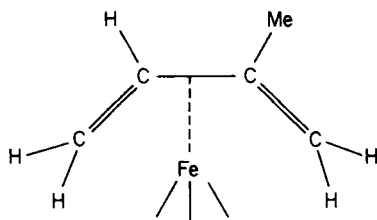
(1) (2)

In metallocarbonyls ^{13}C studies sometimes fail because of rapid relaxation of ^{13}C induced by quadrupolar metal nuclei. Aime et al.[16] have used ^{17}O as well

as ^{13}C NMR to study rotational correlation times of a number of organometallic carbonyl complexes with Fe(2), Fe$_2$, Os$_3$, Co$_2$ and FeCo centres. ^{17}O has relatively short relaxation times (~ 10 ms), so that rapid pulsing can be used to obtain good-quality spectra quickly even at the low natural abundance (0.037%). Lines are quite narrow and well resolved. T_1 values are dominated by an electric quadrupolar mechanism and are easier to interpret in principle than ^{13}C T_1 values. Activation energies of cyclopentadienyl group rotation and molecular tumbling in ferrocene derivatives have been determined using ^{13}C T_1 and NOE enhancement measurements.[17] The latter quantities were used to calculate the dipole–dipole component of T_1, which is a function of correlation time τ_c. Measurements of temperature dependence of τ_c then yielded Arrhenius and Eyring activation-energy parameters.

Proton T_1 measurements have been used[18] to determine the barriers to rotation of the cyclopentadienyl ring in titanium(IV) and molybdenum(I) complexes. In one case two T_1 processes were observed with barriers of 8.9 and 7.7 kJ mol^{-1}, corresponding to two Cp rings rotating at different rates owing to different hindering potentials.

^{199}Hg spin–lattice relaxation times have been measured in diphenylmercury.[19] At high fields the chemical-shielding anisotropy (CSA) mechanism was shown to be important for ^{199}Hg. The activation energy for rotational motion was calculated to be 13.3 kJ mol^{-1} from variable-temperature ^{13}C T_1 experiments. Correlation times for internal rotation around a Pt–N bond and for the overall molecular tumbling in N(n-C$_4$H$_9$)$_4$[PtCl$_3$.py] were determined via ^{13}C T_1 measurements.[20] In these tetracoordinated Pt(II) complexes with pyridine ligands all protonated carbons are relaxed by the dipole–dipole mechanism, DD. The authors also measured ^{195}Pt spin–lattice relaxation times, but the results seem to imply a predominant spin–rotation mechanism, which is inconsistent with other results,[21] which show that ^{195}Pt is predominantly relaxed via CSA at high field strengths.

C. Spin–spin relaxation-time measurements

In principle, it is possible to extract kinetic information from spin-echo NMR experiments. Frahm[22] proposed combining the classic Hahn-echo or Carr–Purcell–Meiboom–Gill (CPMG) pulse sequences with subsequent Fourier transformation of resulting echoes. The introduction of a variable pulse spacing modifies the decaying spectral peak amplitudes in such a way that kinetic data are obtained. The method has been applied to intramolecular exchange in N,N-dimethylbenzamide and can be used for the whole dynamic range from slow to fast exchange. These multipulse experiments are especially suited for thermally unstable samples, since no temper-

ature variations are needed for the evaluation of kinetic parameters. The time evolution of the transverse magnetization in the CPMG sequence in the presence of fast exchange has been treated theoretically.[23] The exchange process is described by a fluctuating Hamiltonian and perturbation theory applied to the equation of motion of the density matrix. A method for determining the rates and types of rotational molecular motions in solids has been proposed.[24] The narrowing of lines due to both random motions (motions of individual molecules) and coherent motions (overall motions of the sample or of the spins) has been discussed. Motional parameters of hexamethylbenzene, hexamethylethane and adamantane have been studied via T_2 measurements of ^{13}C nuclei dipolar-coupled to ^1H under conditions of proton decoupling.

Kaplan and Vasavada[25] have described a procedure for calculating the lineshape of a cluster of isochronous spins embedded in a molecule that is rotating with free or restricted motion. This is useful in the cases of complex motions that cannot be defined unambiguously in terms of an autocorrelation function and/or where some mixture of correlation times would lead to a non-Lorentzian lineshape. More recently[26] the authors extended this procedure to the case of two spins with different chemical shifts interacting via a dipolar coupling and have given expressions for T_2 in systems with and without exchange. They show that for two spins (I and S) with similar half-widths $(T_2^I)^{-1} \approx (T_2^S)^{-1}$ the exchange-collapsed doublet has a half-width $(T_2^I)^{-1} + (T_2^{IS})^{-1}$, where T_2^{IS} is a cross-relaxation-type term. This is contrary to the previously held view that the exchange-collapsed width is equal to that of the nonexchanging pair.

D. Magnetization-transfer experiments

1. Liquids

Magnetization-transfer techniques, such as selective saturation or selective inversion, are extremely useful methods for measuring chemical-exchange rate constants of comparable magnitude to spin–lattice relaxation rates of exchanging spins. The methods have been successfully applied to a number of systems and nuclei. ^{13}C is the obvious candidate for carbonyl scrambling studies, as exemplified on $Ir_4(CO)_{11}PEt_3$ using the DANTE pulse sequence to generate selective $180°$ pulses.[27] Another, similar, example is the study by Hawkes et al.[28] of the ^{13}C-enriched osmium cluster $[Os_3(\mu\text{-}H)_2(CO)_{10}]$ (3), which establishes the existence of localized ^{13}C exchange, involving only 2 of the 4 types of carbonyl ligand, namely ^6CO and ^7CO. A study[29] of the fluxionality of $[Fe(\eta^4\text{-}C_8H_8)(CO)_2(CNCHMe_2)]$ (4) was able to confirm a specific exchange mechanism consistent with the Woodward–Hoffmann

(3)

(4)
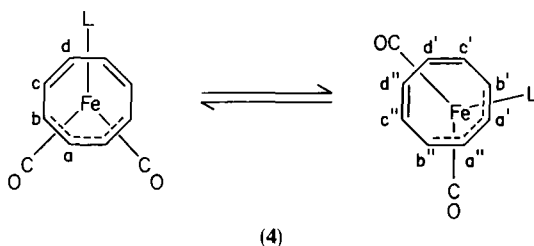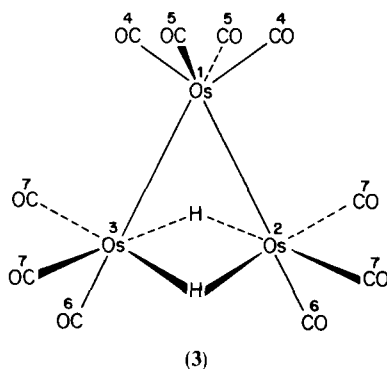
rules and eliminate alternative mechanisms. Compounds with a cyclo-heptatrienyl ring bonded in monohapto fashion to ruthenium, namely (η^5-C_5H_5)Ru(CO)$_2$(7-η'-C_7H_7) were the subjects of an investigation[30] leading to the claim of two concurrent fluxional pathways, 1,2 and 1,4 migration. Olefin insertion into the rhodium–hydrogen bond[31] and into niobium–hydride bonds[32] has been studied using magnetization-transfer techniques, taking advantage of the fact that these techniques enable measurements of slow rates of exchange at low temperatures, thus avoiding the problems of irreversible decomposition at higher temperatures. In addition to common ^{1}H, ^{13}C and ^{31}P nuclei, selective inversion of ^{119}Sn has been used[33] for determining the rate of *cis/trans* isomerization of octahedral SnCl$_4$.2Me$_2$S.

Such determinations are relatively simple for a two-site exchange case, but complications arise when multisite exchanges are involved, because the method ultimately requires solutions to several rate equations and involves the knowledge of several relaxation rates and resonance intensities during saturation of the exchange partner(s). However, recent work[34] has shown that a multisite exchange problem can be reduced to a 2-site exchange. For example, in the system $A \underset{}{\overset{k_1}{\rightleftharpoons}} B \underset{}{\overset{k_2}{\rightleftharpoons}} C$ if C-nuclei are continuously saturated, then the interconversion of A and B spins is essentially reduced to 2-site exchange. Similarly, in the exchange scheme $D \rightleftharpoons A \rightleftharpoons B \rightleftharpoons C$, k_{AB} can be determined essentially as a 2-site exchange provided that both C and D are

continuously saturated. The method is referred to as MST (multiple satur-
ation transfer). Another interesting development is magnetization transfer in
the rotating frame,[35] which is a combination of the magnetization transfer
and the $T_{1\rho}$ method. The experiments are carried out in the rotating frame in
the presence of a nonselective spin-locking field B_1. The method is especially
advantageous in cases when it is difficult to perform the usual magnetization-
transfer experiments, as, for example, in high-resolution solid-state NMR.

2. Solids

Variable-temperature   cross-polarization   magic-angle-spinning   NMR
(VT–CPMAS) has been shown to have considerable potential for elucidating
structure and dynamics in the solid state. Recent reviews[36,37] have included
discussion of a variety of motional effects and chemical exchange in the solid
state. The value of CPMAS experiments to inorganic structural chemistry
was exemplified by cases of tautomerism, polymorphism and hindered
intramolecular motion.[38] Many of the solid-state ^{13}C NMR experiments
centre on the lineshape analysis, because lineshapes are very sensitive to the
microscopic details of molecular reorientation. A good example of such work
is the study of the ring reorientation in permethylferrocene.[39] The CPMAS
analogue of two-dimensional exchange spectroscopy was suggested by
Szeverenyi et al.,[40] who replaced the initial 90° pulse in the standard 2D
experiment by a cross-polarization sequence and demonstrated the technique
on tropolone, alanine, p-dimethoxybenzene and hexamethylbenzene. An
interesting VT–CPMAS experiment on solid dicobalt octacarbonyl has been
reported.[41] At room temperature the ^{13}C spectrum consists of a single
resonance due to a rapid bridge–terminal carbonyl exchange. On lowering
the temperature, the signal first broadens and then splits into a complex
pattern of spinning sidebands. However, application of the TOSS[42,43] (total
suppression of sidebands) pulse sequence reveals the presence of two separate
carbonyl peaks as expected for the complex containing two bridging and six
terminal carbonyls.

E. Two-dimensional experiments

1. Usual 2D exchange methods

Although the idea of two-dimensional Fourier transformation of an NMR
signal obtained as a function of two time variables has been known since
1971, it was not until 1979 that the method, using the basic Jeener[44] pulse
sequence (Fig. 1) was applied to the area of molecular dynamics. The basic
three-pulse experiment is repeated n times (where n depends on the required
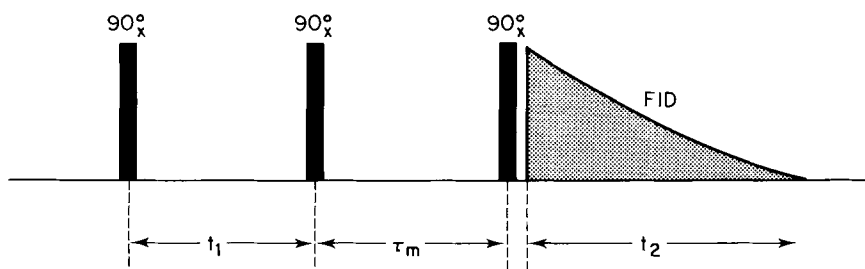
FIG. 1. Pulse sequence for two-dimensional NOESY or EXSY experiments.

resolution) for n different values of t_1 increasing systematically from near zero by an increment Δt_1, whose length depends on the required spectral width. This produces n FIDs, which are first Fourier transformed with respect to the acquisition time t_2, and then with respect to the other time variable, the evolution time t_1. The resulting two-dimensional spectrum contains peaks along the diagonal, which resemble a one-dimensional spectrum, but with changed peak intensities, and depend on exchange rates, relaxation times and mixing time. It also contains off-diagonal or cross-peaks between those diagonal peaks, which are "coupled" by exchange. An illustrative example of such a spectrum is the ^{195}Pt 2D spectrum of the complex [PtIMe$_3$(MeSCH$_2$CH$_2$SMe)][45] shown in Fig. 2. This compound exists at low temperatures as a mixture of three distinct species *meso*-1, *dl* and *meso*-2 (5), which undergo slow exchange due to pyramidal inversion of either sulphur atom:

meso-1   *dl*   *meso*-2

(5)
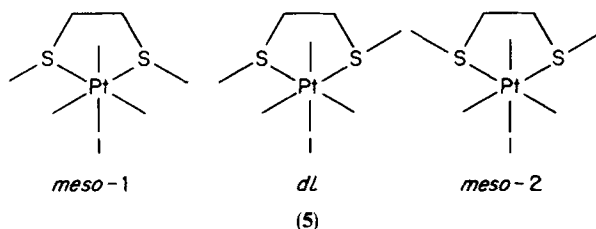
The three strong peaks on the diagonal correspond to these invertomers. The spectrum indicates the presence of direct exchanges $(meso\text{-}1) \overset{k_1}{\rightleftharpoons} (dl)$ and $(dl) \overset{k_2}{\rightleftharpoons} (meso\text{-}2)$. There are also weaker second-order peaks $(meso\text{-}1) \overset{k_3}{\rightleftharpoons} (meso\text{-}2)$, despite the absence of direct exchange between these two invertomers. The peak intensities are a complex function of spin–lattice relaxation rates, rate constants, and mixing time. Macura and Ernst[46] have derived explicit expressions for the intensities in the case of a 2-site spin system coupled by cross-relaxation. More generally, for a multisite exchange problem, the peak
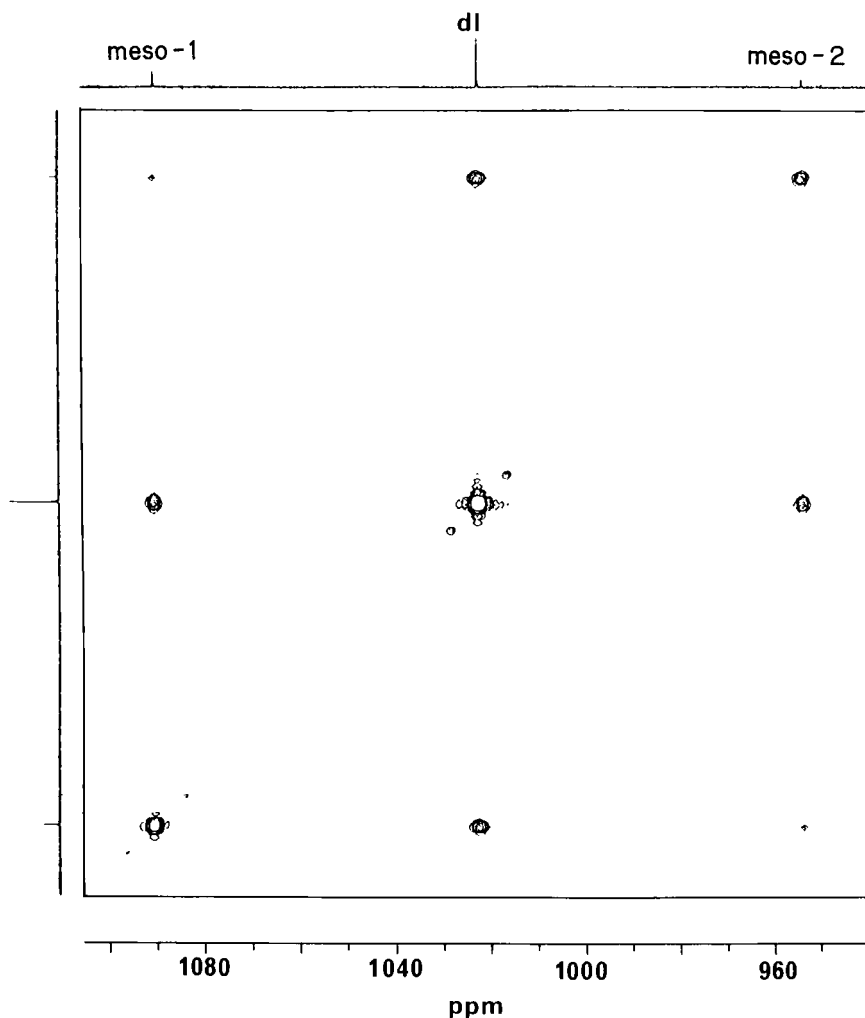
FIG. 2. ^{195}Pt 2D–EXSY spectrum of [PtIMe$_3$(MeSCH$_2$CH$_2$SMe)] at 253 K with mixing time $\tau_m = 0.3$ s. 1D spectra shown along the left-hand and upper edges of contour plot.

intensity for nuclei in sites i and j is given by the matrix equation

$$I_{ij}(\tau_m) = (e^{-L\tau_m})_{ij}M_j^0 \tag{1}$$

where L is the exchange matrix, with elements $L_{ij} = k_{ji}$ and $L_{ii} = -R_i - \Sigma_j k_{ij}$, and M_j^0 is the equilibrium magnetization of the nuclei in site j. The solution of this equation for exchange rates k_{ij} and external spin–lattice relaxation rates R_i as a function of τ_m, M_j^0, and I is not straightforward and involves

diagonalization of the intensity matrix I and iterative numerical methods. The technique has been used mainly for qualitative mechanistic studies of exchange pathways, or for quantitative evaluation of exchange rates in the case of a simple 2-site exchange. However, it has recently been quantitavely applied[47] to a three-site exchange of the CO groups in two of the $Ru(CO)_3$ moieties of $[Ru_3(\mu\text{-H})(CO)_9(MeCCHCMe)]$ (6):

(6)
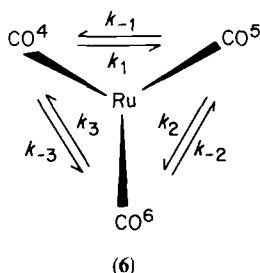
Here the problem is somewhat simplified, because the populations of all sites are equal, i.e. $k_i = k_{-i}$, and the exchange matrix L is symmetrical. The authors used an iterative program to obtain the "best-fit" rate constants that satisfy the experimental intensities given by (1), and found that at 299 K $k_1 = k_2 = k_3 = 3.83\,s^{-1}$.

Another approach is adopted in a study of the kinetics of the halide redistribution reactions occurring in a mixture of $SnCl_4$ and $SnBr_4$.[48] There are four possible pathways for magnetization transfer, namely

$$SnCl_4 \quad \rightarrow SnCl_3Br$$

$$SnCl_3Br \rightarrow SnCl_2Br_2$$

$$SnCl_2Br_2 \rightarrow SnClBr_3$$

$$SnClBr_3 \rightarrow SnBr_4$$
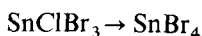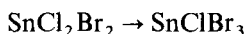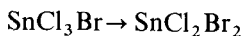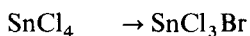
The ^{119}Sn 2D–NOESY spectrum shows five diagonal peaks corresponding to the five species present and four cross-peaks corresponding to the above reactions. Plotting the cross-peak intensities as functions of τ_m gives curves, whose initial slopes determine the exchange rates. This approach requires repeating the experiment for several mixing times, a time-consuming process. However, a more time-efficient method is emerging[45] for the quantitative treatment of multisite exchange of any complexity on the basis of a single experiment.

This involves essentially the reverse procedure of the previous approach,[47] namely calculating exchange-rate information in the form of the kinetic matrix L from measured cross-peak intensities. The method avoids having to

iterate on trial values of k_{ij} and R_i inherent in the previous approach.[47] The new method, which can be applied to systems undergoing exchange between any number of sites between 2 and 8, has been demonstrated for the 3-site exchange of the invertomers of $[PtXMe_3(MeSCH_2CH_2SMe)]$ (5).[45] The results are in good agreement with those based on proton 1D bandshape fittings (Fig. 3). This graph also illustrates how the 2D approach extends the measurable range of rate constants to much lower values. In this work, k_{ij} values down to $0.03\,s^{-1}$ can be evaluated with high accuracy.

There are several sources of experimental artefacts that can lead to spurious peaks in 2D NOESY spectra. Most of these can be removed by the process of symmetrization, which compares the intensities of all pairs of points related by symmetry about the diagonal and makes them equal to the smaller value within a pair.

It is important to realize that the standard pulse sequence described above cannot distinguish between cross-relaxation processes (NOE) and processes where magnetization is transferred by chemical exchange. Thus cross-peak intensities may sometimes be a composite of both. In fact, the basic Jeener experiment is very often referred to as NOESY (Nuclear Overhauser effect spectroscopy), although in the present context it is preferable to call it EXSY (exchange spectroscopy). This ambiguity can be removed by a variation of the 2D exchange experiment that is referred to as "zz-exchange spectroscopy".[49]
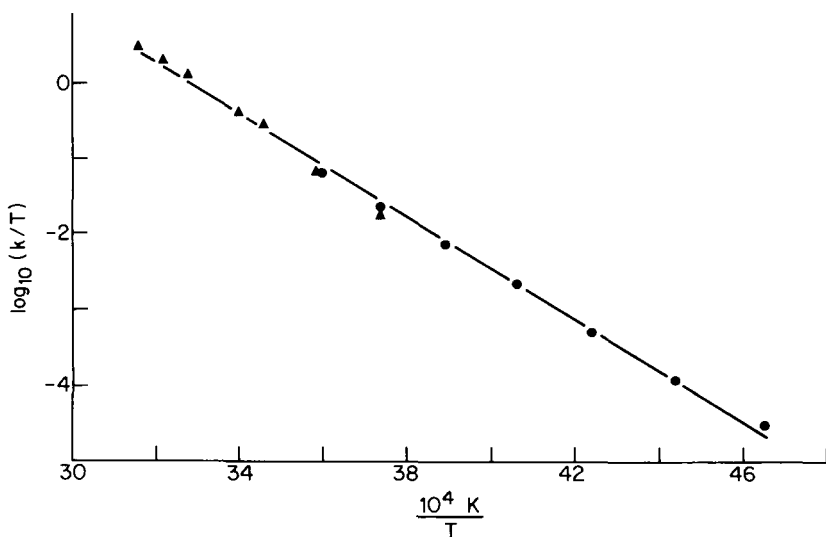
FIG. 3. Eyring energy plot for $[PtIMe_3(MeSCH_2CH_2SMe)]$ using both ^{195}Pt 2D ($\bullet$) and ^{1}H 1D ($\blacktriangle$) data.

This modified pulse sequence in effect monitors the transfer of polarization associated with a set of spins rather than of individual spins.

Another complication often encountered in ^{1}H EXSY spectra is the presence of so-called J cross-peaks. This problem is discussed by Macura et al.,[50] who point out that in systems of coupled spins, J-couplings can lead to cross-peaks analogous to cross peaks in 2D autocorrelated spectroscopy (COSY). They reflect a coherent magnetization transfer, in contrast with the incoherent processes responsible for chemical exchange. There are several methods of selective suppression of J cross-peaks: (a) application of a magnetic-field gradient pulse; (b) phase cycling; (c) two-dimensional digital filtering; (d) random variation of the mixing time τ_m; and (e) incremented mixing technique.[51] The last-mentioned technique permits distinction between different orders of multiple-quantum coherence during the mixing time and leads to a displacement of all J cross-peaks from their original positions along the ω_1 direction. Thus the symmetry of J peaks is destroyed and they can be easily eliminated by symmetrization. Recently, a systematic approach to the suppression of J cross-peaks has been suggested.[52] This involves introducing an additional refocusing 180° pulse during the mixing period and averaging signals from experiments with different delay times at which this pulse is inserted in the mixing interval.

Usually in the final stages of data processing sine-bell window functions are used and magnitude-mode rather than pure absorption-mode spectra are computed. This removes complications with phasing and reduces data-storage requirements by a factor of two. However, it has been suggested[53] that pure absorption-phase spectra in four quadrants have several advantages including substantial increase in resolution and discrimination. This view is supported by other workers,[54] who conclude that pure-phase 2D exchange spectroscopy is best suited for quantitative studies as it systematically suppresses several artefacts, including certain types of J peaks.

In some cases it is desirable to suppress diagonal peaks, which would otherwise obscure nearby cross-peaks, a situation often arising with macromolecules. Bodenhausen and Ernst[55] proposed a type of two-dimensional exchange-difference spectroscopy that in effect subtracts diagonal signals in such a way that the algebraic sums over rows or columns of the 2D data table vanish.

The 2D NMR EXSY technique has been applied to many inorganic and organometallic systems using a number of nuclei. Starting with ^{1}H, Kook et al.[56] studied molybdenum alkyne complexes (7) undergoing cis–trans intramolecular exchange as a result of alkyne rotations and found the 2D technique very effective for studying these thermally sensitive compounds under slow-exchange conditions. Intramolecular mobilities of phosphine η^3-allylpalladium chloride complexes have been investigated by using 2D ^{1}H
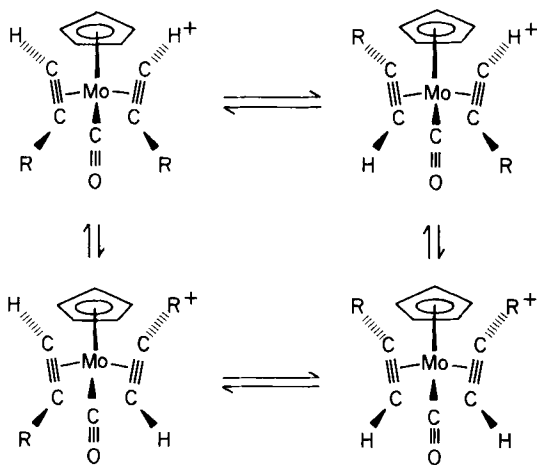
(7)

NMR, and several mechanisms of exchange in these compounds have been reported.[57,58] Perrin and Gipe[59] have reported a ^{1}H study on the acid-catalysed proton exchange of acrylamide and thioacetamide between three sites. They were able to determine the rate constants quantitatively and to draw mechanistic conclusions from them.

The first ^{13}C application of EXSY was suggested by Huang et al.,[60] who pointed out two important advantages of this nucleus over ^{1}H. First, J cross-peaks are completely absent for low-abundance nuclei, whereas the second advantage arises from the longer spin–lattice relaxation times. As a general rule, the slower the exchange process, the longer the mixing period τ_m required to obtain appreciable intensities of the cross-peaks. On the other hand, τ_m cannot be chosen to be much longer than T_1 because of the loss of magnetization due to external relaxation during the mixing period. As a rule of thumb, therefore, the measurable exchange rate should satisfy the condition $k \gtrsim T_1^{-1}$. ^{13}C relaxation times are normally considerably longer than those of protons, and thus the carbon nuclei have a longer-lasting memory, permitting the investigation of slower exchange processes, which require long mixing times. A typical inorganic example of ^{13}C 2D EXSY is the work[61] on ^{13}C-enriched $Os_3H_2(CO)_{10}$ (3). The exchange occurs only between ^{6}CO and ^{7}CO with $k = 1.21\,s^{-1}$, this dynamic problem being treated as 2-site exchange, since two of the sites are equivalent. A qualitative ^{13}C investigation of exchange processes in tetra-allyldichromium $(\eta^3\text{-}C_3H_5)_4Cr_2$ has been reported.[62]

Among other nuclei, ^{31}P has been used[63] in determining rearrangement mechanisms of octahedral organometallic complexes of type

$[\{(RO)_3P\}_nCr(CO)_{5-n}(CX)]$ $(R = alkyl, aryl; X = O, n = 2, 3, X = S, Se,$ $n = 1, ..., 3)$. *Fac* and *mer* complexes of type (**8**) are shown to rearrange exclusively via a trigonal–prismatic pathway.[63]

fac   mer I   mer II

(8)

(9)
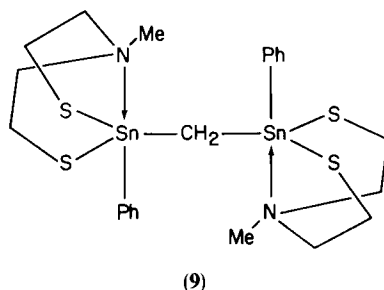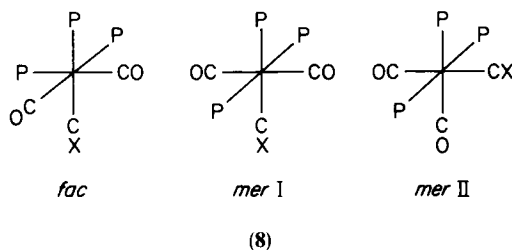
The first ^{119}Sn 2D EXSY spectra were reported by Wynants et al.,[64] who investigated dynamic stereochemistry of the ditin compound (**9**).

The compound isomerizes at the Sn centres in an uncorrelated way thus forming three isomers: aa, ae and ee. The authors discuss the importance of choosing correct mixing times for the correct qualitative interpretation of results. For longer mixing times, cross-peaks may appear between sites even in the absence of a direct exchange pathway. (See Fig. 2 for example.)

In conclusion, it would appear that 2D chemical exchange spectroscopy is an ideal alternative to magnetization-transfer techniques, as *all* exchange pathways can be investigated simultaneously. It only requires the application of nonselective pulses, which is another advantage especially for closely spaced resonances, where selective perturbation of a single line may be impossible. Turner[65] draws an interesting comparison between 2D EXSY and conventional selective-transfer experiments from the point of view of sensitivity. He concludes that the 2D experiment offers $1.28\ p_A p_B n^{1/2}$ of the sensitivity obtainable with a series of selective experiments, where n is the number of pairs of exchanging resonances, and p_A and p_B are the mole fractions in each site. This represents a considerable gain for complex systems, even when exchange

occurs solely within pairs of signals. For more complicated exchange networks the advantages could be even greater.

A few special 2D techniques deserve special mention.

2. 2D accordion spectroscopy

Bodenhausen and Ernst[66,67] have proposed an alternative class of NMR exchange experiments based on systematic variation of three time variables. The problem with 2D EXSY is, that for quantitative measurement of rate constants it is not often sufficient to record one 2D spectrum with a single τ_m value. In other words, a three-dimensional data set is required as a function of three time variables t_1, t_2 and τ_m, which is very time-demanding. To reduce the time requirements, the authors proposed to increment two variables simultaneously by defining $\tau_m = kt_1$. Because of this concerted "stretching" of the pulse sequence, the experiment is referred to as "accordion" spectroscopy.

The spectral lines obtained by this technique have characteristic shapes. Diagonal peaks consist of sums of two Lorentzians with line widths R and $R + 2k$, where R and k are relaxation and exchange rates respectively. Cross-peaks are composed of the differences of the same pair of Lorentzians. Such lineshapes can be easily analysed by least-squares fitting procedures yielding the exchange rate k. Thus it is no longer necessary to obtain a set of 2D spectra for different τ_m delays.

3. Skewed exchange spectroscopy

A novel experiment called SKEWSY or skewed NOESY has recently been described.[68] The pulse sequence of this technique differs from the basic NOESY sequence by an additional 180° pulse applied in the preparation period. The experiment results in a spectrum in which symmetrical cross-peaks are not necessarily of equal intensity. This asymmetry or "skewness" reflects differences in T_1. All exchange information is obtainable from the cross-peaks, thus avoiding the diagonal region of the 2D spectrum, which is sometimes crowded. Another advantage lies in the absence of J-coupling effects.

4. 2D magnetization transfer in the rotating frame

This is an extension of the one-dimensional NMR technique.[35,69] The pulse sequence is D1–90$^\circ_x$–D0–P2$_y$–AQ, where D1 is the relaxation delay, AQ means acquisition and D0 is the incremented delay. Switching from the high-power range of the transmitter (for the first pulse) to the low-power range (for the spin-locking pulse, P2$_y$) is required, and occurs during the time interval D0.

The length of the spin-locking pulse is of the order of $T_{1\rho}$. The technique could be useful for situations where a 2D–EXSY experiment is desirable, but the resonances do not have a large enough frequency separation.

5. 2D exchange NMR in rotating solids

A proposed extension to the 2D exchange NMR experiment to make it capable of detecting very slow molecular reorientations in solids is based on measuring the spinning sideband intensities of the 2D spectrum under conditions of slow magic-angle-spinning (MAS).[70] Diagonal as well as off-diagonal spinning sideband peaks normally appear in the spectrum, even when there is no exchange, as a result of sample rotation. However, it turns out that off-diagonal peaks disappear in the absence of exchange when the mixing time τ_m is chosen as an integral number of spinner periods. It is necessary to synchronize τ_m with spinning, and De Jong et al. used an optical sensor to generate short trigger pulses synchronous with the spinner rotation. The method was applied to dimethyl sulphone $(CH_3)_2SO_2$, which is known to exhibit a molecular reorientation in the millisecond region. A different approach was recently adopted by Harbison et al.,[71] who modified the standard pulse sequence of Jeener[44] to include scaling cycles in the evolution period t_1. Such chemical-shift scaling during t_1 ensures isotropic evolution, and, as a result, one dimension contains isotropic shifts while the second contains isotropic plus anisotropic shifts. The method yields better quality spectra, i.e. without sidebands and with improved signal-to-noise ratio. The technique was demonstrated on ^{13}C MAS spectra of p-nitroanisole and other compounds containing aromatic rings that undergo twofold flips.

F. Oriented solute studies

The NMR spectra of molecules partially oriented in liquid-crystal solvents are often dominated by large interactions such as direct dipole–dipole or quadrupolar couplings. Such couplings, which are absent (i.e. averaged to zero) in ordinary isotropic solvents, lead to very large characteristic splittings in the NMR spectra, often of the order of several kilohertz. This opens the possibility of studying chemical exchange processes by lineshape analysis over a wider range of rates than would be possible in isotropic solvents. In certain cases oriented-solute studies provide the only method of measuring rates of intramolecular processes. As an example, all eight protons of cyclooctatetraene are equivalent in an isotropic medium, and the NMR spectrum consists of a singlet, which is totally insensitive to any exchange process. When dissolved in a liquid-crystalline solvent, however, the compound gives a very complicated spectrum, which is strongly temperature-

dependent and yields the rate constant for the intramolecular bond shift.[72]

The subject has been reviewed and the limitations of the method have been discussed.[73, 74] The principal disadvantage is that the spectra are very difficult to analyse if more than about six spins are involved. Sometimes it is possible to take advantage of the symmetry of the molecule and simplify the calculations using group theory.[75] Although potentially very useful, the technique has been applied to only a few simple organic molecules to date.

III. COORDINATION COMPLEXES AND ORGANOMETALLIC COMPOUNDS

A. Ring-conformational changes

1. 5,6-membered rings

The study of conformational analysis of five- and six-membered chelate ring systems by NMR has been reviewed.[76] Here we mention only a few illustrative studies. Shaver and McCall[77] have estimated inversion barriers of metallocyclosulphanes Cp_2MS_5 and $(Me_5Cp)_2MS_3$, where M = Ti, Zr or Hf, and Cp = cyclopentadienyl. In the case of the ME_5 ring the barriers follow the order Ti > Hf > Zr for E = S and Se, with those for the selenanes being slightly greater than those for the sulphanes. Buchanan et al.[78] have performed lineshape analysis on ^1H NMR spectra of complexes of cis-dioxomolybdenum(VI) with the (R)- and (S)-enantiomers of penicillamine O-methyl ester. Inversion of the configuration about molybdenum is observed over the temperature range 24–112 °C, and $\Delta G^{\neq}$ for the process of $\Delta \rightleftharpoons \Lambda$ interconversion (10), which occurs via partial chelate dissociation and without geometrical isomerization, was found to be 76.4 kJ mol^{-1}:
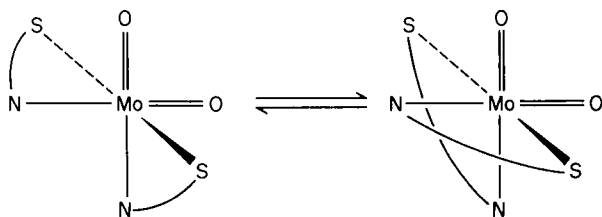
(10)

Selenium-77 NMR has been used[79] to estimate ring-reversal barriers in phenylselenylcyclohexane derivatives PhSeR (R = cyclohexyl) with the results $\Delta G^{\neq}_{ea} = 49.1$ and $\Delta G^{\neq}_{ae} = 44.1$ kJ mol^{-1}. Accurate energy data for the

bridge reversal of [3]-ferrocenophanes with a variety of bridging atoms (11) have been obtained[80, 81] using the cyclopentadiene protons as probe nuclei:

(11)
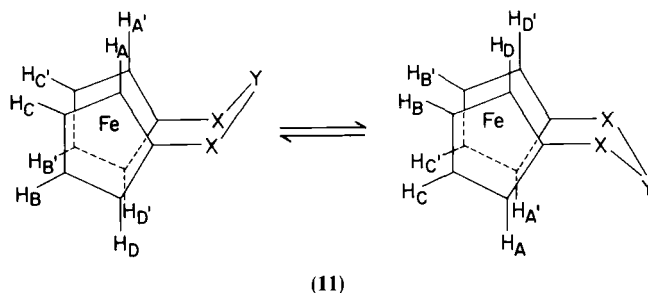
The dynamic problem is treated as $ABCD \rightleftharpoons DCBA$. The energy barriers depend on the types of the bridging atoms. The compounds studied include $X = S$; $Y = CH_2$, CMe_2, S, Se or Te. $X = CH_2$; $Y = CH_2$, O, or S. $X = Se$; $Y = S$, Se or Te.

The values of $\Delta G^{\neq}$ are in the range $35–81\, kJ\, mol^{-1}$, and the data allow estimates to be made of the relative magnitudes of torsional barriers about single bonds involving like and unlike Group VI atoms. For example, the S–S torsion is $3.9\, kJ\, mol^{-1}$ higher in energy than S–Se torsion and $5.8\, kJ\, mol^{-1}$ higher than the Se–Se torsion. Czech et al.[82] extended this work to [5]-ferrocenophane where $X = S$, $Y = C(CH_2Br)_2$, and found $\Delta G^{\neq}$ (bridge reversal) $= 58.2\, kJ\, mol^{-1}$. They were able to demonstrate correlation of $\Delta G^{\neq}$ values and total bridge length. Ferrocenylsulphide–palladium(II) and –platinum(II) complexes have also been studied by variable-temperature NMR.[83] However, the bridge-reversal process in these complexes was found to be too rapid for ^1H NMR detection, even at $-100\,°C$, due presumably to the smaller torsional barriers associated with Pd–S or Pt–S bonds compared with C–S bonds. Abel et al.[84] also reported conformational studies of the five-membered rings of dithiastannolanes $SnRR'(SCH_2CHR''S)$ where $R,R' = Me$ or Ph and $R'' = H$ or Me (12).

(12)
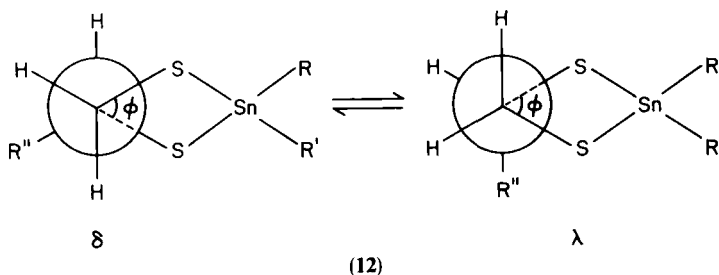
The chelate rings exist as half-chair conformations with the $-CH_2CHR''-$ moiety in a fully staggered configuration. Bandshape analysis of ^1H spectra of the methylene/methine ring protons yield $\Delta G^{\neq}$ values in the range $30-32 \, kJ \, mol^{-1}$, which are essentially independent of the substituents, but strikingly high in magnitude for 5-membered ring pseudorotation processes.

2. 7,8-Membered rings

Brown and Chaloner[85] have investigated the dynamic behaviour of the bis palladium complex of the ligand DIOP (13):
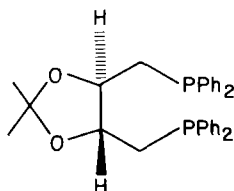
(13)

The 7-membered chelate rings undergo conformational changes such that ^{31}P NMR shows a singlet at $300 \, K$ and an A_2B_2 spectrum at $190 \, K$. Complete bandshape analysis gives $\Delta G^{\neq} = 41.2 \, kJ \, mol^{-1}$. This work has been extended to bis(diphosphine) complexes of rhodium and iridium.[86] The conformations of the 7-membered chelate rings in complexes such as $[(DIOP)Rh(COD)]BF_4$, where $COD = 1,5$-cyclooctadiene, may be modelled on cycloheptane. However, the barrier to interconversion of chair and boat forms is expected to be lower than that for cycloheptane owing to increased bond lengths. In fact, such a lowering of the barrier is not observed, probably because of opposite effects caused by interactions of the P-phenyl rings with the COD ligands.

Conformational behaviour of 7- and 8-membered organosilicon hetero-cycles has been observed.[87] A $\Delta G^{\neq}$ value of $58.4 \, kJ \, mol^{-1}$ is obtained for ring inversion of the dioxasilocin (14), $X = CH_2$, $R^1 = R^2 = Me$). The ^1H NMR spectrum below $6 \, °C$ shows 2 nonequivalent methyls.

Conformational changes in binuclear complexes $[Pt_2Me_4(\mu-R_2PCH_2PR_2)_2]$ (15) have also been reported.[88] The 8-membered $Pt_2P_4C_2$ dimetallacycles adopt twist–chair or twist–boat conformations. For $R = Me$, $\Delta G^{\neq}$ for the inversion of the twist–chair form was estimated to be $56 \, kJ \, mol^{-1}$. When $R = Ph$ there are two processes: a twisting motion with $\Delta G^{\neq} = 54.7 \, kJ \, mol^{-1}$, and ring inversion with $\Delta G^{\neq} = 61 \, kJ \, mol^{-1}$.
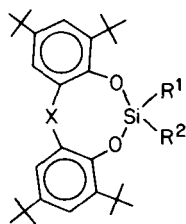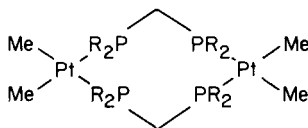
(14)   (15)

3. Larger rings

Aalmo and Krane[89] have reported investigations on lithium-cation complexes of 1,5,9,13-tetraoxacyclohexadecanes. The octamethyl derivative of this 16-membered cyclic oligoether exhibits conformational changes with $\Delta G^{\neq} = 36.8 \, \text{kJ mol}^{-1}$.

An example of conformational changes in 10-membered ring systems has been given by Van Stein *et al.*[90] These authors have studied some silver(I) and copper(I) dication complexes with polydentate N_4-donor ligands L (**16**). ^{1}H
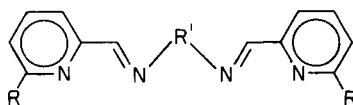
(16)

NMR data show that in complexes with ethanediyl bridging R' groups a fast conformational movement takes place between two identical structures. In contrast, this movement does not occur in complexes with (*R,S*)-cyclohexanediyl bridging groups.

B. Pyramidal inversions

1. Group V atoms

Inversion of configuration of an atom bonded to three substituents in a pyramidal geometry is referred to as pyramidal inversion. The process normally involves the interchange of two equivalent configurations or invertomers via a planar transition state.

Most molecules with pyramidal phosphorus atoms are configurationally stable, i.e. their inversion barriers are higher than *ca.* 100 kJ mol^{-1} and beyond the range measurable by NMR methods. Among the few cases of

phosphorus inversion investigated by NMR are the pyramidal terminal phosphide complexes $(\eta^5\text{-}C_5H_5)Re(NO)(PPh_3)(PRR')$.[91] Variable-temperature ^1H, ^{31}P and ^{13}C NMR have been used to estimate P inversion barriers from coalescence measurements. These are among the lowest known for phosphorus, namely $\Delta G^{\neq} = 48.3\,kJ\,mol^{-1}$ for (17) and $54.6\,kJ\,mol^{-1}$ for (18):

(RS,SR) (RR,SS)

(17)   (18)
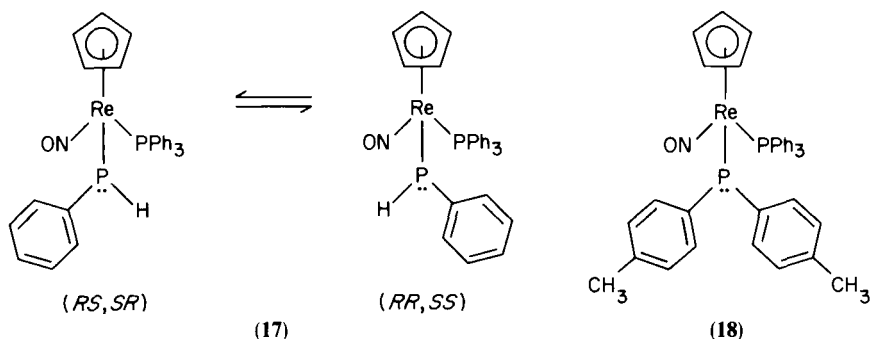
Newman et al.[92] have studied P inversion in the heterocyclic diphosphasilanes, $(PhP)_2(SiMe_2)_n$ $(n = 2,3,4)$, these being 4-, 5- and 6-membered heterocycles. The free energies of activation for inversion in $(PhP)_2.(SiMe_2)_3$ and $(PhP)_2.(SiMe_2)_4$ are similar and estimated to be around $12.5\,kJ\,mol^{-1}$. This low value is explained by a minimal angle strain in the transition state. In the smaller 4-membered ring $(PhP)_2.(SiMe_2)_2$ the angle strain is increased and the barrier to inversion is raised by ca. $10.5\,kJ\,mol^{-1}$.

The only recent NMR study of the inversion of configuration of nitrogen atoms is that by Mirti[93] on the cadmium(II) complex of ethylenediaminetetraacetic acid in water–dioxane mixtures. The rate of N inversion appears to increase with the amount of dioxane present in the solvent.

2. Group VI atoms

By far the largest number of NMR studies of pyramidal atomic inversion have involved inversions at sulphur or selenium atoms in transition-metal complexes. A comprehensive review of the subject was published in 1984.[94] Coordination of a sulphur or selenium atom to a transition metal lowers the barrier to pyramidal inversion, so that the process is observable on the NMR time scale. The considerable range of results obtained will be classified according to the transition metal attached to the inverting centre(s).

(a) Coordination to chromium, molybdenum and tungsten. Sulphur and selenium inversions at metal carbonyl compounds of Group VI metals have

been extensively studied. Sulphur-bridged dimers $[R_2Ti(\mu\text{-SH})_2M(CO)_4]$ (M = Mo, W; R = Cp) were found to exist as a 2:1 mixture of *syn* and *anti* isomers (19):[95]

(19)
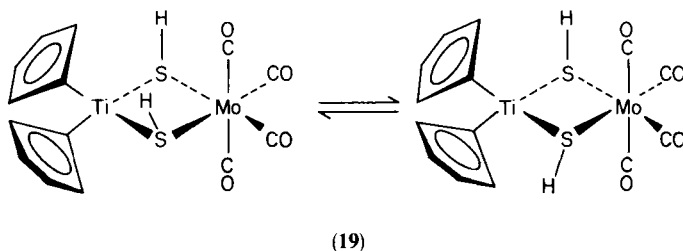
Bandshape analysis yields activation energies of *ca.* $72\,kJ\,mol^{-1}$ for inter-conversion by a unimolecular pyramidal inversion pathway. However, addition of 10 mol% of triethylamine approximately halves the activation energy. This result suggests another isomerization mechanism, namely a base-catalysed pathway involving a deprotonation–reprotonation sequence.

A series of dimolybdenum complexes $[Mo_2(CO)_2L(\mu\text{-SMe})_3(\eta\text{-C}_7H_7)]$ (L = $P(OMe)_3$, $PMePh_2$, PMe_2Ph, PMe_3; C_7H_7 = cycloheptatrienyl) (20),

(20)
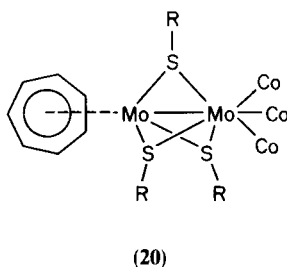
have been reported,[96] and their free energies of activation for S inversion de-rived from coalescence temperatures. Values are found to vary between 46 and $59\,kJ\,mol^{-1}$, depending on the nature of L. The energies refer to the inversion for the sulphur atom *trans* to the phosphine, and are much lower than in the unsubstituted complexes (L = CO), except for L = $P(OMe)_3$ where the energy is essentially unchanged. The chromium tetracarbonyl complex of the ligand 1,1,2,2-tetrakis(methylthio)ethane, $[Cr(CO)_4\{(MeS)_2CHCH(SMe)_2\}]$, exists as a mixture of the *cis* and *trans* configurational isomers, with the *trans* predominating.[97] At low temperature, where sulphur inversion is slow, both isomers give rise to several distinct invertomers. (The *trans* case is shown: (21).)

dl - 1   dl - 2

dl - 3   dl - 1
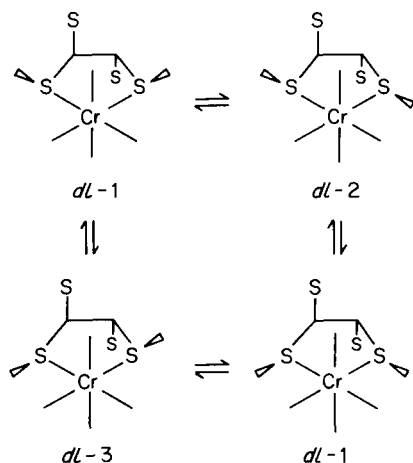
(21)

The different invertomers of each configurational isomer have been identified by two-dimensional ^{1}H EXSY experiments, and the barriers to S inversion determined by total bandshape analysis. $\Delta G^{\neq}$ values are in the range 45–54 kJ mol^{-1}.

Numerous M(CO)$_5$L complexes where M = Cr, Mo or W and L is a sulphur or selenium ligand have been studied. Their free energies of activation for chalcogen inversion are collected in Table 1. Factors influencing atomic inversion energies have been discussed in ref. 94.

Selenium inversion barriers are *ca.* 20 kJ mol^{-1} greater than sulphur barriers in corresponding complexes. Also, inversion barriers in the molybdenum complexes are *ca.* 3.5–6 kJ mol^{-1} lower than in chromium complexes, which in turn are *ca.* 1–2.5 kJ mol^{-1} lower than in the tungsten complexes. This can be rationalized on the basis of relative magnitudes of the electronegativities of the metals and conjugation effects.[102,103] In diselenide complexes the barrier is *ca.* 4 kJ mol^{-1} lower than in the corresponding monoselenide complex. This effect of chalcogenic substitution may be explained in terms of π-conjugation effects.[102] When an inverting atom is incorporated in a ring,[103] the energy barrier increases owing to the ligand ring constraining access to the planar transition state of the inverting atom.

(b) Coordination to rhenium. There have been a variety of DNMR studies performed on the inversion characteristics of S or Se atoms coordinated to rhenium in [ReX(CO)$_3$L] or [ReX(CO)$_3$L$_2$] complexes. Dimethyl sulphide and dimethyl selenide form complexes of type [ReX(CO)$_3$(Me$_2$E)$_2$] (X = Cl, Br, I, E = S or Se) (22).[104]

TABLE 1

Activation energies for pyramidal chalcogen inversion in the complexes [M(CO)$_5$L].

M	L	$\Delta G^{\ast}$ (kJ mol^{-1})	Ref.
Cr	$\overline{SCH_2SCH_2CH_2CH_2}$	50.6	98
Cr	$\overline{SCH_2SCH_2SCH_2}$	51.2	98
W	$\overline{SCH_2SCH_2SCH_2}$	53.0	98
Cr	$\overline{SCH_2SCH_2SCH_2SCH_2}$	38.2	100
W	$\overline{SCH_2SCH_2SCH_2SCH_2}$	41.3	100
Cr	MeS(CH$_2$S)$_2$Me	41.6	101
W	MeS(CH$_2$S)$_2$Me	42.5	101
Cr	Me$_3$SiCH$_2$SeSeCH$_2$SiMe$_3$	53.0	102
Mo	Me$_3$SiCH$_2$SeSeCH$_2$SiMe$_3$	49.7	102
W	Me$_3$SiCH$_2$SeSeCH$_2$SiMe$_3$	54.8	99, 102
W	Me$_3$SiCH$_2$SSCH$_2$SiMe$_3$	37.3	102
W	Me$_3$SiCH$_2$SeCH$_2$SiMe	58.5	102
Cr	$\overline{Me_2CCH_2SeSeCH_2}$	67.6	103
Mo	$\overline{Me_2CCH_2SeSeCH_2}$	60.5	103
W	$\overline{Me_2CCH_2SeSeCH_2}$	69.4	103
Cr	$\overline{Me_2CCH_2SSCH_2}$	47.6	103
Mo	$\overline{Me_2CCH_2SSCH_2}$	41.4	103
W	$\overline{Me_2CCH_2SSCH_2}$	48.6	103
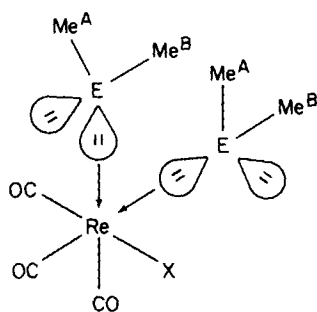
(22)

The *fac* geometry of this isomer imposes chemical-shift nonequivalence on the geminal E-methyl pairs, which is removed by the onset of rapid E pyramidal inversion. The energy barriers are found to be *ca.* 48 kJ mol^{-1} for S inversion and 65 kJ mol^{-1} for Se inversion. The chelate ligand complexes [ReX(CO)$_3$L] form the largest class of rhenium compounds wherein

ligand atom inversions have been studied. When $L = MeE(Z)EMe$, $Z = -(CH_2)_2-,^{105}-(CH_2)_3-,^{105}-CH=CH-,^{105}-o-C_6H_4-,^{105}-CH_2-S-CH_2-,^{106}$ four diastereoisomers (invertomers) exist at below-ambient temperatures when pyramidal E inversion does not occur at a measurable rate. These invertomers consist of two distinct *meso* forms (*meso*-1 and *meso*-2) and a degenerate *dl* pair. When $L = MeS(Z)SeMe$, $Z = -(CH_2)_2-$ or $-o-C_6H_4-$, four doubly degenerate *dl* pairs exist.[107] Independent pyramidal inversion of either E atom interchanges the four invertomers. The case of $E = S$, $E' = Se$ is illustrated (23):

(23)
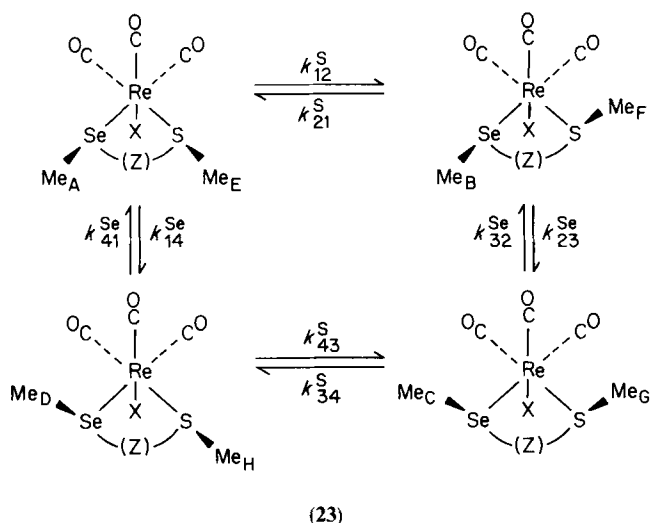
The dynamic spin system for the E—Me protons is either (A) or (B) below, depending on whether $E = E' = S$ or Se, or $E = S$, $E' = Se$, respectively:

$$AA' \rightleftharpoons BC \qquad\qquad AE \rightleftharpoons BF$$
$$\updownarrow \qquad\quad \updownarrow \qquad\qquad\qquad \updownarrow \qquad\quad \updownarrow$$
$$CB \rightleftharpoons DD' \qquad\qquad DH \rightleftharpoons CG$$
$$(A) \qquad\qquad\qquad\qquad (B)$$
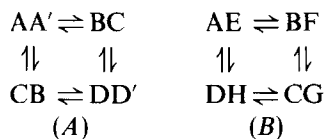
However, these two-spin systems can be further subdivided into pairs of interconverting one-spin systems, since no observable spin–spin coupling arises between E-methyls in any species. Detailed bandshape fittings of the ^1H E-methyl spectra yield precise $\Delta G^{\neq}$ values for the systems. A representative set of these values is collected in Table 2, where they can be seen to vary with (i) the nature of the inverting centre (Se > S), and (ii) the nature of the aliphatic Z backbone of the ligand. Regarding the latter, replacement of a saturated aliphatic backbone $-CH_2-CH_2-$ by an aromatic moiety $o-C_6H_4$

TABLE 2

Chalcogen pyramidal-inversion energies in selected $ReBr(CO)_3L$ complexes.

L	$\Delta G^{\neq}$ (kJ mol^{-1})	Ref.
$MeS(CH_2)_2SMe$	65.2 (S^1) 63.9 (S^2)	105
$MeSe(CH_2)_2SeMe$	86.7	105
$MeSCH{=}CHSMe$	57.1 (S^1) 51.8 (S^2)	105
$o\text{-}MeSC_6H_4SMe$	54.9 (S^1) 53.5 (S^2)	105
$o\text{-}MeSC_6H_4SeMe$	51.8 (S^1) 52.8 (S^2) 82.2 (Se)	107
$MeSCH_2SCH_2SMe$	95.1	106

causes a lowering of S inversion energy of *ca.* 10 kJ mol^{-1}. The change from aromatic to olefinic $-CH{=}CH-$ backbone is somewhat less well defined, but the majority of available data indicate an additional lowering of 1–2 kJ mol^{-1}. These trends almost certainly arise from (p–p)π conjugation between the chalcogen lone pair and ligand backbone being more effective in the planar transition state than in the pyramidal ground state. When the chalcogen ligand (L) is RCH_2EECH_2R (R = Ph, Me_3Si, E = S or Se), dinuclear complexes of type $[Re_2X_2(CO)_6L]$ are preferentially formed.[108] Sulphur inversion was now found to be more facile ($\Delta G^{\neq} = 47$–49 kJ mol^{-1}) than in the mononuclear $[ReX(CO)_3L]$ complexes.

(c) Coordination to ruthenium. Pyramidal inversion of S or Se atoms coordinated to Group VIII transition metals, particularly palladium and platinum, has been very extensively investigated. Pyramidal inversion of S or Se atoms attached to ruthenium was studied in complexes $[Ru(NO)X_3L_2]$ (X = Cl, Br; L = Et_2S, EtPhS, $(PhCH_2)_2S$, Et_2Se).[109] The inversion was followed by the methylene protons of the ethyl groups, the ^1H signals of which constituted the AB part of an ABX_3 system at low temperatures. Inversion exchanges the diastereotopic protons, and at high inversion rates they become the A_2 part of an A_2X_3 system. Total bandshape fittings yield S inversion energies, expressed as $\Delta G^{\neq}(298\,K)$ data, in the range 54–59 kJ mol^{-1} and a Se energy for the complex X = Cl, L = Et_2Se of 78.7 kJ mol^{-1}.

(d) Coordination to palladium and platinum. As part of an ongoing programme of studies of pyramidal atomic inversion and other related fluxions of transition-metal complexes, Abel *et al.* have employed total bandshape fitting methods for measuring quantitatively pyramidal inversion of S or Se atoms coordinated to palladium(II), platinum(II) and platinum(IV)

atoms in a wide range of coordination complexes. Much of this work has been reviewed elsewhere,[94] and thus only the most salient points are reported here. In the palladium(II) complexes $[PdX_2\{Se(CH_2)_n\}_2]$ ($n = 4, ..., 6, X = Cl$, Br, I) and $[PdX_2\{\overline{SeCH_2CMe_2CH_2}\}_2]$ (X = Cl, Br, I), the variable-temperature ^1H spectra over the temperature range 20–140 °C are attributed to varying rates of Se inversion in the presence of rapid ligand-ring pseudorotation or, in the case of the 6-membered rings, to rapid chair–chair reversal.[110] In the static structure of the 6-membered ring complex (24), the ten ring protons consist of five anisochronous pairs:

(24)
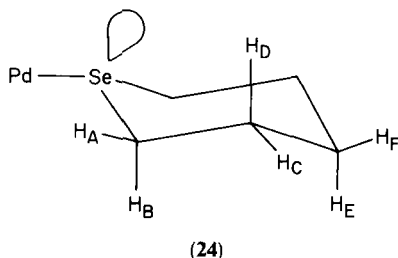
However, by neglecting cross-ring coupling between the A,B and C,D pairs and restricting the bandshape fittings to the α-methylene (i.e. A,B) proton region, the dynamic spin problem may be treated as $ABCD \rightleftharpoons BADC$, and may be computed without difficulty. $\Delta G^{\neq}$ values for selenium inversion are in the range 66–78 kJ mol^{-1} and are observed to increase with decreasing ring size. This is attributed to the ease whereby the pyramidal Se atom achieves a trigonal planar transition state with a C–Se–C angle of 120°. The inversion energies also reflect a *cis* halogen influence of 5–7 kJ mol^{-1}. In Section III.A, reference is made to 3-ferrocenophanes with bridging Group VI atoms undergoing a bridge-reversal process[80] somewhat akin to chair–chair reversal of 6-membered alicyclic rings. Complexation of 3-ferrocenophanes with palladium and platinum leads to species of the type $[Fe(C_5H_4SR)_2MX_2]$ (M = Pd^{II}, Pt^{II}; X = Cl, Br; R = Ph, Pr^i, Bu^i), which have the potentiality to undergo both bridge reversal and pyramidal S inversion. A careful evaluation

(25)
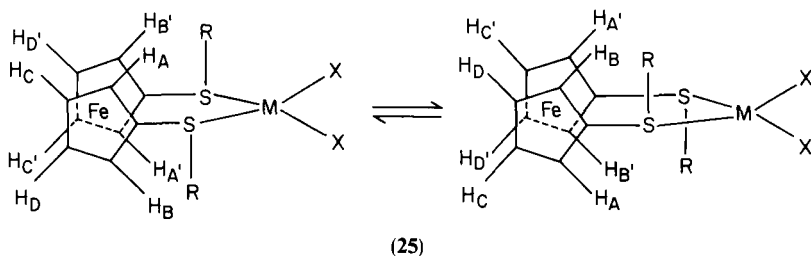
of the ^{1}H spectra of these complexes[83] leads to the conclusions that the bridge-reversal process is fast on the NMR time scale at all temperatures, and the ^{1}H spectral changes are due purely to interconversion of the pair of *dl* invertomers by S inversion (25).

In view of the absence of inter-ring proton J couplings, bandshape fittings are performed for an ABCD $\rightleftharpoons$ BADC problem and full activation-energy data calculated. Sulphur inversion energies ($\Delta G^{\neq}(298 \text{ K})$ data) in the range 47–65 kJ mol^{-1} are obtained, values being dependent on transition metal (Pt^{II} > Pd^{II}), halogen (Cl > Br), and S-substituent (Pr^i > Bu^i > CH$_2$Ph > Ph). Similar trends in inversion energies can be deduced from studies of complexes of type *cis*-[MX$_2$L] (M = Pd^{II}, Pt^{II}, X = Cl, Br, I; L = MeS(CH$_2$)$_2$SMe, MeS(CH$_2$)$_2$SMe, *o*-(SMe)$_2$C$_6$H$_3$Me, and *cis*-MeSCH=CHSMe), and [PtXMe{MeE(CH$_2$)$_2$E'Me}] (E = E' = S or Se and E = S, E' = Se; X = Cl, Br, I).[111] In the homochalcogen ligand complexes, E inversion interconverts the *syn* and *anti* species (26), whereas in the S/Se ligand complexes two

(26)
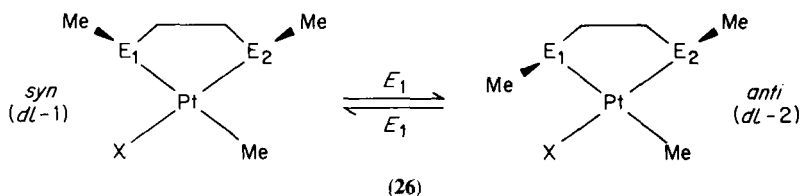
distinct *syn* and *anti* species exist at low temperatures where E inversion is arrested. Barrier energies are in the range 48–81 kJ mol^{-1} and decrease by 10–12 kJ mol^{-1} on going from aliphatic through aromatic to olefinic ligand backbones. This work also illustrates the different *trans* influences of halogen atoms and methyl groups. In *cis*-[PtXMeL] (L = MeE(CH$_2$)$_2$EMe) complexes compared with the corresponding *cis*-[PtX$_2$L] complexes, the inversion energy of the chalcogen *trans* to methyl is 15–20 kJ mol^{-1} lower than that *trans* to halogen.

Trimethylhalogenoplatinum(IV) complexes of coordinated chalcogen ligands are notably stable in solution. The symmetries of these complexes and their particular arrangements of methyl groups allow several means of observing and accurately quantifying chalcogen inversion. The complexes [PtXMe$_3$(EMe$_2$)$_2$] (X = Cl, Br; E = S, Se)[112] adopt the *fac* geometry analogous to the rhenium complex structure (22). The absence of a symmetry plane through either of the E–Pt bonds means that rotation about an E–Pt bond is not a route to averaging the geminal methyl environments, whereas E inversion is. Accordingly, the low-temperature ligand methyl AX spectrum changes on increasing temperature to an A$_2$ system with ^{195}Pt coupling being retained throughout. $\Delta G^{\neq}$ data for the inversion process are given in Table 3.

TABLE 3

Activation-energy data for chalcogen inversion in mononuclear platinum(IV) complexes [PtXMe$_3$L].

L	X	$\Delta G^{\neq}$ (kJ mol^{-1})	Ref.
(SMe$_2$)$_2$	Br	47.8	112
(SeMe$_2$)$_2$	Br	57.0	112
MeS(CH$_2$)$_2$SeMe	Cl	60.8 S^a	113
		54.9 S^b	
		73.1 Se	
o-MeS(C$_6$H$_4$)SeMe	Br	49.6 S^a	113
		47.8 S^b	
		65.7 Se	
MeSCH$_2$SCH$_2$SMe	Cl	55.7^c	114
		58.0^d	
MeSCH=CHSMe	Br	53.4^c	115
		48.6^d	
MeSeCH=CHSeMe	Br	63.4^c	115
		60.1^d	

$^a dl$-1 → dl-2; $^b dl$-3 → dl-4; $^c meso$-1 → dl; $^d dl$ → $meso$-2.

The corresponding *fac* complexes [PtXMe$_3$(MeSZSeMe)] (X = Cl, Br, I; Z = –(CH$_2$)$_2$–, or o-C$_6$H$_4$) exist as four distinct *dl* invertomers at low temperatures where S or Se inversion is slow (**27**):[113]

(27)
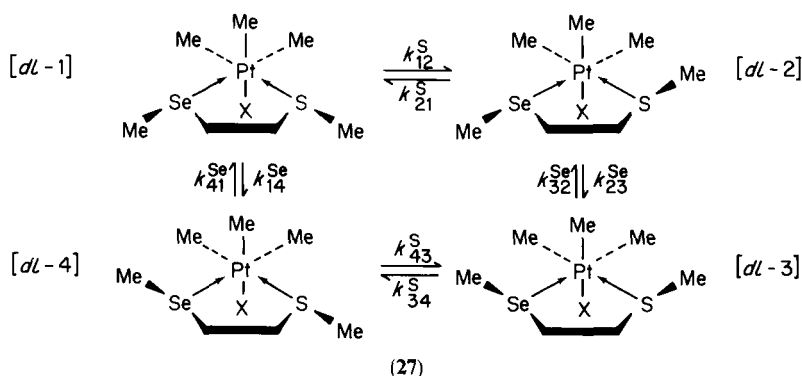
All four species are detectable in the low-temperature ^{1}H spectra. Interchange involves four forward and four reverse rate constants as illustrated in the above scheme (**27**) and in Fig. 4. The low-temperature spectrum of [PtIMe$_3$\{MeS(CH$_2$)$_2$SeMe\}] (Fig. 5) illustrates how the different exchange pathways interchange the appropriate pairs of ligand methyl signals. Detailed analyses of the ^{1}H spectra enabled two S inversion energies and one Se energy
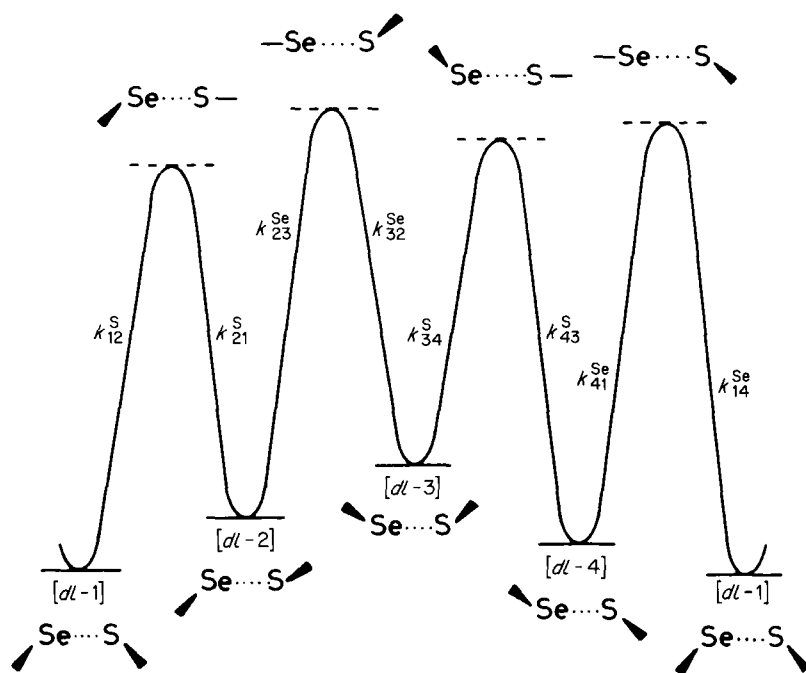
FIG. 4. Potential-energy profile for pyramidal atomic inversions in [PtXMe$_3$(MeSCH$_2$CH$_2$SeMe)].

to be calculated for each complex (Table 3). The homochalcogen *fac* complexes [PtXMe$_3$(MeEZEMe)] (X = Cl, Br, I; E = S, Se, Z = –CH$_2$S— CH$_2$–,[114] –CH=CH–[115]) exist as two distinct *meso* forms and a mirror pair of *dl* invertomers. Independent inversion of E atoms causes exchange between these species, and the spectra are sensitive to two independent rate constants at most temperatures, yielding activation energies for *meso*-1 → *dl* and *dl* → *meso*-2 pathways (Table 3).

Dinuclear platinum(IV) complexes of the general type [(PtXMe$_3$)$_2$L] also exist as stable species. The two Pt centres are bridged by a pair of halogen atoms and by the ligand. The complexes [(PtXMe$_3$)$_2$MeSCH$_2$SeMe] (X = Cl, Br, I),[116] exist only as the *dl* invertomers (**28**), which are exchanged as a result of inversion at both S and Se centres.

(28)
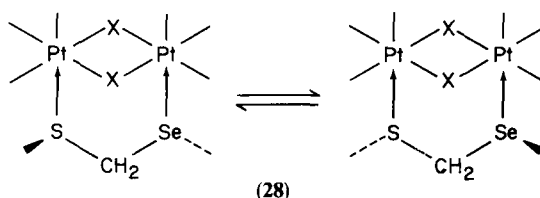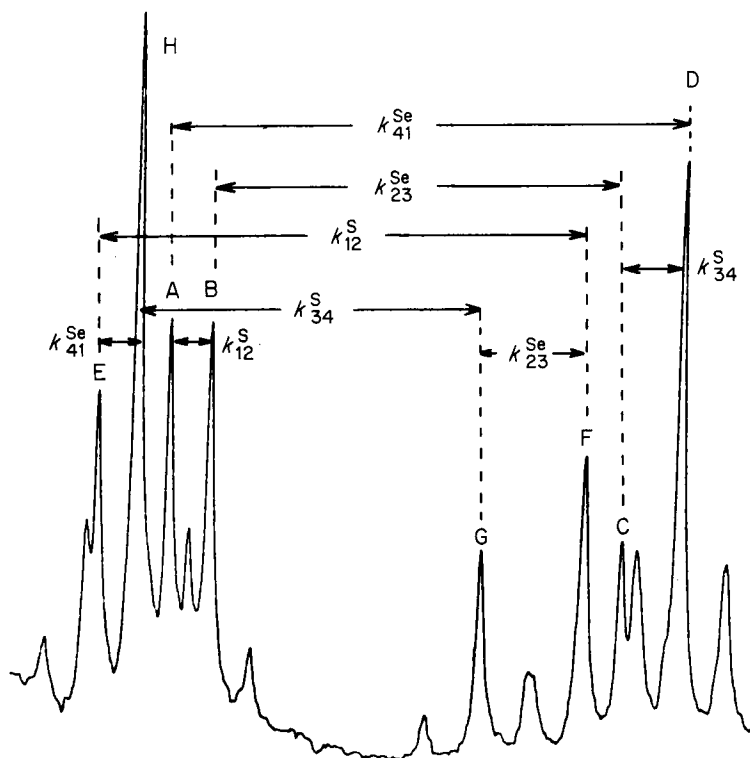
FIG. 5. Ligand-methyl ^{1}H spectrum of [PtIMe$_3$(MeSCH$_2$CH$_2$SeMe)] at low temperature, showing line assignments to individual invertomers. Lines A,E (*dl*-1); B,F (*dl*-2); C,G (*dl*-3); D,H (*dl*-4). Unlabelled lines are ^{195}Pt satellites.

This exchange may be followed by the averaging effect on the equatorial Pt-methyl signals. The spectra are sensitive to a single rate constant, which is attributed to the slower Se inversion process. No independent assessment of the S inversion process is possible and thus the authors were unable to decide in favour of either a synchronous or nonsynchronous double-inversion process. In order to gain further insight into this problem, the complexes [(PtXMe$_3$)$_2$($\overline{ECH_2CMe_2CH_2E}$)] (E = S, Se; X = Cl, Br, I) were studied.[117,118] Here the E atoms are constrained in a ring, and therefore can invert only in a synchronous manner. The process can be followed by the averaging effects on the diastereotopic ring methylenes A,B, ring methyls C,D and the equatorial Pt-methyls E,F. The ligand methylene spectra of [(PtClMe$_3$)$_2$($\overline{SeCH_2CMe_2CH_2Se}$)] and the computer-simulated band-shapes are shown in Fig. 6. The double-inversion process causes a novel
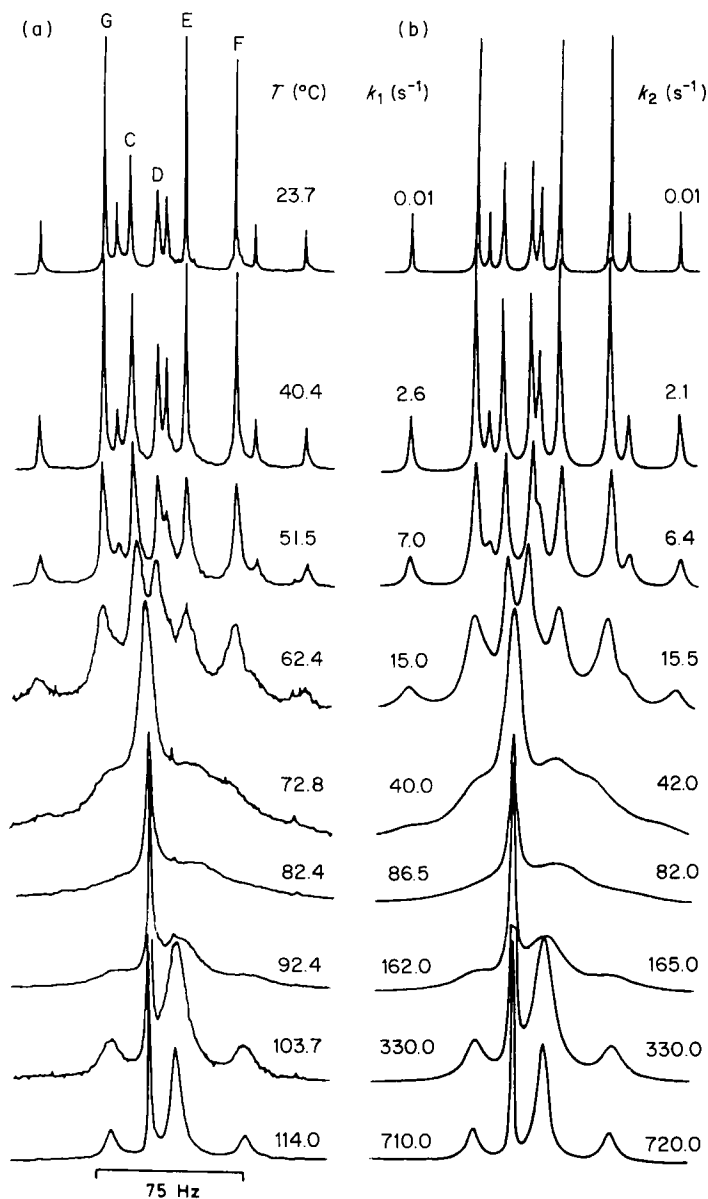
FIG. 6. (a) Experimental and (b) computer-synthesized ^{1}H spectra of the ligand-methyl and Pt-methyl regions of [(PtClMe$_3$)$_2$($\overline{\text{SeCH}_2\text{CMe}_2\text{CH}_2\text{Se}}$)], showing the effects of synchronous Se inversion (k_1) and Pt-methyl scrambling (k_2). Signals are labelled according to Fig. 7.

AB ⇌ BA
CD ⇌ DC
EF ⇌ FE
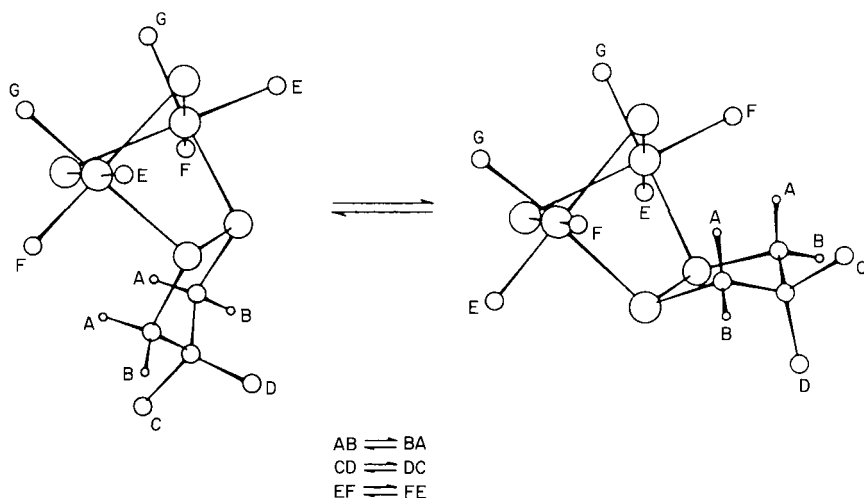
FIG. 7. The effects of synchronous double inversion on the diastereotopic ligand methylene (A,B), ligand methyl (C,D) and equatorial Pt-methyl (E,F) environments. Note that the labelling refers to the chemical environments, not the atoms.

"flapping" of the ligand relative to the $(PtXMe_3)_2$ moiety (Fig. 7). The energy data for this synchronous double-inversion process (Table 4) are in the range 66–75 kJ mol^{-1}. The fact that these values are ca. 20 kJ mol^{-1} higher than usual lends support to the nonsynchronous nature of inversion of chalcogen pairs not constrained to a ring.[94,116] A further study in this series has examined the tris(methylthio)methane complexes $[(PtXMe_3)_2HC(SMe)_3]$ (X = Cl, Br),[119] where the ligand bridges the pair of Pt atoms via two of its SMe groups. Sulphur inversion may be followed by its effects on the Pt-methyl environments. The $\Delta G^{\neq}$ values obtained (Table 4) are similar to those found

TABLE 4

Activation-energy data for chalcogen inversion in dinuclear platinum(IV) complexes $[(PtClMe_3)_2 L]$.

L	$\Delta G^{\neq}$ (kJ mol^{-1})	Ref.
MeSCH$_2$SeMe	55.3 (Se)	116
SeCH$_2$CMe$_2$CH$_2$Se	74.4	117, 118
SCH$_2$CMe$_2$CH$_2$S	66.2	117, 118
HC(SMe)$_3$	45.5	119
MeSCH$_2$SMe	48.5	94
MeSSMe	41.4	94

for other open-chain ligand complexes.[94] The onset of rapid pyramidal inversion in all the above mononuclear and dinuclear platinum(IV) complexes is simply the prelude to a variety of novel high-temperature fluxional rearrangements, which are described in Sections III.D.5(a) and (b).

C. Bond rotations

1. C–C bonds

Hexaethylbenzene (heb) can adopt up to eight possible conformers, depending on which side of the benzene ring plane the methyls are located. Variable-temperature studies of $(\eta^6$-heb)ML_3 and $(\eta^6$-heb)ML_2L' (M = Cr, Mo, L = CO, L' = PEt$_3$, PPh$_3$, CS) provoked an interesting controversy as to whether the observed changes in the ^{13}C spectra at low temperatures (down to ca. 153 K) are due to restricted ethyl-group rotation or to slowed rotation of the tripodal ML_3 or ML_2L' moiety. Hunter and Mislow[120-122] argue in favour of the former process but their reasoning requires that the major isomer of $(\eta^6$-heb)$Cr(CO)_2CS$ in CD_2Cl_2 solution be the 1,2,3,5-distal-4,6-proximal species (29), in contrast with the 1,3,5-distal-2,4,6-proximal isomer (30) known to exist in the solid state:
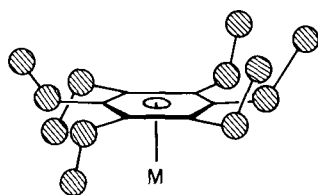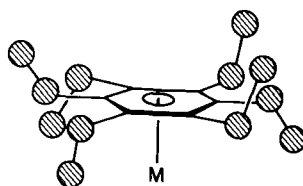
(29)   (30)

McGlinchey *et al.*, however, favour restricted rotation of the tripodal moiety,[123] and from both solid-state and solution ^{13}C spectra are able to establish[124] that isomer (30) is the only detectable species in either phase. The bandshape analyses,[122] which lead to $\Delta G^{\neq}$ values of 32–37 kJ mol^{-1}, can then be reinterpreted in terms of restricted tripodal rotation. Hunter and Mislow's proposal of uncorrelated ethyl rotation as the mechanism for interconverting proximal and distal ethyls is, however, still valid, since once the alkyl groups have rotated out of the path of the carbonyls the tripod can rotate unhindered. The same authors[125] have investigated the ^{13}C spectra of tricarbonyl(hexaethylborazine)chromium(0), and again have interpreted the changes in terms of restricted ethyl-group rotation ($\Delta G^{\neq} = 43.7$ kJ mol^{-1}).

2. C–O bonds

The low temperature ^{1}H spectra of dicarbonyl(triphenylphosphine)(1,3-di-t-butyl-2-methoxyarene)chromium compounds (31) may be fairly unam-

(31)
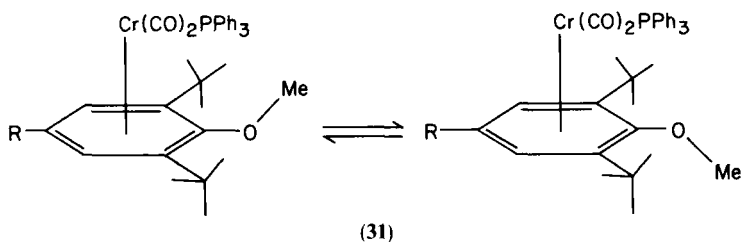
biguously interpreted in terms of restricted rotation about the arenemethoxy C–O bond. DNMR studies[126] using the DNMR5 program[127] yield $\Delta G^{\neq}$ values of 47.2 and 48.1 kJ mol^{-1} for CDCl$_3$ and CD$_2$Cl$_2$ solutions of (31), R = H, respectively.

3. C–N bonds

A number of studies involving dithiocarbamate (dtc) ligands have been reported. One particularly detailed study[128] involves the pentagonal bipyramidal complexes CpM(Me$_2$dtc)$_2$ (32):

(32)
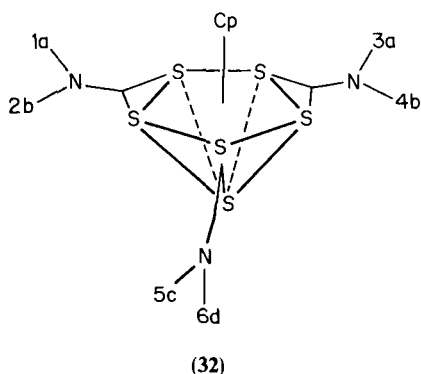
These complexes exhibit three kinetic processes: (i) exchange of methyl groups within the equatorial ligands; (ii) exchange of methyl groups within the unique ligand; and (iii) exchange of the equatorial and unique ligand. Processes (i) and (ii) are believed to involve rotation about the C⋯N bond in the dtc ligands, perhaps preceded by rupture of an equatorial metal–sulphur

bond. The kinetics of methyl-group exchange involves a four-site exchange problem. ^{1}H spectra are fitted for the three rate constants associated with processes (i)–(iii), after carrying out a permutational analysis of the problem. Total bandshape fittings of the ^{1}H spectra yield $\Delta G^{\neq}(343\,\text{K})$ values of 58.8 and 79.8 kJ mol^{-1} for the complexes M = Ti and Zr/Hf respectively. For M = Ti the rate of process (i) is 10^2–10^3 times greater than that of process (ii), whereas for M = Zr or Hf the rates of the two processes are approximately the same. For process (iii) $\Delta G^{\neq}(343\,\text{K}) = 75$–$80\,\text{kJ mol}^{-1}$. A double-facial twist mechanism involving a capped-trigonal-prismatic transition state has been proposed for process (iii), and discussed in terms of steric and electronic effects.

Dithiocarbamate-type ligands have also been used to form rhodium(III),[129] palladium(II)[130] and ferrocene[131] complexes. For Rh(MePhdtc)$_3$ $\Delta G^{\neq}$ for C–N bond rotation is measured to be $61.5 \pm 4.2\,\text{kJ mol}^{-1}$ whereas for ferrocene complexes of types Fe(C$_5$H$_4$dtc)$_2$ and Fe(C$_5$H$_5$)(C$_5$H$_4$dtc) values are in the range 66–67 kJ mol^{-1}. The ligand pyrrole-N-carbodithiate forms molybdenum(II) complexes of type Mo(RC$\equiv$CR)$_2$(S$_2$CNC$_4$H$_4$)$_2$, which undergo two independent fluxional processes.[132] The lower-energy process ($\Delta G^{\neq} = 44.9\,\text{kJ mol}^{-1}$) involves restricted rotation about the ligand C–N bonds, while the higher-energy process ($\Delta G^{\neq} = 57.5\,\text{kJ mol}^{-1}$) corresponds to rotation of the alkyne ligands around the Mo–alkyne bond axis. A detailed DNMR study of hindered rotation in the NC(E) bond fragment (E = S, Se) has been made on metal complexes of 1,1-diethyl-3-benzoylthio(seleno)urea (33):[133]
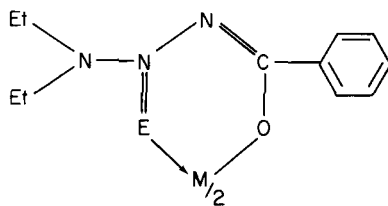
(33)

Some of the metal complexes produce only small internal ^{13}C shifts (i.e. $\Delta\nu = 1.8$–$8\,\text{Hz}$ in most cases), causing the bandshape fittings to be quite demanding. $\Delta G^{\neq}$ data range from 64.4 kJ mol^{-1} for the free ligand to 90.9 kJ mol^{-1} for the M = Ni^{II}, X = Se complex. Rotation about nitrogen–carbon double bonds is normally very slow, with energy barriers exceeding 160 kJ mol^{-1}, such cases not being measurable by DNMR. However, complexation of benzoquinone diimines with pentaammineosmium (NH$_3$)$_5$Os^{2+} sufficiently weakens the coordinated N$=$C bond that

rotation proceeds at a rate within the NMR time scale, yielding a value of $52 \pm 2 \, \text{kJ mol}^{-1}$ for $\Delta G^{\neq}(273 \, \text{K})$.[134] No temperature dependence of the $(NH_3)_5Ru^{2+}$ complex is observed, which accords with the lower back-bonding capacity of Ru^{II} compared with Os^{II}.

4. C–X bonds

Rotation about C–S bonds is hindered in carbene complexes of the type $(\eta^5\text{-Cp})(CO)LFe[C(SCH_3)_2]^+$. Proton studies of a range of such complexes reveal varying rates of C–S bond rotation at below-ambient temperatures.[135] This is attributed to methyl groups exchanging between *syn* and *anti* positions. $\Delta G^{\neq}$ values, based solely on coalescence temperatures, are in the range $42.4 \, \text{kJ mol}^{-1}$ ($L = C_5H_5N$) and $57.1 \, \text{kJ mol}^{-1}$ ($L = CO$). In studies of other carbene complexes, the dynamic process of interest is that of restricted rotation about metal–carbene multiple bonds. In complexes of the type $Cp(CO)_2(L)M(:CHR)^+$ ($M = Mo, W; L = PPh_3, PEt_3; R = H, Ph$),[136] rotation about the $W\!=\!C$ bond involves energy barriers of $35\text{--}38 \, \text{kJ mol}^{-1}$, as evidenced by the coalescence of the methylene signals, whereas rotation about the $Mo\!=\!C$ bond is rapid on the NMR time scale, even at $-90 \, °C$. Barriers to rotation about $Fe\!=\!C$ bonds were measured in the complexes (34).[137] When $R = H$, $\Delta G^{\neq}(189 \, \text{K}) = 40.3 \pm 0.8 \, \text{kJ mol}^{-1}$, and when $R = $ benzo, $\Delta G^{\neq}(205 \, \text{K}) = 43.7 \pm 0.8 \, \text{kJ mol}^{-1}$.

(34)
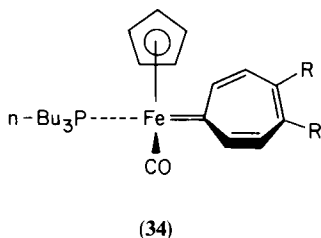
A rather rare example of restricted rotation about a Zr–C bond is provided by the complexes $[Zr\text{-}(\eta\text{-}C_5H_4R)_2\{CH(SiMe_3)_2\}Cl]$.[138] Variable-temperature ^1H NMR shows that the preferred low-temperature conformation possesses diastereotopic pairs of $SiMe_3$ and $\eta\text{-}C_5H_4R$ groups, with restricted rotation about the $Zr\text{-}C(sp^3)$ bond being $59.8\text{--}65.6 \, \text{kJ mol}^{-1}$, with values such that $R = SiMe_3 > Et > CMe_3 > CHMe_2 \approx Me > H$.

The molecules tris[2,6-bis(difluoromethyl)phenyl]phosphine, tris[2,6-bis(difluoromethyl)phenyl]arsine and their oxides afford interesting examples of restricted rotation about C–P and C–As bonds.[139] At low temperatures ^{19}F NMR data unambiguously establish that the molecules adopt chiral
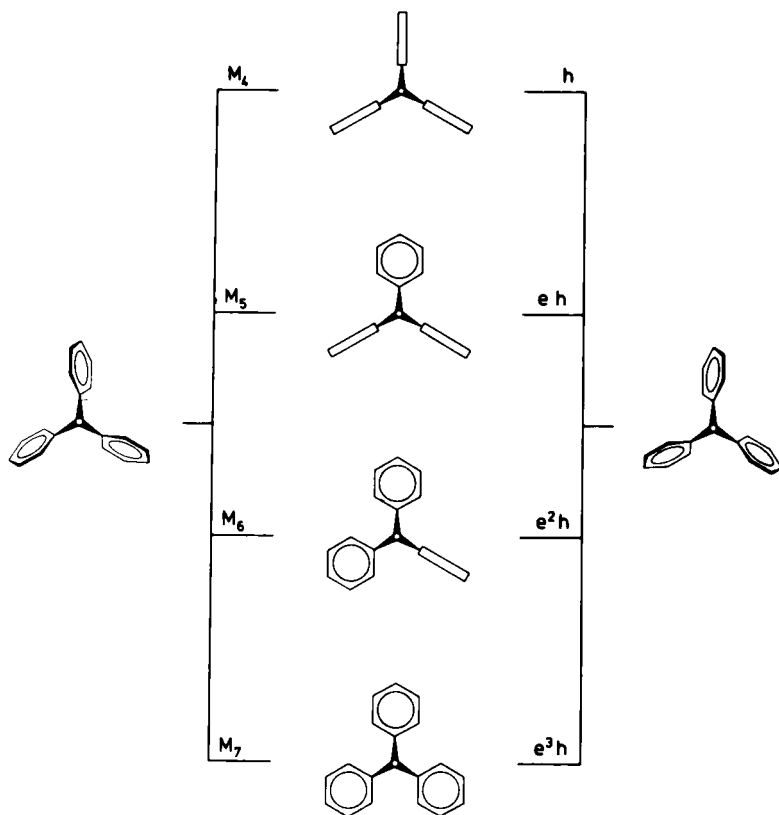
FIG. 8. Idealized transition states for the permutational mechanisms M_4, ..., M_7 of tris[2,6-bis(difluoromethyl)phenyl]phosphine or -arsine.

propeller equilibrium conformations. A theoretical analysis of the conformational dynamics establishes that there are seven differentiable permutational mechanisms (M_1, ..., M_7) of which five (M_1, ..., M_4, M_7) can be excluded from the fast-exchange-limit spectra. Mechanisms M_4, ..., M_7 are shown in Fig. 8, the symbols e and h referring to edge interchange and helicity reversal respectively. Distinction between the two possible mechanisms (M_5, M_6) is more subtle and is made more difficult by the uncertainty in relative shift assignments. Two alternative assignments were tested and bandshape fittings carried out in the most sensitive exchange-broadened temperature range. Iteratively calculated rate constants k_5 and k_6 for the processes M_5 and M_6 in the arsine compound are given in Table 5. For assignment 2, the rate constant k_6 converges to zero within one standard deviation, while k_5 values increase with increasing temperature. For assignment 1, the rate-constant dependence

TABLE 5

Best-fit rate constants for processes M_5 and M_6 of tris[2,6-bis(difluoromethyl)phenyl]arsine.[139]

$T(°C)$	Assignment 1		Assignment 2	
	$k_5 (s^{-1})$	$k_6 (s^{-1})$	$k_5 (s^{-1})$	$k_6 (s^{-1})$
−46.8	405.0(10.5)[a]	2.1(8.9)	415.8(5.6)	0.9(4.7)
−41.1	546.4(15.8)	58.6(15.3)	654.6(5.9)	0.7(4.3)
−38.6	727.0(20.4)	16.1(16.9)	805.3(8.0)	0.8(5.2)
−31.4	569.0(34.9)	543.6(32.8)	1366.0(12.6)	0.6(6.5)

[a]Standard deviations in parentheses.

on temperature is unrealistic, even though the quality of the matchings of experimental and computer synthesized spectra is very high. However, the matchings for assignment 2 are even higher, with the R factor $<3\%$ over the entire temperature range. A typical set of fittings using both assignments is shown in Fig. 9. The results unambiguously prove the exclusive operation of the two-ring-flip mechanism M_5. Precise values of $\Delta H^{\neq}$ and $\Delta S^{\neq}$ are quoted. The relative shift assignment is independently confirmed by a selective population-inversion experiment on the arsenic compound using a DANTE pulse sequence.

In a brief study[140] of the solution structure of $[Rh(COMe)(CO)_2I_3]^-$, restricted rotation about the Rh–COMe bond occurs, with $\Delta G^{\neq}$ being $31.9\,kJ\,mol^{-1}$.

5. Rotation of coordinated alkenes

The rotational barriers associated with alkene–ML_n movements have been well characterized by DNMR. Five-coordinate platinum(II)–alkene complexes have been the subject of a number of more recent studies.[141,142] In complexes of type $[Pt^{II}Cl_2(\eta^2\text{-alkene})L_2]$ $(L_2 = RN{=}CHCR'{=}NR$ or $RN(H)CH_2CH_2N(H)R)$ extensive studies[141] reveal that: (i) the Pt–N interaction of the σN, σN-bonded L_2 ligand is inert on the ^{15}N and ^{195}Pt NMR time scales; (ii) no Pt–alkene bond dissociation occurs up to 34 °C; (iii) the ligand L_2 does not participate in stereoisomerization processes; and (iv) the observed temperature dependence of the spectra can be fully explained in terms of rotation around the Pt–alkene bond axis. $\Delta G^{\neq}$ values for this process range from 55.4 to $66.8\,kJ\,mol^{-1}$. Qualitative observation of Pt–alkene-group rotation is made in the related Pt^{II} complexes (35).[142]

Rates of rotation of alkenes coordinated to square planar platinum(II) complexes vary greatly with the nature of the alkene. Thus in cis-dichloro(p-
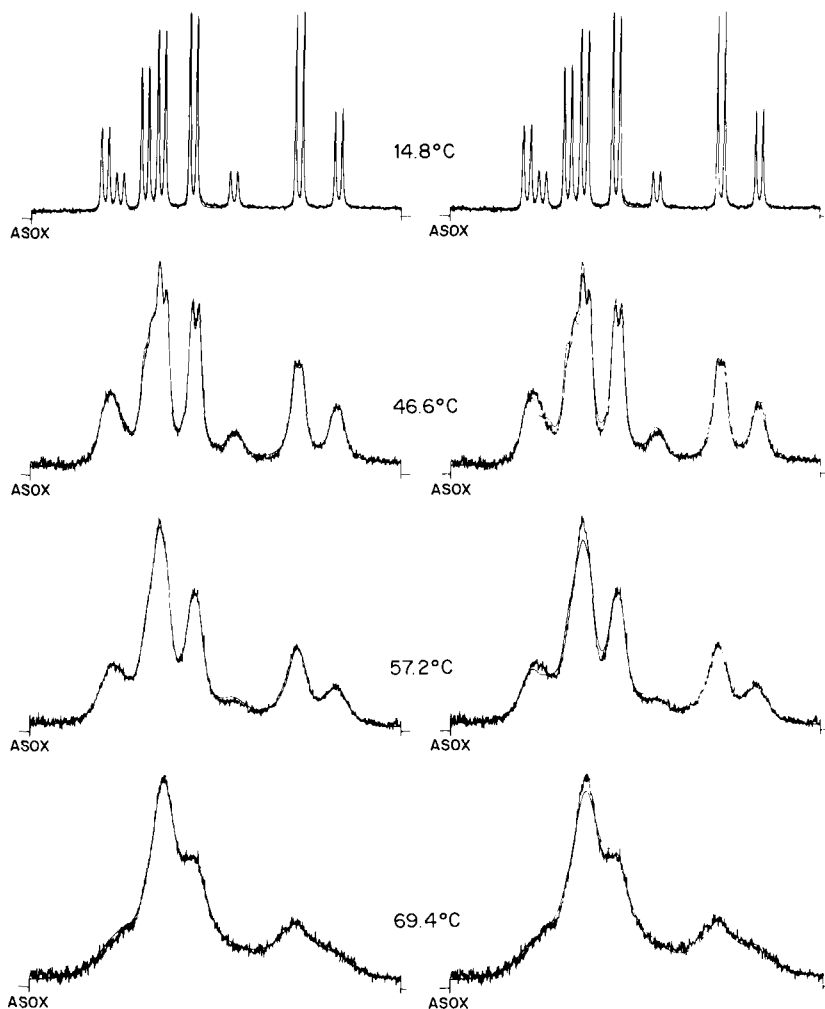
FIG. 9. Experimental and superposed theoretical ^{19}F spectra of tris[2,6-bis(difluoro-methyl)phenyl]arsine oxide in acetone-d_6. The left- and right-hand sets of spectra refer to the two chemical-shift assignments 1 and 2 respectively.

toluidine)(alkene)platinum(II) complexes[143] no evidence of rotation is found up to 50 °C when the alkene is ethyl vinyl ether, whereas in the ethene complex coalescence of the ethene proton signals occurs at *ca.* −25 °C, giving a $\Delta G^{\neq}$ value of 51.7 ± 1.3 kJ mol^{-1} in CD_2Cl_2. This value is somewhat lower than most of those associated with rotation of ethene ligands about W–C_2H_4 bonds in $(\eta^5$-L)W(CO)$_2$(C_2H_4)CH$_3$ (L = cyclopentadienyl or indenyl)[144] and

(35)
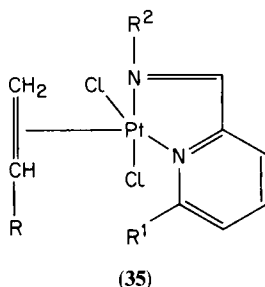
W(CO)$_3$(PMe$_3$)$_2$(olefin)[145] complexes. Restricted rotation of ethene ligands about Ni–C$_2$H$_4$ bonds in (C$_2$H$_4$)$_2$NiPMe$_3$ and CpNiMe(C$_2$H$_4$) has been followed by total bandshape analysis of the ^{1}H spectra.[146,147] There have been a number of studies of rotation of alkenes about Rh–C$_2$H$_4$ bonds. Bisalkene complexes of rhodium(I), for example bis(vinylacetate)rhodium(I), can undergo complex rotameric interconversion, which can be followed by dynamic ^{13}C NMR.[148] For the above complex $\Delta G^{\neq}(223\,\mathrm{K})$ is *ca.* 40 kJ mol^{-1}. Alkene rotation in C$_2$H$_4$ complexes of Rh^I and Ir^I of general type [(C$_2$H$_4$)$_2$MX]$_n$, where X = η^5-Cp, pentane-2,4-dionate and carboxylate, gives values that decrease with increasing electron-acceptor nature of the associated ligand.[149] The greater $\Delta G^{\neq}$ values for Ir^I compared with Rh^I complexes are reflected in the different mass-spectral fragmentation patterns for corresponding members of the two series.

(36)
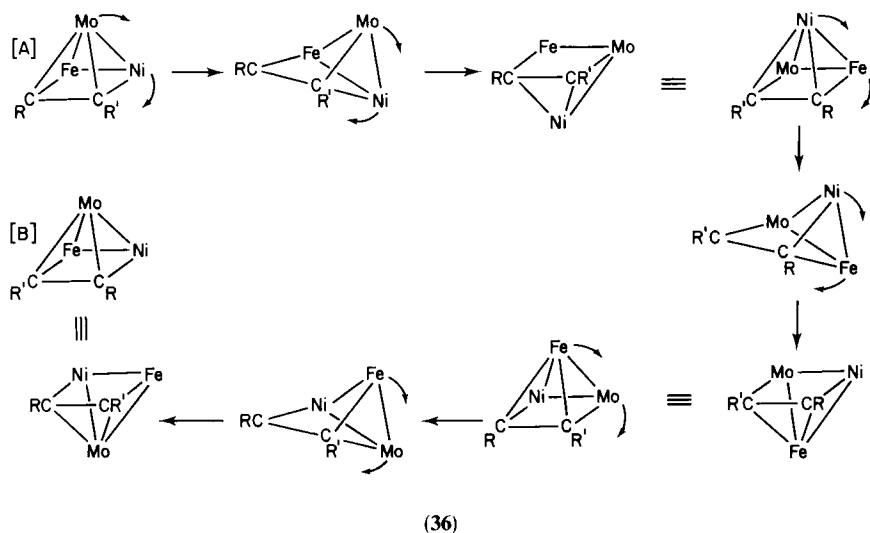
6. Rotation of coordinated alkynes

Ethyne rotation has been closely investigated[150] in mixed clusters of type $CpNiFe(CO)_3(RC\equiv CR')M$, $(M = CpNi, Co(CO)_3$ and $Mo(CO)_2Cp)$. Such complexes are special examples of square-pyramidal chiral clusters of type M_3C_2. These species undergo intramolecular fluxionality, for which a number of mechanisms may be proposed. The observed process leads to racemization of the cluster, thus eliminating a mechanism involving circumambulation about the periphery of the metal triangle. Instead a "windshield-wiper" motion based on an earlier theoretical analysis[151] is proposed. This model, however, requires modification to allow for the additional rotation of the alkyne with respect to its own triple-bond axis. The proposed mechanism is then analogous to that of a $C_5H_5^+$ system (36). ^{1}H NMR bandshape fittings over a temperature range of 290–360 K for the $M = Mo(CO)_2Cp$ complex gave a $\Delta G^{\neq}$ value of $63 \pm 3\,kJ\,mol^{-1}$.

7. Rotation of miscellaneous η-ligands

Allyl ligands have been shown by two-dimensional exchange NMR to undergo two types of $\eta^3 \rightleftharpoons \eta^1$ conversion in allylpalladium chloride complexes of various phosphines.[58] The faster $\eta^3 \rightleftharpoons \eta^1$ conversion (37) involves a preferred C–C rotation, while the slower conversion combines with C–C rotation and C–Pd rotation. Both processes are detected from a qualitative assessment of the cross-peaks in the 2D ^{1}H spectra.

(37)
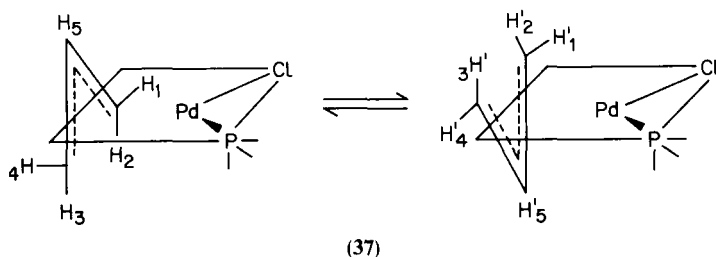
Hindered rotation of an indenyl ligand in the compound $CrRh(\mu\text{-}CO)_2(CO)_2(\eta\text{-}C_9H_7)(\eta\text{-}C_6H_3Me_3\text{-}1,3,5)$ has been examined by $^{13}C\text{-}\{^1H\}$ NMR.[152] At low temperatures the $\overline{Cr(\mu\text{-}CO)_2Rh}$ system gives two ^{13}C doublets (split by $^{103}Rh\text{-}^{13}C$ coupling), which coalesce at higher temperatures, giving a $\Delta G^{\neq}(241\,K)$ value of $45.2 \pm 1\,kJ\,mol^{-1}$.

Restricted rates of diene ligand rotations have been reported in a number of cases. Butadiene ligands (L) undergo rotation and ligand-site rearrangement in $LCr(CO)_2(PMe_3)P(OMe)_3$ complexes.[153] Cyclohexadiene ligands

(L') rotate relatively slowly ($E_a \approx 45\,kJ\,mol^{-1}$)[154] in tricarbonyliron complex salts of the type $[Fe(CO)_3L']^+PF_6^-$, while in the compound (s-*cis*-η-butadiene)bis(η-t-butylcyclopentadienyl)zirconium two fluxional processes are measured in solution.[155] Rotation of the t-butylcyclopentadienyl rings interchanges the two rotational enantiomers of the complex, with $\Delta G^{\neq} = 41.2 \pm 0.8$ kJ mol^{-1}, while at somewhat higher temperatures the butadiene–Zr moiety undergoes a rate process with $\Delta G^{\neq} = 56.7 \pm 0.8\,kJ\,mol^{-1}$. X-ray data show that the butadiene–Zr moiety is best described as a zirconacyclopentene moiety with two C–Zr σ-bonds and a π-bond between Zr and the C=C bond. The $\Delta G^{\neq}$ value above is therefore attributed to a ring-inversion process. Cyclooctadiene (COD) rotation is slowed in the complex $[(CO)_3FeC_8H_8Rh(COD)]$, as evidenced by the observation of two olefinic carbon signals at low temperature due to the COD ligand occupying two nonequivalent coordination sites.[156]

8. Miscellaneous bond rotations

A series of studies of dimesitylboryl compounds has included dynamic ^{13}C investigations. The compounds $(2,4,6\text{-}Me_3C_6H_2)_2BX(Y)(Z)$, X = O, S or N, Y = hydrocarbyl and Z = H or a lone electron pair, undergo restricted rotation about the boron–mesityl bond (i.e. B–O, B–S or B–N), the barrier height varying from 47 to 105 kJ mol^{-1} in the order B–N > B–S > B–O.[157] This order is attributed to the degree of B–X π back-bonding occurring. Rotation about B–C and B–Se bonds in $(2,4,6\text{-}Me_3C_6H_2)_2BR$ (R = SeMe, SePh) has also been investigated,[158] the B–C and B–Se barrier energies being in the ranges 36–39 and 71–77 kJ mol^{-1} respectively.

A detailed investigation of the stereodynamics of rhodium–phosphorus bonds has been carried out using ^{31}P–$\{^1H\}$ NMR on complexes of type *trans*-$[RhX(CO)L_2]$ (L = tertiary phosphine).[159] The observation of ^{103}Rh–^{31}P spin coupling (117–140 Hz) for all the complexes at any temperature shows that phosphine-ligand dissociation is slow on the ^{31}P NMR time scale. Molecular-model considerations indicated that a slowing down of Rh–P bond rotation at low temperatures would lead to four stable rotamers: two *syn* forms and two *anti* forms (**38**).

Complete ^{31}P–$\{^1H\}$ bandshape analyses (Fig. 10) indicate that the best fits incorporate no direct *syn–syn* or *anti–anti* exchange, i.e. rate constants k_{ss} and k_{aa} are zero. Such a stepwise exchange model is consistent with simple rotation about Rh–P bonds. Activation parameters are quoted for conversion from the major *syn* rotamer to one *anti* rotamer and from one *anti* to the minor *syn* rotamer. $\Delta G^{\neq}$ values are in the range 53–58 kJ mol^{-1} in most cases.

A similar magnitude of rotational barrier is associated with Pt–N bond

(38)
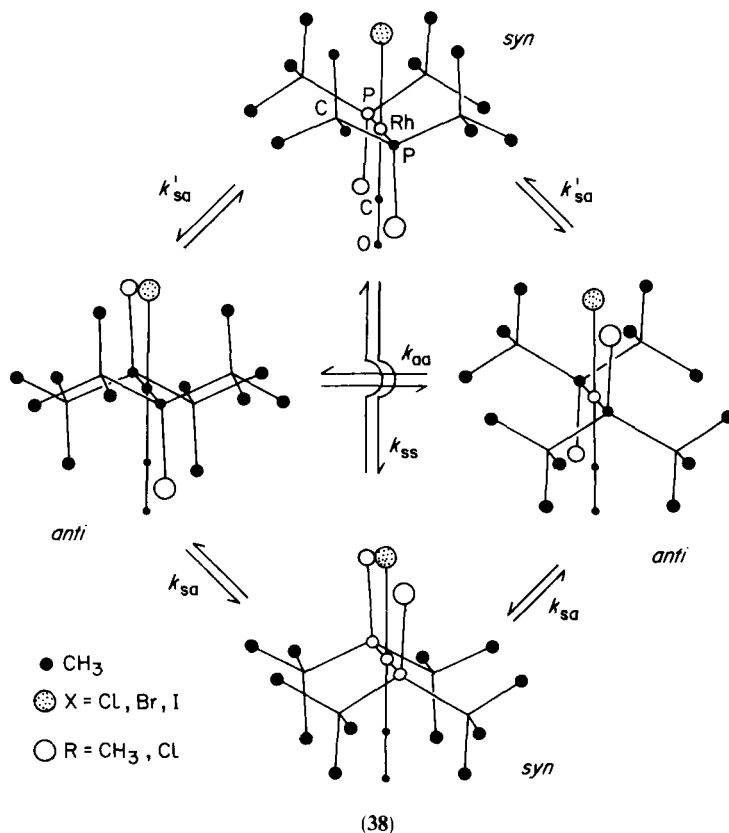
rotation in platinum(II) complexes of bis(pyridin-2-yl)ethane and bis(9-methylhypoxanthine-N^7).[160] Rotation about uranium–nitrogen bonds can be detected by ^{1}H NMR in some uranium(IV) complexes of the type U[η-$(CH_3)_5C_5]_2[\eta^2$-$CONR_2]_2$Cl.[161] These species are paramagnetic, exhibiting isotropic ^{1}H shifts spreading over 100 ppm in some cases. The shifts follow an approximate Curie-law temperature dependence and exhibit very broad coalescence effects. For the complex R = Me, $\Delta G^{\neq}$ (311 K) is estimated to be 52 ± 4 kJ mol^{-1}. Surprisingly, the analogous diamagnetic thorium complexes produce no clearly defined changes in their ^{1}H variable-temperature spectra. One of the first examples of rotation about hafnium–hafnium bonds is afforded by binuclear mixed hydride–tetrahydroborate complexes of hafnium(IV).[162] In [Hf{N(SiMe$_2$CH$_2$PMe$_2$)$_2$}]$_2$(μ-H)$_4$(BH$_4$)$_2$ a barrier energy of 56.3 kJ mol^{-1} has been calculated. The first observation of rotation about a molybdenum–molybdenum triple bond is reported for 1,1- and 1,2-Mo$_2$(NMe$_2$)$_2$(CH$_2$SiMe$_3$)$_4$ from variable-temperature ^{1}H spectra.[163] $\Delta G^{\neq}$
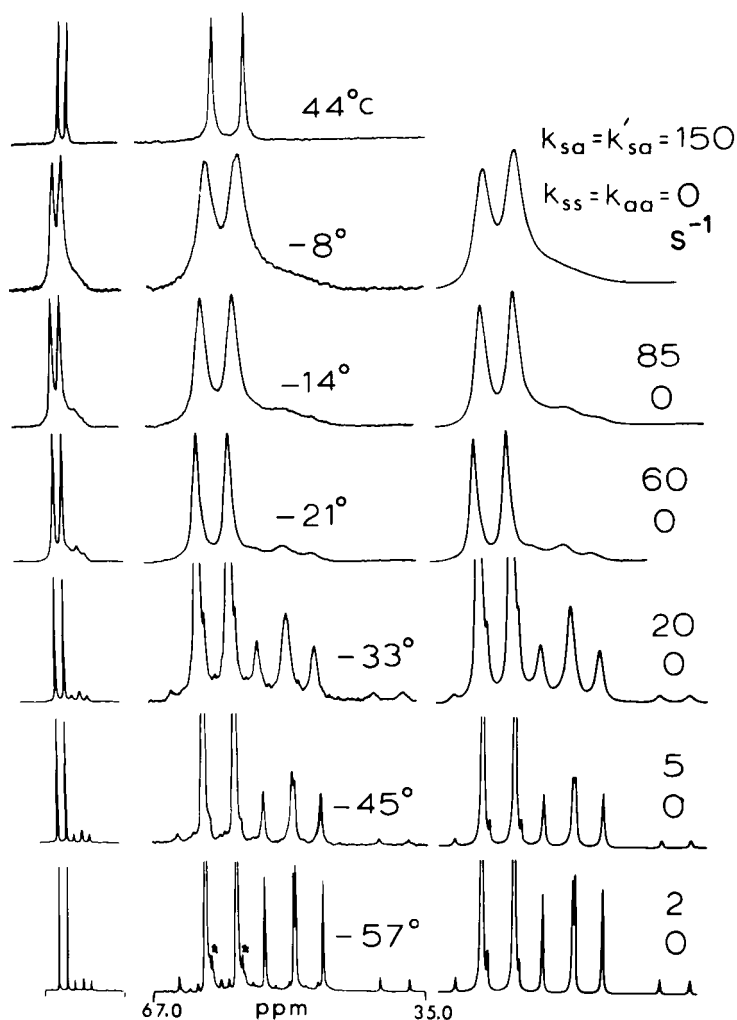
FIG. 10. Experimental and theoretical ^{31}P-$\{^1$H$\}$DNMR spectra (36.43 MHz) of [RhCl(CO)$\{$Bu$^t_2$PCl$\}_2$]. The left-hand and middle columns give the experimental spectra, while the right-hand set of spectra are computer-synthesized using the given values of rate constants. See (38) for definitions of these rate constants.

values for this rotation are 58.8 and 65.5 kJ mol^{-1} respectively. In contrast, the barriers to rotations about Mo–N bonds in these compounds are 43.3 $\pm$ 2 and 63.0 $\pm$ 2 kJ mol^{-1}.

Two new types of fluxional processes that involve formal rotations have been reported. In the chiral tetrahedral organo-transition-metal clusters

$PhC{\equiv}CCO_2CHMe_2[(C_5H_5)NiM]$, $M = (C_5H_5)Mo(CO)_2$, formal rotation of the Ni–Mo and C–C bond vectors takes place at a relatively slow rate $(\Delta G^{\neq} = 86 \pm 2\,kJ\,mol^{-1})$.[164] In the bimetallic complex $MnPt(\mu\text{-}H)(\mu\text{-}CO)(CO)_4(PEt_3)_2(MnPt)$ (39), the ^1H spectra are compatible with an intramolecular fluxion involving apparent rotation of the PtL_2 moiety about the Mn–H bond:[165]

(39)
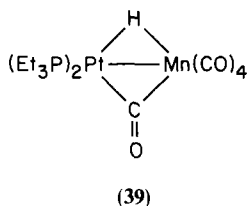
D. Fluxional processes

1. σ-Polyenyl–metal systems

Distinction between 1,2- and 1,3-movements of a metal M around a cyclopentadiene ring is a subtle and challenging DNMR problem, and has been the subject of much debate over the past decade. The weight of evidence strongly favours, but does not conclusively prove, a 1,2-rearrangement. Recent ^{13}C studies[166] on some chiral silylcyclopentadienes $C_5H_5Si*H(R)Cl$ ($R = Me$, Bu^n, or Me_3SiCH_2) and $C_6H_5Si*H(Pr^i)(Me)$ have provided definitive evidence for a 1,2-pathway. The chirality at the Si atom produces anisochronicity among the $C^{2,5}$ and $C^{3,4}$ carbon pairs (40) in the low-temperature ^{13}C spectra:

(40)
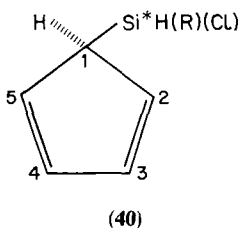
With increasing temperature, the C^2 and C^5 signals, having the greater diastereotopic shift, coalesce more rapidly with C^1 than do C^3 and C^4. This qualitative support for a 1,2-shift mechanism is supported by a full bandshape treatment of this 5-site exchange problem, where it is shown that the 1,2- and 1,3-pathways are distinguishable, and only the former mechanism fits the observed spectral changes. For the $R = Me_3SiCH_2$ and Pr^i

compounds, $\Delta G^{\neq}$ values of 61.3 ± 1.3 and $59.8 \pm 2.7\,\mathrm{kJ\,mol^{-1}}$ respectively are calculated. A study of related compounds has established that the metallotropic rearrangement always occurs with retention of configuration at the migrating centre. The same authors then examined the nature of the metallotropic shifts in indenyl systems (41a–c):[167]
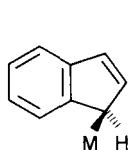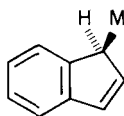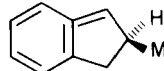
(41a)   (41b)   (41c)

Earlier studies point towards consecutive 1,2-shifts via the energetically less favourable isoindenyl structure (41c). Variable-temperature ^{1}H and ^{13}C studies on polyindenyl derivatives of germanium and tin such as $Ge(ind)_4$, $Sn(ind)_4$, $Bu^nSn(ind)_3$, do not yield any further evidence in favour of a 1,2-shift pathway, but they do show that stereomutation results from the metallotropic shifts. $\Delta G^{\neq}$ values for the process are in the range $60–70\,\mathrm{kJ\,mol^{-1}}$. In compounds of the type $Sn^*MePr^iPh(R)$ ($R = C_5H_4Me$, C_9H_7, C_5Me_5) the chirality of the migrating Sn centre provides further insight into the fluxionality.[168] The NMR spectral changes are consistent with retention of configuration at Sn in all cases. The $R = C_5Me_5$ compound is directly analogous to the unsubstituted cyclopentadienyl systems, and its fluxionality is related to a symmetry-controlled Woodward–Hoffmann [1,5]-migration. For $R = C_5H_4Me$, the dynamic process appears to involve facile epimerization, while for the indenyl derivative ($R = C_9H_7$) stereomutation occurs at elevated temperatures via a suprafacial rearrangement.

Evidence supporting two concurrent metallotropic pathways has been presented from ^{13}C spin-saturation-transfer studies on the cycloheptatrienyl compound $(\eta^5\text{-}C_5H_5)Ru(CO)_2(7\text{-}\eta^1\text{-}C_7H_7)$ (42):[30]
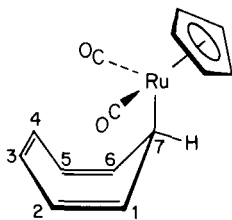
(42)

Saturation at C^7 effected the greatest intensity decrease at $C^{1,6}$, implying that 1,2-migration is clearly occurring. However, smaller intensity decreases at $C^{2,5}$ and $C^{3,4}$ are noted and attributed to 1,4-migrations, the rate constant for the latter being 5–6 times smaller than for the 1,2-migration. Spin-saturation-transfer and line-broadening studies of the E- and Z-isomers of 6,6,6-triphenyl-6-stannahexa-1,3-diene show that only the Z-isomer is fluxional, the probable mechanism being symmetry-allowed suprafacial [1,5]-shifts (43):[169]
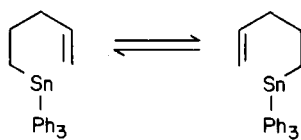
(43)

No evidence for E–Z isomerization is obtained, and the activation energy of the suprafacial shift is calculated to be $81.5 \, kJ \, mol^{-1}$. The fluxionality of η^1-allyl ligands in R_2Zn (R = allyl, methallyl) compounds has been followed by ^1H NMR, and kinetic data have been reported.[170]

2. σ–π-Exchanging polyenyl systems

Fluxional processes that interconvert σ- and π-bonded ligands are well established in polyenyl systems. A recent study[171] of tris(cyclopentadienyl)scandium in THF solvent using ^1H and ^{45}Sc nuclei as NMR probes has established two fluxional processes. The higher-temperature process involves a σ–π exchange between two η^5-Cp rings and one η^1-Cp ring, as evidenced by a 2:1 splitting of the ^1H Cp signal at $-30\,°C$. Further cooling produces a splitting of the smaller peak into a 2:2:1 pattern indicative of a metallotropic 1,5-shift of the $(\eta^5\text{-Cp})_2Sc(THF)$ moiety about the third Cp ring. In toluene-d_8 solvent, dimer formation occurs, complicating the stereodynamics. However, ^{45}Sc NMR has proved a useful diagnostic tool. ^{45}Sc is a high-sensitivity nucleus (relative receptivity $D_H = 0.301$), and its high spin value ($I = \frac{7}{2}$) alleviates the effects of its quadrupole moment to the extent that its line widths are not excessive. Variable-temperature ^{45}Sc spectra provide conclusive evidence for the dimeric species at low temperature.

The reaction of η^5-indenyltricarbonylrhenium $(\eta^5\text{-}C_9H_7)Re(CO)_3$ with trimethylphosphine produces fac-$(\eta^1\text{-}C_9H_7)Re(CO)_3(PMe_3)_2$.[172] A primary aim of this work was to observe the η^3 intermediate, but this proved impossible. It was noted, however, that the rate of $\eta^5 \rightarrow \eta^1$ conversion is much greater than for the corresponding Cp complexes. The η^1 species was obtained as the facial configuration, and this underwent intramolecular 1,3

rhenium migrations, evidence being obtained from the coalescence of the ^{1}H signals from the diastereotopic PMe$_3$ ligands. The $\Delta G^{\neq}$ value for the 1,3-migration is $50.4 \pm 0.4\,\text{kJ mol}^{-1}$, this being substantially higher than for the analogous η^1-Cp compound.

3. π-Polyenyl and π-arene–metal systems

The fluxionality of butadiene–transition-metal complexes has been examined in some detail by ^{1}H NMR. Little was previously known about the fluxional behaviour of η^4-butadiene–metal complexes. Studies on $[(\eta^4$-C$_4$H$_6)$COT]M (M = Ti, Zr, Hf) and related complexes provided evidence of either s-cis-η^4-butadiene (44 a,c) or s-trans-η^4-butadiene conformations:[173]

(44a)   (44b)   (44c)
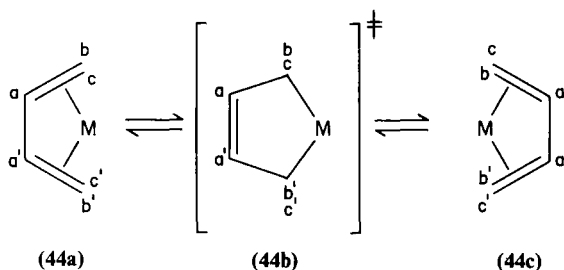
At low temperatures the butadiene protons form an AA'MM'XX' spin system, which changes to an AA'X$_2$X'$_2$ system (Fig. 11). Full bandshape analyses have been performed and activation energy data quoted. In certain cases, the rate process is too slow to fully equilibrate the terminal butadiene protons, and it was necessary to resort to magnetization transfer experiments to confirm the exchange. The fluxional process is thought to proceed via a metallocyclopentene intermediate (44 b). Such a concerted mechanism is favoured, but stepwise mechanisms cannot be totally discounted.

In a series of tetracarbonyl-η-dienechromium(0) complexes $(\eta$-L)Cr(CO)$_4$ (L = open chain and cyclic η-dienes), ^{13}C studies reveal hindered ligand mobility of these formally octahedral complexes.[174] $\Delta G^{\neq}$ data for these movements are in the range $39\text{–}47\,\text{kJ mol}^{-1}$. Trihydridodienerhenium complexes (Ph$_3$P)$_2(\eta$-1,3-diene)ReH$_2$ undergo several rearrangement processes.[175] In order of increasing temperature, these involve ligand interchange, reversible migration of a hydride ligand onto the diene ligand leading to η-allyl species, and, in the case of cyclic dienes, isomerization of the ligand.

The ground-state structures of various transition-metal diene hydride complexes have been shown by NMR to be of the bridge type with a two-electron three-centre M···H···C bond rather than the classical structure
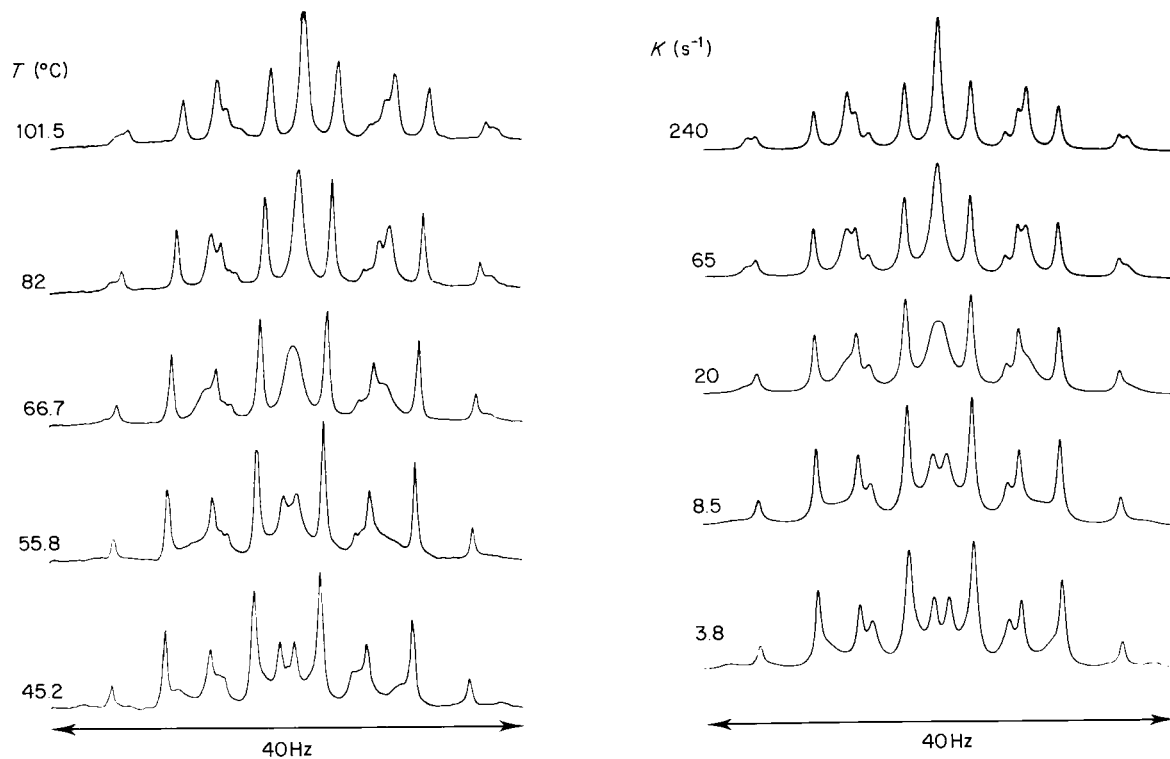
FIG. 11. Experimental (left) and computer-synthesized (right) spectra of the AA′ portion of the AA′MM′XX′ proton spectrum of $[(\eta^4\text{-}C_4H_6)COT]Hf$. The rate constants are based on exchange of proton b with c, and b′ with c′ assuming a concerted mechanism. See (44).

with a terminal metal–hydride bond. In the case of $[IrH(PPh_3)_2L]^+$ ($L = \eta^3$-2,3-dimethylbutenyl),[176] the classical diene dihydride structure (45) is considered as the intermediate for the fluxional process that exchanges the allyl and hydride signals and the Me^2 and Me^3 signals:

(45)
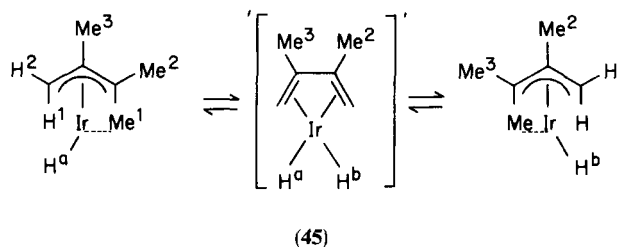
Spin-saturation-transfer experiments show there to be no hydrogen transfer with Me^2 or Me^3. However, deuteriation studies show two D atoms incorporated at Me^1, suggesting a rapid facial rotation of the allyl–Me^1 moiety. Structural characterization of (η^3-cyclohexenyl)manganese tricarbonyl by ^1H and ^{13}C NMR reveal three distinct fluxional processes.[177] The process with lowest activation energy involves the two *endo* C–H bonds adjacent to the π-allyl unit being alternately coordinated to the metal centre (46):

(46)
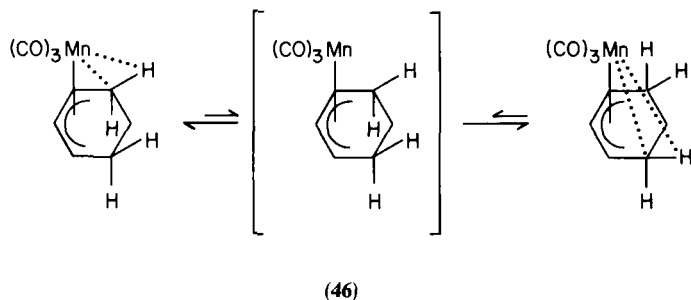
The process is thought to proceed via the symmetrical 16-electron π-allyl species. ^1H NMR spectra in the range -99 to $-9\,^\circ C$ clearly reveal the exchange of bridged and unbridged *endo* C–H signals. The single bridging hydrogen gives rise to an exceptionally low-frequency signal at $\delta = -12.8$. At temperatures between 4 and $119\,^\circ C$ the two *endo*-H signals ($H^n_{1,5}$ and H^n_6) coalesce, as do the remaining *exo*-H (H^x) and olefinic hydrogen signals (Fig. 12). This is clearly indicative of a [1,2]-metal migration about the 6-membered ring (47):
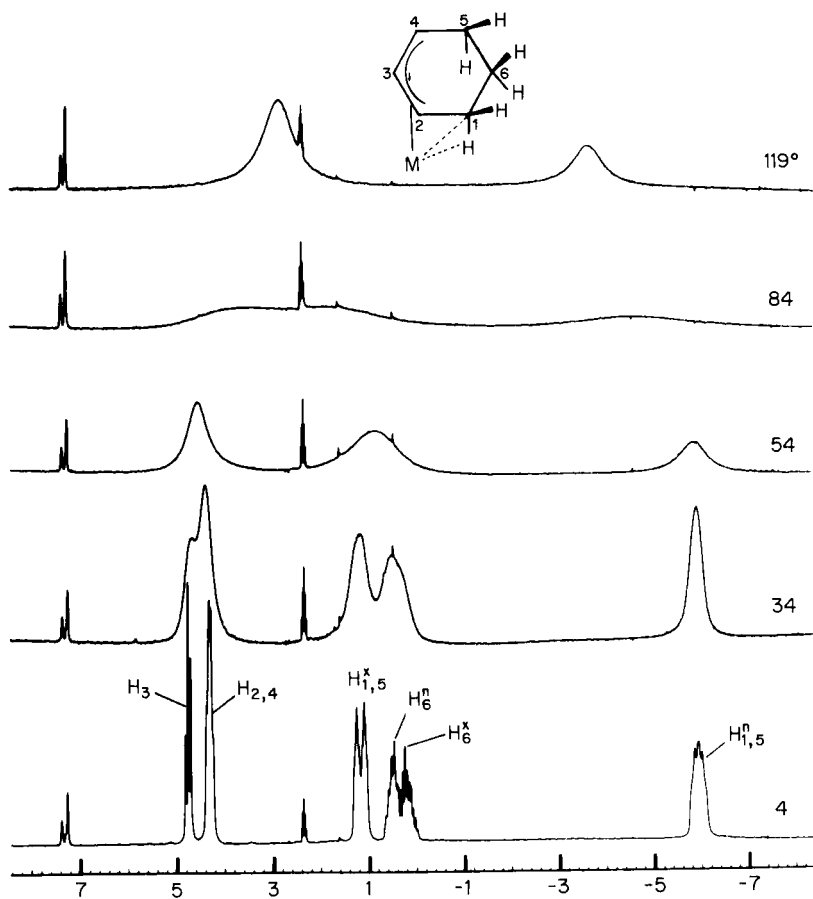
FIG. 12. 100 MHz ^{1}H spectra of cyclohexenylmanganese tricarbonyl in toluene-d_8 solvent.

(47)
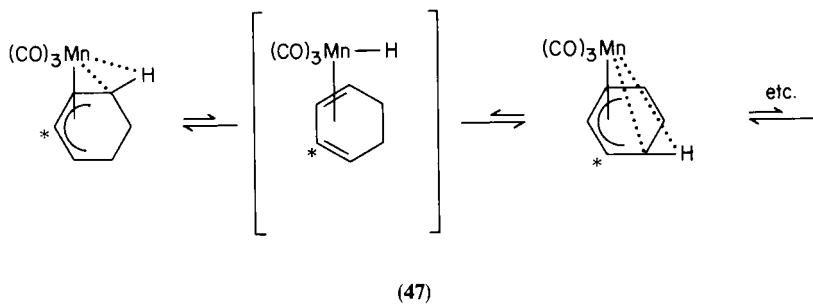
^{13}C–{^{1}H} spectra in the range -40 to $+40\,^\circ$C reveal *cis–trans* carbonyl scrambling as a third isomerization process. Two methyl-substituted butenyl-manganese tricarbonyl complexes also exist as two-electron three-centre M···H···C bond species.[178] They undergo two rearrangement processes. The first involves exchange of the three protons of the bridging methyl group and proceeds through a 16-electron intermediate with free rotation of the methyl group. The process has an activation energy of 37.4 kJ mol^{-1} as determined by bandshape analysis and spin-inversion-transfer experiments. The two methyl derivatives equilibrate at high temperatures via an 18-electron diene hydride species with $\Delta G^{\neq}$ for the process being 72.7 kJ mol^{-1}. It has recently been proposed that the bonding between a metal and a proximal CH bond of a ligand be described as agostic. Systems containing agostic η^3-allylic ligands include η^3-enyl complexes [Ru(η^3-COD)L$_3$]$^+$ (COD = 1,5-cyclooctadiene, L = various phosphines). NMR studies[179] reveal mutual change of the three phosphorus donor ligands, and exchange of the *endo* hydrogens on the two carbons adjacent to the allylic functionality. The complex Cr(COD)(PF$_3$)$_3$H has been characterized by X-ray crystallography. The solid-state structure is retained in solution at temperatures $<80\,^\circ$C. Above this temperature ^{13}C and ^{1}H NMR spectroscopy reveal two fluxional processes as shown in (**48**) and (**49**). The first results in pairwise coalescence of the ^{13}C and ^{1}H signals, while the second leads to two averaged ^{1}H signals (8 : 4 intensity ratio), indicating equivalence of the eight structures of type (**49**).

$$M \equiv Cr(PF_3)_3$$

$$-80\,^\circ C \longrightarrow 60\,^\circ C$$

(**48**)

$$80\,^\circ C \longrightarrow 130\,^\circ C \qquad M \equiv Cr(PF_3)_3$$

(**49**)
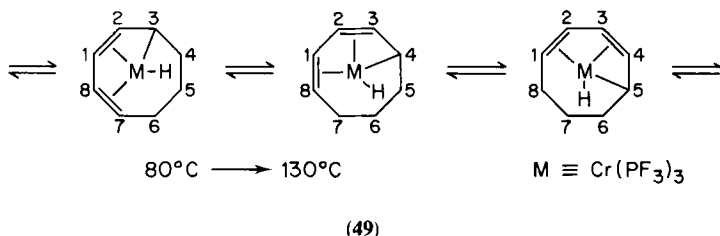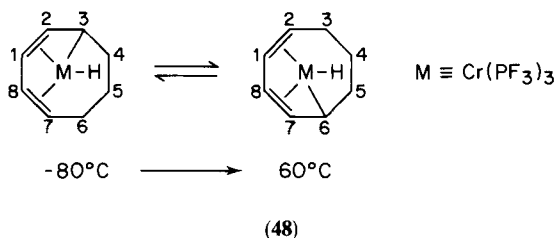
Cyclopentadiene is a highly versatile ligand, exhibiting η^1, η^3 and η^5 hapticities. This list has recently been extended with a recent report of the first η^4-C_5H_6 complex, $(\eta^4$-$C_5H_6)Re(PPh_3)_2H_3$. Variable-temperature and spin-saturation-transfer ^1H experiments have been used to fully characterize the structure and stereodynamics of this complex.[181] At least two distinct fluxional processes occur, one of which involves the *endo* C_5H_6 hydrogen exchanging with the hydride ligands in a manner analogous to the studies described earlier.[176-180] However, further clarification of the precise mechanism is still required. The energies of formation of these two-electron three-centre $M \cdots H \cdots R$ bonds have been measured for aryl complexes $(C_5Me_5)Rh(PMe_3)(R)H$ (R = alkanes, aryl).[182] The aryl complexes are in rapid equilibrium with their η^2-arene derivatives at temperatures above $-15\,^\circ C$. Spin-saturation-transfer studies reveal a [1,2]-shift migration around the ring with $\Delta H^\neq = 68.5 \pm 0.8\,kJ\,mol^{-1}$ and $\Delta S^\neq = -26 \pm 3\,J\,K^{-1}\,mol^{-1}$ for the complex with R = 2,5-$C_6H_3Me_2$. A review has appeared on DNMR studies of fluxional organogold complexes with cyclopentadienyl ligands.[183] The latter ligands are also incorporated in some chiral $(\eta^5$-Cp) zirconium(II) complexes $(\eta^5$-Cp)$(\eta^3$-allyl)Zr$(\eta^4$-butadiene),[184] which undergo fluxional behaviour.

Three interesting studies of fluxionality in cycloheptatriene (CHT) complexes have appeared.[185 187] Proton spin-saturation-transfer experiments have been used to measure the energies of [1,3]-iron shifts in (cycloheptatriene)iron tricarbonyl complexes.[185] $\Delta G^\neq$ values are in the range 84–100 kJ mol^{-1}, and depend on the precise nature of the cycloheptatriene derivative. Extended Hückel MO calculations support the contention that the Fe(CO)$_3$ moiety is shifted towards the interior of the CHT ring in a modified η^2-geometry. Two-dimensional ^{13}C NMR has been used to identify a fluxional process that exchanges carbon 1 with 2, 2 with 5 and 3 with 4 in the cobalt complex (50):[186]

(50)
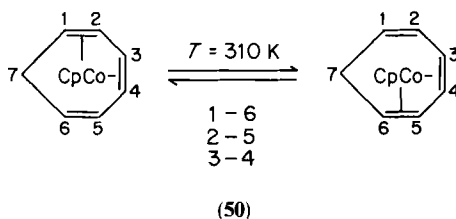
Benn *et al.*[186] were unable to distinguish between a mechanism involving two consecutive 1,2-shifts involving a norcaradiene intermediate and one involving a 1,3-shift. An interesting feature of ref. 186 is the promotion of ^{59}Co as a useful probe for cobalt(I) and cobalt(III) structural studies. In the case of (η^3-

allyl)(η^5-Cp)Co^{III}R complexes (R = Br, benzyl, methyl), shifts range from 1100 to -1300 ppm, relative to $K_3[Co(CN)_6]$. Shifts for cobalt(I) complexes range from -300 to -1300 ppm, with line widths in the range 7–12 kHz. Extended Hückel MO calculations are able to rationalize the variation in ^{59}Co shifts with the HOMO/LUMO energy gap and frontier MO compositions in a series of (η^5-Cp)CoL complexes. In tricarbonyliron complexes with CHT derivatives (51) (E = Si, Ge)[187] the ^{1}H spectra in the temperature range from ambient to 130 °C show coalescences of signals due to H_1 and H_6, H_2 and H_5, and H_3 and H_4, with the H_7 signal remaining sharp:
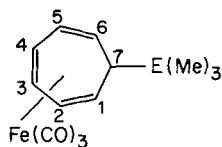
(51)

Rates for this fluxional process have been measured by ^{13}C spin-saturation-transfer experiments, and the activation barriers, based on the coalescence of the ^{1}H signals, are about 75 kJ mol^{-1}. After exploring various possible mechanisms for this fluxion, Li Shing Man et al.[187] favoured a direct [1,3]-iron migration.

4. Carbonyl scrambling

(a) Unimetallic systems. The intramolecular interchange of carbonyl-ligand environments is a well established and well documented area of inorganic stereochemistry. ^{13}C NMR has in the past played a definitive role in describing this phenomenon, and continues to do so. Indeed, the increased sensitivity of modern NMR spectrometers now enables carbonyl fluxionality to be monitored by ^{17}O as well as ^{13}C nuclei.

The activation energies associated with CO scrambling vary greatly. Many unimetallic carbonyl complexes are stereochemically rigid, whereas carbonyl complexes of metal clusters tend in general to be highly fluxional.

Seven-coordinate tungsten complexes of the type $W(CO)_2L(S_2CNR_2)_2$ (L = phosphines, R = Me,Et) are stereochemically nonrigid, and only at -110 °C are the two distinct carbonyl ^{13}C signals observed.[188] No ^{31}P exchange is observed, and various possible mechanisms involving either motion of the phosphine ligands L or of the two chelate ligands have been proposed. In a variety of symmetrically substituted (η-1,3-diene)tricarbonyl iron complexes, the carbonyl groups occupy two distinct environments in the solid state. In solution these environments are rapidly exchanged

($\Delta G^{\neq} \approx 40$–$60\,kJ\,mol^{-1}$) by a probable turnstile-type mechanism consisting of successive $120°$ rotations of the $Fe(CO)_3$ fragment relative to the diene moiety.[189] A number of (η-diene)tricarbonyl complexes of iron, $Cr(CO)_3LL'$ ($L = PMe_3$, $P(OMe)_3$, $L' = \eta^4$-diene), undergo carbonyl scrambling, with activation barriers in the range 40–$50\,kJ\,mol^{-1}$. Mechanisms involving trigonal-prismatic transition-state structures have been proposed.[190] Molybdenum(0) and tungsten(0) complexes of the type $Mo(CO)_2(\eta^4$-diene)$[P(OMe)_3]_2$ exhibit temperature-dependent ^{13}C and ^{31}P spectra associated with hindered ligand mobilities in these formally octahedral complexes.[191] These ligand movements that induce scrambling of the carbonyl environments are again explained in terms of trigonal-prismatic transition states and octahedral intermediates. $\Delta G^{\neq}$ (273 K) values are in the range 42–$64\,kJ\,mol^{-1}$. Carbonyl scrambling arises from a *cis–trans* intramolecular isomerization of $M(CO)_4(^{13}CO)PR_3$ ($M = Cr$, $R = Et$, $M = W$, $R = OMe$, Me, Et, Pr^i) complexes.[192] The rate of scrambling is found to decrease with $PMe_3 > PEt_3 > PPr^i_3$ for the tungsten complexes. The activation parameters suggest a considerable reorganization in the transition state, with little metal–ligand bond breaking.

(b) Bimetallic systems. A short review that highlights certain recent multinuclear NMR studies of transition metal carbonyl clusters has appeared.[193] It covers ^{13}C and ^{17}O studies of bi-, tri- and tetrametallic systems, the metals being iron, cobalt, osmium and ruthenium. The bimetallic (binuclear) species described are $Fe_2(CO)_6X$ ($X = S$, SMe, SPh). Distinction between a localized and delocalized carbonyl exchange can be made from the observation of ^{57}Fe satellites (2.2% relative intensity) ($^1J(Fe–C) = 26.9$–$29.3\,Hz$), which are only consistent with a polytopal rearrangement occurring within each $Fe(CO)_3$ moiety. Detection of such satellites, however, usually requires ^{13}CO-enriched materials.[194]

The triply bonded dimolybdenum complex $Cp_2Mo_2(CO)_3P(OMe)_3$ exhibits temperature-dependent ^{13}C spectra in the range -95 to $33\,°C$,[195] which can be interpreted in terms of localized exchange between the bridging carbonyls, with the third terminal CO being unaffected. Other triply bonded species to exhibit carbonyl scrambling are $Re_2Cl_4(dppm)(CO)_n$ (dppm = bis(diphenylphosphinomethane); $n = 1$ or 2).[196] The likely mechanisms of these movements depend on whether one or two CO ligands are attached. The fluxion of the monocarbonyl species keeps the CO ligand bound to a single ligand, whereas the dicarbonyl compound undergoes a "merry-go-round" process, as has also been observed for $Mn_2(CO)_6(dppm)_2$,[197] where the six carbonyls are exchanged as in (52). In the related compound $Mn_2(CO)_5(dppm)_2$ a concerted wagging process occurs, which disrupts the Dewar–Chatt portion of the 4-electron donor carbonyl.

(52)
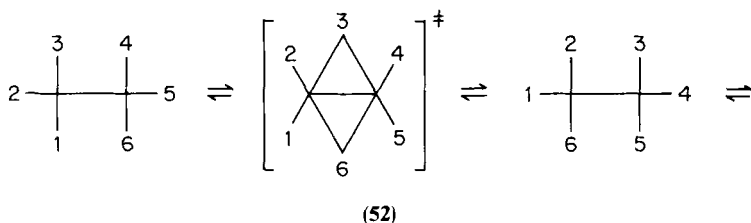
Mixed bimetallic complexes of type $MM'(CO)_6(DAB)$ $(DAB = 1,4\text{-}$ diazabutadiene) $(M = Mn, Re)$ undergo two distinct types of fluxionality.[198] One involves exchange between the σ- and π-coordinated parts of the DAB ligand; the other involves exchange of the semibridging and terminal CO groups. Bridge–terminal carbonyl exchange has also been observed in $Co_2(CO)_8$ in the solid state by variable-temperature MAS ^{13}C NMR spectra.[41] At room temperature a single ^{13}C resonance is observed. On cooling the solid, this signal splits into two, each with its own series of spinning sidebands owing to the sample spin rate being considerably less than the static inhomogeneous line width (estimated to be *ca.* 400 ppm at $-70\,°C$). However, use of the TOSS pulse sequence mentioned earlier[42,43] enables the two isotropic signals due to the bridging and terminal carbonyls to be detected. The activation energy for bridge–terminal CO exchange has been estimated to be approximately $50\,kJ\,mol^{-1}$. This fluxional behaviour of $Co_2(CO)_8$ is unprecedented, since the closely related molecules $Fe_2(CO)_9$ and $(\eta^5\text{-}Cp)_2Fe_2(CO)_4$ are static in the solid state, although the latter is fluxional in solution.[199]

(c) Trimetallic systems. The stereodynamics of the iron-group compounds $M_3(CO)_{12}$ $(M = Fe, Ru, Os)$ have been extensively studied in the past. For the iron and ruthenium compounds the carbonyl exchange is very rapid, while for the osmium compound it is relatively slow and causes carbonyl signal coalescence at *ca.* $70\,°C$. In recent years a wide variety of derivatives of the parent $M_3(CO)_{12}$ structure have been examined in order to shed further light on the bonding and fluxionality in these clusters. For example, mixed osmium/ruthenium complexes $MM'_2(CO)_{12}$ have been examined.[200] In the case of $RuOs_2(CO)_{12}$, a single averaged ^{13}CO signal is observed at high temperatures, but on cooling to $30\,°C$ it splits into two (intensity ratio $10:2$), which are due to the terminal and bridging carbonyls respectively. Replacement of a single carbonyl by another ligand as in $[Fe_3(CO)_{11}L]$ $(L = PR_3$ or $P(OR)_3)$ leads to species that undergo polyhedral rearrangements of the twelve ligands involving icosahedral structures via cube-octahedral transition states as postulated for the parent $Fe_4(CO)_{12}$ compound.[201] The osmium complex $(\mu\text{-}H)Os(CO)_{10}(\mu\text{-}\eta^2\text{-}CPh{=}CHPh)$ contains a triangular array of

Os atoms with the stilbenyl ligand bridging one Os–Os edge and forming a σ-bond to one Os atom and a π-bond to the other. The third osmium atom has four coordinated carbonyls. Low-temperature ^{13}C studies reveal ten separate CO signals due to the static structure. On warming to $-12\,°C$, exchange occurs between four pairs of CO signals, the signals due to the two axial carbonyls of the $Os(CO)_4$ moiety being unaffected. These changes are consistent with a mechanism involving facile exchange of the σ- and π-bonds between the H-bridged Os atoms. A $\Delta G^{\neq}$ value of $47.5\,kJ\,mol^{-1}$ has been calculated for this process.[202]

The complex $[Os_3(CO)_{10}(HC{\equiv}CCMe_2OH)]$, where 3-hydroxy-3-methylbut-1-yne is behaving as a μ_3-ligand, appears to undergo two mechanistically distinct localized CO exchanges at separate $Os(CO)_3$ moieties, followed by total CO scrambling at temperatures above ca. $-25\,°C$.[203] The complexes $H_2Os_3(CO)_{10}L$ (53), where L can be one of a number of Lewis bases such as CO, phosphines, phosphites, arsines, amines, halides, etc, display both hydride and carbonyl fluxionality:[204, 205]

(53)
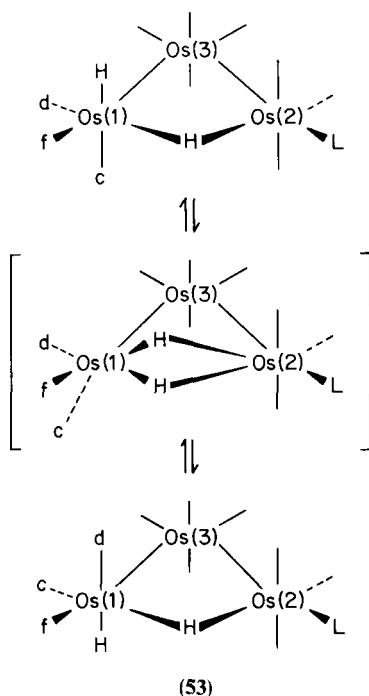
Each of these complexes contains a single axial L ligand, terminal hydride ligand and bridging hydride ligand. Variable-temperature ^1H and ^{13}C studies

reveal that both hydride ligands and two carbonyl ligands undergo simultaneous fluxional exchange. Both Aime *et al.*[204] and Keister and Shapley[205] suggest a turnstile-like movement of the axial and bridging hydrides and axial and equatorial carbonyls about the Os–CO(f) axis (**53**). It is not possible to decide which of the two equatorial carbonyls *cis* to the axial hydride is involved in exchange. In some complexes (L = CNMe and CNBu^t) the ligand occupies an axial position. The same type of turnstile mechanism is proposed in this case, but the averagings of the CO signals are somewhat different. $\Delta G^{\neq}$ data for these fluxions are in the range 46–$58 \, kJ \, mol^{-1}$, but accurate measurements are somewhat limited by sample decomposition.

The osmium cluster $[H_2Os_3(CO)_{10}]$ (**3**) has been the subject of saturation-transfer[28] and 2-dimensional exchange[61] techniques, as mentioned in Section II. Both techniques establish the existence of localized carbonyl exchange involving the two types of carbonyls on the $Os(CO)_3$ moieties. For two-site exchange problems of this type there is little to choose between the two techniques, as they both give reliable quantitative data. Using the saturation-transfer technique, a rate-constant value of $1.08 \, s^{-1}$ (i.e. $0.36 \times 3 \, s^{-1}$) is obtained[28] at 300 K, as opposed to $1.21 \, s^{-1}$ obtained by the 2D NOESY method.[61] It has also been shown[28] how an estimate of the quadrupole coupling of ^{17}O in the enriched complex together with $^{17}O \, T_1$ measurements can provide an estimate of the correlation time for molecular reorientation in solution. Two-dimensional NMR studies provide a more efficient and equally accurate way of studying multisite exchange problems, as has been demonstrated earlier. The ruthenium cluster $[HRu_3(CO)_9(MeCCHCMe)]$ provides an example of a three-site exchange problem, since scrambling occurs between the three types of CO on each $Ru(CO)_3$ moiety. The three derived rate constants are all virtually equal in magnitude, implying a concerted mechanism. Analysis of the 2D data also provides a value for the $^{13}C \, T_1$ relaxation time, which has been checked independently using the 1D inversion-recovery method. Further insight into the mechanism of localized carbonyl scrambling has been obtained from a ^{13}C study of the chiral cluster $HRu_3(CO)_8[PMe(CH_2Ph)Ph](\mu_3\text{-}C_2CMe_3)$.[206] Two mechanisms — successive pairwise exchange of two of the three ligands, and simultaneous pinwheeling of all three ligands (a pseudo-C_3 rotation) — have been considered. The observed low- and high-temperature limiting ^{13}C spectra are consistent only with the C_3 rotation process. Kinetic deuterium isotope effects on the axial–radial carbonyl exchange at the hydride-bridged metal atoms are observed in $H(\mu\text{-}H)Os_3(CO)_{10}L$ and $(\mu\text{-}H)Ru_3(CO)_9L$ complexes, but not in $(\mu\text{-}H)_2Os_3(CO)_{10}$.[207] The sizes of the effect are small, but they do throw some light on the nature of the carbonyl migrations. A detailed study of hydrido metal clusters $[HM_3(CO)_9(MeC\!=\!C\!=\!CMe_2)]$ (M = Ru, Os) has been reported.[208] For the ruthenium complex the variable-temperature ^1H and ^{13}C spectra may be rationalized in terms of edge-hopping of the hydride

ligand and a simultaneous wagging of the organic ligand. A barrier of $56\,kJ\,mol^{-1}$ has been measured for this process. This value is substantially lower than that calculated for the osmium analogue ($81\,kJ\,mol^{-1}$), where the latter refers with certainty to the organic ligand motion but not necessarily to the edge-hopping hydride motion. Variable-temperature ^{13}C NMR has been combined with UV–PES and theoretical studies to investigate the bonding in $Fe_3(CO)_9(\mu_3-\eta^2EtC{\equiv}CEt)$.[209] Localized carbonyl exchange at each $Fe(CO)_3$ moiety occurs. Formation of the cluster anion $[Ru_3(CO)_9(C_2Bu^t)]^-$ enables its fluxionality to be compared with the neutral hydrido cluster compound.[210] Both localized axial–radial and intermetallic carbonyl exchange occur, with both processes having barriers lower than in the parent neutral complex, the difference in energy being $20\,kJ\,mol^{-1}$ in the case of the localized carbonyl exchange. Halogen atoms can act as μ_1- or μ_3-bridging ligands in cluster compounds. The structures of $Ru_3(\mu-H)(\mu-X)(CO)_{10}$ ($X = Cl$, Br or I) and $Ru_3(\mu-H)(\mu_3-I)(CO)_9$ have been established by X-ray data and their carbonyl fluxionality followed by ^{13}C NMR.[211] For the first group of complexes localized CO scrambling occurs in each $Ru(CO)_3$ unit, with a coalescence temperature of $-40\,°C$. In contrast, in the triply bridged iodo complex, total carbonyl scrambling is rapid at temperatures above $-80\,°C$.

Other studies of osmium clusters have been concerned with $[H_3Os_3(CO)_9(SiPh_3)]$,[212] $[Os_3(CO)_{10}(PMe_2Ph)_2]$[213] and $[Os_3(CO)_9(PMe_2Ph)_3]$.[213] The trihydrido cluster contains the formally unsaturated $Os(\mu-H)_2Os$ unit, a singly H-bridged Os–Os bond and an unbridged Os–Os bond. ^1H NMR studies reveal that the hydrides in $Os(\mu-H)_2Os$ undergo mutual exchange and exchange at a slower rate with the third hydride. ^{13}C studies show rapid exchange of the carbonyls associated with the $Os(\mu-H)_2Os$ moiety only. The tertiary-phosphine complexes[213] exist as isomeric mixtures. ^{13}C and ^{31}P NMR studies establish the existence of localized and delocalized carbonyl exchanges and the nonexistence of intramolecular phosphine transfer.

^{13}C and ^1H NMR spectroscopy has been used to investigate the fluxionality of a number of mixed trimetallic carbonyl clusters. In the complex $FeCo_2(\mu_2-CO)(CO)_7(\mu_2-PPh_2)_2$ (54) four distinct carbonyl exchanges occur:[214]

(54)
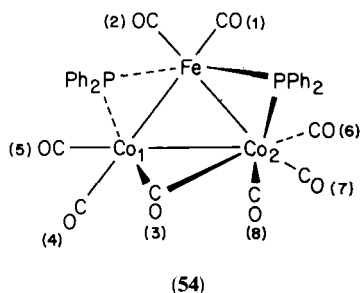
At $-62\,^\circ C$, the carbonyls 3,4,5 associated with Co_1 undergo a turnstile rotation. This is followed at $-35\,^\circ C$ by a similar rotation on Co_2. The carbonyls 1,2 on the Fe atom then undergo mutual site exchange. Finally, at $-15\,^\circ C$, all six cobalt-bound carbonyls exchange. A mixed Fe/As/Mo cluster of type $[(CO)_4Fe(\mu\text{-AsMe}_2)Mo(CO)_2(C_5H_5)]$ undergoes three different fluxional processes, of which two are correlated.[215] These involve mutual exchanges of the As methyls and of the Mo carbonyls with an energy $(\Delta G^{\neq})$ of $47.9 \pm 0.8\,kJ\,mol^{-1}$. The third uncorrelated process involves exchange of the Fe and Mo carbonyls $(\Delta G^{\neq} = 59.6 \pm 2\,kJ\,mol^{-1})$. Finally, the trirhenium cluster $Re_3(\mu\text{-H})(\mu_3\text{-H})(CO)_{10}(\eta^5\text{-}C_7H_9)$ exhibits fluxionality of the cyclo-heptadienyl ligand together with scrambling of the carbonyls on the $Re(CO)_2$ moiety.[216] This is rationalized in terms of a complete interchange of the CO and C_7H_9 coordination sites together with a concerted up/down movement of the triply bridged hydride through the plane of the Re_3 triangle. At $-100\,^\circ C$ all fluxionality is frozen, with the ten CO groups and all the hydrogens of C_7H_9 giving distinct signals.

(d) Polymetallic systems. The use of high-pressure ^{13}C NMR techniques for studying high-nuclearity carbonyl transition-metal clusters has been impressively demonstrated.[217-223] The cluster $[Rh_5(CO)_{15}]^-$ is formed from $[Rh_{12}(CO)_{30}]^{2-}$ with 5 bar pressurization of CO. The cluster is a regular trigonal bipyramid, with six apical carbonyls, three equatorial bridging carbonyls, and six carbonyls bridging the equatorial/apical edges. At room temperature all the carbonyls except the three equatorial carbons undergo exchange. $^{13}C\text{-}\{^{103}Rh\}$ spectra have also been obtained, and the rhodium–carbon coupling $^1J(Rh\text{-}C_{eq})$ found to be $32.7\,Hz$.[217]

The cluster $[Rh_{10}S(CO)_{22}]^{2-}$ has been shown by ^{103}Rh, ^{13}C and $^{13}C\text{-}\{^{103}Rh\}$ NMR to have a solution structure at low temperatures[218]
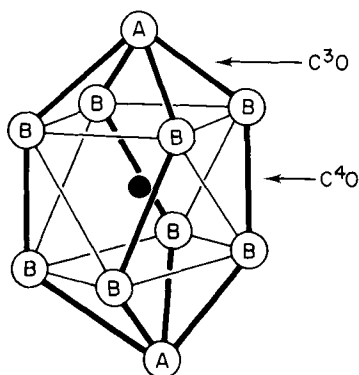
(55)

consistent with that of the solid state. This involves two types of rhodium atoms, two square-capping atoms Rh_A and four square-antiprismatic atoms Rh_B (55).

Warming a solution of this complex to 60 °C produces a poorly resolved multiplet, which collapses to a singlet on irradiation at a *single* rhodium frequency. This implies complete fluxionality of both the carbonyl and metal polyhedra. At 95 °C the cluster converts to $[Rh_{17}(S)_2(CO)_{32}]^{3-}$. The nickel-capped rhodium cluster $[NiRh_6(CO)_{16}]^{2-}$ has also been structurally identified by $^{13}C-^{103}\{Rh\}$ NMR, and its fluxionality examined.[219] Two independent CO migrations occur. The lower-energy process involves concomitant exchange of C_bO, C_dO and C_fO (56) and resembles a rotation on Rh_B:
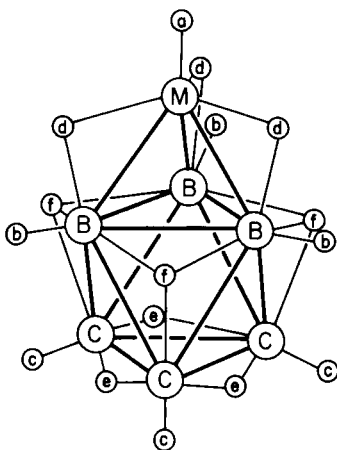
(56)

At higher temperatures (25 °C) the terminal C_cO and edge-bridging C_eO carbonyls also exchange around the Rh_{3c} face. At 90 °C total CO fluxionality occurs. Other bimetallic clusters that have been investigated are $[Fe_2Rh(CO)_{10}]^-$, $[Fe_2Rh(CO)_{11}]^-$, $[FeRh_4(CO)_{15}]^{2-}$, $[Fe_2Rh_4(CO)_{16}]^{2-}$ and $[FeRh_5(CO)_{16}]^-$. Various types of carbonyl fluxionality have been detected, but none of the compounds show rearrangement of the metal polyhedron.[220] Multinuclear NMR studies have been performed on $[Rh_9E(CO)_{21}]^{2-}$, $[Rh_{10}E(CO)_{22}]^{3-}$ (E = P or As) and $[Rh_{12}Sb(CO)_{27}]^{3-}$. The solid-state structure of $[Rh_9E(CO)_{21}]^{2-}$ (57) has been shown[221] to contain three types of terminal carbonyls (C^1O, C^2O and C^3O) associated with Rh_A, Rh_B and Rh_C (ratio 1:4:4). There are also three types of edge-bridging carbonyls C^4O, C^5O and C^6O (ratio 4:4:4).

(57)
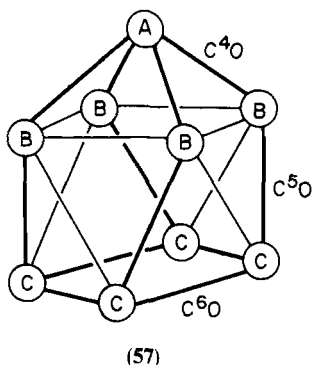
Variable-temperature ^{13}C spectra of $[Rh_9P(CO)_{21}]^{2-}$ are shown in Fig. 13. The cluster was examined as the $[Cs\{Me(OCH_2CH_2)_4OMe\}]^+$ salt. The low-temperature $(-90\,°C)$ spectrum has been unambiguously assigned using $^{13}C-\{^{103}Rh\}$ and $^{13}C-\{^{31}P\}$ experiments. Values of $^1J(Rh–CO)$ are in the range 22–97 Hz, the variation being attributed to asymmetric CO bridging with short Rh–carbonyl bonds giving rise to high values of $^1J(Rh–CO)$. On raising the solution temperature, all the carbon resonances broaden simultaneously until a broad band is observed at room temperature, which collapses to a sharp doublet on irradiation at a single Rh frequency. This implies carbonyl–metal skeletal fluxionality. Mechanisms involving either a D_{3h} tricapped trigonal-prism intermediate or a Rh–Rh bond-breaking/remaking process are proposed. The Rh_{12} cluster compound is highly nonrigid, and its static structure cannot be examined by NMR. The fluxionalities of a variety of mixed platinum–rhodium carbonyl clusters, $[PtRh_5(CO)_{15}]^-$, $[PtRh_4(CO)_{14}]^{2-}$ and $[PtRh_4(CO)_{12}]^{2-}$, have been examined by multi-nuclear NMR.[222] The first two clusters are related to $[Rh_6(CO)_{16}]^-$ and $[Rh_5(CO)_{15}]^-$, where a $Rh(CO)_2$ group has been replaced by a $Pt(CO)$ moiety. In addition to localized carbonyl scramblings in these species an equilibrium exists between $[PtRh_4(CO)_{14}]^{2-}$ and $[PtRh_4(CO)_{12}]^{2-}$. Some novel mixed copper–iron carbonyl clusters, $Na_3[Cu_3Fe_3(CO)_{12}]$, $Na_3[Cu_5Fe_4(CO)_{16}]$ and $Na_2[Cu_6Fe_4(CO)_{16}]$, have been reported.[223] ^{13}C and ^{17}O studies indicate total CO fluxionality at room temperature, and evidence of a reduced rate of CO scrambling has been obtained only in the case of $Na_3[Cu_5Fe_4(CO)_{16}]$. ^{63}Cu NMR data have been reported for these species.

The mixed-metal clusters $H_2FeRu_3(CO)_{12}L$ (L = PMe_2Ph, PMe_3) and $H_2FeRu_3(CO)_{11}L_2$ (L = PMe_3, PPh_3, $P(OMe)_3$, $P(OEt)_3$) undergo a variety of fluxional processes analogous to those exhibited by the parent cluster $H_2FeRu_3(CO)_{13}$. These involve bridge–terminal CO exchange localized on
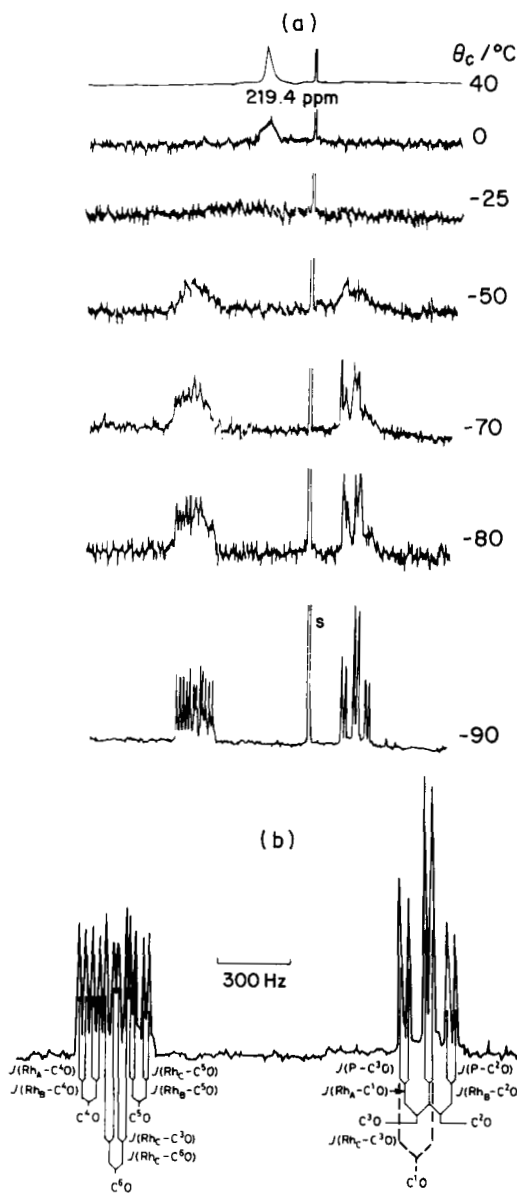
FIG. 13. (a) Variable-temperature 25 MHz ^{13}C spectra of $[Cs\{Me(OCH_2CH_2)_4 OMe\}]_2[Rh_9P(CO)_{21}]$; (b) expansion of spectrum at $-90\,°C$. $S = (CD_3)_2CO$ (solvent).

the iron atom, cyclic exchange of the carbonyls about the triangular face of the cluster that possesses the bridging carbonyls, and rearrangement of the metal framework with a corresponding shift of the hydride and carbonyl ligands.[224] This latter rearrangement leads to a facile $C_s \rightleftharpoons C_i$ isomerization of the monosubstituted derivatives. A study[225] of the solution structures of $Co_4(CO)_{12}$ and $HFeCo_3(CO)_{12}$ using ^{17}O NMR shows them to possess the C_{3v} geometries found in the solid state, previous ^{13}C studies having given ambiguous information. Variable-temperature ^{17}O spectra reveal nonselective CO scrambling in $Co_4(CO)_{12}$, but three distinct types of CO movement in $HFeCo_3(CO)_{12}$. These involve different rates of exchange of the bridging CO with the nonequivalent carbonyls of each $Co(CO)_2$ moiety, followed, at the highest temperatures, by involvement of the $Fe(CO)_3$ carbonyls.

The iron cluster $[HFe_4(CO)_{13}]^-$ exists at room temperature as an equilibrium mixture of two hydride species.[226] Low-temperature $(-80\,^\circ C)$ ^{13}C studies show two hydride signals $(\delta = -24.9$ and $-16.9)$, which are assigned to species with a butterfly Fe_4 geometry and a closed tetrahedral Fe_4 geometry respectively. The latter species undergoes rapid total carbonyl scrambling at $-80\,^\circ C$.

Two recent studies of iridium clusters have appeared.[227,228] Substituted clusters of the types $Ir_4(CO)_{12-n}(RNC)_n$ $(n = 1, ..., 4; R = Bu^t, Me)$ and $Ir_4(CO)_9(\mu_2\text{-}CO)_2(\mu_2\text{-}SO_2)_2$ both have interesting stereodynamics. The isonitrile derivatives,[227] which in most cases have structures related to $Ir_4(CO)_{12}$ and possess only terminal carbonyl ligands, undergo a CO scrambling that is the formal reverse of the $C_{3v} \rightarrow T_d$ scrambling proposed for $Rh_4(CO)_{12}$. The cluster $Ir_4(CO)_9(\mu_2\text{-}CO)_2(\mu_2\text{-}SO_2)$ exhibits variable-temperature ^{13}C spectra that can be rationalized in terms of two different types of CO migration. A DANTE sequence magnetization-transfer experiment has been used to confirm the mechanism of the lower-energy process.

5. Scrambling of organic ligands around metals

This section covers a wide variety of intramolecular rearrangements of ligands coordinated to metals. It is subdivided according to the number of metal centres in the complexes. In the subsection immediately following on unimetallic systems the papers are grouped according to the different ligand types.

(a) Unimetallic systems. There have been a number of reports on dionato ligand complexes. The ligand 1,1,1,5,5,5-hexafluoro-2,4-pentanedione (hfac) forms 5-coordinate complexes with palladium(II)[229,230] and platinum(II)[230] of type $[M(hfac)_2L]$, where L = tertiary phosphine. The solid-state and solution geometries of the complexes have been characterized by X-ray and

NMR methods respectively. All the complexes have distorted square-pyramidal structures. Variable-temperature studies reveal stereochemical nonrigidity. For the complex [Pd(hfac)$_2$P(o-tolyl)$_3$] a ^{19}F total-bandshape study[229] led to values of $\Delta H^{\neq} = 32.3 \pm 4\,\text{kJ mol}^{-1}$ and $\Delta S^{\neq} = -84 \pm 20\,\text{J K}^{-1}\,\text{mol}^{-1}$ for the fluxional process, which is thought to proceed via a C_{2v} square-pyramidal transition state. In the more recent study[230] two kinds of twist mechanisms are proposed. Gallium(III) and indium(III) complexes of the dionato ligands RCOCHCOR', where R = Me, Ph, aryl, etc. and R' = CF$_3$ or CHF$_2$, are also nonrigid at ambient temperatures.[231] The gallium complexes exhibit ^{19}F signal coalescences between 40 and 90 °C, whereas the indium complexes exhibit slow exchange only below -100 °C. The exchange is associated with $fac(cis)$–$mer(trans)$ interconversion of these complexes. $\Delta G^{\neq}$ data for the gallium complexes are around 88 kJ mol^{-1}. Similar values are obtained for Ga(MeCOCHCOCF$_3$)$_3$ and Al(MeCOCHCOCF$_3$)$_3$ from ^{1}H bandshape studies.[232] The configurational inversion $\Delta \rightleftharpoons \Lambda$ of a variety of dionato complexes of titanium(IV) has been followed by ^{1}H NMR.[233] The complexes of type [TiL$_2$(OR)$_2$] (L = MeCOCHCOMe, Bu^{t}COCHCOBu^t; R = CH$_2$Ph, CH$_2$CHMe$_2$, CHMe$_2$ or CMe$_2$Ph) undergo inversion and R-group exchange. Both processes occur at comparable rates by a common intramolecular mechanism. Activation-energy data $\Delta G^{\neq}$ are in the range 65–85 kJ mol^{-1}. The ratio of rate constants $k_{\text{inv}}/k_{\text{ex}}$ decreases from $ca.$ 2 to $ca.$ 1 with increasing size of alkoxide ligand. This is consistent with a twist about the various C_3 axes rather than a bond-rupture mechanism, a conclusion further supported by (i) $\Delta H^{\neq}$ values increasing with increasing bulk of the OR group, (ii) negative values of $\Delta S^{\neq}$, and (iii) lack of solvent effects on the rates. Activation-energy data have also been reported for $\Delta \rightleftharpoons \Lambda$ configuration inversion in [TiL$_2$(OPr^i)$_2$], where HL is a salicylideneamine.[234]

A series of studies have been made of the intra- and intermolecular exchange processes exhibited by metal aminecarboxylates in solution.[235-239] The Zn^{II}–iminodiacetate complex Zn(IDA)$_2^{2-}$ exhibits intramolecular ligand scrambling ($\Delta G^{\neq}$(298 K) $\sim$ 60 kJ mol^{-1}) and intermolecular ligand exchange, the latter being considered to involve both unprotonated and mono-protonated iminodiacetate anions.[235] Exchange studies of ethylenebis(oxy-ethyleneamino)tetraacetic acid (EGTA) complexes are complicated by the uncertainty of the metal chelate structure (**58**) or (**59**):

(58)   (59)
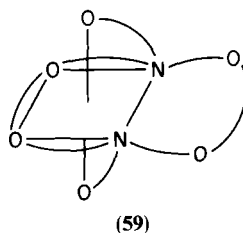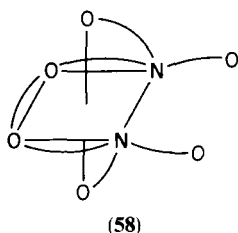
Proton bandshape studies[236] have been performed on M(EGTA) complexes. Ether-oxygen coordination structures (59) have been suggested for M = Sc^{III} and Lu^{III}, but not for M = Mg^{II}, Ca^{II}, Sr^{II}, Ba^{II}, Y^{III}, La^{III}, Zn^{II} and Pb^{II}. The ligand-scrambling process is thought to proceed either by rupture of M–O bonds ($\Delta \rightleftharpoons \Lambda$ inversion) or by rupture of M–O and M–N bonds (N inversion). Complexes of the ligand *meso*-(2,3-butylenediamine)tetraacetic acid (BDTA) have been closely examined by ^{1}H NMR. Alkaline-earth complexes [237] undergo fast $\Delta \rightleftharpoons \Lambda$ inversion on the NMR time scale, while N inversion proceeds at a NMR measurable rate for calcium and strontium complexes. However, the inversion rate is too slow for the magnesium chelate and too rapid for the barium chelate. The lead complex[238] exhibits moderately slow N inversion ($\Delta H^{\neq} = 70 \pm 3\,\text{kJ mol}^{-1}$, $\Delta S^{\neq} = -4 \pm 8\,\text{J K}^{-1}\,\text{mol}^{-1}$) but fast $\Delta \rightleftharpoons \Lambda$ inversion. The same is true for Zn, Cd, Sc and La chelates.[239]

The novel diastereotopic exchange occurring in the chiral square planar complex (N,N'-dimethylethylenediamine)bis(guanosine)platinum(II) has been followed by ^{1}H NMR.[240] Six diastereoisomers, classified into three sets RR, SS and SR, arise from the configuration of the two coordinated ethylenediamine nitrogens. However, the ribose moieties of the guanosine ligands lower the symmetry to such an extent that all six stereoisomers possess different physical and chemical properties. At high temperatures rapid rotation about the Pt–guanosine bond produces exchange within each pair of diastereoisomers. At low temperature ($-32\,^\circ\text{C}$), the complex spectrum is attributed to slow exchange within the SR pair and within either the RR or SS pairs, while exchange in the third pair is appreciably faster. The neutral pyridine–imine ligand (6-R—py—2-CH=N—R') reacts with $[M(O_3SCF_3)]$ (M = Ag^I or Cu^I) to give ionic complexes.[241] When R' is the prochiral group Pr^i or the chiral (S)-CHMePh, the metal centres are tetrahedral, with either Δ or Λ configurations, Λ being more abundant. These complexes have been subjected to a whole range of NMR techniques, namely ^{1}H, ^{1}H-$\{^{109}\text{Ag}\}$, INEPT ^{15}N and INEPT ^{109}Ag. The last mentioned technique establishes a shift difference of 24 ppm for ^{109}Ag in the Δ and Λ configurations. ^{1}H and INEPT ^{15}N studies show that in the case of the Ag^I complex (R = Me, R' = Pr^i) $\Delta \rightleftharpoons \Lambda$ inversion is occurring together with a slower intermolecular exchange process.

The cation complexes $[MCl(PEt_3)_2L]^+$ (M = Pd or Pt, L = pyrazole or 3,5-dimethylpyrazoles) are stereochemically rigid when M = Pt and nonrigid when M = Pd.[242] The palladium complexes exhibit rapid averaging of the two nonequivalent phosphorus nuclei and of the 3,5-groups on the pyrazole ligands. The former process involves pyrazole dissociation as the rate-determining step, whereas the methyl averaging may involve deprotonation followed by an intramolecular metallotropic 1,2-shift. Despite the fact that the energies of the two processes at 273 K are very similar ($\Delta G^{\neq} \approx 60\,\text{kJ mol}^{-1}$),

Bushnell et al.[242] argue in favour of two uncorrelated fluxions. The energy barriers associated with inversion of tetrahedral configuration ($\Delta \rightleftharpoons \Lambda$) of metal(II) bischelates from substituted pyrazoles have been measured for a wide range of metals and ligands.[243]

There have been a number of independent studies on the stereochemical nonrigidity of pyrazolylborate complexes. Rhodium complexes of the type $RhB(pz)_4(diene)$ exhibit intramolecular exchange of free and coordinated pyrazolyl groups at rates that depend on the type of diene.[244,245] The exchange interconverts the complex between 4-coordinate square-coplanar and 5-coordinate trigonal-bipyramidal forms. Activation parameters based on ^1H variable-temperature studies have been quoted and ^{103}Rh measurements have also been performed. Zirconium complexes of the type $[RB(pz)_3]Zr(OBu^t)Cl_2$ ($R = Bu^n$, Pr^i) are fluxional at room temperature but give limiting static spectra at low temperatures.[246] The spectral changes can be explained in terms of a trigonal twist of the poly(pyrazolyl)borate ligand about the Zr–B axis, with $\Delta G^{\neq} = 56.3\,kJ\,mol^{-1}$ when R is Bu^n. The fluxionality of palladium(II) complexes of the type $[PdClB(pz)_4L]$ ($L = PEt_3$ or $P(OEt)_3$) leads to equivalence of all four pz groups at high temperatures.[247] Zinc, cadmium and nickel complexes of the type ML_2 ($L = $ 5-thio-4-formylpyrazole) are tetrahedral diastereoisomeric species. Their inversion of configuration has been followed and activation-energy data determined.[248]

DNMR studies of miscellaneous nitrogen-coordinated ligand complexes include pyrazine,[249] imidazole[249] and triazene[250] complexes of platinum, quinolinol[251] and amine[252,253] complexes of tin, naphthyridine and phthalazine complexes[254] of chromium and tungsten, penicillamine complexes of technetium and rhenium,[255] and a nitrosyl complex of ruthenium.[256] In most cases activation-energy data are given for the various fluxional processes. The tin(IV) quinolinol complexes[251] exhibit isomerization equilibria due to cis–cis–trans and cis–trans–cis species (60):

cis - cis - trans   cis - trans - cis

(60)
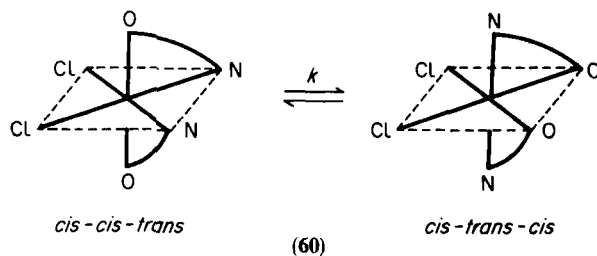
Total bandshape analyses including Sn–H couplings give accurate Arrhenius-energy parameters for the isomerization process. The tin complex

$CH_2[(C_6H_5)Sn(SCH_2CH_2)_2NCH_3]_2$ possesses a structure in which both tin atoms show approximate trigonal-bipyramidal coordination.[252] At low temperatures three isomers are apparent from the ^1H, ^{13}C and ^{119}Sn data, whereas in the fast-exchange situation only one residual isomer is present. These observations suggest that the two Sn atoms rearrange independently, and a mechanism involving a dissociation–inversion pathway is favoured. The ligand 1,8-naphthyridine offers two potential N-donor sites to a metal.[254] Only one of these is involved in coordination with Cr or W at low temperatures. However, on heating to ca. 300 K coordination involves both nitrogens, with the $M(CO)_5$ commuting between both sites via a 1,2-shift process (61):

(61)
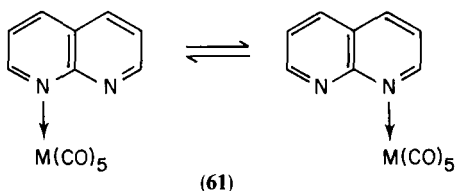
Penicillamine complexes involve coordination via N, O and S atoms. In the study of Te and Re complexes of penicillamine the fluxion involves no spatial movement of the ligand but purely an electronic reorganization involving oxygen and carbon atoms.[255] In the nitrosyl complex[256] ^{15}N NMR shows a rapid intramolecular interconversion between bent and linear NO ligands. Finally, in this section on N-coordinated ligand complexes, there has been a report[257] of the stereochemical nonrigidity associated with complexes of the 20-membered macrocycle L (62):

(62)
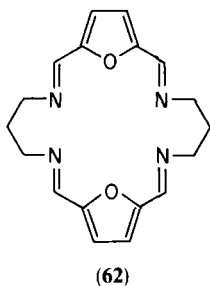
In the complex $[BaL_2(MeCN)_2][BPh_4]$ the Ba atom is bonded to all six heteroatoms of one macrocycle but to only three of the second macrocycle, this being severely folded so that one furan di-imine moiety is uncoordinated. Variable-temperature ^1H studies show exchange involving both the HC=N and C=N—CH$_2$, protons which is attributed to fluxional interconversion

between the four equivalent low-temperature configurations of the complex with $\Delta G^{\neq} \approx 62.5 \, \text{kJ mol}^{-1}$.

Recent reports on phosphine-ligand fluxionality include a study of the complexes PdX_2L_2, PdX_2L_3 and $PdXL_4^+$ and related nickel and platinum complexes.[258] The complexes $PdX_2(PMe_3)_3$ are trigonal bipyramidal when $X = Br$ or I but distorted square-pyramidal when $X = Cl$. Phosphine exchange is rapid at room temperature via an intermolecular double-displacement mechanism. The $PdXL_4^+$ species are square-pyramidal, with phosphine exchange again being intermolecular in nature. The 7-coordinate complex $CrH_2[P(OCH_3)_3]_5$ can in theory undergo a great variety of intramolecular fluxions.[259] These have been carefully followed by ^1H and $^{31}P-\{^1H\}$ NMR studies of this complex $AB_2CC'XX'$ spin system. The distal structure (63), where the arrows refer to distortions from the regular pentagonal bipyramid, is attributed to the static Cr complex:
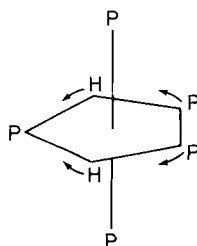
(63)

From a full permutational analysis sixteen basic sets of permutations of the hydride and phosphine ligands have been calculated. NMR bandshapes based on each of these sets have been computed and compared with experimental bandshapes. Only 2 out of the 16 sets give reasonable agreement. The two sets correspond to identical phosphorus permutational behaviour (Fig. 14), and differ only with respect to whether or not the hydrogens permute. These two cases (sets 9, 10) are compared with the experimental ^1H spectra in Fig. 15. The case that did not admit any hydrogen permutation was marginally preferred. This mechanism involves a simultaneous exchange of the two axial phosphines with two of the equatorial phosphines. The total fluxion corresponds to permutation of the CrP_5 framework related to the Berry pseudorotation process in 5-coordinate complexes. The computation of the bandshapes for these exchanging 5- or 7-spin systems is far from trivial. For the 5-spin system of the $^{31}P-\{^1H\}$ spectrum the Liouville space is of dimension 1024×1024, which factorizes to matrices of highest order 34. The 7-spin problems of the ^1H spectra involve
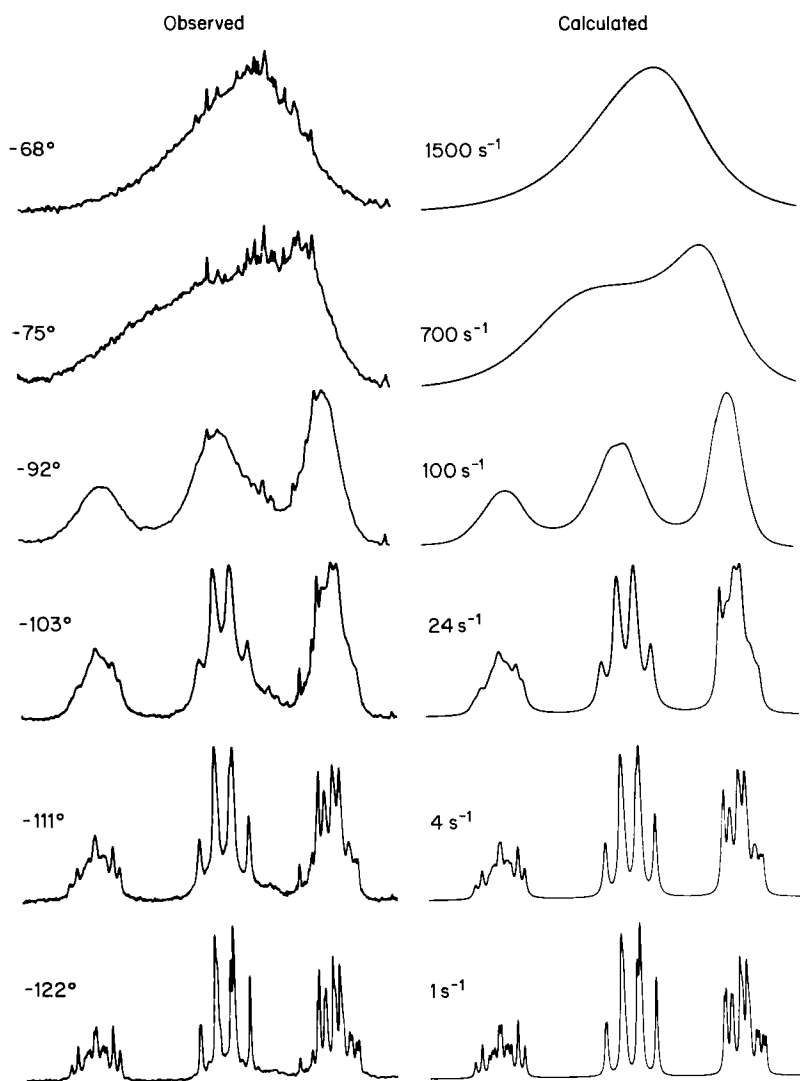
Observed   Calculated

FIG. 14. ^{31}P-$\{^1$H$\}$ spectra of $CrH_2[P(OCH_3)_3]_5$ compared with computer-simulated spectra for the basic permutational set 6.[259]

the diagonalization of 64×64 matrices, each of which requires 29 minutes computing time! By omitting very weak transition intensities, the computational problem can be reduced without significant error. Nevertheless, this work represents one of the most ambitious applications of the total-bandshape method.

Calculated (set 9) | Observed | Calculated (set 10)

1000 s^{-1} | -59° | 1500 s^{-1}

120 s^{-1} | -81° | 160 s^{-1}

40 s^{-1} | -107° | 60 s^{-1}

9 s^{-1} | -118° | 11 s^{-1}

4 s^{-1} | -125° | 4 s^{-1}
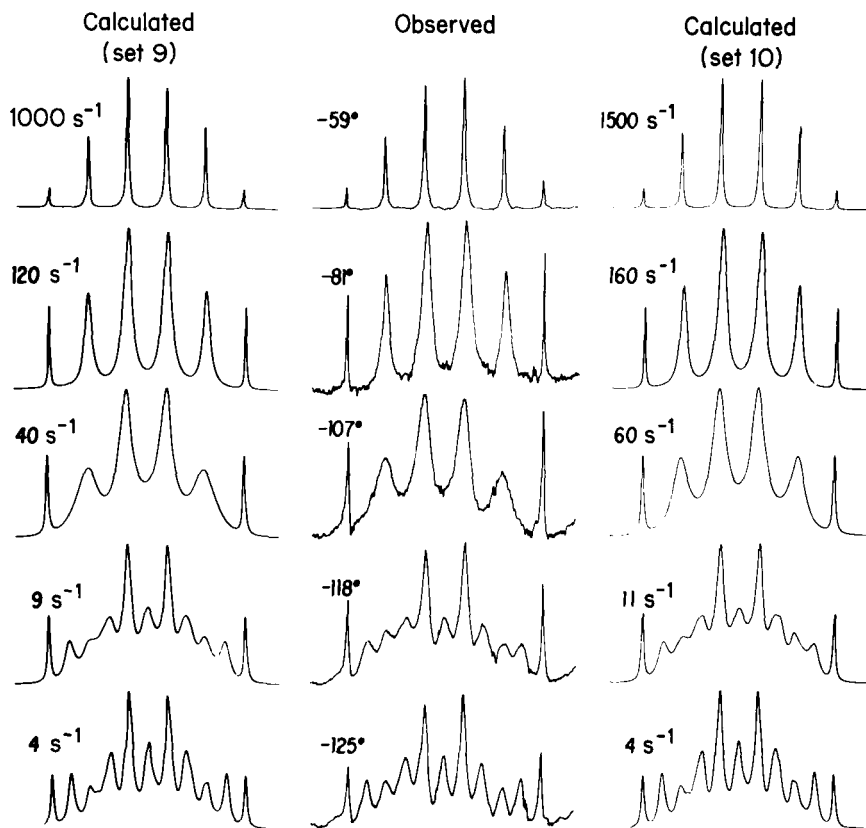
FIG. 15. Experimental ^{1}H spectra of $CrH_2[P(OCH_3)_3]_5$ compared with theoretical spectra based on the permutational sets 9 and 10.[259]

The complex $[Ti(CO)_3(dmpe)_2]$ (dmpe = 1,2-bis(dimethylphosphino)ethane is also 7-coordinate and stereochemically nonrigid at high temperatures.[260] Variable-temperature ^{13}C and ^{31}P spectra are able to quantify two fluxions, one of which appears to involve rotation of a P–P–P triangular face and the other which equilibrates all P and CO sites. The chromium(0) complexes $Cr(CO)_2(PMe_3)_2(\eta$-diene) and $Cr(CO)_2\{P(OMe)_3\}_2(\eta$-diene) are distorted octahedral species, which exhibit intramolecular mutual exchange of the donor ligands. Activation-energy barriers have been measured by ^{31}P DNMR.[261] The latter technique has also been applied to $Ir(CH_2SiMe_3)(CO)\{P(OMe)_3\}_3$, which is fluxional at room temperature ($\Delta G^{\neq} = 29$ kJ mol^{-1}).[262] The ligand o-phenylenebis(methylphenylarsine) and its phosphine analogue form optically active square-planar and square-pyramidal complexes with nickel(II),[263] palladium(II) and platinum(II).[264] The square-planar complexes $[Ni(diars)_2](PF_6)_2$

and [Ni(diphos)$_2$](PF$_6$)$_2$ are kinetically stable, whereas the square-pyramidal cation complexes [NiX(diphos)$_2$]$^+$ undergo rapid axial ligand-site exchange by intramolecular isomerization of the chelate rings and by intermolecular exchange of the halides between sterically compatible complex ions. These ligands, together with the mixed P/As mixed-donor ligand, have been used to form gold(I) complexes.[265] The complexes of the bis(tertiary phosphine) can be separated into racemic and *meso* forms, whereas the complexes of bis(tertiary arsine) and the mixed donor ligands undergo rapid intermolecular ligand redistribution. ^{1}H studies of the complexes $\pm$[Au((R*,S*)-bidentate)$_2$]PF$_6$ lead to a calculated value of 97 $\pm$ 14 kJ mol^{-1} for the barrier to inversion of the tetrahedral gold centre.

Turning now to coordinated sulphur ligand complexes, the stereodynamics of such complexes with both main-group and transition metals have been reviewed.[94] Rates of pyramidal inversions of Group VI atoms are greatly accelerated when such atoms are coordinated to transition metals. These subsequent rates fall neatly within the range of NMR detection, producing temperature-dependent spectra usually in the range $-100\,^\circ$C up to ambient temperatures (Section III.B). Rapid pyramidal inversions of coordinated S or Se atoms often initiate other fluxional processes detectable at above-ambient temperatures. A wide variety of chromium, molybdenum and tungsten complexes of the general type M(CO)$_5$L (L = open-chain or cyclic S or Se ligands) have been studied. With 6-membered cyclic ligands, namely L = $\overline{\text{SCH}_2\text{SCH}_2\text{SCH}_2}$, β-$\overline{\text{SCHMeSCHMeSCHMe}}$, and $\overline{\text{SCH}_2\text{SCH}_2\text{CH}_2\text{CH}_2}$, a commutation of the M(CO)$_5$ moiety between the two or three sulphur atoms occurs via a 1,3-shift process (64):[98,266]


(64)
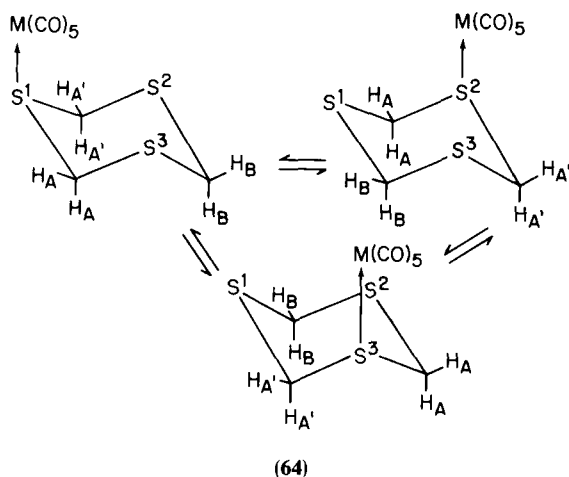
The energy of this process depends on the skeletal flexibility of the cyclic ligand. In the fixed axial conformation of the β-$\overline{\text{SCHMeSCHMeSCHMe}}$ complex the axial lone pairs of the uncoordinated S atoms are held at a constant distance from the $M(CO)_5$ moiety and directed in such a way as to greatly facilitate a 1,3-shift via an easily accessible 7-coordinate intermediate. In the unsubstituted trithian complexes rapid ring reversal and S pyramidal inversion interconvert conformers of similar ground-state energy, thus disturbing the ideal positioning of the $M(CO)_5$ groups and the sulphur lone pairs. This results in the ΔG^* value for the process (in the Cr complexes) increasing from *ca.* $65\,\text{kJ mol}^{-1}$ to $75\,\text{kJ mol}^{-1}$. In the 8-membered ring complexes $(L = \overline{\text{SCH}_2\text{SCH}_2\text{SCH}_2\text{SCH}_2})$[100] the ring flexibility increases the activation-energy barrier by a further $5\,\text{kJ mol}^{-1}$. 1,3-Metallotropic shifts have also been detected with open-chain ligand complexes.[267,268] For example, when $L = \text{MeECH}_2\text{E}'\text{Me}$ ($E = E' = S$ or Se; $E = S$, $E' = Se$), the ^1H spectra in the range $25–100\,^{\circ}\text{C}$ show changes in the Me signals characteristic of the 1,3-metal shift. In the complexes $[M(CO)_5(\text{MeSCH}_2\text{SeMe})]$ the 1,3-shift causes an interconversion between chemically distinct isomers, and the difference in ΔG^* values for Se $\rightarrow$ S and S $\rightarrow$ Se 1,3-shifts closely reflects the different S $\rightarrow$ M and Se $\rightarrow$ M bond strengths. For tungsten complexes the Se $\rightarrow$ W bond is stronger by *ca.* $2.9\,\text{kJ mol}^{-1}$. Open-chain and cyclic ligands of the types $\text{Me}_3\text{SiCH}_2\text{EECH}_2\text{SiMe}_3$ and $\text{Me}_2\overline{\text{CCH}_2\text{EECH}_2}$ ($E = S$, Se) present the coordinated $M(CO)_5$ moiety with the potentiality for undergoing 1,2-metal shifts. Such movements are indeed observed in $M(CO)_5 L$ complexes at above-ambient temperatures when the coordinated E atoms are inverting rapidly on the NMR time scale. The case of $W(CO)_5\text{Me}_3\text{SiCH}_2\text{SeSeCH}_2\text{SiMe}_3$ is shown in (65):[99,102]
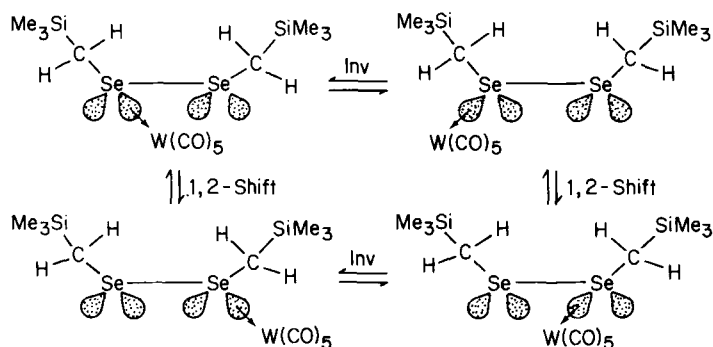
(65)

The energies of the 1,2-shifts are $7-10\,kJ\,mol^{-1}$ lower than 1,3-shifts in the nearest analogous complexes. The effect of ring incorporation of the E atoms[103] increases the $\Delta G^{\neq}$ values of the process by $4-8\,kJ\,mol^{-1}$. The other trends noted are that for both 1,3- and 1,2-shifts the $\Delta G^{\neq}$ values are in the order $W > Cr > Mo$, with the values for Se → M shifts being $3-4\,kJ\,mol^{-1}$ higher in energy than for S → M shifts.

Trimethylplatinum(IV) halide complexes with sulphur- or selenium-coordinated ligands undergo a variety of fluxional rearrangements.[94] At below-ambient temperatures these include ligand ring conformational changes and pyramidal inversions of the coordinated atoms. At higher temperatures more extensive ligand fluxions occur, and these then initiate a scrambling of the platinum-methyl groups. In complexes of the types $[PtXMe_3L]$ (X = Cl, Br, I; L = $MeSCH_2CH_2SeMe$,[113] $MeSCH=CHSMe$,[115] $MeSeCH=CHSeMe$[115]), the axial and equatorial Pt-methyl ^{1}H signals coalesce on increasing the temperature, until a single signal with [195]Pt satellites is observed. At the same time, the methylene-region signals (in the case of the L = $MeSCH_2CH_2SeMe$ complex) change from an ABCD to an AA'BB' pattern. The latter change is only consistent with a 180° rotation fluxion (ligand "pancaking" process) about the platinum centre. The coalescence of the Pt-methyl signals leads to an estimation of the energy of the scrambling process. The energy of the ligand rotation fluxion cannot be separately measured in these complexes, but may be measured in the complexes $[PtXMe_3(MeSCH_2SCH_2SMe)]$,[114] where the process causes chemical-shift averaging of the geminal methylene protons. The novel ligand "pancaking" fluxion depicted in (66) is thought to involve a highly nonrigid 8-coordinate platinum(IV) intermediate, which then activates scrambling of the Pt-methyl environments:

(66)
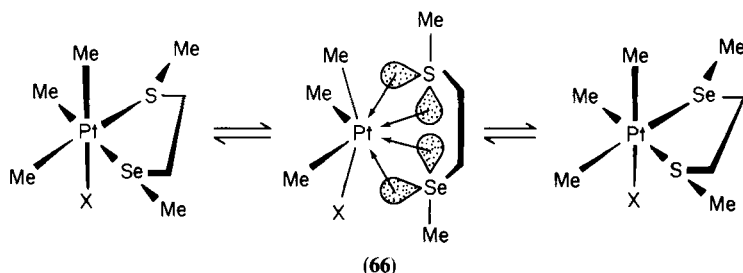
Activation energies for both processes are given in Table 6. It will be observed that most pairs of values are equal within experimental error, implying that the two processes are highly concerted. The analogous ligand-rotation fluxion, with a higher activation energy, is also observed in the complex $[ReX(CO)_3(MeSCH_2SCH_2SMe)]$ (X = Cl, Br, I)[106] (Table 6).

TABLE 6

Ligand-rotation and methyl-scrambling energies in complexes with MeSCH$_2$SCH$_2$SMe(L).

Complex	X	Process[a]	$\Delta G^{\neq}$ (kJ mol^{-1})
[PtXMe$_3$L]	Cl	LR	77.69 ± 0.29
		MeS	79.22 ± 0.19
[PtXMe$_3$L]	Br	LR	77.99 ± 0.75
		MeS	79.20 ± 1.49
[PtXMe$_3$L]	I	LR	78.12 ± 1.01
		MeS	79.16 ± 0.38
[ReX(CO)$_3$L]	Cl	LR	95.63 ± 0.45
[ReX(CO)$_3$L]	Br	LR	95.05 ± 1.27
[ReX(CO)$_3$L]	I	LR	96.33 ± 1.47

[a] LR, ligand rotation; MeS, methyl scrambling.

Dithiolates can act as both mono- and bidentate ligands. Use of ^{31}P NMR to study the dynamic stereochemistry of platinum and palladium complexes of the type M(S$_2$PR$_2$)$_2$PPh$_3$ established monodentate–bidentate ligand exchange, with $\Delta G^{\neq}$ for the process being 52 kJ mol^{-1} for M = Pt^{II}, R = OEt.[269] Two reports on the isomerization of iron–sulphur-ligand complexes have appeared. The isomerization of syn- and anti-[Fe(SMe)(CO)$_3$]$_2$ has been examined and thought to involve Fe–S bond rupture and reformation.[270] The $C_{2h} \rightleftharpoons C_{2v}$ isomerization of Fe$_2$(SMe)$_2$(NO)$_4$ has been investigated by ^{1}H NMR using a wide range of solvents.[271] $\Delta G^{\neq}$ values are around 78 kJ mol^{-1} for most solvents. Dithiocarbamato complexes of osmium(III)[272] and tungsten(IV)[273] are stereochemically nonrigid. The complex Os(S$_2$CNR$_2$)$_3$ is a low-spin d^5 species. The isotropically shifted ^{1}H signals show coalescence features that suggest that the complex rearranges via a trigonal twist mechanism. Oxo-tungsten(IV) acetylene complexes of the type OW(S$_2$CNR$_2$)$_2$(R^{1}C≡CR^2) undergo a rearrangement thought to involve a dissociative 5-coordinate intermediate.[273]

Dynamic ^{19}F NMR has enabled the mechanism of inversion of silicon in siliconates to be probed in detail.[274-276] The inversion of configuration carries a site interchange of geminal CF$_3$ groups in compounds such as (67).

When M = Si the structure is a distorted tetrahedron, whereas when M = PhSi$^-$N$^+$Me$_4$ it is essentially trigonal bipyramidal at sulphur. The configurational inversion proceeds via a nondissociative Berry-type pseudorotation, with $\Delta G^{\neq}$ values for the process being linearly related to the Taft σ^* inductive parameter of the ligand. It is also catalysed by weak nucleo-
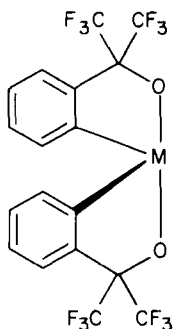
(67)

philes.[276] The 5-coordinate silicon–nitrogen complex (68) also undergoes an intramolecular rearrangement which interchanges F atom sites:[277]
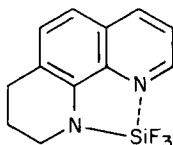
(68)

Hydride fluxionality has also been the subject of recent studies. The exchange of bridging and terminal hydride ligands in $[(MeO)_3P]_2CuH_3BCO_2Et$[278] and $[Co(terpy)H_2BH_2]$ (terpy = 2,2':6',2''-terpyridyl)[279] has been followed, and $\Delta G^{\neq}$ values of 18.1 and 46.6 kJ mol^{-1} obtained for the respective processes. The reaction of $Ni[P(O\!-\!p\text{-tolyl})_3]_4$ with strong acids gives both 4-coordinate (NiP_3H^+) and 5-coordinate (NiP_4H^+) hydride species. Both species are fluxional, but only NiP_4H^+ rearranges at a rate measurable by ^1H NMR.[280] At low temperatures the ^1H spectrum of NiP_4H^+ is consistent with a square-planar arrangement of ligands around the Ni atom. On raising the temperature, the spectral changes imply an intramolecular exchange of cis and trans phosphorus ligands. Activation-energy parameters have been calculated, the large negative $\Delta S^{\neq}$ values and the small $\Delta H^{\neq}$ values implying ion pairing in the transition state.

The species $Te(OTeF_5)_4$ has a trigonal-bipyramidal arrangement of four bonding pairs and one lone pair of electrons, with two axial and two equatorial $OTeF_5$ groups. Distinction between these two environments is observed in the ^{19}F spectrum only at low temperatures (~ 150 K), suggesting Berry pseudorotation via a square-pyramidal transition state ($\Delta G^{\neq} = 30.7$

$\pm 0.3 \, kJ \, mol^{-1}$). This work has additional interest in that ^{125}Te spectra are also used for characterization purposes and $^{125}Te^{VI}-^{125}Te^{IV}$ spin couplings are quoted.[281]

Finally, there have been two reports on alkyl fluxionality. s-Butyllithium exists as a mixture of dimers, hexamers and tetramers that undergo a variety of inter- and intra-aggregate exchanges, as evidenced by ^{13}C and ^{6}Li NMR.[282] ^{13}C NMR provides evidence for bridge–terminal exchange of ligands via a singly bridged intermediate in tricyclopropylaluminium, -gallium and -indium.[283] Low-temperature ^{13}C spin–lattice relaxation times suggest that the bridging and terminal cyclopropyl groups on the same side of the M–C–M–C rings rotate at the same rate, while the terminal groups on the opposite side rotate 5–8 times faster.

(b) Bimetallic systems. Such systems can be further classified in terms of structures with formal metal–metal bonds and those with the two metals linked by bridging ligands. The former category is considered first.

In studies[284,285] of alkyne adducts of dimetal hexa-alkoxides $M_2(OR_6)(\mu\text{-}C_2R_2)py_2$ (M = Mo, W), various types of fluxionality are found. In the molybdenum complexes[284] exchange occurs between the bridging and terminal OR groups and between free and coordinated pyridine. However, no exchange takes place between free and coordinated alkyne. The ditungsten complexes are also fluxional,[285] and in the case of $W_2(OCMe_3)_6(\mu\text{-}C_2H_2)(py)$ an equilibrium exists between ditungsten tetrahydrane $W_2(\mu\text{-}C_2H_2)$ and methylidyne tungsten $(W\equiv CH)_2$ species. The iron complex $[Fe_2(CNR)_9]$ (R = Et, Pr^i) has been shown by X-ray diffraction to involve three bridging isocyanide ligands, with the remaining ligands being terminal, three to each Fe atom. Variable-temperature ^1H and ^{13}C NMR reveal bridge–terminal ligand exchange, the most likely mechanism being synchronous pairwise exchange with inversion at N.[286] The mechanism for one ligand is depicted in (69):

(69)
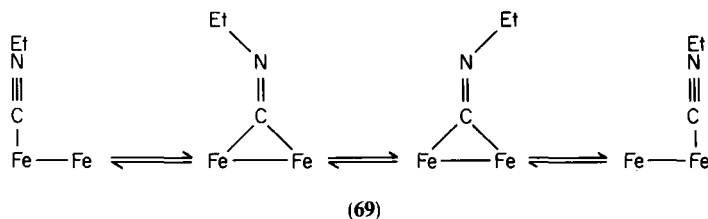
The lateral shift step (windscreen-wiper effect) is considered to be fast, and the calculated energy barrier ($\Delta G^{\neq} = 63 \pm 1 \, kJ \, mol^{-1}$ for R = Et) is for the *syn* or *anti* movements. In a series of studies of diiron, diruthenium and ditungsten

complexes with alkyne and carbon monoxide ligands, new fluxional rearrangements have been detected.[287][289] Thus in the complex $[M_2(CO)(\mu\text{-}CO)\{\mu\text{-}\sigma:\eta^3C(O)C(R^1)C(R^2)\}(\eta\text{-}C_5H_5)_2]$ (M = Fe, Ru) (70),[179] ^{1}H and ^{13}C spectra indicate synchronous carbonyl insertion into, and elimination from, the dimetallacycles when $R^1, R^2 = H$, Me or Ph:


(70)
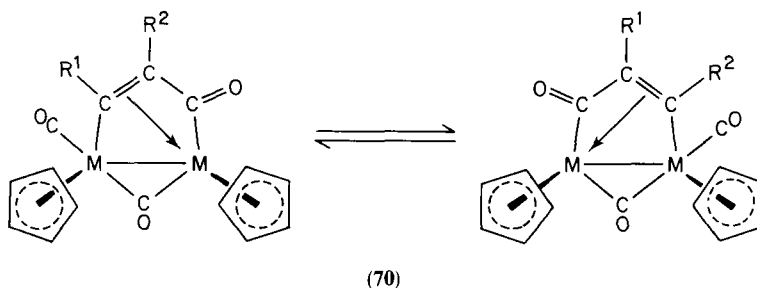
This process involves reversible cleavage of the alkyne–carbonyl link. This link, however, is retained in the proposed fluxion of (70), $R^1 = R^2 = CO_2Me$.[288] The μ-vinyl cation complexes $[M_2(CO)_2(\mu\text{-}CO)\{\mu\text{-}C(R)\equiv C(H)R\}(\eta\text{-}C_5H_5)_2]^+$ exist in solution as isomers with *cis* and *trans* orientations of terminal ligands. These isomers interconvert above $-50\,^\circ$C, and the *cis* species exhibit an additional fluxional oscillation of the μ-vinyl ligand.[289] The solution dynamics of μ-alkyne complexes of dicobalt[290] and dirhodium[291] centres have also been investigated. Variable-temperature ^{1}H and ^{31}P NMR have been used to establish the solution structures of the dirhodium complexes $[Rh_2L_4L']$ (L = RCO_2, L' = $P(OR)_3$)[292] and $[Rh_2(CO)_3(dppm)_2]$.[293] The thiocyanate ligand (SCN) can bind to metals in a linear or bent manner, depending on whether the N or S atoms are coordinated. In the palladium complexes $[\{Ph_2P(CH_2)_nPPh_2\}Pd(CNS)_2]$ (n = 1,2,3) the three types of linkage isomers (bent/bent, bent/linear and linear/linear) have been identified by ^{31}P NMR below $-40\,^\circ$C.[294]

   Turning now to dimetal centres linked by one or more bridging groups or atoms, there has been a report of dyotropic rearrangements of dizirconium complexes where the Zr atoms are bridged by the oxygen atom of aldehyde ligands.[295] The diplatinum complex $[Pt_2H_2Cl(\mu\text{-}dppm)]PF_6$ was originally thought to possess an A-frame structure with a Pt–H–Pt or Pt–Cl–Pt bridged structure. However, a recent variable-temperature ^{195}Pt study has established that such a structure is a time-averaged representation of the fluxional process (71), which involves chloride ion transfer.[296]

   Trimethylplatinum(IV) halides form a variety of very stable dinuclear complexes of the type $[(PtXMe_3)_2L]$, where the Pt atoms are bridged by a

(71)
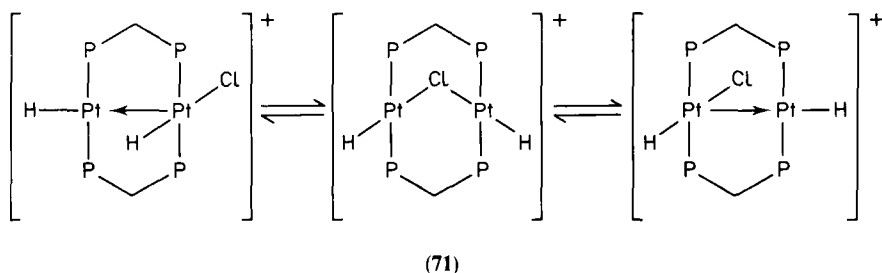
pair of halogens (X) and the ligands (L) are either open-chain or cyclic ligands coordinated via S or Se atoms. In all such complexes, the onset of rapid pyramidal inversion of the coordinated atoms leads to other fluxional rearrangements. When $L = MeSCH_2SeMe$[116] this ligand undergoes 180° switches between the Pt atom pairs. This shows up in the ^1H spectra as mutual exchange of the two axial and two equatorial PtMe signals, and also in the ligand-methyl spectrum, where the SMe or SeMe signals exhibit coupling to both ^{195}Pt atoms producing a quintet of relative intensity $1 : 7.8 : 17.5 : 7.8 : 1$. The PtMe region of the spectrum also shows coalescence features due to axial–equatorial exchanges, and this can only be explained by invoking an intramolecular Pt-methyl scrambling process. Activation-energy calculations for both the ligand-switching (LS) and methyl-scrambling (MS) processes indicate that the two processes are concerted, being consecutive aspects of a single fluxional rearrangement. The ligand-switching process is thought to involve a highly nonrigid 7-coordinate Pt^{IV} intermediate (72):

(72)
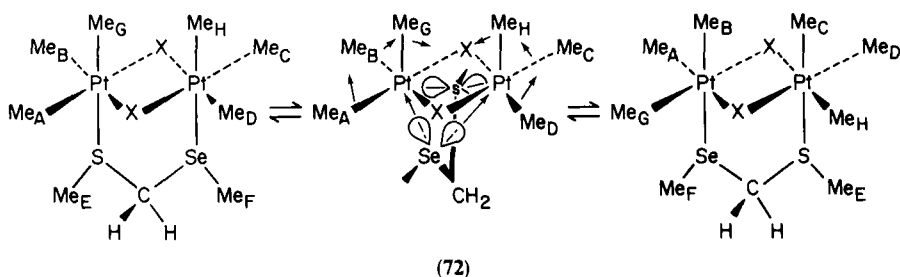
With cyclic ligand complexes $[(PtXMe_3)_2L]$ $(L = \overline{SCH_2SCH_2SC}H_2$[297] and $\overline{SCH_2SCH_2SCH_2SC}H_2$[298]) ^1H studies indicate the onset of a fluxion that averages certain Pt-methyl and ring-methylene signals. In the case of $L = \overline{SCH_2SCH_2SC}H_2$ the exchanges are $R \rightleftharpoons S$, $A \rightleftharpoons D \rightleftharpoons D'$ and $B \rightleftharpoons C \rightleftharpoons C'$ (73):

(73)
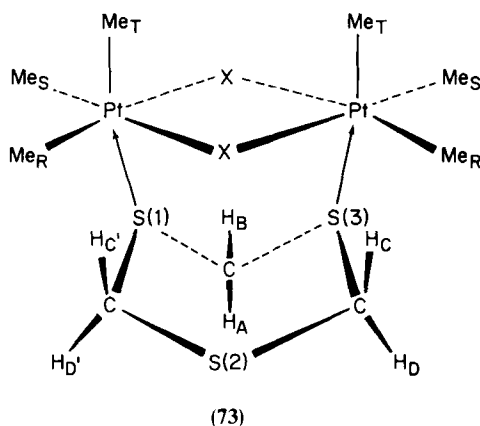
Such changes can be fully accounted for by a series of 60° 1,3-pivots of the ligand about any one S → Pt bond. With the 8-membered ring L = $\overline{SCH_2SCH_2SCH_2SCH_2}$[298] detailed analyses of the spectral changes support a series of 90° 1,5-pivots of the ligand followed by Pt-methyl scrambling. In this case, the latter fluxion is thought to proceed via 120° rotations of the commuting PtMe$_3$ group. In the complexes where L = $\overline{SCH_2CMe_2CH_2S}$,[118] the absence of a third sulphur atom prevents any ligand commutation. Even so, Pt-methyl scrambling does occur at high temperatures ($T_c \approx 80\,°C$), but in this case pairwise axial–equatorial exchange with no direct equatorial–equatorial exchange is indicated. Thus the mechanism of Pt-methyl scrambling in these [(PtXMe$_3$)$_2$L] complexes appears to depend on the precise nature of the ligand movements (viz

TABLE 7

Activation energies of fluxional processes in [(PtXMe$_3$)$_2$L] complexes.

		$\Delta G^{\neq}$ (kJ mol^{-1})		
L	X	LS/LP*[a]	MS[b]	Ref.
MeSCH$_2$SeMe	Cl	69.5 ± 0.1	70.3 ± 0.1	116
MeSCH$_2$SeMe	I	65.6 ± 0.1	64.8 ± 0.1	116
$(\overline{SCH_2})_3$	Cl	58.57 ± 0.08*	71.12 ± 0.08	297
$(\overline{SCH_2})_3$	Br	58.80 ± 0.16*	67.42 ± 0.01	297
$(\overline{SCH_2})_4$	Cl	66.18 ± 0.01*	65.82 ± 0.08	298
$\overline{SCH_2CMe_2CH_2S}$	Cl	—	71.38 ± 0.05	118

[a]LS, ligand switching; LP, ligand pivoting.
[b]MS, methyl scrambling.

switching or pivoting). A representative set of energies for the various fluxions (LS, LP and MS) in these Pt^{IV} complexes is given in Table 7.

(c) *Trimetallic systems.* This section deals with triangulo metal structures, with homometallic species considered first. The ethylidene-capped triangulo tungsten species $W_3(\mu_3\text{-CMe})(\mu_2\text{-OR})_3(OR)_6$ has the structure (74):
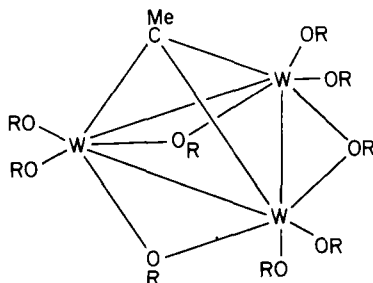

(74)

Variable-temperature ^1H spectra indicate site exchange between the terminal alkoxide ligands, probably via a pseudorotation about each W atom, but no bridge–terminal OR exchange.[299] Reaction of ethene with $[Ru_3(CO)_{12}]$ gives $[Ru_3H_2(CO)_9C_2R_2]$ (R = H, Me and Et) as three of the reaction products. These have been shown by ^1H NMR to possess an apparent symmetry plane as a result of hydride migration.[300] The complexes (R = Me, Et) also undergo other exchange processes. There have been two reports of fluxional Os_3 cluster complexes. $[Os_3H_3(CO)_9\overline{CC(CH_2)_2CH_2}]^+$ gives rise to a single hydride resonance with two sets of ^{187}Os satellites. This is consistent with rapid hydrocarbon-ligand rotation with concomitant rotation of the $Os_3H_3(CO)_9$ moiety.[301] In $Os_3(CO)_7\{P(OMe)_3\}_5$ ^{31}P and ^{13}C spectra imply the phosphite ligand moving between equatorial sites via a trigonal twist mechanism.[302] In the cobalt cluster $Co_3(CO)_9CCHCHMe_2^+$ the energy barrier $\Delta G^{\neq}$ associated with enantiomerization of the cluster is calculated to be $44.1 \pm 0.4 \, kJ \, mol^{-1}$ at $-52 \,^{\circ}C$.[303] A similar barrier energy is attributed to an intramolecular flipping process, which averages the PR_3 ligand environments in the platinum cluster $Pt_3(\mu\text{-SO}_2)_3(PR_3)_2dppp$ (R = cyclohexyl, dppp = 1,3-bis(diphenylphosphino)propane).[304]

Finally, there have been two reports on heteronuclear triangulo clusters. The Pd_2MClL_2 (M = Cr, Mo, W; $L = o\text{-Me}_2NCH_2C_6H_4$ or $o\text{-Me}_2NC_6H_4CH_2$)[305] species undergo an exchange process that creates a plane of symmetry for the molecule. $\Delta G^{\neq}$ values for the process range from 49 to $73 \, kJ \, mol^{-1}$ and depend on *the nature of the σ-bonded carbon of the*

ancillary N͡C ligand, as well as on the metal M. The mixed metal clusters [(RC≡CR')MM'Fe(CO)₃] (M = NiCp, M' = Co(CO)₃, NiCp) possess a square-pyramidal geometry (75):


(75)
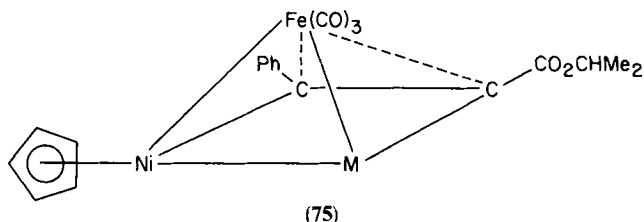
They may be regarded as octahedral clusters with a vacant coordination site, a description that accords with their fluxional behaviour involving formal rotation of the alkyne moiety with respect to the metal triangle.[306]

(d) Polymetallic systems. This subsection includes reports on the stereo-dynamics of transition-metal clusters, carboranes and metallocarboranes. The review[307] by McGlinchey *et al.* shows how the electronic structures of the 4- to 9-atom organotransition-metal clusters are closely analogous to the corresponding boranes using the isolobal principle. This analogical approach can neatly account for the high reactivity and NMR fluxionality of clusters with a vacant site on the polyhedral surface. Thus the chiral tetrahedral alkyne bimetallic cluster (PhC≡CCO₂Pr^i)CpNiCo(CO)₃ (76) undergoes a racemization process, which may be visualized as a migration of a cluster vertex into a vacant site on a surface (77):

(76)

(77)
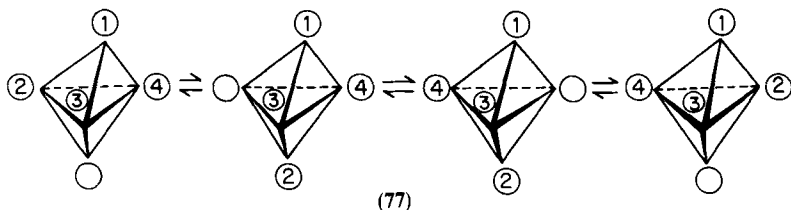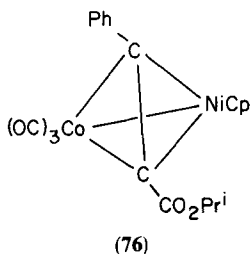
This suggestion of vertex fluxionality is relatively new, but may prove to be a particularly useful rationalization of many stereodynamical changes in metal clusters. Whatever the mechanism, the diastereotopic methyls of the isopropyl group enable an energy barrier of *ca.* $88\,kJ\,mol^{-1}$ to be calculated.

Much effort has been devoted in recent years to locating the active sites of metalloenzymes. The ferredoxins involving the basic Fe_4S_4 cage structure are particularly important and have been very extensively studied. A recent report of two Fe_4S_5 clusters, $Cp_4Fe_4S_5$ and $Cp_4Fe_4S_5^{2+}$, has shown them to exhibit a novel fluxionality of the triply bridging disulphide ligand (78), which is rapid above $-40\,°C$ for the neutral species and above $70\,°C$ for the dication:[308]
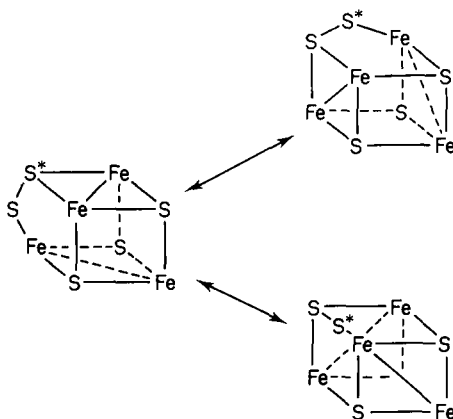

(78)

The mixed-metal cluster $Hg[Pt_3(2,6\text{-}Me_2C_6H_3NC)_6]_2$ may be described as a trigonal prism of Pt atoms whose edges are associated with bridging isocyanide groups, with the remaining ligands terminally attached. The Hg atom forms the pseudocentre of the prism. Variable-temperature ^1H studies reveal inter- and intramolecular ligand exchanges.[309] Finally, there is a report of a fluxional gold–iridium cluster $[IrAu_4(H)_2(PPh_3)_6]BF_4$, which consists of an approximate trigonal bipyramidal $IrAu_4$ core with an $Ir(PPh_3)_2$ unit occupying an equatorial position. ^{31}P NMR spectra show exchange between the axial and equatorial Au sites.[310]

Fluxionality of carboranes is usually too slow for its NMR detection. However, the 12-vertex $R_4C_4B_8H_8$ carboranes are a notable exception.[311] These have now been examined by ^{11}B, ^{13}C and ^1H methods. The compounds exist in solution as a mixture of cage isomers, the equilibrium constant for the system depending on the nature of the alkyl substituent R.

The two isomers undergo an interconversion (79), which involves cleavage of a framework C–C bond:

A   ○ BH   B
           ● CR

(79)
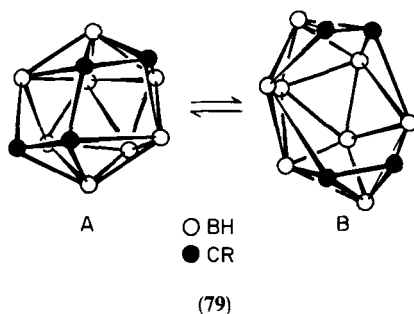
At elevated temperatures more complex modes of cage rearrangement have been noted, but not yet analysed. Stereochemical nonrigidity of polyhedral boranes is fairly widespread, and has been extensively studied over the past 10 years. The first example of intramolecular rearrangement of a 9-boron cluster has now been reported.[312] $B_9H_8SMe_2^-$ exists as two isomers, one with a 5-coordinate capping boron and the other with a 6-coordinate prismatic boron. These interconvert, with an activation-energy barrier of $92 \, kJ \, mol^{-1}$. The cluster $B_9H_7(SMe_2)_2$ is also found to be fluxional, with an activation energy of $80 \, kJ \, mol^{-1}$ due to a cage rearrangement which may follow a $D_{3h} \rightleftharpoons C_{4v} \rightleftharpoons D_{3h}$ sequence.

Turning now to metallaboranes and -carboranes, the *arachno*-1-metallopentaborane $[1,1,1-(CO)PMe_3)_2(1-IrB_4H_9)]$ has been shown by $^1H-\{^{31}P\}$ NMR to be fluxional, with the two PMe_3 groups becoming equivalent and the basal borane ^{11}B and ^1H nuclei (except the unique bridging hydrogen) becoming equivalent in pairs. This suggests a rapid mutual pseudorotation of the η^4-borane and $(PMe_3)_2CO$ groups (80), $L = PMe_3$, $L' = CO$:[313]

(80)
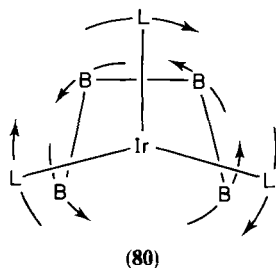
Analogous pseudorotation processes are also postulated for the *nido*-7-platinaundecaborane $[(PMe_2Ph)_2(PtB_{10}H_{12})]^{314}$ and various *nido*-6-

rhenadecaboranes.[315] The latter species undergo dual pseudorotational fluxionality, with $\Delta G^{\neq}$ values of the order of 45–60 and 30 kJ mol^{-1}. A detailed ^{1}H and ^{31}P–$\{^1$H$\}$ study of numerous 12-vertex *closo*-phosphino-metallacarboranes has been undertaken,[316] and activation energies reported for the metal vertex undergoing hindered rotation with respect to the 5-membered face of the carborane cage. Complexes include those of general type [L$_2$HM(carb)] (L = substituted phosphine, carb = 1,2-, 1,7- or 1,12-C$_2$B$_9$H$_{10}$R, M = Rh^{III}, Ir^{III}). $\Delta G^{\neq}$ values for the rotational barriers range from below 35 to above 73 kJ mol^{-1}.

ACKNOWLEDGMENT

REFERENCES

1. B. E. Mann, in *Annual Reports on NMR Spectroscopy*, Vol. 12 (G. A. Webb, ed.), Academic Press, London, 1982, p. 263.
2. J. Kaplan and G. Fraenkel, *NMR of Chemically Exchanging Systems*, Academic Press, New York, 1981.
3. J. Sandström, *Dynamic NMR Spectroscopy*, Academic Press, London, 1982.
4. J. B. Lambert, *NATO ASI Ser., Ser. C*, 1983, **103**, 91–110.
5. J. Schotland and J. S. Leigh, *J. Magn. Reson.*, 1983, **51**, 48.
6. A. K. Roy, A. A. Jones, and P. T. Inglefield, *J. Magn. Reson.*, 1985, **64**, 441.
7. R. Kuespert, *J. Magn. Reson.*, 1982, **47**, 91.
8. R. Laatikainen, *J. Magn. Reson.*, 1985, **64**, 375.
9. V. Gold and L. Z. Zdunek, *J. Chem. Soc., Faraday Trans. II*, 1982, **78**, 1835.
10. L. Z. Zdunek and V. Gold, *J. Chem. Soc., Faraday Trans. II*, 1982, **78**, 1825.
11. P. O. Westlund and H. Wennerstroem, *J. Magn. Reson.*, 1982, **50**, 451.
12. J. I. Kaplan and A. N. Garroway, *J. Magn. Reson.*, 1982, **49**, 464.
13. S. Szymanski, *Mol. Phys.*, 1985, **55**, 763.
14. M. L. Martin, F. Mabon and M. Trierweiler, *J. Phys. Chem.*, 1981, **85**, 76.
15. D. W. Aksnes and K. Ramstad, *Magn. Reson. Chem.*, 1985, **23**, 253.
16. S. Aime, R. Gobetto, D. Osella, G. E. Hawkes and E. W. Randall, *J. Chem. Soc., Dalton Trans.*, 1984, 1863.
17. B. E. Mann, C. M. Spencer, B. F. Taylor and P. Yavari, *J. Chem. Soc., Dalton Trans.*, 1984, 2027.
18. D. F. R. Gilson and G. Gomez, *J. Organomet. Chem.*, 1982, **240**, 41.
19. D. G. Gillies, L. P. Blaauw, G. R. Hays, R. Huis and A. D. H. Clague, *J. Magn. Reson.*, 1981, **42**, 420.
20. K. Lystbaek and H. Bildsoe, *Magn. Reson. Chem.*, 1985, **23**, 263.
21. I. M. Ismail, S. J. S. Kerrison and P. J. Sadler, *Polyhedron*, 1982, **1**, 57.
22. J. Frahm, *J. Magn. Reson.*, 1982, **47**, 209.

23. D. Lankhorst, J. Schriever and J. C. Leyte, *J. Magn. Reson.*, 1983, **51**, 430.

24. W. P. Rothwell and J. S. Waugh, *J. Chem. Phys.*, 1981, **74**, 2721.

25. J. I. Kaplan and K. V. Vasavada, *J. Magn. Reson.*, 1983, **52**, 475.

26. K. V. Vasavada and J. I. Kaplan, *J. Magn. Reson.*, 1985, **62**, 37.

27. B. E. Mann, C. M. Spencer and A. K. Smith, *J. Organomet. Chem.*, 1983, **244**, C17.

28. G. E. Hawkes, E. W. Randall, S. Aime, D. Osella and J. E. Elliot, *J. Chem. Soc., Dalton Trans.*, 1984, 279.

29. M. J. Hails, B. E. Mann and C. M. Spencer, *J. Chem. Soc., Dalton Trans.*, 1985, 693.

30. D. M. Heinekey and W. A. G. Graham, *J. Am. Chem. Soc.*, 1982, **104**, 915.

31. D. C. Roe, *J. Am. Chem. Soc.*, 1983, **105**, 7770.

32. N. M. Doherty and J. E. Bercaw, *J. Am. Chem. Soc.*, 1985, **107**, 2670.

33. C. T. G. Knight and A. E. Merbach, *J. Am. Chem. Soc.*, 1984, **106**, 804.

34. K. Ugurbil, *J. Magn. Reson.*, 1985, **64**, 207.

35. J. Hennig and H. H. Limbach, *J. Magn. Reson.*, 1982, **49**, 322.

36. J. R. Lyerla, C. S. Yannoni and C. A. Fyfe, *Acc. Chem. Res.*, 1982, **15**, 208.

37. C. A. Fyfe *et al., Phil. Trans. R. Soc. Lond.*, 1982, **A305**, 591.

38. G. E. Balimann, C. J. Groombridge, R. K. Harris, K. J. Packer, B. J. Say and S. F. Tanner, *Phil. Trans. R. Soc. Lond.*, 1981, **A299**, 643.

39. D. E. Wemmer, D. J. Ruben and A. Pines, *J. Am. Chem. Soc.*, 1981, **103**, 28.

40. N. M. Szeverenyi, M. J. Sullivan and G. E. Maciel, *J. Magn. Reson.*, 1982, **47**, 462.

41. B. E. Hanson, M. J. Sullivan and R. J. Davis, *J. Amer. Chem. Soc.*, 1984, **106**, 251.

42. W. T. Dixon, J. Schaefer, M. D. Sefcik, E. O. Stejskal and R. A. McKay, *J. Magn. Reson.*, 1982, **49**, 341.

43. W. T. Dixon, *J. Chem. Phys.*, 1982, **77**, 1800.

44. J. Jeener, B. H. Meier, P. Bachmann and R. R. Ernst, *J. Chem. Phys.*, 1979, **71**, 4546.

45. E. W. Abel, T. P. J. Coston, K. G. Orrell, V. Šik and D. Stephenson, *J. Magn. Reson.*, 1986, **70**, 34.

46. S. Macura and R. R. Ernst, *Mol. Phys.*, 1980, **41**, 95.

47. G. E. Hawkes, L. Y. Lian, E. W. Randall and K. D. Sales, *J. Magn. Reson.*, 1985, **65**, 173.

48. R. Ramachandran, C. T. G. Knight, R. J. Kirkpatrick and E. Oldfield, *J. Magn. Reson.*, 1985, **65**, 136.

49. G. Wagner, G. Bodenhausen, N. Mueller, M. Rance, O. W. Soerensen, R. R. Ernst and K. Wuethrich, *J. Am. Chem. Soc.*, 1985, **107**, 6440.

50. S. Macura, Y. Huang, D. Suter and R. R. Ernst, *J. Magn. Reson.*, 1981, **43**, 259.

51. S. Macura, K. Wuethrich and R. R. Ernst, *J. Magn. Reson.*, 1982, **46**, 269.

52. M. Rance, G. Bodenhausen, G. Wagner, K. Wuethrich and R. R. Ernst, *J. Magn. Reson.*, 1985, **62**, 497.

53. D. J. States, R. A. Haberkorn and D. J. Ruben, *J. Magn. Reson.*, 1982, **48**, 286.

54. E. T. Olejniczak, J. C. Hoch, C. M. Dobson and F. M. Poulsen, *J. Magn. Reson.*, 1985, **64**, 199.

55. G. Bodenhausen and R. R. Ernst, *Mol. Phys.*, 1982, **47**, 319.

56. A. M. Kook, P. N. Nickias, J. P. Selegue and S. L. Smith, *Organometallics*, 1984, **3**, 499.

57. A. Zschunke, H. Meyer and I. Nehls, *Z. Anorg. Allg. Chem.*, 1982, **494**, 189.

58. H. Meyer and A. Zschunke, *J. Organomet. Chem.*, 1984, **269**, 209.

59. C. L. Perrin and R. K. Gipe, *J. Am. Chem. Soc.*, 1984, **106**, 4036.

60. Y. Huang, S. Macura and R. R. Ernst, *J. Am. Chem. Soc.*, 1981, **103**, 5327.

61. G. E. Hawkes, L. Y. Lian, E. W. Randall, K. D. Sales and S. Aime, *J. Chem. Soc., Dalton Trans.*, 1985, 225.

62. R. Benn, *Agnew. Chem., Int. Ed. Engl.*, 1982, **21**, 626.

63. A. A. Ismail, F. Sauriol, J. Sedman and I. S. Butler, *Organometallics*, 1985, **4**, 1914.

64. C. Wynants, G. Van Binst, C. Muegge, K. Jurkschat, A. Tzchach, H. Pepermans, M. Gielen and R. Willem, *Organometallics*, 1985, **4**, 1906.
65. D. L. Turner, *J. Magn. Reson.*, 1985, **61**, 28.
66. G. Bodenhausen and R. R. Ernst, *J. Magn. Reson.*, 1981, **45**, 367.
67. G. Bodenhausen and R. R. Ernst, *J. Amer. Chem. Soc.*, 1982, **104**, 1304.
68. J. Bremer, G. L. Mendz and W. J. Moore, *J. Am. Chem. Soc.*, 1984, **106**, 4691.
69. H. Bleich and J. Wilde, *J. Magn. Reson.*, 1984, **56**, 149.
70. A. F. De Jong, A. P. M. Kentgens and W. S. Veeman, *Chem. Phys. Lett.*, 1984, **109**, 337.
71. G. S. Harbison, D. P. Raleigh, J. Herzfeld and R. G. Griffin, *J. Magn. Reson.*, 1985, **64**, 284.
72. R. Naor and Z. Luz, *J. Chem. Phys.*, 1982, **76**, 5662.
73. Z. Luz, *Isr. J. Chem.*, 1983, **23**, 305.
74. Z. Luz, *NATO ASI Ser., Ser. C*, 1985, **141**, 315.
75. Z. Luz and R. Naor, *Mol. Phys.*, 1982, **46**, 891.
76. C. J. Hawkins and J. A. Palmer, *Coord. Chem. Rev.*, 1982, **44**, 1.
77. A. Shaver and J. M. McCall, *Organometallics*, 1984, **3**, 1823.
78. I. Buchanan, C. D. Garner and W. Clegg, *J. Chem. Soc., Dalton Trans.*, 1984, 1333.
79. H. Duddeck, P. Wagner and S. Gegner, *Tetrahedron Lett.*, 1985, **26**, 1205.
80. E. W. Abel, M. Booth and K. G. Orrell, *J. Organomet. Chem.*, 1981, **208**, 213.
81. E. W. Abel, M. Booth, C. A. Brown, K. G. Orrell and R. L. Woodford, *J. Organomet. Chem.*, 1981, **214**, 93.
82. B. Czech, A. Piorko and R. Annunziata, *J. Organomet. Chem.*, 1983, **255**, 365.
83. K. G. Orrell, V. Šik, C. H. Brubaker and B. McCulloch, *J. Organomet. Chem.*, 1984, **276**, 267.
84. E. W. Abel, S. K. Bhargava, K. G. Orrell and V. Šik, *J. Chem. Soc., Dalton Trans.*, 1982, 2073.
85. K. Brown and P. A. Chaloner, *J. Organomet. Chem.*, 1981, **217**, C25.
86. P. A. Chaloner, *J. Organomet. Chem.*, 1984, **266**, 191.
87. S. D. Pastor, J. D. Spivack, R. K. Rodebaugh and D. Bini, *J. Org. Chem.*, 1984, **49**, 1297.
88. L. Manojlovic-Muir, K. W. Muir, A. A. Frew, S. S. M. Ling, M. A. Thomson and R. J. Puddephatt, *Organometallics*, 1984, **3**, 1637.
89. K. M. Aalmo and J. Krane, *Acta Chem. Scand.*, 1982, **A36**, 219.
90. G. C. Van Stein, G. Van Koten, K. Vrieze and C. Brevard, *Inorg. Chem.*, 1984, **23**, 4269.
91. W. E. Buhro and J. A. Gladysz, *Inorg. Chem.*, 1985, **24**, 3505.
92. T. H. Newman, J. C. Calabrese, R. T. Oakley, D. A. Stanislawski and R. West, *J. Organomet. Chem.*, 1982, **225**, 211.
93. P. Mirti, *Transition Met Chem.*, 1984, **9**, 357.
94. E. W. Abel, S. K. Bhargava and K. G. Orrell, *Prog. Inorg. Chem.*, 1984, **32**, 28.
95. C. J. Ruffing and T. B. Rauchfuss, *Organometallics*, 1985, **4**, 524.
96. I. B. Benson, S. A. R. Knox, P. J. Naish and A. J. Welch, *J. Chem. Soc., Dalton Trans.*, 1981, 2235.
97. E. W. Abel, K. M. Higgins, K. G. Orrell, V. Šik, E. H. Curzon and O. W. Howarth, *J. Chem. Soc., Dalton Trans.*, 1985, 2195.
98. E. W. Abel, M. Booth, K. G. Orrell and G. M. Pring, *J. Chem. Soc., Dalton Trans.*, 1981, 1944.
99. E. W. Abel, S. K. Bhargava, P. K. Mittal, K. G. Orrell and V. Šik, *J. Chem. Soc., Chem. Commun.*, 1982, 535.
100. E. W. Abel, G. D. King, K. G. Orrell and V. Šik, *Polyhedron*, 1983, **2**, 1363.
101. E. W. Abel, M. Z. A. Chowdhury, K. G. Orrell and V. Šik, *J. Organomet. Chem.*, 1984, **262**, 293.
102. E. W. Abel, S. K. Bhargava, P. K. Mittal, K. G. Orrell and V. Šik, *J. Chem. Soc., Dalton Trans.*, 1985, 1561.

103. E. W. Abel, P. K. Mittal, K. G. Orrell and V. Šik, *J. Chem. Soc., Dalton Trans.*, 1985, 1569.
104. E. W. Abel, M. M. Bhatti, K. G. Orrell and V. Šik, *J. Organomet. Chem.*, 1981, **208**, 195.
105. E. W. Abel, S. K. Bhargava, M. M. Bhatti, K. Kite, M. A. Mazid, K. G. Orrell, V. Šik, B. L. Williams, M. B. Hursthouse and K. M. A. Malik, *J. Chem. Soc., Dalton Trans.*, 1982, 2065.
106. E. W. Abel, M. Z. A. Chowdhury, K. G. Orrell and V. Šik, *Polyhedron*, 1984, **3**, 331.
107. E. W. Abel, S. K. Bhargava, K. Kite, K. G. Orrell, V. Šik and B. L. Williams, *J. Chem. Soc., Dalton Trans.*, 1984, 365.
108. E. W. Abel, S. K. Bhargava, M. M. Bhatti, M. A. Mazid, K. G. Orrell, V. Šik, M. B. Hursthouse and K. M. A. Malik, *J. Organomet. Chem.*, 1983, **250**, 373.
109. C. T. Page and J. E. Fergusson, *Austr. J. Chem.*, 1983, **36**, 855.
110. E. W. Abel, T. E. MacKenzie, K. G. Orrell and V. Šik, *J. Chem. Soc., Dalton Trans.*, 1986, 205.
111. E. W. Abel, S. K. Bhargava, K. Kite, K. G. Orrell, V. Šik and B. L. Williams, *Polyhedron*, 1982, **1**, 289.
112. E. W. Abel, A. R. Khan, K. Kite, K. G. Orrell and V. Šik, *J. Organomet. Chem.*, 1982, **225**, 357.
113. E. W. Abel, S. K. Bhargava, K. Kite, K. G. Orrell, V. Šik and B. L. Williams, *J. Chem. Soc., Dalton Trans.*, 1982, 583.
114. E. W. Abel, M. Z. A. Chowdhury, K. G. Orrell and V. Šik, *J. Organomet. Chem.*, 1983, **258**, 109.
115. E. W. Abel, S. K. Bhargava, K. G. Orrell, A. W. G. Platt, V. Šik and T. S. Cameron, *J. Chem. Soc., Dalton Trans.*, 1985, 345.
116. E. W. Abel, K. Kite, K. G. Orrell, V. Šik and B. L. Williams, *J. Chem. Soc., Dalton Trans.*, 1981, 2439.
117. E. W. Abel, P. K. Mittal, K. G. Orrell, V. Šik and T. S. Cameron, *J. Chem. Soc., Chem. Commun.*, 1984, 1312.
118. E. W. Abel, P. K. Mittal, K. G. Orrell and V. Šik, *J. Chem. Soc., Dalton Trans.*, 1986, 961.
119. E. W. Abel, T. E. MacKenzie, K. G. Orrell and V. Šik, *J. Chem. Soc., Dalton Trans.*, 1986, 2173.
120. D. J. Iverson, G. Hunter, J. F. Blount, J. R. Damewood, and K. Mislow, *J. Am. Chem. Soc.*, 1981, **103**, 6073.
121. J. F. Blount, G. Hunter and K. Mislow, *J. Chem. Soc., Chem. Commun.*, 1984, 170.
122. G. Hunter and K. Mislow, *J. Chem. Soc., Chem. Commun.*, 1984, 172.
123. M. J. McGlinchey, J. L. Fletcher, B. G. Sayer, P. Bougeard, R. Faggiani, C. J. L. Lock, A. D. Bain, C. Rodger, E. P. Kundig, D. Astruc, J.-R. Hamon, P. Le Maux, S. Top and G. Jaouen, *J. Chem. Soc., Chem. Commun.*, 1983, 634.
124. M. J. McGlinchey, P. Bougeard, B. G. Sayer, R. Hofer and C. J. L. Lock, *J. Chem. Soc., Chem. Commun.*, 1984, 789.
125. G. Hunter, W. S. Wadsworth, and K. Mislow, *Organometallics*, 1982, **1**, 968.
126. E. M. Campi, B. M. K. Gatehouse, W. R. Jackson, I. D. Rae and M. G. Wong, *J. Chem. Soc., Chem. Commun.*, 1984, 175.
127. D. S. Stephenson and G. Binsch, *J. Magn. Reson.*, 1978, **32**, 145.
128. R. C. Fay, J. R. Weir and A. H. Bruder, *Inorg. Chem.*, 1984, **23**, 1079.
129. B. M. Mattson, A. E. Madera and M. C. Palozzotto, *J. Coord. Chem.*, 1984, **13**, 321.
130. I. J. B. Lin, *J. Chin. Chem. Soc. (Taipei)*, 1983, **30**, 17.
131. B. McCulloch and C. H. Brubaker, *Organometallics*, 1984, **3**, 1707.
132. R. S. Herrick, S. J. Nieter-Burgmayer and J. L. Templeton, *Inorg. Chem.*, 1983, **22**, 3275.
133. E. Kleinpeter, S. Behrendt and L. Beyer, *Z. Anorg. Allg. Chem.*, 1982, **495**, 105.
134. S. Joss, P. Bigler and A. Ludi, *Inorg. Chem.*, 1985, **24**, 3487.
135. F. B. McCormick and R. J. Angelici, *J. Organomet. Chem.*, 1981, **205**, 79.

136. S. E. Kegley, M. Brookhart and G. R. Husk, *Organometallics*, 1982, **1**, 760.
137. F. J. Manganiello, M. D. Radcliffe and W. M. Jones, *J. Organomet. Chem.*, 1982, **228**, 273.
138. M. F. Lappert, P. I. Riley, P. I. W. Yarrow, J. L. Atwood, W. E. Hunter and M. J. Zaworotko, *J. Chem. Soc., Dalton Trans.*, 1981, 814.
139. E. E. Wille, D. S. Stephenson, P. Capriel and G. Binsch, *J. Amer. Chem. Soc.*, 1982, **104**, 405.
140. A. G. Kent, B. E. Mann and C. P. Manuel, *J. Chem. Soc., Chem. Commun.*, 1985, 728.
141. H. Van der Poel and G. Van Koten, *Inorg. Chem.*, 1981, **20**, 2941.
142. H. Van der Poel and G. Van Koten, *Inorg. Chem.*, 1981, **20**, 2950.
143. R. Lazzaroni, G. Uccello-Barretta, S. Bertozzi and P. Salvadori, *J. Organomet. Chem.*, 1984, **275**, 145.
144. C. G. Kreiter, K. Nist and H. G. Alt, *Chem. Ber.*, 1981, **114**, 1845.
145. U. Koemm and C. G. Kreiter, *J. Organomet. Chem.*, 1982, **240**, 27.
146. R. Benn, *Org. Magn. Reson.*, 1983, **21**, 723.
147. H. Lehmkuhl, J. Elsaesser, R. Benn, B. Gabor, A. Rufinska, R. Goddard and C. Krueger, *Z. Naturforsch.*, 1985, **40b**, 171.
148. D. Parker, *J. Organomet. Chem.*, 1982, **240**, 83.
149. M. A. Arthurs and S. M. Nelson, *J. Coord. Chem.*, 1983, **13**, 29.
150. M. Mlekuz, P. Bougeard, B. G. Sayer, S. Peng, M. J. McGlinchey, A. Marinetti, J. Y. Saillard, J. Ben Naceur, B. Mentzen and G. Jaounen, *Organometallics*, 1985, **4**, 1123.
151. B. E. R. Schilling and R. Hofmann, *Acta Chem. Scand.*, 1979, **B33**, 231.
152. R. D. Barr, M. Green, T. B. Marder and F. G. A. Stone, *J. Chem. Soc., Dalton Trans.*, 1984, 1261.
153. G. Michael and C. G. Kreiter, *Z. Naturforsch* 1984, **39b**, 1738.
154. L. Harland, G. R. Stephenson and M. J. Whittaker, *J. Organomet. Chem.*, 1984, **263**, C30.
155. G. Erker, T. Muellenbernd, R. Benn, A. Rufinska, Y. H. Tsay and C. Krueger, *Angew. Chem., Int. Ed. Engl.*, 1985, **24**, 321.
156. A. Salzer, T. Egolf and W. Von Philipsborn, *J. Organomet. Chem.*, 1981, **221**, 351.
157. N. M. D. Brown, F. Davidson and J. W. Wilson, *J. Organomet. Chem.*, 1981, **210**, 1.
158. R. I. Baxter, R. J. M. Sands and J. W. Wilson, *J. Chem. Res., Synop.*, 1983, 94.
159. C. H. Bushweller, S. Hoogasian, A. D. English, J. S. Miller and M. Z. Lourandos, *Inorg. Chem.*, 1981, **20**, 3448.
160. A. T. M. Marcelis, H. J. Korte, B. Krebs and J. Reedijk, *Inorg. Chem.*, 1982, **21**, 4059.
161. P. J. Fagan, J. M. Manriquez, S. H. Vollmer, C. S. Day, V. W. Day and T. J. Marks, *J. Amer. Chem. Soc.*, 1981, **103**, 2206.
162. M. D. Fryzuk, S. J. Rettig, A. Westerhaus and H. D. Williams, *Inorg. Chem.*, 1985, **24**, 4316.
163. M. H. Chisholm, K. Folting, J. C. Huffman and I. P. Rothwell, *Organometallics*, 1982, **1**, 251.
164. G. Jaouen, A. Marinetti, J. Y. Saillard, B. G. Sayer and M. J. McGlinchey, *Organometallics*, 1982, **1**, 225.
165. P. Braunstein, G. L. Geoffroy and B. Metz, *Nouv. J. Chim.*, 1985, **9**, 221.
166. A. Bonny, R. D. Holmes-Smith, G. Hunter and S. R. Stobart, *J. Am. Chem. Soc.*, 1982, **104**, 1855.
167. A. D. McMaster and S. R. Stobart, *J. Am. Chem. Soc.*, 1982, **104**, 2109.
168. A. D. McMaster and S. R. Stobart, *J. Chem. Soc., Dalton Trans.*, 1982, 2275.
169. M. J. Hails, B. E. Mann and C. M. Spencer, *J. Chem. Soc., Dalton Trans.*, 1983, 729.
170. E. G. Hoffmann, H. Nehl, H. Lehmkuhl, K. Seevogel and W. Stempfle, *Chem. Ber.*, 1984, **117**, 1364.
171. P. Bougeard, M. Mancini, B. G. Sayer and M. J. McGlinchey, *Inorg. Chem.*, 1985, **24**, 93.
172. C. P. Casey and J. M. O'Connor, *Organometallics*, 1985, **4**, 384.
173. R. Benn and G. Schroth, *J. Organomet. Chem.*, 1982, **228**, 71.
174. M. Kotzian, C. G. Kreiter and S. Oezkar, *J. Organomet. Chem.*, 1982, **229**, 29.

175. D. Baudry, M. Ephritikhine, H. Felkin and J. Zakrzewski, *J. Organomet. Chem.*, 1984, **272**, 391.

176. O. W. Howarth, C. H. McAteer, P. Moore and G. E. Morris, *J. Chem. Soc., Chem. Commun.*, 1981, 506.

177. M. Brookhart, W. Lamanna and M. B. Humphrey, *J. Amer. Chem. Soc.*, 1982, **104**, 2117.

178. F. Timmers and M. Brookhart, *Organometallics*, 1985, **4**, 1365.

179. T. V. Ashworth, A. A. Chalmers, E. Meintjies, H. E. Oosthuizen and E. Singleton, *Organometallics*, 1984, **3**, 1485.

180. J. R. Blackborow, C. R. Eady, F. W. Grevels, E. A. Koerner von Gustorf, A. Scrivanti, O. S. Wolfbeis, R. Benn, D. J. Brauer and C. Krueger, *J. Chem. Soc., Dalton Trans.*, 1981, 661.

181. W. D. Jones and J. A. Maguire, *Organometallics*, 1985, **4**, 951.

182. W. D. Jones and F. J. Feher, *J. Am. Chem. Soc.*, 1984, **106**, 1650.

183. K. C. Dash, *Indian J. Chem.*, 1985, **A24**, 265.

184. G. Erker, K. Berg, R. Benn, and G. Schroth, *Chem. Ber.*, 1985, **118**, 1383.

185. K. J. Karel, T. A. Albright and M. Brookhart, *Organometallics*, 1982, **1**, 419.

186. R. Benn, K. Cibura, P. Hofmann, K. Jonas and A. Rufinska, *Organometallics*, 1985, **4**, 2214.

187. L. K. K. Li Shing Man, J. G. A. Reuvers, J. Takats and G. Deganello, *Organometallics*, 1983, **2**, 28.

188. J. L. Templeton and B. C. Ward, *J. Am. Chem. Soc.*, 1981, **103**, 3743.

189. P. Bischofberger and H. J. Hansen, *Helv. Chim. Acta*, 1982, **65**, 721.

190. M. Kotzian, C. G. Kreiter, G. Michael and S. Oezkar, *Chem. Ber.*, 1983, **116**, 3637.

191. S. Ozkar and C. G. Kreiter, *J. Organomet. Chem.*, 1983, **256**, 57.

192. D. J. Darensbourg and R. L. Gray, *Inorg. Chem.*, 1984, **23**, 2993.

193. S. Aime, *Inorg. Chim. Acta*, 1982, **62**, 51.

194. S. Aime and D. Osella, *J. Organomet. Chem.*, 1981, **214**, C27.

195. J. Wachter, J. G. Riess and A. Mitschler, *Organometallics*, 1984, **3**, 714.

196. F. A. Cotton, L. M. Daniels, K. R. Dunbar, L. R. Falvello, S. M. Tetrick and R. A. Walton, *J. Am. Chem. Soc.*, 1985, **107**, 3524.

197. J. A. Marsella and K. G. Caulton, *Organometallics*, 1982, **1**, 274.

198. L. H. Staal, J. Keijsper, L. H. Polm and K. Vrieze, *J. Organomet. Chem.*, 1981, **204**, 101.

199. H. C. Dorn, B. E. Hanson and E. J. Motell, *J. Organomet. Chem.*, 1982, **224**, 181.

200. A. A. Koridze, O. A. Kizas, N. M. Astakhova and P. V. Petrovskii, *Izv. Akad. Nauk SSSR, Ser. Khim*, 1981, 1181.

201. R. E. Benfield, P. D. Gavens, B. F. G. Johnson, M. J. Mays, S. Aime, L. Milone and D. Osella, *J. Chem. Soc., Dalton Trans.*, 1981, 1535.

202. A. D. Clauss, M. Tachikawa, J. R. Shapley and C. G. Pierpont, *Inorg. Chem.*, 1981, **20**, 1528.

203. S. Aime and A. J. Deeming, *J. Chem. Soc., Dalton Trans.*, 1981, 828.

204. S. Aime, D. Osella, L. Milone and E. Rosenberg, *J. Organomet. Chem.*, 1981, **213**, 207.

205. J. B. Keister and J. R. Shapley, *Inorg. Chem.*, 1982, **21**, 3304.

206. E. Rosenberg, C. B. Thorsen, L. Milone and S. Aime, *Inorg. Chem.*, 1985, **24**, 231.

207. E. Rosenberg, E. V. Anslyn, C. Barner-Thorsen, S. Aime, D. Osella, R. Gobetto and L. Milone, *Organometallics*, 1984, **3**, 1790.

208. S. Aime, R. Gobetto, D. Osella, L. Milone and E. Rosenberg, *Organometallics*, 1982, **1**, 640.

209. G. Granozzi, E. Tondello, M. Casarin, S. Aime and D. Osella, *Organometallics*, 1983, **2**, 430.

210. C. Barner-Thorsen, K. I. Hardcastle, E. Rosenberg, J. Siegel, A. M. M. Lanfredi, A. Tiripicchio and C. M. Tiripicchio, *Inorg. Chem.*, 1981, **20**, 4306.

211. C. E. Kampe, N. M. Boag, C. B. Knobler and H. D. Kaesz, *Inorg. Chem.*, 1984, **23**, 1390.

212. A. C. Willis, F. W. B. Einstein, R. M. Ramadan and R. K. Pomeroy, *Organometallics*, 1983, **2**, 935.

213. A. J. Deeming, S. Donovan-Mtunzi, S. E. Kabir and P. J. Manning, *J. Chem. Soc., Dalton Trans.*, 1985, 1037.

214. D. A. Young, *Inorg. Chem.*, 1981, **20**, 2049.
215. C. P. Casey and R. M. Bullock, *J. Organomet. Chem.*, 1981, **218**, C47.
216. T. Beringhelli, G. Ciani, G. D'Alfonso, P. Romiti, A. Sironi and M. Freni, *Inorg. Chem.*, 1984, **23**, 2849.
217. B. T. Heaton, L. Strona, J. Jonas, T. Eguchi and G. A. Hoffman, *J. Chem. Soc., Dalton Trans.*, 1982, 1159.
218. L. Garlaschelli, A. Fumagalli, S. Martinengo, B. T. Heaton, D. O. Smith and L. Strona, *J. Chem. Soc., Dalton Trans.*, 1982, 2265.
219. B. T. Heaton, R. Della Pergola, L. Strona, D. O. Smith and A. Fumagalli, *J. Chem. Soc., Dalton Trans.*, 1982, 2553.
220. A. Ceriotti, G. Longoni, R. Della Pergola, B. T. Heaton and D. O. Smith, *J. Chem. Soc., Dalton Trans.*, 1983, 1433.
221. B. T. Heaton, L. Strona, R. Della Pergola, J. L. Vidal and R. C. Schoening, *J. Chem. Soc., Dalton Trans.*, 1983, 1941.
222. A. Fumagalli, S. Martinengo, P. Chini, D. Galli, B. T. Heaton and R. Della Pergola, *Inorg. Chem.*, 1984, **23**, 2947.
223. G. Doyle, B. T. Heaton and E. Occhiello, *Organometallics*, 1985, **4**, 1224.
224. W. L. Gladfelter, J. R. Fox, J. A. Smegal, T. G. Wood and G. L. Geoffroy, *Inorg. Chem.*, 1981, **20**, 3223.
225. S. Aime, D. Osella, L. Milone, G. E. Hawkes and E. W. Randall, *J. Am. Chem. Soc.*, 1981, **103**, 5920.
226. C. P. Horwitz and D. F. Shriver, *Organometallics*, 1984, **3**, 756.
227. G. F. Stuntz and J. R. Shapley, *J. Organomet. Chem.*, 1981, **213**, 389.
228. D. Braga, R. Ros and R. Roulet, *J. Organomet. Chem.*, 1985, **286**, C8.
229. A. R. Siedle, R. A. Newmark and L. H. Pignolet, *J. Am. Chem. Soc.*, 1982, **104**, 6584.
230. S. Okeya, T. Miyamoto, S. Ooi, Y. Nakamura and S. Kawaguchi, *Bull. Chem. Soc. Jpn*, 1984, **57**, 395.
231. D. T. Haworth, J. W. Beery and M. Das, *Polyhedron*, 1982, **1**, 9.
232. D. L. Grossmann and D. T. Haworth, *Inorg. Chim. Acta*, 1984, **84**, L17.
233. R. C. Fay and A. F. Lindmark, *J. Am. Chem. Soc.*, 1983, **105**, 2118.
234. A. D. Garnovskii, I. S. Vasil'chenko, S. G. Kochin, L. S. Minkina, V. D. Khavryuchenko and L. E. Nivorozhkin, *Koor. Khim.*, 1985, **11**, 1156.
235. M. C. Gennaro and P. Mirti, *J. Inorg. Nucl. Chem.*, 1981, **43**, 1711.
236. P. Mirti and M. C. Gennaro, *J. Inorg. Nucl. Chem.*, 1981, **43**, 3221.
237. M. C. Gennaro and P. Mirti, *Nouv. J. Chim.*, 1981, **5**, 495.
238. M. C. Gennaro, P. Mirti and M. Vallinotto, *Nouv. J. Chim.*, 1981, **5**, 501.
239. P. Mirti, M. C. Gennaro and M. Vallinotto, *Transition Met. Chem.*, 1982, **7**, 2.
240. R. E. Cramer and P. L. Dahlstrom, *Inorg. Chem.*, 1985, **24**, 3420.
241. G. C. Van Stein, G. Van Koten, B. De Bok, L. C. Taylor, K. Vrieze and C. Brevard, *Inorg. Chim. Acta*, 1984, **89**, 29.
242. G. W. Bushnell, K. R. Dixon, D. T. Eadie and S. R. Stobart, *Inorg. Chem.*, 1981, **20**, 1545.
243. L. E. Nivorozhkin, M. S. Korobov, A. L. Nivorozhkin, L. E. Konstantinovskii and V. I. Minkin, *Zh. Obsch. Khim*, 1985, **55**, 1125.
244. M. Cocivera, T. J. Desmond, G. Ferguson, B. Kaitner, F. J. Lalor and D. J. O'Sullivan, *Organometallics*, 1982, **1**, 1125.
245. M. Cocivera, G. Ferguson, F. J. Lalor and P. Szczecinski, *Organometallics*, 1982, **1**, 1139.
246. D. L. Reger and M. E. Tarquini, *Inorg. Chem.*, 1983, **22**, 1064.
247. M. Onishi, K. Hiraki, A. Ueno, Y. Yamaguchi and Y. Ohama, *Inorg. Chim. Acta*, 1984, **82**, 121.
248. A. L. Nivorozhkin, M. S. Korobov, L. E. Konstantinovskii and V. E. Minkin, *Zh. Obshch. Khim*, 1985, **55**, 946.

249. G. A. Foulds, G. E. Jackson and D. A. Thornton, *J. Mol. Struct.*, 1983, **98**, 323.
250. C. J. Creswell, M. A. M. Queiros and S. D. Robinson, *Inorg. Chim. Acta*, 1982, **60**, 157.
251. J. L. Nieto, F. Galindo and A. M. Gutierrez, *Polyhedron*, 1985, **4**, 1611.
252. R. Willem, M. Gielen, J. Meunier-Piret, M. Van Meerssche, K. Jurkschat and A. Tzschach, *J. Organomet. Chem.*, 1984, **277**, 335.
253. M. Oki and M. Ohira, *Chem. Lett.*, 1982, 1267.
254. K. R. Dixon, D. T. Eadie and S. R. Stobart, *Inorg. Chem.*, 1982, **21**, 4318.
255. D. L. Johnson, A. R. Fritzberg, B. L. Hawkins, S. Kasina and D. Eshima, *Inorg. Chem.*, 1984, **23**, 4204.
256. J. Mason, D. M. P. Mingos, D. Sherman and R. W. M. Wardle, *J. Chem. Soc., Chem. Commun.*, 1984, 1223.
257. M. G. B. Drew, F. S. Esho and S. M. Nelson, *J. Chem. Soc., Dalton Trans.*, 1983, 1653.
258. R. Favez and R. Roulet, *Inorg. Chem.*, 1981, **20**, 1598.
259. F. A. Van-Catledge, S. D. Ittel and J. P. Jesson, *Organometallics*, 1985, **4**, 18.
260. P. J. Domaille, R. L. Harlow and S. S. Wreford, *Organometallics*, 1982, **1**, 935.
261. C. G. Kreiter, M. Kotzian, U. Schubert, R. Bau and M. A. Bruck, *Z. Naturforsch*, 1984, **39b**, 1553.
262. L. Dahlenburg and F. Mirzaei, *J. Organomet. Chem.*, 1983, **251**, 123.
263. N. K. Roberts and S. B. Wild, *Inorg. Chem.*, 1981, **20**, 1892.
264. N. K. Roberts and S. B. Wild, *Inorg. Chem.*, 1981, **20**, 1900.
265. J. A. L. Palmer and S. B. Wild, *Inorg. Chem.*, 1983, **22**, 4054.
266. E. W. Abel, G. D. King, K. G. Orrell, G. M. Pring, V. Šik and T. S. Cameron, *Polyhedron*, 1983, **2**, 1117.
267. E. W. Abel, S. K. Bhargava, T. E. MacKenzie, P. K. Mittal, K. G. Orrell and V. Šik, *J. Chem. Soc., Chem. Commun.*, 1982, 983.
268. E. W. Abel, S. K. Bhargava, T. E. MacKenzie, P. K. Mittal, K. G. Orrell and V. Šik, *J. Chem. Soc., Dalton Trans.*, Accepted for publication.
269. J. P. Fackler, L. D. Thompson, I. J. B. Lin, T. A. Stephenson, R. D. Gould, J. M. C. Alison and A. J. F. Fraser, *Inorg. Chem.*, 1982, **21**, 2397.
270. A. Mueting and B. M. Mattson, *J. Inorg. Nucl. Chem.*, 1981, **43**, 749.
271. C. Glidewell and A. R. Hyde, *Polyhedron*, 1985, **4**, 1155.
272. L. J. Maheu, G. L. Miessler, J. Berry, M. Burow and L. H. Pignolet, *Inorg. Chem.*, 1983, **22**, 405.
273. J. L. Templeton, B. C. Ward, G. J. J. Chen, J. W. McDonald and W. E. Newton, *Inorg. Chem.*, 1981, **20**, 1248.
274. W. B. Farnham and R. L. Harlow, *J. Am. Chem. Soc.*, 1981, **103**, 4608.
275. W. H. Stevenson, S. Wilson, J. C. Martin and W. B. Farnham, *J. Am. Chem. Soc.*, 1985, **107**, 6340.
276. W. H. Stevenson and J. C. Martin, *J. Amer. Chem. Soc.*, 1985, **107**, 6352.
277. G. Klebe and K. Hensen, *J. Chem. Soc., Dalton Trans.*, 1985, 5.
278. J. C. Bommer and K. W. Morse, *Inorg. Chim. Acta*, 1983, **74**, 25.
279. D. J. Wink and N. J. Cooper, *J. Chem. Soc., Dalton Trans.*, 1984, 1257.
280. D. R. Eaton, M. J. McGlinchey, K. A. Moffat and R. J. Buist, *J. Amer. Chem. Soc.*, 1984, **106**, 8110.
281. M. J. Collins and G. J. Schrobilgen, *Inorg. Chem.*, 1985, **24**, 2608.
282. G. Fraenkel, M. Henrichs, M. Hewitt and B. M. Su, *J. Am. Chem. Soc.*, 1984, **106**, 255.
283. R. D. Thomas and J. P. Oliver, *Organometallics*, 1982, **1**, 571.
284. M. H. Chisholm, K. Folting, J. C. Huffman and I. P. Rothwell, *J. Amer. Chem. Soc.*, 1982, **104**, 4389.
285. M. H. Chisholm, K. Folting, D. M. Hoffman and J. C. Huffman, *J. Am. Chem. Soc.*, 1984, **106**, 6794.

286. J. M. Bassett, G. K. Barker, M. Green, J. A. K. Howard, F. G. A. Stone and W. C. Wolsey, *J. Chem. Soc., Dalton Trans.*, 1981, 219.

287. A. F. Dyke, S. A. R. Knox, P. J. Naish and G. E. Taylor, *J. Chem. Soc., Dalton Trans.*, 1982, 1297.

288. S. R. Finnimore, S. A. R. Knox and G. E. Taylor, *J. Chem. Soc., Dalton Trans.*, 1982, 1783.

289. A. F. Dyke, S. A. R. Knox, M. J. Morris and P. J. Naish, *J. Chem. Soc., Dalton Trans.*, 1983, 1417.

290. B. E. Hanson and J. S. Mancini, *Organometallics*, 1983, **2**, 126.

291. R. S. Dickson, G. S. Evans and G. D. Fallon, *Austr. J. Chem.*, 1985, **38**, 273.

292. E. B. Boyar and S. D. Robinson, *J. Chem. Soc., Dalton Trans.*, 1985, 629.

293. C. Woodcock and R. Eisenberg, *Inorg. Chem.*, 1985, **24**, 1285.

294. C. T. Hunt and A. L. Balch, *Inorg. Chem.*, 1982, **21**, 1242.

295. G. Erker and K. Kropp, *Chem. Ber.*, 1982, **115**, 2437.

296. M. C. Grossel, R. P. Moulding and K. R. Seddon, *J. Organomet. Chem.*, 1983, **247**, C32.

297. E. W. Abel, M. Booth, G. D. King, K. G. Orrell, G. M. Pring and V. Šik, *J. Chem. Soc., Dalton Trans.*, 1981, 1846.

298. E. W. Abel, G. D. King, K. G. Orrell, V. Šik, T. S. Cameron and K. Jochem, *J. Chem. Soc., Dalton Trans.*, 1984, 2047.

299. M. H. Chisholm, K. Folting, J. A. Heppert, D. M. Hoffman and J. C. Huffman, *J. Am. Chem. Soc.*, 1985, **107**, 1234.

300. J. Evans and G. S. McNulty, *J. Chem. Soc., Dalton Trans.*, 1981, 2017.

301. A. A. Koridze, O. A. Kizas, N. E. Kolobova, P. V. Petrovskii and E. I. Fedin, *J. Organomet. Chem.*, 1984, **265**, C33.

302. R. F. Alex and R. K. Pomeroy, *J. Organomet. Chem.*, 1985, **284**, 379.

303. R. T. Edidin, J. R. Norton and K. Mislow, *Organometallics*, 1982, **1**, 561.

304. M. F. Hallam, N. D. Howells, D. M. P. Mingos and R. W. M. Wardle, *J. Chem. Soc., Dalton Trans.*, 1985, 845.

305. M. Pfeffer, J. Fischer and A. Mitschler, *Organometallics*, 1984, **3**, 1531.

306. G. Jaouen, A. Marinetti, B. Mentzen, R. Mutin, J. Y. Saillard, B. G. Sayer and M. J. McGlinchey, *Organometallics*, 1982, **1**, 753.

307. M. J. McGlinchey, M. Mlekuz, P. Bougeard, B. G. Sayer, A. Marinetti, J. Y. Saillard and G. Jaouen, *Can. J. Chem.*, 1983, **61**, 1319.

308. G. J. Kubas and P. J. Vergamini, *Inorg. Chem.*, 1981, **20**, 2667.

309. Y. Yamamoto, H. Yamazaki and T. Sakurai, *J. Am. Chem. Soc.*, 1982, **104**, 2329.

310. A. L. Casalnuovo, J. A. Casalnuovo, P. V. Nilsson and L. H. Pignolet, *Inorg. Chem.*, 1985, **24**, 2554.

311. T. L. Venable, R. B. Maynard and R. N. Grimes, *J. Am. Chem. Soc.*, 1984, **106**, 6187.

312. E. H. Wong, M. G. Gatter and R. M. Kabbani, *Inorg. Chem.*, 1982, **21**, 4022.

313. J. Bould, N. N. Greenwood and J. D. Kennedy, *J. Chem. Soc., Dalton Trans.*, 1982, 481.

314. S. K. Boocock, N. N. Greenwood, J. D. Kennedy, W. S. McDonald and J. Staves, *J. Chem. Soc., Dalton Trans.*, 1981, 2573.

315. M. A. Beckett, N. N. Greenwood, J. D. Kennedy and M. Thornton-Pett, *J. Chem. Soc., Dalton Trans.*, 1985, 1119.

316. T. B. Marder, R. T. Baker, J. A. Long, J. A. Doi and M. F. Hawthorne, *J. Am. Chem. Soc.*, 1981, **103**, 2988.

This Page Intentionally Left Blank

Nuclear Magnetic Resonance of Cyclophosphazenes

S. S. KRISHNAMURTHY AND MICHAEL WOODS*

Department of Inorganic and Physical Chemistry, Indian Institute of Science, Bangalore 560012, India

I. INTRODUCTION

The phenomenal growth of the applications of NMR spectroscopy in solving diverse chemical problems continues unabated. As a consequence of the commercial availability of Fourier-transform (FT) spectrometers capable of operating at high fields and equipped with tunable multinuclear probes and heteronuclear decoupling accessories, the era of dominance of proton NMR measurements is coming to an end, and NMR studies of other nuclei are gaining in popularity.[1-4] This trend is clearly visible in the chemistry of

*Present address: 80, Shrewsbury Lane, London SE18, UK.

cyclophosphazenes, an important class of inorganic heterocyclic compounds containing an $-\!\!-\![N\!=\!PX_2]\!-\!\!-$ repeating unit in a valence-unsaturated skeleton. These compounds occur in varied ring sizes and shapes, and thus offer some of the best examples of multispin systems that have been studied by NMR techniques. Phosphorus NMR spectroscopy has proved an invaluable structural tool for cyclophosphazenes, and ^{31}P parameters are now reported routinely for this class of compounds. Phosphorus NMR measurements can also be gainfully employed to monitor the course of reactions and to identify unstable intermediates or products that cannot be easily separated from reaction mixtures. In this review we shall present a comprehensive survey of the extensive ^{31}P NMR data that have accumulated for cyclophosphazenes in the last two decades. In addition, major findings involving other familiar nuclei (^{1}H, ^{13}C, ^{15}N, ^{19}F) are summarized and significant trends assessed. Formally saturated cyclophospha*zanes* and cyclic phosphorus–nitrogen compounds containing other heteroatoms in the ring are excluded from this review.

Earlier surveys of NMR data for cyclophosphazenes are understandably limited in scope, and reflect the "state of the art" at that time. The general works on the NMR spectra of organophosphorus compounds[5-7] include some early results for cyclophosphazenes. Data published before 1971 have been tabulated[8]; lists are also to be found in Allcock's book devoted to phosphorus-nitrogen compounds.[9] Finer and Harris[10] have discussed some aspects of P $\cdots$ P couplings observed for cyclophosphazenes and general reviews of the chemistry of these compounds[11-15] contain useful summaries of the applications of NMR spectroscopy. Annual surveys in the *Specialist Periodical Reports on Organophosphorus Chemistry*[16] and on *NMR Spectroscopy*[17] also give brief annotations of significant NMR studies of cyclic phosphorus–nitrogen compounds.

For all the NMR data presented in this review, shifts to low frequency of the reference standard, 85% aqueous phosphoric acid, are assigned a negative sign in accordance with the convention recommended by IUPAC. We have encountered several problems in compiling the data. In numerous papers, authors do not specify the sign convention employed or the solvent used for the measurements. All these data have been standardized to conform to the sign convention adopted in this review. Many earlier papers quote data with reference to standards that are different from the ones in general use today, and in these cases we have applied standard conversions.

The literature has been surveyed until the end of 1984. Structural elucidation and empirical correlations have been given prominance in the text. Theoretical treatments of NMR parameters for cyclophosphazenes are still very limited, and such results are alluded to only briefly. In spite of numerous attempts by several authors to develop unified theoretical foundations for ^{31}P NMR parameters for all classes of phosphorus compounds,[3,4]

the classic work of Letcher and Van Wazer[18] on this subject has not yet been superseded.

The nomenclature and numbering system adopted in this chapter correspond closely to that suggested by Shaw *et al.*[19] and used extensively by Keat and Shaw in their compilation.[8] The structures of cyclotri- and cyclotetraphosphazenes (1) and (2) are shown below:

(1)   (2)
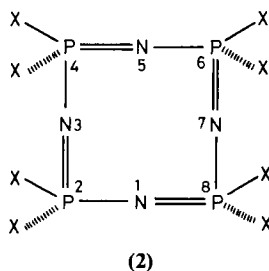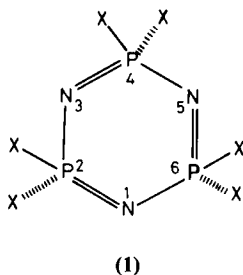
II. CYCLOTRIPHOSPHAZENES

The bulk of NMR studies in cyclophosphazenes chemistry is concerned with the 6-membered cyclotriphosphazene system (1). Proton and ^{31}P NMR data have proved very useful for deducing the structures of the products obtained in the reactions of chloro- and bromocyclophosphazenes with various nucleophiles. The utility of ^{19}F NMR studies for the elucidation of the structure of fluorocyclophosphazenes is well established. The ^{13}C NMR technique appears to be useful only for alkyl- and aryl-substituted cyclophosphazenes as they contain phosphorus–carbon bonds. NMR measurements of ^{15}N in its natural abundance have not been reported for cyclophosphazenes, but NMR investigations have been carried out on ^{15}N-labelled derivatives in some detail. In addition to providing structural information, the NMR data permit conclusions to be drawn regarding the nature of the electronic interactions within the phosphazene ring as well as of the interaction between the ring and an exocyclic substituent.

A. Proton NMR data

1. Proton chemical shifts and assignment of structures to positional and geometrical isomers

Proton NMR spectra of organo-substituted cyclophosphazenes can give valuable information regarding the positional and geometrical disposition of the substituents. For example, the three isomers of tris(dimethyl-

amino)trichlorocyclotriphosphazenes $N_3P_3(NMe_2)_3Cl_3$, viz geminal, non-geminal *trans* and nongeminal *cis*, can be readily distinguished by the appearance in their ^1H NMR spectra of three, two and one dimethylamino doublets respectively (coupling with ^{31}P).[20] In general, the shielding of NMe_2 protons increases with the increasing degree of chlorine replacement.[20,21] Furthermore, the shielding of N$\underline{Me}_2$ protons for the *trans* nongeminal bis(dimethylamino) derivative is less than that for the corresponding *cis* isomer (Fig. 1). Using this criterion, assignments of *cis* and *trans* isomers of several bis(amino)cyclotriphosphazenes $N_3P_3R_2Cl_4$ (R = NHMe,[25] NHEt,[26]

$D = -N(CH_3)_2$; $T = -NPPh_3$

$Ar = -C_6H_4Me - p$, $Ar' = Ph$
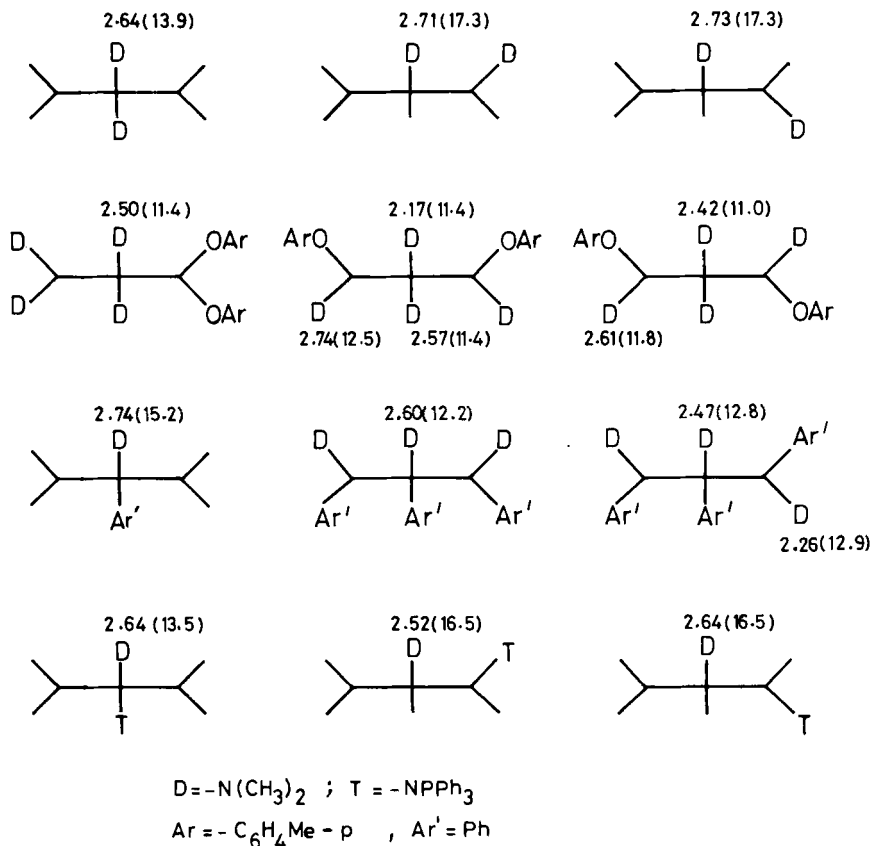
FIG. 1. The chemical shifts and ^3J(P–H) values of NMe_2 protons for selected cyclotri-phosphazenes $N_3P_3(NMe_2)_2Cl_4$, $N_3P_3(OAr)_2(NMe_2)_4$, $N_3P_3Ph(NMe_2)Cl_4$, $N_3P_3Ph_3(NMe_2)_3$ and $N_3P_3(NMe_2)(NPPh_3)Cl_4$ (data from refs. 20, 22–24). The phosphazene ring is shown as a plane projection, with substituents above and below the ring plane; ring nitrogen atoms and chlorines attached to phosphorus atoms are not shown.

NC_2H_4,[27] NEt_2[28] or $NMePh$[29]) have been made. These assignments are confirmed by the ^{19}F NMR spectra of fluorinated derivatives (Section II.C) and also by the determination of the X-ray crystal structures of *cis*- and *trans*-$N_3P_3Cl_4(NMe_2)_2$.[30] A similar shielding is observed for the two nongeminal bis(dimethylamino)fluoro-[31] and bromo-[32] and bis(ethylamino)bromo-[33] cyclotriphosphazenes.

The shielding of the protons of an amino group is accentuated when it is flanked by a phenyl,[24,34-36] phenoxy,[22,37] triphenylphosphazenyl ($N=PPh_3$)[23,38,39] (Fig. 1) or a phenylthio substituent.[40] The shielding of $N\underline{Me}_2$ protons by an anilino group[41] is less than that by a phenyl group.[35] In the reaction of $N_3P_3Cl_6$ with sodium *p*-cresoxide, eleven out of the possible twelve *p*-cresoxy derivatives $N_3P_3Cl_{6-n}[OC_6H_4(Me)-p]_n$ ($n = 1, ..., 6$) have been identified by conversion to their respective dimethylamino derivatives $N_3P_3(NMe_2)_{6-n}[OC_6H_4(Me)-p]_n$, and by examining their ^{1}H NMR spectra.[22] Figure 2 shows the spectrum of the mixture of isomers of $N_3P_3(NMe_2)_4[OC_6H_4(Me)-p]_2$; the chemical shifts and couplings are shown in Fig. 1. This "exhaustive-dimethylamination" technique should be used with caution, as *cis–trans* isomerization may occur under certain experimental conditions.[42] Methoxylation can be used instead for structural assignments, as demonstrated for (*p*-cresoxy)chloro-[43] and (aryl-
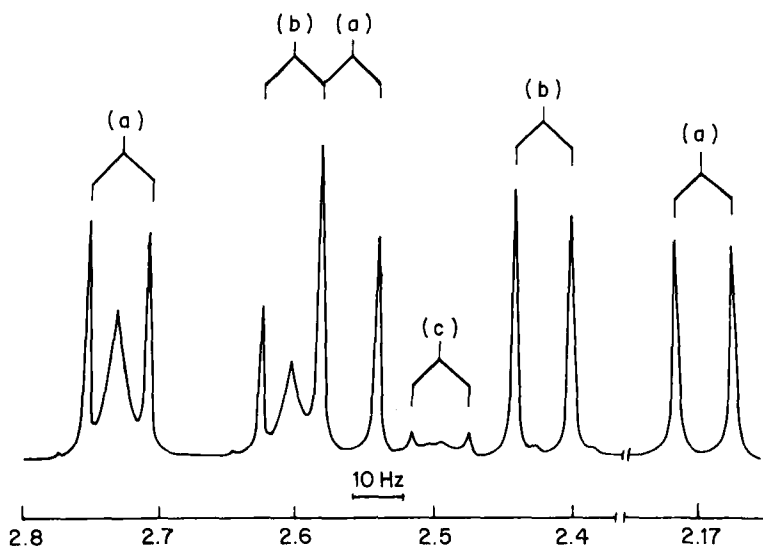
FIG. 2. The ^{1}H NMR (270 MHz, CDCl$_3$) spectrum (NMe region only) of $N_3P_3(NMe_2)_4(OC_6H_4Me-p)_2$, a mixture of (a) 2-*cis*-4, (b) 2-*trans*-4 and (c) 2,2-geminal isomers. (Reproduced from ref. 22 with permission of Johann Ambrosius Barth, Leipzig, DDR.)

amino)chloro-[44] cyclotriphosphazenes. The "methoxylation" procedure is particularly useful for fluorocyclophosphazenes, as complete replacement of fluorine atoms by amino groups is very difficult. The isomeric compositions at the bis, tris and tetra stages of substitution of fluorine atoms from $N_3P_3F_6$ by phenoxide have been determined by conversion of the fluoro(phenoxy) precursors to the respective methoxy derivatives $N_3P_3(OMe)_{6-n}(OPh)_n$ ($n = 2, 3, 4$) and recording their ^{1}H NMR spectra.[45]

Structural assignments for the products of the reactions of pentachloro and pentafluoro(triphenyl phosphazenyl)cyclotriphosphazenes, $N_3P_3X_5(N{=}PPh_3)$ ($X = F$, Cl) (3) with methoxide are based partly on the "shielding" exerted by the $-N{=}PPh_3$ group on the protons of the adjacent *cis* OMe groups:[46,47]
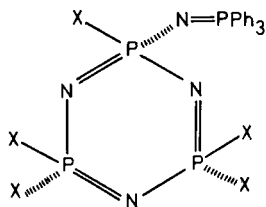
(3)

For the triphenyl phosphazenyl derivatives $N_3P_3(N{=}PPh_3)R_5$ ($R = NMe_2$, OMe, or OCH_2CF_3) the order of shielding of the protons of the R groups is *cis* > *gem* > *trans*. However, for the penta(aziridino)derivative $N_3P_3(N{=}PPh_3)(NC_2H_4)_5$ the shielding sequence of the aziridino protons is *gem* > *cis* > *trans*. This difference is readily explained in terms of the X-ray structure[48] of the penta(aziridino) derivative $N_3P_3(N{=}PPh_3)(NC_2H_4)_5$; the $N{=}PPh_3$ group adopts a novel conformation that causes the protons of the geminal aziridino group to lie in the shielding zone of one of the phenyl rings. An AA'BB' type nonequivalence has been observed for the aziridino protons of (triphenylphosphazenyl)(aziridino)cyclotriphosphazenes in their 270 MHz-^{1}H NMR spectra recorded at ambient temperature; no such nonequivalence is detected for the hexa(aziridino) derivative $N_3P_3(NC_2H_4)_6$, even at $-55\,°C$. Presumably the bulky $-N{=}PPh_3$ substituent renders the aziridino protons nonequivalent by hindering either pyramidal inversion at the aziridino nitrogen atom or rotation around the P–N bond.[48]

The chemical shifts of N–H protons have been utilized for distinguishing geminal and nongeminal (primary alkylamino) cyclotriphosphazenes. The N–$\underline{H}$ resonances for the nongeminal compounds occur at 3.6–3.9δ, whereas those for the geminal derivatives lie at 2.2–2.9δ[26,33,42,49,50] The N–H chemical shifts are known to vary with trace acidic impurities in the solvent and also with temperature. In the absence of detailed studies of these effects,

the infallibility of the above criterion for structural assignments remains to be established.

High-field (270 MHz) ^{1}H NMR spectra of the (oxo)phosphazadienes $N_3(H)P_3(O)(OMe)_3(N{=}PPh_3)(R)$ (4, R = NMe$_2$ or OMe) consist of two sets of four doublets, and this observation clearly shows the existence of two isomers, which differ in the disposition of the $-N{=}PPh_3$ group with respect to the phosphoryl group (cis or trans):
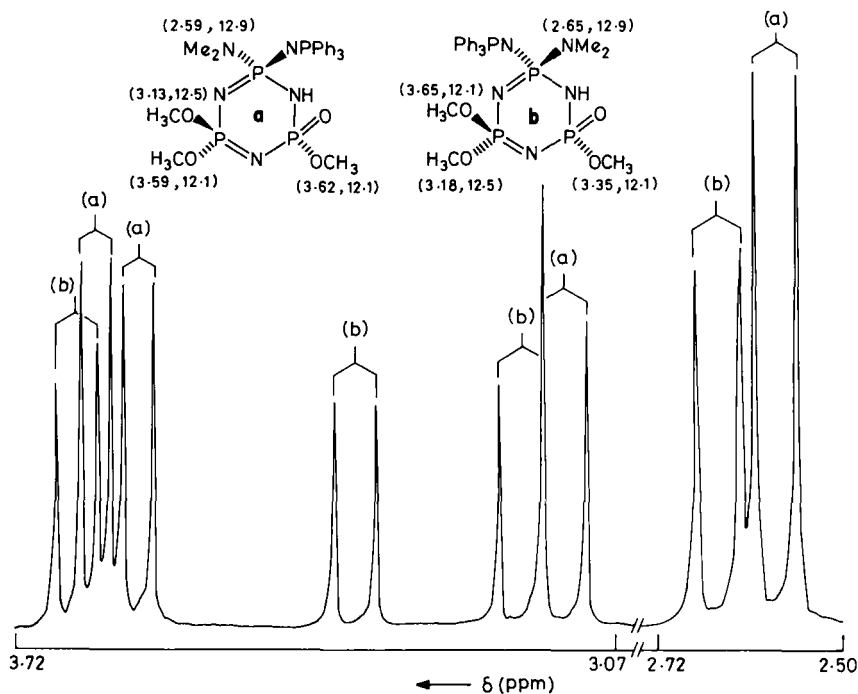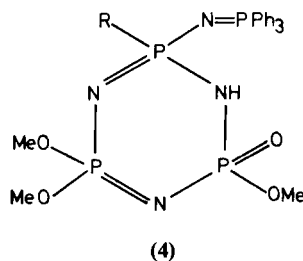

(4)

FIG. 3. The ^{1}H NMR (270 MHz, CDCl$_3$) spectrum of isomeric oxophosphazadienes, $N_3HP(O)(OMe)_3(NPPh_3)(NMe_2)$ (4, R = NMe$_2$) along with assignments.

The spectrum of (4, R = NMe$_2$) is illustrated in Fig. 3 along with the NMR parameters. The assignment of *cis* and *trans* structures is again based on the shielding of the protons of the substituent in a *cis* disposition to the –N=PPh$_3$ substituent.[46,51]

Solvent effects on proton chemical shifts have been investigated in a few instances.[21,31,52,53] Often the use of benzene in place of CDCl$_3$ or CCl$_4$ leads to a better resolution of the spectra on account of differential shielding effects on chemically nonequivalent protons in the molecule.

2. "Virtual-coupling" effects

The ^{1}H NMR spectra of organo substituted cyclophosphazenes often consist of a "hump", or unresolved extra lines between the components of a multiplet, which one might expect from first-order considerations (Fig. 2). This so called "virtual coupling" arises as a consequence of the multispin system inherently present in these compounds. Thus compounds of the type *gem*-N$_3$P$_3$R$_2$(NMe$_2$)$_4$ or *cis*-N$_3$P$_3$Cl$_3$(OMe)$_3$ may be represented as belonging to the general class of $[AX_n]_3$ spin systems, where A is the phosphorus and X is the proton. Spectra of this type of spin system have been computed for various values of the spin parameters appropriate to cyclotriphosphazenes. The dependence of the band shapes of the X-region on the number of X-nuclei in each group (n) has been considered, and it is shown that differences between the cases $n = 3$ and $n = 4$ are negligible. The observed bandshapes cannot be reproduced by these computations if a single line width is used for all the transitions. Possible reasons for this discrepancy are discussed. The most likely explanation for the failure to obtain agreement between observed and computed spectra is that different transitions may have different line widths.[54]

The essential conditions for observing "virtual coupling" in a cyclo-triphosphazene constituting an $[AX_n]_3$ spin system is that $|N| = |J_{AX} + 2J_{AX'}| \leqslant J_{AA}$ (where $|N|$ is the separation between the sharp and intense doublet usually observed) and the difference in chemical shifts between the $A(^{31}P)$ nuclei giving rise to these effects is small or zero.[54,55] For example, in the ^{1}H NMR spectrum of the nongeminal isomers of N$_3$P$_3$(OAr)$_2$(NMe$_2$)$_4$ (Fig. 2) the NMe$_2$ signals of the P(OAr)(NMe$_2$) group show intense "virtual coupling" because of the presence of another such (magnetically nonequiva-lent) ^{31}P nucleus; on the contrary, the signals of the P(NMe$_2$)$_2$ protons do not exhibit "virtual coupling", because the chemical shift of this phosphorus differs from that of the other two phosphorus nuclei by ~ 5.5 ppm. This effect has been noted in earlier studies on the ^{1}H NMR spectra of the ethoxy derivatives N$_3$P$_3$(OEt)$_{6-n}$Ph$_n$ ($n = 0, 2, 4$)[56] and of the homologous series [NP(NMe$_2$)$_2$]$_n$ ($n = 3, ..., 8$).[57] In the latter case, the intensity of the central

"hump" is enhanced relative to that of the doublet as the ring-size increases. The appearance of "virtual coupling" (or its absence) can provide useful structural information[12,13] as has been demonstrated for the spirocyclic derivatives $N_3P_3R_4[NH(CH_2)_2NH]$ (5, $n = 2$, $R^1 = R^2 = Cl$ or NMe_2)[58] and (triphenylphosphazenyl)(methoxy) derivatives $N_3P_3(NPPh_3)X_{5-n}(OMe)_n$ ($X = Cl$ or F, $n = 1, ..., 4$).[47]
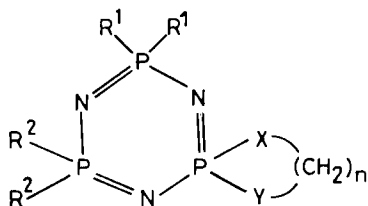
(5)

3. Phosphorus–proton couplings

Because of the second-order effects discussed in the previous subsection, phosphorus–proton couplings measured directly from the spectra of organo-substituted cyclophosphazenes are slightly different from their true values. However, P–H couplings are still of great diagnostic value for distinguishing geminal and nongeminal structures in many systems. The P–H couplings observed for different types of structural units in cyclophosphazenes are listed in Table 1. Coupling of phosphorus and hydrogen separated by more than 4 bonds has been observed only in a few instances.[22,40,86]

(a) One-bond P–H couplings. For hydridophosphazenes (6) the one-bond P–H couplings range from 502 to 719 Hz (Table 2). This feature of the ^{1}H NMR spectra of hydridophosphazenes clearly rule out the alternative N–H tautomeric structure (7) shown below:

(6)   (7)
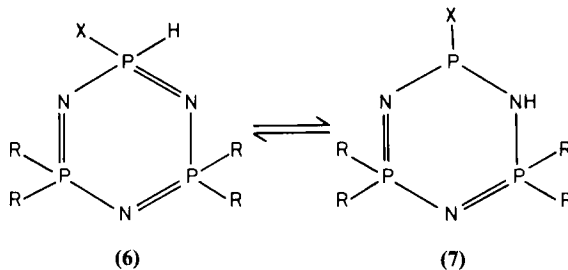
TABLE 1

Phosphorus–proton couplings.

Structural unit	$J(P–H)$ (Hz)	Refs.
One-bond couplings		
P(H)(R)	502–579	59–62
(R = alkyl, aryl)		
P(H)(OR)	670–719	60, 63
P(H)(NMe$_2$)	553, 611	64, 65
Two-bond couplings		
P(Me)(X)	16.5–17.5	66, 67
(X = Cl, Br, I)		
P(Me)(R)	13.5–16	66, 68–70
(R = alkyl, aryl)		
P(NHBu^t)	6–6.5	71
P(NHAr)	8–12	29, 44, 72
P(XCH$_2$CH$_2$NH)	10–13	71, 73
(X = O, NH)		
Three-bond couplings		
R$_2$PNPH	4–14.5	60–62
P(alkyl)X	23–29	67
(X = Cl, Br, I)		
P(alkyl)$_2$	18–21.5	68
P(F)(C$_6$H$_5$)	15.5–16.5	74, 75
P(C$_6$H$_5$)$_2$	13	74, 75
P(NC$_2$H$_4$)Cl	21–22	27, 48, 76
P(NC$_2$H$_4$)(R)	15.5–17.5	27, 48, 76, 77
(R = NC$_2$H$_4$, NRR′, OR)		
P(NMe$_2$)F	12–12.5	31, 53, 78, 79
P(NMe$_2$)Cl	15.5–17.5	20, 21, 32, 53
P(NMe$_2$)Br	18–20	32, 52
P(NMe$_2$)(OR)	12–12.5	22
P(NMe$_2$)$_2$	10–14	20, 21, 24, 53
P(NMe$_2$)(NPPh$_3$)	12.8–14.3	23, 38
P(NHEt)Cl	14–15	49
P(NHEt)Br	14.5–15.5	33
P(NHEt)$_2$	10.5–11.5	33, 49
P(OMe)F	12–13	46, 47
P(OMe)Cl	15–15.5	46, 47, 54
P(OMe)$_2$	12–13	46, 47
P(OMe)(NPPh$_3$)	12–13	46, 47
PF(SEt)	17.5–19	81
P(SEt)$_2$	17.5–18	81, 82
PNR(CH$_2$)$_2$NR (R = H, Me)	10–12.5	71, 73, 83
PNH(CH$_2$)$_3$NH	15–15.5	73, 84, 236

TABLE 1 (*cont.*)

Structural unit	J(P–H) (Hz)	Refs.
Four-bond couplings		
P(NRR')	1	28, 33, 49
R$_2$P̲NPC̲H̲ ^{a}	2–3	67, 68
P(OR)	1	56
P(OCOMe)	2	85
P(SC$_6$H$_4$X)	2–2.5	40, 86
P(R)X	1.5–2	67
PF(C$_6$H$_4$X)	3.5–4.5	75
P—(CH=C=CH$_2$)	11.5–12.5	69
P—(C≡C—CH$_3$)	4	69
P—(CH$_2$—C≡CH̲)	6.5–7	69

^{a}Coupling of proton to the remote phosphorus nuclei.

TABLE 2

(Hydrido)cyclotriphosphazenes (6): ^{1}H chemical shifts and P–H couplings.

R	X	δ(H)	^1J(P–H) (Hz)	^3J(P–N–P–H) (Hz)	Ref.
Cl	Me	7.44	568	11	61
Cl	Et	7.33	553	12	61
Cl	Pr^n	7.33	554	12	61
Cl	Pr^i	7.10	548	13	61
Cl	Bu^n	7.33	554	12	61
Cl	Bu^i	7.36	553	12	61
Cl	Bu^t	6.83	543	13	61
Cl	Ph	7.89	579	4.5	62
Cl	OPr^i	6.40	719	c	63
Me	Me	7.43	504	5.8	60
Ph	Me	7.65	509	3.8	60
Ph	Et	7.58	506	4.6	60
Ph	NMe$_2$	7.55	611	c	64
Ph	OPh	7.36	676	10.0	60
Me, Ph^a	OPh	7.32	675	10.4	60
Me$_2$N	Me	7.33	502	c	60
Me$_2$N	OPh	7.10	670	c	60
H, NMe$_2$ ^{b}	NMe$_2$	6.96	553	c	65

^{a}Geminal derivative; ^{b}nongeminal derivative; ^{c}value not stated.

In metal complexes of hydridophosphazenes the coordination occurs to the phosphorus atom in the N–H tautomeric form (7), and the large one-bond P–H coupling is not observed in the ^{1}H NMR spectra of the complexes (Section V). Schmidpeter and coworkers have shown that the magnitude of ^1J(P–H) depends strongly on the electronegativity of the group X attached to the phosphorus atom bonded to hydrogen (Table 2); this variation also parallels the increase in P–H stretching vibration with the electronegativity of X.[60] In line with this trend, the highest value of ^1J(P–H) has been observed for the isopropoxy derivative $N_3P_3Cl_4(OPr^i)(H)$.[63]

(b) Two-bond P–H couplings. Two-bond P–H couplings are observed for many alkyl-substituted cyclophosphazenes, and can be of diagnostic value (Table 3).[66][69] Schmidpeter and Högel[66] have noted that for the methylcyclophosphazenes (**8**, R = Ph) the value of ^2J(P–C–H) increases with the electronegativity of X, as shown in Fig. 4. The values for bromo and iodo substituents deviate appreciably from the linear relationship, presumably because of widening of the X–P–C angle. The reasons for the deviation of SMe and H from the linearity is not clear, but it is noticeable that both groups have an electronegativity close to that of phosphorus.

Another series of compounds for which ^2J(P–H) can be observed (in principle) consists of (primary-amino)cyclophosphazenes or spirocyclic compounds containing a P—NH grouping. For most of these derivatives, the N–*H* resonances appear as unresolved humps, and the coupling to phosphorus cannot usually be discerned. However when an aromatic primary amino group is present, for example $N_3P_3Cl_2(NMePh)_3(NHPh)$[29] or $N_3P_3Cl_5(NHAr)$,[44] the N–*H* signals are sharp and ^2J(P–H) ranges from 7.0 to 12.0 Hz. For the spirocyclic phosphazenes $N_3P_3Cl_2R_2(XCH_2CH_2NH)$ (R = Ph or $NHBu^t$; X = NH or O), the value of ^2J(P–H) for the spiro unit lies between 10.0 and 13.0 Hz; for the $NHBu^t$ group the ^2J(P–H) value is 6.0–6.5 Hz.[71] The NH resonance for the fluorospirocyclic derivative $N_3P_3F_4[NH(CH_2)_2NH]$ also appears as a sharp doublet, with a ^2J(P–H) value of 11.4 Hz. The N–H resonances of analogous spirocyclic phosphazenes containing a six-membered spiro ring do not show this splitting.[73,84] Presumably, hydrogen-bonding effects, which would lock the hydrogen in certain preferred conformations, are responsible for the observed differences.

(c) Three-bond P–H couplings. The magnitude of ^3J(P–H) has proved a useful and reliable criterion for distinguishing geminal and nongeminal structures for numerous (amino)chlorocyclophosphazenes N_3P_3 $(NRR')_{6-n}Cl_n$ (Table 1; Fig. 1). In general, the geminal coupling constant is 3–4 Hz lower than the nongeminal one.[12,13,20] The highest ^3J(P–H) value observed is for the $PCl(NC_2H_4)$ group.[27,48,76] A similar distinction between

TABLE 3

Variation of ^2J(P–C–H) for methyl-substituted cyclotriphosphazenes (8).

(8)
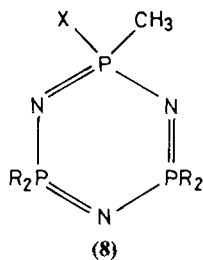
R	X	^2J(P–C–H) (Hz)	Ref.
Cl	H	16.0	68
Cl	Me	14.4	68
Cl	Et	14.5	68
Cl	Pr^i	13.5	68
Cl	Bu^t	14.0	68
Cl	CH_2—CH=CH_2	14.5	68
Cl	CH_2C≡CH	14.5	69
Cl	CH=C=CH_2	15.1	69
Cl	C≡$C.CH_3$	16.0	69
Cl	CH_2C≡$C.CH_3$	14.3	69
Cl	Cl	17.5	67
Cl	Br	17.0	67
Cl	I	17.0	67
Cl	OMe	18.5	67
Cl	OPh	18.1	67
Cl	NHBu^n	17.8	67
Ph	H	15.1	60
Ph	Me	14.3	66
Ph	C(O)Me	13.4	66
Ph	SiMe$_3$	10.6	66
Ph	SnMe$_3$	10.7	66
Ph	NMe$_2$	15.6	66
Ph	PMe$_2$	12.3	66
Ph	PMe$_2$N(tos)	14.9	66
Ph	OMe	17.4	66
Ph	SMe	15.9	66
Ph	Cl	17.4	66
Ph	Br	17.0	66
Ph	I	16.8	66
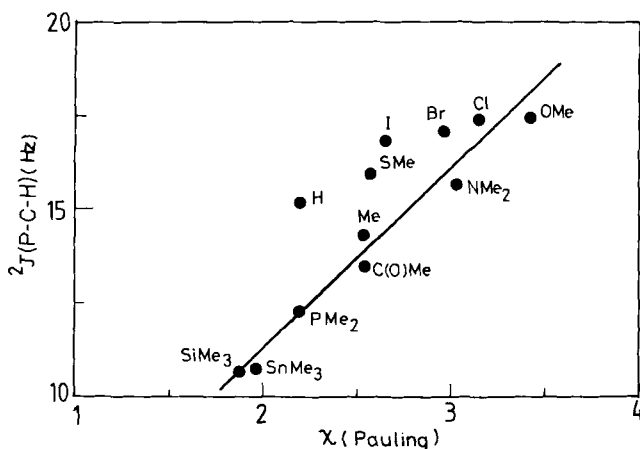
FIG. 4. A plot of ^2J(P–C–H) for $N_3P_3Ph_4MeX$ (8, R = Ph) (Table 3) *versus* electronegativity (χ) of the X group (Pauling scale[87]).

geminal and nongeminal structures can be made for (amino)bromocyclo-phosphazenes[32,33,52] and (methoxy)chlorocyclophosphazenes[46,47] on the basis of ^3J(P–H) values. This structural criterion is not informative for (amino) and (alkoxy)fluorocyclophosphazenes; the ^3J(P–H) for $P(NMe_2)_2$, $P(NMe_2)F$, $P(OMe)_2$ and $P(OMe)F$ lie more or less in the same range, viz 10–13 Hz (Table 1).

Allen has reported the three-bond phosphorus–proton couplings for aryl-substituted fluorocyclophosphazenes. The value of J(P–H_{ortho}) is slightly lower for a geminal configuration at phosphorus compared with that for a nongeminal disposition. This difference presumably arises from the smaller exocyclic bond angle (and hence less s-character) at a PAr_2 centre compared with a PF(Ar) centre, although owing to the proximity of the *ortho*-proton to the phosphorus nucleus, orbital and dipolar terms may make significant contributions to the magnitude of J(P–H_{ortho}).[74,75] For the pentafluoro-mono(aryl)cyclophosphazenes $N_3P_3F_5[C_6H_4X$-$p]$ (X = F, Cl, OCH_3, CH_3) the value of ^3J(P–H_{ortho}) increases in the order F < OCH_3 < Cl < Me, although the overall change (1–2 Hz) is small. The more the electron density in the aryl ring, the lower is the effective charge on the *ortho* hydrogen atom, and hence a reduction in the value of J(P–H_{ortho}) results. Thus better π-donors (F, OCH_3) lower the values of ^3J(P–H_{ortho}), whereas the poorer electron donors (Cl, Me) increase it.[75] In alkyl-substituted cyclophos-phazenes the $P(alkyl)_2$ group[68] is associated with a ^3J(P–H) value that is 6–7 Hz less than that for P(alkyl)X (X = Cl, Br or I).[67] It is noteworthy that for the series, $N_3P_3Cl_4MeR$ (R = Et, Pr^i, Bu^t), the ^3J(P–H) of the R group

decreases from 21.0 to 18.0 Hz. However, there is no regular trend for the series of dialkyl compounds containing isopropyl or t-butyl groups.[68]

The coupling of hydrogen to the remote phosphorus nuclei [^3J(P–N–P–H)] ranges in value from 11 to 14.5 Hz for hydridophosphazenes containing chlorine atoms at the remote P nuclei. If the ring is substituted with several alkyl or aryl substituents, this coupling is very much attenuated (Table 2).

An interesting feature of the proton NMR spectra of spirocyclic cyclophosphazenes is that ^3J(P–H) for five-membered spiro rings is smaller than that for the analogous six-membered spiro rings.[71,73,84] This difference is particularly apparent for $N_3P_3Cl_4[HN(CH_2)_2NH]$ (^3J(P–H) = 11.4 Hz) and $N_3P_3Cl_4$ [$HN(CH_2)_3NH$] (^3J(P–H) = 15.4 Hz). The former value is close to ^3J(P–H) values observed for numerous geminally substituted (amino)cyclophosphazenes. The smaller bond angle at the phosphorus within the five-membered ring and the consequent decrease in π-bonding of the two nitrogen atoms of the spiro ring to the phosphorus atom may be responsible for the appreciable decrease of ^3J(P–H) for 5-membered spiro rings (Section II.B.2.f).

(d) Four-bond P–H couplings. Four-bond P–H couplings for (amino) and (alkoxy)cyclophosphazenes are usually < 1.0 Hz and seldom resolved in their ^{1}H NMR spectra. For alkyl-substituted cyclophosphazenes ^4J(P–C–C–C–H) is ~ 2.0 Hz.[67] However, when an aryl group is considered, the ^4J(P–H$_{meta}$) can be as high as 3.5–4.5 Hz.[75] The highest ^4J(P–C–C–C–H) coupling (11.5–12.6 Hz) observed is for the –CH=C=CH$_2$ group attached to phosphorus; here an extended conjugation between the phosphazene ring and the exocyclic π-system can be envisaged. Conformational effects must also be important since a five-bond coupling of 6.6 Hz is observed for the group, $\underline{P}$—CH$_2$—C≡C—C$\underline{H}_3$ whereas the four-bond coupling for $\underline{P}$—C≡C—C$\underline{H}_3$ and $\underline{P}$—CH$_2$—C≡C$\underline{H}$ is 4.0 and 6.5 Hz respectively.[69]

For P—Me and P—CH$_2$ groups of alkyl-substituted cyclophosphazenes, the four-bond P–H coupling involving the remote phosphorus nuclei ^4J(P–N–P–C–H) is only slightly higher for PRCl (3–3.2 Hz) compared with the value for the PR$_2$ (2–2.5 Hz) group.[67,68]

B. ^{31}P NMR spectra

1. Different types of spin systems observed and structural assignments

Proton-decoupled ^{31}P NMR spectra of cyclotriphosphazenes provide examples of different types of a three-spin system (A$_3$, AB$_2$, AX$_2$, ABC, ABX or AMX). The form of the spectra in conjunction with the chemical shifts

yield structural information, particularly for those compounds for which proton NMR data are uninformative. The assignment of geminal structures to $N_3P_3Cl_2(NHBu^t)_4$,[55,88] $N_3P_3Cl_4(NCS)_2$,[89] $N_3P_3Br_4(NH_2)_2$[90] and the geminal and nongeminal isomers of $N_3P_3Cl_4(NHPh)_2$[41,44] and $N_3P_3Cl_4(NHPr^i)_2$[50] serve to illustrate this point. The geminal structure of $N_3P_3Cl_4(SEt)_2$ is clearly revealed by its proton-coupled ^{31}P NMR spectrum, which shows a quintet of triplets because of coupling with four equivalent protons and two equivalent $\underline{P}Cl_2$ groups.[91] Similarly the ^{31}P NMR spectrum of the mono(1,3-diaminopropane) derivative $N_3P_3Cl_4[NH(CH_2)_3NH]$ (5, $n = 3$; X = Y = NH; $R^1 = R^2 = Cl$) shows a triplet of quintets,[92] which is only consistent with a spirocyclic structure for this compound and not the *ansa* structure assumed previously.[9] Subsequently many monospiro- (5) and dispirocyclotriphosphazenes (9) have been prepared; these compounds generally show either AB_2 or AX_2 type ^{31}P{^{1}H} NMR spectra:[71,73,93-99]

(9)
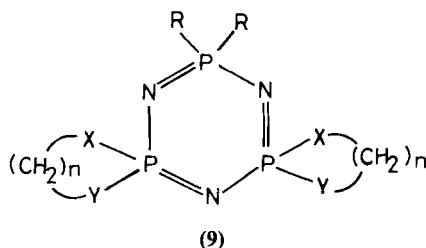
Fluorination of spirocyclic chloro derivatives with potassium fluoride in methyl cyanide affords the fluoro analogues. Their ^{31}P NMR spectra show a triplet with a large J spacing of $\sim 900\,Hz$ (presence of PF_2 groups only), and so this technique can be conveniently used for assigning structures to spirocyclic chloro precursors.[73]

Most cyclotriphosphazenes contain only two differently substituted phosphorus centres, and consequently give rise to AB_2 or AX_2 type spectra. Examples of cyclotriphosphazenes exhibiting ABC, ABX or AMX type spectra are rare (for example the spiro derivatives $N_3P_3Cl_2R_2[NH(CH_2)_2X]$ (R = Ph, NHBu^t, X = NH or O)[71] and the recently reported *ansa* derivative, $N_3P_3Cl_3Me[NH(CH_2)_3O]$[100]).

The ^{31}P-{^{1}H} NMR spectra of phosphazenyl ($N=PX_3$) substituted cyclotriphosphazenes constitute examples of a four-spin system, and in many cases recourse to high-field ($> 80\,MHz$) measurements is necessary for the analysis of the complex spectra.[46-48] The spectrum of *gem*-$N_3P_3Cl_2(OMe)_3(NPPh_3)$ is shown in Fig. 5, and the signals due to $\underline{P}(OMe)_2$, $\underline{P}Cl_2$, $\underline{P}(OMe)(NPPh_3)$ and $NP\underline{P}Ph_3$ can be readily assigned. The geminal and nongeminal isomers of $N_3P_3Cl_4(NPPh_3)(NEt_2)$(10, 11) have been distin-
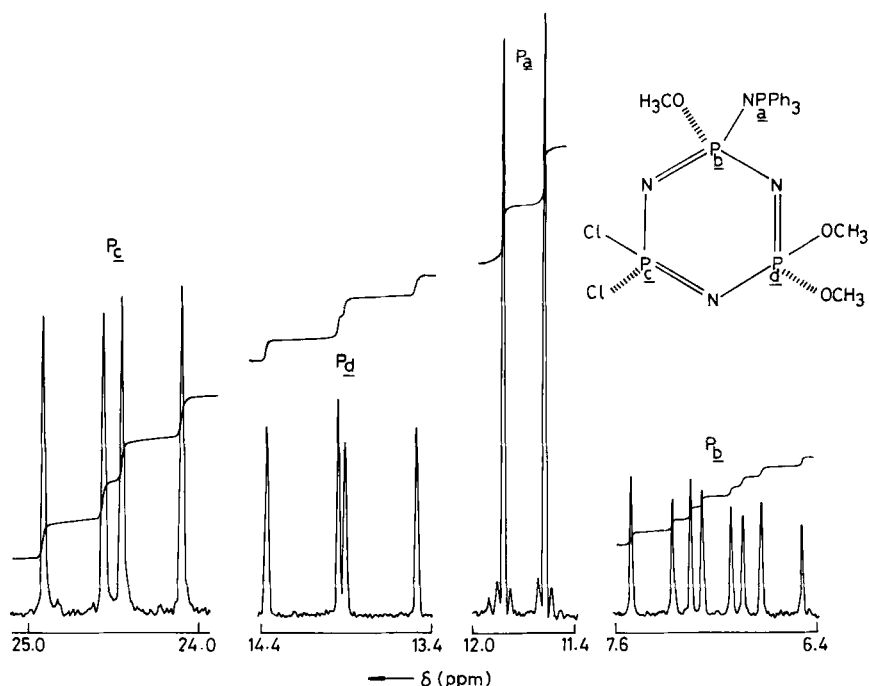
FIG. 5. The $^{31}P-\{^1H\}$ (162 MHz, CDCl$_3$) spectrum of gem-N$_3$P$_3$Cl$_2$(OMe)$_3$(NPPh$_3$).

guished by the observation of three and four distinct phosphorus environ-
ments respectively in their $^{31}P-\{^1H\}$ NMR spectra.[101] The ^{31}P NMR
spectrum of gem-N$_3$P$_3$Cl$_4$(N=PCl$_3$)$_2$ (12) clearly establishes its structure,
and this result has dispelled the doubts concerning the geminal structure of its
precursor N$_3$P$_3$Cl$_4$(NH$_2$)$_2$.[102,103]
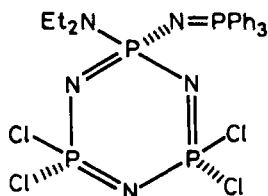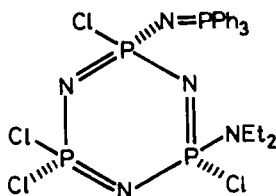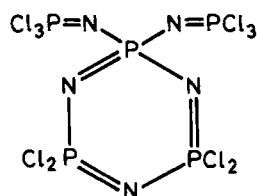
The NMR spectra of fluorinated cyclotriphosphazenes containing Cl, Br
or NMe$_2$ substituents provide examples of [AX]$_3$, A[BX]$_2$, AX[BY]$_2$ and

AB_2XY (A and B denote ^{31}P; X and Y refer to ^{19}F) spin systems, which have been analysed by iterative computation, often relying on the $^{19}F-\{^1H\}$ part of the spectra (Section II.C).[104] In addition, ^{31}P spectra for cis- and trans-2,4-$N_3P_3F_2Cl_4$, 2,2:4-cis-6:4,6 and 2,2:4-trans-6:4,6-$N_3P_3Cl_2F_2(NMe_2)_2$, 2,2:4-trans-6:4,6-$N_3P_3F_2Cl_2(NMe_2)_2$ (A[BX]$_2$ spin system) and 2,2:4-cis-6:4,6-$N_3P_3F_2Cl_2(NMe_2)_2$ (AB_2XY spin system) have been used in the iterative computational analysis, and couplings and chemical shifts evaluated.

Allcock and coworkers have used ^{31}P NMR spectroscopy to great advantage for monitoring the course of reactions of $N_3P_3Cl_6$ with Grignard[105] and organo-copper reagents;[61,68] the intermediacy of a metallo-phosphazene derivative has been established in these reactions, although it could not be isolated. The ^{31}P NMR technique has also been used to study the rates of hydrolysis of several (amino)cyclotriphosphazenes.[106]

2. ^{31}P chemical shifts and empirical trends

In one of the early compilations of ^{31}P chemical shifts for many cyclic and acyclic phosphorus–nitrogen compounds, Schmidpeter and Schumann[107] pointed out that the observed ^{31}P shielding for PN_4-type compounds is increased with changes in nitrogen hybridization in the order $p^3 \rightarrow sp^3 \rightarrow sp^2 \rightarrow sp$. For cyclotriphosphazenes with P–N–P angles close to 120° the ^{31}P shifts often lie to high frequency compared with analogous acyclic systems. On the other hand, for cyclotetraphosphazenes the P–N–P angle is much wider (130–135°), signifying a greater tendency towards sp hybridization: consequently the phosphorus chemical shifts lie between the values for cyclotriphosphazenes and open-chain compounds.

The confusion prevailing in the interpretation of the ^{31}P chemical shifts of many organophosphorus compounds MPZ_3 (M = lone pair, O or S), has been discussed[3,4] on the basis of the theory of Letcher and Van Wazer.[18] Electron withdrawal from phosphorus can lead to either shielding or deshielding, and anomalies can arise by a simplistic application of the above theory.[18] The latter assumes that the phosphorus chemical shift is the sum of p- and d-orbital terms:

$$\delta = \delta_0 + \delta_p + \delta_d \qquad (1)$$

where δ_0 is a constant determined by the reference standard and δ_p and δ_d are the paramagnetic shielding contributions arising from p- and d-orbital unbalancing terms. Substituent effects on phosphorus chemical shifts will thus depend on a complex interplay of electronegativity, bond angles and the changes in occupancy of phosphorus p- and d-orbitals. No satisfactory method is yet available to quantify each of these effects separately. Theoretical interpretation of ^{31}P chemical shifts for cyclophosphazenes is even more

difficult than for acyclic phosphorus compounds, because the nature of bonding in cyclophosphazenes is complex and has been a continuing challenge to theoreticians.[9,13,108]

[31]P chemical shifts are now available for a large number of cyclophosphazenes containing different substituents, and the data are given in 24 tables in the Appendix. We shall confine our discussion to empirical trends, and devote particular attention to papers that have attempted to rationalize the observed ^{31}P chemical shifts. The available data on the ^{31}P chemical shifts (and P–P couplings) for pairs of geometrical (cis and trans) isomers are still very limited, and no clear trends can be discerned which differentiate them unequivocally.

(a) Halogeno and pseudohalogeno derivatives. The ^{31}P chemical shifts for halogeno and pseudohalogeno derivatives range from -45.4 for $N_3P_3Br_6$[109] to 26.7 for $2,4,6,6:2$-cis-4-$N_3P_3Cl_4F_2$[104]. The shielding sequence is PBr_2 $> P(NCS)_2 > PFBr > PF_2 > P(N_3)_2 > PFCl > PCl_2$.[104] For the (chloro)-(bromo)cyclotriphosphazenes $N_3P_3Cl_{6-n}Br_n$ ($n = 1, ..., 5$) and the end-members of the series ($N_3P_3Br_6$ and $N_3P_3Cl_6$), the $\underline{P}Cl_2$, $\underline{P}ClBr$ and $\underline{P}Br_2$ nuclei become more shielded upon progressive replacement of chlorine by bromine.[109] The variations for each of these three groupings are linear with respect to the degree of chlorine replacement, and the three lines have almost identical slopes.

(b) Alkyl and aryl cyclotriphosphazenes. Data for a large number of monoalkyl(aryl)- or geminally substituted dialkyl(aryl)chloro- and fluoro-cyclotriphosphazenes are available. In contrast, data for fully substituted derivatives or alkyl/aryl halogenocyclophosphazenes with different degrees of halogen replacement are somewhat limited (Table A.2). For phenyl substituted chlorocyclophosphazenes, $\delta(PPh_2)$ is only slightly downfield (2.5 ppm) from the values for $\delta(PCl_2)$; $\delta(PPhCl)$ on the other hand is markedly deshielded (15 ppm) with respect to either $\delta(PPh_2)$ or $\delta(PCl_2)$.[34,55,110,111] The changes are represented graphically in Fig. 6(a). Similar linear variations of $\delta(PF_2)$, $\delta(PPhF)$ and $\delta(PPh_2)$ with the number n of phenyl groups are observed for the fluorocyclotriphosphazenes $N_3P_3F_{6-n}Ph_n$ ($n = 2$, 3, 4).[112,113]

Harris[114] has analysed the ^{31}P chemical shifts of a series of alkyl- and aryl-substituted cyclotriphosphazenes, and evaluated the partial contributions of the alkyl groups to the chemical shift of the alkyl/aryl-substituted phosphorus nucleus. These values allow an accurate prediction of the observed chemical shifts. For the geminal dialkyl compounds $N_3P_3Cl_4(R)(R')$ the sequence of partial chemical-shift contribution is $CH_3 < C_2H_5 < i\text{-}C_3H_7 <$ $t\text{-}C_4H_9$. This order is the reverse of that expected from simple inductive effect
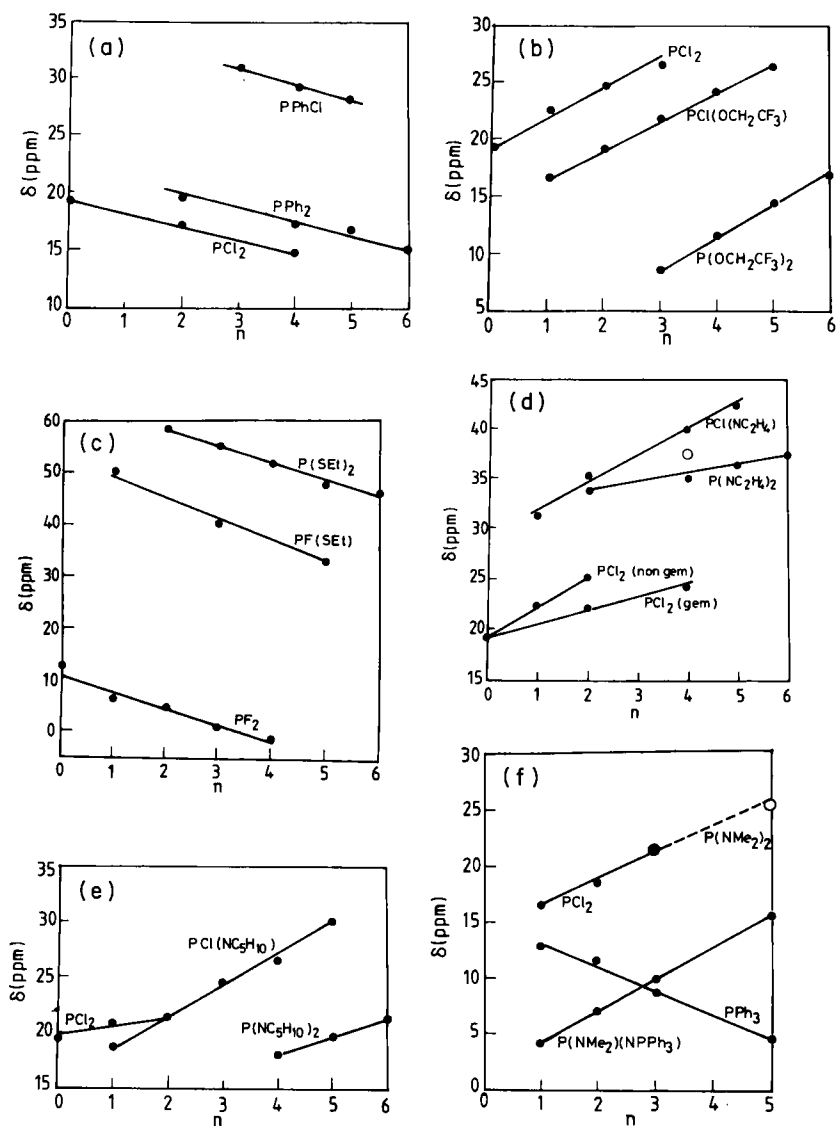
FIG. 6. Variation of $\delta(^{31}P)$ with the degree of halogen substitution n for the series (a) $N_3P_3Cl_{6-n}Ph_n$, (b) $N_3P_3Cl_{6-n}(OCH_2CF_3)_n$, (c) $N_3P_3F_{6-n}(SEt)_n$, (d) $N_3P_3Cl_{6-n}(NC_2H_4)_n$, (e) $N_3P_3Cl_{6-n}(NC_5H_{10})_n$ and (f) $N_3P_3(NPPh_3)Cl_{5-n}(NMe_2)_n$. In (d) the open circle represents $\delta(P)$ of $\underline{P}(NC_2H_4)_2$ for nongeminal compound; in (f) there are only two points for $\underline{P}(NMe_2)_2$ chemical shifts. For sources of data see Tables A.2, A.3, A.6, A.7 and A.11(a).

arguments, and can be rationalized by invoking "hyperconjugation" between the α-protons of the alkyl group and phosphorus d-orbitals (structures (13) and (14)) and/or by considering the variation of electron density within the phosphazene ring:

(13)   (14)
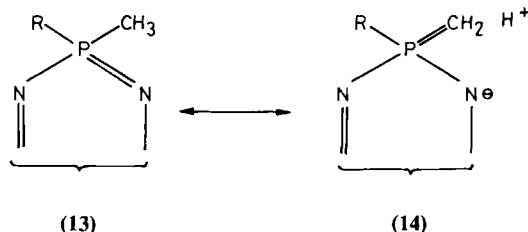
The presence of an electron-donating alkyl group at one end of the P–N–P island will cause the drift of electron density from the phosphorus carrying the alkyl group towards the other end of the island. This electron drift effectively deshields the alkylated phosphorus nucleus, and would also account for the slight shielding observed for the adjacent PCl_2 group (from 19.8δ for $N_3P_3Cl_6$ to 17.7–19.3δ for the 2,2-dialkyl compounds. Similar deshieldings of $P(Bu^t)(F)$ and $P(Bu^t)_2$ are observed for fluorocyclo-triphosphazenes.[115] For 2,2-alkyl,aryl compounds, the ^{31}P shifts of $P(R)(Ar)$ can be accurately estimated from the partial shift contribution of the aryl group calculated from the $\delta(PPh_2)$ value for gem-$N_3P_3Cl_4Ph_2$.[114]

The shielding sequence for 2-alkyl, 2-halo/hydrido derivatives $N_3P_3Cl_4(R)(X)$ $(X = Cl, Br, I$ or $H)$ is $H > Cl < Br < I$ if the same R group is considered. Attempts to fit the data in terms of partial chemical-shift contributions give poor agreement with the experimental values for bromo and iodo compounds. This anomaly is ascribed to a widening of the exocyclic angle for compounds containing branched alkyl groups and iodo or bromo substituents. The chemical shifts are rationalized by using a "bulk coefficient" to account for the variation in the exocyclic bond angle:

observed chemical shift = partial shift contribution of halogen

$$+ \text{(partial shift contribution for alkyl)}$$

$$\times \text{(bulk coefficient)} \qquad (2)$$

The significance of the "bulk coefficient" is not clear.[114] For the methyl compounds, the bulk coefficient is less than unity and decreases from $X = Cl$ (0.93) to $X = I$ (0.47). Such a trend would imply a decrease of the CH_3–P–X bond angle in the same order. Undoubtedly other factors must be considered for rationalizing the chemical shifts for the bromo and iodo compounds.

For the series of compounds $2,2\text{-}N_3P_3Cl_4(Me)[C_6H_4(X)\text{-}p]$ (X = H, Cl, F, CH_3, OCH_3, CF_3, $N(CH_3)_2$, $N(C_2H_5)_2$ or C_6H_5), there is a good correlation between the chemical shift of the P(Ar)(R) centre and the Hammett σ-parameter. This result indicates a strong interaction between the phosphazene ring and the aromatic ring.[114] The nature of this interaction has been examined in the light of ^1H, ^{13}C and ^{19}F NMR data (Section II.D).

(c) (Alkoxy) and (aryloxy)cyclotriphosphazenes. The introduction of the first alkoxy,[116,117] vinyloxy[118,119] or aryloxy group[22,120,121] into the chlorocyclophosphazene ring (1, X = Cl) leads to a slight high frequency shift of PCl_2, whereas the PCl(OR) signal appears considerably to low frequency of those of $\underline{P}Cl_2$. However from an examination of the ^{31}P chemical shifts for a given series of compounds $N_3P_3Cl_{6-n}$ (n = 0, ..., 6), it is clear that PCl_2, PCl(OR) and $P(OR)_2$ nuclei are deshielded as the number of OR group increases. A linear relationship between $\delta(^{31}P)$ and the degree of substitution n can be demonstrated for aryloxy,[22] vinyloxy[119] and trifluoroethoxy[117] derivatives. Figure 6(b) shows the data for trifluoroethoxy derivatives. The linear relationship is reasonable when one considers the same type of substituted derivatives (viz geminal or nongeminal). Slight deviations occur if the trends for the two types of derivatives are considered together. It is clear that the chemical shift of a particular phosphorus atom is not only dependent on the substituents attached to it, but also on the nature of the substituents on the remote phosphorus nuclei. This effect can be envisaged to operate via a competition of the phosphorus nuclei for π-interaction with the skeletal nitrogen atoms, the extent of competition being determined by the substituents attached to the phosphorus atoms and their propensity to engage in (exocyclic) π-bonding. If the data for the series $N_3P_3Cl_5(OR)$ (R = Me, Et, Pr^i) and $N_3P_3(OR)_6$ (R = Me, Et, Pr^n, Bu^n), are considered then the variation of $\delta[P(OR)Cl]$ for the former and that of $\delta[P(OR)_2]$ for the latter closely parallel the trend observed for the ^{31}P shifts of trialkyl phosphates $(RO)_3P{=}O$ (Table 4). In rationalizing these variations, the effect of chemical-shift anisotropy should also be taken into account, in addition to the stereoelectronic effect of alkyl groups, which would operate by distorting the tetrahedral symmetry around the phosphorus atom.[3,4]

(d) Mercapto derivatives. For mercaptocyclotriphosphazenes, the $\underline{P}F(SR)$ and $\underline{P}Cl(SR)$ shifts lie between the shifts of $\underline{P}(SR)_2$ and $\underline{P}F_2$ or $\underline{P}Cl_2$ groups.[81,124] There is a linear decrease in the shift values with increasing number of mercapto groups except for $\underline{P}Cl(SEt)$. The changes in the chemical shifts of $\underline{P}(SEt)_2$, $\underline{P}F(SEt)$ and $\underline{P}F_2$ with n run parallel to each other for the fluoro series $N_3P_3(SEt)_nF_{6-n}$ (Fig. 6c).[81] The large deshielding of $\underline{P}(SR)_2$ may be linked to the increased covalency in the P–S bond and the consequent

TABLE 4

^{31}P chemical shifts for $N_3P_3Cl_5(OR)$ $N_3P_3(OR)_6$ and $(RO)_3PO$.

R	$\delta(P)$ $(RO)_3PO^a$	$\delta[P(OR)Cl]$ $N_3P_3Cl_5(OR)$	$\delta[P(OR)_2]$ $N_3P_3(OR)_6{}^c$
Me	+ 2.1	16.7	21.7
Et	− 1.0	13.6	14.3
Pr^n	− 0.7		17.7
Pr^i	− 3.3	12.6	
Bu^n	− 1.0		16.9
Bu^t	− 13.3		

^{a}Data from ref. 4; ^{b}Data from ref. 116; ^{c}Data from refs. 80, 122, 123.

increase in the contribution to the chemical shift from p-orbital unbalancing terms.

(e) (Amino)cyclotriphosphazenes. The proton-decoupled ^{31}P NMR spectra of a series of primary and secondary aminocyclotriphosphazenes were first reported by Keat and coworkers in 1976, and since then extensive data have become available for numerous such compounds[55] (Tables A.3 and A.4). For secondary amino derivatives the order of shielding is $PCl(NR_2) < PCl_2 < P(NR_2)_2$;[55] however, for piperidino[55] and *N*-methylanilino derivatives[125] the $PCl(NR_2)$ signal is slightly to low frequency of the PCl_2 signal. For a series of compounds $N_3P_3Cl_{6-n}(NR_2)_n$ all three resonances — PCl_2, $PCl(NR_2)$ and $P(NR_2)_2$ — are deshielded with increasing degree of chlorine replacement *n*, and the variations are linear if either the nongeminal or the geminal derivatives are considered separately (Figs. 6d,e). The lines depicting the variations of $\delta(PCl_2)$ and $\delta[P(NR_2)_2]$ with *n* are more or less parallel; however, the increase of $\delta[PCl(NR_2)]$ with *n* is steeper. Cooperative electron withdrawal by chlorine and mesomeric electron release from the exocyclic nitrogen to the phosphorus[127,128] presumably cause the pronounced deshielding of $PCl(NR_2)$ signals.

(Primary amino)cyclotriphosphazenes are characterized by the low frequency shifts of $PCl(NHR)$ and $P(NHR)_2$ signals.[55] Exceptions to this general rule are the values for methylamino derivatives.[25,129] This trend may be contrasted with the high frequency phosphorus shifts for both primary and secondary amino derivatives of phosphoryl chloride[130] compared with the parent compound $(POCl_3)$ (Table 5). The most complete series for which data are available are the isopropylamino and *p*-anisidino derivatives $N_3P_3Cl_{6-n}(NHPr^i)_n$ ($n = 1, 2, 4$ or 6)[50] and $N_3P_3Cl_{6-n}[NHC_6H_4(OCH_3)-p]_n$ ($n = 1, ..., 4$ or 6).[44] As observed for secondary amino series, the chemical

TABLE 5

[31]P chemical shifts for $Cl_2P(O)(R)$, $N_3P_3R_4Cl_2$ and $N_3P_3R_6$ (R = Cl or primary amino).

R	$\delta(P)^a$ $Cl_2P(O)(R)$	$\delta(PR_2)^b$ $N_3P_3R_4Cl_2$	$\delta(PR_2)^b$ $N_3P_3R_6$
Cl	3	19.3	19.3
NHMe	18	—	21.5
NHEt	16	—	18.0
NHPr[i]	13	9.4	12.6
NHBu[t]	10	3.9	7.0[c]

[a]From ref. 130; [b]from refs. 50 and 55; [c]Estimated value from the observed shifts of $P(NHBu^t)_2$ for $N_3P_3(NHBu^t)_2Cl_4$ and $N_3P_3(NHBu^t)_4Cl_2$[55] and also from the trends for the isopropylamino derivatives $N_3P_3Cl_{6-n}(NHPr^i)_n$ (n = 2, 4, 6).[50]

shifts of $\underline{P}Cl_2$, $\underline{P}Cl(NHR)$ and $\underline{P}(NHR)_2$ move to high frequency in a linear fashion upon progressive replacement of chlorine atoms. On the basis of this trend and the data for $N_3P_3Cl_4(NHBu^t)_2$ and $N_3P_3Cl_2(NHBu^t)_4$, the $PCl(NHBu^t)$ chemical shift value of -5.3 reported for the mono (t-butylamino) derivative $N_3P_3Cl_5(NHBu^t)$ appears unlikely.[55] It is clear from Table 5 that for both the phosphoryl chloride derivatives and cyclo-phosphazenes, increased branching of the alkyl chain leads to shielding of the phosphorus nuclei. This trend may be contrasted with the deshielding observed for alkylcyclotriphosphazenes with increasing branching of the alkyl group (Section II.B.2b).

(f) Spirocyclic phosphazenes. The chemical shift of the phosphorus nucleus incorporated in a five-membered spiro ring occurs at a much higher frequency than that observed for P_{spiro} in derivatives containing six- or seven-membered rings (Table A.10).[71,73,93-99] The five-membered ring is subject to steric strain (as reflected in the angle at the spiro phosphorus within the five-membered ring),[98] and as a result there is a decrease of π-electron release to the phosphorus atom from the substituents. Theoretical calculations also show that the phosphorus atom incorporated in a five-membered ring has a greater positive charge than that in an acyclic or six-membered analogue.[131] A similar trend is reported for monocyclic phosphate esters,[132,133] A decrease in the smallest O–P–O bond angle (obtained from X-ray data) in the molecule leads to a deshielding of the phosphorus nucleus.

(g) Phosphazenyl-substituted cyclotriphosphazenes. The ^{31}P chemical shifts of phosphazenyl derivatives (Table A.11(a)–11(c)) follow the trends

established for other amino derivatives discussed earlier. The most extensive series for which data are available consists of the triphenylphosphazenyl derivatives $N_3P_3Cl_{5-n}R_n(NPPh_3)$ ($n = 1, ..., 5$; $R = NMe_2$[23,134] NC_2H_4[48] or OMe[46,47]). In all the series the signals arising from $\underline{P}(NPPh_3)(R)$, $\underline{P}Cl_2$, $\underline{P}ClR$ or $\underline{P}R_2$ move to higher frequency upon progressive replacement of chlorine atoms. On the other hand, the chemical shift of the exocyclic phosphorus nucleus ($NPPh_3$) undergoes progressive shielding, which may be a consequence of a decreased participation of the lone pair of electrons on the nitrogen of the $-NPPh_3$ group in π-bonding with the ring phosphorus atom.[47,48] The trends are shown graphically in Fig. 6(f) for the dimethyl-amino derivatives $N_3P_3Cl_{5-n}(NPPh_3)(NMe_2)_n$ ($n = 1, 2, 3, 5$). By far the most affected chemical shift is that of $\underline{P}(NPPh_3)(R)$ group, which varies from -20.3 ($R = NPCl_3$) to 14.4 ($R = Ph$) (Table 6). The pronounced deshielding of phosphorus by an aziridino group and shielding by a t-butylamino group (Table A.3) are once again evident from these data.

TABLE 6

^{31}P chemical shifts of $X\underline{P}(NPPh_3)$ for $N_3P_3Cl_4X(NPPh_3)$.

X	$\delta(^{31}P)$	Ref.	X	$\delta(^{31}P)$	Refs.
F	7.4^a	47, 136	NHBu^t	-5.9	23
Cl	0.1	134	NC$_2$H$_4$	10.3	48
Ph	14.4	134	NMe$_2$	3.9	134
OMe	7.0^b	47	NEt$_2$	1.0	23, 101
NH$_2$	-1.6	137, 138	NPCl$_3$	-20.3	103
NHMe	0.8	23	NPPh$_3$	-10.9	137, 138

^{a}For the fluoro compound, $N_3P_3F_5(NPPh_3)$; ^{b}for the geminal tris-derivative, $N_3P_3Cl_2(OMe)_3(NPPh_3)$.

(h) Cyclotriphosphazenes with mixed substituents. The phosphorus chemical shifts of cyclotriphosphazenes containing mixed substituents can be predicted by and large from the data for homogeneously substituted derivatives. For example, $\delta[\underline{P}(NHEt)(NMe_2)]$ for (dimethylamino)(ethyl-amino)cyclotriphosphazenes is in between the ^{31}P shifts for $P(NMe_2)_2$ and $P(NHEt)_2$ groups.[55] Such an "additivity" rule also operates for the cyclo-tetraphosphazenes compiled in Table A.16(b).

3. Spectra in the nematic phase and ^{31}P chemical-shift anisotropies

The ^{31}P spectra of partially oriented $N_3P_3X_6$ ($X = F$, Cl) and $N_4P_4Cl_8$ in a liquid-crystal solvent have been reported.[139] The spectra of the hexachloride

and the hexafluoride are analysed by assuming the rings to be planar. The spectrum of the octachloride is consistent with D_{4h} symmetry for the molecule in the liquid-crystal environment. The shielding anisotropies for the hexachloride and hexafluoride are $+10.4 \pm 3$ and $+58.3 \pm 3$ ppm respectively. These values are regarded as positive on the assumption of a substantial π-electron delocalization. While the average shielding in the molecular plane remains virtually unaltered, the shielding component along the threefold axis of symmetry is appreciably greater for $N_3P_3F_6$ compared with that for $N_3P_3Cl_6$. This result signifies a more effective electron delocalization in the hexafluoride.

NMR measurements on other cyclophosphazenes in liquid-crystal solvents would yield valuable information on their molecular geometries in solution.

4. Phosphorus–phosphorus couplings

As with phosphorus chemical shifts, a comprehensive theoretical treatment of P–P couplings for cyclophosphazenes has not yet emerged. In this section empirical trends in two-bond P–P couplings are dealt with first, followed by a brief discussion of four-bond P–P couplings observed for phosphazenyl substituted cyclotriphosphazenes. Two-bond P–P couplings for homogeneously substituted cyclophosphazenes have been obtained from measurements on ^{15}N-labelled cyclophosphazenes, and this aspect is discussed in Section II.E.

(a) Two-bond P–P couplings. Heatley and Todd[116] have suggested that ^2J(P–P) for cyclotriphosphazenes $N_3P_3Cl_5X$ is dependent on the electronegativity of the substituent X. Finer[140] has developed an empirical quantitative relationship between the P–P couplings and substituent electronegativity by assigning a parameter, λ_X to each substituent X such that the effects of the two substituents attached to a given phosphorus atom are additive. Thus for compounds of the type (15) an expression ^2J(P–P) $= (\lambda_B + \lambda_C)(\lambda_D + \lambda_E)$ is proposed for calculating P–P couplings:
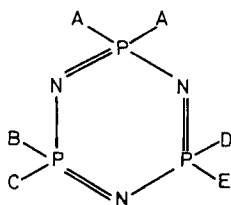
(15)

On the basis of the above expression, the couplings calculated agree reasonably well with experimental values for many cyclophospha-zenes.[10,140,141] However, Allen has shown that the application of this equation leads to serious discrepancies for compounds containing phenyl and fluoro substituents.[142] Similarly, Keat and coworkers[55] have pointed out that although the correct trend is established for the decrease of J(P–P) for (dimethylamino)chlorocyclotriphosphazenes with increasing degree of amin-ation, variations in J(P–P) occur, depending on the geometrical disposition of substituents and, more importantly, the nature of the substituents on the third phosphorus atom not involved in the coupling. Harris, Sowerby and coworkers[104] note that there is a significant, albeit small, effect of stereo-chemistry on ^2J(P–P). For example, for the trifluorotrichloroderivative 2-$trans$-4,6-$N_3P_3F_3Cl_3$, the two values of ^2J(P–P) differ by $ca.$ 4 Hz, and both differ from that observed for 2-cis-4,6-$N_3P_3F_3Cl_3$. For the bromo analogue 2-$trans$-4,6-$N_3P_3F_3Br_3$ the difference between the two values of ^2J(P–P) is even larger ($ca.$ 10 Hz) (Table A.1).

The value of ^2J(P–P) for 2-cis-4-$N_3P_3F_2Cl_4$ (100.2 Hz) is equal to that for gem-$N_3P_3Cl_4F_2$ (100 Hz) within experimental error. Both compounds con-tain the same grouping (PCl$_2$) at the uninvolved phosphorus. It appears that J($\underline{P}$FCl–$\underline{P}$FCl) cannot be distinguished from J($\underline{P}$F$_2$–$\underline{P}$Cl$_2$) for similar sub-stituent change in the chlorofluoro series of compounds. The value of J($\underline{P}$FCl–$\underline{P}$FCl) changes from 105.3 Hz for 2-cis-4,6–$N_3P_3F_3Cl_3$ to 100.2 Hz for 2-cis-4-$N_3P_3F_2Cl_4$; J($\underline{P}$FCl–$\underline{P}$Cl$_2$) changes from 81.6 Hz for 2-cis-4-$N_3P_3F_2Cl_4$ to 78.3 for $N_3P_3Cl_5F$. Thus the introduction of a second chlorine atom at the "uninvolved" phosphorus reduces ^2J(P–P) by factors of 0.95 and 0.96 in the two examples cited above. The change in ^2J(P–P) from gem-$N_3P_3Cl_4F_2$ (100 Hz) to $N_3P_3Cl_5F$ (78.3 Hz) represents a reduction by a factor of 0.78 when fluorine is replaced by chlorine. Treating this reduction factor and that for replacement at the "uninvolved" phosphorus (0.95–0.96) as constants, the value of ^2J(P–P) for $N_3P_3F_6$ is estimated as $ca.$ 179 Hz.[104] This value is in good agreement with that (190 ± 20 Hz) determined experiment-ally[143] from the ^{19}F-decoupled ^{31}P NMR spectrum of $^{15}N_3P_3F_6$ (Section II.E).* It must, however, be stressed that the use of such empirical reduction factors may minimize but not altogether eliminate all the discrepancies (e.g. ^2J(P–P) values for (phenyl)fluorocyclotriphosphazenes).[142]

The value of ^2J(P–P) increases linearly with the degree of chlorine replacement for (alkoxy)[117,119] or (aryloxy)chlorocyclotriphosphazenes.[22] The linearity is quite striking in view of the different parameters under consideration, viz J[$\underline{P}$Cl$_2$–$\underline{P}$Cl(OR)] for the mono and bis(alkoxy) or (aryloxy) derivatives and J[$\underline{P}$Cl(OR)–P(OR)$_2$] for the tetra and pentasub-

*The ^{19}F[91] and ^{31}P[139] spectra of $N_3P_3F_6$ have been published, but have not been analysed.

stituted derivatives. The incremental change in ^2J(P–P) with the degree of chlorine replacement for alkoxy or aryloxy chlorocyclotriphosphazenes appears to be constant.

For secondary amino derivatives the variation of ^2J(P–P) with the degree of chlorine replacement is somewhat erratic.[55] The ^2J(P–P) value of 40 Hz, determined for $N_3P_3(NMe_2)_6$ from ^1H-$\{^{31}P\}$ INDOR measurements,[55] is the same as that obtained from the NMR spectrum of $^{15}N_3P_3(NMe_2)_6$.[144] For *gem*-$N_3P_3(NMe_2)_3Cl_3$, $J[\underline{P}Cl_2$–$\underline{P}Cl(NMe_2)]$ and $J[\underline{P}Cl(NMe_2)$–$\underline{P}(NMe_2)_2]$ are identical. Mono(primary amino) derivatives exhibit a smaller ^2J(P–P) than $N_3P_3Cl_5(NMe_2)$; however, further replacement of chlorine atoms increases ^2J(P–P) for geminal isopropylamino and *t*-butyl amino derivatives relative to the values for dimethylamino derivatives.[55] These trends would imply that at the mono stage of substitution a primary amino group is more effective in supplying electron density to phosphorus than a secondary amino group, but that with increasing number of chlorine replacement, the electron release from primary amino groups is less than that of secondary amino groups.

For phosphazenyl substituted cyclotriphosphazenes, ^2J(P–P) involving the exocyclic phosphorus nucleus changes with the electronegativity of the substituents in a manner similar to that observed for P–P couplings within the phosphazene ring. If one considers the triphenyl phosphazenyl (NPPh$_3$) derivatives (3), ^2J(P–P) involving NPPh$_3$ and the ring phosphorus is 20–30 Hz when the substituent attached to the latter is chlorine or an amino group.[23,47,48,134] When the chlorine at the ring phosphorus is replaced by methoxide or fluorine this coupling shows an increase of ~ 10 Hz.[47] Thus the magnitude of ^2J(P–P) involving the NPPh$_3$ group can be used to assign the structures of the products formed in the reactions of $N_3P_3Cl_5(NPPh_3)$ with methoxide.[46,47] For most amino derivatives ^2J(P–P) within the ring is never below 30 Hz (Table A.11a) The value of 14.7 Hz for $^2J[\underline{P}(NHBu^t)_2$–$\underline{P}(NPPh_3)(NHBu^t)]$ of *gem*-$N_3P_3Cl_2(NHBu^t)_3(NPPh_3)$[23] is unusually low, and may reflect a considerable puckering of the ring owing to the presence of the bulky t-butylamino and –NPPh$_3$ substituents.

The value of ^2J(P–P) for the hydrochloride adduct $N_3P_3(NMe_2)_2$ $(NHEt)_4$.HCl (30.0 Hz) is much lower when compared with the value (42.1 Hz) for the free base. This result might be anticipated if the coupling were to be dominated by the contact term, because upon protonation the endocyclic P–N bond lengths increase relative to those in the free base.[55] A similar reduction in ^2J(P–P) is observed for cyclophosph*azanes*,[80] and also for the phosph*azane* segment of phosphazadienes (Section II.B.4) and bicyclic phosphazenes (Section IV.A), where again the P–N bonds are longer than those for cyclophosphazenes.[145,146]

(b) Sign of $^2J(P-P)$ in cyclophosphazenes. It has been shown by analysis that $^2J(P-P)$ is of opposite sign to $^1J(P-F)$ for $N_3P_3Cl_5F$,[116] *gem*-$N_3P_3Cl_4F_2$[147] and several fluorocyclotriphosphazenes containing chloro, bromo or dimethylamino substituents.[104] Since $^1J(P-F)$ is negative,[6] $^2J(P-P)$ must be positive. The $^1H-\{^{31}P\}$ INDOR studies on *cis*-$N_3P_3Cl_3(NMe_2)_3$ and $N_3P_3(NMe_2)_6$ also show that values of $^2J(P-P)$ for these compounds are positive. It is therefore reasonable to assume that $^2J(P-P)$ for most cyclotriphosphazenes has a positive sign, although when $^2J(P-P)$ is small (e.g. for phenyl and mercapto derivatives) it may be prudent to await relative sign determinations.[55]

(c) Four-bond phosphorus–phosphorus couplings. An interesting aspect of the ^{31}P NMR spectra of phosphazenyl-substituted cyclotriphosphazenes is the observation of four-bond coupling between the exocyclic phosphorus and the remote ring-phosphorus nuclei. This coupling was first observed[102] for $N_3P_3Cl_5(NPCl_3)$ (9.5 Hz) and *gem*-$N_3P_3Cl_4(NPCl_3)_2$ (**12**) (4.2 Hz). From a computer analysis of the ^{31}P NMR spectra of these two compounds, $^2J(P-P)$ and $^4J(P-P)$ are shown to have the same signs. Since $^2J(P-P)$ is known to be positive, $^4J(P-P)$ for these compounds must also be positive. Biddestone *et al.* have determined the magnitude and sign of $^4J(P-P)$ for triphenyl-phosphazenyl derivatives, and the values range from $+4.5$ Hz for $N_3P_3Cl_5(NPPh_3)$ to -0.4 Hz for *gem*-$N_3P_3Cl_4Ph(NPPh_3)$.[134] These values are correlated with the conformations of the $NPPh_3$ group with respect to the phosphazene ring.[148] However, in view of the small magnitude of this coupling and the limited structural data available, the correlation is some-what tenuous. In general, values of $^4J(P-P)$ for geminally substituted amino derivatives of $N_3P_3Cl_5(NPPh_3)$ are < 1.0 Hz.[23] For methoxy derivatives this coupling varies from 4.5 to 1.0 Hz.[47]

5. Oxocyclotriphosphazadienes and dynamic aspects

It is now evident that cyclotriphosphazene derivatives containing a hydroxy substituent exist in the oxocyclotriphosphazadiene from both in solution and in the solid state.[111,146,149-151] The tautomeric behaviour of these derivatives is revealed in a striking manner by dynamic ^{31}P NMR spectroscopy.[149] The $^{31}P-\{^1H\}$ NMR spectrum of the penta(methoxy)derivative (**16**, R^1, R^2 = OMe) at $-40\,^{\circ}C$ consists of twelve lines (ABX) as the proton exchange between the two equivalent *alpha* ring nitrogen sites is "frozen", thereby conferring nonequivalence on the phosphorus nuclei of the two $P(OMe)_2$ groups:

(16b)   (16a)   (16c)
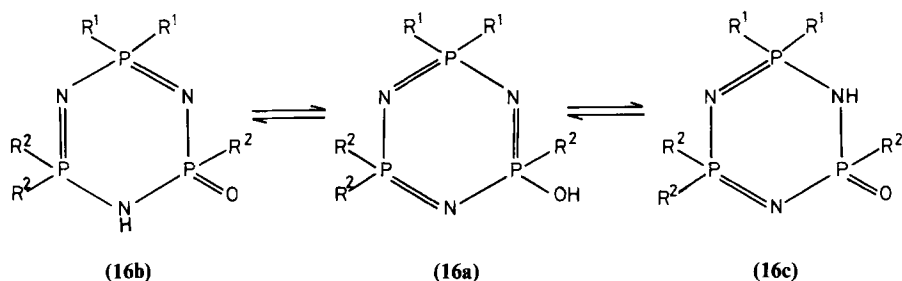
At ambient temperature, the exchange is fast and an AX_2 spectrum results. The 60 MHz ^{1}H NMR spectrum has been reported.[152] The N–H resonance occurs to high frequency (δ7.78), as anticipated for strongly hydrogen-bonded protons.[146,150] Only three methoxy doublets are resolved, with the most shielded one (δ3.60) assigned to the methoxy protons of the P(O)(OMe) group.

For the phenylcyclophosphazenes $N_3P_3Ph_4(OMe)OH$[149] and $N_3P_3Ph_5OH$,[111,153] exchange between the two equivalent *alpha* ring nitrogen atoms is very slow, even at ambient temperature; three groups of signals are seen in the ^{31}P NMR spectra of both compounds (Table A.13).

Exchange between two nonequivalent *alpha* sites is observed for the alkoxy derivatives $N_3P_3Ph_2(OR)_3OH$. Their ^{31}P–$\{^1H\}$ NMR spectra vary considerably with temperature.[146,149] At $-40\,°C$ two tautomers are present in solution, and two overlapping ABX spectra can be readily discerned (slow proton exchange). Exchange becomes more rapid as the temperature is raised, and at $30\,°C$ the spectrum consists only of broad, featureless signals (Fig. 7). At $100\,°C$ a single ABX spectrum is obtained (fast exchange) with chemical shifts and coupling constants ^2J(P–P) that are close to the average of the values for the individual tautomers obtained at $-40\,°C$. The magnitude of ^2J(P–P) across the phosph*azane* segment P—NH—P(O) observed for either tautomer is lower than that observed for the formal phosphazene links. The considerable variation in ^2J(P–P) values associated with the phosphazene segment and also the marked differences in the values of δ(PPh$_2$) suggest that there are conformational differences between the tautomeric P–N rings.

The ^{31}P–$\{^1H\}$ NMR spectra of the geminal derivatives, $N_3P_3(NHBu^t)_2(OR)_3OH$ (R = Me, Et)[149] and $N_3P_3Cl_2(NEt_2)_3OH$[149,150] each consist of a twelve-line ABX pattern, which is independent of temperature. This evidence indicates the absence of the exchange phenomenon. The tautomeric form with a proton *alpha* to P(NHBu^t)$_2$ (or P(NEt$_2$)$_2$)[150] and the phosphoryl group is clearly indicated by the NMR parameters (Table A.13). This tautomer is also anticipated on electronic grounds, as the base-
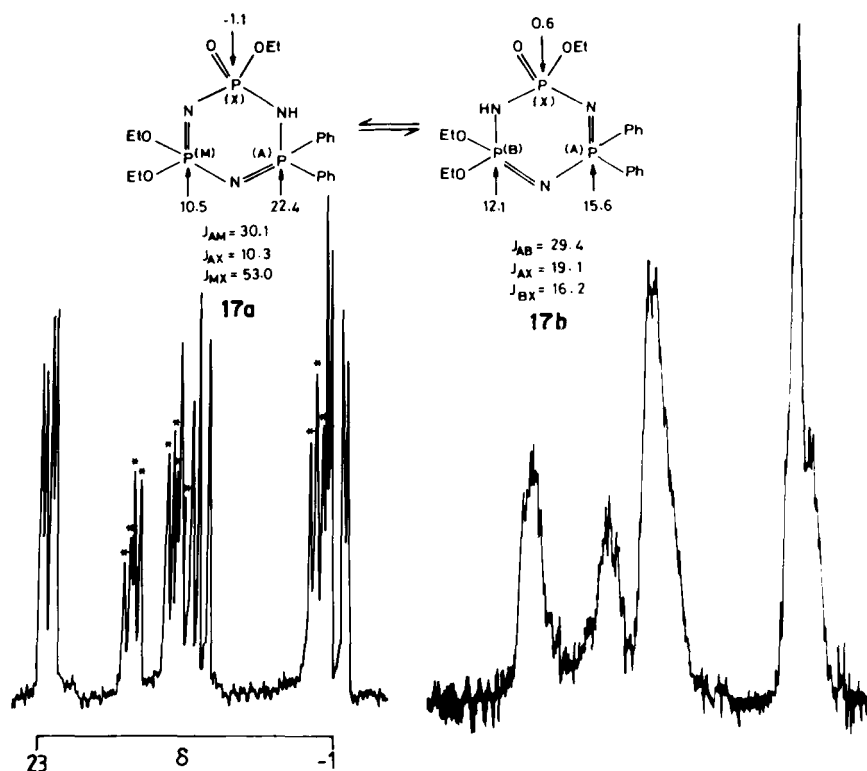
FIG. 7. The ^{31}P-$\{^{1}H\}$ NMR spectrum (36.43 MHz, $CDCl_3$) of $N_3P_3Ph_2(OEt)_3(OH)$ at $-40\,°C$; the spectrum on the right is as ambient temperature. NMR parameters for the two tautomeric forms are indicated on the structural diagrams. The lines marked with an asterisk are due to **17b**. (Reproduced from ref. 216(a) with permission of the Indian Institute of Science, Bangalore.)

strengthening effect of amino groups on an adjacent ring nitrogen atom is considerably greater than that of methoxy groups.[14]

The 162 MHz ^{31}P-$\{^{1}H\}$ NMR spectrum of the triphenylphosphazenyl derivative (**4**, R = OMe) establishes the presence of *cis*- and *trans*-oxophosphazadienes, with the former predominating. The proton resides at a ring nitrogen atom adjacent to the $P(NPPh_3)(OMe)$ group.[51] The anion $[N_3HP_3Cl_4O_2]^-$ also exists in *cis* and *trans* forms[154] (Table A.13).

Data for other mono("hydroxy")cyclophosphazenes are given in Table A.13. There is no compelling evidence that any of them contain a formal $P(OH)$ group. Oxophosphazadienes containing a ring *N*-methyl group are detected by both ^{31}P and ^{1}H NMR spectroscopy as intermediates in the thermal rearrangement of *gem*-$N_3P_3R_2(OMe)_4$ (R = Ph or $NHBu^t$).[80]

Another example, viz $N_3(Me)P_3(O)Ph_4Me$, is described by Schmidpeter and coworkers.[155]

In addition to the neutral species discussed above, proton scrambling within the P–N ring has been observed for cyclotriphosphazenium ions. Variable-temperature NMR measurements (^{31}P, ^{13}C, ^1H) for hexamethyl-cyclotriphosphazenium dimethyltrihalogenostannate(IV) indicate an inter-molecular dissociative mechanism for the proton exchange. The barrier for the exchange process has been calculated from ^{31}P data to be $31.4\,kJ\,mol^{-1}$.[156] Such an intermolecular mechanism is also considered likely for the prototropic behaviour of the hydrochloride adducts of *gem*-$N_3P_3(NMe_2)_4(NPPh_3)_2$ at elevated temperatures.[138]

C. ^{19}F NMR Spectra

^{19}F NMR data* have now been reported for a variety of fluorocyclophospha-zenes. Complex spectra are inevitable for compounds with several phosphorus–fluorine bonds, as P–F coupling is very marked (760–1033 Hz) between directly bonded nuclei and other couplings $^3J(P–F)$, $^2J(F–F)$ and $^4J(F–F)$ are significant. Fortunately, a complete analysis of the spectrum is seldom required for most purposes, as chemical shift differences between $P\underline{F}_2$ and $P\underline{F}R$ groups are usually significant and informative. As a result, the assignment of a geminal or a nongeminal structure to a particular derivative is usually straightforward.

By far the most detailed analysis of ^{19}F NMR spectra of cyclophos-phazenes containing fluorine substituents is a study[104] of the derivatives *cis*- and *trans*-$N_3P_3X_3F_3$, X = Cl, Br; *cis*- and *trans*-$N_3P_3X_4F_2$, X = Cl, Br; and four isomers of $N_3P_3Cl_2F_2(NMe_2)_2$. For these derivatives the ^{19}F spectra have been analysed using iterative fitting by computer, and consequently the values of chemical shifts and couplings given in Table A.25 are of much greater accuracy than those reported for other fluorocyclophosphazenes. The couplings are discussed first, followed by trends in ^{19}F chemical shifts and structural assignments.

1. One-bond P–F couplings

This coupling has a negative sign, and its magnitude depends on several factors, including the electronegativity and the position of substituents in the Periodic Table.[6,157] The order for $^1J(P–F)$ for simple halogeno substituents is $PFBr > PFCl > PF_2$ (Table A.25). Values for $PF(NRR')$ (*ca.* 870–940 Hz) are somewhat higher than anticipated,[104] and clearly variations in phosphorus

*All chemical shifts are relative to $CFCl_3$.

hybridization and subsequent geometrical changes need to be considered. Steric effects may also be important, but no clear-cut trend is discernible from the considerable body of data now available.

It is tempting to correlate the magnitude of $^1J(P-F)$ with structural features. For example, a Cl or Br *trans* to a fluorine nucleus in mixed halogenocyclophosphazenes usually results in a higher value of $^1J(P-F)$ than that observed for a *cis* halogen. Also, there are often appreciable differences in $^1J(P-F)$ between PF$_2$ and PFR groups.[112,113,115,158] A scrutiny of the data presented in Table A.25 suggest that it is unwise to rely solely on such criteria, particularly as there are significant experimental errors in most determinations of $^1J(P-F)$ owing to the use of first-order approximations.

2. Three-bond P–F couplings

For fluorinated cyclophosphazenes three influences on this coupling have been considered:[104] (a) the nature of X for the group PFX; (b) substituents at the other P atom involved in the coupling and their *cis* or *trans* orientation; and (c) similar effects at the third ring P atom, which is not involved in the coupling. Data for some halogenofluorocyclophosphazenes are given in Table 7, and show that *cis* and *trans* isomers may be differentiated, as $^3J(P-F)$ for the latter is 3–5 Hz greater. Only a few examples are available from (amino)cyclophosphazenes, but they tend to show that there is no great

TABLE 7

Values of $^3J(P-F)$ and $^4J(F-F)$ for some fluorocyclotriphosphazenes.[a]

Compound	$^3J(P-F)$[b] (Hz)	$^4J(F-F)$[b] (Hz)
cis-N$_3$P$_3$Cl$_3$F$_3$	8.9	−1.0
trans-N$_3$P$_3$Cl$_3$F$_3$	12.6, 12.1, 16.0	12.5
cis-N$_3$P$_3$Br$_3$F$_3$	3.7	−0.5
trans-N$_3$P$_3$Br$_3$F$_3$	8.7, 10.5, 13.5	11.9
cis-N$_3$P$_3$Cl$_4$F$_2$	11.2, 8.8	−1.2
trans-N$_3$P$_3$Cl$_4$F$_2$	14.0, 12.1	12.5
cis-N$_3$P$_3$Br$_4$F$_2$	2.8, 5.7	< 1.5
trans-N$_3$P$_3$Br$_4$F$_2$	7.5, 11.8	11.9
N$_3$P$_3$Cl$_2$F$_2$(NMe$_2$)$_2$ (2,2:4-*cis*-6:4, 6)	5.8, 8.6	−1.1
N$_3$P$_3$Cl$_2$F$_2$(NMe$_2$)$_2$ (2,2:4-*trans*-6:4, 6)	11.5, 12.4	14.0

[a]Data from ref. 104; [b]standard errors from computer fitting (0.1–0.5 Hz).

distinction in the value of $^3J(P-F)$ (usually 11–15 Hz) between *cis* and *trans* isomers.[159] The limited measurements available preclude firm conclusions.

3. Fluorine–fluorine couplings

The values of $^4J(F-F)$ are in two distinct groups, *ca.* +12 and *ca.* −1 Hz, which have been assigned to *trans* and *cis* fluorine pairs respectively (Table 7). This coupling is undoubtedly extremely useful for structural assignments, but its general application will clearly remain limited given the considerable difficulties involved in computing its value. A few measurements of $^2J(F-F)$ have been reported for the compounds $N_3P_3Cl_2F_2(NRR')_2$, in which the amino groups are in a *cis* disposition; the values lie in the range 60–80 Hz.[104,159] It is unclear whether this measurement has general diagnostic value.

4. ^{19}F chemical shifts and structural assignments

In view of the extensive NMR data available for primary and secondary amino derivatives of $N_3P_3Cl_6$, it is not unduly surprising to find substantial ^{19}F NMR data for their fluorinated analogues $N_3P_3F_{6-n}$ $(NRR')_n$.[31,53,78,79,104,158-162] For (dimethylamino)fluorocyclotriphosphazenes, Sowerby and Green have demonstrated that the fluorine nucleus is a sensitive probe for different isomeric configurations.[31,79,161] Fluorine atoms *cis* to each other appear at higher frequency than fluorine atoms *cis* to dimethylamino groups and, $\delta(P\underline{F}_2)$ is *ca.* 7 ppm upfield from $\delta[P\underline{F}(NMe_2)]$. Thus the isomeric tris derivatives $N_3P_3F_3(NMe_2)_3$ exhibit three, two and one ^{19}F environments for geminal, *trans* and *cis* isomers respectively (Table A.25).

The preferential fluorination of PCl_2 centres observed with KSO_2F has led to an unambiguous method of determining the structures of nongeminal isomers of $N_3P_3Cl_4(NRR')_2$ (18, 20):[31,159]

No inversion occurs at the PCl(NRR') centres, as can be demonstrated by using individual isomers of known configuration.[159] *Trans* products (**21a**) show one ^{19}F environment ($\delta(F_A)$ *ca.* -68); two are observed for *cis* compounds (**19**) ($\delta(F_A)$ *ca.* -66, $\delta(F_B)$ *ca.* -70). This method seems to be less reliable for derivatives with two primary amino substituents, as isomerization can occur.[163] In addition, fluorination with KSO_2F proceeds to completion to give $N_3P_3F_4(NHR)_2$.[158] Partial fluorination can also be achieved with SbF_3, but in this case fluorination occurs solely at a PCl(NRR') centre: the reaction appears to proceed largely with retention of structure (**21b**). The ^{19}F shift of P$\underline{F}$(NRR') moves to higher frequency with an increase in size of the amino substituents (e.g. $\delta(PFNMe_2)_2$ -62.3, $\delta(PFNEt_2)$ -55.9; $\delta(PFNHMe)$ -58.2, $\delta(PFNHPr^i)$ -53.8).[31,158]

An examination of the ^{19}F NMR spectra of the compounds $N_3P_3F_4[RN(CH_2)_nNR]$ ($n = 2$, R = H, Me; $n = 3$, R = H) provides convincing evidence[73,83] for their spirocyclic structures (**5**), thus providing another simple spectroscopic method of solving the apparent "spiro versus ansa" dilemma.[95]

Fluorine NMR data for numerous monosubstituted fluorocyclotriphosphazenes containing phosphazenyl side groups (NPX$_2$R, X = F, R = OMe, OEt, Ph, NHSiMe$_3$, NPCl$_3$) are reported in earlier literature.[164-166] More detailed work[167] on isomeric phosphazenyl compounds $N_3P_3F_4(NPR_2R')_2$ (R = R' = Me, Ph, NMe$_2$; R = Me, R' = Ph) shows that *cis* and *trans* isomers are easily distinguished, with $\delta[P\underline{F}(cis)] > \delta[P\underline{F}(trans)]$. The usefulness of ^{19}F NMR for structural assignments has been convincingly demonstrated for the (methoxy)triphenylphosphazenyl derivatives $N_3P_3(NPPh_3)(OMe)_nF_{5-n}$ ($n = 1, ..., 4$). The P(NPPh$_3$)$\underline{F}$ signals (-40 to -45δ) are considerably deshielded with respect to those of P(OMe)F or PF$_2$ (-67 to -71δ). Fluorine nuclei *cis* to the NPPh$_3$ group are more shielded than fluorine nuclei with a *trans* disposition, as anticipated from ^{1}H NMR data for triphenylphosphazenyl compounds.[23,46,47] Data for three isomers are summarized below:

$$T = -NPPh_3 \, , \, O = -OMe$$
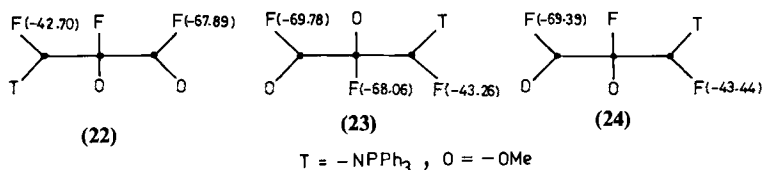
The structures of chloro-[104,116,160,162,168-170] and bromo-[104,160,162,171] fluorocyclotriphosphazenes have been established largely by ^{19}F NMR spectroscopy. Data for fluorocyclophosphazenes containing pseudohalogeno substituents CN,[172] NCO,[173] NCS[160,173] and N$_3$[172] have also been

reported. Structural assignments to alkyl-[115,174,175] and aryl-[112,113,176,177] fluoro derivatives are greatly facilitated by ^{19}F NMR spectra, particularly as ^{1}H NMR data for the latter class of compounds are often uninformative. Alkenyl-substituted fluorocyclophosphazenes $N_3P_3F_{6-n}R_n$ (R = CH=CH$_2$,[174] CH=CHMe,[178] C(Me)=CH$_2$,[178] C(OEt)=CH$_2$[179]) have been obtained by the organolithium route. Fluorine NMR studies indicate the exclusive formation of geminal disubstituted products as only signals in the range -63 to -69δ (PF$_2$ groups) are observed. In contrast, the ^{19}F NMR spectrum of the (alkynyl)cyclophosphazene $N_3P_3F_4(C{\equiv}CSiMe_3)_2$ shows complex multiplets centred at -42.6 and -44.5δ and a multiplet at -68.6δ, and these observations are only compatible with the presence of a significant amount of geminal and cis–trans nongeminal isomers.[180] The geminal structure of $N_3P_3F_4(C{\equiv}CPh)_2$ was first demonstrated by Chivers,[181] as the ^{19}F NMR spectrum shows only P$\underline{F}_2$ resonances [δ(F) = -68.4, ^1J(P–F) = 860 Hz].

^{19}F chemical shifts are reported for the geminal ethylthio derivatives $N_3P_3F_{6-n}(SEt)_n$ ($n = 1, ..., 5$).[81] In this series of compounds δ(P$\underline{F}_2$) varies linearly with increasing degree of fluorine replacement. There are no detailed studies of the reaction of $N_3P_3F_6$ with alcohols, and only a few values of δ(F) for monosubstituted compounds $N_3P_3F_5$(OR) (R = Me, Et, Ph)[174] and penta(aryloxy) derivatives $N_3P_3(OPh)_3(OC_6H_4R)_2F$[182] are available.

The effect of a substituent R on the chemical shift of P$\underline{F}$R is compared for an extensive range of monosubstituted derivatives of $N_3P_3F_6$ (Table 8). A

TABLE 8

Effect of substituent on the ^{19}F shift of the PFR group in monosubstituted fluorocyclophosphazenes $N_3P_3F_5R$.

R	δ(F)	Ref.	R	δ(F)	Ref.
F	-71.9	160	C$\equiv$C.SiMe$_3$	-45.5	180
Cl	-30.7	160	Ph	-51.5^a	112
Br	-19.6	160	C$_6$H$_4$NMe$_2$-p	-50.6	177
CN	-46.3	172	NHMe	-62.5	162
NCO	-49.6	173	NMe$_2$	-62.1	160
NCS	-52.1	173	NHNH$_2$	-63.0	184
NSO	-57.0	183	N=PPh$_3$	-44.7	167
N$_3$	-55.5	172	N=PF$_2$Ph	-66.5	164
Me	-53.9	174	N=CCl$_2$	-56.8	173
Bu^n	-60.0	115	NS$_3$N$_2$ ^{b}	-69.8	185
Bu^t	-79.3	115	OEt	-66.3	174
C$\equiv$C.Ph	-43.2	181	SEt	-35.5	81

^{a}Value for trans-$N_3P_3F_4Ph_2$; ^{b}N-(1,2,4,3,5-trithiadiazol-1-ylidene)amino.

correlation between the electronegativity of R and the fluorine shift is obvious for simple mixed halides. If the substituent is able to participate in π-bonding to phosphorus (e.g. NMe_2, NCS, Ph) then the paramagnetic contribution to shielding at the fluorine nucleus is reduced, causing a shift to lower frequency than that anticipated solely from electronegativity considerations. The value of $\delta(P\underline{F}R)$ reported for the t-butyl derivative $N_3P_3F_5Bu^t$ is -79.3, almost 20 ppm to low frequency of the value for the n-butyl isomer $N_3P_3F_5Bu^n$, and further to low frequency than most values reported for $\delta(P\underline{F}_2)$ (Table A.25). This considerable shielding is presumably due to a steric effect, as is the concomitant deshielding of the phosphorus nucleus.[115]

^{19}F NMR data have been reported for numerous cyclophosphazenes containing fluorinated side chains, particularly trifluoroalkoxy derivatives.[186-190] The reactions of (trifluoroethoxy)cyclotriphosphazenes with n-butyl lithium at $-78\,°C$ affords metallated intermediates (e.g. $[NP(OCLi{=}CF_2)_2]_3$), which on treatment with electrophiles give cyclophosphazenes with olefinic side groups containing fluorine, These reactions are conveniently monitored by ^{19}F NMR spectroscopy.[190]

D. ^{13}C NMR spectra

The use of ^{13}C NMR spectroscopy is still somewhat limited with regard to cyclophosphazenes, although data are now reported more routinely.[23,156,190-197] The nature of the interaction between the phosphazene ring and an aryl substituent has been studied by both ^{13}C and ^1H NMR spectroscopy.[74,75,198] A Hammett σ^+ value of 0.74 has been calculated for the $N_3P_3F_5$ group. This value decreases with increasing number of aryl groups attached to the phosphazene ring; the values observed for 2,4-$N_3P_3Ar_2F_4$, 2,2-$N_3P_3Ar_2F_4$ and 2,2,4,4-$N_3P_3Ar_4F_2$ groups are 0.66, 0.57 and 0.42 respectively.[74] In this study the resonances due to the ipso-carbon nuclei were not located. The para-carbon shifts for geometrical isomers are the same,[198] whereas those of the para hydrogens are different.[74] This observation underscores the difficulties involved in treating ^1H chemical shifts, which may be subject to a variety of shielding mechanisms. The $^2J(P–C_{ortho})$ and $^3J(P–C_{meta})$ couplings for the PFPh group (17 and 12 Hz respectively) are higher than that for the PPh_2 group (14 and 11 Hz).[198]

A high-field (67.89 MHz) ^{13}C NMR study[199] of phenyl substituted cyclophosphazenes $N_3P_3Ph_{2n}Cl_{6-2n}$ ($n = 1$, 2, 3) and the nongeminal $–N_3P_3Cl_3Ph_3$ isomeric pair clearly shows that the signals of the ipso(C–1) carbon nuclei move to high frequency with increasing number of aryl groups. The signals of the para(C–4) and ortho(C–2) carbon nuclei move to low frequency and those of meta(C–3) carbon nuclei remain unchanged. The observed trends in the chemical shifts for the geminal compounds can be

explained on the basis of concomitant mesomeric electron release from the benzene ring and inductive electron withdrawal by phosphorus. There is an approximate linear relationship between C–1 shifts and the mean P–C(1) bond lengths for the three geminal compounds $N_3P_3Cl_{6-2n}Ph_{2n}$ ($n = 1, 2, 3$). For the nongeminal isomers of $N_3P_3Ph_3Cl_3$ there is an increased deshielding of C–1, C–2 and C–4, and this trend can be attributed to an enhanced mesomeric electron release from the phenyl substituent. The closeness of the respective carbon shifts for the related chloro- and fluorocyclophosphazenes may be rationalized by postulating that electronegativity differences between the halogeno substituents and the relative effectiveness of p–d back donation to the phosphazene ring may balance one another.[199]

The magnitude of ^1J(P–C(1)) for nongeminal compounds is ~40 Hz higher than that observed for geminal compounds. While only a single environment is observed for C–1 to C–4 of the *cis* isomer of $N_3P_3Ph_3Cl_3$, two distinct C–1, C–2 and C–3 environments are seen for the *trans* isomer. The magnitude of ^3J (P–C(1)) decreases with the increase in the number of phenyl substituents, and this attenuation is consistent with the decreasing mesomeric electron release from the benzene ring, as well as with the increase in the mean dihedral angle between the phenyl and phosphazene rings.[199]

In a recent study Harris *et al.*[70] have examined the ^{13}C, ^1H and ^{19}F NMR data for a series of 1-aryl, 1-alkyl tetrachlorocyclotriphosphazenes (**25**), the most extensive series of structurally similar compounds studied so far:
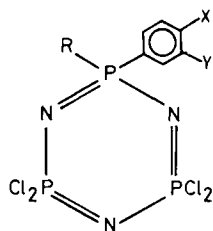
(**25**)

From the ^{13}C and ^1H NMR data, a value of 0.63 has been calculated for the Hammett σ_{para} of the $N_3P_3Cl_4Me$ group, which is close to that of the cyano group. The Taft reactivity parameters (σ_I and σ_R) for the $N_3P_3Cl_4Me$ group are 0.48 and 0.16 respectively (^{19}F NMR data); the σ_I and σ_R values for the cyano group are 0.48 and 0.21 respectively. It is inferred that the inductive withdrawal by the phosphazene ring is similar to that of the cyano group, but that conjugative interaction appears to be less. This inference has also been confirmed by UV spectroscopic data.[70] Although a photoelectron study[200] of phenyl-substituted fluorophosphazenes appears to indicate little or no

mesomeric interaction between the aryl and the phosphazene rings, the bulk of the NMR evidence repudiates this view and points to a π-component, albeit a modest one (Section III.D).

The ^{13}C NMR spectra of an extensive series of geminal dialkyltetra-chlorocyclotriphosphazenes $N_3P_3Cl_4R^1R^2$ (R^1, R^2 = Me, Et, Pr^n, Pr^i, Bu^n, Bu^i, Bu^t, $-CH_2CH{=}CH_2$, $-CH_2C{\equiv}CH$, $-CH{=}C{=}CH_2$, $-C{\equiv}CCH_3$, $-CH_2C{\equiv}C.CH_3$; R^1 not necessarily the same as R^2), have been reported.[68,69] In most cases the spectra are well resolved, and each $\delta(C)$ and $J(P-C)$ could be determined. The resonance due to the carbon nucleus bonded directly to the phosphazene ring always appears as a doublet of triplets because of coupling to the near and far ring-phosphorus nuclei. Carbon nuclei two or three bonds away from phosphorus give rise to doublets, usually with $^3J(P-C) > {}^2J(P-C)$. Typical values for these parameters are given in Table 9.

TABLE 9

Selected values^a of $J(^{31}P-^{13}C)$ for dialkyl cyclotriphosphazenes gem-$N_3P_3Cl_4(Me)R$.

R	$^1J(P-CH_3)$ (Hz)	$^1J(P-C)$ (Hz)	$^2J(P-C-C)$ (Hz)	$^3J(P-C-C-C)$ (Hz)	$^3J(P-N-P-C)$ (Hz)
CH_3	94.0				3.7
CH_2CH_3	92.2	92.3	6.6		3.7^b, 3.3
$CH_2CH_2CH_3$	92.0	91.4	5.2	17.9	3.5, 3.3
$CH(CH_3)_2$	90.3	91.4	2.7		3.6, 3.0
$CH_2CH_2CH_2CH_3$	92.2	91.5	5.5	17.0	3.6, 3.3
$CH_2CH(CH_3)_2$	91.5	90.7	5.0	10.1	3.2, 3.5
$C(CH_3)_3$	88.1	90.2	c		3.5, 2.9
$CH_2CH{=}CH_2$	94.2	87.8	11.7	13.6	4.2, 2.7
$CH_2C{\equiv}CH$	98.5	88.8	14.8	9.5	4.2, 2.7
$CH{=}C{=}CH_2$	104.1	131.7	c	15.6	5.4, 2.9
$C{\equiv}CCH_3$	119.0	213.9	43.4	3.9	6.3, 3.7, 1.3^d
$CH_2C{\equiv}CCH_3$	97.7	88.4	16.2	9.2, 3.5^e	5.2, 1.9

^{a}Data from Allcock et al;[68,69] ^{b}first entry refers to $^3J(\underline{P}-N-P-CH_3)$; ^{c}singlet observed; $^d{}^4J(\underline{P}-N-P-C-C)$; $^e{}^4J(P-C-C-C-C)$.

Analysis of the ^{13}C NMR spectra of the isomeric products gem-$N_3P_3Cl_4(Me)(R)$ ($R = -CH_2C{\equiv}CH$, $-CH{=}C{=}CH_2$, $C{\equiv}C.CH_3$), provides convincing evidence for each structure.[69] The chemical shift of the geminal methyl carbon increases from 17.6 ($R = -CH_2C{\equiv}CH$) to 23.2 ($R = C{\equiv}C.CH_3$) with a parallel increase in the values of $^1J(P-C)$ and $^3J(P-N-P-C)$. The increase in $^1J(P-C)$ for the $alpha$-carbon of the C_3H_3 substituent is particularly marked for these three isomers [88.8 Hz (prop-2-

ynyl); 131.7 (prop-1,2-dienyl; 213.9 (prop-1-ynyl)]. For the series $N_3P_3Cl_4(CH=C=CH_2)(R)$ (R = Me, Et, Pr^i, Bu^t) the ^{13}C shift of the *alpha*-carbon of the prop-2-ynyl substituent decreases from 25.5 (R = Me) to 19.4 (Bu^t). The observation can be rationalized in terms of the electron-donating ability of the alkyl group R increasing the electron density at phosphorus, and thus increasing the shielding of the *alpha*-carbon of the C_3H_3 group. Once again, ^{13}C NMR provides valuable information on the interaction of the P–N ring and an organic side group.[69]

Geminal and nongeminal replacement patterns may be discerned by a study of the ^{13}C NMR spectra of the derivatives, $N_3P_3F_{6-n}R_n$ (R = Bu^n,[115] Bu^t,[115] $C\equiv C-SiMe_3$,[180] $C\equiv C.Ph$,[180] $C(OR)=CH_2$ [179]). The value of $^1J(P-C)$ is considerably smaller for a geminal PR_2 group than that for a PFR group. The disappearance of the coupling $^2J(F-P-C)$ is also diagnostic of geminal substitution.[115,180] The very small attenuation of $^2J(P-C)$, $^3J(P-C)$ and $^3J(P-N-P-C)$ values (wherever applicable) is a less reliable criterion for making this structural distinction. ^{13}C NMR spectra confirm that halo-genocyclophosphazenes react with lithium enolate of acetaldehyde ($LiOCH=CH_2$) to give vinyloxy derivatives; the coupling $^2J(P-O-C)$ is usually $< 10\,Hz$.[118,119] The structure of *trans*-$N_3P_3Cl_2(NC_2H_4)_4$ has been assigned on the basis of the simple appearance of the $P(N^{13}C_2H_4)_2$ region ($\delta(^{13}C) = 23.9$; $^2J(P-C) = 6.9\,Hz$) of the ^{13}C NMR spectrum.[201]

^{13}C NMR spectroscopy is useful for monitoring the thermal rearrangement of the hexamethoxide $N_3P_3(OMe)_6$ and other (methoxy)cyclotriphosphazenes to their respective *N*-methyloxocyclophosphazanes;[80,202–205] new signals due to $N^{13}\underline{C}H_3$ appear in the spectrum, and increase in intensity as the reaction progresses.

E. Nitrogen NMR measurements

1. ^{14}N

There is only one report of the measurement of ^{14}N shifts for cyclo-phosphazenes,[206] and the data are shown in Table 10. The measurements have been carried out by wide-line methods. The nitrogen resonances are spread over a range of 90 ppm and are at relatively low frequency, in contrast with those of azines, which are at medium frequency. In an attempt to correlate the nitrogen resonances with the phosphorus chemical shifts, Mason *et al.* have found that if the shifts are corrected for the rather large variation in the diamagnetic contribution of the substituents (the atom plus ligand paramagnetic terms σ_P^{AL} and σ_N^{AL} are listed in Table 10) then both the ^{14}N and ^{31}P shieldings decrease in the order X = NMe_2 > NCS > OMe > F > Cl > Br. The ^{14}N resonance for $N_3P_3(NCS)_6$ is anomalous, presumably

TABLE 10

$^{14}N^b$ (and ^{31}P shifts^c) and paramagnetic-shielding terms for cyclophosphazenes.^{a}

Compound	$\delta(^{14}N)$	$\sigma_p^{AL}(N)^d$	$\delta(^{31}P)$	$\sigma_p^{AL}(P)^d$
$N_3P_3(NMe_2)_6$ ^{e}	27	−312	25	−796
$N_3P_3(OMe)_6$	35	−322	21.7	−810
$N_3P_3F_6$ ^{e}	59	−347	13.9	−819
$N_3P_3(NCS)_6$	100	−386	30	−802
$N_3P_3Cl_6$ ^{e}	106	−394	20	−872
$N_3P_3Br_6$ ^{f}	115	−402	−45.4	−950
$N_4P_4(OMe)_8$	56	−343	−3.5	−785
$N_4P_4F_8$ ^{e}	55	−349	−17	−791
$N_4P_4Cl_8$	97	−384	−7.4	−854

^{a}From ref. 206. ^{b}Shifts measured with a Varian 4300 B wide-line spectrometer at 3 MHz; external reference $[NH_4]^+$(aq), positive to high frequency. ^{c}From sources quoted in ref. 206; also see tables in the Appendix. ^{d}Atom-plus-ligand paramagnetic term. ^{e}Neat liquid; in other cases Et_2O solution. ^{f}CHCl$_3$ or C_6H_6 solution.

because in this case the resonances for the ring and exocyclic nitrogen atoms are not resolved. The shifts can be interpreted in terms of inductive and conjugative effects of the substituents; conjugation is limited to a P–N–P island and the exocyclic substituents.[206]

2. ^{15}N

Grossmann, Thomas and coworkers have carried out extensive ^{15}N and ^{31}P NMR studies of ^{15}N-labelled cyclophosphazenes.[143,144,207-214a] In addition to ^{15}N and ^{31}P shifts, such investigations can yield other parameters, viz $^1J(P–N)$, $^2J(P–P)$, $^2J(N–N)$ and $^3J(P–N)$ for cyclotriphosphazenes. In particular, $^2J(P–P)$ values for homogeneously substituted derivatives can be readily found that are unobtainable from their normal $^{31}P–\{^1H\}$ NMR spectra. The relevant data are summarized in Tables A.27 and A.28.

^{15}N-labelled cyclotriphosphazenes provide examples of an $[AX]_3$ spin system.[143] Because the couplings $^2J(N–N)$ and $^3J(P–N)$ are very small and can be neglected, the analyses of the ^{31}P and ^{15}N spectra of these derivatives are simplified and depend only on the ratio of the two couplings $^2J(P–P)/^1J(P–N)$. The one-bond P–N coupling $^1J(P–N)$ is directly read from the spectra. Using a series of simulated model spectra, it is shown that $^2J(P–P)$ can be calculated by a graphical procedure instead of simulating the entire spectrum by iterative computation. The error in the graphical determination increases with increasing ratio of $^2J(P–P)/^1J(P–N)$, so that the error in the $^2J(P–P)$ value for $N_3P_3F_6$ is ∼ 10%.[143]

The ^{15}N chemical shifts for homogeneously substituted cyclotriphosphazenes $N_3P_3X_6$ (1) (Table A.27) show that the shielding of the nitrogen for the various substituents decrease in the order $NR_2 \sim Me \sim OR \sim F > SR > Cl > Br.$[144] This sequence is almost the same as the one found for ^{14}N shifts (Section II.E.1).

Semiempirical CNDO/2 calculations have been carried out to provide a theoretical explanation for the ^{31}P and ^{15}N chemical shifts and P–N and P–P couplings.[144,207] The paramagnetic contribution to the shielding is evaluated using Pople's ΔE approximation. The observed ^{15}N shifts can be qualitatively explained on the basis of these calculations, although there are several serious difficulties. If the values for the trimer and tetramer series are compared then the shielding differences among F, OR and NR_2 substituted derivatives are not appreciable; for the chloride, however, the difference between the trimer and tetramer is ~ 60 ppm. Such a large variation for the chloride cannot be satisfactorily accounted for by the changes in $r^{-3}\Sigma Q_{AB}$ term. It has been suggested that inclusion of transannular $P \cdots P$ bonds in the theoretical treatment of chemical shifts and couplings may lead to a better agreement between calculated and experimental values.[143,207] Transannular bonding involves the interaction of p-orbitals, and would influence the orbital–orbital term in the calculation of couplings and chemical shifts. However, the importance of transannular bonding in cyclophosphazenes remains to be evaluated in detail,[108] and further progress in the theoretical description of bonding is needed before a satisfactory explanation can be offered for the variations of ^{15}N chemical shifts and the couplings $^1J(P–N)$ and $^2J(P–P)$.

For the ^{15}N-labelled (mercapto)cyclophosphazenes $^{15}N_3P_3Cl_{6-n}(SR)_n$ (R = Et or Ph; $n = 0, 2, 4$ or 6) the ^{15}N shielding increases in the sequence PCl_2—$^{15}\underline{N}$—$PCl_2 > PCl_2$—$^{15}\underline{N}$—$P(SEt)_2 > P(SEt)_2$—^{15}N—$P(SEt)_2$, whereas the ^{31}P chemical shifts vary in the reverse order, $\underline{P}Cl_2 < \underline{P}Cl(SEt) < \underline{P}(SEt)_2$. Two-bond P–P couplings involving $\underline{P}(SEt)_2$ are smaller than that between two $\underline{P}Cl_2$ groups. An opposite trend is observed for $^1J(P–N)$, which increases with decreasing $^2J(P–P)$ values.[208]

^{13}P and ^{15}N NMR measurements on other geminally disubstituted compounds $^{15}N_3P_3X_4Y_2$ (X = Cl; Y = F or NH_2) have also been carried out.[209] Considering these data along with those for gem-$N_3P_3Cl_4(SEt)_2$ [208] (Table A.27), it is apparent that the couplings II and III (26) lie in between the values for $(^{15}NPCl_2)_3$ and $(^{15}NPY_2)_3$. The value for I is close to that found for $^{15}N_3P_3Cl_6$; II lies nearer that of I, whereas III lies nearer the $^1J(P–N)$ for $(^{15}NPY_2)_3$. It is also shown that $^1J(P–N)$ may be of different signs. The absolute value of $^1J(P–N)$ is significantly influenced only by those substituents bonded to the phosphorus nuclei directly involved in the coupling. The ^{15}N chemical shifts are also only altered by substituents on the directly bonded P atoms.
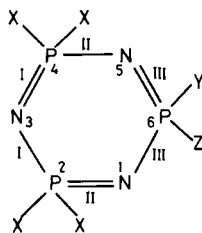
(26)

NMR (^{31}P and ^{15}N) measurements have been carried out for a few exocyclic ^{15}N-labelled cyclotriphosphazenes $N_3P_3Cl_5X$ and $N_3P_3Cl_4X_2$ (X = ^{15}NH$_2$, ^{15}NHMe, ^{15}NMe$_2$ or ^{15}NHC$_6$H$_5$).^{212} ^{15}N shifts for the ^{15}N-labelled hexa(azido)cyclophosphazene $N_3P_3(^{15}N_3)_6$ have also been reported[215] (Table A.28). For the (amino)cyclophosphazenes the P–N couplings have been evaluated by spectral simulation.[212] Both ^1J(P–N) and ^3J(P–N) have the same sign, and, assuming ^2J(P–P) to be positive, these P–N couplings are assigned a positive sign. The ^{15}N shieldings of the exocyclic nitrogen nuclei are lower than the value for the corresponding free amines. The participation of the lone pair of electrons on the nitrogen atoms in pπ–dπ bonding with phosphorus leads to their deshielding. The $\delta(^{15}$N) values for the nongeminal bis(amino) derivatives, $N_3P_3Cl_4R_2$ (R = NHMe, NMe$_2$) are the same as those for the corresponding mono(amino) derivatives. On the other hand, geminal compounds, $N_3P_3Cl_4R_2$ (R = NH$_2$, NHMe or NHC$_6$H$_5$) show a low-frequency ^{15}N shift compared with the corresponding mono(amino) compounds, because two exocyclic nitrogen atoms must compete for the d-orbitals on the same phosphorus atom. If one considers the ^{15}N shifts for the mono- and bis(amino) derivatives separately then it is clear that a deshielding of phosphorus is accompanied by a shielding of the nitrogen nuclei. This trend is consistent with the flow of electron density from the exocyclic nitrogen to phosphorus. The effect of this electronic interaction on the chemical shifts of ring nitrogen atoms (and the remote phosphorus atoms) cannot be assessed from the available data. An increase in shielding of the ring nitrogen adjacent to PR(NHPh) (R = Cl or NHPh) occurs for the endocyclic ^{15}N-labelled cyclotriphosphazene $^{15}N_3P_3Cl_4R(NHC_6H_5)$ compared with $\delta(^{15}$N) for $^{15}N_3P_3Cl_6$.

The one bond P–N coupling constants ^1J(P–N) for the exocyclic ^{15}N-labelled amino derivatives lie in the range 25–39 Hz. For the dimethylamino derivatives $N_3P_3Cl_5(^{15}NMe_2)$ and cis- and trans-$N_3P_3Cl_4(^{15}NMe_2)_2$ the ^1J(P–N) value is $\sim$10 Hz smaller than that for the other compounds. It is also interesting to note that in these compounds the three-bond P–N coupling ^3J(P–N) involving the exocyclic nitrogen and the remote phosphorus nuclei

is $\sim 4\,Hz$; this coupling is not resolved ($< 1\,Hz$) in the spectra of compounds containing ^{15}N-labelled ring nitrogen atoms (Fig. 8). Perhaps dihedral angle can play an important role in determining the magnitude of $^3J(P-N)$ as found for vicinal couplings involving other nuclei. For endocyclic $^3J(P-N)$, the dihedral angle is $0°$, whereas for the $^3J(P-N)$ involving the exocyclic nitrogen the dihedral angle is $\sim 130°$.[212]
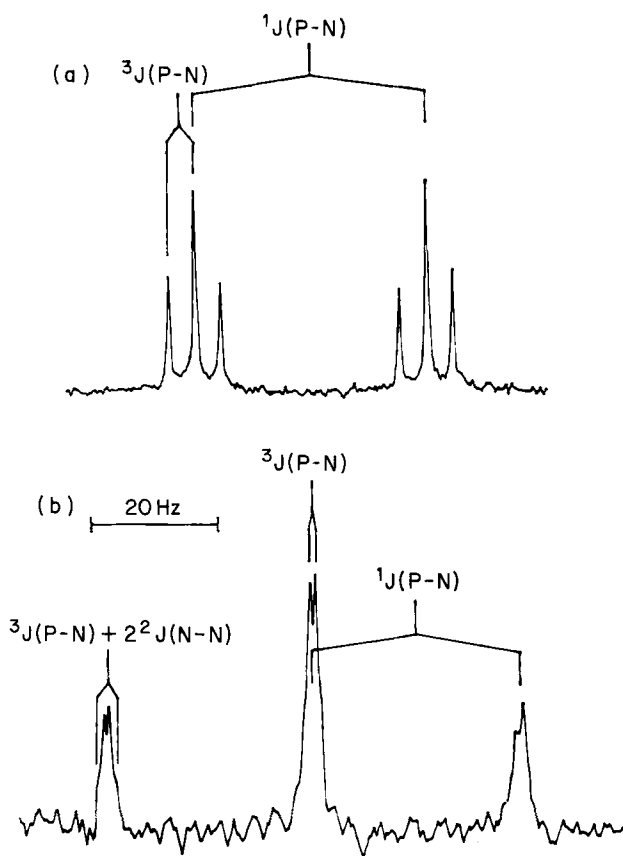
FIG. 8. The $^{15}N-\{^1H\}$ (9.1 MHz, $CDCl_3$) spectrum of (a) exocyclic ^{15}N-labelled $N_3P_3Cl_5(^{15}NHPh)$ and (b) endocyclic ^{15}N-labelled $^{15}N_3P_3Cl_5(NHPh)$ ($Cl_2P-^{15}N-PCl_2$) region only) (Reproduced from ref. 212 with permission of Johann Ambrosius Barth, Leipzig, DDR.)

III. EIGHT-MEMBERED AND HIGHER P–N RINGS

A. Proton NMR spectra of cyclotetraphosphazenes

The chemistry of the eight-membered cyclophosphazenes $(NPX_2)_4$ (2) is considerably more complicated than that of the trimeric analogues owing to the large number of possible isomers.[13] Aminolysis reactions of octachloro-cyclotetraphosphazene $N_4P_4Cl_8$ have been studied in greatest detail,[13,14,216] and proton NMR has proved useful for structural assignments for the derivatives, $N_4P_4Cl_{8-n}R_n$ (R = NMe_2,[217,218] NC_2H_4,[27] $NMePh$,[219] $N(CH_2Ph)_2$[220]) and various mixed(amino) compounds.[72,221] High-field NMR measurements are a prerequisite, but ideally the data obtained should only be assessed in conjunction with ^{31}P NMR data and/or ^{19}F data for derivatives of $N_4P_4F_8$.[222,223] Even in these favourable circumstances, many uncertainties remain with regard to the *cis/trans* stereochemistry of substituents.

The ^1H NMR criteria utilized for assigning structures to derivatives of $N_4P_4X_8$ (X = Cl, F) are identical with those described for trimeric compounds in Section II.A.1. The –NMe regions of the spectra of four of the ten possible N-methylanilino derivatives $N_4P_4Cl_4(NMePh)_4$ illustrate these points (Fig. 9).[219] The observation of a doublet without virtual coupling (^3J(P–H) = 10.5 Hz) indicates a 2,2,6,6-structure for isomer (29), an assignment that is supported by the ^{31}P spectrum (A_2B_2 type). There are four isomers with an N-methylanilino group on each phosphorus atom, but only isomer (30) can have three NMe environments. The ^3J(P–H) values are characteristic of PCl(NMePh) groups.[29] The spectrum of isomer (28) shows a single NMe doublet with strong virtual coupling, but in this case an exact assignment can be made only with the assistance of additional chemical evidence.[219] The spectrum of isomer (27) shows four NMePh environments (two geminal and two nongeminal). The chemical shifts observed are more compatible with the structure shown than with the alternative *cis* structure.

The structures of many isomeric chloro- or fluoro(dimethylamino)cyclo-tetraphosphazenes $N_4P_4X_{8-n}(NMe_2)_n$ have been assigned[217,223-225] with the aid of proton NMR spectra. As the coupling ^3J(P–H) is not diagnostic for nongeminal $PF(NMe_2)$ groups (Table 1), it is essential to use ^{19}F NMR to obtain such information (Section III.C). Crystallographic studies confirm the proposed structures,[13,226,227] except in the case of one pentakis(dimethyl-amino) derivative of $N_4P_4Cl_8$.[228] Chemical shifts of NMe_2 protons for $N_4P_4Cl_{8-n}(NMe_2)_n$ (2.75–2.49) are largely explicable in electronic terms with $\delta[N\underline{Me}_2(gem)] < \delta[N\underline{Me}_2(cis)] < \delta[N\underline{Me}_2(trans)]$.[217] Shifts of N-methyl protons for $N_4P_4Cl_{8-n}(NMePh)_n$ occur over a wide range ($\delta 3.24$–2.64),[219] whereas a much narrower range (0.16 ppm) is found for the N-methyl
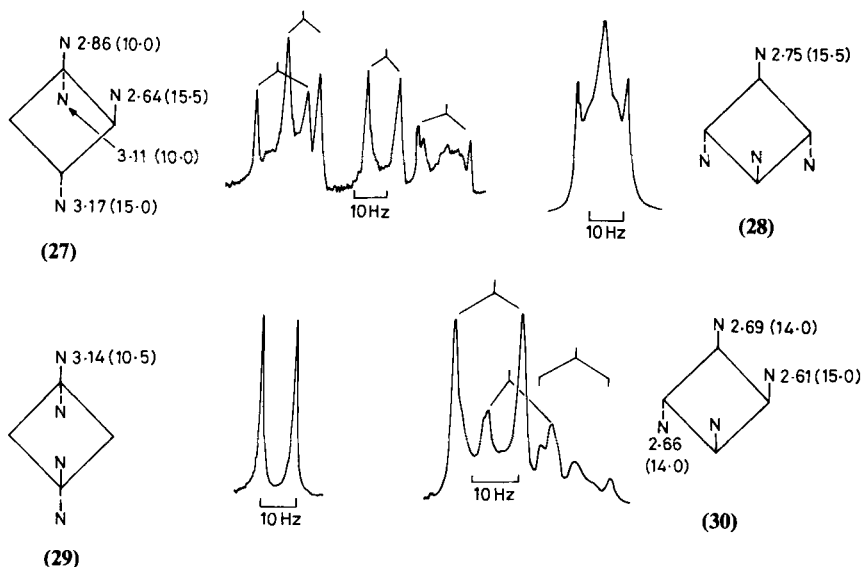
FIG. 9. The ^{1}H NMR spectra (NME region only) of four isomers of $N_4P_4Cl_4(NMePh)_4$ along with their structures. The values shown are the chemical shifts of N-methyl protons with $^3J(P-H)$ in parentheses. The spectrum of (30) was measured in C_6D_6 at 220 MHz; the other spectra were recorded at 100 MHz in $CDCl_3$. (Adapted from ref. 216(b) with permission of the Indian Institute of Science, Bangalore.)

resonances of $N_3P_3Cl_{6-n}(NMePh)_n$.[29] The NMePh shifts in both series are clearly influenced by the aromatic ring-current effects of the substituent. The considerable variation observed for the tetrameric derivatives suggests that conformational changes in the eight-membered P–N ring[13,219,229] may also contribute. As a result, the shielding effects associated with aromatic substituents are less easy to evaluate for cyclotetraphosphazenes, and thus structural assignments are often problematic. Difficulties in assessing the shielding of phenyl groups for nongeminal isomers of $N_4P_4Ph_4(NMe_2)_4$ are discussed.[230]

The absence (or presence) of virtual coupling in the proton NMR spectra of cyclotetraphosphazenes has sometimes been utilized for obtaining structural information.[12,13] For example, the ^{1}H NMR spectra of geminal 2,2,6,6- and 2,2,4,4-$N_4P_4Ph_4(NMe_2)_4$ isomers both contain a single NMe_2 doublet but only the latter shows intense virtual coupling.[231] The ^{1}H NMR spectra of the isomeric pairs, 2,4- and 2,6-$N_4P_4(NMePh)_2X_6$ (X = Cl, OMe), cannot be differentiated on this basis, as both exhibit pronounced virtual coupling.[219] We suggest that this criterion for structural assignment be used

with great discretion. Even in favourable cases it is prudent to have some knowledge of the differences in chemical shifts of the ring phosphorus nuclei.

An increasing feature of the ^{1}H NMR spectrum of the adduct $N_4P_4(NHBu^t)_8 \cdot HCl$, is the appearance of two NH signals in the ratio 1:1 at 3.8 and 2.4δ, suggesting that the exchange of the proton among the four equivalent ring N atoms is slow on the NMR time scale at ambient temperature.[14,232] (An AA'BB' pattern is observed in the ^{31}P spectrum.) The resonance at 3.8δ is assigned to N$\underline{H}$Bu^t protons adjacent to the site of protonation.

B. ^{31}P NMR spectra of cyclotetraphosphazenes

^{31}P NMR spectroscopy is particularly important for distinguishing geminal and nongeminal derivatives of halogenocyclotetraphosphazenes (2, X = F, Cl). The ^{31}P NMR spectra of $N_4P_4R_2X_6$ (31a–c) are of the types A_2BC, AA'BB' and A_2B_2, corresponding to 2,2-, 2,4- and 2,6-structures respectively:[55]
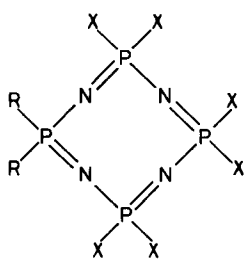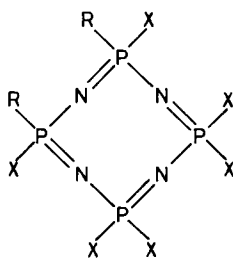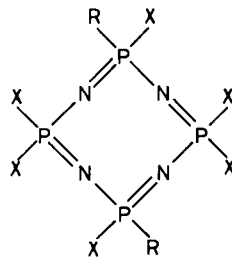
(31a)   (31b)   (31c)

Geometrical isomers cannot be differentiated in this way, since the spin system would remain the same, and any possible differences in ring conformation would be too small to affect the ^{31}P spectra significantly. There is usually no difficulty in recognizing AA'BB' and A_2B_2 spectra (illustrated elsewhere[49,55,72,220,232,233]) although the latter may not always be fully resolved if A and B chemical shifts are close.[72,233] Examples of A_2B_2 spectra are common, as 2,6-substitution is encountered in all reactions of $N_4P_4Cl_8$ with primary or secondary amines.[49,72,232] In contrast, surprisingly few examples are known elsewhere in which true magnetic equivalence of A and B nuclei is found.[234]

Some general trends can be summarized from the NMR data for (amino)cyclotetraphosphazenes (Table A.16). The replacement of Cl atoms by amino groups results in a deshielding of [PCl(NRR')]. Exceptions are

observed during the initial stages of chlorine replacement by bulky arylamino or t-butylamino groups, but the shielding induced is still modest. For compounds containing primary amino groups, [PCl(NHR)] for 2,6-isomers is shielded with respect to (PCl_2), but the reverse is true for 2,4-disubstituted derivatives.[72] The overall range of chemical shifts is much larger than that found for comparable derivatives of the more rigid trimeric ring.[55] There is a noticeable steric effect on $\delta(P)$ for the derivatives $N_4P_4(NHR)_8$, with shielding increasing in the order $R = NHEt < NHPr^i < NHBu^i$.[49,232,235]

Most two bond couplings $^2J(P-P)$ for (amino)cyclotetraphosphazenes are in the range 37–46 Hz, although the value for $N_4P_4(NMe_2)_8$ (60.2 Hz) is somewhat higher, and values for aziridino derivatives are lower. In general, this coupling is less positive than those of analogous trimeric derivatives, an observation that is unexpected considering the larger bond angles at endocyclic nitrogen atoms for cyclotetraphosphazenes.[13,229]

The low coupling $(^2J(P_{spiro}-PCl_2) = 27.1$ Hz) observed for the spirocyclic derivative $N_4P_4Cl_6(MeNCH_2CH_2NMe)$[236] is rather surprising in view of the value of 41.8 Hz observed for the trimeric analogue.[97] A similar decrease is observed for the geminal bis(aziridino) derivatives $N_3P_3Az_2Cl_4$ $(^2J(P-N-P)$ = 30.0 Hz) and $N_4P_4Az_2Cl_6$ $(^2J(P-N-P) = 11.6$ Hz).[27] The two-bond coupling $(\underline{P}Cl_2 \cdots \underline{P}Cl_2)$ is obtained from the AA'BB' spectra of the 2,4-isomers of $N_4P_4Cl_6(NRR')_2$ $(R = H, R' = CH_2Ph, Bu^t, Ph; R = Me, R' = Ph; R = R'$ $= CH_2Ph),$[214,220,233] and falls in the range 33–35 Hz. For exact computer simulation of this type of spectrum a small negative four-bond coupling (*ca.* -1.0 Hz) must be included.

Thomas *et al.*[211] have determined the value of $^2J(P-N-P)$ from ^{31}P and ^{15}N NMR spectra of labelled octasubstituted cyclotetraphosphazenes $^{15}N_4P_4R_8$ $(R = F, Cl, Br, OMe, OPh, SEt, NMe_2, NHEt, Me)$. They range from 155.0 Hz for the octafluoride to 10.7 Hz for the octamethyl derivative, and correlate reasonably with the electronegativity of the substituent (Table A.27).

^{31}P NMR spectroscopy is invaluable for the structural elucidation of the many products obtained in the reactions of $N_4P_4Cl_8$ with either sodium ethanethiolate[124] or sodium phenoxide.[237] Thioethoxy derivatives $N_4P_4Cl_{8-n}(SEt)_n$ $(n = 2, ..., 6, 8)$ have geminal structures, and pairs of isomers are obtained when $n = 3, ..., 5$. Chemical shifts of $(\underline{P}Cl_2)$, $\underline{P}Cl(SEt)$ and $\underline{P}(SEt)_2$ fall in the narrow ranges -7.1 to -9.5, 12.2 to 14.6, and 25.1 to 30.4δ respectively, with modest low frequency shifts with increasing degree of thioalcoholysis. Values of $^2J[\underline{P}Cl_2-\underline{P}(SEt)_2]$ are low (11.6–17.4 Hz), as observed for other thiochlorocyclophosphazenes.[82,86,208] Data for some alkoxy and amido derivatives of 2,2,6,6-$N_4P_4Cl_4(SEt)_4$ have also been reported[238] (Table A.18).

Chloro(phenoxy)cyclotetraphosphazenes $N_4P_4Cl_{8-n}(OPh)_n$ and their di-

methylamino and methoxy derivatives provide other examples of ^{31}P NMR spectra arising from four-spin systems.[237] At 162 MHz the ^{31}P–{^{1}H} spectrum of a mixture of nongeminal bis isomers of $N_4P_4Cl_6(OPh)_2$ consists of three sets of symmetrical lines. Two sets are of an A_2X_2 type and arise from 2,6-isomers. The chemical shifts are very similar: $\delta(PCl_2) = -4.69$, $\delta[PCl(OPh)] = -11.56$; $\delta(PCl_2) = -3.64$, $\delta[PCl(OPh)] = -11.16$ and their assignment to individual *cis/trans* isomers is not obvious. The remaining lines constitute an AA'XX' pattern and arise from isomers with 2,4-structures (*cis* and *trans* not distinguished even at high field). Data are given in Table A.17 and show that [PCl(OPh)] (-11.6 to -6.9δ) is always deshielded with respect to [P(OPh)$_2$] but shielded in relation to (PCl$_2$). Both δ[PCl(OPh)] and δ[P(OPh)$_2$] move to high frequency with increasing replacement of chlorine atoms. Two-bond couplings ^2J(P–N–P) are in the range 25–79 Hz, and reflect the influence of the electronegativity of the substituents at phosphorus.[237]

^{31}P NMR data are available for a few fluoro- and chlorocyclotetraphosphazenes with alkyl (or aryl) substituents (Table A.15). The relative magnitude of the chemical shifts observed for the geminal derivatives, $N_4P_4F_{8-n}Me_n$ ($n = 1, ..., 4, 8$), is $\delta(PF_2) > \delta(PMe_2) > \delta(PFMe)$; the shielding of the most-shielded nucleus (PF$_2$) gradually decreases as the number of methyl groups on other phosphorus atoms increases.[222] ^{31}P NMR data for the mixed methyl(phenyl)cyclotetraphosphazene (32a) and its methyl iodide adduct (32b)[239] are shown below:

(32a)   (32b)
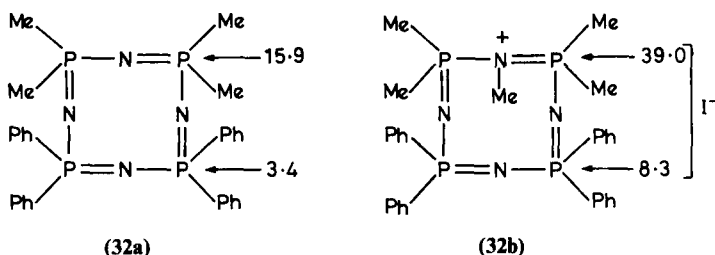
There is a pronounced high frequency shift of the PMe$_2$ nuclei on quaternization of the most-basic ring-nitrogen atom. Similar observations pertain to $N_4P_4Me_8 \cdot MeI$.[240]

C. ^{19}N, ^{15}N and ^{13}C NMR studies of cyclotetraphosphazenes

The utility of ^{19}F NMR spectroscopy for structural assignments is elegantly demonstrated[222] in the case of (methyl)fluorocyclotetraphosphazenes $N_4P_4F_{8-n}Me_n$ ($n = 1, 2$ (two isomers), 3 (two isomers), 4 and 8), which are formed in the reaction of $N_4P_4F_8$ with methyl lithium. Fluorine atoms are

replaced in a predominantly geminal sequence ($\delta(P\underline{F}_2) = -66.4$ to -69.7; $\delta(P\underline{F}Me) = -55.3$ to -56.6). Second-order effects in these spectra are pronounced, although they diminish with increasing methylation. With the aid of heteronuclear decoupling, the two geminal tris isomers (33a,b) are distinguished, as the 2,2,4-isomer gives rise to two distinct PF_2 multiplets, with nonequivalent fluorine nuclei being observed for one such group. A $^4J(F-F)_{cis}$ of 13.5 Hz is observed for the 2,2,6-isomer.
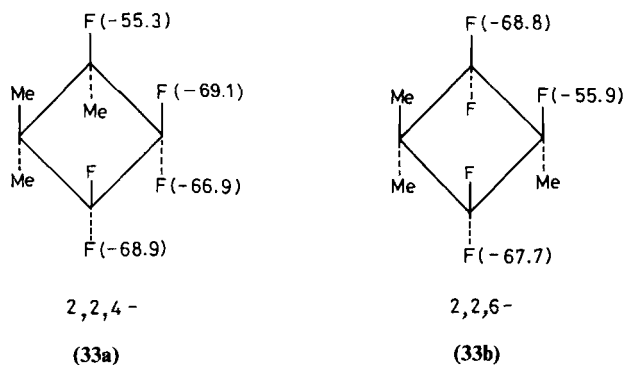
Structural assignments for (dimethylamino)fluorocyclotetraphosphazenes, $N_4P_4F_{8-n}(NMe_2)_n$ ($n = 1, ..., 6$ (many isomers)) by ^{19}F NMR spectroscopy are considerably more difficult than for the corresponding cyclotriphosphazenes, but this challenge has been taken up by Sowerby and Millington.[223-225] The principles employed parallel those for trimeric analogues (Section II.C): a fluorine atom *cis* to an NMe_2 group on adjacent P atoms resonates to low frequency of one *cis* to other fluorine substituents. The problem arises in assessing the contribution made by substituents that are in a *trans* position on adjacent phosphorus and by groups on the antipodal P atoms (this may be negligible in most cases). Thus the non-equivalence of the fluorine atoms of a PF_2 group is not always observed when anticipated.[223] Also, the nonplanarity of these eight-membered rings[226,227] does not make this task any easier. Some typical data are given in Table A.26.

The 2,4-transannular bridged fluorocyclotetraphosphazene $N_4P_4F_6(NSN)$ (34)[241] exhibits complex multiplets at -66.2 $\delta(PF_2)$ and -59.8 $\delta(P\underline{F}N)$ in its ^{19}F NMR spectrum.[242]

^{15}N NMR data for cyclotetraphosphazenes ($^{15}NPR_2)_4$ are reported (Table A.27).[207,208,211] The shielding of nitrogen for the various substituents decrease in the same order as the one found for the trimeric series ($^{15}NPR_2)_3$ (Section II.E.2). The values of $\delta(^{15}N)$ do not have a direct correlation with the base strength of the cyclophosphazenes. For example, the ^{15}N chemical shifts
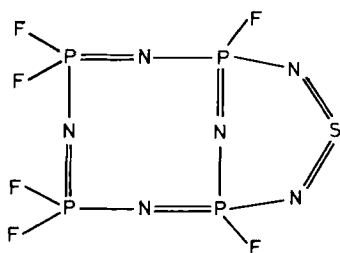
(34)

of $^{15}N_4P_4F_8$ and $^{15}N_4P_4(NMe_2)_8$ are virtually the same, although the latter is a much stronger base. Since the charge on nitrogen should be important in determining the chemical shift, it seems obvious that the chemical shift is very much dependent on a balance of forces involving ring π and π' bonding as well as exocyclic P–X bonding.[211] Values of $^1J(P-N)$ vary linearly with the electronegativity of the substituents, except for the bromide. With the exception of $^2J(P-P)$ for the fluoride, $^1J(P-N)$ and $^2J(P-P)$ are higher for the tetramer than for the trimer, and this observation can be correlated with the smaller P–N bond lengths in the tetrameric compounds.[211] It is difficult to explain these trends in terms of the semiempirical quantum-mechanical calculations using the CNDO/2 formalism.[210] If one considers only the contact term, the calculated sequences of $^1J(P-N)$ and $^2J(P-P)$ values are opposite to the experimentally observed trends. There is thus no simple correlation between the couplings and the s-character of the respective bonds.[143,207]

The trends observed for ^{15}N chemical shifts, $^1J(P-N)$ and $^2J(P-P)$ for the derivatives $^{15}N_4P_4Cl_{8-n}(SEt)_n$ $(n = 0, 4, 8)$ are similar to those noted for analogous cyclotriphosphazenes[208] (Section II.E.2).

^{13}C NMR data for octa(methoxy)cyclotetraphosphazene $N_4P_4(OMe)_8$ and its thermally rearranged products have been reported;[80,202,203] the rearrangement can be monitored by ^{13}C NMR measurements.[202] The ^{13}C data for the two phenylated derivatives $2,2,6,6-N_4P_4Cl_4Ph_4$ and $N_4P_4Ph_8$ show that the ipso-carbon is more shielded (by ~ 5.6 ppm), whereas the ortho- and para-carbon nuclei are more deshielded (by ~ 1 and 2 ppm respectively) for the latter. Both $^1J[P-C(1)]$ and $^3J[P-C(1)]$ decrease with increasing number of phenyl substituents.[199] These trends are similar to those observed for phenyl-substituted cyclotriphosphazenes (Section II.D).

D. Higher rings

NMR data for the higher homologues $(NPX_2)_n$ $(n > 4)$ are very limited, as might be anticipated: the compounds are difficult to obtain in any quantity
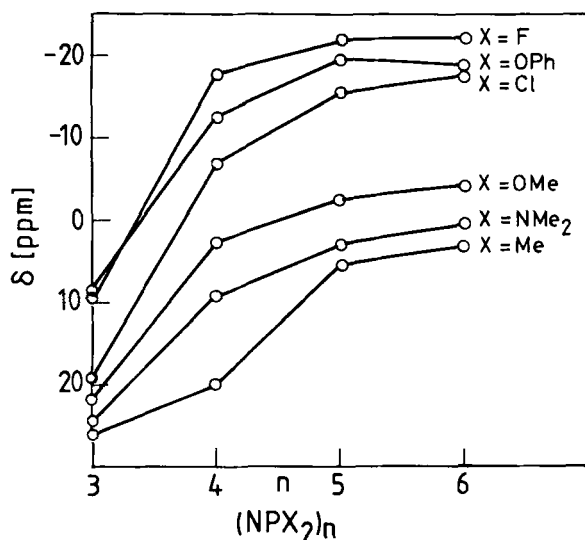
FIG. 10. Variation of $\delta(^{31}P)$ with ring size n for $(NPX_2)_n$ ($X = Cl$, NMe_2[55,213]; F[207,213]; Me[144,211,344]; OMe[80]; OPh[144,237,345]).

and their chemistry has hardly been explored.[9,13] ^{31}P NMR data are listed in Table A.19. Most derivatives show negative shifts, whereas analogous cyclotriphosphazenes have a positive $\delta(P)$. The variation of $\delta(P)$ with ring size for some fully substituted derivatives $(NPX_2)_n$ ($n = 3, \ldots, 6$) is shown graphically in Fig. 10. Recently the first example of the four-membered cyclodiphosphazene ring system (35) has been reported, and its ^{31}P signal (40δ) is deshielded with respect to those of (amino)cyclotriphosphazenes (Table A.3), but shielded with respect to that of an amino-substituted λ^3-phosphorus nucleus:[243]
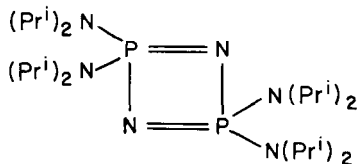
(35)

Dynamic nuclear polarization has been observed for the fluorocyclo-phosphazenes $(NPF_2)_n$ ($n = 3, \ldots, 7$), with three free radicals.[244] Much-weaker scalar coupling between the free radicals and the ^{31}P nucleus is found than for the corresponding chlorides.[245] It is concluded that exocyclic F

atoms behave towards radical probes as though they are not conjugated to the P–N ring π-orbitals.

Flourine NMR data[176] for the homologous fluorocyclophosphazenes $(NPF_2)_n$ ($n = 3, ..., 9$) are given in Table 11. All PF_2 groups are equivalent,

TABLE 11

Variation[a] of $\delta(F)$ and $^1J(P–F)$ with ring size for $(NPF_2)_n$.[b]

n	3	4	5	6	7	8	9
$\delta(F)$	-71.90	-71.85	-69.05	-68.60	-68.00	-68.00	-67.95
$^1J(P–F)$	868	836	874	885	901	903	901

[a]Data from ref. 76; [b]measured as neat liquid.

and the shifts decrease with increase in ring size, albeit not regularly: the shifts of even-numbered rings exceed the mean shifts of their odd-numbered neighbours. The pattern of ^{19}F shifts for PClF in the homologous series $N_nP_nCl_{2n-1}F$ and $N_nP_nF_{2n-1}Cl$ ($n = 3, ..., 6$) is the same, with $N_3P_3 < N_4P_4 > N_5P_5 < N_6P_6$. The corresponding parameters for the two series are remarkably similar, suggesting that chloro- and fluorophosphazene rings have a comparable electronic influence on a PClF group. Other mono-substituted derivatives studied by ^{19}F NMR for different-sized rings include $N_nP_nF_{2n-1}X$ (X = Br, NCS or NMe$_2$; $n = 3, ..., 6$).[160]

The first detailed NMR study of the interaction of an aryl group with the cyclophosphazene ring was reported by Chivers and Paddock.[176] The ^{19}F chemical shifts of the fluorine attached to the aryl ring of the derivatives $N_nP_nF_{2n-1}Ar_F$ ($n = 3, ..., 8$, $Ar_F = C_6F_5$, C_6H_4F-p, C_6H_4F-m) indicate a strong inductive and conjugative withdrawal by the fluorocyclophosphazene ring. Although meta-^{19}F shifts hardly vary with ring size, the para-^{19}F shifts decrease steadily with ring size, particularly for the pentafluorophenyl substituent (4 ppm). The alternation of the value of the parameter, $\delta\{F(meta)\} - \delta\{F(para)\}$ (15–16 ppm), is experimentally significant, and can be taken as evidence for the conjugation of the homomorphic π-system of the C_6F_5 ring with the homomorphic π-system of the P–N ring; the transfer of charge will be greatest to the ring containing $4n + 2$ π-electrons. Similarly, 1-methylpyrrol-2-yl derivatives $N_nP_nF_{2n-1}(C_4H_3NMe)$ have been studied, and $\delta[PF_2(n = 3, 4)] < \delta[PF_2(n = 5, 6)]$; $\delta(PFC)$ for the tetrameric and hexameric rings occurs at lower frequency (-49.7 ppm) than for the trimer or pentamer.[197] In conjunction with ^{13}C and ^{31}P data, these results indicate a withdrawal of electrons by the fluorophosphazene ring, but a detailed discrimination of the effects is not possible.

The pentameric chloride, $N_5P_5Cl_{10}$, reacts with KSO_2F to give the chlorofluoro derivatives $N_5P_5Cl_{10-n}F_n$.[246] A detailed analysis of the ^{19}F NMR spectra was understandably not attempted, but a partial one suffices, as compounds containing more than one PClF group are not formed. ^{19}F shifts for this group ($\delta(PFCl) = -36.4$ to -33.6) are well separated from $\delta(PF_2) = -68.6$ to -66.3, and they move to high frequency as fluorination proceeds. An additional structural aid is that $^3J(P-F)$ of 24–27 Hz can be observed for a PClF group flanked by two PCl_2 groups.

The ^{15}N chemical shifts for homogeneously substituted cyclophosphazenes $(^{15}NPX_2)_n$ ($n = 3, \ldots, 6$) (Table A.27) do not show a large variation with ring size. Invariably, the $\delta(^{15}N)$ values for cyclotriphosphazenes are to low frequency compared to those for cyclotetraphosphazenes ($N_3P_3F_6$ and $N_4P_4F_8$ are exceptions to this general statement).[211] It is worth noting that for the chloro- and methoxy-substituted derivatives there is an alternation of $\delta(^{15}N)$ with ring size from trimer to the pentamer.[213] Generally, $\delta(^{15}N)$ shifts reach a limiting value as the ring size increases.[207,213]

IV. BICYCLIC PHOSPHAZENES, BI(CYCLOTRIPHOSPHAZENES) AND OTHER POLYCYCLIC SYSTEMS

A. Bicyclic phosphazenes

Transannular bridged bicyclic phosphazenes are formed in many aminolysis reactions of $N_4P_4Cl_8$.[220,235,247-250] The ^{31}P chemical shifts of this novel P_4N_5 ring system occur at ca. 15–22δ, a region more characteristic of (amino)cyclotriphosphazenes (Table A.3) and considerably to high frequency of the shifts associated with (amino)cyclotetraphosphazenes. Consequently, ^{31}P NMR spectroscopy is a useful analytical tool for examining the mixture of products obtained in the aminolysis reactions of chlorocyclotetraphosphazenes.[235,249,250] Symmetrical bicyclic phosphazenes $N_4P_4(NHR)_6(NR)$ (36), give rise to $^{31}P-\{^1H\}$ NMR spectra of the A_2B_2 type. An examination of the data in Table A.20 suggests that the chemical shift of the junction phosphorus atoms [P(2)(6)] remains more or less constant (18.5–19.5δ), irrespective of the substituent. We have thus reversed the previous assignments[235] for P(2)(6) and P(4)(8) for the symmetrical compounds (36, R = Et, Pr^n and Bu^n). The $^{31}P-\{^1H\}$ NMR spectra of the hydrochloride adducts, $N_4P_4(NHR)_6(NR) \cdot HCl$ (R = Me, Et), are also of the A_2B_2 type, an observation that is consistent only with protonation at the bridge nitrogen atom.[247] Protonation at any of the four ring nitrogen atoms would destroy the symmetry of the spin system unless the proton exchange is very rapid. The phosphorus

nuclei of the adducts are more shielded than those of their respective bases, a trend that is characteristic of most adducts of (amino)cyclophosphazenes.[55,72]
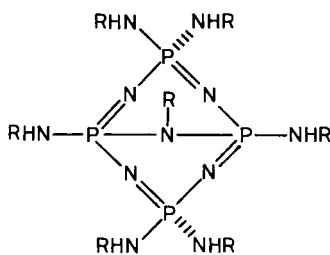
(36)

R = Me , Et , Pr^n, Pr^i, Bu^n

(37)
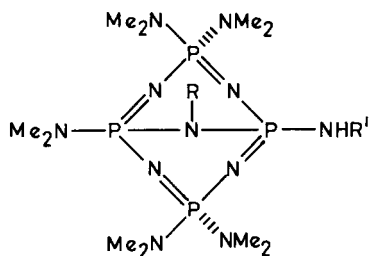
R = R^1 = Me , Et , Pr^n , Bu^n , CH$_2$Ph

R = Et , R^1 = Bu^t

Unsymmetrical bicyclic compounds, $N_4P_4(NMe_2)_5(NHR)(NR')$ (37) generate $^{31}P-\{^1H\}$ NMR spectra of the A_2BC type, as shown in Fig. 11. NMR parameters are listed in Table A.20, and in most cases the values have been
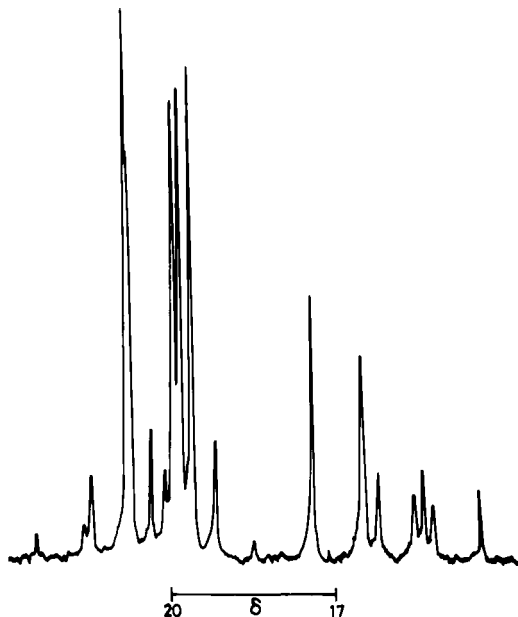
FIG. 11. The $^{31}P-\{^1H\}$ (36.43 MHz, CDCl$_3$) spectrum of the unsymmetrical bicyclic derivative $N_4P_4(NMe_2)_5(NHBu^i)(NEt)$ (37, R = Et, R' = Bu^t). (Reproduced from ref. 235 with permission of the Council of Scientific and Industrial Research, New Delhi.)

confirmed by computer simulation.[235,247] The couplings ^2J(P–P) within the phosphazene framework are of a similar magnitude to those observed for other (amino)cyclophosphazenes. The magnitude of ^2J(P–P) across the phosph*azane* bridge is significantly less (particularly for the compound with a benzyl group attached to the bridge nitrogen atom), but still somewhat higher than might be anticipated from PN̲P couplings for amino derivatives of bis(dichlorophosphino)amines.[251]

(38)
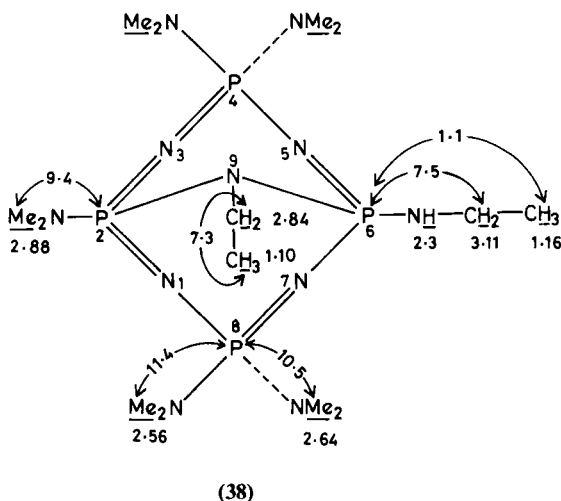
The proton NMR spectrum of $N_4P_4(NMe_2)_5(NHEt)(NEt)$(38) shows the characteristic features associated with this class of bicyclic P–N ring compounds. The methyl protons of the NMe_2 group attached to the junction phosphorus atom P(2) are deshielded compared with those of the NMe_2 groups attached to P(4) and P(8). Similarly, the shifts of the NCH_2CH_3 protons at P(6) are to high frequency of those of the NCH_2CH_3 protons at the bridgehead.[247] The assignment of the latter is straightforward, as this NCH_2 multiplet is more complex owing to major couplings to two phosphorus nuclei. The two NMe_2 groups at both P(4) and P(8) are nonequivalent: the lower-frequency NMe_2 doublet has been assigned to the dimethylamino protons *cis* to the bridge nitrogen atoms. Supporting evidence for this assertion stems from the changes observed in the spectrum on the addition of the shift reagent $Eu(fod)_3$. Thus, if it is assumed that the bridge N atoms coordinates to the shift reagent then the NMe_2 protons which are most shifted and broadened should be those in closest proximity to the europium ion.[247] The assignments (270 or 400 MHz spectrum) are depicted on the structural diagram (38), and are more accurate than those reported previously.[247]

MeNH NHMe
2.48 2.52
P 4
N N
N
MeHN—P 2 6 P—NHMe
2.61 Me
2.63
N 8 N
P
MeHN NHMe

(39a)

MeHN NHMe
2.52 2.56
P 4
N N
H
N+
MeHN—P 2 6 P—NHMe
2.67 Me
2.78
N 8 N
P Cl⁻
Me NH NHMe

(39b)

2.65 δ 2.45   2.80 δ 2.50
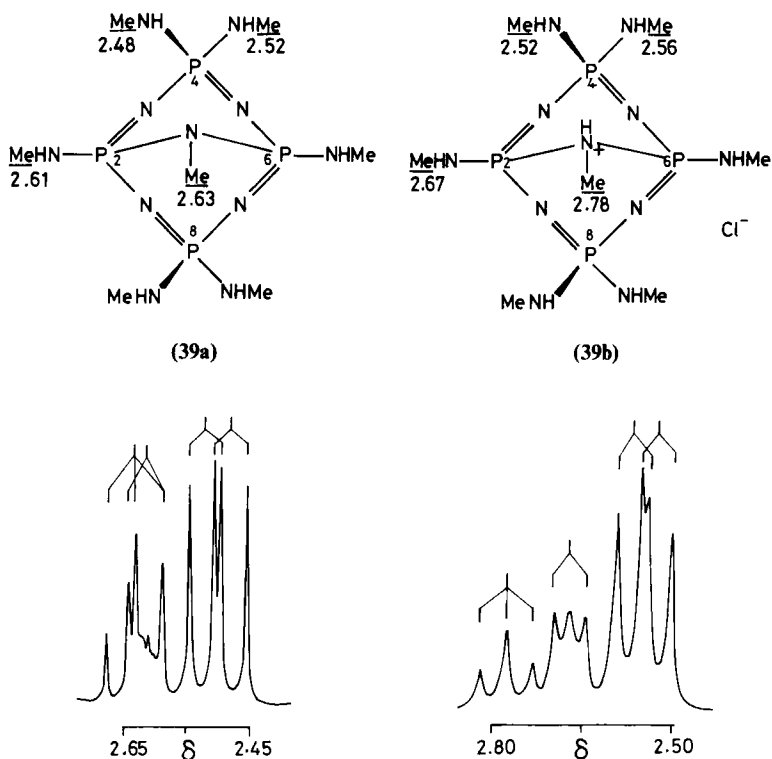
FIG. 12. The ^{1}H NMR (270 MHz, D$_2$O, Reference Standard TSP) of the bicyclic derivative N$_4$P$_4$(NHMe)$_6$(NMe) [39a] and its hydrochloride adduct [39b]. (Reproduced from ref. 248 with permission of the Royal Society of Chemistry, London.)

The 270 MHz NMR spectrum of the methylamino derivative (39a) or its hydrogen-chloride adduct (39b) contains a triplet and three doublets (Fig. 12). The assignments shown are analogous to those discussed above. The considerable deshielding of the N-methyl protons at the bridge for the hydrogen-chloride adduct (39b) relative to those of the base (39a) provide strong evidence for protonation at the bridge N atom rather than at other ring N atoms.[248]

B. Bi(cyclotriphosphazenes)

The methyl region of the ^{1}H NMR spectra of bi(cyclotriphosphazenes) [N$_3$P$_3$X$_4$R]$_2$ (40, X = Cl, Ph or OPh; R = Me)[105,252,253] with a direct P–P bond or those connected by an intervening oxygen atom (41, R = R′

= Me)[254] can be treated as the X-part of an $[AB_2X_3]_2$ or $[AM_2X_3]_2$ spin system:
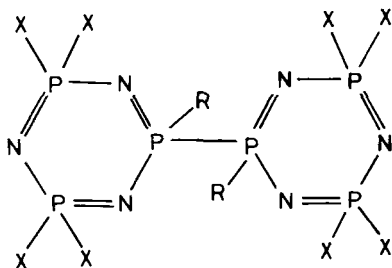
(40)
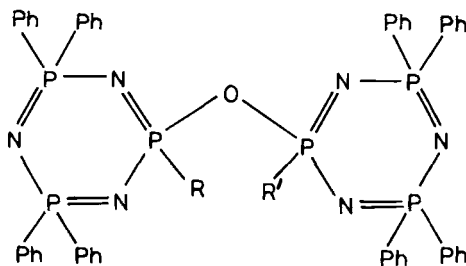
(41)

Since $J_{BX'(MX')}$, which is equal to $J(P-N-P-P-C-H)$ or $J(P-N-P-O-P-C-H)$, is negligible, the spin system can be approximated as $M_2[AX_3]_2$. The spectra of (40, R = Me, X = Cl) and (41, R = R' = Me) are illustrated in Fig. 13. The "deceptively simple" X-region of the $[AX_3]_2$ part is split into a triplet by the M-part of the spin system. The coupling $J_{MX} = {}^4J(P-N-P-C-H)$, can be read from the spectra directly, and has a value of 2.7 and 1.3 Hz for compounds (40, R = Me, X = Cl) and (41, R, R' = Me) respectively. The value of N that equals $|J_{AX} + J_{A'X}| = |J(P-C-H) + J(P-P-C-H)|$ or $|J(P-C-H) + J(P-O-P-C-H)|$ can also be found from the spectrum readily. Assuming the value of J_{AX} ($J(P-C-H)$) from the values for related compounds, one can calculate $J_{AX'}$, and from this L, which equals $|J_{AX} - J_{AX'}|$, can be obtained. From the value of L and the observed line width $\Delta v_{1/2}(2.1\ Hz)$ of the innermost line, an upper limit for J_{PP} (164 Hz for (40, R = Me, X = Cl)) can be ascertained. For other bi(cyclotriphosphazenes) of type (40) similar analyses of the respective ${}^1H$ and ${}^{31}P$ spectra (see below) yield values of $J(P-P)$ in the range 100–200 Hz.[253] In the spectrum of (41, R = R' = Me) the inner line splitting $S_i(1)$,[255] is visible (4.4 Hz), and from the observed weak outer lines $J_{AA'}$ can be evaluated. Hence all the couplings can be readily calculated for (41, R = R' = Me)[254] (Table A.22).

(a)

5.0 Hz

1.95   1.85

ppm

(b)

N

$J_{AA'}$ S_i (1)
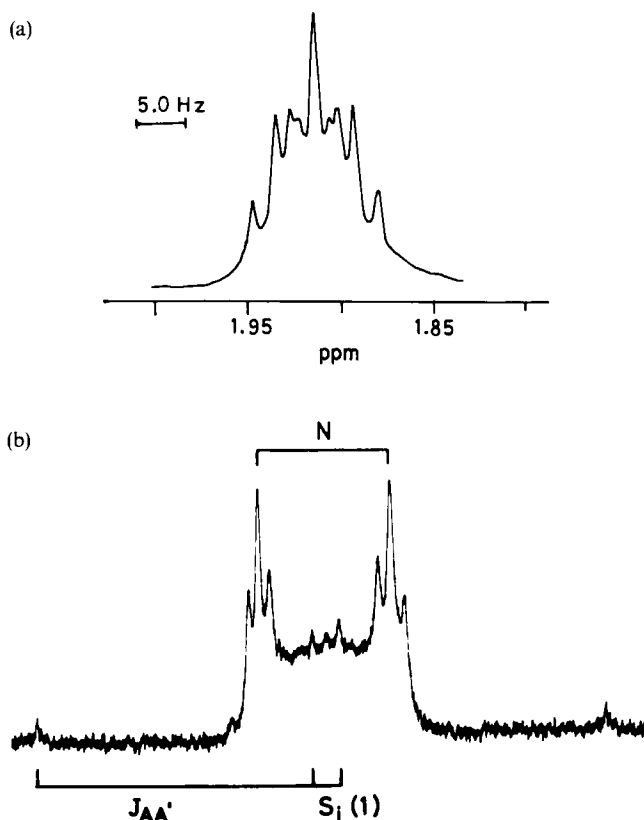
FIG. 13. The ^{1}H NMR spectra of (a) the bi(cyclotriphosphazene) (**40**, R = Me, X = Cl) and (b) (**41**, R = R' = Me). (a) Reprinted with permission from *J. Am. Chem. Soc.*, **104**, 2482, Copyright 1982 American Chemical Society. (b) Reprinted from *Z. Naturforsch.* **31b**, 1466 (1976) with permission of Verlag der Zeitschrift für Naturforschung, Tübingen, Federal Republic of Germany.)

The proton-decoupled ^{31}P NMR spectra of bi(cyclotriphosphazenes) (**40**, **41**) can be interpreted as an $[M_2A]_2$ spin system. The exact value of $J_{AA'}$ could not be determined for (**40**) because of the "deceptive simplicity" of the spectrum and the failure to observe the outer lines. Only an average value of $J_{AM} + J_{AM'} = J$ (P–N–P) + J(P–P–N–P) can be found from the spectra. By making assumptions for the value of J(P–N–P) and from the line width of the innermost line, a lower limit for J(P–P) can be obtained.[253] The ^{31}P data for compounds of the type (**40**) are summarized in Table A.21.

The ^{31}P–{^{1}H} NMR spectrum of (**41**, R = R' = Ph) has been analysed

by computer simulation,[111] and the values of ^2J(P–O–P) and ^4J(P–O–P–N–P) determined (Table A.22).

For the unsymmetrically substituted derivative (**41**, R = OPh, R' = Me) the ^{31}P–$\{^1$H$\}$ NMR spectrum (M_2ABN_2 spin system) is well resolved, and ^2J(P–N–P) within each ring is different. The value for the methyl-substituted cyclotriphosphazene ring (7.3 Hz) is close to that found for *gem*-$N_3P_3Ph_4$-(Me)(OMe) (7.4 Hz). The value of ^2J(P–O–P) (28.7 Hz) is *ca.* 6 Hz less than that for the symmetrically substituted compound (**41**, R = R' = Me).[254] The unsymmetrical derivative (**40**, X = OPh, R = Me, Bu^n) provides another example of a $M_2ABN_2X_3$ spin system, and in this case the J(P–P) value is estimated as > 168 Hz.[253]

The bicyclotriphosphazene (**42a**) is the first example of a triphosphini-dimine. The central phosphorus atom of the –N=P–P–P=N–unit has a δ(P) of -63.0 ppm, with ^1J(P–P) = 215 Hz. A related bi(cyclotriphosphazene) cation (**42b**) contains the HN–P–P–P–NH arrangement.[256] Data for both compounds are given in Table A.22.

(42a)   (42b)
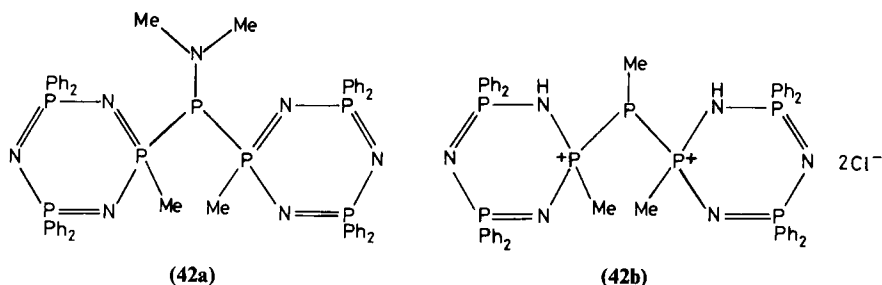
Some ^{31}P NMR parameters have been reported recently for two bi(cyclotetraphosphazenes) (**43**, R = Me, Et), but a complete analysis of the spectrum requires computer simulation:[257]

(43)
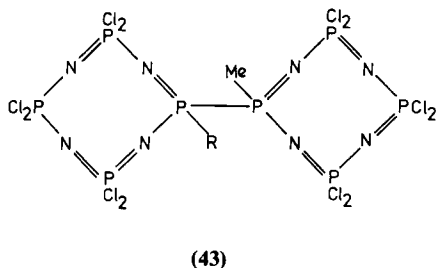
C. Other bicyclic and polycyclic systems

^{31}P NMR data have been reported for spirobi(cyclotriphosphazenes) (e.g. (**44**, **45**)) and related species (**46–48**).[258-263] The low-frequency shift of $\delta(P_{spiro})$ (Table 12) is characteristic of PN_4 compounds.[107]
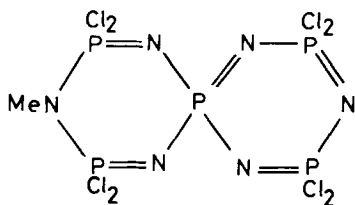
(44)
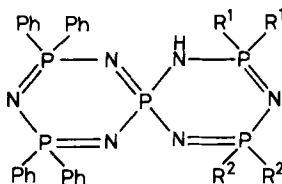
(45)
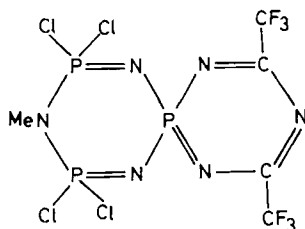
(46)
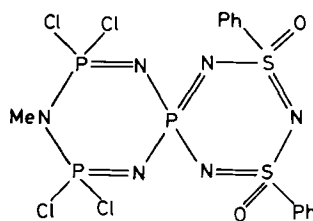
(47)
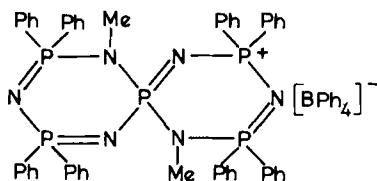
(48)

The ^{31}P NMR spectrum of the condensed tricyclic phosphazene $N_7P_6Cl_9$ (**49**) consists of peaks of equal intensity at $\delta 20.2$ (PCl$_2$) and -3.5 (PClN). In its reaction with dimethylamine, one of the central bonds is broken and two of the bridgehead chlorine atoms remain unsubstituted. The ^{31}P NMR spectrum of the product (**50**) consists of a triplet at $\delta 13.7$ and broad singlets at $\delta 3.7$ and -1.9 (ratio 1:2:3), corresponding to P(1), P(2, 6) and P(3, 4, 5). The ^{1}H NMR spectrum shows four doublets at $\delta 2.55$ (J(P–H) = 12.7 Hz) 2.58 (10.7), 2.61 (10.7) and 2.63 (10.7) in the ratio 2:3:2:1, and δ(N$\underline{H}$) 6.15. A complete assignment of these shifts is difficult.[264]

TABLE 12

^{31}P NMR data for spirobi(cyclotriphosphazenes) and related compounds.

Compound	δ(P)	^2J(P–P) (Hz)	Ref.
(44)	20.1, 6.1, -15.8^a	60	258
(45) (a) $R^1 = R^2 = Ph$	18.5, -7.5^a	11.8	260
(b) $R^1 = Ph$, $R^2 = Me^b$	38.1^c, 19.1, 18.0, -7.0^a	—	261
(c) $R^1 = R^2 = Me^d$	32.4^c, 15.2, -5.7^a	15.4^e	261
$Na^+[N_6P_5Ph_8]^{-f}$	13.2, -2.3^a		261
(46)	6.5, 3.9^a	23	262
(47)^g	9.6, -16.8^a	38.6	263
(48)	35.0 (A)	4.4 (AM)	
	19.4 (M)	16.9 (AX)	261
	-3.0 (X)^a	12.1 (MX)	

^{a}P(spiro); ^{b}MeOH solvent; ^{c}PMe$_2$; ^{d}C$_6$D$_5$NO$_2$ solvent; ^eJ[$\underline{P}$(spiro)–$\underline{P}$Ph$_2$]; ^{f}sodium salt of (45a), thf solvent; ^{g}MeCN solvent.


(49)

(50)
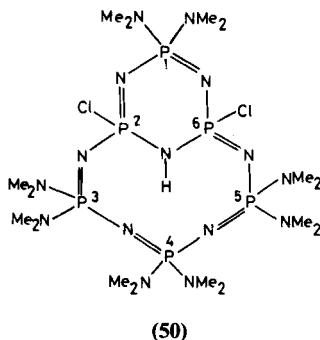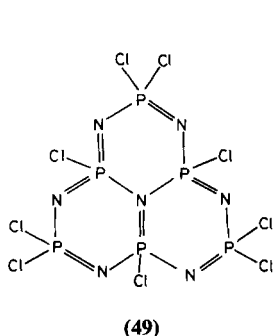
## V. METALLO CYCLOPHOSPHAZENES AND METAL COMPLEXES OF CYCLOPHOSPHAZENES

There has been a revival of interest since 1981 in the metal complexes of cyclophosphazenes, and a consequent increase in the availability of NMR data. Earlier work consists largely of isolated examples of complexes involving coordination through ring and/or exocyclic nitrogen atoms or of ionic species where the cyclophosphazene functions merely as a counter-ion.[13,216a] NMR studies are negligible, and structural assignments usually required X-ray crystallography.[13,265,266] The systematic studies of Allcock and coworkers[193-195,267-272] have extended the range of metallocyclophosphazenes available, and the diverse structural types encountered are repre-

sented by (**51–70**). The ^{31}P NMR data are summarized in Tables A.23 and A.24. A salient feature to emerge is the large high frequency shift observed when a phosphorus atom is attached directly to a transition metal (e.g. $N_3P_3Cl_4Fe_2(CO)_8$ (**53**), $\delta(\underline{P}Fe)$ 222.5).[271] This pronounced deshielding is partly a consequence of the constrained metal–phosphorus–metal bond angle (*ca.* 75°). High-frequency shifts for phosphorus bonded to metal are also characteristic of the spectra of metallocenofluorocyclophosphazenes containing iron and/or ruthenium[193,267,269] and of chromium, molybdenum- and tungsten-bonded chlorocyclophosphazenes.[194] Other metallocene derivatives of cyclophosphazenes contain carbon–phosphorus bonds (e.g. **58**, R′ = X = F or Cl; R = H).[193] The high-frequency shift observed for $\delta[PX(\text{ferrocenyl})]$ is again significant (X = F, $\delta44.3$; X = Cl, $\delta36.1$), albeit much less pronounced.

(51)

(52)

(53)

(54)

(55a)

(55b)

(56)

(57)
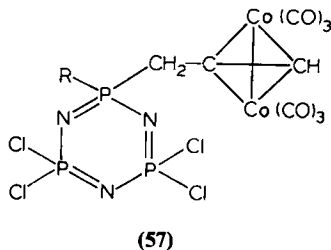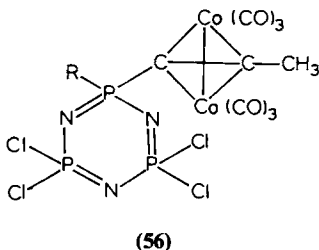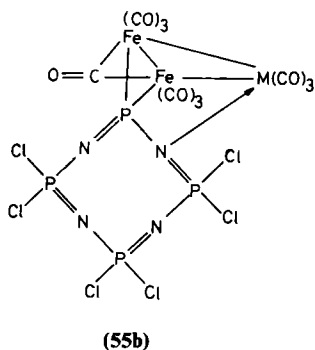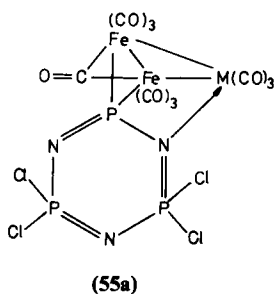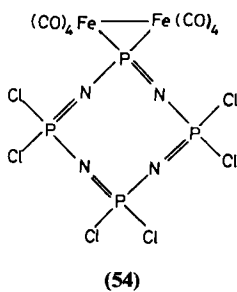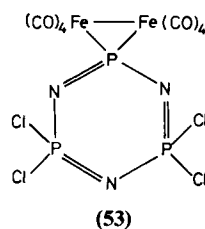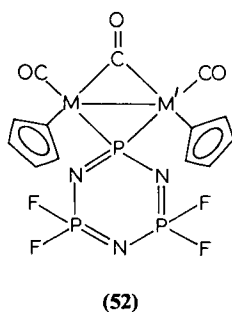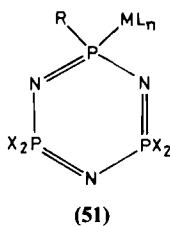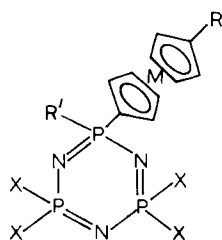
(58)
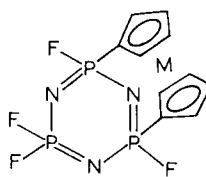
(59)
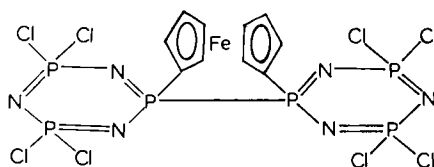
(60)
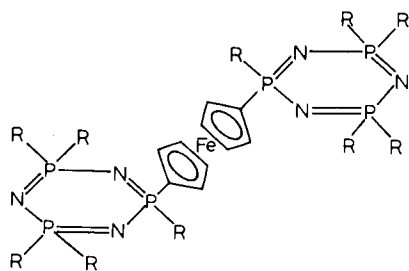
(61)
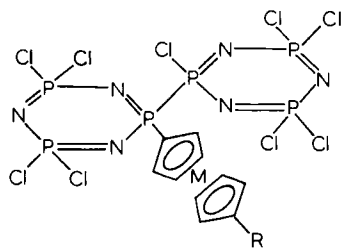
(62)
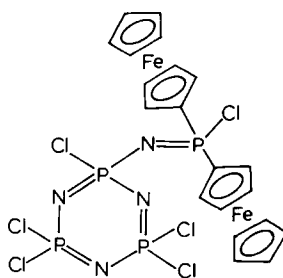
(63)
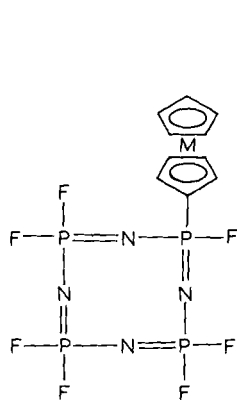
(64)
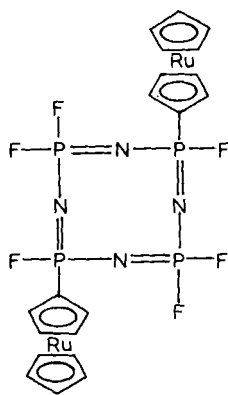
(65)
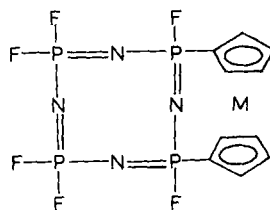
(66)
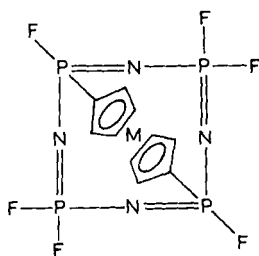
(67)
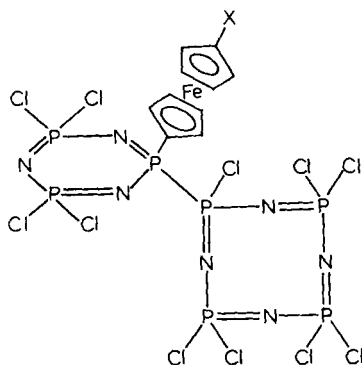
(68)
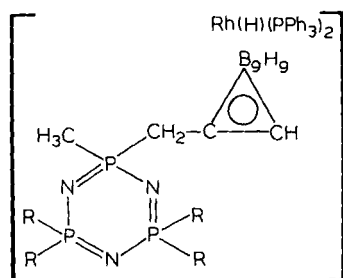
(69)
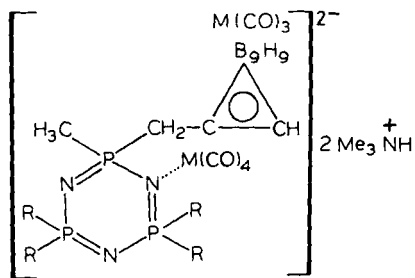
(70)

The ^{19}F NMR spectra of cyclophosphazenes in which phosphorus is directly bound to a transition-metal organometallic species show exceptionally high-frequency shifts and high ^1J(P–F) values for the fluorine at the PFM (M = metal) centre (e.g. $N_3P_3F_5Ru(CO)_2(\eta-C_5H_5)$ (51), (PFM) + 11.1, ^1J(P–F) = 1123 Hz).[269] Fluorine data are available for other metallocyclophosphazenes,[193] including those with metal–metal bonds.[267,269] Most values of δ(PF$_2$) (ca. -68 to -70) and δ(PFR) (ca. -45 to -50) are unexceptional. However, the latter shows pronounced low-frequency shift for trans-annular bridged derivatives $N_3P_3F_4(\eta-C_5H_4)_2M$ (59).[193] ^{19}F NMR data for 2,6-metallocenyl bridged cyclotetraphosphazene compounds $N_4P_4F_6(\eta-C_5H_4)_2M$ (67) have been reported; the fluorine nuclei of the PF$_2$ groups are nonequivalent (-67.4, -70.0δ for M = Ru).[193]

NMR data for P-coordinated metal complexes have been reported.[273,274] The (hydrido)cyclophosphazene $N_3P_3Ph_4Me(H)$ reacts with the nitrile complexes of PdCl$_2$ and PtCl$_2$ to give a product (71) in which the metal displaces the hydrogen at phosphorus towards the adjacent ring-nitrogen atom.

M = Pd , Pt
X = Cl , Br

(71)

a M = AuCl
b M = Me$_2$AuCl

(72)
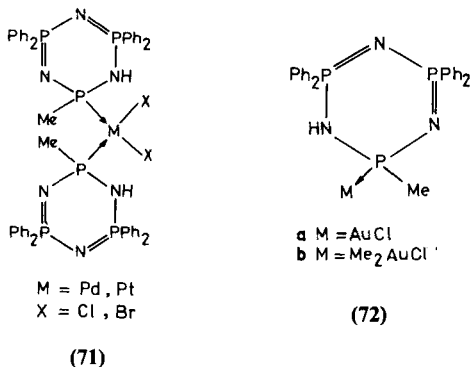
The ^{31}P NMR spectrum has the characteristic high-frequency shift of phosphorus directly bonded to a metal (Table A.23); the other phosphorus nuclei are anisochronous unless the exchange of the proton between equivalent nitrogen atoms becomes rapid (as in nitrobenzene solution), when they then appear equivalent at an averaged ^{31}P shift.[273] The gold complexes (72) behave similarly.[274] The ^{31}P–{^{1}H} NMR spectrum of $N_3HP_3Ph_4Me(AuCl)$ (72a) is temperature-dependent. At 30 °C an AX$_2$ pattern is observed, which changes to an AXY spin system at -80 °C (i.e. the two PPh$_2$ phosphorus nuclei becomes nonequivalent as the proton transfer between NH—P=N and N=P—NH becomes slower). The gold(III) complex $N_3HP_3Ph_4Me$ (Me$_2$AuCl) (72b) exhibit nonequivalence of PPh$_2$ groups at room temperature (AXY pattern), indicating that the prototropic shift is even slower in this case. The proton NMR spectrum shows two doublets at δ2.00 and 2.27 for MeAu groups, which provides evidence for a cis configuration at the metal centre. The

complimentary $^{13}\underline{C}H_3Au$ signals observed in the ^{13}C NMR spectrum have very different *cis*- and *trans*-^{13}C–Au–^{31}P coupling, $^2J = 4.9\,Hz$ (*cis*), $157.2\,Hz$ (*trans*).[274]

The ^{31}P NMR spectrum of the complex $N_3P_3Ph_4(Me_2Pz)_2 \cdot PdCl_2$ (73) is an ABX type with the two $\underline{P}Ph_2$ groups distinctly different:
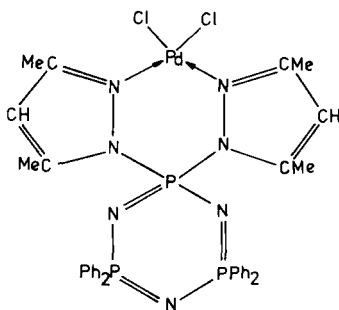
(73)

For the complex $N_3P_3Ph_2(Me_2Pz)_4 \cdot PdCl_2$ coordination could occur at two pyrazolyl groups on the same or on different P atoms. The ABX pattern ' observed in the ^{31}P spectrum excludes the second possibility. The coordination of the metal to phosphazene ring N atoms does not occur, presumably because of the considerable electron-withdrawing properties of this ligand.[275] The diamagnetic nickel-chloride complex $NiCl_2 \cdot 2[N_3P_3(NMe_2)_4$ $(HNCH_2CH_2NH)]$ also involves coordination through an exocyclic nitrogen (one N atom from each ethylenediamino moiety). The ^{31}P NMR spectra of the complex and of the free ligand are both of the AB_2 type. The ^{31}P shieldings increase on coordination, particularly so for P(spiro) (by $10\,ppm$).[276] A similar trend is discerned for the complexes of pyrazolyl cyclophosphazenes.[275]

The palladium-chloride complex of $N_6P_6Me_{12}$ is square-planar, and the phosphazene ligand forms six- and ten-membered chelate rings (74):[196]

M = Pd , Pt
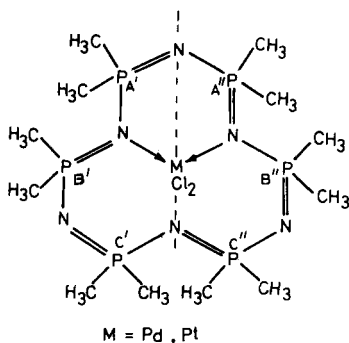
(74)

Five different ^{31}P resonances are observed from 6.74 to 29.06 ppm; three of them are considerably to high frequency of the resonance position of the uncoordinated ligand at 3.0δ.[344] The ^1H NMR spectrum shows six distinct Me environments from 1.59 to 2.78 ppm (Fig. 14), and assignments have been made by selective decoupling. The two methyl groups attached to a particular P atom are strongly differentiated, especially those nearest to the metal. Similar NMR data are obtained for the analogous platinum complex $N_6P_6Me_{12}\cdot PtCl_2$.[196]
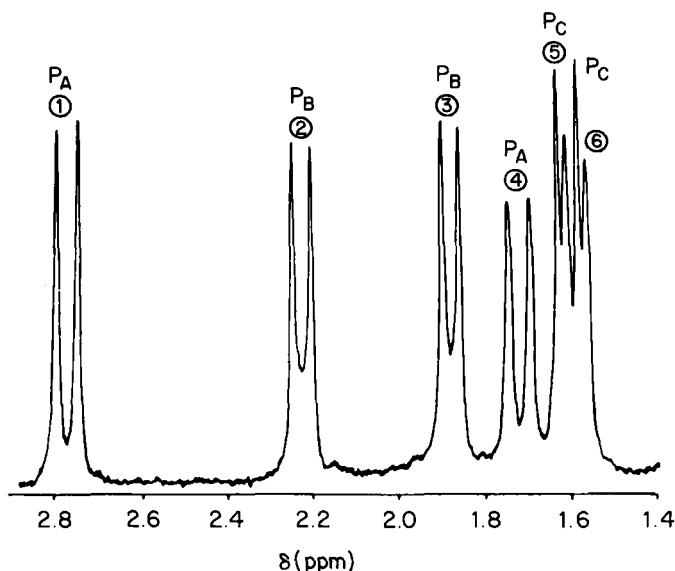
FIG. 14. The ^1H NMR (270 MHz, $CDCl_3$) of the palladium complex $PdCl_2\cdot N_6P_6Me_{12}$ [74]. (Reproduced from ref. 196 with permission of the National Research Council of Canada, Ottawa.)

   The coordination of organometallic units to phosphine donors linked to the cyclic P–N skeleton by aryloxy spacer groups has been reported.[270] Their ^{31}P NMR spectra resemble those of analogous (triphenylphosphine)metal complexes. The δ value of the PPh$_2$ group for the free ligand (-6 to -8) undergoes a high-frequency shift upon complexation (-3 to $+93\delta$), whereas the chemical shift of the phosphorus nuclei of the cyclophosphazene ring is hardly affected (8–9δ). A variable-temperature study of the rhodium complex $N_3P_3(OC_6H_4PPh_2)_6[RhCl(CO)]$ (**75a, b**) provides evidence for a facile exchange among the rhodium bound and uncoordinated phosphine units.[270]
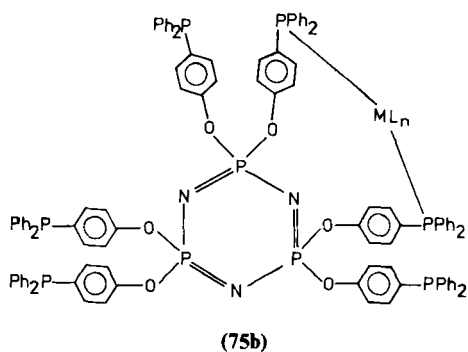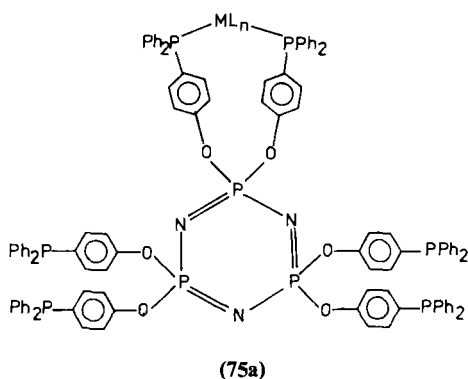
(75a)

(75b)

ACKNOWLEDGMENTS

APPENDIX: TABLES OF NMR DATA

There are 24 tables here that list ^{31}P NMR data for cyclophosphazenes. All values are quoted with reference to aqueous 85% phosphoric acid (external standard). The substituent-group categories appear in the following order:[8,9]

 halogeno, hydrido or pseudohalogeno;
 alkyl/aryl;
 amino;
 alkoxy/aryloxy;
 thioalkyl/thioaryl.

Phosphazenyl cyclotriphosphazenes, spirocyclotriphosphazenes, carboranyl derivatives, oxophosphazadienes and their salts, metal complexes of cyclophosphazenes and (metallo)cyclophosphazenes are listed in separate tables.

^{19}F NMR data for cyclotriphosphazenes and cyclotetraphosphazenes are given in Tables A.25 and A.26; ^{15}N data are in Tables A.27 and A.28.

When there is more than one set of values for a compound, we have chosen the one from the most recent measurements or that which we regard as the most reasonable. No mention is made of the solvent if it is $CDCl_3$, CD_2Cl_2 or C_6D_6 or their ^{1}H analogues; only other less-common solvents (e.g. thf, D_2O, dioxane) are specified in the tables. [31]P chemical shifts are quoted to the first decimal place, except where the measurements have been made at very high field strength (162 MHz) and when distinction between closely spaced values (for isomers) is required.

TABLE A.1

^{31}P NMR data for halogeno- and pseudohalogenocyclotriphosphazenes.

Compound	$\delta(PX_2)$	$\delta(PXY)$	$\delta(PY_2)$	$^2J(P-P)$ (Hz)	Refs.
$N_3P_3F_6$			13.9		113
$N_3P_3Br_3F_3$ [a]		$2.64(2)$ [b]		87.2	104
		$3.31(1)$		77.0 [c]	
$N_3P_3Cl_4F_2$ [d]	26.7	18.5		81.6 [c]	104
				100.2	
$N_3P_3Cl_4F_2$ [e]	26.4	18.4		83.0 [c]	104
				97.6	
$N_3P_3Cl_5F$	22.8	14.5		79.0	116, 168
$N_3P_3Cl_6$	19.3				55
$N_3P_3Cl_5Br$	17.7	-7.8			109
$nongem$-$N_3P_3Cl_4Br_2$	16.1	-8.7			109
$nongem$-$N_3P_3Cl_3Br_3$		-9.8			277
gem-$N_3P_3Cl_3Br_3$	14.0	-10.0	-39.8		109
$nongem$-$N_3P_3Cl_2Br_4$		-12.1	-41.3		109
$N_3P_3ClBr_5$		-14.0	-42.5		109
$N_3P_3Br_6$			-45.4		109
$N_3P_3(N_3)_6$			11.4		278
gem-$N_3P_3Cl_4(NCS)_2$	22.0		-31.5	72.9	89
$N_3P_3(NCS)_6$			-30		279

[a] 2,4,6:2-*trans*-4,6 structure; [b] relative intensities in parentheses; [c] coupling involving the unique phosphorus; [d] 2,4,6,6:2-*cis*-4 structure; [e] 2,4,6,6:2-*trans*-4 structure.

TABLE A.2

^{31}P NMR data for alkyl(aryl)cyclotriphosphazenes.

Compound	$\delta(PX_2)$	$\delta(PXR)$	$\delta(PR_2)$	$^2J(P-P)$ (Hz)	Refs.
$N_3P_3F_5Me$	8.1	46.2			174
gem-$N_3P_3F_4Me_2$	8.0		41.3	45.0	175
trans-$N_3P_3Me_3[CH_2C(O)Ph]_3$			12.4(1)[a]		280
			13.0(2)		
cis-$N_3P_3Me_3(CH_2Br)_3$			24.1		280
trans-$N_3P_3Me_3(CH_2Br)_3$			25.2		280
$N_3P_3Me_5H$		6.5	28.0		60
$N_3P_3Me_6$			31.7[b]		240
			25.9		156, 280
$[N_3P_3Me_6H]^+I^{-\,b}$			35.7		240
			48.1[c]		
$[N_3P_3Me_6H]^+[SnMe_2Cl_3]^{-\,d}$			31.7	10.0	156
			36.4[c]		
$[N_3P_3Me_6H]^+[SnMe_2Br_3]^{-\,d}$			31.4	10.0	156
			35.8[c]		
$N_3P_3F_5Bu^n$	9.5	50.2		63.4	115
gem-$N_3P_3F_4(Bu^n)_2$	9.8		48.3	35.4	115
$N_3P_3F_5Bu^t$	9.1	56.5			115
trans-$N_3P_3F_4(Bu^t)_2$	9.6	56.2		51.3	115
trans-$N_3P_3F_3(Bu^t)_3$		33.2(1)[a]			115
		31.1(2)			
$N_3P_3F_5(C_4H_3NMe)^e$	6.9	23.8		90.0	197
$N_3P_3F_5(CH{=}CH_2)$	9.6	9.8			174
$N_3P_3(CH_2CH_2Me)_6$			29.8		188
$N_3P_3(CH_2CH_2CF_3)_6$			28.8		188
gem-$N_3P_3F_4Ph_2$	12.1		30.4	86.0	113

cis-N$_3$P$_3$F$_4$Ph$_2$	12.4	38.4		58.0	112
trans-N$_3$P$_3$F$_4$Ph$_2$	10.8	38.3		65.0	112
gem-N$_3$P$_3$F$_3$Ph$_3$	8.6	31.2	27.3	25.0, 44.0, 57.0	113
gem-N$_3$P$_3$F$_2$Ph$_4$	6.2		27.3	32.9	113
N$_3$P$_3$Ph$_6$			15.2		34
N$_3$P$_3$Ph$_6$·HCl			21.9		347
N$_3$P$_3$Cl$_5$(Me)	21.3	39.2		7.8	67
[N$_3$P$_3$Cl$_4$Me]$^-$Li$^+$	2.9	97.1		93.0	69
N$_3$P$_3$Cl$_4$(Me)$_2$	18.0		35.7	8.9	68
gem-N$_3$P$_3$Cl$_4$Br(Me)	21.1	21.4		2.0	67
gem-N$_3$P$_3$Cl$_4$I(Me)	21.0	−16.3			67
gem-N$_3$P$_3$Cl$_4$(H)(Me)^f	17.6	24.4		12.0	61
gem-N$_3$P$_3$Cl$_4$(D)(Me)	18.6	11.4		12.0	61
gem-N$_3$P$_3$Cl$_4$(Me)(Et)	18.3		41.8	<2	68
gem-N$_3$P$_3$Cl$_4$(Me)(Pr^n)	18.2		39.6	2.8	68
gem-N$_3$P$_3$Cl$_4$(Me)(Pr^i)	17.9		46.1	<2	68
gem-N$_3$P$_3$Cl$_4$(Me)(Bu^n)	18.0		39.9	2.1	68
gem-N$_3$P$_3$Cl$_4$(Me)(Bu^i)	17.7		38.3	<2	68
gem-N$_3$P$_3$Cl$_4$(Me)(Bu^t)	18.1		50.4	<2	68
gem-N$_3$P$_3$Cl$_4$(Me)(CH$_2$CH=CH$_2$)	18.5		36.9	<2	68
gem-N$_3$P$_3$Cl$_4$(Me)(CH$_2$COMe)	19.2		31.4	9.7	281(a)
gem-N$_3$P$_3$Cl$_4$(Me)(CH$_2$COPh)	19.3		32.4	9.7	281(a)
gem-N$_3$P$_3$Cl$_4$(Me)[CH$_2$C(OMe)=CH$_2$]	18.3		37.4	4.1	281(a)
gem-N$_3$P$_3$Cl$_4$(Me)[CH=C(OMe)Me]	18.1		27.0	12.2	281(a)
gem-N$_3$P$_3$Cl$_4$(CH$_2$C≡CH)	19.4		34.3	6.0	69
gem-N$_3$P$_3$Cl$_4$(Me)(CH=C=CH$_2$)	18.6		25.9	9.0	69
gem-N$_3$P$_3$Cl$_4$(Me)(C≡CMe)	18.8		2.5	14.0	69
gem-N$_3$P$_3$Cl$_4$(Me)(CH$_2$C≡CMe)	19.4		36.3	<2	69
gem-N$_3$P$_3$Cl$_4$(Me)(CH$_2$C$_6$HPh$_4$)	18.9		38.4	—	195
gem-N$_3$P$_3$Cl$_4$(Me)(CH$_2$C$_6$H$_3$Ph$_2$)	18.8		38.0	—	195
gem-N$_3$P$_3$Cl$_4$(Me)(CH$_2$C$_6$H$_3$Ph$_2$)	19.0		37.7	—	195
gem-N$_3$P$_3$Cl$_4$(Me)(Ph)	18.6		29.0	11.0	62, 70
gem-N$_3$P$_3$Cl$_4$(Me)(C$_6$H$_2$MePh$_2$)	16.9		27.5	8.0	195

Compound	$\delta(PX_2)$	$\delta(PXR)$	$\delta(PR_2)$	$^2J(P\text{--}P)$ (Hz)	Refs.
gem-$N_3P_3Cl_4(Me)(C_6H_2Ph_3)$	15.7		27.9	10.8	195
gem-$N_3P_3Cl_4(Me)(C_6MePh_4)$	18.9		37.0		195
gem-$N_3P_3Cl_4(Me)(C_6H_4Cl\text{-}p)$	19.0		28.3	11.0	70
gem-$N_3P_3Cl_4(Me)(C_6H_4F\text{-}p)$	18.7		28.4	10.3	70
gem-$N_3P_3Cl_4(Me)(C_6H_4Me\text{-}p)$	18.7		29.4	9.8	70
gem-$N_3P_3Cl_4(Me)[C_6H_4(OMe)\text{-}p)$	18.6		29.3	8.8	70
gem-$N_3P_3Cl_4(Me)[C_6H_4(CF_3)\text{-}p]$	19.1		27.7	11.7	70
gem-$N_3P_3Cl_4(Me)[C_6H_4(NMe_2)\text{-}p]$	18.3		30.0	8.8	70
gem-$N_3P_3Cl_4(Me)[C_6H_4(NEt_2)\text{-}p]$	18.2		30.0	9.7	70
gem-$N_3P_3Cl_4(Me)[C_6H_4Bu^t\text{-}p]$	18.3		29.2	9.8	70
gem-$N_3P_3Cl_4(Me)(C_6H_4Ph\text{-}p)$	18.8		29.1	10.3	70
gem-$N_3P_3Cl_4(Me)[C_6H_4(NMe_2)\text{-}m]$	18.1		30.6	7.3	70
gem-$N_3P_3Cl_4(Me)[C_6H_4(OMe)\text{-}m]$	18.5		29.4	9.8	70
gem-$N_3P_3Cl_4(Me(C_6H_4F\text{-}m)$	18.7		27.7	11.7	70
gem-$N_3P_3Cl_2Me_4$	16.6		31.6	3.6	281(b)
$N_3P_3Cl_5(Et)$	21.7	46.0		2.0	67
gem-$N_3P_3Cl_4(Et)_2$	19.2		48.1	<2	68
gem-$N_3P_3Cl_4(Br)(Et)$	21.6	34.8		2.0	67
gem-$N_3P_3Cl_4I(Et)$	21.3	0.7		9.8	67
gem-$N_3P_3Cl_4H(Et)^f$	18.4	20.4		8.0	61
gem-$N_3P_3Cl_4(Et)(Pr^n)$	18.7		45.8	<2	68
gem-$N_3P_3Cl_4(Et)(Pr^i)$	18.8		52.5	3.7	68
gem-$N_3P_3Cl_4(Et)(Bu^n)$	18.7		46.3	<2	68
gem-$N_3P_3Cl_4(Et)(Bu^i)$	18.3		44.7	<2	68
gem-$N_3P_3Cl_4(Et)(Bu^t)$	18.6		56.8	7.0	68
gem-$N_3P_3Cl_4(Et)(CH_2CH{=}CH_2)$	18.5		36.9	<2	68
gem-$N_3P_3Cl_4(Et)(CH_2C{\equiv}CH)$	20.5		40.3	<2	69

gem-$N_3P_3Cl_4(Et)(CH{=}C{=}CH_2)$	19.5		31.6	<2	69
gem-$N_3P_3Cl_4(Et)(C{\equiv}CMe)$	19.9		9.9	14.0	69
gem-$N_3P_3Cl_4(Et)(Ph)$	18.9		35.4	4.0	62, 70
gem-$N_3P_3Cl_5(Pr^n)$	21.3	43.7		2.0	67
gem-$N_3P_3Cl_4(Pr^n)_2$	18.5		43.6	<2	68
gem-$N_3P_3Cl_4(Br)(Pr^n)$	21.7	32.4		2.8	67
gem-$N_3P_3Cl_4I(Pr^n)$	21.0	−2.9		9.7	67
gem-$N_3P_3Cl_4H(Pr^n)^f$	19.0	17.1		8.0	61
gem-$N_3P_3Cl_4(Pr^n)(Pr^i)$	18.6		50.3	3.8	68
gem-$N_3P_3Cl_4(Pr^n)(Bu^n)$	18.5		44.1	<2	68
gem-$N_3P_3Cl_4(Pr^n)(Bu^i)$	18.0		42.4	<2	68
gem-$N_3P_3Cl_4(Pr^n)(Bu^t)$	18.2		54.3	7.2	68
gem-$N_2P_3Cl_4(Pr^n)(CH_2CH{=}CH_2)$	18.9		40.9	<2	68
gem-$N_3P_3Cl_4(Pr^n)(CH_2C{\equiv}CH)$	19.9		37.9	<2	69
gem-$N_3P_3Cl_4(Pr^n)(CH{=}C{=}CH_2)$	18.9		29.2	<2	69
gem-$N_3P_3Cl_4(Pr^n)(C{\equiv}CMe)$	19.0		7.0	14.0	69
gem-$N_3P_3Cl_4(Pr^n)(Ph)$	18.7		32.5	4.2	62, 70
$N_3P_3Cl_5(Pr^i)$	21.7	51.8		2.0	67
$N_3P_3Cl_4(Pr^i)_2$	18.8		56.6	7.4	62
$N_3P_3Cl_4Br(Pr^i)$	21.6	43.6		9.5	67
$N_3P_3Cl_4I(Pr^i)$	21.3	16.3		15.5	67
gem-$N_3P_3Cl_4H(Pr^i)^f$	18.4	26.5		8.0	61
gem-$N_3P_3Cl_4(Pr^i)(CH_2CH{=}CH_2)$	18.9		47.6	5.5	68
gem-$N_3P_3Cl_4(Pr^i)(CH_2C{\equiv}CH)$	20.1		44.5	<2	69, 195
gem-$N_3P_3Cl_4(Pr^i)(CH{=}C{=}CH_2)$	19.0		35.9	<2	69
gem-$N_3P_3Cl_4(Pr^i)(C{\equiv}CMe)$	19.2		14.7	9.2	69
gem-$N_3P_3Cl_4(Pr^i)(Ph)$	18.6		38.0	<2	62
gem-$N_3P_3Cl_4(Pr^i)(CH_2C_6HPh_4)$	19.4		49.8		195
gem-$N_3P_3Cl_4(Pr^i)(C_6MePh_4)$	15.6		40.3		195
$N_3P_3Cl_5(Bu^n)$	21.4	44.2		2.0	67
gem-$N_3P_3Cl_4(Bu^n)_2$	18.4		44.5	<2	68
$N_3P_3Cl_4Br(Bu^n)$	21.5	32.7		2.0	67
$N_3P_3Cl_4I(Bu^n)$	21.0	−2.3		10.5	67

TABLE A.2 (cont.)

Compound	$\delta(PX_2)$	$\delta(PXR)$	$\delta(PR_2)$	$^2J(P-P)$ (Hz)	Refs.
gem-$N_3P_3Cl_4H(Bu^n)^f$	19.4	17.9		4.0	61
gem-$N_3P_3Cl_4(Bu^n)(Pr^i)$	19.0		51.1	4.3	68
gem-$N_3P_3Cl_4(Bu^n)(Bu^i)$	17.9		42.9	<2	68
gem-$N_3P_3Cl_4(Bu^n)(Bu^t)$	18.2		54.2	7.2	68
gem-$N_3P_3Cl_4(Bu^n)(CH_2CH{=}CH_2)$	18.9		41.4	<2	68
gem-$N_3P_3Cl_4(Bu^n)(CH_2C{\equiv}CH)$	19.7		38.2	<2	69
gem-$N_3P_3Cl_4(Bu^n)(CH{=}C{=}CH_2)$	18.7		29.3	3.0	69
gem-$N_3P_3Cl_4(Bu^n)(C{\equiv}CMe)$	19.2		7.5	13.0	69
gem-$N_3P_3Cl_4(Bu^n)(Ph)$	18.8		33.0	4.0	62, 70
gem-$N_3P_3Cl_4(H)(Bu^i)^f$	19.0	15.7		6.0	61
gem-$N_3P_3Cl_4(Bu^i)(CH_2CH{=}CH_2)$	18.5		39.8	<2	68
gem-$N_3P_3Cl_4(Bu^i)(CH_2C{\equiv}CH)$	19.5		36.8	<2	69
gem-$N_3P_3Cl_4(Bu^i)(CH{=}C{=}CH_2)$	18.5		28.3	<2	69
gem-$N_3P_3Cl_4(Bu^i)(C{\equiv}CMe)$	19.2		6.4	13.0	69
$N_3P_3Cl_5(Bu^t)$	21.8	57.1		6.9	67
$N_3P_3Cl_4Br(Bu^t)$	21.7	51.4		15.0	67
$N_3P_3Cl_4I(Bu^t)$	20.3	26.0		20.8	67
gem-$N_3P_3Cl_4H(Bu^t)^f$	18.4	32.3		2.0	61
$N_3P_3Cl_4(Bu^t)(CH_2CH{=}CH_2)$	19.2		52.3	9.3	68
$N_3P_3Cl_4(Bu^t)(CH_2C{\equiv}CH)$	20.7		49.3	<2	69
$N_3P_3Cl_4(Bu^t)(CH{=}C{=}CH_2)$	18.9		39.8	<2	69
$N_3P_3Cl_4(Bu^t)(C{\equiv}CMe)$	19.7		20.9	6.0	69
gem-$N_3P_3Cl_4(CH_2CH{=}CH_2)_2$	19.3		37.8	2.3	68
gem-$N_3P_3Cl_4(CH_2CH{=}CH_2)(CH_2C{\equiv}CH)$	19.9		34.6	<2	69
gem-$N_3P_3Cl_4(CH_2CH{=}CH_2)(CH{=}C{=}CH)$	18.9		25.8	<2	69
gem-$N_3P_3Cl_4(CH_2CH{=}CH_2)(C{\equiv}CMe)$	19.2		3.7	15.0	69

gem-N$_3$P$_3$Cl$_4$(CH$_2$CH=CH$_2$)(Ph)	18.8		28.6	<2	62
N$_3$P$_3$Cl$_5$Ph	21.2	28.9		15.5	62
gem-N$_3$P$_3$Cl$_4$H(Ph)	18.2	6.9		10.3	62
gem-N$_3$P$_3$Cl$_4$(Ph)(BEt$_3$)$^-$Li$^+$	7.4		72.8	74.4	62
gem-N$_3$P$_3$Cl$_4$F(Ph)	22.4	23.8^g		34.1	62
gem-N$_3$P$_3$Cl$_4$Br(Ph)	21.1	15.3		8.6	62
gem-N$_3$P$_3$Cl$_4$I(Ph)	20.6	−23.9			62
gem-N$_3$P$_3$Cl$_4$Ph$_2$	17.1		19.5	12.1	55
trans-N$_3$P$_3$Cl$_3$Ph$_3$		30.2(2) 32.8(1)		5.4	55, 110
cis-N$_3$P$_3$Cl$_3$Ph$_3$		29.6			55, 110
gem-N$_3$P$_3$Cl$_2$Ph$_4$	14.8		17.1	9.3	55
trans-N$_3$P$_3$Cl$_2$Ph$_4$		28.5	19.0		34
cis-N$_3$P$_3$Cl$_2$Ph$_4$		30.2	19.0		34
N$_3$P$_3$ClPh$_5$		28.6	16.8	2.5	111
gem-N$_3$P$_3$ClPh$_4$(Me)		38.4	15.3		155
gem-N$_3$P$_3$BrPh$_4$(Me)		38.3	14.9		155
gem-N$_3$P$_3$HPh$_4$(Me)		6.9	12.9		155
gem-N$_3$P$_3$Ph$_4$Me$_2$			27.1^h 14.1		280
gem-N$_3$P$_3$Ph$_4$Me$_2$.HCl			39.6^h 18.8		282
gem-[N$_3$P$_3$Ph$_4$Me$_3$]$^+$I$^-$		48.5^h	31.0^c 18.8		60, 283
gem-N$_3$P$_3$Ph$_4$Me[CH$_2$(SnMe$_3$)]			13.0 31.5^i		280
gem-N$_3$P$_3$Ph$_4$Me[CH$_2$C(O)Ph]			14.0 24.8^i		280
gem-N$_3$P$_3$Ph$_4$Me(CH$_2$Br)			14.1 23.3^i		280
gem-N$_3$P$_3$Ph$_4$Me(CH$_2$COOH)			15.5 25.7^i		280

TABLE A.2 (cont.)

Compound	$\delta(PX_2)$	$\delta(PXR)$	$\delta(PR_2)$	$^2J(P-P)$ (Hz)	Refs.
[N$_3$P$_3$Ph$_4$Me(CH$_2$)]$_2$SiMe$_2$			12.9		280
			29.1[i]		
[N$_3$P$_3$Ph$_4$Me(CH$_2$)]$_2$		30.4[i]	13.3		280
gem-N$_3$P$_3$Ph$_4$Me[CH(OH)Ph]		30.8[i]	14.3		155
gem-N$_3$P$_3$Ph$_4$Me[CH(OH)C$_6$H$_4$Me-p]		30.2[i]	14.0		155
gem-N$_3$P$_3$Ph$_4$Me[CH(OH)C$_6$H$_4$Cl-p]		30.1[i]	13.9		155
gem-N$_3$P$_3$Ph$_4$Me[CH(OH)C$_6$H$_4$(NO$_2$)-p]		30.1[i]	13.8		155
N$_3$P$_3$Ph$_4$Me[CH(OH)C$_6$H$_4$(NO$_2$)-o]		30.0[i]	13.7		155
N$_3$P$_3$Ph$_4$Me[C(OH)Me$_2$]		35.4[i]	12.7		155
N$_3$P$_3$Ph$_4$Me[C(OH)Me(COMe)]		31.0[i]	13.3		155
N$_3$P$_3$Ph$_4$Me[C(OH)Ph(COPh)]		33.3[i]	14.2		155
N$_3$P$_3$Ph$_4$Me[C(S)NMHe]		18.1[i]	14.1		155
N$_3$P$_3$Ph$_4$Me[C(S)NHPh]		19.3[i]	14.4		155
N$_3$P$_3$Ph$_4$Me[CHPhCH$_2$NO$_2$]		38.1[i]	13.8		155
N$_3$P$_3$Ph$_4$Me[CHCO$_2$EtCH$_2$CO$_2$Et]		26.9[i]	13.8		155
gem-N$_3$P$_3$Ph$_4$Me(SiMe$_3$)		26.6[i]	9.9		66
gem-N$_3$P$_3$Ph$_4$Me(SnMe$_3$)		29.5[i]	11.0		66
gem-N$_3$P$_3$Ph$_4$Me(Me$_2$PNSO$_2$C$_6$H$_4$Me-p)[j]		24.4[i]	13.1		66
gem-N$_3$P$_3$Ph$_4$Me(PMe$_2$)[k]		40.2[i]	12.6		256
gem-N$_3$P$_3$Ph$_4$Me(PMe$_2$).HCl[l]		54.0[i]	18.7		256
gem-N$_3$P$_3$Ph$_4$Me[P(Me)Ph][m]		27.2[i]	10.4		256
gem-N$_3$P$_3$Ph$_4$Me[P(Me)Ph].HCl[n]		49.2[i]	18.8		256
gem-N$_3$P$_3$Ph$_4$Me(PPh$_2$)[o]		34.8[i]	11.8		256
gem-N$_3$P$_3$Ph$_4$Me(PPh$_2$).HCl[p]		45.0[i]	45.0		256
gem-N$_3$P$_3$Ph$_4$Me(Me$_2$PS)[q]		27.5[i]	13.5		66

gem-N₃P₃Ph₄Me(Et₂PS)ʳ		30.4[i]	13.4	66
gem-N₃P₃Ph₄EtH		12.5	15.5	60
cis-N₃P₃Br₃Ph₃		16.4		284
trans-N₃P₃Br₃Ph₃		20.1 (1)		284
		18.0 (2)		
N₉P₉Cl₁₂(Me)₃[C₆H₃(CH₂)₃](76, R = Me)ˢ	19.0		38.1	4.4	195
	18.6		37.5		
			36.0		
N₉P₉Cl₁₂(Prⁱ)₃[C₆H₃(CH₂)₃](76, R = Prⁱ)ˢ	19.3		49.8	4.5	195
	19.1		48.7	8.1	
	19.1		47.1	7.0	

^{a}Relative intensities in parentheses; ^{b}D$_2$O solvent; ^{c}$\underline{P}$R$_2$N$^+$; ^{d} $-30\,^\circ$C; ^{e}1-methylpyrrol-2-yl; ^{f}thf solvent; ^{g} ^{1}J(P–F) = 1003 Hz; ^{h}$\underline{P}$Me$_2$; ^{i}$\underline{P}$Me(R); ^{j}$\delta(\underline{P}_{exo})$ = 17.2; ^{k}$\delta(\underline{P}_{exo})$ = -62, ^{l}J(P–P) = 178 Hz; ^{l}$\delta(\underline{P}_{exo})$ = -50.5, ^{1}J(P–P) = 234 Hz; ^{m}$\delta(\underline{P}_{exo})$ = -42.5, ^{1}J(P–P) = 185 Hz; ^{n}$\delta(\underline{P}_{exo})$ = -35.1, ^{1}J(P–P) = 250 Hz; ^{o}$\delta(\underline{P}_{exo})$ = -16.1, ^{1}J(P–P) = 190 Hz; ^{p}$\delta(\underline{P}_{exo})$ = -14.6, ^{1}J(P–P) = 249 Hz; ^{q}$\delta(\underline{P}_{exo})$ = 26.9; ^{r}$\delta(\underline{P}_{exo})$ = 29.6; ^{s}(76) is
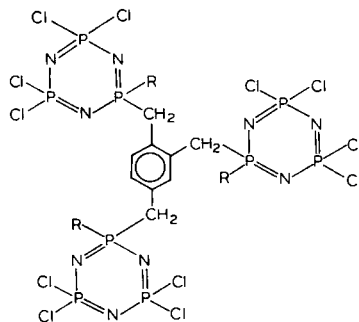
(76)

TABLE A.3

^{31}P NMR data for (amino)cyclotriphosphazenes.

Compound	$\delta(PX_2)$	$\delta(PXR)$	$\delta(PR_2)$	$^2J(P-P)$ (Hz)	Refs.
$N_3P_3F_5(NMe_2)$	10.3	24.2	—	100–200	160
gem-$N_3P_3F_4(NMe_2)_2$	14.0	—	29.2	100–105	160
cis-$N_3P_3F_4(NMe_2)_2$	8.4	23.7	—	101.0	78
$trans$-$N_3P_3F_4(NMe_2)_2$	8.0	23.6	—	102.8	78
$N_3P_3F_2Cl_2(NMe_2)_2$ (2-cis-4:6, 6:2, 4)	26.1	18.9	—	67.1[a], 70.5[b]	104
$N_3P_3F_2Cl_2(NMe_2)_2$ (2-$trans$-4: 6, 6:2, 4)	25.6	19.0	—	69.1[a], 75.8[b]	104
$N_3P_3F_2Cl_2(NMe_2)_2$ (2, 2:4-cis-6:4, 6)	4.6	31.9	—	82.3[c]	104
$N_3P_3F_2Cl_2(NMe_2)_2$ (2, 2:4-$trans$-6:4, 6)	3.6	31.3	—	82.0[c]	104
$N_3P_3Cl_5(NH_2)$	20.4	19.0	—	46.5	102
gem-$N_3P_3Cl_4(NH_2)_2$	18.3		9.0	48.5	102, 103
gem-$N_3P_3Cl_4[NHC(OMe)S]_2$[d]	24.3		−10.8		89
gem-$N_3P_3Cl_4[NHC(OEt)S]_2$[d]	24.0		−12.0		89
gem-$N_3P_3Cl_4(NHPOCl_2)_2$	15.6	—	−1.2		258
$N_3P_3(NH_2)_6$[e]			18.0		106, 285
$N_3P_3Cl_5(NHMe)$	21.7	21.0	—	47.3	25, 129
$N_3P_3Cl_5[N(Me)(SCCl_3)]$	21.5	23.5	—	52.1	129
gem-$N_3P_3Cl_4(NHMe)_2$	20.1	—	12.3	—	25
cis-$N_3P_3Cl_4(NHMe)_2$	21.6	21.6	—	—	25
$trans$-$N_3P_3Cl_4(NHMe)_2$	22.2	22.2	—	—	25
$N_3P_3(NHMe)_6$	—	—	23.0[e]		106, 286
$N_3P_3Cl_5(NHEt)$	20.3	18.7	—	43.0	55
cis-$N_3P_3Cl_4(NHEt)_2$	20.8	20.8	—	—	55
$N_3P_3(NHEt)_6$	—	—	18.0	—	55

$N_3P_3(NHCH_2CF_3)_6$	—	—	17.4	—	188
$N_3P_3Cl_5(NHCH_2COOEt)$	20.8	18.3		35.9	287
gem-$N_3P_3Cl_4(NHCH_2COOEt)_2$	21.6		10.0	47.4	287
gem-$N_3P_3Cl_2(NHCH_2COOEt)_4$	24.9		14.0	51.4	287
$N_3P_3(NHCH_2COOEt)_6{}^e$			18.9		106
$N_3P_3(NHCH_2CONHMe)_6{}^e$			20.3		106
$N_3P_3Cl_5(NHPr^i)$	20.4	17.0	—	46.5	50, 55
gem-$N_3P_3Cl_4(NHPr^i)_2$	19.8	—	6.2	45.5	50
cis-$N_3P_3Cl_4(NHPr^i)_2$	21.9	19.0	—	48.8	50
trans-$N_3P_3Cl_4(NHPr^i)_2$	21.3	19.1	—	48.8	50
gem-$N_3P_3Cl_2(NHPr^i)_4$	22.2	—	9.4	49.4	55
$N_3P_3(NHPr^i)_6$	—	—	12.6	—	55
$N_3P_3(NHBu^n)_6$	—	—	18.1^d	—	286
gem-$N_3P_3Cl_4(NHBu^t)_2$	17.5	—	0.7	44.7	55
gem-$N_3P_3Cl_2(NHBu^t)_4$	19.7	—	3.9	52.6	55
$N_3P_3[NH(CH_2)_3Si(OEt)_3]_6$			17.4		348
$N_3P_3Cl_5(NHC_6H_5)$	21.2	11.7	—	47.1	44
gem-$N_3P_3Cl_4(NHC_6H_5)_2$	20.5	—	-2.6	48.2	44
cis-$N_3P_3Cl_4(NHC_6H_5)_2$	22.3	13.7	—	49.4	44
trans-$N_3P_3Cl_4(NHC_6H_5)_2$	22.2	13.5	—	49.0	44
gem-$N_3P_3Cl_3(NHC_6H_5)_3{}^g$	23.0	14.2	-1.0	—	44
cis-$N_3P_3Cl_3(NHC_6H_5)_3$	—	15.5	—	—	44
trans-$N_3P_3Cl_3(NHC_6H_5)_3$	—	15.3	—	—	44
$N_3P_3Cl_5(NHCH_2C_6H_5)$	21.3	18.1	—	46.6	55
nongem-$N_3P_3Cl_4(NHCH_2C_6H_5)_2$	21.1	21.1	—	—	55
gem-$N_3P_3Cl_4(NHCH_2C_6H_5)_2$	21.0	—	9.4	44.4	55
$N_3P_3Cl_5(NHC_6H_4Me\text{-}p)$	21.6	12.2	—	48.2	44
gem-$N_3P_3Cl_4(NHC_6H_4Me\text{-}p)_2$	21.8	—	-1.6	48.5	44
cis-$N_3P_3Cl_4(NHC_6H_4Me\text{-}p)_2$	22.5	14.0	—	49.6	44
trans-$N_3P_3Cl_4(NHC_6H_4Me\text{-}p)_2$	22.3	13.9	—	49.6	44
gem-$N_3P_3Cl_3(NHC_6H_4Me\text{-}p)_3{}^g$	21.3	14.0	0.0	—	44
cis-$N_3P_3Cl_3(NHC_6H_4Me\text{-}p)_3$	—	15.9	—	—	44
trans-$N_3P_3Cl_3(NHC_6H_4Me\text{-}p)_3$	—	15.8	—	—	44
$N_3P_3Cl_5[NHC_6H_4(OMe)\text{-}p]$	21.3	13.0	—	47.6	44

TABLE A.3 (cont.)

Compound	$\delta(PX_2)$	$\delta(PXR)$	$\delta(PR_2)$	$^2J(P–P)$ (Hz)	Refs.
gem-$N_3P_3Cl_4[NHC_6H_4(OMe)$-$p]_2$	21.3	—	−1.0	46.2	44
cis-$N_3P_3Cl_4[NHC_6H_4(OMe)$-$p]_2$	22.7	15.2	—	51.6	44
trans-$N_3P_3Cl_4[NHC_6H_4(OMe)$-$p]_2$	22.2	15.0	—	47.1	44
gem-$N_3P_3Cl_3[NHC_6H_4(OMe)$-$p]_3$[g]	22.8	17.1	1.5	—	44
cis-$N_3P_3Cl_3[NHC_6H_4(OMe)$-$p]_3$[h]	—	17.3	—	—	44
trans-$N_3P_3Cl_3[NHC_6H_4(OMe)$-$p]_3$[h]	—	18.0(1)[i] 17.2(2)	—	43.6	44
gem-$N_3P_3Cl_2[NHC_6H_4(OMe)$-$p]_4$	23.6	—	2.1	50.8	44
$N_3P_3[NHC_6H_4(OMe)$-$p]_6$	—	—	6.4	—	44
cis-$N_3P_3Cl_4(NHC_6H_4Me$-$p)$-$[NHC_6H_4(OMe)$-$p]$	22.3	14.8	—	44.6	44
trans-$N_3P_3Cl_4(NHC_6H_4Me$-$p)$-$[NHC_6H_4(OMe)$-$p]$	22.8	14.6	—	46.6	44
$N_3P_3Cl_4[NHC_6H_2Me_3(-2, 4, 6)]_2$	20.0	—	3.2	40.0	288
$N_3P_3[NH$-$C_6H_4(CO_2Et)$-$p]_6$[j]	—	—	2.9	—	289
$N_3P_3[NH$-$C_6H_4(CO_2Bu^n)$-$p]_6$[j]	—	—	3.1	—	289
$N_3P_3[NH$-$C_6H_4(CO_2CH_2CH_2NEt_2$-$p)]_6$[j]	—	—	2.9	—	289
N_3P_3(2-amino-4-picoline)$_6$[j]	—	—	3.5	—	289
N_3P_3(chloroprocaine)$_6$[j]	—	—	3.8	—	289
gem-$N_3P_3Br_4(NH_2)_2$[d]	−43.0	—	5.0	—	90
$N_3P_3Cl_5(NC_2H_4)$	22.3	31.2	—	39.0	27, 126
gem-$N_3P_3Cl_4(NC_2H_4)_2$	21.9	—	34.2	29.9	27, 76, 126
nongem-$N_3P_3Cl_4(NC_2H_4)_2$[k]	24.9 25.0	34.7 34.1	—	38.2 38.0	27, 126
gem-$N_3P_3Cl_2(NC_2H_4)_4$	25.1	—	35.5	25.5	290
trans-$N_3P_3Cl_2(NC_2H_4)_4$	—	40.0	37.6	29.7	27, 201

$N_3P_3Cl(NC_2H_4)_5$	—	42.6	37.2	29.4	76, 291
$N_3P_3(NC_2H_4)_6$	—	—	37.0	—	292
$N_3P_3Cl_5(NMe_2)$	20.5	21.6	—	49.1	55
cis-$N_3P_3Cl_4(NMe_2)_2$	21.6	24.9	—	46.3	55
$trans$-$N_3P_3Cl_4(NMe_2)_2$	21.5	25.2	—	44.4	55
gem-$N_3P_3Cl_3(NMe_2)_3$	21.7	27.3	21.7	44.8	55
cis-$N_3P_3Cl_3(NMe_2)_3$	—	27.5	—	---	55
$trans$-$N_3P_3Cl_3(NMe_2)_3$	—	27.7(2)[i] 28.3(1)		44.4	55
$nongem$-$N_3P_3H_3(NMe_2)_3$		−3.3			65
cis-$N_3P_3Cl_2(NMe_2)_4$		32.2	24.8	38.4	55
$trans$-$N_3P_3Cl_2(NMe_2)_4$		30.4	23.1	—	21
$N_3P_3(NMe_2)_6$	—	—	24.6	—	55, 293
$N_3P_3(NMe_2)_6.HCl$	—	—	20.5	—	265
cis-$N_3P_3Cl_4(NC_4H_8)_2$	21.0	21.0	---	—	294
$trans$-$N_3P_3Cl_4(NC_4H_8)_2$	21.0	21.0	—	—	294
cis-$N_3P_3Cl_3(NC_4H_8)_3$	—	23.0	—	—	294
$trans$-$N_3P_3Cl_3(NC_4H_8)_3$	—	23.8	—	—	294
cis-$N_3P_3Cl_2(NC_4H_8)_4$	—	27.2	15.8	36.3	294
$trans$-$N_3P_3Cl_2(NC_4H_8)_4$	—	27.7	16.4	34.9	294
$N_3P_3(NC_4H_8)_6$	—	—	17.8	—	294
$N_3P_3Cl_5(NC_4H_8O)$	19.0	21.3	—	47.3	294
cis-$N_3P_3Cl_4(NC_4H_8O)_2$	22.2	22.2	—	—	294
$trans$-$N_3P_3Cl_4(NC_4H_8O)_2$	21.6	21.6	—	—	294
cis-$N_3P_3Cl_3(NC_4H_8O)_3$	—	24.8	—	—	294
$trans$-$N_3P_3Cl_3(NC_4H_8O)_3$	—	24.8 } 24.0 }	—	40.0	294
cis-$N_3P_3Cl_2(NC_4H_8O)_4$	—	27.0	18.0	39.3	294
$trans$-$N_3P_3Cl_2(NC_4H_8O)_4$	—	26.6	18.2	37.3	294
$N_3P_3Cl(NC_4H_8O)_5$	—	29.5	19.0	41.6	77
$N_3P_3(NC_4H_8O)_6$	—	—	20.0	—	294
$trans$-$N_3P_3Cl_3(NEt_2)_3$	—	24.4	—	—	55
$N_3P_3(NEt_2)_6$	—	—	22.5	—	55

TABLE A.3 (*cont.*)

Compound	δ(PX$_2$)	δ(PXR)	δ(PR$_2$)	^2J(P–P) (Hz)	Refs.
N$_3$P$_3$Cl$_5$(NC$_5$H$_{10}$)	20.8	18.7	—	48.0	55
cis-N$_3$P$_3$Cl$_4$(NC$_5$H$_{10}$)$_2$	21.6	21.6	—	—	55
trans-N$_3$P$_3$Cl$_4$(NC$_5$H$_{10}$)$_2$	21.2	21.2	—	—	55
cis-N$_3$P$_3$Cl$_3$(NC$_5$H$_{10}$)$_3$		24.9	—	—	294
trans-N$_3$P$_3$Cl$_3$(NC$_5$H$_{10}$)$_3$	—	24.3(2)^i 25.2(1)	—	40.5	55
cis-N$_3$P$_3$Cl$_2$(NC$_5$H$_{10}$)$_4$	—	26.4	18.0	37.4	55
trans-N$_3$P$_3$Cl$_2$(NC$_5$H$_{10}$)$_4$	—	26.8	18.5	36.3	294
N$_3$P$_3$Cl(NC$_5$H$_{10}$)$_5$	—	30.4	19.6	40.7	77
N$_3$P$_3$(NC$_5$H$_{10}$)$_6$	—	—	21.2	—	55
N$_3$P$_3$Cl$_5$[N(Me)P(O)(OEt)$_2$]	21.0	17.1	0.9^l	52.5 18.2^m	295
nongem-N$_3$P$_3$Cl$_4$[N(Me)P(O)(OEt)$_2$]$_2$	20.3	18.0	0.8^l	51.8 18.2^m	295

gem-$N_3P_3Cl_3[N(Me)(PO)(OEt)_2]_3$	19.4	16.9	10.9	54.0[n]	295
			2.2(2)[i,l]	50.0[o]	
			1.2(1)[i,l]	58.0[p]	
				27.0[q]	
				19.0[m]	
$N_3P_3(N_2C_3H_3)_6$[d,r]			−2.2		286
$N_3P_3(N_2C_3H_3)_6$[s]	—	—	0.4	—	275
$N_3P_3(N_2C_3H_2Me)_6$[t]	—	—	−0.5	—	275
$N_3P_3(N_2C_3HMe_2)_6$[u]	—	—	−2.0	—	275
$N_3P_3Cl_5(NMePh)$	19.7	16.9	—	48.6	125
$N_3P_3(NMePh)_6$	—	—	13.3	—	125
$N_3P_3Br_5(NMe_2)$	−39.3	4.5	—	18[d]	32
cis-$N_3P_3Br_4(NMe_2)_2$	−36.8	9.2	—	18[d]	32
trans-$N_3P_3Br_4(NMe_2)_2$	−36.6	10.0	—	18[d]	32
trans-$N_3P_3Br_3(NMe_2)_3$	—	15.4	—	—	32

[a] $J[\underline{P}Cl_2-\underline{P}F(NMe_2)]$; [b] $J[\underline{P}F(NMe_2)-\underline{P}F(NMe_2)]$; [c] $J[\underline{P}F_2-\underline{P}Cl(NMe_2)]$; [d] thf solvent; [e] H_2O/D_2O; [f] ^{14}N and ^1H decoupled spectrum; [g] poor resolution for determination of Js; [h] 109.3 MHz spectrum; [i] relative intensities in parentheses; [j] dioxane; [k] cis–trans mixture; [l] P_{exo}; [m] $J[\underline{P}_{exo}-\underline{P}ClR]$; [n] $J[\underline{P}Cl_2-\underline{P}ClR]$; [o] $J[\underline{P}Cl_2-\underline{P}R_2]$; [p] $J[\underline{P}R_2-\underline{P}ClR]$; [q] $J[\underline{P}R_2-\underline{P}_{exo}]$; [r] imidazolyl; [s] 1-pyrazolyl; [t] 3-methyl-1-pyrazolyl; [u] 3,5-dimethyl 1-pyrazolyl.

TABLE A.4(a)

^{31}P NMR data for cyclotriphosphazenes with mixed amino substituents.

Compound	δ(P)	^2J(P–P) (Hz)	Ref.
gem-$N_3P_3(NH_2)_2(NMe_2)_4$	$P(NH_2)_2$ 19.2; $P(NMe_2)_2$ 26.0	41.5	55
$N_3P_3(NH_2)_2[N(Me)P(O)(OEt)_2]Cl_3$	PCl_2(a) 20.8; PClR(b) 19.9;	a–b 65.5	285
(2, 2:4, 6, 6)	$P(NH_2)_2$(c) 12.5; P_{exo}(d) 2.0	a–c 44.3	
		b–c 50.5	
		b–d 24.0	
$N_3P_3(NH_2)_2[N(Me)P(O)(OEt)_2]_2Cl_2$	PClR(a) 20.9; $P(NH_2)_2$(b) 13.8;	a–b 47.7	285
(2, 2:4, 6:4, 6)	P_{exo}(c) 2.6	a–c 22.0	
gem-$N_3P_3(NH_2)_3[N(Me)P(O)(OEt)_2]_3$	$P(NH_2)_2$(a) 16.4; PR_2(b) 13.4;	a–b 52.5	285
	$P(NH_2)(R)$(c) 17.2; P_{exo}(d)	b–c 55.0	
	6.1, 5.1, 4.9	a–c 50.0	
		b–d 29.0, 28.0	
		c–d 25.5	
nongem-$N_3P_3(NH_2)_4[N(Me)P(O)(OEt)_2]_2^a$	$P(NH_2)_2$(a) 17.0; $P(NH_2)R$(b)	a–c 48.5	285
	16.7; P_{exo}(c) 6.1	b–c 22.0	

$N_3P_3(NH_2)_5[N(Me)P(O)(OEt)_2]^b$	$P(NH_2)_2(a)$ 15.8; $P(NH_2)(R)(b)$ 15.6; $P_{exo}(c)$ 6.5	a–b 48.5 b–c 21.0	285
cis-$N_3P_3(NHEt)_2(NMe_2)_4$	$P(NMe_2)_2$ 26.6; $P(NMe_2)(NHEt)$ 22.8	42.2	55
trans-$N_3P_3(NHEt)_4(NMe_2)_2$	$P(NMe_2)(NHEt)$ 22.8; $P(NHEt)_2$ 18.9	42.1	55
trans-$N_3P_3(NHEt)_4(NMe_2)_2$.HCl	$P(NHEt)(NMe_2)$ 17.3; $P(NHEt)_2$ 12.3	30.0	55
nongem-$N_3P_3(NHPr^i)_2(NMe_2)_4$	$P(NMe_2)_2$ 24.8; $P(NMe_2)(NHPr^i)$ 20.0	41.9	55
$N_3P_3(NHPr^i)(NMe_2)_5$	$P(NMe_2)_2$ 25.4; $P(NMe_2)(NHPr^i)$ 20.2	43.7	55
gem-$N_3P_3(NHPr^i)_4(NMe_2)_2$	$P(NMe_2)_2$ 25.8; $P(NHPr^i)_2$ 14.2	45.7	55
gem-$N_3P_3(NHBu^t)_4(NMe_2)_2$	$P(NMe_2)_2$ 22.4; $P(NHBu^t)_2$ 8.2	45.2	55
nongem-$N_3P_3(NHBu^t)_4(NMe_2)_2$	$P(NMe_2)(NHBu^t)$ 19.1; $P(NHBu^t)_2$ 12.0	49.1	55
$N_3P_3[NHC_6H_4Me-p](NMe_2)_5$	$P(NMe_2)(NHAr)(NMe_2)$ 15.0; $P(NMe_2)_2$ 25.3	42.3	44
gem-$N_3P_3[NHC_6H_4Me-p]_2(NMe_2)_4$	$P(NMe_2)_2$ 25.9; $P(NHAr)_2$ 5.6	44.5	44
cis-$N_3P_3[NHC_6H_4Me-p]_2(NMe_2)_4$	$P(NMe_2)_2$ 26.2; $P(NHAr)(NMe_2)$ 15.3	43.6	44
trans-$N_3P_3[NHC_6H_4Me-p]_2(NMe_2)_4$	$P(NMe_2)_2$ 26.8; $P(NHAr)(NMe_2)$ 15.8	40.6	44
$N_3P_3[NHC_6H_4(OMe)-p](NMe_2)_5$	$P(NMe_2)_2$ 26.3; $P(NHAr)(NMe_2)$ 16.3	42.2	44
nongem-$N_3P_3[NHC_6H_4(OMe)-p]_2(NMe_2)_4$	$P(NMe_2)_2$ 26.3; $P(NHAr)(NMe_2)$ 16.3	43.6	44

^{a}MeOH solvent; ^{b}H$_2$O solvent.

TABLE A.4(b)

^{31}P NMR data for mixed (aziridino) (amino) cyclotriphosphazenes.

Compound	$\delta[P(NC_2H_4)_2]$	$\delta(PR_2)$	$\delta\begin{bmatrix}P(NC_2H_4)Cl\\ \text{or}\\ P(NC_2H_4)R\end{bmatrix}$	$^2J(P-P)$ (Hz)	Refs.
cis-$N_3P_3Cl_2(NC_2H_4)_2(NC_4H_8)_2$	36.0	—	27.4	31.7	77
trans-$N_3P_3Cl_2(NC_2H_4)_2(NC_4H_8)_2$	36.0	—	27.5	30.4	77
cis-$N_3P_3Cl_2(NC_2H_4)_2(NC_4H_8O)_2$	36.9	—	27.7	32.4	77
trans-$N_3P_3Cl_2(NC_2H_4)_2(NC_4H_8O)_2$	36.7	—	27.2	31.9	77
cis-$N_3P_3Cl_2(NC_2H_4)_2(NC_5H_{10})_2$	36.8	—	28.0	32.7	77
trans-$N_3P_3Cl_2(NC_2H_4)_2(NC_5H_{10})_2$	36.6	—	27.7	31.9	77
$N_3P_3Cl(NC_2H_4)_4(NC_4H_8)(2:4, 4, 6, 6:2)$	36.5	—	32.0	32.0	77
$N_3P_3Cl(NC_2H_4)_4(NC_4H_8O)(2:4, 4, 6, 6:2)$	36.9	—	31.3	33.6	77, 126
$N_3P_3Cl(NC_2H_4)_4(NC_5H_{10})(2:4, 4, 6, 6:2)$	36.8	—	31.7	33.3	77, 126
gem-$N_3P_3(NC_2H_4)_2(NHCH_2COOEt)_4$	38.5	18.1	—	39.8	287
trans-$N_3P_3(NC_2H_4)_3(NC_4H_8)_3$	—	—	27.1	34.9	201
			27.7		
cis-$N_3P_3(NC_2H_4)_3(NC_4H_8)_3$	—	—	26.7	—	201

gem-N$_3$P$_3$(NC$_2$H$_4$)$_4$(NH$_2$)$_2$	37.4	18.6	—	36.6	201, 296
gem-N$_3$P$_3$(NC$_2$H$_4$)$_4$(NHMe)$_2$	37.6	21.6	—	36.1	201
gem-N$_3$P$_3$(NC$_2$H$_4$)$_4$(NHCH$_2$COOEt)$_2$	37.5	18.5	—	37.3	287
gem-N$_3$P$_3$(NC$_2$H$_4$)$_4$(NHBu)$_2$	37.6	18.5	—	36.2	201
gem-N$_3$P$_3$(NC$_2$H$_4$)$_4$(NC$_4$H$_8$)$_2$	36.9	16.5	—	35.8	201
gem-N$_3$P$_3$(NC$_2$H$_4$)$_4$(NC$_4$H$_8$O)$_2$	36.7	20.2	—	37.6	201
gem-N$_3$P$_3$(NC$_2$H$_4$)$_4$(NC$_5$H$_{10}$)$_2$	36.8	20.7	—	36.5	201
gem-N$_3$P$_3$(NC$_2$H$_4$)$_4$(NHPh)$_2$.THF	38.1	7.0	—	38.5	201
trans-N$_3$P$_3$(NC$_2$H$_4$)$_4$(NC$_4$H$_8$)$_2$	36.8	—	27.4	33.8	201
cis-N$_3$P$_3$(NC$_2$H$_4$)$_4$(NC$_4$H$_8$)$_2$	36.6	—	26.8	33.3	201
trans-N$_3$P$_3$(NC$_2$H$_4$)$_4$(NC$_4$H$_8$O)$_2$	37.1	—	28.5	33.0	201
trans-N$_3$P$_3$(NC$_2$H$_4$)$_4$(NC$_5$H$_{10}$)$_2$	37.4	—	28.7	33.3	201
cis-N$_3$P$_3$(NC$_2$H$_4$)$_4$(NC$_5$H$_{10}$)$_2$	37.1	—	27.4	32.6	201
N$_3$P$_3$(NC$_2$H$_4$)$_5$(NH$_2$)	37.7	—	28.1	38.2	296
N$_3$P$_3$(NC$_2$H$_4$)$_5$(NHNH$_2$)	37.6	—	30.6	—	76
N$_3$P$_3$(NC$_2$H$_4$)$_5$(NHMe)	37.3	—	29.7	—	76
N$_3$P$_3$(NC$_2$H$_4$)$_5$(NHCH$_2$COOEt)	36.8	—	28.0	33.8	287
N$_3$P$_3$(NC$_2$H$_4$)$_5$(N$_2$C$_3$H$_3$)[a]	37.1	—	20.8	35.4	201
N$_3$P$_3$(NC$_2$H$_4$)$_5$(NC$_4$H$_8$)	36.7	—	27.3	33.5	77, 126
N$_3$P$_3$(NC$_2$H$_4$)$_5$(NC$_4$H$_8$O)	36.9	—	28.4	33.2	77
N$_3$P$_3$(NC$_2$H$_4$)$_5$(NC$_5$H$_{10}$)	36.9	—	28.6	32.8	77, 126

[a]Imidazolyl.

TABLE A.5

^{31}P NMR data for (alkyl/aryl)(amino)cyclotriphosphazenes.

Compound	$\delta[P(NRR')_2]$	$\delta[P(NRR')R'']$	$\delta(PR''_2)$	$^2J(P–P)$ (Hz)	Refs.
gem-N$_3$P$_3$Cl$_4$(Me)(NHBu^n)	19.7^a	24.4	—	20.6	67
gem-N$_3$P$_3$Cl$_4$(Me)(NHBu^t)	19.5^a	18.3	—	21.0	67
gem-N$_3$P$_3$Cl$_4$(Me)[NH(CH$_2$)$_3$OH]	19.8^a	25.0	—	19.5	100
gem-N$_3$P$_3$(Me)(H)(NMe$_2$)$_4$	23.9	—	12.8		60
gem-N$_3$P$_3$(Me)(NEt$_2$)(NMe$_2$)$_4$	23.6	43.5			60
gem-N$_3$P$_3$(Me)[NMe(CH$_2$Ph)](NMe$_2$)$_4$	24.3	30.2			155
[N$_3$(H)P$_3$(Me)$_2$(NMe$_2$)$_4$]$^+$I$^-$	20.6	—	37.9		60
gem-N$_3$P$_3$Cl$_4$Ph(NEt$_2$)	18.4^a	18.4	—		36
gem-N$_3$P$_3$Ph$_2$(NMe$_2$)$_4$	24.1	—	16.1	21.6	55
gem-N$_3$P$_3$Ph$_2$(NC$_2$H$_4$)$_4$	36.2	—	18.9	15.6	201
gem-N$_3$P$_3$Ph$_2$[N$_2$C$_3$H(Me)$_2$]$_4$ ^{b}	−3.5	—	21.7	25.0	275
gem-N$_3$P$_3$Ph$_4$(NH$_2$)$_2$	11.7	—	16.4	16.8	283
gem-N$_3$P$_3$Ph$_4$(NMe$_2$)$_2$	21.0	—	15.5	16.0	55

gem-$N_3P_3Ph_4[N_2C_3H_2(Me)]_2$[c]	-6.1	—	19.1	19.9	275
gem-$N_3P_3Ph_4[N_2C_3H(Me)_2]_2$[b]	-5.2	—	18.2	19.9	275
gem-$N_3P_3Ph_4(H)(NMe_2)$	—	7.5	14.1		60
gem-$N_3P_3Ph_4(Me)(NH_2)$	—	21.8	13.9		283
gem-$N_3P_3Ph_4(Me)(NHMe)$	—	21.8	13.9		155
gem-$N_3P_3Ph_4(Me)(NMe_2)$	—	28.2	14.1		155
gem-$N_3P_3Ph_4(Me)(NHCH_2Ph)$	—	22.0	14.4		155
gem-$N_3P_3Ph_4(Me)[N(Me)CH_2Ph]$	—	26.6	14.3		155
gem-$N_3P_3Ph_4(Me)(NHPh)$	—	16.7	18.8		155
gem-$N_3P_3Ph_4(Me)N(Me)Ph$	—	23.8	18.8		155
gem-$[N_3P_3Ph_4(NH_2)_2Me]^+I^-$	13.0	—	35.2		283
			19.5		
gem-$[N_3P_3Ph_4(NH_2)_2Me]^+[BPh_4]^-$[d]	11.9	—	35.0		283
			19.4		
gem-$[N_3P_3Ph_4(NH_2)_2Me]^+[SbCl_6^-]^-$	12.4	—	36.7		283
			22.9		
gem-$[N_3P_3Ph_4(NH_2)Me_2]^+I^-$	—	33.2	29.9		283
			20.2		

[a] PCl_2; [b] 3-5-dimethyl-1-pyrazolyl; [c] 3-methyl-1-pyrazolyl; [d] in MeCN medium.

TABLE A.6

^{31}P NMR data for (alkoxy) and (aryloxy)cyclotriphosphazenes.

Compound	$\delta(PX_2)^a$	$\delta(PXR)^a$	$\delta(PR_2)^a$	$^2J(P-P)$ (Hz)	Refs.
$N_3P_3F_5(OMe)^b$	9.7	13.5	—		174
$N_3P_3F_5(OEt)^b$	9.6	12.5	—		174
$N_3P_3F_5(OCH{=}CH_2)^b$	11.0	11.2	—		118
$N_3P_3F(OCH_2CF_3)_5$	14.4	16.7	—	103.4	189
$N_3P_3F_5(OPh)^c$	15.5	14.6	—		45
$trans\text{-}N_3P_3F_4(OPh)_2{}^c$	15.4	13.6	—		45
$trans\text{-}N_3P_3F_3(OPh)_3{}^c$	—	15.5	—	—	45
$nongem\text{-}N_3P_3F_2(OPh)_4{}^c$	—	16.7	15.5	—	45
$N_3P_3F(OPh)_5$	—	10.4	8.6	100.0	45, 182
$N_3P_3F[OC_6H_4(Me)\text{-}p]_5$		10.7	9.3	98.4	182
$N_3P_3F[OC_6H_4(Me)\text{-}m]_5$		10.3	8.5	101.2	182
$N_3P_3F[OC_6H_4(OMe)\text{-}p]_5$		11.6	10.3	97.0	182, 189
$N_3P_3F[OC_6H_4(OMe)\text{-}m]_5$		9.8	8.0	101.7	182
$N_3P_3Cl_5(OMe)$	22.5	16.7	—	63.3	116
$N_3P_3(OMe)_6$	—	—	21.7	—	80
$N_3P_3Cl_5(OEt)$	21.3	13.6	—	63.3	116
$N_3P_3(OEt)_6$	—	—	14.3	—	80
$N_3P_3Cl_5(OPr^i)$	21.7	12.6	—	62.7	116
$N_3P_3(OPr^n)_6$	—	—	17.7	—	122
$N_3P_3Cl(OBu^n)_5$		12.5	15.0	79	349
$N_3P_3(OBu^n)_6$	—	—	16.9	—	123
$N_3P_3Cl_5(OCH{=}CH_2)$	23.4	13.2	—	64.7	118, 281^a
$N_3P_3Cl_5[OC(Me){=}CH_2]$	22.3	10.2	—	62.4	281^a
$N_3P_3Cl_5[OC(Ph){=}CH_2]$	23.0	12.4	—	62.0	281^a
$gem\text{-}N_3P_3Cl_4(OCH{=}CH_2)_2$	24.5	—	−0.6	68.4	119
$cis\text{-}N_3P_3Cl_4(OCH{=}CH_2)_2$	24.8	15.8	—	67.3	119
$trans\text{-}N_3P_3Cl_4(OCH{=}CH_2)_2$	24.8	15.6	—	67.5	119

gem-$N_3P_3Cl_3(OCH{=}CH_2)_3$[b]	27.3	18.0	3.0		119
gem-$N_3P_3Cl_2(OCH{=}CH_2)_4$	28.9	—	5.7	75.7	119
cis-$N_3P_3Cl_2(OCH{=}CH_2)_4$	—	21.6	6.1	83.4	119
$N_3P_3Cl(OCH{=}CH_2)_5$	—	23.9	8.7	85.0	119
$N_3P_3(OCH{=}CH_2)_6$	—	—	11.3	—	119
$N_3P_3Cl_5(OCH_2CF_3)$	22.5	16.1	—	66.0	116, 117
trans-$N_3P_3Cl_4(OCH_2CF_3)_2$	24.8	19.0	—	69.6	117
gem-$N_3P_3Cl_3(OCH_2CF_3)_3$[b]	26.5	21.0	8.4	—	117
trans-$N_3P_3Cl_3(OCH_2CF_3)_3$	—	$\begin{cases} 21.9(2) \\ 21.7(1) \end{cases}$	—	—	117
cis-$N_3P_3Cl_2(OCH_2CF_3)_4$	—	24.3	11.6	85.4	117
$N_3P_3Cl(OCH_2CF_3)_5$	—	26.3	14.2	87.0	117
$N_3P_3(OCH_2CF_3)_6$	—	—	16.7 17.7[d]	—	117 286
$N_3P_3Cl_5(OCH_2CF_2CF_2H)$	22.6	17.5	—	64	297
trans-$N_3P_3Cl_4(OCH_2CF_2CF_2H)_2$	24.8	19.1	—	68	297
trans-$N_3P_3Cl_3(OCH_2CF_2CF_2H)_3$	—	22.5	—	—	297
nongem-$N_3P_3Cl_2(OCH_2CF_2CF_2H)_4$	—	24.9	12.2	83	297
$N_3P_3Cl(OCH_2CF_2CF_2H)_5$	—	27.0	14.8	87	297
$N_3P_3(OCH_2CF_2CF_2H)_6$	—	—	17.0	—	297
nongem-$N_3P_3Cl_4(OCH_2C_2F_5)_2$	18.0	16.1	—	—	298
nongem-$N_3P_3Cl_3(OCH_2C_2F_5)_3$	—	21.3	—	—	298
nongem-$N_3P_3Cl_2(OCH_2C_2F_5)_4$	—	25.3	22.9	—	298
$N_3P_3(OCH_2C_2F_5)_6$	—	—	16.7	—	298
$N_3P_3Cl_5[OCH(CF_3)_2]$	22.6	17.9	—	68.2	188
gem-$N_3P_3Cl_4[OCH(CF_3)_2]_2$	22.3	—	6.8	78.0	188
nongem-$N_3P_3Cl_4[OCH(CF_3)_2]_2$	26.9	22.5	—	69.2	188
$N_3P_3[OCH(CF_3)_2]_6$	—	—	13.8	—	188
nongem-$N_3P_3Cl_3(OCH_2C_3F_7)_3$	—	20.9	—	—	298
nongem-$N_3P_3Cl_2(OCH_2C_3F_7)_4$	—	24.3	21.9	—	298
$N_3P_3(OCH_2C_3F_7)_6$	—	—	16.7	—	298
nongem-$N_3P_3Cl_4[OCH_2(CF_2)_3CF_2H]_2$	25.2	19.4	—	67.0	299
nongem-$N_3P_3Cl_3[OCH_2(CF_2)_3CF_2H]_3$	—	22.2	—	—	299
nongem-$N_3P_3Cl_2[OCH_2(CF_2)_3CF_2H]_4$	—	24.5	12.2	85	299

TABLE A.6 (cont.)

Compound	$\delta(PX_2)^a$	$\delta(PXR)^a$	$\delta(PR_2)^a$	$^2J(P-P)$ (Hz)	Refs.
$N_3P_3[OCH_2(CF_2)_5CF_2H]_6$	—	—	16.9	—	299
trans-$N_3P_3Cl_3(OPh)_3$	—	18.3	—	—	121, 300
nongem-$N_3P_3(NCS)_3(OPh)_3$	—	−2.8	—	—	300
$N_3P_3Cl(OPh)_5$	—	22.1	6.9	83.1	120, 191, 301
$N_3P_3(OPh)_6$	—	—	8.3	—	120, 121
$N_3P_3Cl[OC_6H_4F-p]_5$	—	22.5	7.3	83.0	301
$N_3P_3[OC_6H_4F-p]_6$	—	—	8.9	—	302
$N_3P_3(OC_6F_5)_6$	—	—	10.3	—	302
$N_3P_3[OC_6H_4Cl-p]_6$	—	—	9.6	—	302
$N_3P_3Cl_5(OC_6H_4Me-p)^e$	22.5	12.2	—	60.0	22
gem-$N_3P_3Cl_4(OC_6H_4Me-p)_2$			−1.5	—	22
cis-$N_3P_3Cl_4(OC_6H_4Me-p)_2$	23.9	14.2	—	65.4	22
trans-$N_3P_3Cl_4(OC_6H_4Me-p)_2$	23.9	14.4	—	63.4	22
nongem-$N_3P_3Cl_3(OC_6H_4Me-p)_3$	—	18.3	—	—	22
cis-$N_3P_3Cl_2(OC_6H_4Me-p)_4$	—	20.1	4.6	79.5	22
trans-$N_3P_3Cl_2(OC_6H_4Me-p)_4$	—	19.9	4.4	77.6	22
$N_3P_3Cl(OC_6H_4Me-p)_5$	—	22.4	6.9	83.0	22
$N_3P_3(OC_6H_4Me-p)_6$	—	—	9.2	—	22
$N_3P_3(OMe)_5(OC_6H_4Me-p)$	19.7	15.5	—	84.2	205
cis-$N_3P_3(OMe)_4(OC_6H_4Me-p)_2$	18.7	14.7	—	85.2	205
trans-$N_3P_3(OMe)_4(OC_6H_4Me-p)_2$	18.8	14.7	—	84.3	205
cis-$N_3P_3(OMe)_3(OC_6H_4Me-p)_3$	—	14.1	—	—	205

trans-N$_3$P$_3$(OMe)$_3$(OC$_6$H$_4$Me-p)$_3$	—	14.3	—	—	205
gem-N$_3$P$_3$(OMe)$_3$(OC$_6$H$_4$Me-p)$_3$	18.7(A)	14.5(B)	9.9(C)	84.0(AB) 88.4(BC) 85.2(AC)	205
cis-N$_3$P$_3$(OMe)$_2$(OC$_6$H$_4$Me-p)$_4$	—	14.0	9.4	87.3	205
trans-N$_3$P$_3$(OMe)$_2$(OC$_6$H$_4$Me-p)$_4$	—	14.2	9.5	87.0	205
N$_3$P$_3$(OMe)(OC$_6$H$_4$Me-p)$_5$	—	13.3	8.7	87.2	205
N$_3$P$_3$(OBu^n)(OPh)$_5$	—	12.6	9.4	88.8	303^f
N$_3$P$_3$(OSiPh$_3$)(OC$_6$H$_4$Me-p)$_5$		2.9	8.4	70.6	303
cis-N$_3$P$_3$(OEt)$_3$(OC$_6$H$_4$Me-p)$_3$	—	12.7	—	—	205
trans-N$_3$P$_3$(OEt)$_3$(OC$_6$H$_4$Me-p)$_3$	—	12.9	—	—	205
N$_3$P$_3$(OCH$_2$CF$_3$)$_5$(OC$_6$H$_4$Me-p)	16.2	13.0	—	93.8	205
N$_3$P$_3$[OC$_6$H$_4$(CHO)-p]$_6$	—	—	7.2	—	304, 305
N$_3$P$_3$[OC$_6$H$_4$(CH$_2$OH)-p]$_6$	—	—	8.7	—	305
N$_3$P$_3$[OC$_6$H$_4$(COMe)-p]$_6$	—	—	7.5	—	306^f
N$_3$P$_3$[OC$_6$H$_4$(NO$_2$)-p]$_6$	—	—	6.9^d	—	307
N$_3$P$_3$[OC$_6$H$_4$(NH$_2$)-p]$_6$	—	—	11.2^d	—	307
N$_3$P$_3$[OC$_6$H$_4$(PPh$_2$)-p]$_6$	—	—	8.1, −7.2^g	—	191
				—	
N$_3$P$_3$(OC$_6$H$_4$Br-p)(OPh)$_5$	—	—	8.0	—	191
N$_3$P$_3$[OC$_6$H$_4$(CN)-p](OPh)$_5$	—	—	9.4	—	308
N$_3$P$_3$[OC$_6$H$_4$CH$_2$(NH$_2$)-p](OPh)$_5$	—	—	9.4	—	308^f
N$_3$P$_3$[OC$_6$H$_4$(OH)-p]$_3$(OPh)$_3$	—	9.0	—	—	309^f
N$_3$P$_3$(OC$_{18}$H$_{21}$O)$_6^{d,h}$	—	—	8.4	—	350

^{a}For halogen derivatives, X = F, Cl; R = alkoxy, aryloxy; for mixed(alkoxy)(aryloxy) derivatives, X = alkoxy, R = aryloxy. ^{b}Approximate values — coupling constants not reported. ^{c} ^1J(P–F$_2$) ≈ 940–960 Hz; ^1J[P(OPh)–F] ≈ 900–930 Hz; ^2J(P–P) ≈ 100 Hz. ^{d}thf solvent. ^{e}Data for a similar series of phenoxy derivatives reported;[120,121] chemical shifts and coupling constants almost identical with p-cresoxy derivatives. ^{f}The chemical shifts for (aryloxy) derivatives with other substituents attached to the aryl ring are also reported; the values lie in the range 7–10δ. ^{g}PPh$_2$. ^{h}C$_{18}$H$_{22}$O$_2$ = 1,3,5-estratrien-3-ol-17-one.

TABLE A.7

^{31}P NMR data for (alkylthio) and (arylthio)cyclotriphosphazenes.

Compound	$\delta(PX_2)$	$\delta[PX(SR)]$	$\delta[P(SR)_2]$	$^2J(P-P)$ (Hz)	Refs.
$N_3P_3F_5(SMe)$	6.3	47.9	—	—	174
$N_3P_3F_5(SEt)$	6.0	50.0	—	—	81
gem-$N_3P_3F_4(SEt)_2$	5.0		59.0	—	81
gem-$N_3P_3F_3(SEt)_3$	1.0	40.0	55.0	—	81
gem-$N_3P_3F_2(SEt)_4$	−1.0		52.0	—	81
$N_3P_3F(SEt)_5$		33.0	48.0	—	81
$N_3P_3Cl_5(SMe)^a$	21	41	—	—	310
gem-$N_3P_3Cl_4(SMe)_2{}^a$	23	—	59	—	310
gem-$N_3P_3Cl_2(SMe)_4{}^a$	17	—	50	—	310
$N_3P_3(SMe)_6{}^a$	—	—	46	—	310
$N_3P_3Cl_5(SEt)$	21.0	33.1		32.9	124
gem-$N_3P_3Cl_4(SEt)_2$	18.7		51.4	5.0	82, 124
gem-$N_3P_3Cl_3(SEt)_3$	18.1	38.5	50.6	17.3^b	124
				3.5^c	
				14.1^d	
gem-$N_3P_3Cl_2(SEt)_4$	17.4		49.2	5.2	124
$N_3P_3Cl(SEt)_5$	—	37.1	48.0	9.9	124
$N_3P_3(SEt)_6$	—	—	46.5	—	124
$N_3P_3F_5(SPh)$	7.3	44.1	—	—	174
gem-$N_3P_3Cl_4(SPh)_2$	18.6		46.8	—	82
gem-$N_3P_3Cl_4[SC_6H_4(Me)\text{-}p]_2$	18.9	—	47.4	—	311
$N_3P_3(SCB_{10}H_{10}CH)_6{}^e$	—	—	30.0	—	312

^{a}Approximate values ± 2 ppm; $^bJ[\underline{P}Cl_2-\underline{P}Cl(SEt)]$; $^cJ[\underline{P}Cl_2-\underline{P}(SEt)_2]$; $^dJ[\underline{P}Cl(SEt)-\underline{P}(SEt)_2]$; ^{e}carborane derivative.

TABLE A.8

^{31}P NMR data for alkyl (aryl)cyclotriphosphazenes containing alkoxy or alkylthio groups.[a]

Compound	$\delta[P(OR)_2/PCl_2]$	$\delta[P(OR)R']$	$\delta(PR'_2)$	$^2J(P-P)$ (Hz)	Refs.
gem-$N_3P_3Cl_4(Me)(OMe)$	21.1	31.6	—	23.1	67
gem-$N_3P_3Cl_4(Me)[OCH{=}CH_2]$	21.6	29.6	—	21.9	281
gem-$N_3P_3Cl_4(Me)[OC(Me){=}CH_2]$	21.2	30.0	—	20.8	281[a]
gem-$N_3P_3Cl_4(Me)[OC(Ph){=}CH_2]$	23.4	32.8	—	21.0	281[a]
gem-$N_3P_3Cl_4(Me)(OPh)$	20.5	29.8	—	18.6	67
gem-$N_3P_3Cl(Me)(OCH_2CF_3)_4$	47.6	14.7	—	32.4	253
gem-$N_3P_3Cl(Me)(OPh)_4$	6.4	45.7	—	33.0	253
$N_3P_3(Me)(OCH_2CF_3)_5$	14.3	38.3	—	47.6	253, 313
gem-$N_3P_3(Me)(OCH_2CF_3)(OPh)_4$	8.7	38.5	—	49.2	253
gem-$N_3P_3H(Me)(OCH_2CF_3)_4$	15.0	—	17.2	30.6	253
gem-$N_3P_3H(Me)(OPh)_4$	7.3	—	16.2	28.4	253
$N_3P_3(Me)(OPh)_5$	8.7	35.9	—	49.2	253, 313
gem-$N_3P_3(Me)(CH_2CH{=}CH_2)(OCH_2CF_3)_4$	15.5	—	37.9	27.3	253
gem-$N_3P_3(Me)(CH_2CH{=}CH_2)(OPh)_4$	8.0	—	36.5	26.0	253
gem-$N_3P_3HMe_2Ph_2(OPh)$	—	6.0	$\begin{cases} 29.2^b \\ 16.4 \end{cases}$	—	60
$N_3P_3(Et)(OCH_2CF_3)_5$	16.1	43.8	—	43.1	313
$N_3P_3(Et)(OPh)_5$	8.9	40.1	—	43.3	313
$N_3P_3(Pr^n)(OCH_2CF_3)_5$	16.0	42.1	—	42.9	313
$N_3P_3(Pr^n)(OPh)_5$	8.7	38.4	—	42.3	313
$N_3P_3(Pr^i)(OCH_2CF_3)_5$	16.5	46.7	—	40.2	313
$N_3P_3(Pr^i)(OPh)_5$	9.7	43.3	—	43.3	313
$N_3P_3(Bu^n)(OCH_2CF_3)_5$	16.1	42.5	—	43.6	313
$N_3P_3(Bu^n)(OPh)_5$	8.8	38.7	—	43.3	313
$N_3P_3(Bu^t)(OCH_2CF_3)_5$	16.4	67.3	—	20.1	313
$N_3P_3(Bu^t)(OPh)_5$	8.1	65.5	—	16.7	313

TABLE A.8 (*cont.*)

Compound	$\delta[P(OR)_2/PCl_2]$	$\delta[P(OR)R']$	$\delta(PR'_2)$	$^2J(P-P)$ (Hz)	Refs.
gem-N$_3$P$_3$Cl(Ph)(OCH$_2$CF$_3$)$_4$	14.8	—	37.7	39.0	253
gem-N$_3$P$_3$Cl(Ph)(OPh)$_4$	6.5	—	36.4	40.0	253
N$_3$P$_3$(Ph)(OEt)$_5$	16.5	25.8	—	50.4	253
N$_3$P$_3$(Ph)(OCH$_2$CF$_3$)$_5$	16.1	29.2	—	53.0	253
N$_3$P$_3$(Ph)(OPh)$_5$	8.2	24.4	—	53.9	253
gem-N$_3$P$_3$(Ph)(OCH$_2$CF$_3$)(OPh)$_4$	9.5	28.2	—	53.2	253
gem-N$_3$P$_3$H(Ph)(OCH$_2$CF$_3$)$_4$	14.9	—	12.4	32.2	253
gem-N$_3$P$_3$(H)(Ph)(OPh)$_4$	7.1	—	12.1	30.3	253
N$_3$P$_3$Cl$_2$Ph$_2$(OPh)$_2$^{c}	—	16.6	21.9		314
gem-N$_3$P$_3$Ph$_2$(OMe)$_4$	18.3	—	21.0	34.3	80
gem-N$_3$P$_3$Ph$_2$(OEt)$_4$	15.2	—	20.1	34.8	153
gem-N$_3$P$_3$Ph$_2$(OPr^n)$_4$	15.7	—	20.7	34.2	153
nongem-N$_3$P$_3$Ph$_3$[O(CH$_2$)$_4$OH]$_3$^{d}	—	25.7⎰ 22.9⎱	—		315
gem-N$_3$P$_3$Ph$_4$(OEt)$_2$	9.8	—	19.8	24.0	153
N$_3$P$_3$HPh$_4$(OPh)	—	5.8	14.5	—	59
gem-N$_3$P$_3$Ph$_4$(Me)(SMe)	—	38.6	14.1		316
gem-N$_3$P$_3$Ph$_4$(OPh)(SMe)	—	30.9	15.2		316
gem-N$_3$P$_3$Ph$_4$[C$_6$H$_4$(OMe)-*p*](SMe)	—	27.0	14.1		316

^{a}Values quoted from ref. 313 are measured in thf. ^{b}PMe$_2$; ^{c}2, 4:6, 6:2, 4 derivative; ^{d}*cis* and *trans* isomers.

TABLE A.9

^{31}P NMR data for (alkoxy)(amino)cyclotriphosphazenes, $N_3P_3(OR)_n(NR'R'')_{6-n}$.

Compound	$\delta[P(OR)_2]$	$\delta[P(OR)(NR'R'')]$	$\delta[P(NR'R'')_2]$	$^2J(P-P)$ (Hz)	Refs.
gem-$N_3P_3(OMe)_4(NHBu^t)_2$	18.9	—	11.6	63.7	80
gem-$N_3P_3(OMe)_2(NHBu^t)_4$	11.7	—	6.1	60.8	153
$N_3P_3(OMe)_5(NMe_2)$	20.2	26.5	—	67.3	122
trans-$N_3P_3(OMe)_4(NMe_2)_2$	14.8	20.7	—	64.5	80
trans-$N_3P_3(OMe)_3(NMe_2)_3$	—	26.0	—	—	80
gem-$N_3P_3(OMe)_2(NC_2H_4)_4$	20.1		38.0	—	76
$N_3P_3(OMe)(NC_2H_4)_5$	—	29.6	38.2	—	76
gem-$N_3P_3(OMe)(NH_2)(NC_2H_4)_4$	—	23.6	38.1	44.0	318
$N_3P_3(OMe)_5[NHC_6H_4(OMe)-p]$	19.1	16.5	—	71.4	44
gem-$N_3P_3(OMe)_4[NHC_6H_4(OMe)-p]_2$	18.7	—	7.7	66.0	44
cis-$N_3P_3(OMe)_4[NHC_6H_4(OMe)-p]_2$	18.4	16.2	—	69.1	44
trans-$N_3P_3(OMe)_4[NHC_6H_4(OMe)-p]_2$	18.4	16.0	—	68.3	44
nongem-$N_3P_3(OMe)_3[NHC_6H_4(OMe)-p]_3$ [a]	—	15.0	—	—	44
gem-$N_3P_3(OMe)_2[NHC_6H_4(OMe)-p]_4$	17.5	—	6.8	59.2	44
cis-$N_3P_3(OMe)_4(NHPh)_2$	18.7	15.8	—	67.6	44
trans-$N_3P_3(OMe)_4(NHPh)_2$	18.7	15.6	—	71.7	44
gem-$N_3P_3(OMe)_4(NHC_6H_4Me-p)_2$	18.9		6.8	65.9	44
cis-$N_3P_3(OMe)_4(NHC_6H_4Me-p)_2$	17.9	15.1	—	69.9	44
trans-$N_3P_3(OMe)_4(NHC_6H_4Me-p)_2$	17.9	15.0	—	70.3	44
gem-$N_3P_3(OEt)_4(NHBu^t)_2$	15.9	—	11.3	62.3	153
gem-$N_3P_3(OCH_2CF_3)_4(NHPh)_2$	16.4	—	6.4	72.0	319
gem-$N_3P_3(OCH_2CF_3)_4(NHC_6H_4Cl-m)_2$	16.2	—	6.9	—	319
$N_3P_3(OCH_2CF_3)(C_3H_3N_2)_5$ [c]	—	5.6	−1.0	61.8	286
$N_3P_3(OCH_2CF_3)(NHMe)_5$ [b]	—	21.2	23.0	55.1	350
trans-$N_3P_3(OPr^n)_4(NH_2)_2$	16.5	21.4	—	66.4	320
gem-$N_3P_3H(OPh)(NMe_2)_4$	11.6 [d]	—	23.6	30.2	60
gem-$N_3P_3(OPh)_4(NH_2)_2$	16.5	—	8.7	36.0	321

TABLE A.9 (*cont.*)

Compound	$\delta[P(OR)_2]$	$\delta[P(OR)(NR'R'')]$	$\delta[P(NR'R'')_2]$	$^2J(P-P)$ (Hz)	Refs.
gem-$N_3P_3(OC_6H_4Me-p)_4(NH_2)_2$	16.9	—	13.5	17.7	321
gem-$N_3P_3(OC_6H_4F-p)_4(NH_2)_2$	15.6	—	8.8	38.4	321
gem-$N_3P_3(OC_6H_4Cl-p)_4(NH_2)_2$	15.5	—	8.4	36.9	321
gem-$N_3P_3(OPh)_5(NH_2)$	8.5	18.3	—	76.2	322
gem-$N_3P_3[OC_6H_4(OMe)-p]_5(NH_2)$	10.0	19.0	—	72.8	322
$N_3P_3(OC_6H_4Me-p)_5(NMe_2)$	9.0	20.7	—	74.1	22
cis-$N_3P_3(OC_6H_4Me-p)_4(NMe_2)_2$	8.9	20.7	—	71.8	22
trans-$N_3P_3(OC_6H_4Me-p)_4(NMe_2)_2$	8.8	20.5	—	70.0	22
nongem-$N_3P_3(OC_6H_4Me-p)_3(NMe_2)_3$	—	20.0	—	—	22
cis-$N_3P_3(OC_6H_4Me-p)_2(NMe_2)_4$	—	20.6	26.2	49.5	22
trans-$N_3P_3(OC_6H_4Me-p)_2(NMe_2)_4$	—	20.6	25.9	48.8	22
$N_3P_3(OC_6H_4Me-p)(NMe_2)_5$	—	21.6	25.9	47.5	22

[a]*Cis–trans* mixture; [b]thf solvent; [c]$C_3H_3N_2$ = imidazolyl; [d]$P(H)(OPh)$.

TABLE A.10

^{31}P NMR data for spirocyclic derivatives of cyclotriphosphazenes.

Compound	$\delta(P_{spiro})$	$\delta(PX_2/PR_2)$	$^2J(P–P)$ (Hz)	Refs.
$N_3P_3F_4[O(CH_2)_3O]^a$	15.2	9.0	—	73
$N_3P_3F_4[HN(CH_2)_3O]^a$	15.1	10.2	—	73
$N_3P_3F_4[(Me)N(CH_2)_2O]^a$	30.6	14.0	—	73
$N_3P_3F_4[HN(CH_2)_2NH]^a$	30.1	10.2	—	73
$N_3P_3F_4[HN(CH_2)_3NH]^a$	16.3	10.6	ca. 95	73
$N_3P_3F_2[HN(CH_2)_3O]_2{}^{a,b}$	17.7	10.1	84.0	73
	17.7	9.2	84.0	
$N_3P_3F_2[(Me)N(CH_2)_2O]_2{}^a$	31.6	14.4	98.0	73
$N_3P_3F_2[HN(CH_2)_3NH]_2{}^a$	17.1	10.1	74.0	73
$N_3P_3Cl_4[O(CH_2)_2O]$	23.8	22.5	67	94, 351
$N_3P_3Cl_2[O(CH_2)_2O]_2$	30.3	30.3	—	323
$N_3P_3[O(CH_2)_2O]_3$	36.5			323
$N_3P_3(OMe)_4[O(CH_2)_2O]^c$	31.9	17.0	79.5	94
$N_3P_3(NMe_2)_4[O(CH_2)_2O]$	35.9	27.9	52.3	84
$N_3P_3Cl_4[OCH(Me)CH_2O]^c$	24.3	24.3		94
$N_3P_3Cl_4[OCHClCH_2O]^c$	25.1	25.1		94
$N_3P_3Cl_4[O(CHCl)_2O]^c$	24.9	24.9		94
$N_3P_3Cl_4[O(CCl_2)_2O]^c$	26.6	11.1	79.2	94
$N_3P_3Cl_4[OCCl(Me)CHClO]^c$	15.3	20.3	70.0	94
$N_3P_3Cl_4[O(CH_2)_3O]^c$	2.2	23.0	70.8	94
$N_3P_3Cl_2[O(CH_2)_3O]_2$	8.3	25.9	70.6	323
$N_3P_3[O(CH_2)_3O]_3$	13.2			323
$N_3P_3[OCH_2CH(CH_2Cl)O]_3{}^c$	30.0			94
$N_3P_3Cl_4[O(CH_2)_4O]^c$	9.3	23.0	74.3	94
$N_3P_3Cl_4[OCHCl(CCl_2)_3O]^c$	−9.7	19.5	79.9	94
	−17.1	18.2	88.7	
$N_3P_3(OC_6H_4O-o]_3{}^{d,e}$	10.8			324
$N_3P_3Cl_4[O(C_{10}H_6)_2O]^f$	13.6	24.3	71.0	325
$N_3P_3Cl_4[O(C_{10}H_6)_2O]^g$	15.0	23.5	71.0	325
$N_3P_3Cl_2[O(C_{10}H_6)_2O]_2{}^g$	20.3	28.6	57.3	325
$N_3P_3Cl_2(OPh)_2[O(C_{10}H_6)_2O]^{f,h}$	22.6	18.3	108.5	326
$N_3P_3Cl_2(OPh)_2[O(C_{10}H_6)_2O]^{g,h}$	22.1	17.0	—	326
$N_3P_3(OPh)_4[O(C_{10}H_6)_2O]^f$	28.2	8.6	91.6	326
$N_3P_3(OPh)_4[O(C_{10}H_6)_2O]^g$	26.1	8.8	91.8	326
$N_3P_3Cl_2[OC_8H_{12}O]_2{}^i$	7.2	24.0	—	327
$N_3P_3[OC_8H_{12}O]_3{}^i$	13.8	—	—	327
$N_3P_3Cl_4[O(CH_2)_2NH]$	24.3	24.9	53.9	328
$N_3P_3Cl_2[O(CH_2)_2NH]_2$	29.0	29.0		71
gem-$N_3P_3Cl_2Ph_2[O(CH_2)_2NH]$	25.8	22.9^j	39.3^l	71
		20.8^k	21.1^m	
			21.3^n	
gem-$N_3P_3Cl_2(NHBu^t)_2[O(CH_2)_2NH]$	27.1	23.3^j	58.6^l	71
		6.7^k	51.2^m	
			55.0^n	

TABLE A.10 (cont.)

Compound	$\delta(P_{spiro})$	$\delta(PX_2/$ $PR_2)$	$^2J(P-P)$ (Hz)	Refs.
$N_3P_3(NMe_2)_4[O(CH_2)_2NH]$	36.5	27.3	46.0	71
$N_3P_3Cl_4[O(CH_2)_2N(Me)]$	22.4	25.1	53.9	98
$N_3P_3Cl_2[O(CH_2)_2N(Me)]_2$	28.5	30.7	62.3	98
$N_3P_3[O(CH_2)_2N(Me)]_3$	25.4(2)^o 33.6(1)		58.6	98
$N_3P_3(OMe)_4[O(CH_2)_2N(Me)]$	33.7	21.9	67.5	98
gem-$N_3P_3Cl_2(NHBu^t)_2[O(CH_2)_2N(Me)]$	25.3	25.3^j 7.7^k	53.0	84
$N_3P_3(NMe_2)_4[O(CH_2)_2N(Me)]$	32.5	28.3	46.0	98
$N_3P_3Cl_4[O(CH_2)_3NH]$	7.2	22.4	54.0	73, 328
$N_3P_3Cl_2[O(CH_2)_3NH]_2^b$	12.7 12.5	23.8 23.7	50.5 53.8	73
$N_3P_3Ph_4[N(Me)C(O)N(Me)]$	11.9	21.1	13.0	259
$N_3P_3Cl_4[HN(CH_2)_2NH]$	22.8	23.5	45.7	71, 328
gem-$N_3P_3Cl_2Ph_2[HN(CH_2)_2NH]$	25.3	21.4^j 18.9^k	31.8^l 18.5^m 23.7^n	71
gem-$N_3P_3Cl_2(NHBu^t)_2[HN(CH_2)_2NH]$	26.0	22.2^j 6.0^k	49.2^l 54.0^m 54.8^n	71
$N_3P_3(NMe_2)_4[HN(CH_2)_2NH]$	35.5	26.7	40.0	71
$N_3P_3Cl_4[N(Me)(CH_2)_2N(Me)]$	20.4	23.8	41.8	97, 328
$N_3P_3Cl_2[N(Me)(CH_2)_2N(Me)]_2$	24.9	29.1	54.0	97, 328
$N_3P_3[N(Me)(CH_2)_2N(Me)]_3$	29.4			97
$N_3P_3Cl_4[HN(CH_2)_3NH]$	7.5	21.5	45.5	92, 93, 95
$N_3P_3Cl_2[HN(CH_2)_3NH]_2$	12.3	23.1	43.7	84, 93
$N_3P_3(NMe_2)_4[HN(CH_2)_3NH]$	17.8	26.7	39.8	84
$N_3P_3Cl_4[HN(CH_2)_4NH]$	12.8	21.2	46.0	93, 96
$N_3P_3(NMe_2)_4[HN(CH_2)_4NH]$	21.3	25.4	40.0	84
$N_3P_3Cl_4[HNC_6H_4NH$-$o]^p$	19.0	19.0		324
$N_3P_3[HNC_6H_4NH$-$o]_3$	22.0			324

^{a} $^1J(P-F) = 900-990\,Hz$; ^{b} cis and $trans$ mixture; ^{c} Cl_3CNO_2 solvent; ^{d} DMF (100 °C); ^{e} 1,2-phenylenedioxy; ^{f} 1,1'-dioxy-2,2'-binaphthyl; ^{g} 2,2'-dioxy-1,1'-binaphthyl; ^{h} 2,4:2,4:6,6 structure; ^{i} cyclohexene-4,4'-di(oxymethyl); ^{j} $\underline{P}Cl_2$; ^{k} $\underline{P}R_2$; ^{l} $J[\underline{P}(spiro)-\underline{P}Cl_2]$; ^{m} $J[\underline{P}(spiro)-\underline{P}R_2]$; ^{n} $J[\underline{P}Cl_2-\underline{P}R_2]$; ^{o} relative intensities in parentheses; ^{p} thf solvent.

TABLE A.11(a)

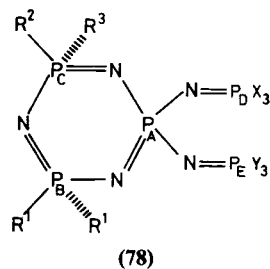^{31}P NMR data for (phosphazenyl)cyclotriphosphazenes (77):

(77)

R¹	R²	R³	R⁴	R⁵	X	δ^a A	B	C	D	J(Hz) AB	AC	BC	CD	AD/BD	Refs.
Cl	Cl	Cl	Cl	Cl	Cl	20.5	20.5	−2.2	−3.3	—	58.4	58.4	40.0	9.5	102
Cl	Cl	Cl	Cl	Cl	Me	20.9	20.9	1.1	25.4	—	44.5	44.5	16.0	7.5	134, 167
Cl	Cl	Cl	Cl	Cl	OPr^i	20.5	20.5	−5.3	−8.2	—	50.2	50.2	69.4	8.3	167
Cl	Cl	Cl	Cl	Cl	NMe$_2$	19.4	19.4	−8.2	22.3	—	47.6	47.6	62.0	4.0	167
Cl	Cl	Cl	Cl	Cl	Me$_2$,Ph	19.6	19.6	0.5	19.6	—	46.0	46.0	20.0	—	167
F	F	F	F	F	Ph	10.2	10.2	7.4	16.4	—	—	—	47.3	—	135, 136
F	OMe	OMe	OMe	OMe	Ph	20.64	20.64	13.34	11.73	—	78.0	78.0	44.5	—	47
Cl	Cl	Cl	Cl	Cl	Ph	20.3	20.3	0.1	15.4	—	47.5	47.5	27.8	3.4	134, 137
Cl	Cl	Cl	Cl	OMe	Ph	23.75	20.38	4.53	14.76	75.8	52.4	59.4	28.8	3.0/4.5	47
Cl	Cl	Cl	OMe	Cl	Ph	23.90	20.75	5.08	15.02	72.0	54.8	56.0	27.5	3.5/3.7	47
Cl	Cl	OMe	Cl	OMe	Ph	24.20	24.20	8.44	13.97	—	63.8	63.8	29.6	4.5	47
Cl	Cl	Cl	OMe	OMe	Ph	c	13.01	8.74	13.95	74.1	56.6	67.5	29.6	4.0	47
OMe	Cl	Cl	Cl	OMe	Ph	23.5	21.40	5.20	13.80	74.0	55.1	63.1	41.1	<2.0	47
OMe	Cl	Cl	OMe	Cl	Ph	23.5	21.80	4.40	13.90	74.0	52.7	64.1	40.5	<2.0	47
OMe	Cl	Cl	OMe	OMe	Ph	24.50	13.92	7.03	11.73	74.1	56.6	67.7	39.0	<1.0	47
OMe	OMe	Cl	OMe	OMe	Ph	28.56	17.24	10.00	11.00	79.3	66.9	68.4	38.1	3.1/5.0	47
OMe	OMe	OMe	OMe	OMe	Ph	21.01	21.01	13.48	9.42	—	70.9	70.9	37.0	2.0	51

R¹	R²	R³	R⁴	R⁵	X	δ^a A	B	C	D	J (Hz) AB	AC	BC	CD	AD/BD	Refs.
OEt	Cl	Cl	Cl	Cl	Ph	18.5	18.5	−1.6	13.5	—	49.5	49.5	39.0	0.9	134
NH₂	Cl	Cl	Cl	Cl	Ph	18.3	18.3	−4.9	13.4	—	45.6	45.6	29.4	—	137, 138
NHMe	Cl	Cl	Cl	Cl	Ph	18.2	18.2	0.8	13.5	—	41.2	41.2	27.9	—	23
Cl	Cl	Cl	Cl	NHMe	Ph	21.3	23.3	3.6	13.5	52.6	47.1	44.1	27.9	3.5	23
Cl	Cl	Cl	NHMe	Cl	Ph	21.2	23.4	4.1	13.6	52.7	44.1	42.7	26.5	3.5	23
NHBuᵗ	Cl	Cl	Cl	Cl	Ph	15.9	15.9	−5.9	10.7	—	42.7	42.7	26.5	—	23
NHBuᵗ	NHBuᵗ	NHBuᵗ	Cl	Cl	Ph	5.0	15.0	−6.2	11.2	49.3	14.7	38.2	20.6	—	23
NC₂H₄	Cl	Cl	Cl	Cl	Ph	18.09	18.09	10.32	14.43	—	34.2	34.2	24.7	<1.0	48
Cl	Cl	Cl	NC₂H₄	Cl	Ph	23.81	34.38	5.54	14.63	46.7	46.7	40.8	27.4	<1.0	48
Cl	Cl	Cl	NC₂H₄	NC₂H₄	Ph	24.63	35.28	8.75	13.02	39.0	49.4	34.1	29.4	3.0/3.0	48
NC₂H₄	Cl	Cl	NC₂H₄	Cl	Ph	21.38	33.84	13.17	11.63	36.9	33.5	33.2	26.2	<1.0	48
NC₂H₄	Cl	Cl	NC₂H₄	NC₂H₄	Ph	23.01	35.04	13.71	10.06	36.5	36.5	36.5	23.4	<1.0	48
NC₂H₄	Cl	NC₂H₄	NC₂H₄	NC₂H₄	Ph	41.61	37.10	16.66	7.87	35.5	35.3	35.1	25.0	<1.0	48
NC₂H₄	NC₂H₄	NC₂H₄	NC₂H₄	NC₂H₄	Ph	37.38	37.38	18.69	7.77	—	34.7	34.7	19.5	<1.0	48
NMe₂	Cl	Cl	Cl	Cl	Ph	16.6	16.6	3.9	12.8	—	36.8	36.8	28.0	<0.1	23, 134
Cl	Cl	Cl	Cl	NMe₂	Ph	21.4	25.5	3.2	13.1	57.4	48.5	42.0	28.0	—	23
Cl	Cl	Cl	NMe₂	Cl	Ph	21.4	26.4	4.4	14.6	56.9	46.4	42.9	26.2	5.3/3.3	23
NMe₂	NMe₂	Cl	Cl	Cl	Ph	26.9	18.4	7.0	11.4	60.3	40.0	30.9	27.9	—	23
NMe₂	NMe₂	NMe₂	Cl	Cl	Ph	21.3	21.3	9.8	8.6	—	44.9	44.9	20.6	—	23
NMe₂	NMe₂	NMe₂	NMe₂	NMe₂	Ph	25.1	25.1	15.3	4.5	—	39.7	39.7	20.6	—	23
NEt₂	Cl	Cl	Cl	Cl	Ph	16.0	16.0	1.0	12.4	—	37.4	37.4	27.9	—	23
Cl	Cl	Cl	NEt₂	Cl	Ph	20.3	22.5	4.3	14.3	58.8	49.1	42.6	26.5	4.9	23
NEt₂	NEt₂	Cl	Cl	Cl	Ph	23.1	17.3	4.6	10.8	63.2	38.2	35.3	26.5	—	23
NC₅H₁₀	Cl	Cl	Cl	Cl	Ph	16.6	16.6	1.9	13.0	—	35.3	35.3	26.5	—	23
Cl	Cl	Cl	NC₅H₁₀	Cl	Ph	20.4	22.4	4.2	13.8	57.7	45.8	42.0	26.5	—	23
NC₅H₁₀	NC₅H₁₀	Cl	Cl	Cl	Ph	23.5	18.2	5.3	10.9	60.3	36.8	30.9	25.0	—	23
Ph	Cl	Cl	Cl	Cl	Ph	16.1	16.1	14.4	2.9	—	21.9	21.9	5.8	−0.4	134

[a] Values quoted to two significant decimal places obtained from spectra recorded at 162 MHz. [b] $^1J(P_C-F) = 845$ Hz; $^3J(P_D-F) = 18.1$ Hz; $^3J(P_A-F)$ = $^3J(P_B-F) < 15.0$ Hz. [c] Could not be measured owing to overlap with signals arising from isomers present in the sample.

TABLE A.11(b)

^{31}P NMR of bis(phosphazenyl)cyclotriphosphazenes (78):

(78)

R^1	R^2	R^3	X	Y	δ P$_A$	P$_B$	P$_C$	P$_D$	P$_E$	^2J(A–B) (Hz)	^2J(A–D) (Hz)	Refs.
Cl	Cl	Cl	Cl	Cl	−20.4	17.5	17.5	−13.5	−13.5	61.0	35.5[a]	102, 103
Cl	Cl	Cl	Cl	Ph	−20.3	18.5	18.5	19.0	−11.8	27.0[b]	—	103
Cl	Cl	Cl	Ph	Ph	−10.9	13.4	13.4	5.9	5.9	35.8	20.6	137, 138
Cl	Cl	NMe$_2$	Ph	Ph	−8.0	15.5	24.4	4.28	4.34	37.6[c]	22.5	138
Cl	NMe$_2$	NMe$_2$	Ph	Ph (78a)	−4.7	18.9	20.5	1.8	1.8	43.4[d]	16.6	138
			(78a).HCl		−11.0	15.4	21.5	8.8	8.8	21.1[e]	13.8	138
NMe$_2$	NMe$_2$	NMe$_2$	Ph	Ph (78b)	1.9	25.0	25.0	2.6	2.6	40.1	10.3	138
			(78b).HCl		6.0	19.6	21.9	5.9	5.9	29.5[f]	11.6	138
			(78b).2HCl		−14.2	18.9	18.9	10.2	10.2		16.6[b]	138

^{a}^4J(C–D) = 4.2 Hz. ^{b}Insufficient resolution for other couplings. ^{c}^2J(A–C) = 36.3; ^2J(B–C) = 59.5; ^2J(A–E) = 19.3 Hz. ^{d}^2J(A–C) = 39.7; ^2J(B–C) = 47.7 Hz. ^{e}^2J(A–C) = 18.2; ^2J(B–C) = 40.4 Hz. ^{f}^2J(A–C) = 26.1; ^2J(B–C) = 38.9 Hz.

TABLE A.11(c)

^{31}P NMR data for other (phosphazenyl)cyclotriphosphazenes.[a]

Compound	$\delta(\underline{P}X_2)$	$\delta[\underline{P}(X)(NPX_3)]$	$\delta(N\underline{P}X_3)$	$J(P–P)$ (Hz)
$N_3P_3F_5[NPCl_2(NHSiMe_3)]$	9.5	4.0	6.0	
$N_3P_3F_5[NPF_2(NHSiMe_3)]$	9.0	3.0	−3.5	
$N_3P_3F_5[NPCl_2(NPCl_3)]$	9.0	3.0	4.5	33.0[d]
			−18.0[b]	
$N_3P_3F_5[NPF_2(NPCl_3)]$	8.5	4.0	8.5	78.0[e]
			−28.0[c]	
$N_3P_3F_5[NPCl_2(NPCl_2.NPCl_3)]$	9.0	3.0	7.5	31.0[d]
			16.0[b]	
			18.0[b]	
$N_3P_3F_5[NPF_2(NPCl_2.NPCl_3)]$	9.0	3.0	6.5	38.0[d]
			−25.0[c]	
			−13.0[b]	78.0[f]
$N_3P_3Cl_5[NP(Ph)(NPPh_3)_2]^g$	19.8	−5.1	−9.6	
			−5.1[h]	

[a]From ref. 166, which includes data for other similar compounds — data for a few selected compounds given here. [b]exocyclic $\underline{P}Cl_2$; [c]exocyclic $\underline{P}F_2$; [d]$\underline{P}Cl_2$–$\underline{P}Cl_3$; [e]$\underline{P}F_2$–$\underline{P}Cl_2$; [f]$\underline{P}F_2$–$\underline{P}Cl_2$; [g]ref. 329; [h]$\underline{P}(Ph)$.

TABLE A.12

^{31}P NMR data for carboranyl phosphazenes.[a]

(79a) (79b)

(80a) (80b)
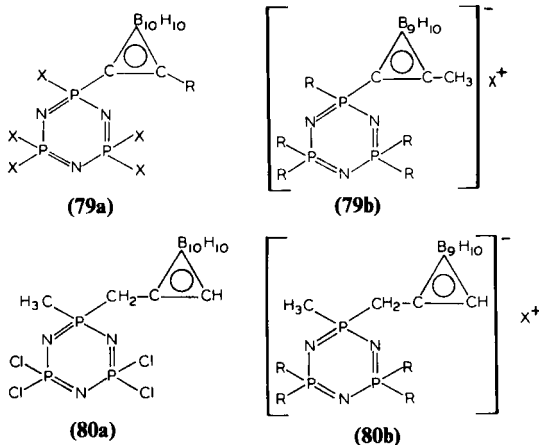
Compound	$\delta(P_A)$[b]	$\delta(P_B)$
$N_3P_3Cl_5[C_2(R)B_{10}H_{10}]$ (79a)[c,d]	—— 19.0[e] ——	
$N_3P_3(OCH_2CF_3)_5[C_2(R)B_{10}H_{10}]$ (79a)[c,d]	26.0	13.0
gem-$N_3P_3(NC_5H_{10})_5[C_2(Me)B_9H_{10}]^-[H_2NC_5H_{10}]^+$ (79b)[f]	22.0	14.0
gem-$N_3P_3Cl_4(Me)[CH_2(C_2HB_{10}H_{10})]$ (80a)[c]	30.0	19.0
gem-$N_3P_3(NC_5H_{10})_4(Me)[CH_2(C_2HB_9H_{10})]^-H^+$ (80b)[f,g]	39.4	13.5
gem-$N_3P_3(NC_5H_{10})_4(Me)[CH_2(C_2HB_9H_{10})]^-[NHEt_3]^+$ (80b)[f]	34.0	17.0
gem-$N_3P_3(NC_5H_{10})_4(Me)[CH_2(C_2HB_9H_9)]^{2-}2Na^+$ (80b)[f]	32.2	19.0

[a] From refs. 268 and 330; solvent thf. [b] Carborane-linked phosphorus. [c] o-carboranyl derivative. [d] R = Me or Ph. [e] Centre of AB_2 spectrum. [f] nido-carboranyl derivative. [g] In CDCl$_3$, ABB' spectrum; $\delta_A = 39.5$, $\delta_B = 14.5$, $\delta_{B'} = 13.6$.

TABLE A.13

^{31}P NMR data for oxocyclophosphazadienes and their salts:

(81)

Compound							^2J(P–P)	
R^1	R^2	Y	Solvent	δ[P(2)]	δ[P(4)]	δ[P(6)]	(Hz)	Refs.
NH$_2$	NH$_2$	NH$_2$	H$_2$O	—— 14.5 ——		5.2	31.4	106
NHMe	NHMe	NHMe	EtOH/H$_2$O	—— 19.2 ——		7.7	28.5	106
N$_2$C$_3$H$_3$ ^{a}	N$_2$C$_3$H$_3$	N$_2$C$_3$H$_3$	THF	—— −9.5 ——		−1.9	52.5	286
NHCH$_2$CO$_2$Et	NHCH$_2$CO$_2$Et	NHCH$_2$CO$_2$Et	EtOH	—— 15.3 ——		3.6	33.0	106
			Et$_2$O	—— 15.0 ——		2.6	39.6	106
NHCH$_2$CONHMe	NHCH$_2$CONHMe	NHCH$_2$CONHMe	EtOH	—— 16.9 ——		5.4	31.4	106
Cl	NEt$_2$	NEt$_2$	CDCl$_3$	13.7	19.7	0.1	33.8^b 13.3 42.7	149
OMe	NHBu^t	OMe	CD$_2$Cl$_2$	8.3	13.7	3.1	24.3^b 63.7 63.7	149
			C$_6$D$_5$NO$_2$	7.8	13.9	0.9	23.5^b 60.3 63.2	153
OEt	NHBu^t	OEt	CD$_2$Cl$_2$	7.3	10.2	1.2	25.1^b 58.8 63.2	149

OMe	OMe, NPPh$_3$[c]	OMe	CDCl$_3$[e]	14.45	7.18	2.65	62.0[b] 28.4 67.0	51
OMe	OMe, NPPh$_3$[d]	OMe	CDCl$_3$[e]	14.06	7.11	3.15	62.3[b] 26.0 68.0	51
OMe	OMe	OMe	CD$_2$Cl$_2$	—— 14.9 ——		2.1	48.8	149
			CDCl$_3$				30.9[b]	153
			(−40 °C)	15.8	12.7	1.9	67.7 75.0	
			CD$_2$Cl$_2$ (−95 °C)	15.8	12.3	1.1	30.8[b] 69.2 80.0	149
OCH$_2$CF$_3$	OCH$_2$CF$_3$	OCH$_2$CF$_3$	Et$_2$O	—— 19.2 ——		11.2	71.5	106
OPh	OPh	OPh	CDCl$_3$	—— 2.4 ——		−5.8	52.2	149
			CD$_2$Cl$_2$ (−84 °C)	6.2	0.4	−6.1	38.2[b] 73.5 79.4	149
OC$_6$H$_4$F-p	OC$_6$H$_4$F-p	OC$_6$H$_4$F-p		—— 4.7 ——		−3.5		302
OC$_6$H$_4$Cl-p	OC$_6$H$_4$Cl-p	OC$_6$H$_4$Cl-p		—— 4.1 ——		−4.7		302
NMe$_2$	NMe$_2$	OC$_6$H$_4$Me-p	CDCl$_3$	—— 22.5 ——		−5.1	30.1	332
Ph	Ph	Ph	CDCl$_3$ (ambient)	24.0	16.7	2.7	—	111
			CDCl$_3$ (−50 °C)	24.7	17.2	3.7	2.5, 5.5	111
OMe	Ph	OMe	CDCl$_3$[f] (−50°C)	23.7	13.8	1.1	54.4[b] 10.3 30.9	146, 149
				16.6	15.9	2.3	17.7[b,g] 18.9 30.0	146, 149
			C$_6$D$_5$NO$_2$ (100 °C)	18.8	14.4	−0.5	13.2[h] 36.8 29.4	153

TABLE A.13 (*cont.*)

Compound							^2J(P–P)	
R^1	R^2	Y	Solvent	δ[P(2)]	δ[P(4)]	δ[P(6)]	(Hz)	Refs.
OEt	Ph	OEt	CDCl$_3$ [f] (−40 °C)	22.4	10.5	−1.1	53.0[b] 10.3 30.1	149, 216[a]
				14.6	12.1	0.6	16.2[b,g] 19.1 29.4	149, 216[a]
OPr^n	Ph	OPr^n	CDCl$_3$ [f] (−40 °C)	22.3	11.1	−0.6	51.5[b] 9.6 30.8	149
				15.9	12.8	1.1	14.7[b,g] 17.7 29.4	

Ph	Ph	OMe		24.0	18.0	−2.1		149
Ph	Ph	Me	$C_6H_5NO_2$	—— 18.2 ——		9.1		155
Ph	Ph	OPh	$C_6H_5NO_2$	21.4	14.7	−7.0		155
Ph	Ph	Me, OMe[i]	CH_2Cl_2	—— 21.1 ——		31.4		155
Ph	Ph	Me[j]	CH_2Cl_2	14.3	31.0	12.9		155
Ph	Ph	[C_6H_4(OMe)-p]	CH_2Cl_2	—— 21.6 ——		45.8[k]		317
Cl	Cl, O⁻	Cl[l]	$CDCl_3$	18.6		−4.2	35.1	154
Cl	Cl, O⁻	Cl[m]	$CDCl_3$	15.4		−5.1	41.5	154
Cl	Cl	Cl[n]	$CDCl_3$	—— 21.1 ——		−1.9	44.0	331
Cl	Cl	NHPh	$CDCl_3$	—— 16.7 ——		−9.6	43.9	332
Cl	Cl	[NHC_6H_4Me-p][n]	$CDCl_3$	—— 16.7 ——		−8.5	43.1	332
Cl	Cl	[NHC_6H_4(OMe)-p][n]	$CDCl_3$	—— 16.9 ——		−6.5	43.4	332
Cl	Cl	[OC_6H_4(CN)-p][n]	$CDCl_3$	—— 18.5 ——		−6.9	—	333

[a] Imidazolyl. [b] The three coupling constants quoted in the order P(2)–P(6), P(4)–P(6) and P(2)–P(4). [c] Isomer with $NPPh_3$ *cis* to P=O; other data are $\delta(\underline{P}Ph_3) = 14.32$, $^2J(P–P) = 33.7$ Hz (see structure **4**). [d] Isomer with $NPPh_3$ *trans* to P=O; other data are $\delta(\underline{P}Ph_3) = 13.20$, $^2J(P–P) = 36.5$ Hz (see structure **4**). [e] 162 MHz spectrum. [f] Broad featureless signals at ambient temperature. [g] Tautomeric form with proton at N(1). [h] Rapid exchange of proton between N(1) and N(5). [i] [P(6)Me(OMe)]⁺, Cl⁻ salt. [j] N(5)Me derivative. [k] P(6) = S. [l] [$AsPh_4$]⁺ salt, *cis* isomer. [m] [$AsPh_4$]⁺ salt, *trans* isomer. [n] [Et_3NH]⁺ salt.

TABLE A.14

^{31}P NMR data for halogeno- and pseudohalogenocyclotetraphosphazenes.

Compound	$\delta(P)$	$^2J(P-P)$ (Hz)	Refs.
$N_4P_4F_8$	-17.7	155.0	210
$N_4P_4Cl_8$	-6.5	>69.0	210
$N_4P_4Br_8$	-69.9	27.2	210
$N_4P_4(NCS)_8$	-49.1		7
$N_4P_4(N_3)_8$	-8.9		278
$N_4P_4Cl_7F$	$-6.6, -11.2^a$		168

^{a} $\underline{P}ClF$.

TABLE A.15

^{31}P NMR data for alkyl(aryl)cyclotetraphosphazenes.

Compound	Structure^a	$\delta(PR_2)$	$\delta(PRX/PX_2)$	$^2J(P-P)$ (Hz)	Refs.
$N_4P_4F_7Me$			$-12.9^b, 25.6$		222
$N_4P_4F_6Me_2$	2, 2	19.3	-14.2		222
$N_4P_4F_5Me_3$	2, 2, 6	18.6	$22.4^c, -13.5$		222
$N_4P_4F_5Me_3$	2, 2, 4	17.1	$22.3^c, -13.7$		222
$N_4P_4F_4Me_4$	2, 2, 6, 6	19.5	-8.5		222

	^{a}				
$N_4P_4F_7(C_4H_3NMe)^d$			$0.7, -15.6^b$		197
$N_4P_4Cl_7Me$			$-7.8^e, -4.5^f$	32.8^g	257
			12.8	$<2^h$	
$N_4P_4Cl_6(H)Me$	i		$-6.4^f, 4.3$	26.3^j	257
$N_4P_4Me_6(CH_2COPh)_2$	2, 2, 4, 4, 6, 8	16.9	10.0	—	280
$N_4P_4Me_6(CH_2SiMe_3)_2$	2, 2, 4, 6, 6, 8	17.2	12.7	12	280
$N_4P_4Me_6(CH_2GeMe_3)_2$	2, 2, 4, 6, 6, 8	18.2	12.7	12	280
$N_4P_4Me_6(CH_2SnMe_3)_2$	2, 2, 4, 6, 6, 8	19.5	12.3	12	280
$N_4P_4Me_4(CH_2SiMe_3)_4$	2, 4, 6, 8		12.2		280
$N_4P_4Me_4(CH_2GeMe_3)_4$	2, 4, 6, 8		14.2		280
$N_4P_4Me_4(CH_2SnMe_3)_4$	2, 4, 6, 8		15.8		280
$N_4P_4Me_4(CH_2Br)_4$	2, 4, 6, 8		12.7		280
$N_4P_4Me_4(CH_2I)_4$	2, 4, 6, 8		10.1		280
$N_4P_4Me_4(AsMe_2)_4$	2, 4, 6, 8		12.6		280
$N_4P_4Me_4(AsMe_2)_4.4MeI$			12.6^k		280
$N_4P_4Me_4Et_4$	2, 4, 6, 8		22.9		280
$N_4P_4Me_4Et_4.2HCl$			41.1^k		280
$N_4P_4Me_8$		19.9		10.7	210
		26.1^k			240
$N_4P_4Me_8.MeI$		$28.8, 42.3^k$			240
$N_4P_4Cl_4Ph_4$	2, 2, 4, 4	5.9	-4.5^f	<2	55
$N_4P_4Cl_4Ph_4$	2, 2, 6, 6	2.9	-3.1^f	<2	55
$N_4P_4Me_4Ph_4$	2, 2, 4, 4	3.4, 15.9			239
$N_4P_4Me_4Ph_4.MeI$	2, 2, 4, 4	8.5, 39.0			239
$N_4P_4(NMe_2)_4Ph_4$	2, 2, 6, 6	0.3	15.6	17.5	55
$N_4P_4[O(CH_2)_4OH]_4Ph_4$	2, 4, 6, 8		$8.5, 7.6^l$	—	315

^{a}Disposition of alkyl(aryl)substituent; ^{b} $\underline{P}F_2$; ^{c} $\underline{P}FMe$; ^{d} 1-methyl-pyrrol-2-yl; ^{e} $\underline{P}Cl_2$ adjacent to two $\underline{P}Cl_2$ groups; ^{f} $\underline{P}Cl_2$; ^{g} $\underline{P}Cl_2-\underline{P}Cl_2$; ^{h} $\underline{P}Cl_2-\underline{P}ClMe$; ^{i}contains geminal PHMe; ^{j} $\underline{P}Cl_2-\underline{P}MeH$; ^{k}in D_2O; ^{l}two isomers.

TABLE A.16(a)

^{31}P NMR data for (amino)cyclotetraphosphazenes.

Compound[a]	$\delta(PX_2)$	$\delta(PXR)$	$\delta(PR_2)$	$^2J(P–P)$ (Hz)	Refs.
$N_4P_4Cl_6(NH_2)_2$ (2, 6)	—— -5.8^b ——		—		334
$N_4P_4Cl_4(NH_2)_4$ (2, 2, 6, 6)	-13.1	—	0.0		334
$N_4P_4(NH_2)_8$	—	—	10.0	—	7
$N_4P_4Cl_6(NHMe)_2$ (2-trans-6)	—— -2.2^b ——				72
$N_4P_4(NHMe)_8$	—	—	12.2^c	—	248
$N_4P_4Cl_6(NHEt)_2$ (2-trans-6)	-3.4	-4.9	—	46.0	49
$N_4P_4Cl_4(NHEt)_2(NMe_2)_2$ (2-trans-6:4-trans-8)	—	0.9 5.6^d	—	43.8	250
$N_4P_4Cl_4(NHEt)_4$ (2-cis-4-cis-6-trans-8)		0.9		—	49
$N_4P_4Cl_4(NHEt)_4$ (2-cis-4-trans-6-trans-8)		2.3			49
$N_4P_4(NHEt)_8$			4.3		49
$N_4P_4Cl_6(NHPr^n)_2$ (2-trans-6)	-3.4^b		—		72
$N_4P_4(NHPr^n)_8$	—	—	6.5	—	235
$N_4P_4(NHC_3H_5)_8$ [e]	—	—	5.5	—	323
$N_4P_4Cl_6(NHPr^i)_2$ (2-trans-6)	-4.0	-7.4	—	38.3	72
$N_4P_4(NHPr^i)_8$	—	—	1.1	—	235
$N_4P_4Cl_6(NHBu^n)_2$ (2-trans-6)	-3.4	-4.6	—	40.0	72
$N_4P_4(NHBu^n)_8$	—	—	6.9	—	235
$N_4P_4Cl_6(NHBu^t)_2$ (2, 4)	-8.7	-7.3	—	37.4^f 33.9^g 33.0^h -0.7^i	233
$N_4P_4Cl_6(NHBu^t)_2$ (2-trans-6)	-5.8	-10.6	—	38.1	232
$N_4P_4(NHBu^t)_8$	—	—	-3.1	—	232
$N_4P_4Cl_6(NHCH_2Bu^t)_2$ (2-trans-6)	—— -4.2^b ——		—	—	335
$N_4P_4(NHC_5H_9)_8$ [j]	—	—	1.9	—	323
$N_4P_4Cl_6(NHCH_2Ph)_2$ (2, 4)	-6.1	-0.8	—	38.1^f 36.9^g 33.3^h -1.1^i	233
$N_4P_4Cl_6(NHCH_2Ph)_2$ (2-trans-6)	-2.9	-5.5	—	39.2	72

TABLE A.16(a) (cont.)

Compound[a]	$\delta(PX_2)$	$\delta(PXR)$	$\delta(PR_2)$	$^2J(P-P)$ (Hz)	Refs.
$N_4P_4(NHCH_2Ph)_8$	—	—	4.8	—	235
$N_4P_4Cl_7(NHPh)$	−11.1	−5.1	—	40.0	214
	−7.7			34.2[h]	
$N_4P_4Cl_6(NHPh)_2$ (2, 4)	−8.5	−5.6	—	43.4[f]	214
				36.7[g]	
				35.4[h]	
$N_4P_4Cl_6(NHPh)_2$ (2-trans-6)	−3.0	−12.0	—	40.3	72
$N_4P_4Cl_6(NHC_6H_3Me_2 − 2, 6)_2$ (2, 6)	−5.9	−11.6	—		336
$N_4P_4Cl_6(NHC_6H_3Me_2 − 3, 5)_2$ (2,6)	−5.6	−13.5	—	—	336
$N_4P_4F_7(NMe_2)$	−15.6	3.3	—	—	160
$N_4P_4F_6(NMe_2)_2(2, 6)$	−15.5	4.3	—	—	160
$N_4P_4Cl_6(NMe_2)_2(2-trans-6)$	−3.7	−0.2	—	39.7	55
$N_4P_4Cl_4(NMe_2)_4$ (2-cis-4-trans-6-trans-8)	—	5.2	—		55
$N_4P_4Cl_2(NMe_2)_6$ (2-trans-6)	—	4.4	9.9	47.1	55
$N_4P_4(NMe_2)_8$	—	—	9.6	—	55
			10.0	60.2	211
$N_4P_4Cl_7(NC_2H_4)$	−7.2[k]	8.6	—	27.6	27
	−4.7			30.6[h]	
$N_4P_4Cl_6(NC_2H_4)_2$ (2, 2)	−6.5[k]	—	18.8	11.6	27
	−5.9			26.1[h]	
$N_4P_4Cl_6(NC_2H_4)_2$ (2-trans-4)	−4.9	11.8	—	25.4[f]	27
				31.1[h]	
				27.6[g]	
				−0.9[i]	
$N_4P_4Cl_6(NC_2H_4)_2$ (2-cis-4)	−5.0	10.3	—	27.1[f]	27
				32.7[h]	
				29.2[g]	
				−0.8[i]	
$N_4P_4Cl_6(NC_2H_4)_2$ (2-trans-6)	−1.9	8.4	—	27.9	27
$N_4P_4Cl_6(NC_2H_4)_2$ (2-cis-6)	−2.6	8.7	—	28.4	27
$N_4P_4Cl_2(NC_2H_4)_6$ (2-trans-6)	—	13.7	19.5	24.3	27
$N_4P_4(NC_2H_4)_8$	—	—	17.8	—	27
$N_4P_4(N_2C_3H_3)_8{}^l$	—	—	−25.5	—	275
$N_4P_4(N_2C_3H_2Me)_8{}^m$	—	—	−25.3	—	275
$N_4P_4(N_2C_3HMe_2)_8{}^n$	—	—	−18.8	—	275
$N_4P_4(NC_4H_8)_8$	—	—	0.8	—	323

TABLE A.16(a) (*cont.*)

Compound[a]	$\delta(PX_2)$	$\delta(PXR)$	$\delta(PR_2)$	$^2J(P-P)$ (Hz)	Refs.
$N_4P_4Cl_6(NC_4H_8O)_2$ (*nongeminal*)	—— -3.5^b ——		—		7
$N_4P_4(NC_4H_8O)_8$	—	—	4.4	—	323
$N_4P_4Cl_6(NC_5H_{10})_2$ (*nongeminal*)	—— -4.1^b ——		—	—	7
$N_4P_4Cl_4(NC_5H_{10})_4$ (2, 4, 6, 8)	—	1.7	—	—	337
$N_4P_4Cl_6(NMePh)_2$ (2-*trans*-4)	-7.2	-3.2	—	41.6^f 44.0^g 32.8^h -0.8^i	233
$N_4P_4Cl_6(NMePh)_2$ (2-*trans*-6)	—— -5.3^b ——		—		219
$N_4P_4Cl_4(NMePh)_4$ (2-*cis*-4-*trans*-6-*trans*-8)	—	-2.2	—		338
$N_4P_4Cl_4(NMePh)_4$ (2-*cis*-4-*cis*-6-*trans*-8)	—	-2.1	—		219
$N_4P_4Cl_4(NMePh)_4$ (2-*trans*-4-*cis*-6-*trans*-8)	—	-1.4	—	—	125
$N_4P_4Cl_4(NMePh)_4$ (2, 2, 6, 6)	-11.5	—	-5.4	37.1	219
$N_4P_4Cl_6[N(CH_2Ph)_2]_2$ (2, 4)	-6.8	-0.2	—	38.1^f 40.0^g 36.9^h -1.0^i	220
$N_4P_4Cl_6[N(CH_2Ph)_2]_2$ (2-*trans*-6)	—— -3.9^b ——		—		220
$N_4P_4Cl_4[N(CH_2Ph)_2]_4$ (2-*cis*-4-*cis*-6-*trans*-8)	—	2.0	—		220
$N_4P_4Cl_4[N(CH_2Ph)_2]_4$ (2-*trans*-4-*cis*-6-*trans*-8)	—	2.0	—		220
$N_4P_4Cl_4[N(CH_2Ph)_2]_4$ (2-*cis*-4-*trans*-6-*trans*-8)	—	2.2	—		220
$N_4P_4Cl_6(MeNCH_2CH_2NMe)^o$	-6.2^k -8.3	—	6.1^q	42.1^h 27.1^p -1.1^i	236
$N_4P_4(NMe_2)_6[NH(CH_2)_3NH]^o$	—	—	1.6^q 7.2 8.9	42.2^r 36.8^s -1.1^i	236
$N_4P_4Cl_7(NPMe_3)$	-11.0 -7.0	-18.9	—	$28.8^{h,t}$	135
$N_4P_4Cl_7(NPPh_3)$	-11.3 -7.4	-19.0	—	u	340
$N_4P_4Cl_6(NPCl_3)_2$ (2, 6)	-8.0	-23.5	—		334

TABLE A.16(a) *(cont.)*

Compound[a]	$\delta(PX_2)$	$\delta(PXR)$	$\delta(PR_2)$	$^2J(P-P)$ (Hz)	Refs.
$N_4P_4Cl_4(NPCl_3)_4$ (2, 2, 6, 6)	-11.4	—	-34.1		334, 339
$N_4P_4Cl_6(NVCl_3)_2$ (2, 2)	-7.3	-3.2	—		339
$N_4P_4F_7(NS_3N_2)^v$	-17.0	-7.0	—		341

[a]Disposition of one set of substituents given within parentheses; [b]$\underline{P}X_2$ and $\underline{P}XR$ not distinguished; [c]in $CDCl_3/CD_3OD$; [d]$\delta[PCl(NMe_2)]$; [e]cyclopropyl derivative; [f]$^2J(\underline{P}Cl_2-\underline{P}ClR)$; [g]$^2J(\underline{P}ClR-\underline{P}ClR)$; [h]$^2J(\underline{P}Cl_2-\underline{P}Cl_2)$; [i]$^4J(P-P)$; [j]cyclopentyl derivative; [k]antipodal PCl_2; [l]pyrazolyl; [m]3-methylpyrazolyl; [n]3,5-dimethylpyrazolyl; [o]spirocyclic compound; [p]$^2J(\underline{P}(spiro)-\underline{P}Cl_2)$; [q]$\delta[P(spiro)]$; [r]$^2J(\underline{P}R_2-\underline{P}R_2)$; [s]$^2J(\underline{P}(spiro)-\underline{P}R_2)$; [t]$\delta(\underline{P}R_3) = 27.3$, $^2J(\underline{P}R_3-\underline{P}Cl) = 14.8$ Hz; [u]$\delta(\underline{P}R_3) = 14.4$, $^2J(\underline{P}R_3-\underline{P}Cl) = 23.5$ Hz; [v]N-(1,2,4,3,5-trithiodiazo(-1-ylidene)amino.

TABLE A.16(b)

^{31}P NMR data for mixed(amino)cyclotetraphosphazenes (82):[a]

(82)
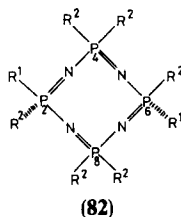
R^1	R^2	$\delta[P(2, 6)]$	$\delta[P(4, 8)]$	$^2J(P-P)$ (Hz)	Refs.
NHMe	NMe_2	10.2	9.4	42.5	72
NHEt	NMe_2	6.8	9.2	41.2	49
NHPr^n	NMe_2	7.2	9.4	41.5	72
NHPr^i	NMe_2	4.6	7.7	41.9	72
NHBu^n	NMe_2	7.4	9.4	41.2	72
NMe_2	NHEt	6.2	3.6	37.5	250
NHBu^t	NHEt	-0.9	2.2	32.4	335
$NHCH_2Ph$	NMe_2	7.1	9.6	40.3	72
NHPh	NMe_2	0.8	11.6	40.8	72
NMePh	NHEt	-0.2	2.6	37.4	335
$N(CH_2Ph)_2$	NHEt	5.6	3.6	39.7	335
NHEt, NHBu^t	NMe_2	$2.0^b, 5.9^c$	8.3	$39.0,^b 41.0^c$	235

[a]Compounds have 2-*trans*-6 structure; [b]$P(2)(NMe_2)(NHBu^t)$, $^2J[P(2)-P(4)]$; [c]$P(6)(NMe_2)(NHEt)$, $^2J[P(4)-P(6)]$.

TABLE A.17

^{31}P NMR data for alkoxy- and aryloxycyclotetraphosphazenes, $N_4P_4X_{8-n}(OR)_n$ (X = Cl, amino).

Compound	Structure	$\delta(PX_2)$	$\delta[PX(OR)]$	$\delta[P(OR)_2]$	$^2J(P–P)$ (Hz)	Refs.
$N_4P_4Cl_6H(OPr^i)$	2,2,4,4,6,6	$\begin{cases} -6.3 \\ -6.5 \end{cases}$	−13.5		18.8^a	257
$N_4P_4(OMe)_8$				$\begin{cases} 2.8 \\ 2.4 \end{cases}$	74.3	80 211
$N_4P_4(OEt)_8$				−0.6		153
$N_4P_4(OCH_2CF_3)_8$				−2.0		342, 343
$N_4P_4(OCH_2CF_3)_6(NMe_2)_2$	2-*trans*-6		8.80	−0.96	65.0	343
$N_4P_4Cl_6(OPh)_2$	2-*trans*-6	−4.69	−11.56		53.7	237
$N_4P_4Cl_6(OPh)_2$	2-*cis*-6	−3.64	−11.16		51.8	237
$N_4P_4Cl_6(OPh)_2$	2,4	−5.10	−9.55		54.9^b 29.0^c 73.0^d −1.2^e	237

$N_4P_4Cl_4(OPh)_4$	2,4,6,8		−9.7			237
$N_4P_4Cl_2(OPh)_6$	2-trans-6		−6.9	−15.1	79.4	237
$N_4P_4(OPh)_8$				$\begin{cases} -12.6 \\ -12.4 \end{cases}$	80.6	237 / 211
$N_4P_4(OC_6F_5)_8$				−10.4		302
$N_4P_4(OC_6H_4F\text{-}p)_8$				−9.0		302
$N_4P_4(NMe_2)_5(OPh)_3$	2,4,6	10.3	2.7(1)		50.5^f	237
			2.9(2)		38.1^q	
			38.1^x		−2.2^e	
$N_4P_4(NMe_2)_2(OPh)_6$	2,6		1.4	−11.6	75.8	237
$N_4P_4(OMe)_6(OPh)_2$	2,6		−6.3	−0.8	78.0	237
$N_4P_4(NMePh)_4(OMe)_4$	2-cis-4-trans-6-trans-8		1.1			219
$N_4P_4(NMePh)_4(OMe)_4$	2-trans-4-cis-6-trans-8		1.7			291
$N_4P_4[N(CH_2Ph)_2]_2(OMe)_6$	2-trans-6		−4.0	1.5	65.0	220
$N_4P_4[N(CH_2Ph)_2]_2(OCH_2CF_3)_6$	2-trans-6		−3.6	5.9	67.0	220

^{a} $^2J[\underline{P}Cl_2–\underline{P}H(OPr^i)]$; ^{b} $^2J[\underline{P}Cl_2–\underline{P}Cl(OPh)]$; ^{c} $^2J[\underline{P}Cl_2–\underline{P}Cl_2]$; ^{d} $^2J[\underline{P}Cl(OPh)–\underline{P}(Cl)(OPh)]$; ^{e} $^4J(P–P)$; ^{f} $^2J[\underline{P}(NMe_2)_2–\underline{P}(NMe_2)(OPh)]$; ^{g} $^2J[\underline{P}(NMe_2)(OPh)–\underline{P}(NMe_2)(OPh)]$.

TABLE A.18

^{31}P data for (alkythio) and (arythio)cyclotetraphosphazenes.

Compound	Structure	$\delta(\underline{P}Cl_2/\underline{P}R_2)$	$\delta(\underline{P}Cl.SR)$	$\delta[\underline{P}(SR)_2]$	$^2J[\underline{P}Cl_2-\underline{P}(SR)_2]$ (Hz)	Other $^2J(P-P)$ (Hz)	Refs.
$N_4P_4Cl_6(SEt)_2$	(2,2)	$\begin{cases}-7.1\\-8.2\end{cases}$		30.4	13.1	30.9[a]	124
$N_4P_4Cl_5(SEt)_3$	(2,2,6)	-8.2	14.6	29.4	17.4	1.5[b]	124
$N_4P_4Cl_5(SEt)_3$	(2,2,4)	$\begin{cases}-8.0\\-8.9\end{cases}$	13.5	29.7	13.5	29.9[a] 1.5[b] 32.4[c]	124
$N_4P_4Cl_4(SEt)_4$	(2,2,66)	-8.8		29.4	11.8		124
$N_4P_4Cl_4(SEt)_4$	(2,2,44)	-8.7		27.9	14.7	$\begin{cases}ca.\,48^a\\ca.\,28^d\end{cases}$	124
$N_4P_4Cl_3(SEt)_5$	(2,2,6)	-9.5	12.2	28.1	11.6	30.1[c]	124
$N_4P_4Cl_3(SEt)_5$	(2,2,4)	$ca.\,-9.4$	$ca.\,12.7$	$ca.\,26.9$			124
$N_4P_4Cl_2(SEt)_6$	(2,2)	-9.5		$\begin{cases}26.9\\26.0\end{cases}$	12.1	33.1[d]	124
$N_4P_4(SEt)_8$				25.1		31.6[d]	124, 238
$N_4P_4Cl_2(NH_2)_2(SEt)_4$	(2,2:6,6:4,4,8,8)	-8.1^e		27.8	11.7	4.0[f]	238
$N_4P_4(NH_2)_4(SEt)_4$	(2,2,6,6)	3.6		27.9		4.4	238
$N_4P_4(OMe)_4(SEt)_4$	(2,2,6,6)	-1.5		28.8		20.0	238
$N_4P_4Cl_2(OEt)_2(SEt)_4$	(2-trans-6:2,6:4,4,8,8)		-5.4^g	29.0		10.6	238
$N_4P_4Cl_2(OEt)_2(SEt)_4$	(2-cis-6:2,6:4,4,8,8)		-5.1^g	28.4		9.6	238
$N_4P_4Cl(OEt)_3(SEt)_4$	(2:2,6,6:4,4,8,8)	-4.2	-5.4^g	28.2	10.1[h]	18.5	238
$N_4P_4(OEt)_4(SEt)_4$	(2,2,6,6)	-4.6		27.7		18.5	238
$N_4P_4Cl_4(SPh)_4$	(2,2,6,6)	-9.5		22.9	17.6		86
$N_4P_4Cl_4(SC_6H_4Cl\text{-}p)_4$	(2,2,6,6)	-10.3		19.9			86

[a] $J(\underline{P}Cl_2-\underline{P}Cl_2)$; [b] $J(\underline{P}Cl_2-\underline{P}Cl(SEt))$; [c] $J[\underline{P}ClSEt-\underline{P}(SEt)_2]$; [d] $J[\underline{P}(SEt)_2-\underline{P}(SEt)_2]$; [e] $\delta[\underline{P}(NH_2)_2]=2.4$; [f] $J[\underline{P}(NH_2)_2-\underline{P}(SEt)_2]$; [g] $\underline{P}Cl(OEt)$; [h] $J[\underline{P}Cl(OEt)-\underline{P}(SEt)_2]$.

TABLE A.19(a)

^{31}P NMR data for cyclopenta and cyclohexaphosphazenes.

Pentamers	$\delta(P)$	Hexamers	$\delta(P)$	Refs.
$N_5P_5F_{10}$	-21.9	$N_6P_6F_{12}$	-22.2	213, 344
$N_5P_5F_9(NMe_2)$	-16.3^a	$N_6P_6F_{11}(NMe_2)$	-17.0^a	160
	3.8		3.7	
$N_5P_5F_8(NMe_2)_2$	-16.3^a	$N_6P_6F_{10}(NMe_2)_2$	-20.7^a ⎫	160
(nongeminal)	4.0	(nongeminal)	3.7 ⎬	
		$N_6P_6F_9(NMe_2)_3$	-16.7^a	160
		$(2,6,10)^b$		
$N_5P_5F_9(C_4H_3NMe)^c$	$-22.1^{a,d}$ ⎫	$N_6P_6F_{11}(C_4H_3NMe)$	$-22.5^{a,d}$ ⎫	197
	-3.7 ⎬		-2.3 ⎬	
$N_5P_5Cl_{10}$	-15.5	$N_6P_6Cl_{12}$	-17.5	207, 352
$N_5P_5Cl_9F$	-16.6 ⎫	$N_6P_6Cl_{11}F$	-15.8 ⎫	168
	$-15.3^{e,f}$ ⎬		$-15.2^{e,g}$ ⎬	
$N_5P_5Me_{10}$	5.6	$N_6P_6Me_{12}$	3.0	344
$N_5P_5(NHBu^n)_{10}$	5.6	$N_6P_6(NHBu^n)_{12}$	4.5	345
$N_5P_5(NMe_2)_{10}$	3.1	$N_6P_6(NMe_2)_{12}$	0.5	213
$N_5P_5(N_2C_3H_3)_{10}^h$	-24.8	$N_6P_6(N_2C_3H_3)_{12}$	-24.6	275
$N_5P_5(N_2C_3H_2Me)_{10}^i$	-24.9	—	—	275
$N_5P_5(OMe)_{10}$	-2.5	$N_6P_6(OMe)_{12}$	-4.2	80
$N_5P_5(OPh)_{10}$	-19.5	$N_6P_6(OPh)_{12}$	-18.5	345

^{a}PF$_2$. ^{b}Disposition of NMe$_2$ groups. ^{c}1-Methylpyrrol-2-yl. $^d\,^2J$(P–N–P) $\approx$ 80 Hz. ^{e}PCl$_2$, averaged. $^{f\,2}J$(P–N–P) = 65 Hz; ^{19}F: δ(PCl$\underline{F}$) = -33.9, ^1J(P–F) = 952 Hz. $^{g\,2}J$(P–N–P) = 48 Hz, ^3J(P–F) = 20 Hz; ^{19}F: δ(PCl$\underline{F}$) = -32.8, ^1J(P–F) = 974 Hz. ^{h}Pyrazolyl. ^{i}3-Methylpyrazolyl.

TABLE A.19(b)

^{31}P NMR data for cyclohepta- and cyclooctaphosphazenes.

Compound	$\delta(P)$	Refs.
$N_7P_7Cl_{14}$	-18.1	213, 352
$N_8P_8Cl_{16}$	-18	9
$N_7P_7(NHBu^n)_{14}$	4.5	345
$N_7P_7(OPh)_{14}$	-21.0	345

TABLE A.20

^{31}P NMR data for *trans*-annular bridged(amino)cyclotetraphosphazenes (83):

(83)

R^1	R^2	R^3	δ[P(2)]	δ[P(6)]	δ[P(4), P(8)]	^2J(P–P)(Hz)			Refs.
NHMe	Me	Me	—— 18.5 ——		21.5	39.0	—	—	248
NHMe	Me	Me^a	—— 15.6 ——		18.0	37.0	—	—	248
NHEt	Et	Et	—— 18.6 ——		15.3	40.9	—	—	247
NHEt	Et	Et^a	—— 14.3 ——		11.8	36.4	—	—	247
NHPr^n	Pr^n	Pr^n	—— 18.5 ——		15.5	41.2	—	—	235
NHPr^i	Pr^i	Pr^i	——— 12.0^b ———						235
NHBu^n	Bu^n	Bu^n	—— 18.7 ——		15.5	41.4	—	—	235
NMe$_2$, NHEt^c	Et	Et	——— 18.6^b ———						250
NMe$_2$, NHEt^d	Et	Et	——— 19.6^b ———						335
NMe$_2$	Et	Et	19.7	18.9	22.5	42.7^e	42.7^f	33.0^g	247
NMe$_2$	Me	Me	20.7	20.6	21.7	44.0^e	43.9^f	32.5^g	235
NMe$_2$	Pr^n	Pr^n	—— 19.5 ——		22.4	43.4			249
NMe$_2$	Bu^n	Bu^n	—— 19.6 ——		22.4	43.3			249
NMe$_2$	Bu^t	Et	19.6	16.1	20.6	46.5^e	41.2^f	34.6^g	235
NMe$_2$	NCH$_2$Ph	CH$_2$Ph	19.3	18.9	22.0	47.1^e	40.7^f	23.4^g	235
N(CH$_2$Ph)$_2$	h	CH$_2$Ph	——— 21.0^b ———						220

^{a}Hydrogen chloride adduct; ^{b}chemical shifts of P(2)P(6) and P(4)P(8) almost identical (<0.5 ppm difference); ^{c}P(2)NHEt, P(4,8)NMe$_2$(NHEt); ^{d}P(2)NMe$_2$, P(4,8)NMe$_2$(NHEt); ^e2J[P(2)–P(4)]; ^f2J[P(4)–P(6)]; ^g2J[P(2)–P(6)]; ^{h}P(6)N(CH$_2$Ph)$_2$.

TABLE A.21

^{31}P NMR data for bicyclotriphosphazenes $[N_3P_3X_4(R)]_2$ (40).

Compound	δ(PPR)	δ(PX$_2$)	^2J(P–P) (Hz)	Refs.
$[N_3P_3Cl_4(Me)]_2$	26.4	19.8	a	253
$[N_3P_3Cl_4(Ph)]_2$	17.7	19.8	8.7[b]	253
$[N_3P_3(OPh)_4(Me)]_2$	29.9	6.8	26.5[b]	253
$[N_3P_3(OPh)_4(Ph)]_2$	20.6	6.3	33.2[b]	253
$[N_3P_3(Ph)_4(Me)]_2$	24.7	12.0	a	252
$[N_3P_3Cl_4(Et)]_2$	31.9	20.4	a	105
$[N_3P_3Cl_4(Pr^n)]_2$	30.0	20.1	a	105
$[N_3P_3Cl_4(Bu^n)]_2$	30.5	20.0	a	105

[a] Unresolved; [b] ^2J(P–N–P) + ^3J(P–P–N–P).

TABLE A.22

^{31}P NMR data for bi(cyclotriphosphazenes) containing P–O–P or P–P–P groups.

Compound	δ(PPh$_2$)	δ[P(R)XP]	^2J(P–N–P) (Hz)	^2J(P–X–P) (Hz)	Refs.
$[N_3P_3(Ph)_4(Me)]_2O$ (41)	15.5	21.1	5.0	35.0	254
$[N_3P_3(Ph)_4(OPh)]O[N_3P_3(Ph)_4(Me)]$ (41)[a]	15.5, 19.9	21.8, −5.5	7.3, 28.3	28.7	254
$[N_3P_3(Ph)_5]_2O^b$	15.4	10.1	11.4	37.9	111
$[N_3P_3Ph_4Me]_2PMe_2$ (42a)	12.5	36.5, −63.0[c]	215[d]	—	256
$[N_3HP_3Ph_4Me]_2^{2+}PMe, 2Cl^-$ (42b)	19.5	44.5, −57.8[c]	241[d]	—	256

[a] Two different values of δ and J refer to PPh$_2$(Me) and PPh$_2$(OPh) respectively; [b] ^4J(P–N–P–O–P) = 0.2 Hz; [c] bridge P nucleus; [d] ^1J(P–P): ^2J(P–N–P) unresolved.

TABLE A.23

^{31}P NMR data for metal complexes of cyclophosphazenes.

Complex	δ(P)	^2J(P–P) (Hz)	Refs.
$N_3HP_3Ph_4Me(AuCl)$ **(72a)**[a]	{16.0[b] {66.0	21.2	274
$N_3P_3Ph_4Me(AuCl)$ **(72a)**[c]	{13.5,[b] 14.9[b] {64.2	36.6, 15.3	274
$[(N_3HP_3Ph_4Me)_2AuCl_2]^+[AuCl_4]^-$	23.1,[b] 38.7	11.8	274
$N_3HP_3Ph_4Me(Me_2AuCl)$ **(72b)**	15.7,[b] 20.0[b] 94.7	43.1, 20.9[d]	274
$(N_3HP_3Ph_4Me)_2MX_2$ **(71)**			
(a) M = Pd	17.9,[b] 13.3[b]		273
X = Cl	69.8		
(b) M = Pd	18.4,[b] 15.2[b]		273
X = Br	70.5		
(c) M = Pt	16.8,[b] 13.5[b]	f	273
X = Cl	36.3		
(d) M = Pt	15.1,[b] 37.5		273
X = Br[e]			
$[N_3P_3Ph_4(R)S]_2M$			
(a) R = OPh	11.9,[b] 27.9[b]	—	316
M = Pd	49.0		

(b) R = OPh	10.4,[b] 28.1[b]	—	316
M = Pt	52.9		
(c) R = Me	9.1,[b] 27.1[b]	—	316
M = Pt	57.9		
(d) R = C_6H_4(OMe)-p	16.5,[b] 26.6[b]	—	316
M = Ni	60.6		
(e) R = C_6H_4(OMe)-p	10.9,[b] 26.2[b]	—	316
M = Pd	48.7		
gem-$N_3P_3Ph_4(N_2C_3HMe_2)_2$.$PdCl_2$ (73)[g]	19.3 (A),[b] 17.3 (B)[b]	0 (AB), 14.2 (AX)	275
	−10.4 (X)	27.3 (BX)	
gem-$N_3P_3Ph_2(N_2C_3HMe_2)_4$.$PdCl_2$ [g]	20.8 (X)[b]	49.7 (AB), 18.1 (AX)	275
	−1.5 (A), −5.8 (B)	32.7 (BX)	
$N_3P_3(N_2C_3HMe_2)_6$.$3PdCl_2$ [g]	−11.5		275
$N_3P_3(HNCH_2CH_2NH)(NMe_2)_4$.$NiCl_2$	21.9,[h] 25.5	31.6	276
$N_4P_4(NHMe)_8$.$NiCl_2$	8.0		276
$N_6P_6Me_{12}$.$PdCl_2$(74, M = Pd)	29.06, 28.69 (AA′)		196
	26.24 (BB′)		
	7.03, 6.74 (CC′)[i]		
$N_6P_6Me_{12}$.$PtCl_2$ (74, M = Pt)	29.54, 28.98 (AA′)	j	196
	27.14 (BB′)		
	7.58, 7.14 (CC′)[i]		

[a] At 30 °C; [b] PPh_2; [c] at −80 °C (AXY spectrum interpreted using first-order approximation); [d] approximate values; [e] measured in nitrobenzene; [f] ^1J(Pt–P) = 4590 Hz; [g] $N_2C_3HMe_2$ = 3,5-dimethylpyrazolyl; [h] $P(NMe_2)_2$; [i] AA′, BB′, CC′ marked on structural diagram (74); [j] ^2J(Pt–P) = 99.0 Hz.

TABLE A.24

^{31}P NMR data for metallocyclophosphazenes.

Compound	$\delta(PX_2/PR_2)$	$\delta[P(M)]^a$	$^1J(P–F)^b$ (Hz)	$^2J(P–P)$ (Hz)	Refs.
$N_3P_3F_5[Fe(CO)_2(\eta\text{-}C_5H_5)]$ (51)	1.4	133.2	920, 1141	—	269
$N_3P_3F_5[Ru(CO)_2(\eta\text{-}C_5H_5)]$ (51)	1.6	103.9	901 1117	—	269
$gem\text{-}N_3P_3F_4[Fe(CO)_2(\eta\text{-}C_5H_5)]_2$ (51)	−0.3	158.4	891.4	—	269
$gem\text{-}N_3P_3F_4[Ru(CO)_2(\eta\text{-}C_5H_5)][Fe(CO)_2(\eta\text{-}C_5H_5)]$ (51)	−1.5	126.1	889	—	269
$N_3P_3Cl_5[Cr(CO)_3(\eta\text{-}C_5H_5)]$ (51)	12.6	140.3	—	88	194
$gem\text{-}N_3P_3Cl_4(C_5H_5)[Mo(CO)_3(\eta\text{-}C_5H_5)]$ (51)	9.0	86.0	—	49	194
$gem\text{-}N_3P_3Cl_4Me[W(CO)_3(\eta\text{-}C_5H_5)]$ (51)	8.8	58.9	—	39	194
$gem\text{-}N_3P_3Cl_4(C_5H_5)[W(CO)_3(\eta\text{-}C_5H_5)]$ (51)	12.4	58.5	—	48	194
$gem\text{-}N_3P_3F_4[Fe_2(CO)_3(\eta\text{-}C_5H_5)_2]$ (52)	3.3	272.3	918	—	269
$gem\text{-}N_3P_3F_4[Ru_2(CO)_3(\eta\text{-}C_5H_5)_2]$ (52)	2.5	229.9	898	—	269
$gem\text{-}N_3P_3F_4[FeRu(CO)_3(\eta\text{-}C_5H_5)_2]$ (52)	2.3	249.7	917	—	269
$gem\text{-}N_3P_3Cl_4[Fe_2(CO)_8]$ (53)	13.1	222.5	—	51	271
$gem\text{-}N_3P_3Cl_4[Fe_3(CO)_{10}]$ (55a)	14.5(A) 27.1(M)	217.9 (X)	—	33(AM) 61(AX) 12(MX)	271
$gem\text{-}N_3P_3Cl_4[Fe_2Ru(CO)_{10}]$ (55a)	13.6(A) 24.6(M)	226.3 (X)	—	32(AM) 61(AX) 18(MX)	271
$N_4P_4Cl_6[Fe_2(CO)_8]$ (54)	−5.3(A) −12.8(M)	185.0 (X)	—	33(AM) 85(MX)	271
$N_4P_4Cl_6[Fe_3(CO)_{10}]$ (55b)	−11.3(A) −5.9(M) 2.5(R)	183.8 (X)	—	19(AM) 90(AX) 39(MR) 41(RX)	271

$N_3P_3Cl_4Me[C.C(Me)\{Co(CO)_3\}_2]$ (56)	16.4	29.1		9.5	195[c]
$N_3P_3Cl_4Me[CH_2C(CH)\{Co(CO)_3\}_2]$ (57)	18.6	32.0		—	195[c]
$N_3P_3Cl_4(CH_2—CH=CH_2)[CH_2C(CH)\{Co(CO)_3\}_2]$ (57)	18.8	31.5		—	195
$N_3P_3F_5[(\eta-C_5H_4)Fe(\eta-C_5H_5)]$ (58)	8.9	44.3	933 965	80	193
$N_3P_3(OCH_2CF_3)_5[(\eta-C_5H_4)Fe(\eta-C_5H_5)]$ (58)	16.0	37.4	—	53	193
$N_3P_3Cl_5[(\eta-C_5H_4)Fe(\eta-C_5H_5)]$ (58)	20.2	36.1	—	15	193
$N_3P_3Cl_5[(\eta-C_5H_4)Fe(\eta-C_5H_4Cl)]$ (58)	20.2	35.0	—	17	193
$N_3P_3(OCH_2CF_3)_5[\eta-C_5H_4)Fe(\eta-C_5H_4X)]$ (58, X = H, Cl) (58)	16.5	35.6	—	56	272
gem-$N_3P_3Cl_4Me[(\eta-C_5H_4)Fe(\eta-C_5H_5)]$ (58)	20.7	29.2	—	23	193
$N_3P_3F_5[(\eta-C_5H_4)Ru(\eta-C_5H_5)]$ (58)	9.1	42.9	910 960	80	193
$N_3P_3Cl_5[(\eta-C_5H_4)Ru(\eta-C_5H_5)]$ (58)	20.3	33.7	—	17	193
$N_3P_3Cl_5[(\eta-C_5H_4)Ru(\eta-C_5H_4Cl)]$ (58)	20.1	32.5	—	18	193
gem-$N_3P_3Cl_4Me[(\eta-C_5H_4)Ru(\eta-C_5H_5)]$ (58)	21.0	28.8	—	22	193
gem-$N_3P_3Cl_4H[(\eta-C_5H_4)Ru(\eta-C_5H_5)]$ (58)	8.0	18.6	—	11	193
$nongem$-$N_3P_3F_4[(\eta-C_5H_4)Fe(\eta-C_5H_5)]_2$	5.9	41.2	902 938	70	193
$N_3P_3F_4[(\eta-C_5H_4)_2Fe]$ (59)	15.4	46.6	890 930	60	193
$N_3P_3F_4[(\eta-C_5H_4)_2Ru]$ (59)	16.7	43.6	920 920	80	193
$N_3P_3(OCH_2CF_3)_4[(\eta-C_5H_4)_2Ru]$	22.8	38.8	—	54	193
$N_6P_6Cl_8[(\eta-C_5H_4)_2Fe]$ (60)	18.9[d]	22.5[d]	—	—	193
$N_6P_6F_{10}[(\eta-C_5H_4)_2Ru]$ (61)	8.5	38.3	890 970	80	193
$N_6P_6Cl_{10}[(\eta-C_5H_4)_2Fe]$ (61)	21.1	35.0	—	17.4	193
$N_6P_6(OCH_2CF_3)_{10}[(\eta-C_5H_4)_2Fe]$ (61)	16.4	35.6	—	56.2	193
$N_6P_6Cl_9[(\eta-C_5H_4)Fe(\eta-C_5H_5)]$ (62)	21.1[d]	25.8[d]	—	—	193
$N_6P_6Cl_9[(\eta-C_5H_4)Fe(\eta-C_5H_4Cl)]$ (62)	21.4[d]	25.3[d]	—	—	193
$N_6P_6Cl_9[(\eta-C_5H_4)Ru(\eta-C_5H_5)]$ (62)	21.3[d]	24.9[d]	—	—	193
$N_6P_6Cl_9[(\eta-C_5H_4)Ru(\eta-C_5H_4Cl)]$ (62)	21.2[d]	24.6[d]	—	—	193
$N_3P_3Cl_5[NPCl\{(\eta-C_5H_4)Fe(\eta-C_5H_5)\}_2]$ (63)[e]	20.0	36.9	—	52	272

TABLE A.24 (cont.)

Compound	$\delta(PX_2/PR_2)$	$\delta[P(M)]_j^a$	$^1J(P\text{-}F)^b$ (Hz)	$^2J(P\text{-}P)$ (Hz)	Refs.
$N_4P_4F_7[(\eta\text{-}C_5H_4)Fe(\eta\text{-}C_5H_5)]$ **(64)**	ca. −16	21.4	850 929	—	193
$N_4P_4(OCH_2CF_3)_7[(\eta\text{-}C_5H_4)Fe(\eta\text{-}C_5H_5)]$ **(64)**	ca. −2.0	18.4	—	—	193
$N_4P_4F_7[(\eta\text{-}C_5H_4)Ru(\eta\text{-}C_5H_5)]$ **(64)**	−16.9	17.1 10.2	870 910 890	70 80	193
$N_4P_4F_6[(\eta\text{-}C_5H_4)Ru(\eta\text{-}C_5H_5)]_2$ **(65)**	−22.8	13.7	870 890	90	193
$N_4P_4F_6[(\eta\text{-}C_5H_4)_2Fe]$ **(66)**	−13.3	35.8	870 850	80	193
$N_4P_4F_6[(\eta\text{-}C_5H_4)_2Fe]$ **(67)**	−15.0	23.3	870 850	80	193
$N_4P_4F_6[(\eta\text{-}C_5H_4)_2Ru]$ **(67)**	−12.7	15.0	870 840	80	193
$N_7P_7Cl_{11}[(\eta\text{-}C_5H_4)Fe(\eta\text{-}C_5H_4X)]$ (X = H or Cl) **(68)**	−1.1^d −6.9^d	22.0^d	—	—	272
(69)^f	16.0	29.0	—	—	268
(70)(M = W)	14.0^d 11.0^d	41.5^d	—	—	268

^{a} Phosphorus nucleus attached to metal or metal-containing substituent. ^{b} First value for PF_2; second for $PF(M)$. ^{c} Data for higher alkyl analogues are also reported. ^{d} Centre of multiplets. $^e\delta[\underline{P}ClNP] = -2.7$, $^2J(\underline{P}_{exo}-\underline{P}_{ring}) = 28.0$ Hz, $^4J(P-P) = 4.0$ Hz. $^f\delta(PPh_3) = 34.5$, $^1J(Rh-P) = 112$ Hz.

TABLE A.25

¹⁹F NMR data for representative fluorocyclotriphosphazenes.[a]

Compound	Structure[b]	$\delta(P\underline{F}_2)$	$\delta(P\underline{F}R)$	$^{1}J(P\text{–}F)^{c}$ (Hz)	Refs.
$N_3P_3F_6$		−71.9			160
$N_3P_3ClF_5$		−70.2		886	160
			−30.7	994	
$N_3P_3Cl_2F_4$	2,2	−71.9			160
$N_3P_3Cl_2F_4$	2,2		−31.5	960	162
$N_3P_3Cl_3F_3$	2,2,4	−71.7	−31.9		170
$N_3P_3Cl_3F_3$	2-cis-4-cis-6		−31.68	−1001.6	104
$N_3P_3Cl_3F_3$	2-trans-4-cis-6		−30.81	−997.7	104
			−29.73[d]	−966.1	104
$N_3P_3Cl_4F_2$	2,2,4,4	−72.3			170
$N_3P_3Cl_4F_2$	2-cis-4,6,6		−31.01	−1002.5	104
$N_3P_3Cl_4F_2$	2-trans-4,6,6		−29.95	−998.8	104
$N_3P_3Cl_5F$			−30.1	1026	168
$N_3P_3BrF_5$		−70.0	−19.6	—	160
$N_3P_3Br_2F_4$	2,4		−20	1000	162
$N_3P_3Br_3F_3$	2-cis-4-cis-6		−22.24	−1051.6	104
$N_3P_3Br_3F_3$	2-trans-4-cis-6		−20.49	−1048.2	104
			−18.26[d]	−1042.3	
$N_3P_3Br_4F_2$	2-cis-4,6,6		−21.19	−1051.2	104
$N_3P_3Br_4F_2$	2-trans-4,6,6		−18.86	−1048.1	104
$N_3P_3BrClF_4$	2:4:2,4,6,6		−30.5	980	162
			−20	1040	
$N_3P_3F_5Me$		−70.6	−53.9		115
$N_3P_3F_5Bu^n$		−69.7		934.4	115
		−67.9		929.7	115
			−60.0	1009.5	

Compound	Structure[b]	$\delta(P\underline{F}_2)$	$\delta(P\underline{F}R)$	$^1J(P-F)^c$ (Hz)	Refs.
$N_3P_3F_4(Bu^n)_2$	2,2,4,4 : 6,6	−68.6		928.1	115
$N_3P_3F_5(Bu^t)$		−68.6 ⎫ −69.8 ⎭		900.7 894.4	115
			−79.3	1032.2	
$N_3P_3F_4(Bu^t)_2$	2-*trans*-4	−68.9		902.8	115
			−78.0	1022.9	
$N_3P_3F_3(Bu^t)_3$	2-*trans*-4-*cis*-6		−72.1^d ⎫ −77.1 ⎭	1011.7 1007.1	115
$N_3P_3F_5[CH_2C(O)Ph]$		−62.0	—	788	346
			−58.0	778	
$N_3P_3F_5(CH{=}CHMe)$		−63		810	178
			−52	830	
$N_3P_3F_4(CH{=}CHMe)_2$	2,2,4,4	−64		840	178
$N_3P_3F_5(C{\equiv}CPh)$		−69.5 ⎫ −68.5 ⎭		941.2	180
			−44.0	910.8	
$N_3P_3F_4(C{\equiv}CPh)_2$	2,2,4,4	−68.6		889.1	180
$N_3P_3F_5(C{\equiv}CSiMe_3)$		−68.4 ⎫ −69.7 ⎭		920 880	180
			−45.5	900	
$N_3P_3F_5[C(OMe){=}CH_2]$		−67.85 ⎫ −69.23 ⎭		933.5 933.5	179
			−66.85	1003.7	
$N_3P_3F_4Ph_2$	2,2,4,4	−69.7		890	113
$N_3P_3F_4Ph_2$	2-*cis*-4	−69.3 ⎫ −65.2 ⎭		898 879	112
			−49.3	965	

$N_3P_3F_4Ph_2$	2-*trans*-4	−67.7		879	112
			−51.5	939	
$N_3P_3F_3Ph_3$	2,2,4	−68.6		895	113
		−66.0		895	
			−49.1	958	
$N_3P_3F_5(C_6H_4NMe_2-p)$		−67.0		910⎫	177
				969⎭	
			−50.6	997	
$N_3P_3F_4(C_6H_4NMe_2-p)_2$	2-*cis*-4	−67.5		879	177
		−65.2		851	
			−47.6	952	
$N_3P_3F_4(C_6H_4NMe_2-p)_2$	2-*trans*-4	−67.0		938	177
			−51.3	875	
$N_3P_3F_5(NMe_2)$		−70.9		809	160
			−62.1	870	
$N_3P_3F_4(NMe_2)_2$	2,2,4,4	−70.1		863	160
$N_3P_3F_4(NMe_2)_2$	2-*cis*-4	−68.5ᵉ		900	31
			−61.0	900	
$N_3P_3F_4(NMe_2)_2$	2-*trans*-4	−69.4		890	31
$N_3P_3F_3(NMe_2)_3$	2,2,4	−68.9⎫		900ᶠ	79
		−68.1⎭			
			−61.9	905	
$N_3P_3F_3(NMe_2)_3$	2-*cis*-4-*cis*-6		−60.4	907	79
$N_3P_3F_3(NMe_2)_3$	2-*trans*-4-*cis*-6		−63.1ᵈ	860ᶠ	79
			−62.1	850ᶠ	
$N_3P_3F_2(NMe_2)_4$	2-*cis*-4		−62.0	920	79
$N_3P_3F_2(NMe_2)_4$	2-*trans*-4		−63.5	905	79
$N_3P_3F(NMe_2)_5$			−63.5	904	53
$N_3P_3F_4(NEt_2)_2$	2-*trans*-4	−69.1		830	158
			−55.1	915	
$N_3P_3F_4(NC_5H_{10})_2$	2-*trans*-4	−69.4		930	158
			−60.1	870	
$N_3P_3F_4(NHMe)_2$	2-*trans*-4	−69.2		914	353
			−58.2	920	

Compound	Structure[b]	δ(P$\underline{\text{F}}_2$)	δ(P$\underline{\text{F}}$R)	^1J(P–F)[c] (Hz)	Refs.
$N_3P_3F_4(NHEt)_2$	2-*trans*-4	−69.4		910	158
			−54.8	880	
$N_3P_3F_4(NHPr^i)_2$	2-*trans*-4	−62.2		855	158
			−53.8	940	
$N_3P_3F_4(NHBu^t)_2$	2,2,4,4	−70		860	158
$N_3P_3Cl_4F(NMe_2)$	2,2,4,4:6:6		−63.0	950	161
$N_3P_3Cl_4F(NMe_2)$	2,2,4,6:4-*cis*-6		−30.5	1010	161
$N_3P_3Cl_4F(NMe_2)$	2,2,4,6:4-*trans*-6		−27.8	1010	161
$N_3P_3Cl_2F_2(NMe_2)_2$	2,2:4,6:4-*trans*-6		−66.34	−901.1	104
$N_3P_3Cl_2F_2(NMe_2)_2$	2,2:4,6:4-*cis*-6		−64.89	−925.7	104
$N_3P_3Cl_2F_2(NMe_2)_2$	2-*trans*-4:6,6:2,4	−71.32		−905.3	104
$N_3P_3Cl_2F_2(NMe_2)_2$	2-*cis*-4:6, 6:2, 4	−69.53		−904.6	104
		−73.61		−909.5	
$N_3P_3Cl_3F_2(NMe_2)$	2,2,4:6,6:4	$\begin{cases} -68.4 \\ -70.7 \end{cases}$		$\begin{cases} 910 \\ 1020 \end{cases}$	104
$N_3P_3Cl_2F_3(NMe_2)$	2-*cis*-4:2,6:2,6,6:4	−66.1[g]		1020	161
			−31.9	880	
$N_3P_3Cl_2F_3(NMe_2)$	2-*trans*-4:2,6,6:4	−66.1[g]		995	161
			−29.4	880	
$N_3P_3Cl_2F_2(NC_5H_{10})_2$	2,2:4,6:4-*trans*-6		−68.2	894	159
$N_3P_3Cl_2F_2(NC_5H_{10})_2$	2,2:4,6:4-*cis*-6		−70.5	891	159
			−65.7	888	
$N_3P_3Cl_2F_2(NC_4H_8O)_2$	2,2:4,6:4-*trans*-6		−69.4	894	159
$N_3P_3Cl_2F_2(NC_4H_8O)_2$	2,2:4,6:4-*cis*-6		−71.9	880	159
			−66.9	891	
$N_3P_3Cl_2F_2(NHEt)_2$	2.2:4.6:4-*trans*-6		−55.0	905	158
$N_3P_3Cl_2F_2(NHPr^i)_2$	2,2:4,6:4-*trans*-6		−53.8	940	158
$N_3P_3F_5(C_4H_3NMe)$[h]		−67.0		903	197
			−47.9	937	

$N_3P_3F_4[HN(CH_2)_2NH]$	2,2,4,4	−76.1		990	73
$N_3P_3F_4[MeN(CH_2)_2NMe]$	2,2,4,4	−68.4		930	83
$N_3P_3F_2[MeN(CH_2)_2NMe]_2$	2,2	−65.5		800	83
$N_3P_3F_4[HN(CH_2)_3NH]$	2,2,4,4	−76.62		910	73
$N_3P_3F_2[HN(CH_2)_3NH]_2$	2,2	−77.44		898	73
$N_3P_3F_2[HN(CH_2)_3O]_2$	2,2(cis)[i]	−78.68⎫ −75.92⎭		962	73
$N_3P_3F_2[HN(CH_2)_3O]_2$	2,2(trans)[i]	−76.90		962	73
$N_3P_3F_5(NPMe_3)$		−70.15		881.8	167
			−43.58	881.8	
$N_3P_3F_4(NPMe_3)_2$	2-trans-4	−69.64		875	167
			−44.04	825	
$N_3P_3F_5[NP(Me)_2Ph]$		−70.39		890	167
			−43.64	870	
$N_3P_3F_5(NPPh_3)$		−70.39		890	167
			−44.70	850	
$N_3P_3F_4(NPPh_3)_2$	2-trans-4	−70.45		895	167
			−44.0 ⎫	821	
$N_3P_3F_3(OMe)_2(NPPh_3)$ (22)	2-cis-4-cis-6:2,4:6		−67.89 ⎭	878	47
			−42.70[j]	863	
			−68.06 ⎫	856	47
$N_3P_3F_3(OMe)_2(NPPh_3)$ (23)	2-trans-4-cis-6:2,4:6		−69.78[k]⎬	851	
			−43.26[j]⎭	850	
$N_3P_3F_3(OMe)_2(NPPh_3)$ (24)	2-cis-4-trans-6:2,4:6		−69.39 ⎫	844	47
			−43.44[j]⎭	851	
$N_3P_3F_5(OMe)$		−71.2	−69.5	—	174
$N_3P_3F_5(OPh)$		−70.7	−67.9	—	174
$N_3P_3F_5(SMe)$		−70.7	−40.2		174
$N_3P_3F_5(SPh)$		−70.2	−46.8		174

[a]Chemical shifts are with reference to $CFCl_3$. [b]Disposition of one set of substituent groups only defined when adequate. [c]Sign stated only when determined. [d]Unique ^{19}F. [e]Average: 2 similar ^{19}F environments. [f]Approximate. [g]Two environments not resolved. [h]1-methylpyrrol-2-yl. [i]cis or trans exocyclic N or O. [j] ^{19}F gem to –NPPh$_3$. [k] ^{19}F cis to –NPPh$_3$.

TABLE A.26

^{19}F NMR data for selected nongeminal (dimethylamino)fluorocyclotetraphosphazenes.[a]

Compound	Structure[b]	PFNMe$_2$	^1J(P–F) (Hz)	Refs.
N$_4$P$_4$F$_2$(NMe$_2$)$_6$	2-*cis*-4	-59.1	920	224
N$_4$P$_4$F$_2$(NMe$_2$)$_6$	c	-60.4	910	224
		-61.4	870	
N$_4$P$_4$F$_2$(NMe$_2$)$_6$	2-*cis*-6	-59.5	900	224
N$_4$P$_4$F$_3$(NMe$_2$)$_5$	2-*trans*-4-*cis*-6	$-61.4\,(2)^d$	870	224
		$-62.9\,(1)$	850	
N$_4$P$_4$F$_3$(NMe$_2$)$_5$	2-*cis*-4-*trans*-6	$-58.1\,(1)$	880	224
		$-59.6\,(1)$	840	
		$-60.8\,(1)^e$	830	
N$_4$P$_4$F$_4$(NMe$_2$)$_4$	2-*cis*-4-*trans*-6-*trans*-8 ^{f}	-58.8	870	223
N$_4$P$_4$F$_4$(NMe$_2$)$_4$	2-*trans*-4-*cis*-6-*trans*-8 ^{g}	-61.5	830	223
N$_4$P$_4$F$_4$(NMe$_2$)$_4$	2-*trans*-4-*cis*-6-*cis*-8	$-55.4\,(1)$	870	223
		$-58.3\,(2)$	880	
		$-60.1\,(1)^e$	840	
N$_4$P$_4$F$_5$(NMe$_2$)$_3$	2-*cis*-4-*trans*-6,8,8	$-58.9\,(1)^h$	950	223
		$-61.2\,(1)$	920	
		$-62.2\,(1)$	910	
N$_4$P$_4$F$_6$(NMe$_2$)$_2$	2-*trans*-6,4,4,8,8	-59.8^i	900	225

[a]With reference to CFCl$_3$; [b]disposition of F atoms only;[19] [c]mixture of 2-*trans*-4 and 2-*trans*-6 isomers; [d]relative intensities in parentheses; [e]*cis* to two NMe$_2$ groups; [f]X-ray structure;[226] [g]X-ray structure;[227] [h]δ(P$\underline{\text{F}}_2$) -69.2, ^1J(P–F) = 920 Hz; [i]δ(P$\underline{\text{F}}_2$) $= -69.3$, ^1J(P–F) = 880 Hz.

TABLE A.27

^{15}N NMR data^a for endocyclic ^{15}N-labelled cyclophosphazenes.

Compound	$\delta(^{15}N)$	$^1J(P-N)$ (Hz)	$^2J(P-P)$ (Hz)	Refs.
$^{15}N_3P_3F_6$	-314.5	$+24.9$	~ 190	144
$^{15}N_3P_3Cl_6$	-258.8	-31.7	50	144, 207
$^{15}N_3P_3Br_6$	-240.1	55.8	4.8	144
$^{15}N_3P_3Me_6$	-319.5	26.1	4.4	144
$^{15}N_3P_3(NH_2)_6$	-298.3	1.6^b	c	209
$^{15}N_3P_3(NHMe)^6$	-315.1	7.7	~ 60	144
$^{15}N_3P_3(NMe_2)_6$	-320.8	7.5	~ 40	144
$^{15}N_3P_3(NHEt)_6$	-312.4	7.8	~ 35	144
$^{15}N_3P_3(NEt_2)_6$	-316.3	6.1	~ 50	144
$^{15}N_3P_3(NHPh)_6$	d	6.6	~ 45	144
$^{15}N_3P_3(OMe)_6$	-317.8	7.5	~ 70	211, 214^a
$^{15}N_3P_3(OEt)_6$	-314.3	6.4	~ 65	144, 214^a
$^{15}N_3P_3(OPh)_6$	-305.9	7.1	~ 70	144
$^{15}N_3P_3(SEt)_6$	-284.2	51.0	14.7	208
$^{15}N_3P_3(SPh)_6$	-285.0	53.3	23.5	208
$^{15}N_3P_3Cl_4F_2^{\ e}$	$-286.9(1,5)$	-30.7 (I)		
	$-259.8(3)$	-21 (II)	97.9	209
		$+13.4$ (III)		
$^{15}N_3P_3Cl_4(NH_2)_2^{\ e}$	$-272.9(1,5)$	-35.8 (I)		
	$-255.5(3)$	-33.0 (II)	50.8	209
		-7.4 (III)		
$^{15}N_3P_3Cl_4(SEt)_2^{\ e}$	$-270.9(1,5)$	-34.1 (I)		
	$-255.9(3)$	-38.8 (II)	5.0	208
		-48.1 (III)		
$^{15}N_3P_3(SEt)_4Cl_2^{\ f}$	—	40.3 (III)	$5.2(P_4-P_6)$	
		47.6 (II)	$17.8(P_4-P_2)$	208
		49.4 (I)		
$^{15}N_3P_3(SPh)_2Cl_4^{\ e}$	$-258.6(3)$	33.7 (I)	$54.0(P_4-P_2)$	
	$-270.0(1,5)$	39.4 (II)	$5.6(P_4-P_6)$	208
		50.6 (III)		
$^{15}N_3P_3(SPh)_4Cl_2^{\ f}$	$-268.3(1,5)$	39.7 (III)	$1.0(P_4-P_6)$	
	$-283.8(3)$	50.9 (II)	$28.5(P_4-P_2)$	208
		53.5 (I)		
$^{15}N_3P_3Cl_5(NHPh)^g$	$-256.3(3)$	32.2 (I)		
	$-268.1(1,5)$	30.4 (II)	48.6	212
		17.9 (III)		
$^{15}N_3P_3Cl_4(NHPh)_2^h$	$-255.1(3)$	34.4 (I)		
	$-279.1(1,5)$	32.3 (II)	49.0	212
		5.8 (III)		
$^{15}N_4P_4F_8$	-314.4	68.8	155.0	211
$^{15}N_4P_4Cl_8$	-248.0	-6.9	> 69	211
$^{15}N_4P_4Br_8$	-230.8	-35.3	27.2	211
$^{15}N_4P_4Me_8$	-300.0	-23.8	10.7	211

TABLE A.27 (cont.)

Compound	$\delta(^{15}N)$	$^1J(P-N)$ (Hz)	$^2J(P-P)$ (Hz)	Refs.
$^{15}N_4P_4(NMe_2)_8$	-314.8	14.2	60.2	211
$^{15}N_4P_4(NHEt)_8$	-306.7	5.5	>55	211
$^{15}N_4P_4Cl_7(NHPh)$	-246.7^j	k		214
	-260.1^j			
$^{15}N_4P_4Cl_6(NHPh)_2$	-259.2	-3.5^l		214
(2, 6)		$+6.6$		
$^{15}N_4P_4Cl_6(NHPh)_2$	-244.5^i			
(2, 4)	-259.2^j	n		214
	-275.5^m			
$^{15}N_4P_4(OMe)_8$	-313.7	32.7	74.3	211, 214^a
$^{15}N_4P_4(OPh)_8$	-302.5	37.5	80.6	211
$^{15}N_4P_4(SEt)_8$	-270.0	-34.0	31.6	211
$^{15}N_4P_4Cl_4(SEt)_4$	-259.8	15.5^i	11.9^k	208
		30.6^j		
$^{15}N_5P_5F_{10}$	-322.8	$+71.8$	m	213
$^{15}N_5P_5(OMe)_{10}$	-318.9	$+39.0$	m	213
$^{15}N_5P_5(NMe_2)_{10}$	-317.0	$+19.4$	m	213
$^{15}N_5P_5Cl_{10}$	-253.1	-3.0	m	213
$^{15}N_6P_6Cl_{12}$	-253.3	-2.0	m	213
$^{15}N_6P_6(OMe)_{12}$	-320.0	$+41.5$	m	213
$^{15}N_6P_6(NMe_2)_{12}$	-317.6	$+29.3$	m	213

^{a}9.1 MHz: external standard Me^{15}NO$_2$; downfield shifts positive. ^{b}Because of the small value, the relative sign was not determined. ^{c}Could not be determined because $^1J(P-N)$ is very small. ^{d}Owing to low solubility there was no ^{15}N spectrum; values from ^{31}P spectrum. ^{e}For numbering of atoms and labelling of coupling constants, see structure (26, X = Cl; Y = Z = F, NH$_2$ or SR). ^{f}Structure (26, X = SR, Y = Z = Cl). ^{g}Structure (26, X = Cl; Y = NHPh; Z = Cl). ^{h}Structure (26, X = Cl; Y = Z = NHPh). ^{i}Cl$_2$P = $\underline{N}$-PCl$_2$. ^{j}Cl$_2$P = $\underline{N}$-PCl(NHPh). $^{k\,1}J$(PN) values are -6.2, -7.0, -2.9 and $+5.7$ Hz. $^{l\,1}J$(Cl$_2\underline{P}$-$\underline{N}$). ^{m}Cl(NHPh)P = N-PCl(NHPh). $^{n\,1}J$(PN) values are -6.8, -3.0, $+6.7$ and $+8.0$ Hz. $^o\underline{P}$Cl$_2$-$\underline{N}$. $^p\underline{P}$(SR)$_2\underline{N}$. $^q\underline{P}$Cl$_2$-$\underline{P}$(SR)$_2$. $^{y\,2}J$(PP) could not be determined.

TABLE A.28

^{15}N NMR data for exocyclic ^{15}N-labelled (amino)cyclotriphosphazenes.^{a}

Compound	$\delta(^{15}N)$	$\delta(^{15}N)$ free amine	$^1J(\text{P–N})$ (Hz)	$^2J(\text{P–N})$ (Hz)
$N_3P_3Cl_5(^{15}NH_2)$	−318.8	−338	33.5	4.4
gem-$N_3P_3Cl_4(^{15}NH_2)_2$	−332.0		33.6	4.0
$N_3P_3Cl_5(^{15}NHMe)$	−326.6		33.8	4.2
gem-$N_3P_3Cl_4(^{15}NHMe)_2$	−342.5	−378	36.3	4.0
trans-$N_3P_3Cl_4(^{15}NHMe)_2$	−325.1		32.1	4.3/2.5^c
cis-$N_3P_3Cl_4(^{15}NHMe)_2$	−327.0		33.0	4.5/4.5^c
$N_3P_3Cl_5(^{15}NMe_2)$	−331.2	−371	25.7	3.6
trans-$N_3P_3Cl_4(^{15}NMe_2)_2$	−329.6		25.3	3.1/1.8^c
cis-$N_3P_3Cl_4(^{15}NMe_2)_2$	b		26.0	3.5/3.5^c
$N_3P_3Cl_5(^{15}NHPh)$	−286.6	−320	36.1	4.1
gem-$N_3P_3Cl_4(^{15}NHPh)_2$	−298.1		38.9	3.4

^{a}From ref. 212. $^{b\,15}$N spectrum was not recorded owing to the small quantity of the sample.
^{c}The first value is for coupling with $\underline{P}Cl_2$ and the second value for coupling with $\underline{P}Cl(NRR')$.

REFERENCES

1. R. K. Harris and B. E. Mann (eds), *NMR and the Periodic Table*, Academic Press, London, 1978.
2. J. W. Akitt, *NMR and Chemistry — An Introduction to the Fourier-Transform Multinuclear Era*, 2nd edn, Chapman and Hall, London, 1983.
3. D. G. Gorenstein, in *Phosphorus-31 NMR Principles and Applications*, Academic Press, 1984, Chaps 1 and 2.
4. D. G. Gorenstein, *Prog. NMR Spectrosc.*, 1983, **16**, 1.
5. G. Mavel, *Prog. NMR Spectrosc.*, 1966, **1**, 251.
6. G. Mavel, in *Annual Reports on NMR Spectroscopy*, Vol. 5B (E. F. Mooney, ed.), Academic Press, London, 1973.
7. V. Mark, C. H. Dungan, M. M. Crutchfield and J. R. Van Wazer, *Top. Phosphorus Chem.*, 1967, **5**, 391.
8. R. Keat and R. A. Shaw, in *Organophosphorus Compounds*, Vol. 6 (G. M. Kosolapoff and L. Maier, eds), Wiley-Interscience, New York, 1973, pp. 833–940.
9. H. R. Allcock, *Phosphorus–Nitrogen Compounds*, Academic Press, New York, 1972.
10. E. G. Finer and R. K. Harris, *Prog. NMR Spectrosc.*, 1971, **6**, 61.
11. M. Bermann, *Top. Phosphorus Chem.*, 1972, **7**, 311.
12. R. A. Shaw, *Z. Naturforsch.*, 1976, **31b**, 641.
13. S. S. Krishnamurthy, A. C. Sau and M. Woods, *Adv. Inorg. Chem. Radiochem.*, 1978, **21**, 41.
14. R. A. Shaw, *Pure Appl. Chem.*, 1980, **52**, 1063.
15. V. V. Kireev, V. I. Astrina and E. A. Chernyshev, *Russ. Chem. Rev.* (Engl. Transl.), 1981, **50**, 1186.

16. *Specialist Periodical Report on Organophosphorus Chemistry*, Vols 1–14, The Chemical Society, London, 1970–84.

17. *Specialist Periodical Report on Nuclear Magnetic Resonance Spectroscopy*, Vols 1–14, The Chemical Society, London, 1972–85.

18. J. H. Letcher and J. R. Van Wazer, *Top. Phosphorus Chem.*, 1967, **5**, 75.

19. R. A. Shaw, B. W. Fitzsimmons and B. C. Smith, *Chem. Rev.*, 1962, **62**, 247.

20. R. Keat, S. K. Ray and R. A. Shaw, *J. Chem. Soc.*, 1965, 7193.

21. B. Green and D. B. Sowerby, *J. Inorg. Nucl. Chem.*, 1971, **33**, 3687.

22. S. Karthikeyan and S. S. Krishnamurthy, *Z. Anorg. Allg. Chem.*, 1984, **513**, 231.

23. S. S. Krishnamurthy, P. Ramabrahmam, A. R. Vasudeva Murthy, R. A. Shaw and M. Woods, *Z. Anorg. Allg. Chem.*, 1985, **522**, 226.

24. S. K. Das, R. A. Shaw and B. C. Smith, *J. Chem. Soc., Dalton Trans.*, 1973, 1883.

25. W. Lehr, *Z. Anorg. Allg. Chem.*, 1967, **352**, 27.

26. R. Das, R. A. Shaw, B. C. Smith and M. Woods, *J. Chem. Soc., Dalton Trans.*, 1973, 709.

27. A. A. Van der Huizen, "Aziridinyl Cyclophosphazenes", Ph.D. thesis, University of Groningen, Netherlands, 1984.

28. W. Lehr and N. Rosswag, *Z. Anorg. Allg. Chem.*, 1974, **406**, 221.

29. S. S. Krishnamurthy, M. N. Sudheendra Rao, A. R. Vasudeva Murthy, R. A. Shaw and M. Woods, *Indian J. Chem.*, 1976, **A14**, 823.

30. F. R. Ahmed and S. Fortier, *Acta Crystallogr.* 1980, **B36**, 1456.

31. B. Green and D. B. Sowerby, *J. Chem. Soc. A*, 1970, 987.

32. G. Engelhardt, E. Steger and R. Stahlberg, *Z. Naturforsch.*, 1966, **21b**, 586.

33. S. S. Krishnamurthy, M. N. Sudheendra Rao and M. Woods, *J. Inorg. Nucl. Chem.*, 1979, **41**, 1093.

34. B. Grushkin, M. G. Sanchez, M. V. Ernest, J. L. McClanahan, G. E. Ashby and R. G. Rice, *Inorg. Chem.*, 1965, **4**, 1538.

35. V. B. Desai, R. A. Shaw and B. C. Smith, *J. Chem. Soc.*, 1969, 1977.

36. S. K. Das, M. Hasan, R. A. Shaw, B. C. Smith and M. Woods, *Z. Naturforsch.*, 1979, **34b**, 58.

37. D. Dell, B. W. Fitzsimmons, R. Keat and R. A. Shaw, *J. Chem. Soc. A*, 1966, 1680.

38. M. Biddlestone and R. A. Shaw, *J. Chem. Soc., Dalton Trans.*, 1973, 2740.

39. M. Biddlestone and R. A. Shaw, *J. Chem. Soc. A*, 1970, 1750.

40. M. Woods, Unpublished results.

41. V. B. Desai, R. A. Shaw and B. C. Smith, *J. Chem. Soc. A*, 1970, 2023.

42. M. Hasan, R. A. Shaw and M. Woods, *J. Chem. Soc., Dalton Trans.*, 1975, 2202.

43. S. Karthikeyan, "Synthesis, thermal rearrangement and silylation reactions of (alkoxy)-(aryloxy)cyclotriphosphazenes", Ph.D. thesis, Indian Institute of Science, Bangalore, 1985.

44. S. Ganapathiappan and S. S. Krishnamurthy, *J. Chem. Soc., Dalton Trans.*, 1987, 579.

45. K. V. Katti and S. S. Krishnamurthy, Unpublished results.

46. K. C. Kumara Swamy and S. S. Krishnamurthy, *Phosphorus Sulfur*, 1983, **18**, 241.

47. K. C. Kumara Swamy and S. S. Krishnamurthy, *Inorg. Chem.*, 1986, **25**, 920.

48. K. C. Kumaraswamy, M. D. Poojary, S. S. Krishnamurthy and H. Manohar, *Z. Naturforsch.*, 1984, **B39**, 615; *J. Chem. Soc., Dalton Trans.*, 1985, 1881.

49. S. S. Krishnamurthy, A. C. Sau, A. R. Vasudeva Murthy, R. Keat, R. A. Shaw and M. Woods, *J. Chem. Soc., Dalton Trans.*, 1976, 1406.

50. D. J. Lingley, R. A. Shaw, M. Woods and S. S. Krishnamurthy, *Phosphorus Sulfur*, 1978, **4**, 379.

51. K. C. Kumaraswamy and S. S. Krishnamurthy, *J. Chem. Soc., Dalton Trans.*, 1985, 1431.

52. R. Keat and R. A. Shaw, *J. Chem. Soc. A*, 1968, 703.

53. P. Clare and D. B. Sowerby, *J. Inorg. Nucl. Chem.*, 1974, **36**, 729.

54. E. G. Finer, R. K. Harris, M. R. Bond, R. Keat and R. A. Shaw, *J. Mol. Spectrosc.* 1970, **33**, 72.
55. R. Keat, R. A. Shaw and M. Woods, *J. Chem. Soc., Dalton Trans.*, 1976, 1582.
56. C. Hewlett and R. A. Shaw, *J. Chem. Soc. A*, 1966, 56.
57. G. Allen, D. J. Oldfield, N. L. Paddock, F. Rallo, J. Serregi and S. M. Todd, *Chem. Ind. (London)*, 1965, 1032.
58. S. S. Krishnamurthy, K. Ramachandran, A. R. Vasudeva Murthy, R. A. Shaw and M. Woods, *Inorg. Nucl. Chem. Lett.*, 1977, **13**, 407.
59. A. Schmidpeter and J. Ebeling, *Angew. Chem. Int. Ed. Engl.* 1968, **7**, 209.
60. A. Schmidpeter, J. Ebeling, H. Stary and C. Weingand, *Z. Anorg. Allg. Chem.*, 1972, **394**, 171.
61. H. R. Allcock and P. J. Harris, *J. Am. Chem. Soc.*, 1979, **101**, 6221.
62. H. R. Allcock, M. S. Connolly and R. R. Whittle, *Organometallics*, 1983, **2**, 1514.
63. H. Winter and J. C. Van de Grampel, *J. Chem. Soc., Chem. Commun.*, 1984, 489.
64. M. Bermann and J. R. Van Wazer, *Inorg. Chem.*, 1972, **11**, 209.
65. A. Schmidpeter and H. Rossknecht, *Chem. Ber.*, 1974, **107**, 3146.
66. J. Högel and A. Schmidpeter, *Z. Anorg. Allg. Chem.*, 1979, **458**, 168.
67. H. R. Allcock and P. J. Harris, *Inorg. Chem.*, 1981, **20**, 2844.
68. H. R. Allcock, P. J. Harris and M. S. Connolly, *Inorg. Chem.*, 1981, **20**, 11.
69. H. R. Allcock, P. J. Harris and R. A. Nissan, *J. Am. Chem. Soc.*, 1981, **103**, 2256.
70. P. J. Harris, K. B. Williams and B. L. Fisher, *J. Org. Chem.*, 1984, **49**, 406.
71. S. S. Krishnamurthy, K. Ramachandran, A. R. Vasudeva Murthy, R. A. Shaw and M. Woods, *J. Chem. Soc., Dalton Trans.*, 1980, 840.
72. S. S. Krishnamurthy, K. Ramachandran and M. Woods, *Phosphorus Sulfur*, 1981, **9**, 323.
73. K. C. Kumaraswamy and S. S. Krishnamurthy, *Indian J. Chem.*, 1984, **A23**, 717.
74. C. W. Allen and A. J. White, *Inorg. Chem.*, 1974, **13**, 1220.
75. C. W. Allen, G. E. Brunst and M. E. Perlman, *Inorg. Chim. Acta*, 1980, **41**, 265.
76. G. Ottmann, H. Agahigian, H. Hooks, G. D. Vickers, E. Koher and R. Rätz, *Inorg. Chem.*, 1964, **3**, 753.
77. A. A. Van der Huizen, A. P. Jekel, J. K. Bolhuis, D. Keekstra, W. H. Ousema and J. C. Van de Grampel, *Inorg. Chim. Acta*, 1982, **66**, 85.
78. E. Niecke, H. Thamm and D. Böhler, *Inorg. Nucl. Chem. Lett.*, 1972, **8**, 261.
79. B. Green, D. B. Sowerby and P. Clare, *J. Chem. Soc. A*, 1971, 3487.
80. K. S. Dhathathreyan, S. S. Krishnamurthy, A. R. Vasudeva Murthy, R. A. Shaw and M. Woods, *J. Chem. Soc., Dalton Trans.*, 1981, 1928.
81. E. Niecke, O. Glemser and H. W. Roesky, *Z. Naturforsch.*, 1969, **24b**, 1187.
82. N. Boden, J. W. Emsley, J. Feeney and W. H. Sutcliffe, *Chem. Ind. (London)*, 1962, 1909.
83. T. Chivers and R. Hedgeland, *Can. J. Chem.*, 1972, **50**, 1017.
84. V. Chandrasekhar, "Spirocyclic phosphazenes and metal complexes of (amino)cyclophosphazenes", Ph.D. thesis, Indian Institute of Science, Bangalore, 1982.
85. K. V. Katti and S. S. Krishnamurthy, *Indian J. Chem.*, 1985, **A24**, 384.
86. A. P. Carroll, R. A. Shaw and M. Woods, *J. Chem. Soc., Dalton Trans.*, 1973, 2736.
87. J. E. Huheey, *Inorganic Chemistry*, 3rd edn, Harper and Row, New York, 1983.
88. S. K. Das, R. Keat, R. A. Shaw and B. C. Smith, *J. Chem. Soc.*, 1965, 5032.
89. R. L. Dieck and T. Moeller, *J. Inorg. Nucl. Chem.*, 1973, **35**, 75.
90. R. L. Dieck and T. Moeller, *J. Inorg. Nucl. Chem.*, 1973, **35**, 737.
91. J. W. Emsley, J. Feeney and L. H. Sutcliffe, *High Resolution Nuclear Magnetic Resonance Spectroscopy*, Vol. 2, Pergamon Press, Oxford, 1966.
92. B. Cardillo, G. Mattogno, A. Melera and F. Tarli, *Atti Accad. Naz. Lincei, Rend Classe Sci., Fis Mat. Nat.*, 1964, **37**, 194.

93. V. Chandrasekhar, S. S. Krishnamurthy, A. R. Vasudeva Murthy, R. A. Shaw and M. Woods, *Inorg. Nucl. Chem. Lett.*, 1981, **17**, 181.
94. H. Manns and H. Specker, *Z. Anal. Chem.*, 1975, **275**, 103.
95. G. Guerch, M. Graffeuil, J.-F. Labarre, R. Enjalbert, R. Lahana and F. Sournies, *J. Mol. Struct.*, 1982, **95**, 237.
96. G. Guerch, J.-F. Labarre, R. Roques and F. Sournies, *J. Mol. Struct.*, 1982, **96**, 113.
97. B. de Ruiter, G. Kuipers, J. H. Bijlaart and J. C. Van de Grampel, *Z. Naturforsch.*, 1982, **37b**, 1425.
98. V. Chandrasekhar, S. S. Krishnamurthy, H. Manohar, A. R. Vasudeva Murthy, R. A. Shaw and M. Woods, *J. Chem. Soc., Dalton Trans.*, 1984, 621.
99. N. El Murr, R. Lahana, J.-F. Labarre, and J. P. Declercq, *J. Mol. Struct.*, 1984, **73**, 117.
100. P. J. Harris and K. B. Williams, *Inorg. Chem.*, 1984, **23**, 1495.
101. S. S. Krishnamurthy, P. Ramabrahmam, A. R. Vasudeva Murthy, R. A. Shaw and M. Woods, *Inorg. Nucl. Chem. Lett.*, 1980, **16**, 215.
102. G. R. Feistel and T. Moeller, *J. Inorg. Nucl. Chem.*, 1967, **29**, 2731.
103. W. Lehr, *Z. Anorg. Allg. Chem.*, 1967, **350**, 18.
104. P. Clare, D. B. Sowerby, R. K. Harris and M. I. M. Wazeer, *J. Chem. Soc., Dalton Trans.*, 1975, 625.
105. H. R. Allcock, J. L. Desorcie and P. J. Harris, *J. Am. Chem. Soc.*, 1983, **105**, 2814.
106. H. R. Allcock, T. J. Fuller and K. Matsumura, *Inorg. Chem.*, 1982, **21**, 515.
107. A. Schmidpeter and K. Schumann, *Z. Naturforsch.*, 1970, **25b**, 1364.
108. H. G. Heal, *The Inorganic Heterocyclic Chemistry of Sulfur, Nitrogen and Phosphorus*, Academic Press, London, 1980, pp. 242–246.
109. G. Engelhardt, E. Steger and R. Stahlberg, *Z. Naturforsch.*, 1966, **21b**, 1231.
110. B. Grushkin, M. G. Sanchez and R. G. Rice, *Inorg. Chem.*, 1964, **3**, 623.
111. R. Keat, D. S. Rycroft, V. R. Miller, C. D. Schmulbach and R. A. Shaw, *Phosphorus Sulfur*, 1981, **10**, 121.
112. C. W. Allen and T. Moeller, *Inorg. Chem.*, 1968, **7**, 2177.
113. C. W. Allen, F. Y. Tsang and T. Moeller, *Inorg. Chem.*, 1968, **7**, 2183.
114. P. J. Harris, *Inorg. Chim. Acta*, 1983, **71**, 233.
115. K. Ramachandran and C. W. Allen, *J. Am. Chem. Soc.*, 1982, **104**, 2396.
116. F. Heatley and S. M. Todd, *J. Chem. Soc. A*, 1966, 1152.
117. J. L. Schmutz and H. R. Allcock, *Inorg. Chem.*, 1975, **14**, 2433.
118. C. W. Allen, K. Ramachandran, R. P. Bright and J. C. Shaw, *Inorg. Chim. Acta*, 1982, **64**, L109.
119. K. Ramachandran and C. W. Allen, *Inorg. Chem.*, 1983, **22**, 1445.
120. W. Sulkowski, A. A. Volodin, K. Brandt, V. V. Kireev and V. V. Korshak, *Zh. Obshch. Khim.*, 1981, **51**, 1221.
121. S. A. Ali, E. Herrmann and B. Thomas, *Z. Chem.*, 1984, **24**, 133.
122. K. S. Dhathathreyan, Unpublished results.
123. M. Kajiwara, Y. Mori and H. Saito, *Polymer*, 1976, **17**, 898.
124. B. Thomas and G. Grossmann, *Z. Anorg. Allg. Chem.*, 1979, **448**, 100.
125. M. N. Sudheendra Rao, "Aminolysis reactions of chloro- and bromo-cyclophosphazenes", Indian Institute of Science, Bangalore, 1976.
126. A. A. Van der Huizen, A. P. Jekel, J. Rusch, and J. C. Van de Grampel, *Rec. Trav. Chim.*, 1981, **100**, 343.
127. G. J. Bullen and P. A. Tucker, *J. Chem. Soc., Dalton Trans.*, 1972, 2437.
128. G. J. Bullen and P. E. Dann, *J. Chem. Soc., Dalton Trans.*, 1973, 1453.
129. B. Thomas and U. H. Scheler, *Z. Chem.*, 1978, **18**, 342.
130. G. Bulloch and R. Keat, *J. Chem. Soc., Dalton Trans.*, 1974, 2010.

131. R. L. Collin, *J. Am. Chem. Soc.*, 1966, **88**, 3281.

132. G. M. Blackburn, J. S. Chohen and I. Weatherall, *Tetrahedron*, 1971, **27**, 2903.

133. D. G. Gorenstein, *J. Am. Chem. Soc.*, 1975, **97**, 898.

134. M. Biddlestone, R. Keat, H. Rose, D. S. Rycroft and R. A. Shaw, *Z. Naturforsch.*, 1976, **31b**, 1001.

135. D. Dahmann, "Darstellung und Struktur von N-cyclophosphazenyl- und N-pentafluoro-phenylphosphiniminen", Dissertation, Ruhr Universität, Bochum, Federal Republic of Germany, 1978.

136. K. C. Kumaraswamy, P. Ramabrahmam and S. S. Krishnamurthy, *Synth. React. Inorg. Metal-Org. Chem.*, 1985, **15**, 1023.

137. M. K. Feldt and T. Moeller, *J. Inorg. Nucl. Chem.*, 1968, **30**, 2351.

138. C. Lensink, B. de Ruiter and J. C. Van de Grampel, *J. Chem. Soc., Dalton Trans.*, 1984, 1521.

139. N. Zumbulyadis and B. P. Dailey, *J. Magn. Reson.*, 1974, **13**, 189.

140. E. G. Finer, *J. Mol. Spectrosc.*, 1967, **23**, 104.

141. K. Schumann and A. Schmidpeter, *Phosphorus*, 1973, **3**, 51.

142. C. W. Allen, *J. Magn. Reson.*, 1971, **5**, 435.

143. B. Thomas and G. Grossmann, *J. Magn. Reson.*, 1979, **36**, 333.

144. B. Thomas, G. Seifert and G. Grossmann, *Z. Chem.*, 1980, **20**, 217.

145. T. S. Cameron and Kh. Mannan, *Acta Crystallogr.*, 1977, **B33**, 443.

146. K. S. Dhathathreyan, S. S. Krishnamurthy, A. R. Vasudeva Murthy, T. S. Cameron, C. Chan, R. A. Shaw and M. Woods, *J. Chem. Soc., Chem. Commun.*, 1980, 231.

147. M. L. Heffernan and R. F. M. White, *J. Chem. Soc.*, 1961, 1382.

148. Y. S. Babu, H. Manohar and R. A. Shaw, *J. Chem. Soc., Dalton Trans.*, 1981, 599.

149. K. S. Dhathathreyan, S. S. Krishnamurthy, A. R. Vasudeva Murthy, R. A. Shaw and M. Woods, *J. Chem. Soc., Dalton Trans.*, 1982, 1549.

150. G. J. Bullen, P. E. Dann, M. L. Evans, M. B. Hursthouse, R. A. Shaw, K. Wait, M. Woods and H. S. Yu, *Z. Naturforsch.*, 1976, **31b**, 995.

151. B. W. Fitzsimmons, C. Hewlett, K. Hills and R. A. Shaw, *J. Chem. Soc.* A, 1967, 679.

152. R. Vilceanu and P. Schulz, *Phosphorus*, 1976, **6**, 231.

153. K. S. Dhathathreyan, "Synthetic and spectroscopic studies of alkoxycyclophosphazenes, phosphazadienes and phosphazanes", Ph.D. thesis, Indian Institute of Science, Bangalore, 1981.

154. B. de Ruiter, H. Winter, T. Wilting and J. C. Van de Grampel, *J. Chem. Soc., Dalton Trans.*, 1984, 1027.

155. A. Schmidpeter, K. Blanck, H. Eiletz, H. Smetana and C. Weingand, *Synth. React. Inorg. Metal-Org. Chem.*, 1977, **7**, 1.

156. V. Ramamoorthy, T. Ranganathan, G. S. Rao and P. T. Manoharan, *J. Chem. Res.*, 1982, (S) 316; (M) 3074–3094.

157. R. K. Harris, J. R. Woplin, M. Murray and R. Schmutzler, *J. Chem. Soc., Dalton Trans.*, 1972, 1590.

158. T. T. Bamgboye and D. B. Sowerby, *J. Inorg. Nucl. Chem.*, 1981, **43**, 2253.

159. Z. Biran and J. M. E. Goldschmidt, *J. Chem. Soc., Dalton Trans.*, 1979, 1017.

160. T. Chivers, R. T. Oakley and N. L. Paddock, *J. Chem. Soc.* A, 1970, 2324.

161. B. Green, *J. Chem. Soc., Dalton Trans.*, 1974, 1113.

162. O. Glemser, E. Niecke and H. Thamm, *Z. Naturforsch.*, 1970, **25b**, 754.

163. Z. Biran and J. M. E. Goldschmidt, *Synth. React. Inorg. Metal-Org. Chem.*, 1978, **8**, 323.

164. H. W. Roesky, *Z. Naturforsch.*, 1970, **25b**, 777.

165. H. W. Roesky and W. G. Böwing, *Z. Anorg. Allg. Chem.*, 1971, **386**, 191.

166. H. W. Roesky, W. G. Böwing and E. Niecke, *Chem. Ber.*, 1971, **104**, 653.

167. D. Dahmann, H. Rose and W. Walz, *Z. Naturforsch.*, 1980, **35b**, 964.

168. N. L. Paddock and D. J. Patmore, *J. Chem. Soc., Dalton Trans.*, 1976, 1029.
169. O. Glemser, E. Niecke and H. W. Roesky, *J. Chem. Soc., Chem. Commun.*, 1969, 282.
170. J. Emsley and N. L. Paddock, *J. Chem. Soc. A*, 1968, 2590.
171. P. Clare, D. Millington and D. B. Sowerby, *J. Chem. Soc., Dalton Trans.*, 1972, 2374.
172. H. W. Roesky and M. Banek, *Z. Naturforsch.*, 1979, **34b**, 752.
173. H. W. Roesky and E. Janssen, *Z. Naturforsch.*, 1974, **29b**, 174.
174. E. Niecke, H. Thamm and O. Glemser, *Z. Naturforsch.*, 1971, **26b**, 366.
175. A. W. Cordes, P. N. Swepston, R. T. Oakley, N. L. Paddock and T. N. Ranganathan, *Can. J. Chem.*, 1981, **59**, 2364.
176. T. Chivers and N. L. Paddock, *Inorg. Chem.*, 1972, **11**, 848.
177. C. W. Allen and P. L. Toch, *Inorg. Chem.*, 1981, **20**, 8.
178. J. G. Dupont and C. W. Allen, *Inorg. Chem.*, 1978, **17**, 3093.
179. C. W. Allen and R. P. Bright, *Inorg. Chem.*, 1983, **22**, 1291.
180. C. W. Allen, J. L. Desorcie and K. Ramachandran, *J. Chem. Soc., Dalton Trans.*, 1984, 2843.
181. T. Chivers, *Inorg. Nucl. Chem. Lett.*, 1971, **7**, 827.
182. A. A. Volodin, V. V. Kireev, A. A. Fomin, M. G. Edelev and V. V. Korshak, *Dokl. Akad. Nauk SSSR*, 1973, **209**, 98.
183. E. Niecke, O. Glemser and H. Thamm, *Chem. Ber.*, 1970, **103**, 2864.
184. H. W. Roesky and E. Janssen, *Z. Naturforsch.*, 1974, **29b**, 177.
185. H. W. Roesky and E. Janssen, *Chem.-Ztg.*, 1974, **98**, 260.
186. M. Biddlestone and R. A. Shaw, *J. Chem. Soc. A*, 1971, 2715.
187. V. N. Prons, N. B. Zaitsev, V. P. Sass and A. L. Klebanskii, *Zh. Obshch. Khim.*, 1980, **50**, 17.
188. H.-G. Horn and F. Kolkmann, *Chem.-Ztg.*, 1981, **105**, 213.
189. H.-G. Horn and F. Kolkmann, *Makromol. Chem.*, 1982, **88**, 1843.
190. H. R. Allcock, P. R. Suszko and T. L. Evans, *Organometallics*, 1982, **1**, 1443.
191. H. R. Allcock, T. L. Evans and T. J. Fuller, *Inorg. Chem.*, 1980, **19**, 1026.
192. R. J. Ritchie, P. J. Harris and H. R. Allcock, *Inorg. Chem.*, 1980, **19**, 2483.
193. H. R. Allcock, K. D. Lavin, G. H. Riding, P. R. Suszko and R. R. Whittle, *J. Am. Chem. Soc.*, 1984, **106**, 2337.
194. H. R. Allcock, G. H. Riding and R. R. Whittle, *J. Am. Chem. Soc.*, 1984, **106**, 5561.
195. H. R. Allcock, R. A. Nissan, P. J. Harris and R. R. Whittle, *Organometallics*, 1984, **3**, 432.
196. N. L. Paddock, T. N. Ranganathan, S. S. Rettig, R. D. Sharma and J. Trotter, *Can. J. Chem.*, 1981, **59**, 2429.
197. R. D. Sharma, S. S. Rettig, N. L. Paddock and J. Trotter, *Can. J. Chem.*, 1982, **60**, 535.
198. C. W. Allen, *J. Organomet. Chem.*, 1977, **125**, 215.
199. S. S. Krishnamurthy, P. Ramabrahmam and M. Woods, *Org. Magn. Reson.*, 1981, **15**, 205.
200. C. W. Allen and J. C. Green, *Inorg. Chem.*, 1980, **19**, 1719.
201. A. A. Van der Huizen, J. C. Van de Grampel, W. Akkerman, P. Lelieveld, A. Van der Meer-Kelverkamp and H. B. Lamberts, *Inorg. Chim. Acta*, 1983, **78**, 239.
202. V. D. Mochel and T. C. Cheng, *Macromolecules*, 1978, **11**, 176.
203. T. C. Cheng, V. D. Mochel, H. E. Adams and T. F. Longo, *Macromolecules*, 1980, **13**, 158.
204. W. T. Ferrar, F. V. DiStefano and H. R. Allcock, *Macromolecules*, 1980, **13**, 1345.
205. S. Karthikeyan and S. S. Krishnamurthy, Unpublished results.
206. J. Mason, W. Van Bronswijk and J. G. Vinter, *J. Chem. Soc., Dalton Trans.*, 1977, 2337.
207. B. Thomas, G. Seifert, G. Grossmann and D. Scheller, *Z. Phys. Chem. Leipzig*, 1979, **260**, 225.
208. B. Thomas, G. Grossmann and D. Scheller, *Z. Anorg. Allg. Chem.*, 1979, **448**, 107.
209. B. Thomas, G. Grossmann and D. Scheller, *Z. Anorg. Allg. Chem.*, 1981, **480**, 163.
210. B. Thomas, W. Bieger and G. Grossmann, *Z. Chem.*, 1981, **21**, 292.
211. B. Thomas, G. Grossmann and H. Meyer, *Phosphorus Sulfur*, 1981, **10**, 375.

212. B. Thomas, A. John and G. Grossmann, *Z. Anorg. Allg. Chem.*, 1982, **489**, 131.
213. B. Thomas and G. Grossmann, *Z. Chem.*, 1983, **23**, 27.
214. B. Thomas, G. Grossmann, W. Bieger and A. Porzel, *Z. Anorg. Allg. Chem.*, 1983, **504**, 138.
    (a) B. Thomas, G. Grossman and H. Meyer, *Z. Anorg. Allg. Chem.*, 1982, **490**, 121.
215. J. Müller and H. F. Schroder, *Z. Anorg. Allg. Chem.*, 1979, **450**, 149.
216. (a) S. S. Krishnamurthy and M. Woods, *J. Indian Inst. Sci.*, 1983, **B64**, 143; (b) S. S. Krishnamurthy, A. R. Vasudeva Murthy, R. A. Shaw and M. Woods, *J. Indian Inst. Sci.* 1979, **B61**, 57.
217. D. Millington and D. B. Sowerby, *J. Chem. Soc., Dalton Trans.*, 1972, 2035.
218. G. J. Bullen, P. E. Dann, V. B. Desai, R. A. Shaw, B. C. Smith and M. Woods, *Phosphorus*, 1973, **3**, 67.
219. S. S. Krishnamurthy, R. A. Shaw, M. N. Sudheendra Rao, A. R. Vasudeva Murthy and M. Woods, *Inorg. Chem.*, 1978, **17**, 1527.
220. S. S. Krishnamurthy, P. M. Sundaram and M. Woods, *Inorg. Chem.*, 1982, **21**, 406.
221. P. Ramabrahmam, S. S. Krishnamurthy and M. Woods, *Z. Naturforsch.*, 1981, **36b**, 894.
222. T. N. Ranganathan, S. M. Todd and N. L. Paddock, *Inorg. Chem.*, 1973, **12**, 316.
223. D. Millington and D. B. Sowerby, *J. Chem. Soc., Dalton Trans.*, 1973, 2649.
224. D. Millington and D. B. Sowerby, *J. Chem. Soc., Dalton Trans.*, 1974, 1070.
225. D. Millington and D. B. Sowerby, *Phosphorus*, 1974, **5**, 51.
226. D. Millington, T. J. King and D. B. Sowerby, *J. Chem. Soc., Dalton Trans.*, 1973, 396.
227. M. J. Begley, D. Millington, T. J. King and D. B. Sowerby, *J. Chem. Soc., Dalton Trans.*, 1974, 1162.
228. T. T. Bamgboye, M. J. Begley and D. B. Sowerby, *J. Chem. Soc., Dalton Trans.*, 1975, 2617.
229. S. S. Krishnamurthy, R. A. Shaw and M. Woods, *Current Sci.*, 1976, **45**, 433.
230. B. Grushkin, *t.*. J. Berlin, J. L. McClanahan and R. G. Rice, *Inorg. Chem.*, 1966, **5**, 172.
231. M. Biddlestone, S. S. Krishnamurthy, R. A. Shaw, M. Woods, G. J. Bullen and P. E. Dann, *Phosphorus*, 1973, **3**, 179.
232. S. S. Krishnamurthy, A. C. Sau, A. R. Vasudeva Murthy, R. Keat, R. A. Shaw and M. Woods, *J. Chem. Soc., Dalton Trans.*, 1977, 1980.
233. S. S. Krishnamurthy, K. Ramachandran, A. C. Sau, M. N. Sudheendra Rao, A. R. Vasudeva Murthy, R. Keat and R. A. Shaw, *Phosphorus Sulfur*, 1978, **5**, 117.
234. R. J. Abraham, *Analysis of High-Resolution NMR Spectra*, Elsevier, Amsterdam, 1971.
235. P. Ramabrahmam, K. S. Dhathathreyan, S. S. Krishnamurthy and M. Woods, *Ind. J. Chem.*, 1983, **A22**, 1.
236. V. Chandrasekhar, S. Karthikeyan, S. S. Krishnamurthy and M. Woods, *Ind. J. Chem.*, 1985, **A24**, 379.
237. K. S. Dhathathreyan, S. S. Krishnamurthy and M. Woods, *J. Chem. Soc., Dalton Trans.*, 1982, 2151.
238. B. Thomas and G. Grossmann, *Z. Chem.*, 1981, **21**, 152.
239. K. D. Gallicano, R. T. Oakley and N. L. Paddock, *J. Inorg. Nucl. Chem.*, 1980, **42**, 923.
240. H. T. Searle, J. Dyson, T. N. Ranganathan and N. L. Paddock, *J. Chem. Soc., Dalton Trans.*, 1975, 203.
241. A. Gieren and B. Dederer, *Z. Anorg. Allg. Chem.*, 1980, **467**, 68.
242. H. W. Roesky and E. Janssen, *Agnew. Chem. Int. Ed. Engl.* 1976, **15**, 39.
243. A. Baceiredo, G. Bertrand, J. P. Majoral, G. Sicard, J. Jaud and J. Galy, *J. Am. Chem. Soc.*, 1984, **106**, 6088.
244. E. H. Poindexter, R. D. Bates, N. L. Paddock and J. A. Potenza, *J. Am. Chem. Soc.*, 1973, **95**, 1714.
245. R. A. Dweck, N. L. Paddock, J. A. Potenza and E. H. Poindexter, *J. Am. Chem. Soc.*, 1969, **91**, 5436.

246. N. L. Paddock and J. Serreqi, *Can. J. Chem.*, 1974, **52**, 2546.
247. S. S. Krishnamurthy, A. C. Sau, A. R. Vasudeva Murthy, R. A. Shaw, M. Woods and R. Keat, *J. Chem. Res.*, 1977, (S) 70, (M) 0860–0884.
248. S. S. Krishnamurthy, K. Ramachandran and M. Woods, *J. Chem. Res.*, 1979, (S) 92, (M) 1258–1265.
249. S. S. Krishnamurthy, K. Ramachandran, A. C. Sau, A. R. Vasudeva Murthy, R. A. Shaw and M. Woods, *Inorg. Chem.*, 1979, **18**, 2010.
250. P. Y. Narayanaswamy, K. S. Dhathathreyan and S. S. Krishnamurthy, *Inorg. Chem.*, 1985, **24**, 640.
251. G. Hägele, R. K. Harris, M. I. M. Wazeer and R. Keat, *J. Chem. Soc., Dalton Trans.*, 1974, 1985.
252. A. Schmidpeter, J. Högel and F. R. Ahmed, *Chem. Ber.*, 1976, **109**, 1911.
253. H. R. Allcock, M. S. Connolly and P. J. Harris, *J. Am. Chem. Soc.*, 1982, **104**, 2482.
254. A. Schmidpeter, K. Blanck and J. Högel, *Z. Naturforsch.*, 1976, **31b**, 1466.
255. E. G. Finer and R. K. Harris, *Mol. Phys.*, 1967, **12**, 457; R. K. Harris, *Can. J. Chem.*, 1964, **42**, 2275.
256. A. Schmidpeter and J. Högel, *Chem. Ber.*, 1978, **111**, 3867.
257. H. Winter and J. C. Van de Grampel, *Rec. Trav. Chim.*, 1984, **103**, 241.
258. W. Lehr, *Z. Anorg. Allg. Chem.*, 1969, **371**, 225.
259. M. Bermann and J. R. Van Wazer, *J. Chem. Soc., Dalton Trans.*, 1973, 813.
260. A. Schmidpeter and H. Eiletz, *Chem. Ber.*, 1975, **108**, 1454.
261. A. Schmidpeter and H. Eiletz, *Phosphorus*, 1976, **6**, 113.
262. G. Schoening and O. Glemser, *Chem. Ber.*, 1977, **110**, 3231.
263. H. Winter and J. C. Van de Grampel, *Z. Naturforsch.*, 1983, **38b**, 7.
264. R. T. Oakley and N. L. Paddock, *Can. J. Chem.*, 1973, **51**, 520.
265. H. R. Allcock, E. C. Bissell and E. T. Shawl, *Inorg. Chem.*, 1973, **12**, 2963.
266. R. W. Allen, J. P. O'Brien and H. R. Allcock, *J. Am. Chem. Soc.*, 1977, **99**, 3987.
267. H. R. Allcock, P. P. Greigger, L. J. Wagner and M. Y. Bernheim, *Inorg. Chem.*, 1981, **20**, 717.
268. H. R. Allcock, A. G. Scopelianos, R. R. Whittle and N. M. Tollefson, *J. Am. Chem. Soc.*, 1983, **105**, 1316.
269. H. R. Allcock, L. J. Wagner and M. L. Levin, *J. Am. Chem. Soc.*, 1983, **105**, 1321.
270. H. R. Allcock, K. D. Lavin, N. M. Tollefson and T. L. Evans, *Organometallics*, 1983, **2**, 267.
271. H. R. Allcock, P. R. Suszko, L. J. Wagner, R. R. Whittle and B. Boso, *J. Am. Chem. Soc.*, 1984, **106**, 4966.
272. H. R. Allcock, K. D. Lavin, G. H. Riding and R. R. Whittle, *Organometallics*, 1984, **3**, 663.
273. A. Schmidpeter, K. Blanck, H. Hess and H. Riffel, *Angew. Chem. Int. Ed. Engl.*, 1980, **19**, 650.
274. K. C. Dash, A. Schmidpeter and H. Schmidbauer, *Z. Naturforsch.*, 1980, **35b**, 1286.
275. K. D. Gallicano and N. L. Paddock, *Can. J. Chem.*, 1982, **60**, 521.
276. V. Chandrasekhar, S. S. Krishnamurthy and M. Woods, *ACS Symp. Ser.*, 1981, **171** (*Phosphorus Chem.*), 418.
277. G. E. Coxon and D. B. Sowerby, *Inorg. Chim. Acta*, 1967, **1**, 381.
278. K. B. Dillon, A. W. G. Platt and T. C. Waddington, *J. Chem. Soc., Dalton Trans.*, 1980, 1036.
279. H. P. Latscha, *Z. Anorg. Allg. Chem.*, 1968, **362**, 7.
280. K. D. Gallicano, R. T. Oakley, N. L. Paddock and R. D. Sharma, *Can. J. Chem.*, 1981, **59**, 2654.
281. (a) P. J. Harris, M. A. Schwalke, V. Liu and B. L. Fisher, *Inorg. Chem.*, 1983, **22**, 1812; (b) P. J. Harris and L. A. Jackson, *Organometallics*, 1983, **2**, 1477.
282. M. Bermann and K. Utvary, *J. Inorg. Nucl. Chem.*, 1969, **31**, 271.
283. A. Schmidpeter and H. Eiletz, *Chem. Ber.*, 1976, **109**, 2340.
284. T. Moeller and P. Nannelli, *Inorg. Chem.*, 1963, **2**, 659.

285. B. Thomas, P. Gehlert, H. Schadow and H. Scheler, *Z. Anorg. Allg. Chem.*, 1978, **438**, 249.
286. H. R. Allcock and T. J. Fuller, *J. Am. Chem. Soc.*, 1981, **103**, 2250.
287. A. A. Smaardijk, B. de Ruiter, A. A. Van der Huizen and J. C. Van de Grampel, *Rec. Trav. Chim.*, 1982, **101**, 270.
288. R. Visalakshi, T. N. Ranganathan, G. S. Rao and K. V. Muralidharan, *Current Sci.*, 1982, **51**, 508.
289. H. R. Allcock, P. E. Austin and T. X. Neenan, *Macromolecules*, 1982, **15**, 689.
290. Y. Kobayashi, L. A. Chasin and L. B. Clapp, *Inorg. Chem.*, 1963, **2**, 212.
291. J. C. Van de Grampel, A. A. Van der Huizen, A. P. Jekel, D. Wiedijk, J.-F. Labarre and F. Sournies, *Inorg. Chim. Acta*, 1981, **53**, L169.
292. J. L. Butour, J.-F. Labarre and F. Sournies, *J. Mol. Struct.*, 1980, **65**, 51.
293. M. Becke-Goehring, K. John and E. Fluck, *Z. Anorg. Allg. Chem.*, 1959, **302**, 103.
294. J. K. Bolhaus, D. Keekstra, W. H. Ousema and J. C. Van de Grampel, Unpublished results.
295. B. Thomas, P. Gehlert, H. Schadow and H. Scheler, *Z. Anorg. Allg. Chem.*, 1975, **418**, 171.
296. A. Mahmoun, P. Castera and J.-F. Labarre, *Inorg. Chim. Acta*, 1984, **86**, L41.
297. V. G. Derendyaeva, Yu. V. Kolodyazhnyi, S. G. Fedorov, S. K. Alieva, S. F. Zapuskalova, G. S. Gol'din and O. A. Osipov, *Zh. Obshch. Khim.*, 1977, **47**, 2502.
298. V. N. Sharov, V. N. Prons, V. V. Korol'ko, A. L. Klebanskii and G. P. Kondratenkov, *Zh. Obshch. Khim.*, 1975, **45**, 1953.
299. G. S. Gol'din, S. G. Federov, S. F. Zapuskalova and A. D. Naumov, *Zh. Obshch. Khim.*, 1976, **46**, 688.
300. K. Brandt, V. V. Kireev, V. V. Korshak and B. R. Tsokolaev, *Zh. Obshch. Khim.*, 1978, **48**, 358.
301. I. B. Telkova, V. V. Kireev, V. V. Korshak, A. A. Volodin and A. A. Fomin, *Zh. Obshch. Khim.*, 1973, **43**, 1257.
302. P. O. Gitel', L. F. Osipova and O. P. Solovova, *Zh. Obshch. Khim.*, 1975, **45**, 1749.
303. A. A. Volodin, S. N. Zelenetskii, V. V. Kireev and V. V. Korshak, *Zh. Obshch. Khim.*, 1975, **45**, 37.
304. H. R. Allcock and P. E. Austin, *Macromolecules*, 1981, **14**, 1616.
305. M. Gleria, S. Lora, F. Minto, L. Busulini and G. Paolucci, *Chim. Ind. (Milan)*, 1981, **63**, 719.
306. M. Gleria, A. Paolucci, F. Minto and S. Lora, *Chim. Ind. (Milan)*, 1982, **64**, 479.
307. H. R. Allcock, P. E. Austin and T. F. Rakowsky, *Macromolecules*, 1981, **14**, 1622.
308. H. R. Allcock, T. X. Neenan and W. C. Kossa, *Macromolecules*, 1982, **15**, 693.
309. L. A. Alekseenko, V. V. Kireev and D. F. Kutepov, *Zh. Obshch. Khim.*, 1978, **48**, 1260.
310. B. Thomas, H. Schadow and H. Scheler, *Z. Chem. (Leipzig)*, 1975, **15**, 26.
311. R. A. Dwek, R. E. Richards, D. Taylor and R. A. Shaw, *J. Chem. Soc. A*, 1970, 1173.
312. V. V. Korshak, A. I. Solomatina, N. I. Bekasova, M. A. Andreyeva, Ye. G. Bulycheva, S. V. Vinogradova, V. N. Kalinin and L. I. Zakharkin, *Polymer Sci. (USSR)*, 1980, **22**, 2180.
313. H. R. Allcock, R. J. Ritchie and P. J. Harris, *Macromolecules*, 1980, **13**, 1332.
314. C. T. Ford, J. M. Barr, F. E. Dickson and I. I. Bezman, *Inorg. Chem.*, 1966, **5**, 351.
315. K. Brandt, T. I. Guseva, V. V. Kireev, V. V. Korshak and A. A. Kudryashov, *Zh. Obshch. Khim.*, 1978, **48**, 2468.
316. A. Schmidpeter, K. Blanck and F. R. Ahmed, *Angew. Chem. Int. Ed. Engl.*, 1976, **15**, 488.
317. A. Schmidpeter and C. Weingand, *Z. Naturforsch.*, 1969, **24b**, 177.
318. G. Guerch, J.-F. Labarre, J. Oiry and J.-L. Imbach, *Inorg. Chim. Acta, Bioinorg. Sect.*, 1982, **67**, L5.
319. H. Lederle, G. Ottmann and E. Kober, *Inorg. Chem.*, 1966, **5**, 1818.
320. J. K. Fincham, M. B. Hursthouse, H. G. Parkes, L. S. Shaw and R. A. Shaw, *J. Chem. Soc., Chem. Commun.*, 1985, 252.

321. M. Kajiwara and Y. Kurachi, *Polyhedron*, 1983, **2**, 1211.
322. A. A. Volodin, V. V. Kireev, V. V. Korshak and A. A. Fomin, *Zh. Obshch. Khim.*, 1973, **43**, 2206.
323. S. R. Contractor, "Studies of spirocyclic and bicyclic phosphazenes", Ph.D. thesis, University of London, 1983.
324. H. R. Allcock and R. L. Kugel, *Inorg. Chem.*, 1966, **5**, 1016.
325. K. Brandt and Z. Jedlinski, *J. Org. Chem.*, 1980, **45**, 1672.
326. K. Brandt. *J. Org. Chem.*, 1981, **46**, 1918.
327. H. Rose and H. Specker, *Z. Anorg. Allg. Chem.*, 1976, **426**, 275.
328. H. G. Parkes and R. A. Shaw, Paper presented at 3rd Int. Symp. on Inorganic Ring Systems, Graz, Austria, 1981.
329. M. Biddlestone, R. A. Shaw and D. Taylor, *J. Chem. Soc., Chem. Commun.*, 1969, 320.
330. H. R. Allcock, A. G. Scopelianos, J. P. O'Brien and M. Y. Bernheim, *J. Am. Chem. Soc.*, 1981, **103**, 350.
331. F. Di Gregorio, W. Marconi and L. Caglioti, *J. Org. Chem.*, 1981, **46**, 4569.
332. S. Ganapathiappan and S. S. Krishnamurthy, *J. Chem. Soc. Dalton Trans.*, 1987, 585.
333. E. J. Wash and J. Smegal, *Inorg. Chem.*, 1976, **15**, 2565.
334. W. Lehr and J. Pietschmann, *Chem-Ztg.*, 1970, **94**, 362.
335. P. Y. Narayanaswamy and S. S. Krishnamurthy, Unpublished results.
336. K. John, T. Moeller and L. F. Audrieth, *J. Am. Chem. Soc.*, 1960, **82**, 5616.
337. K. John, T. Moeller and L. F. Audrieth, *J. Am. Chem. Soc.*, 1961, **83**, 2608.
338. M. N. Sudheendra Rao, Unpublished results.
339. A. Slawisch and J. Pietschmann, *Z. Naturforsch.*, 1970, **25b**, 321.
340. P. Ramabrahmam, Ph.D. Thesis, Indian Institute of Science, Bangalore, 1981.
341. H. W. Roesky and E. Janssen, *Chem. Ber.*, 1975, **108**, 2531.
342. T. L. Evans and H. R. Allcock, *Inorg. Chem.*, 1979, **18**, 2342.
343. K. C. Kumaraswamy, S. S. Krishnamurthy, A. R. Vasudeva Murthy, R. A. Shaw and M. Woods, *Indian J. Chem.*, 1986, **A25**, 1004.
344. K. D. Gallicano, N. L. Paddock, S. J. Rettig and J. Trotter, *Inorg. Nucl. Chem. Lett.*, 1979, **15**, 417.
345. G. I. Mitropol'skaya, V. V. Kireev, V. V. Korshak and A. A. Goryaev, *Zh. Obshch. Khim.*, 1982, **52**, 2486.
346. J. G. Dupont and C. W. Allen, *Inorg. Chem.*, 1977, **16**, 2964.
347. T. Chivers and M. N. S. Rao, *Can. J. Chem.*, 1983, **61**, 1957.
348. V. V. Kireev, V. A. Kovyazin, V. M. Kopylov, M. G. Zaitsava and G. I. Mitropol'skaya, *Zh. Obshch. Khim.*, 1984, **54**, 1899.
349. V. G. Sartaniya, V. V. Kireev and V. V. Korshak, *Zh. Obshch. Khim.*, 1973, **43**, 681.
350. H. R. Allcock, T. J. Fuller and K. Matsumura, *J. Org. Chem.*, 1981, **46**, 13.
351. S. R. Contractor, M. B. Hursthouse, L. S. Shaw, R. A. Shaw and H. Yilmaz, *Acta Crystallogr.*, 1985, **418**, 122.
352. G. I. Mitropol'skaya and V. V. Kireev, *Z. Neorg. Khim.*, 1983, **28**, 1914.
353. T. T. Bambgboye and O. A. Bambgboye, *Spectrochim Acta.*, 1984, **40A**, 329.

INDEX

This Page Intentionally Left Blank